

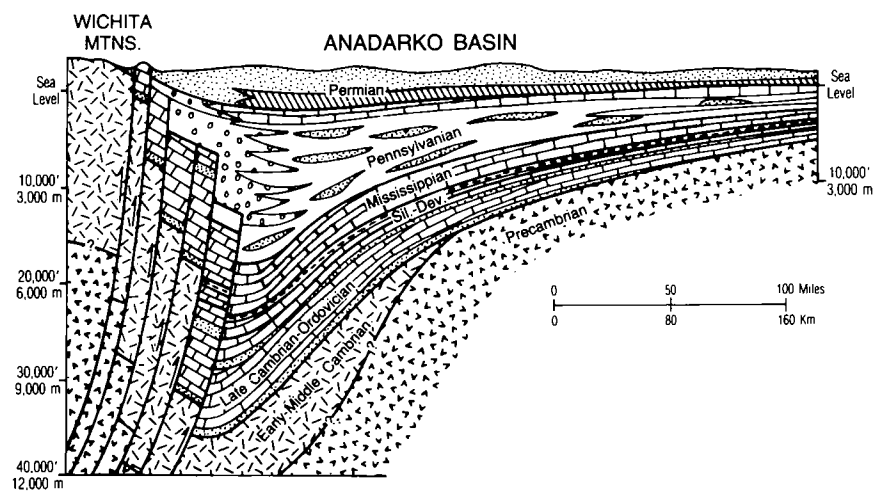
OKLAHOMA GEOLOGICAL SURVEY
Charles J. Mankin, *Director*

CIRCULAR 90

ISSN 0078-4397

ANADARKO BASIN SYMPOSIUM, 1988

KENNETH S. JOHNSON, *Editor*



Proceedings of a symposium held April 5-6, 1988, at Norman, Oklahoma; cosponsored by the Oklahoma Geological Survey and the U.S. Geological Survey.

The University of Oklahoma
Norman
1989

OKLAHOMA GEOLOGICAL SURVEY

CHARLES J. MANKIN, *Director*
KENNETH S. JOHNSON, *Associate Director*

SURVEY STAFF

JAMES H. ANDERSON, <i>Cartographic Technician I</i>	LEROY A. HEMISH, <i>Coal Geologist</i>
ROBERT H. ARNDT, <i>Economic Geologist</i>	PAULA A. HEWITT, <i>Supervisor, Copy Center</i>
BETTY D. BELLIS, <i>Word-Processor Operator</i>	RONA L. HOWARD, <i>Receptionist-Clerk</i>
TOM L. BINGHAM, <i>Geologist I</i>	SHIRLEY A. JACKSON, <i>Research Specialist I</i>
MITZI G. BLACKMON, <i>Clerk-Typist</i>	JAMES IRVIN JONES, <i>Facilities Maintenance Helper</i>
HELEN D. BROWN, <i>Assistant to Director</i>	JAMES W. KING, <i>Clerk</i>
JOCK A. CAMPBELL, <i>Petroleum Geologist</i>	JAMES E. LAWSON, JR., <i>Chief Geophysicist</i>
BRIAN J. CARDOTT, <i>Organic Petrologist</i>	KENNETH V. LUZA, <i>Engineering Geologist</i>
KEITH A. CATTO, JR., <i>Chemist</i>	DAVID O. PENNINGTON, <i>Operations Assistant</i>
JAMES R. CHAPLIN, <i>Geologist</i>	ADAM P. RADZINSKI, <i>Cartographic Technician I</i>
CHRISTIE L. COOPER, <i>Assistant Editor</i>	MASSOUD SAFAVI, <i>Cartographic Technician II</i>
VELMA L. COTTRELL, <i>Chief Clerk</i>	JUDY A. SCHMIDT, <i>Secretary I</i>
ELDON R. COX, <i>Manager, Core and Sample Library</i>	CONNIE G. SMITH, <i>Promotion and Information Specialist</i>
TAMMIE K. CREEL, <i>Data-Entry Operator</i>	LARRY N. STOUT, <i>Editor/Geologist</i>
CHARLES DYER III, <i>Drilling Technician</i>	MICHELLE J. SUMMERS, <i>Coordinator Geological Computer Systems</i>
WALTER C. ESRY, <i>Core and Sample Library Assistant</i>	NEIL H. SUNESON, <i>Stratigrapher</i>
ROBERT O. FAY, <i>Geologist</i>	DANNY L. SWINK, <i>Drilling Technician</i>
SAMUEL A. FRIEDMAN, <i>Senior Coal Geologist</i>	RICHARD L. WATKINS, <i>Electronics Technician</i>
T. WAYNE FURR, <i>Manager of Cartography</i>	JANE L. WEBER, <i>Organic Chemist</i>
JIMMY L. GIBSON, <i>Laboratory Assistant</i>	STEPHEN J. WEBER, <i>Chief Chemist</i>
DIANA L. GILSTRAP, <i>Publications Clerk</i>	GWEN C. WILLIAMSON, <i>Office Manager</i>
JOY HAMPTON, <i>Petroleum Geologist</i>	
PATRONALIA HANLEY, <i>Chemist</i>	

Title-Page Illustration

Schematic cross section of the Anadarko basin.

This publication, printed by Darby Printing Company, Atlanta, Georgia, is issued by the Oklahoma Geological Survey as authorized by Title 70, Oklahoma Statutes, 1981, Section 3310, and Title 74, Oklahoma Statutes, 1981, Sections 231-238. 1,000 copies have been prepared for distribution at a cost of \$13,077.95 to the taxpayers of the State of Oklahoma. Copies have been deposited with the Publications Clearinghouse of the Oklahoma Department of Libraries.

PREFACE

The Anadarko basin is one of the greatest oil and gas provinces in the United States. Cumulative production from the greater Anadarko basin through 1985 was >5 billion barrels of oil and 82 trillion cubic feet of gas, production coming primarily from ~50 significant fields in the basin (Davis and Northcutt, this volume). The Oklahoma Geological Survey and the U.S. Geological Survey have been conducting and sponsoring research programs in the Anadarko basin for a number of years. On April 5–6, 1988, the two agencies cosponsored a symposium comprising invited papers and posters to present data on these programs and other Anadarko basin research. The symposium was held at the Oklahoma Center for Continuing Education, The University of Oklahoma, in Norman, and this volume contains the proceedings of that conference.

Cooperative efforts of the OGS and USGS to jointly study the Anadarko basin were initiated in 1984 when the USGS began its Evolution of Sedimentary Basins (ESB) program. The ESB program—which utilizes sedimentary basins as natural geologic laboratories to address geologic topics and processes important in assessing our nation's natural resources—meshed perfectly with ongoing OGS studies in the Anadarko basin. Funding of the USGS part of the Anadarko basin program has been from their ESB program and the Onshore Oil and Gas program.

Research reported upon at the symposium includes work on basin history, sedimentation, stratigraphy, tectonics, petroleum exploration, source rocks, thermal history, oil characterization and migration, and hydrogeology. It is our hope that the symposium and these proceedings will bring such research to the attention of the geoscience community, and will help foster exchange of information and increased research interest in the Anadarko basin. Twenty-one invited papers were presented orally, and an additional 20 reports were presented as posters during the two-day session. All 21 of the orally presented papers are presented here as full papers or abstracts, and 14 of the poster presentations are presented as abstracts or short reports.

Stratigraphic nomenclature and age determinations used by the various authors in this volume do not necessarily agree with those of the OGS or the USGS.

Persons included in the organization and planning of this symposium include Kenneth Johnson and Charles Mankin of the OGS, and Tom Fouch, Gary Hill, Janet Pitman, Dudley Rice, and Jim Schmoker of the USGS. Appreciation is expressed to them and to the many authors who worked toward a highly successful symposium.

KENNETH S. JOHNSON
General Chairman

CONTENTS

iii Preface

PART I—Papers Presented at the Symposium

- 3 **Geologic Evolution of the Anadarko Basin**
Kenneth S. Johnson
- 13 **The Greater Anadarko Basin: An Overview of Petroleum Exploration and Development**
Herbert G. Davis and Robert A. Northcutt
- 25 **Thermal Maturity of the Anadarko Basin**
James W. Schmoker
- 32 **Thermal Maturation of the Woodford Shale in the Anadarko Basin**
Brian J. Cardott
- 47 **Characterization and Origin of Natural Gases of the Anadarko Basin**
Dudley D. Rice, Charles N. Threlkeld, and April K. Vuletich
- 53 **Geochemistry of Oils and Hydrocarbon Source Rocks, Greater Anadarko Basin: Evidence for Multiple Sources of Oils and Long-Distance Oil Migration**
R. C. Burruss and J. R. Hatch
- 65 **An Organic Geochemical Study of Oils, Source Rocks, and Tar Sands in the Ardmore and Anadarko Basins**
R. P. Philp, P. J. Jones, L. H. Lin, G. E. Michael, and C. A. Lewis
- 77 **Structural Evolution of the Southeastern Portion of the Anadarko Basin Region**
William J. Perry, Jr.
- 78 **Structural Imprint on the Slick Hills, Southern Oklahoma**
R. Nowell Donovan, W. R. David Marchini, David A. McConnell, Weldon Beauchamp, and David J. Sanderson
- 85 **Constraints on Magnitude and Sense of Slip Across the Northern Margin of the Wichita Uplift, Southwest Oklahoma**
David A. McConnell
- 97 **Horizontal Stresses from Well-Bore Breakouts and Lithologies Associated with Their Formation, Oklahoma and Texas Panhandle**
Richard L. Dart
- 121 **Neotectonics and Seismicity of the Anadarko Basin**
Kenneth V. Luza
- 133 **Anadarko Basin Conodont Studies**
John E. Repetski
- 134 **Diagenesis of Hydrocarbon-Bearing Rocks in the Middle Ordovician Simpson Group, Southeastern Anadarko Basin, Oklahoma**
Janet K. Pitman and Robert C. Burruss
- 143 **Depositional and Post-Depositional History of Middle Paleozoic (Late Ordovician through Early Devonian) Strata in the Ancestral Anadarko Basin**
Thomas W. Amsden

- 147 **Depositional Facies, Petrofacies, and Diagenesis of Siliciclastics of Morrow and Springer Rocks, Anadarko Basin, Oklahoma**
C. William Keighin and Romeo M. Flores
- 162 **Quantitative Petrographic Analysis of Desmoinesian Sandstones from Oklahoma**
Thaddeus S. Dyman
- 176 **Paleohydrology of the Anadarko Basin, Central United States**
Donald G. Jorgensen
- 194 **Mineralogic and Textural Relations in Deeply Buried Rocks of the Simpson Group (Middle Ordovician)—Implications in Diagenesis and Petroleum Geology**
Richard M. Pollastro
- 209 **Sulfide Mineralization and Magnetization, Cement Oil Field, Oklahoma**
Richard L. Reynolds, Neil S. Fishman, Michael W. Webring,
Richard B. Wanty, and Martin B. Goldhaber
- 210 **Natural Resources Information System (NRIS) of Oklahoma: Anadarko Basin Data**
Mary K. Grasmick

***PART II—Abstracts and Short Reports
Related to Poster Presentations***

- 221 **Anadarko Basin History from Stratigraphic Response Patterns**
Glenn S. Visher
- 225 **Regional Gravity of the Anadarko Basin Area and a More Detailed Look at the Wichita Frontal Fault Zone**
S. L. Robbins, Meridee Jones-Cecil, and G. R. Keller, Jr.
- 228 **Constraints on the Anadarko Basin—Wichita Uplift Boundary Interpreted from Aeromagnetic Data**
Meridee Jones-Cecil and Anthony J. Crone
- 233 **Genetic-Sequence Stratigraphy of the Upper Desmoinesian Oswego Limestone along the Northern Shelf Margin of the Anadarko Basin, West-Central Oklahoma**
Timothy P. Derstine
- 236 **Analysis of Sedimentary Facies and Petrofacies of Lower Morrowan—Upper Chesterian Sandstones, Anadarko Basin, Oklahoma**
C. William Keighin and Romeo M. Flores
- 239 **Structural Anomalies in the Deep Anadarko Basin, Caddo and Canadian Counties, Oklahoma**
Jock A. Campbell, Harold McIntire, and Richard A. Haines
- 245 **Subsurface Geology of the Northern Shelf of the Anadarko Basin**
Dorothy J. Smith
- 252 **Habitat of Petroleum in Permian Rocks of the Greater Anadarko Basin**
Jock A. Campbell and Charles J. Mankin
- 255 **Thermal Regime of the Anadarko Basin**
Jaquidon D. Gallardo and Larry S. Carter

- 257 Relationship of Clay-Mineral Diagenesis to Temperature, Age, and Hydrocarbon Generation—An Example from the Anadarko Basin, Oklahoma**
Richard M. Pollastro and James W. Schmoker
- 262 Formation Resistivity as an Indicator of the Onset of Oil Generation in the Woodford Shale, Anadarko Basin, Oklahoma**
James W. Schmoker and Timothy C. Hester
- 267 Evidence of Early Oil Generation in the Woodford Shale, Witcher Field, Central Oklahoma**
Terry Smith
- 268 Modeling of Hydrocarbon Generation and Migration for the Woodford Shale in the Anadarko Basin**
Longjiang Wang
- 271 Biomarker Characterization of Woodford-Type Oil and Correlation to Source Rock, Aylesworth Field, Marshall County, Oklahoma**
Jennifer Reber
- 273 Collected References**

PART I

PAPERS PRESENTED AT THE SYMPOSIUM

GEOLOGIC EVOLUTION OF THE ANADARKO BASIN

KENNETH S. JOHNSON

Oklahoma Geological Survey

Abstract.—The Anadarko basin of western Oklahoma and the Texas Panhandle is the deepest basin in the cratonic interior of the United States. Paleozoic sedimentary rocks as much as 40,000 ft thick were deposited along the axis near the south margin of this asymmetrical basin, and Cambrian igneous rocks, perhaps as much as 20,000 ft thick, underlie the sediments. The boundaries of the Anadarko basin—which include the Wichita–Amarillo uplift on the south, the Nemaha uplift on the east, and the Cimarron arch on the west—resulted from Early Pennsylvanian orogenic activity. Prior to that time the proto-Anadarko basin was the depocenter of the greater Oklahoma basin, which extended across the entire southern Midcontinent region.

The history of the Anadarko basin is divided into four major episodes:

1) Early and Middle Cambrian basement rocks were emplaced during an episode of igneous activity in the area that later would become the Wichita uplift and the deep Anadarko basin. They were emplaced within and/or upon a suite of preexisting Precambrian metasedimentary and igneous rocks.

2) About 15,000 ft of Late Cambrian through Mississippian shallow-marine carbonates and some fine clastics were deposited across the vast Oklahoma basin during an early epeirogenic episode.

3) During the Pennsylvanian orogenic episode, the Anadarko basin, as now defined, was created by sharp uplift of the Wichita–Amarillo block and other positive features, and by downwarping of the crust beneath the basin to receive ~18,000 ft of mostly marine sediments. Early in the Pennsylvanian the Wichita–Amarillo uplift was separated from the basin by a series of reverse faults, with vertical displacements which ultimately aggregated as much as 40,000 ft. Orogenic activity, which persisted through the remainder of the Pennsylvanian, resulted in faulting, folding, uplift, and downwarping; no igneous or metamorphic activity accompanied the tectonism.

4) The basin was finally filled with ~7,000 ft of sediments, mainly red beds and evaporites, during a late epeirogenic episode, extending from the Permian through the Holocene. Permian strata make up almost all of these late epeirogenic sediments, with Triassic, Jurassic, Cretaceous, Tertiary, and Quaternary strata being represented largely by erosional remnants.

INTRODUCTION

The purpose of this paper is to briefly describe the geologic setting and evolution of the Anadarko basin, in order to help set the stage for the other reports that follow in this symposium volume. A number of major reports dealing with the entire basin, or with significant packages of rocks in the basin, have been published in recent years, including those by Huffman (1959); Jordan and Vosburg (1963); Ham and others (1964); Ham and Wilson (1967); McKee, Oriel, and others (1967b); Dixon (1967); MacLachlan (1967); Adler and others (1971); Amsden (1975); McKee, Crosby, and others (1975); Frezon and Dixon (1975); Craig, Connor, and others (1979); Frezon and Jordan (1979); Mapel and others (1979); Rascoe and Adler (1983); Donovan (1986); Gilbert (1986); and Johnson and others (1988).

The current report draws upon each of these earlier reports, and relies heavily upon a recently completed discussion of the Anadarko basin by Bailey Rascoe, Jr., and me in Johnson and others (1988). Appreciation is expressed to Rascoe, Ralph H. Espach, and Robert A. Northcutt for their review of the current manuscript.

GENERAL GEOLOGIC SETTING

The Anadarko basin is the deepest sedimentary and structural basin in the cratonic interior of the United States (Fig. 1). Paleozoic sedimentary rocks as much as 40,000 ft thick are present along the axis, near the south margin of this asymmetrical basin, and Cambrian layered igneous rocks perhaps as much as 20,000 ft thick underlie the sediments. The basin is bounded on the south by the Wichita and Amarillo uplifts, on the east by the Nemaha uplift, and on the west by the Cimarron arch. The northern shelf of the Anadarko basin extends across much of western Kansas, and part of it is referred to as the Hugoton embayment. The Hugoton embayment is bounded by the central Kansas uplift and the Cambridge arch on the east and north, and by the Las Animas arch on the west.

The basin is one of the greatest oil and gas provinces in the United States, and the extensive exploration for hydrocarbons since the beginning of this century has established a tremendous data base for understanding the geology of the basin and surrounding areas.

The Anadarko basin did not exist as currently

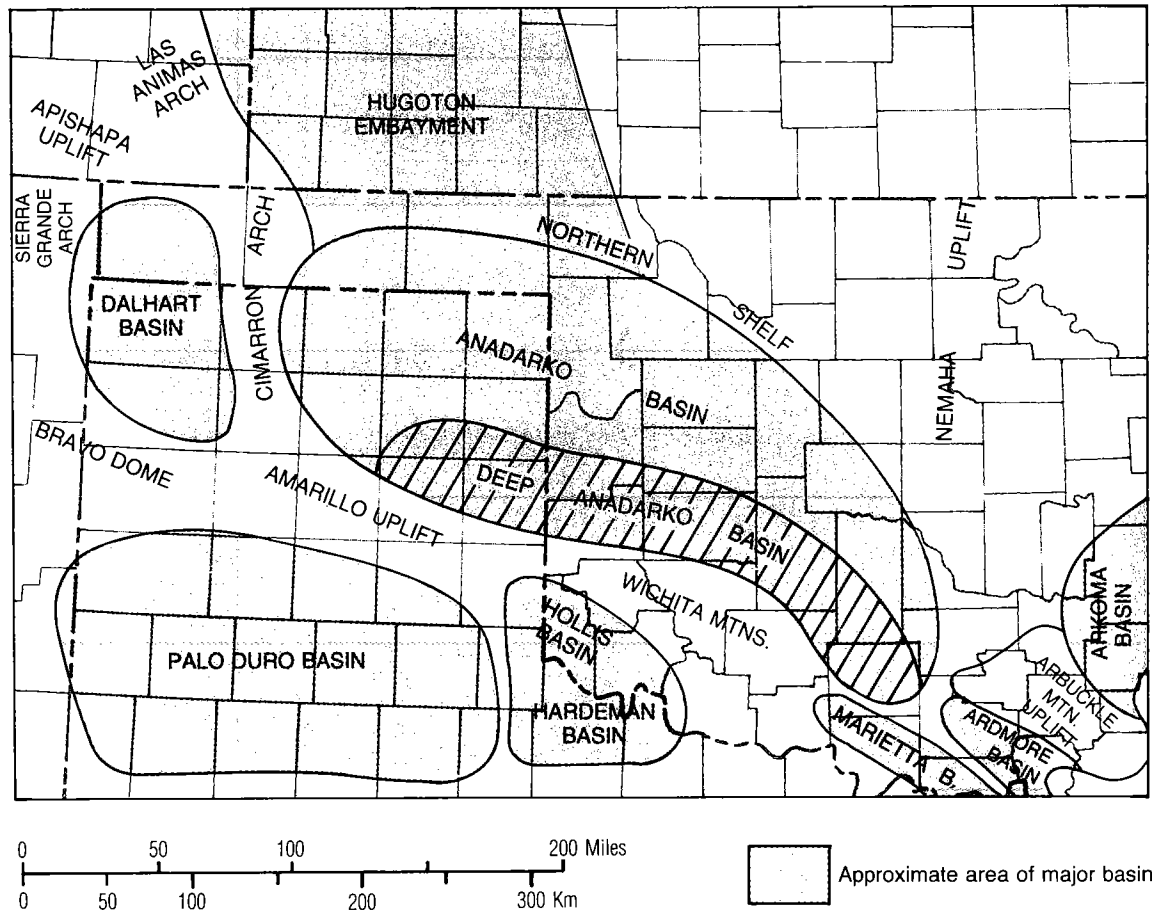


Figure 1. Location of Anadarko basin and surrounding geologic provinces (after Johnson and others, 1988).

defined until early in the Pennsylvanian Period. From late Cambrian through Mississippian time the area of the Anadarko basin was part of a broad epicontinental sea, the Oklahoma basin (Johnson and others, 1988), which extended across most parts of the southern Midcontinent (Fig. 2). The Oklahoma basin was a broad embayment or shelf-like area that received a sequence of thick and extensive carbonates interbedded with thinner shales and sandstones. These strata thickened into protobasins in those areas that would later become the Anadarko, Arkoma, and Ardmore basins, and they also were deposited upon and across the present-day major uplifts. The depocenter for the Oklahoma basin has been variously called the southern Oklahoma geosyncline (Ham and others, 1964; Ham and Wilson, 1967), or the southern Oklahoma aulacogen (Gilbert, 1983c, 1986; Brewer and others, 1983); this depocenter eventually became the site of the

deep Anadarko basin and the Wichita–Amarillo uplift.

The history of the Anadarko basin can be divided into four major episodes:

- 1) An igneous episode, during Precambrian and Early and Middle Cambrian time, when intrusive and extrusive basement rocks were emplaced in the area of the Wichita uplift and the southern part of what would become the Anadarko basin.

- 2) An early epeirogenic episode, ranging from Late Cambrian through Mississippian time, when marine sediments were deposited in a broad epicontinental sea referred to as the Oklahoma basin (Fig. 2).

- 3) An orogenic episode, during the Pennsylvanian, when the Oklahoma basin was broken into a series of sharp uplifts and major basins, including the Anadarko basin. This orogenic activity consisted of folding, faulting, uplift, and downwarping, and was not accompanied by igne-

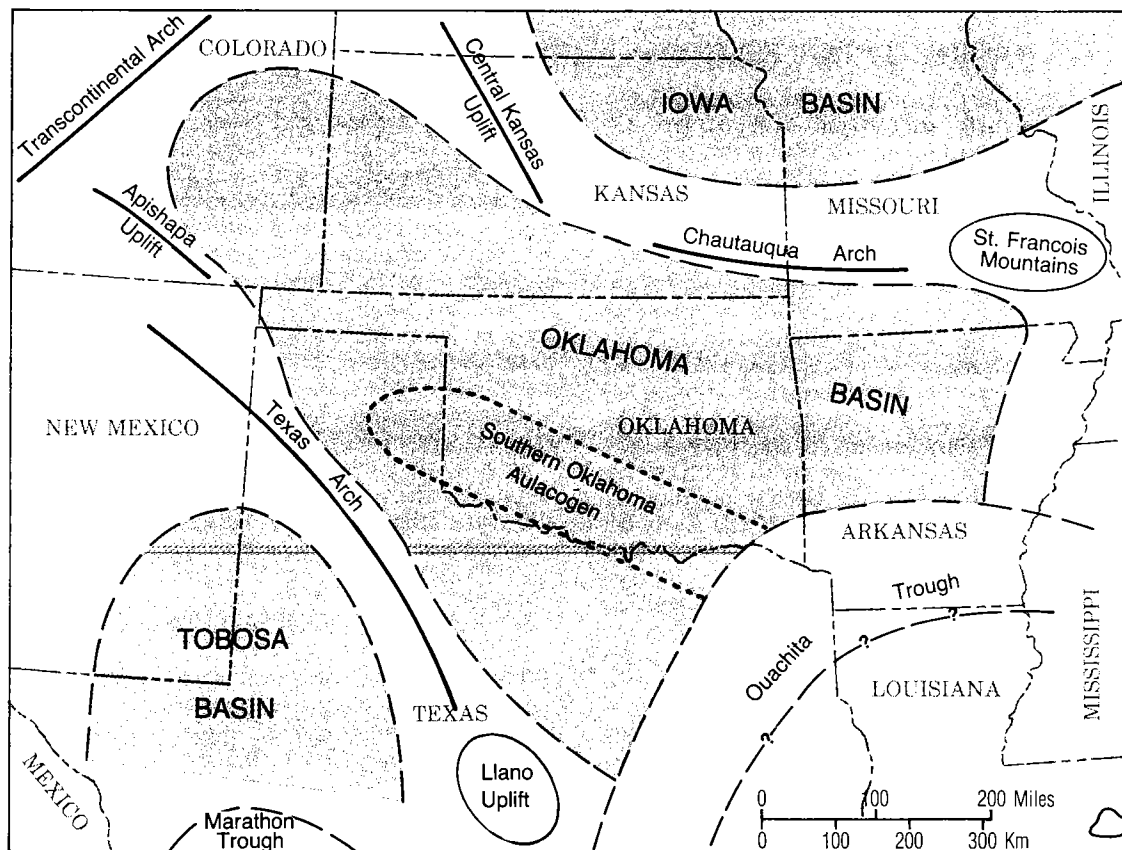


Figure 2. Map of southwestern United States, showing approximate boundary of the Oklahoma basin and other major features that existed in early and middle Paleozoic time (after Johnson and others, 1988).

ous or metamorphic activity in or near the Anadarko basin. Pennsylvanian sediments deposited in the Anadarko basin include coarse clastics near the uplifts, and mostly marine shales, sandstones, and limestones throughout most of the remainder of the basin.

4) A late epeirogenic episode that began in Permian time and has persisted till today. This episode included infilling of the basin with Permian red beds, evaporites, and carbonates, and deposition of thin post-Permian strata uniformly across the Anadarko basin and surrounding areas. Most of these post-Permian strata have been eroded from the basin.

PRECAMBRIAN THROUGH MIDDLE CAMBRIAN TIME

Precambrian and Cambrian basement rocks around the flanks of the Anadarko basin consist mainly of igneous rocks, but some low-rank

metasedimentary rocks are also present. Precambrian units have not been drilled in the deeper parts of the basin, but around the east, north, and west sides of the basin they are massive mesozonal granitic and related igneous rocks. The age of these Precambrian rocks is 1,300–1,600 m.y. (Denison and others, 1984).

Basement rocks on the south side of the Anadarko basin include Early and Middle Cambrian granites, rhyolites, gabbros, anorthosites, and basalts emplaced in the southern Oklahoma aulacogen (Ham and others, 1964; Gilbert, 1986). They were emplaced about 525–550 m.y. ago into and upon a sequence of sedimentary rocks (the Tillman Metasedimentary Group) in the Wichita uplift area, but they have an uncertain relationship to the Precambrian basement within the Anadarko basin. Total thickness of the suite of Cambrian igneous rocks in the Wichita uplift is ~20,000 ft; the thickness is unknown within the basin, but it may range from 5,000 to 20,000 ft in much of the deeper parts of the basin.

LATE CAMBRIAN THROUGH MISSISSIPPIAN TIME

The early epeirogenic phase of Anadarko basin history included shallow-marine deposition of a thick sequence of carbonates, with lesser amounts of shales and sandstones, in the Oklahoma basin. Strata deposited during this early epeirogenic episode commonly extend throughout most of the Oklahoma basin and thus are readily traced and correlated well beyond the boundaries of the southern Oklahoma aulacogen or the Anadarko basin (Johnson and others, 1988).

A basal, transgressive sandstone, the Reagan Sandstone, was deposited across a moderately mature erosion surface of low relief throughout the area. The sand grades up into an overlying succession of shallow-water marine limestones and dolomites (the Arbuckle Group) deposited almost continuously until the end of the Early Ordovician (Fig. 3). The dolomites are secondary and have been formed at the expense of primary limestones. Total thickness of the Late Cambrian and Early Ordovician strata is >6,000 ft along the depocenter of the Oklahoma basin, and they thin positionally northward to ~2,000 ft in northwestern Oklahoma (Johnson and others, 1988); the upper part of the Arbuckle Group also is truncated on the north flank of the basin and in the Hugoton embayment.

Middle Ordovician through earliest Mississippian sediments throughout the Oklahoma basin consist of fossiliferous shallow-water marine carbonates interbedded with fine-grained to moderately coarse-grained clastic sediments derived from northeastern and eastern sources (Johnson and others, 1988). Simpson Group sandstones and limestones at the bottom of this sequence are overlain successively by limestones of the Viola Group, gray and green-gray shales of the Sylvan Shale, carbonates of the Hunton Group, and the organic-rich, black Woodford Shale which was deposited in euxinic seas. Simpson through Woodford strata are still present throughout most parts of the Anadarko basin, and their cumulative thickness ranges from about 500 to 4,000 ft, from north to south. Deposition was interrupted by two major epeirogenic uplifts (Amsden, 1975): pre-middle Early Devonian (pre-Frisco) and pre-Late Devonian (pre-Woodford) unconformities result from these two broad upwarplings, with maximum uplift affecting local structures on the flanks of the basin. The pre-Woodford unconformity is one of the most widespread unconformities in the entire Midcontinent area. Little, if any, folding or faulting accompanied these epeirogenic uplifts, except for the faulting that occurred along the Nemaha uplift. A more complete discussion of Simpson through Woodford strata is given elsewhere in this volume by Amsden.

Mississippian sediments in the Anadarko basin area consist mainly of shallow-marine limestones, cherty limestones, and shales (Craig, Connor, and others, 1979; Frezon and Jordan, 1979; Mapel and others, 1979; Johnson and others, 1988). Euxinic seas of the Late Devonian–Early Mississippian, in which the Woodford Shale was deposited, were replaced by shallow, well-oxygenated, marine waters; in these waters fossiliferous limestones (commonly crinoidal) were deposited, some oolitic and some interbedded with shale and siltstone. Chert, which occurs mainly in Osagean and Meramecian rocks, is a replacement of carbonate. Chert generally comprises 10–30% of the cherty limestones. Shale makes up a large part of Late Mississippian strata in the southern part of the Anadarko basin area. Total thickness of Mississippian strata ranges from about 2,500–3,000 ft along the depocenter to about 1,000–2,000 ft along the northern shelf (Craig, Connor, and others, 1979).

PENNSYLVANIAN PERIOD

The Pennsylvanian was a time of major changes in the history of the Anadarko basin. Prior to Pennsylvanian time, the proto-Anadarko basin and the Wichita–Amarillo block subsided together as a single unit (southern Oklahoma aulacogen) and received as much as 15,000 ft of sediments. These epeirogenic movements and deposition of shallow-marine shelf carbonates over vast areas ended with a series of Pennsylvanian orogenic movements that subdivided the Oklahoma basin into the tectonic provinces easily recognized today. Regional discussions of the Pennsylvanian system are provided in McKee, Crosby, and others (1975) and Frezon and Dixon (1975).

Late Mississippian–Early Pennsylvanian epeirogenic uplift occurred in much of the region. It was accompanied by erosion that initiated development of the pre-Pennsylvanian unconformity that is present in all areas—except in the deep Anadarko basin, where Mississippian–Pennsylvanian sedimentation (Springer Group) was apparently continuous.

In Early Pennsylvanian time the Wichita–Amarillo block was uplifted along a series of WNW-trending reverse faults. Thrusting was northward toward the rapidly sinking Anadarko basin. Faulting began at the southeast end of the basin in early Morrowan time (Ham and Wilson, 1967), whereas farther west it began in late Morrowan time; faulting persisted through the rest of the Pennsylvanian, and probably died out during the Early Permian. Total vertical displacement across these faults is as much as 40,000 ft (Fig. 4), and left-lateral displacement along the main Mountain View fault may be as much as 15 mi

SYSTEM/SERIES		FORMATION OR GROUP	
		HUGOTON EMBAYMENT	ANADARKO BASIN
QUATERNARY		Alluvium, terraces	Alluvium and terrace deposits
TERTIARY		Ogallala Formation	Ogallala Formation
CRETACEOUS		Dakota Group	Dakota Group
JURASSIC		Morrison Formation	
TRIASSIC		Dockum Group	
PERMIAN	OCHOAN		Elk City Sandstone Doxey Shale Alibates Bed
	GUADALUPIAN	Cloud Chief Formation	Cloud Chief Formation
		Whitehorse Formation	Rush Springs Ss. Whitehorse Group Marlow Fm.
		Nippewalla Group	Dog Creek Shale Yelton salt El Reno Group Blaine Formation
		Cedar Hills Ss.	Flowerpot salt Flowerpot Shale Glorieta Ss. Duncan Ss.
	LEONARDIAN	Sumner Group	Hennessey Sh. Hennessey Group Cimarron Evaps. Garber Sandstone Hennessey Sh.
			Wellington Evaps. Wellington Fm.
	WOLFCAMPIAN	Chase Group Council Grove Group Admire Group	Chase Group Council Grove Group Admire Group
	VIRGILIAN	Wabaunsee Group Shawnee Group Douglas Group	Wabaunsee Group Shawnee Group Douglas Group
PENNSYLVANIAN	MISSOURIAN	Lansing Group Kansas City Group Pleasanton Group	Ochelata Group Skiatook Group
	DESMOINESIAN	Marmaton Group Cherokee Group	Marmaton Group Cherokee Group
	ATOKAN	Atoka Group	Atoka Group
	MORROWAN	Morrow Group	Morrow Group
	CHESTERIAN	Chester Group	Springer Formation Chester Group
MISSISSIPPIAN	MERAMECIAN		Meramec Lime
	OSAGEAN	Mississippian Lime	Osage Lime
	KINDERHOOKIAN		
DEVONIAN	UPPER		Woodford Shale
	MIDDLE		
	LOWER		
SILURIAN			Hunton Group
ORDOVICIAN	UPPER	Viola Formation	Sylvan Shale Viola Formation
	MIDDLE	Simpson Group	Simpson Group
	LOWER		Arbuckle Group
CAMBRIAN	UPPER	Arbuckle Group	Reagan Sandstone
	MIDDLE	Reagan Sandstone	
	LOWER		Granite, mylonite, gabbro, and metasediments
PRECAMBRIAN		Rhyolite, granite, and related rocks	Granite and related igneous and metaigneous rocks

Figure 3. Stratigraphic column for the Anadarko basin and Hugoton embayment (modified from Hills and Kottlowski, 1983, and Johnson and others, 1988). Height of formation/group boxes is not related to thickness of unit.

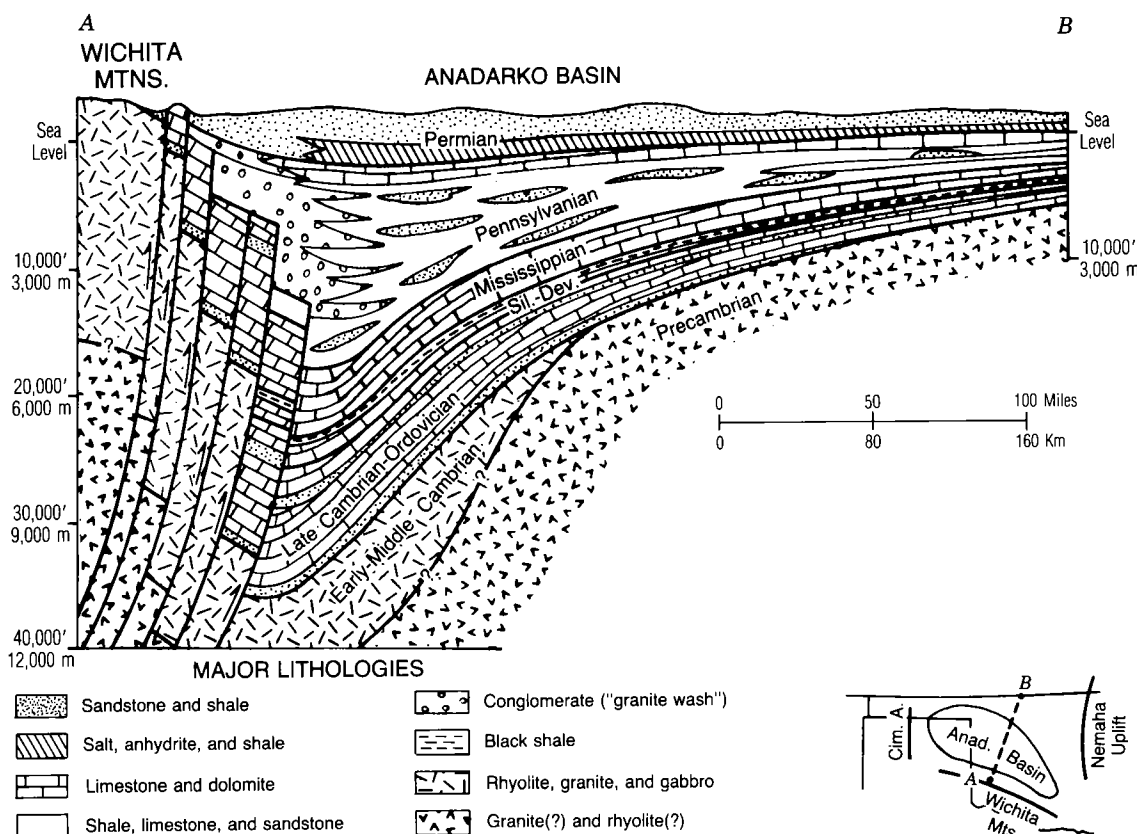


Figure 4. Generalized north-south structural cross section through the Anadarko basin of western Oklahoma (modified from unpublished cross section by Herbert G. Davis).

(McConnell, this volume).

The western margin of the Anadarko basin is formed by the Cimarron arch. The absence of Atokan and uppermost Morrowan strata from parts of this uplift indicates that the Cimarron arch probably was formed toward the end of the tectonic activity that created the Wichita-Amarillo uplift. Still farther west, the Sierra Grande arch and the Apishapa uplift (both part of the Ancestral Rockies) were intermittently lowland or mountain terranes that shed arkosic detritus into the western part of the Anadarko basin. On the east, the Nemaha uplift forms the axis or backbone of the broad, gently raised central Oklahoma arch. The Nemaha structure consists of a discontinuous series of block-faulted uplifts, each of which is generally 5-20 mi long (north-south) and 3-5 mi wide.

Orogenic movements of the Wichita-Amarillo block and of other positive elements surrounding the Anadarko basin consisted only of faulting, folding, uplift, and downwarping. No igneous or metamorphic activity accompanied the tectonism.

The Anadarko basin subsided throughout the Pennsylvanian orogenic activity, and it received as much as 18,000 ft of Pennsylvanian clastics and carbonates. These Pennsylvanian strata are sequences of marine (and some nonmarine) shale, sandstone, conglomerate, and limestone that thicken markedly into the rapidly subsiding basin. Thick wedges of clastics were eroded from the rising Wichita-Amarillo mountain chain. Early-formed coarse clastics are carbonate conglomerates that resulted from erosion of the thick sequence of early and middle Paleozoic carbonates that mantled the uplift; later conglomerates are arkosic sediments (referred to as "granite wash") that resulted from the eventual exposure and erosion of granites and rhyolites in the core of the Wichita-Amarillo Mountains.

Morrowan sediments of the Anadarko basin were deposited on a surface of eroded Mississippian rocks, except in the deep part of the basin where they overlie lithologically similar Springer strata of Late Mississippian and/or Early Pennsylvanian age. The Morrowan/Springer contact is

difficult to identify in the deep Anadarko basin, and Late Mississippian–Early Pennsylvanian sedimentation may have been continuous. Morrowan (and Springer) strata are as much as 4,000 ft thick in the deep Anadarko basin, thinning northward onto the shelf.

Strata in the lower Morrow Group consist of shallow-marine shales, sandstones, and limestones. They were deposited in a transgressive sea and onlap the surface of eroded Mississippian rocks toward the north and northeast. Upper Morrow strata are mainly shales with lenticular, discontinuous sandstones and minor conglomerates, coals, and thin, dark limestones; these are mainly the product of a deltaic sequence that prograded toward the southeast (Swanson, 1979) (Fig. 5B). Evidence of a late Morrowan initiation of uplift along most of the Wichita–Amarillo block is the upper Morrow fan-delta chert conglomerates, derived from weathering of Mississippian cherty limestones and dolomites that mantled the rising Wichita–Amarillo uplift.

Atokan strata consist of a series of southward-thickening marine shales, sandstones, and limestones. These sediments, the so-called “thirteen-finger limestone” of the Atoka Group, are generally 50–200 ft thick in the north and west. Atokan strata locally overlap the northeastern limit of the underlying Morrowan Series in northwestern Oklahoma and southwestern Kansas, and thus they locally rest directly upon Mississippian strata. Toward the south, Atokan limestones and shales grade into a thick sequence consisting mainly of shales, and these in turn grade abruptly into massive clastic deposits consisting of igneous-rock and carbonate-rock fragments (Fig. 5C). In this “granite wash” sequence the boundaries of the Atokan Series are uncertain, but Atokan strata along the depocenter of the basin in Oklahoma apparently are >4,000 ft thick.

Desmoinesian seas finally covered all of the central Oklahoma arch and the northern shelf area (Fig. 5D), extending into central Kansas (Fig. 5E). Desmoinesian strata consist mostly of cyclic marine limestones and shales: the lower part, the Cherokee Group, is mainly shale with numerous thin limestones and some lenticular point-bar and channel-fill sandstones; the upper part, the Marmaton Group, is composed of the Oswego Limestone, overlain by the Big Limestone. This marine sequence, typically 200–1,000 ft thick in the north, grades southward into 4,000–5,000 ft of “granite wash” in the deep Anadarko basin near the Wichita uplift. In the far west, some of the clastics eroded from the Ancestral Rockies are red beds.

The Missourian Series in southwestern Kansas and the Oklahoma Panhandle consists mostly of marine limestones, with some shale interbeds. To the south and southeast these strata grade into a

sequence of shales and sandstones with minor carbonate units, and these in turn grade into thick arkosic and carbonate “wash” sediments eroded from the Wichita–Amarillo block (Fig. 5F). Along the western margin of the Hugoton embayment, the Missourian Series consists of a clastic sequence of shales, siltstones, and sandstones, which are commonly red. The thickness of Missourian strata ranges from 500 to 1,000 ft in most of the northern shelf and Hugoton embayment area to >2,500 ft in the depocenter in the southeast part of the Anadarko basin.

The major positive tectonic elements present during Missourian time were the Wichita–Amarillo uplift (which yielded coarse detritus), the Apishapa uplift (fine-grained detritus), and the Arbuckle uplift (conglomeratic detritus). In the east, the first influence of the rising Ouachita Mountains is seen in Missourian strata. Deformation and uplift of the Ouachitas began during the Desmoinesian, but it was not until late Missourian time that several delta-front clastic wedges were deposited from streams that drained the Ouachitas and flowed into the eastern part of the Anadarko basin (Fig. 5F).

Virgilian strata in the Hugoton embayment and nearby shelf areas are marine limestones with shale interbeds. In central Oklahoma the Virgilian Series consists of continental to shallow-marine shales, sandstones, and mudstones, which grade westward into delta-plain sandstones and pro-delta shales. These strata interfinger with a thick interval of “granite wash” along the front of the Wichita uplift. Red-bed sandstones and shales were deposited in the far west, and red beds make up a major part of the outcropping and shallow-subsurface Virgilian strata in central Oklahoma. The Virgilian Series ranges from about 500–1,500 ft thick in the north and west to >4,500 ft thick in the far southeast end of the basin.

The Ouachitas continued to contribute clastics to the east side of the Anadarko basin during Virgilian time (Fig. 5G), and sharp uplift of the Arbuckle Mountains produced coarse detritus that was deposited in the southeast part of the basin. The rate of uplift of the Wichita block was decreasing; thus, the height of the Wichita Mountains was being reduced by erosion.

PERMIAN THROUGH HOLOCENE TIME

The late epeirogenic history of the Anadarko basin began in the Permian and has lasted through the Holocene. This episode was characterized mainly by filling of the basin with Permian carbonates, red beds, and evaporites, and subsequent deposition of thin sequences of post-Permian strata. Most of the post-Permian strata

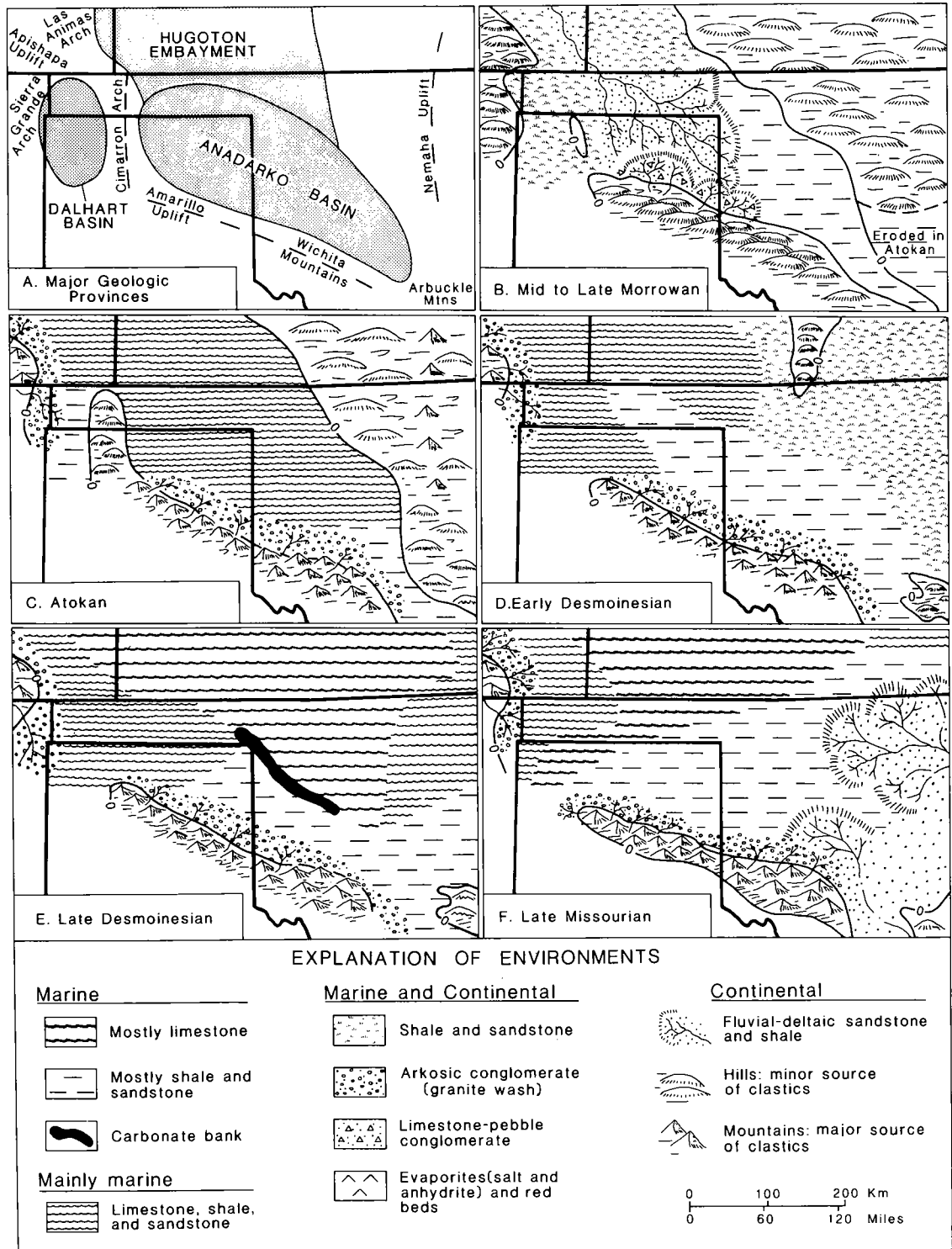
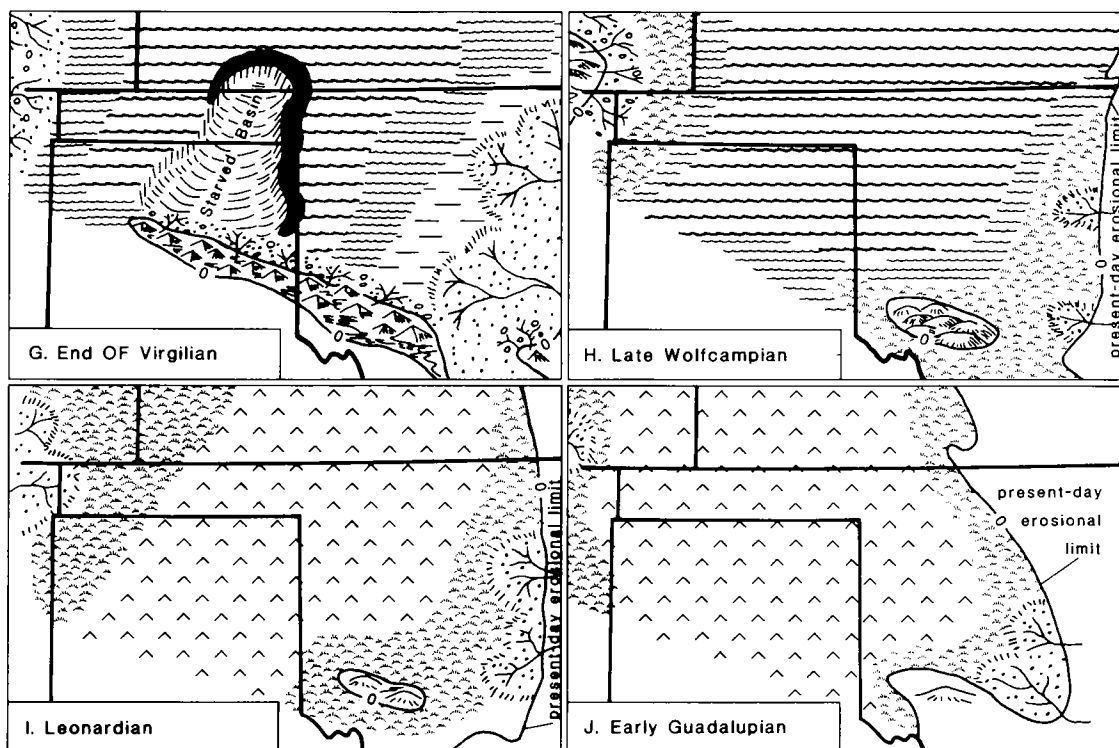


Figure 5. Paleogeography of the Anadarko basin and surrounding areas in Pennsylvanian and Permian times (reproduced from Johnson and others, 1988).

Figure 5. *Continued.*

were eroded from the basin, mainly during Late Jurassic/Early Cretaceous (pre-Dakota Group) and Late Cretaceous/middle Tertiary (pre-Ogallala) epeirogenic uplifts, and thus our knowledge about post-Permian basin history is limited.

Regional studies of Permian strata in the Anadarko basin include those of Jordan and Vossburg (1963); McKee, Oriel, and others (1967b); Dixon (1967); MacLachlan (1967); Johnson (1978); and Johnson and others (1988).

By Early Permian time, uplift in the Wichita-Amarillo block apparently had ceased, and the block began to subside, but at a rate slower than that of the Anadarko basin. The Amarillo segment of the block was completely inundated by Early Permian clastic debris. The Wichitas, however, remained as low mountains that were still a source of Early Permian continental sandstones and shales that interfingered to the north with marine and evaporite deposits in the Anadarko basin. The low mountains and hills on the Wichita block eventually were buried in their own debris during Late Permian time. The Anadarko basin continued to subside during the Permian, but far more slowly than in the Pennsylvanian. The total thickness of Permian strata is as much as 7,000 ft along the depocenter, located just north of the Wichita-Amarillo uplift.

In Wolfcampian time, a fairly well-defined seaway extended southwest to northeast across the western half of the Anadarko basin (Fig. 5H). Shallow-marine cyclic limestones and shales were deposited across the main seaway. Fine-grained clastic red beds border this belt of limestones and shales on the east and west; the red beds were deposited in mixed marine and continental environments and resulted from a general regression of normal marine waters from the region. The clastic sediments were the products of erosion of the Ouachita Mountains on the east, the Ancestral Rockies on the west, and the remnants of the Wichita Mountains on the south. Wolfcampian strata reach a maximum of >2,000 ft thick in the Texas part of the basin.

Leonardian time was marked by continued slow subsidence of the Anadarko basin and continued regression of the sea from the region. A broad, shallow, hypersaline sea inundated most of the Anadarko basin (Fig. 5I), and a thick sequence of evaporites and red beds was deposited. Red-bed clastic units that crop out on the east side of the Anadarko basin were deposited near the eastern shore of the hypersaline sea. The Garber Sandstone and Wellington Formation comprise a complex system of alluvial and deltaic sandstones and shales derived by erosion of low

land areas in the Ouachitas and eastern Oklahoma. These strata, and the overlying Hennessey Shale, grade westward into two thick evaporite units called the Wellington and Cimarron evaporites (Jordan and Vosburg, 1963). The Wellington contains 300–500 ft of interbedded salt, anhydrite, and shale in a unit referred to as the Hutchinson salt, whereas the Cimarron evaporites consist of 300–1,100 ft of interbedded salt and shale.

The Wichita uplift continued to have a modest influence on sedimentation in the Anadarko basin during Leonardian time. Clastic debris was shed northward into the south part of the basin, where it interfingered with the Wellington evaporites, and to a lesser extent with the Cimarron evaporites. Leonardian strata range from ~2,000 ft thick in the north and west to nearly 3,000 ft along the depocenter, in southwest Oklahoma and adjacent Texas.

The Anadarko basin continued to subside in Guadalupian time, and it received as much as 1,500 ft of red beds and evaporites along its depocenter. The Wichita block subsided at a somewhat slower rate than the basin, and all but the highest peaks were probably buried by fine clastics (Fig. 5J). The sources of clastics deposited in the eastern part of the basin were the low land areas of eastern Oklahoma and the deeply eroded Ouachita belt of southeastern Oklahoma and northeastern Texas. During a marine transgression, 100–200 ft of Blaine dolomite, anhydrite, and shale were deposited over almost all of the Anadarko basin and Hugoton embayment. The Blaine Formation is underlain and overlain by several hundred feet of salt and shale (Jordan and Vosburg, 1963). This evaporite deposition was followed by regression and deposition of red-bed sandstones and some anhydrites in the Whitehorse Group and Cloud Chief Formation. In the eastern part of the basin the Cloud Chief locally contains 100 ft of massive anhydrite (gypsum on the outcrop).

Ochoan rocks are mainly red-bed sandstones and shales, but they contain some anhydrite and dolomite (Alibates Bed) in the western part of the Anadarko basin. Little is known about Ochoan paleogeography, but probably it was similar to that of late Guadalupian time. Total thickness of the Ochoan Series along the axis of the basin is >400 ft.

Outcropping Ochoan strata typically contain chaotic structures, collapse features, and other evidence of disturbed bedding due to dissolution of underlying Guadalupian halite beds along the flanks of the Anadarko basin. Such collapse features also occur in some of the Guadalupian and post-Permian strata.

Post-Permian strata in the Anadarko basin

area include remnants of Triassic, Jurassic, Cretaceous, Tertiary, and Quaternary rocks. Deposition of these sediments was not influenced by the tectonic elements that were so pronounced during the Pennsylvanian and were somewhat reduced during the Permian. Triassic and Jurassic strata consist mainly of red-bed sandstones and shales deposited in mixed fluvial, deltaic, and lacustrine environments. Perhaps 500–1,000 ft of Triassic and Jurassic strata originally were deposited in the Anadarko basin, but subsequent (pre-Dakota Group, Cretaceous) erosion has removed all but 25–200 ft which remains in the far western part of the basin (Johnson and others, 1988).

The Cretaceous seaway extended across the western half (and perhaps all) of the Anadarko basin during the last great inundation of the western interior of the United States. At least several hundred feet (and perhaps up to 1,000 ft) of marine limestones, shales, and sandstones were deposited across the western part of the basin, and now only isolated erosional remnants remain (Johnson and others, 1988). Small outliers of these strata in western Oklahoma consist of chaotic blocks and masses (typically 50–2,000 ft across) that have collapsed downward about 50–300 ft, due to dissolution of underlying Permian salts, and are now juxtaposed against Permian outcrops. Formation of the Rocky Mountains during the Laramide orogeny of Late Cretaceous and early Tertiary time raised the entire region and imparted an eastward and south-eastward tilt to the entire region and eventually caused withdrawal of the Cretaceous sea. Most of the Cretaceous strata were eroded from the Anadarko basin area during epeirogenic uplift of Late Cretaceous through middle Tertiary time.

Tertiary strata, mainly the Ogallala Formation of Miocene–Pliocene age, are widespread across the western half of the Anadarko basin (Johnson and others, 1988). The Ogallala is a light-colored sequence of interbedded fluvial and eolian sediments deposited upon an erosional surface cut into Permian red beds (and locally into Triassic, Jurassic, or Cretaceous strata). The Ogallala was deposited by low-gradient alluvial systems that flowed east and southeast from the Rocky Mountains (Seni, 1980). Whereas the eastward-thinning wedge of Ogallala strata probably mantled almost all of the Anadarko basin originally, post-Tertiary erosion has removed much of it, and now 200–600 ft of Ogallala strata remain in most of the western part of the basin.

Quaternary sediments are alluvial, eolian, and lacustrine deposits derived from rivers and streams flowing eastward and southeastward across the Anadarko basin (Johnson and others, 1988); they mainly include terrace deposits and present-day alluvium, which commonly are 10–50 ft thick and locally are >100 ft thick.

THE GREATER ANADARKO BASIN: AN OVERVIEW OF PETROLEUM EXPLORATION AND DEVELOPMENT

HERBERT G. DAVIS

Consulting Petroleum Geologist,
Edmond

ROBERT A. NORTHCUTT

Consulting Petroleum Geologist,
Oklahoma City

Abstract.—The Anadarko basin is located in northwestern Oklahoma, the Oklahoma Panhandle, the northern Texas Panhandle, southwestern Kansas, and southeastern Colorado, encompassing an area of ~60,000 mi². Tectonically, the basin is bounded on the south by the Amarillo–Wichita Mountains, on the west by the Sierra Grande uplift, on the northwest by the Las Animas arch, on the north by the Cambridge arch–central Kansas uplift, on the northeast by the Nemaha Range, on the east by the central Oklahoma fault zone, and on the southeast by the Harrisburg trough.

The earliest exploration for petroleum in the greater Anadarko basin was conducted by surface-mapping parties. They discovered the Cement field (anticline) in 1917. Since this first major field discovery, continued exploration has established production from reservoirs in the Permian, Carboniferous (Pennsylvanian and Mississippian), Devonian, Silurian, Ordovician, and Cambrian Systems.

Cumulative production by the end of 1985 was >5 billion barrels of oil and 82 trillion cubic feet of gas. This production is obtained primarily from ~50 significant fields in the greater Anadarko basin. Many hundreds of additional fields contribute to the total production from structural and stratigraphic traps in this important oil and gas province.

INTRODUCTION

The greater Anadarko basin contains a major accumulation of petroleum. Its geologic history, stratigraphy, and structure have been topics for geologic study and speculation since 1905 (Freie, 1930). These studies continue today, and this workshop attests to that work. It is hoped that this overview will increase the participant's understanding of the importance of this prolific basin as a supplier of our country's energy needs and as a model for exploration in other geologic basins of similar architecture.

The Anadarko basin was first defined by Charles N. Gould (1924) on the basis of surface mapping of the Permian red beds in western Oklahoma. Subsequent studies of subsurface information gained from decades of drilling activity and geophysical surveys have shown the greater Anadarko basin to underlie northwestern Oklahoma, the Oklahoma Panhandle, the northern Texas Panhandle, southwestern Kansas, and southeastern Colorado (Fig. 1). This area encompasses ~60,000 mi².

The basin is tectonically bounded on the south by the Amarillo–Wichita Mountains uplift, on the west by the Sierra Grande uplift, on the northwest by the Las Animas arch, on the north by the

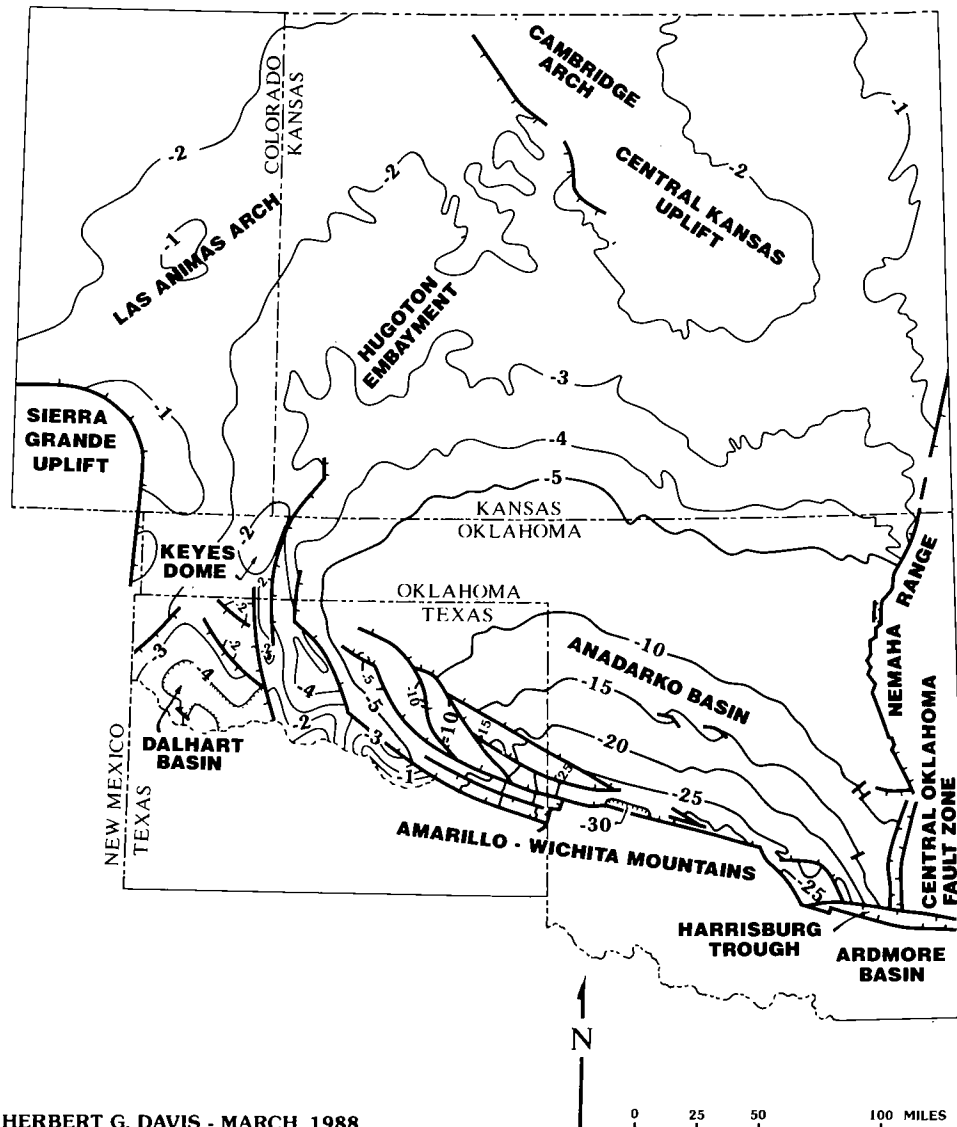
Cambridge arch–central Kansas uplift, on the northeast by the Nemaha Range, on the east by the central Oklahoma fault zone, and on the southeast by the Harrisburg trough, a recognized separation from the Ardmore basin (Fig. 2).

Within the greater Anadarko basin are the lesser tectonic features of the Hugoton embayment, Keyes dome, Dalhart basin, and Cyril basin.

Initial exploration for oil and gas in the Anadarko basin was accomplished by geological surface mapping to delineate structural domes and anticlines. Similar features had been found to be productive in other producing areas in the Midcontinent. The first wells drilled in the basin were shallow cable-tool holes and tested only the Permian red beds. Although shows of oil and gas were reported, no production was established until 1917.

EARLY EXPLORATION AND DISCOVERIES, 1917–41

In 1916, Frank Buttram and D. W. Ohern mapped the Cement anticline in Caddo County, Oklahoma. The discovery of gas and oil from the Permian Fortuna sand was made in 1917 (Becker,



HERBERT G. DAVIS - MARCH, 1988

Figure 2. Arbuckle structure map of the greater Anadarko basin. Contour intervals are 1,000 ft in Colorado, Kansas, Oklahoma, and Texas, and 5,000 ft in Oklahoma and Texas (thousands eliminated). Modified from Merriam (1961) and Cole (1975) in Kansas; modified from Gatewood (1985) in Oklahoma and Texas; also modified from personal maps.

1927), opening what is now a major producing area of the Cement field (Fig. 3). Subsequent development at this field has found production from numerous Pennsylvanian sands to depths below 13,000 ft (Herrmann, 1961). Through 1985 this major field has produced 185 million barrels of oil and 516 billion cubic feet of gas. (Major fields as defined for this paper are those that have produced at least 100 million barrels of oil, 600 billion cubic feet of gas or barrels of oil

equivalent at 6,000 cubic feet of gas per barrel of oil [Northcutt, 1985].)

A surface structure was also mapped in Garfield County, Oklahoma, in 1916, which led to the discovery of the Garber field, another significant Permian-sand producing area in which production was subsequently established from multiple zones in Pennsylvanian sandstones, Mississippian limestone, and Arbuckle limestone (Gish and Carr, 1929).

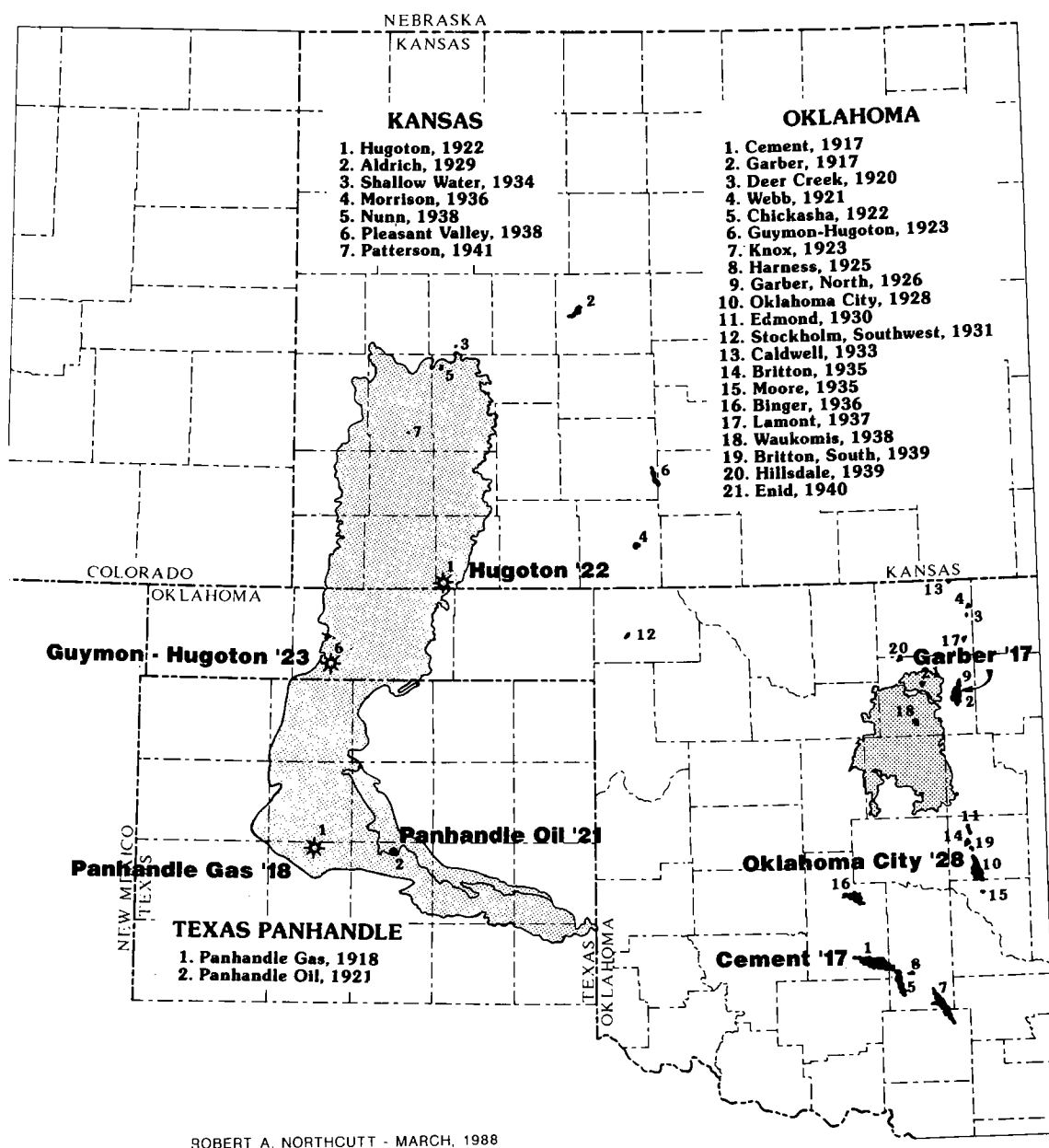


Figure 3. Oil and gas field map of fields discovered through 1941 in the greater Anadarko basin. Stippled areas indicate developed limits of initial field discoveries. Fields are indicated by numerals and names and listed in chronological order of discovery by state.

Surface mapping in the Texas Panhandle by Charles N. Gould in 1917 located the John Ray dome in Potter County, Texas. The huge Panhandle gas field (Fig. 4) was discovered by a well drilled on this dome in 1918 (Mason, 1968). Subsequent drilling in Carson County, Texas, during 1921 discovered the giant Panhandle oil field,

where oil production, largely controlled by structural relationships, is approaching 1.5 billion barrels. ("A giant oil field is defined as one which has 500 million bbls of reserves recoverable by present methods, and a giant gas field as one which has 3.5 trillion cubic feet of reserves recoverable by present methods" [Halbouty, 1970].)

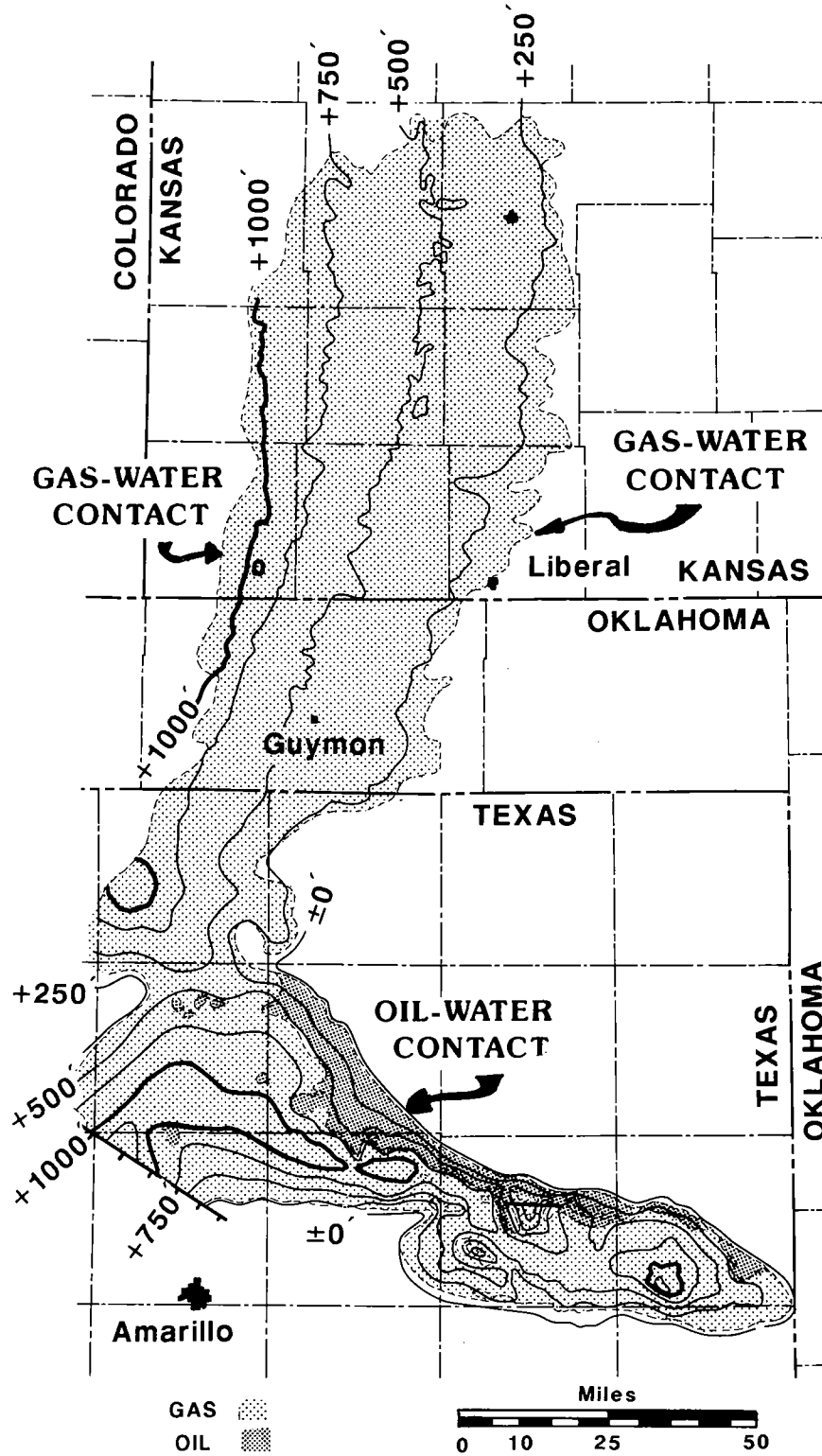


Figure 4. Hugoton-Panhandle gas area, Kansas, Oklahoma, and Texas. Structure on top of Hugoton pay units. Contour interval 250 ft. Modified from Mason (1968, fig. 1).

To the north in Seward County, Kansas, a well completed in 1922 (Pippin, 1970) discovered gas from a large stratigraphic trap in the Permian Chase Group. Another Permian gas discovery in 1923 in Texas County, Oklahoma, set up the eventual linkage of these areas into the Panhandle-Guymon-Hugoton gas field, the largest gas field in North America, covering 8,500 mi², which has produced 48 trillion cubic feet of gas.

As early as 1917, surface evidence of a large structure was noted in Oklahoma County, Oklahoma. It was finally drilled in 1928, and the prolific Oklahoma City field was discovered (Gatewood, 1970). During its rapid development, producing horizons were established in rocks ranging in age from Pennsylvanian to Cambrian. The Second Wilcox sandstone (Ordovician, Simpson) is the largest reservoir in this great structural oil field, which has now produced nearly 750 million barrels of oil (Gatewood, 1970, figs. 4,5,11).

In the 1920s, core drilling was utilized to map structures where satisfactory outcrops were not readily apparent. In northern Oklahoma and western Kansas this method was used to discover some small structural fields.

The seismograph began to be used as an exploration tool in the 1930s and made it possible to delineate subsurface structures not easily found by surface mapping. This resulted in the discovery of several small structural fields in Oklahoma and Kansas.

The small but prolific Patterson oil field was discovered by using seismograph surveys late in 1941 in Kearny County, Kansas, then just north of the Hugoton gas field limits (R. Davis, 1959). This three-well field has now produced over 1 million barrels of oil; it was the earliest discovery of petroleum in the Morrow sand, which later became one of the major objectives in the Anadarko basin.

EXPLORATION AND DEVELOPMENT, 1942-60

Significant fields discovered in the greater Anadarko basin during the period 1942 through 1960 are illustrated on Figure 5. Most of these fields have become major or giant gas fields and/or oil and gas fields. All but three are stratigraphic accumulations.

The Bradshaw and Byerly fields, discovered in 1957 in Hamilton and Greely Counties, Kansas, produce gas from the Permian Chase Group. Although reservoirs extend over a large area, production through 1985 has been only 180 billion cubic feet of gas. More significantly, this production illustrates the fact that as long as reservoir rocks were present updip, the gas that migrated into the Hugoton field continued until it reached a final trap. Explorationists may ask if we have

found the updip limit of the Chase gas production in western Kansas and southeastern Colorado. Has it found a way to migrate into younger traps farther updip?

A major accumulation of gas was later found in the lower Permian Council Grove Group below the Chase Group production inside the giant Hugoton field (D. Davis, 1976). The Panoma field was discovered in 1956, and through 1985 the 2,237 wells in Kansas have produced 1.3 trillion cubic feet of gas. Detailed study of the Panoma field in the 1960s revealed that many of the old Hugoton wells were actually producing from the Council Grove and Chase Groups. The Kansas Corporation Commission designated the Permian Council Grove Group a separate common source of supply in 1959.

A structural accumulation of Permian oil and gas was encountered north of the giant Panhandle oil field in Roberts County, Texas. The Quinduno field, discovered in 1952, has produced 22.5 million barrels of oil and 115 billion cubic feet of gas, primarily from the "Brown" dolomite. Deeper Pennsylvanian and Mississippian pays also contribute to the gross production.

The only other Permian production discovered in the greater Anadarko basin during this period was from small, structurally controlled fields, primarily in the Oklahoma Panhandle and southwestern Kansas.

The hydrocarbon-bearing Upper Pennsylvanian section is represented by gas production discovered in 1952 at the stratigraphically controlled Greenwood field, in extreme southwestern Kansas and southeastern Colorado (Wingerter, 1958). Here, Virgilian limestones produce in a stratigraphic trap similar to the Hugoton trap (see Pippin, 1970, fig. 16). The Greenwood field has produced 955 billion cubic feet of gas through 1985.

The Upper Pennsylvanian was found to be productive of oil and gas in the deep basin at the Elk City field in Beckham and Washita Counties, Oklahoma, in 1947. On this large structure, granite washes in the Missourian Series have produced 50 million barrels of oil and 276 billion cubic feet of gas through 1985. No other structural accumulation has been found in the Upper Pennsylvanian rocks along the front of the Amarillo-Wichita Mountains to date.

A "reef-like" trend of Middle Pennsylvanian Oswego limestone was discovered to be oil- and gas-bearing at the Putman field in 1959 in Dewey County, Oklahoma. Since then, 54 million barrels of oil and 1 trillion cubic feet of gas have been produced through 1985. The Putman field is located at the hingeline of the basin and on an obscure N-S tectonic feature which seems to extend southward from the Pratt anticline of Kansas. The Marmaton (Kansas), Big Lime (Texas), or Oswego (Oklahoma) is productive throughout the

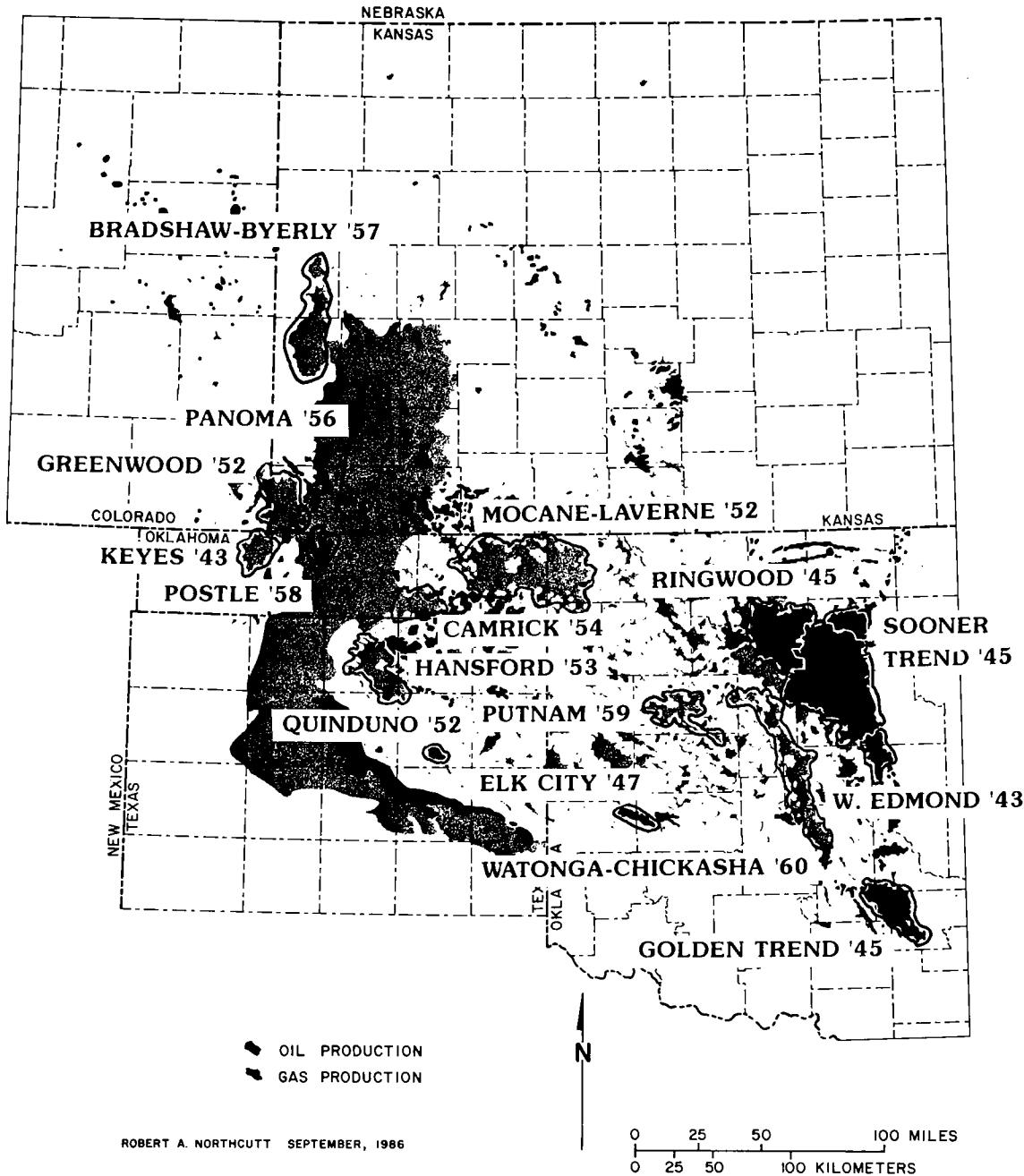


Figure 5. Significant fields, 1942–60, in the greater Anadarko basin. Indicated fields are discussed in the text.

greater Anadarko basin in small, isolated fields.

Lower Pennsylvanian sands in the Morrow Group account for most of the pre-Permian oil and gas production in the greater Anadarko basin. The first Morrow-sand gas was discovered on Keyes dome in Cimarron County, Oklahoma, in 1943. The lower Morrow Keyes sand on this

structure has produced 500 billion cubic feet of gas and 1.7 million barrels of oil through 1985.

The upper Morrow sands have produced 103 million barrels of oil and 52 billion cubic feet of gas through 1985 at the Postle field, discovered in 1958, and 1 trillion cubic feet of gas and 14 million barrels of oil through 1985 at the Camrick

field, discovered in 1954. These two fields are in a large upper-Morrow deltaic plain, which would contain a giant oil and gas field if all significant fields from southeastern Colorado, Morton County (Kansas), Texas and Beaver Counties (Oklahoma), and Hansford, Ochiltree, and Lipscomb Counties (Texas) were combined. The best documentation of this deltaic sequence is contained in Swanson (1979).

The Mocane-Laverne field in Beaver and Harper Counties, Oklahoma, is a true giant field. Production through 1985 has been 4.4 trillion cubic feet of gas and 22 million barrels of oil from the Pennsylvanian Virgilian Hoover sand, Missourian Tonkawa sand, upper and lower Morrow sands, and the Mississippian Chester limestone. Durwood Pate published a classic paper on this stratigraphic accumulation in AAPG Memoir 9, "Natural Gases of North America" (1968).

The Hansford field in Hansford, Ochiltree, Hutchinson, and Roberts Counties, Texas, is a major stratigraphic accumulation discovered in 1953 in the Texas Panhandle. The primary reservoirs are the upper and lower Morrow sands, which have produced 1.1 trillion cubic feet of gas and 10.7 million barrels of oil through 1985.

The Deese sands (Desmoinesian) were found to be productive at the extreme southeast end of the basin in the giant Golden trend in 1945. Through 1985, 500 million barrels of oil and 1 trillion cubic feet of gas have been produced from the onlapping, stratigraphically trapped Deese sands and other reservoirs in Devonian, Silurian, and Ordovician rocks.

The Watonga-Chickasha trend, the last major field designated in the basin to date, was discovered in 1960 in Blaine County, Oklahoma. This trend, which includes reservoirs of Atokan, Morrowan, and Springerian age, now extends from Dewey County through Blaine and into Canadian, Caddo, and Grady Counties, Oklahoma. Through 1985, 1.8 trillion cubic feet of gas and 44 million barrels of oil have been produced from this major field. Multiple sands in many varied trapping conditions are present throughout the trend.

The Ringwood field, discovered in 1945 in the northeastern part of the basin, produces from the Chester. Chesterian limestones and sandstones produce oil and gas which are stratigraphically trapped throughout the basin from western Kansas across the northeastern shelf area to their updip porosity pinchouts. Ringwood is the largest single trap and has produced 84 million barrels of oil and 558 billion cubic feet of gas through 1985.

Older Mississippian rocks, the Meramec and Osage, produce in the giant Sooner trend, discovered in 1945. Here, fractured carbonates have produced 300 million barrels of oil and nearly 1 trillion cubic feet of gas through 1985. There are multiple pay zones ranging in age from Penn-

sylvanian through Ordovician in this large area.

The West Edmond field in Oklahoma County, Oklahoma, was discovered in 1943 by an "exotic" technique. The discovery well of this large stratigraphic trap in the Hunton (Bois d'Arc) limestone was located by a "doodlebugger" or dowser, as reported in Swesnik (1948). Oil production from this major field, which was unitized in 1947, is now >160 million barrels of oil.

THE DEEP ANADARKO BASIN, 1960-87

Several significant wells, fields, and trends of production in the "deep Anadarko basin" are identified in Figure 6.

The Lone Star #1 Baden, located in sec. 28, T. 10 N., R. 22 W., Beckham County, Oklahoma, reached a total depth of 30,050 ft in the Viola, February 29, 1972 (Rowland, 1974a). This exploratory test in the "deep basin" was historic because it was the deepest test in the world at the time and proved that the petroleum industry's geologists, geophysicists, engineers, and drilling and service companies were up to the task of exploring the deep part of the basin.

The depth record was short-lived, as the Lone Star #1 Bertha Rogers, located in sec. 27, T. 10 N., R. 19 W., Washita County, Oklahoma, reached a total depth of 31,441 ft in the Arbuckle, April 13, 1974 (Rowland, 1974b). Bottom-hole pressure was 24,835 lb/in². A small show of high-sulfur gas was detected at the surface, and after the well was controlled, sulfur crystals were circulated to the surface. It is theorized that when the sulfur crystallized at 15,200 ft the drill pipe parted at that depth. The well, which is still the deepest hole in the free world, added the valuable geologic knowledge that the Precambrian basement is ~43,600 ft deep in the Anadarko basin.

The Mills Ranch field, a multiple-reservoir field located on a thrust block in the deep basin in Wheeler County, Texas, is the site of the world's deepest producer (Jemison, 1979). The Chevron-Freeport #1 Ruth Ledbetter, sec. 21, Block L, Jim Lindsay Survey, produces gas from the Arbuckle at 26,536 ft. The field was originally discovered by a Morrow gas producer in June 1971. The Hunton gas discovery occurred in October 1973; Atoka gas was added in July 1975; and the Arbuckle gas discovery was made in August 1976. Gas reserves for the Mills Ranch complex are estimated at 400 billion cubic feet from over 40 producers.

The West Mayfield field, located immediately east, across the state line in Beckham County, Oklahoma, was discovered in May 1954, producing gas and oil from the Pennsylvanian (Virgilian) arkose. Three miles west of the discovery

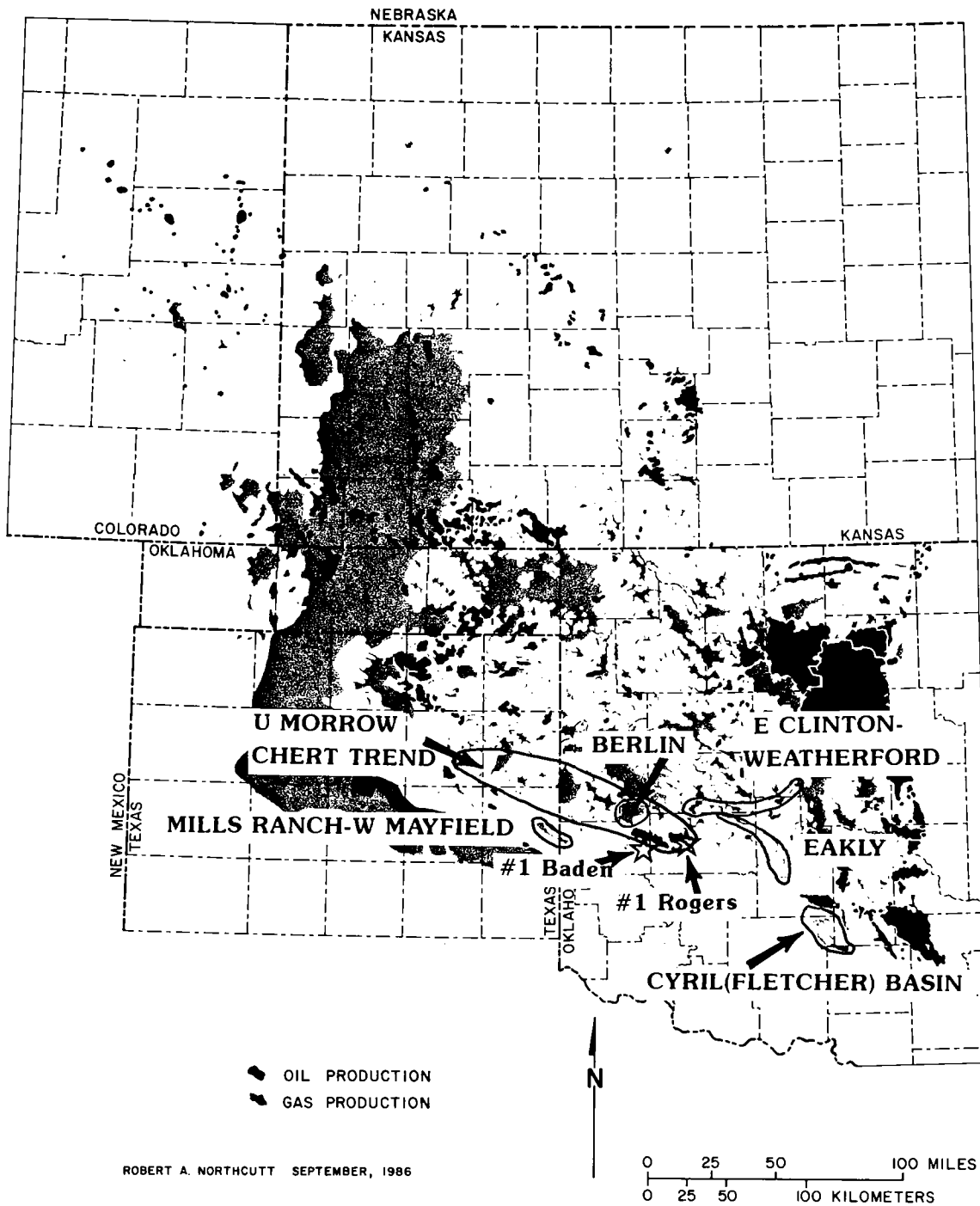


Figure 6. Significant wells, fields, and trends, 1960-87, in the deep portion of the greater Anadarko basin. Indicated wells, fields, and trends are discussed in the text.

well, Continental Oil Co. completed a Pennsylvanian granite-wash gas discovery in September 1972, after having shows of gas in the Hunton and Arbuckle. The first Arbuckle gas well was the Helmerick and Payne #1 Cupp, completed in July 1975. The field's production through 1985 totals 194 billion cubic feet of gas. Gas reserves for the West Mayfield complex are estimated to be >350 BCF from 26 Hunton, Viola, and Arbuckle producers. In-fill Hunton and off-structure Atokan and Morrowan gas reservoirs will add to the ultimate gas recovery at the Mills Ranch-West Mayfield complex.

The Reydon field in Roger Mills County, Oklahoma, was a significant gas discovery in the deep Anadarko basin. The Gulf #1 Hartley discovered upper Morrow gas in January 1962. The field was extended by the Texas Pacific #1-29 Hollis in December 1970.

Geologic studies in the late 1970s indicated that upper-Morrow chert reservoirs extended from eastern Roberts County, Texas, to Washita County, Oklahoma, a distance >100 miles. Jerry Shelby, an independent geologist in Amarillo, Texas, presented the first of many papers on this trend. His exhibit presented at the Deep Drilling and Production Symposium in April 1979, in Amarillo, Texas, located the trend (see Shelby, 1980, fig. 2). Significant fields in the trend to date are the Shreikay field, Roberts County, Texas; Buffalo Wallow field, Hemphill County, Texas; Reydon and Cheyenne fields, Roger Mills County, Oklahoma; and Elk City field, Washita County, Oklahoma.

The structural cross section of Shelby (1980, fig. 9) illustrates the massive chert conglomerate in the upper Morrow, generated by erosion of the Amarillo-Wichita Mountains to the south. The obvious source for this chert is the Lower Mississippian rocks, which were being stripped off the mountains and deposited as a fan-delta system in the subsiding basin during Morrowan time. A second source during late Morrowan time was to the northwest, where large quantities of quartz sand were being carried into the fluvial channels which locally intertongue in a southeasterly direction into the fan-delta cherts.

Current estimates are that the upper-Morrow trend in the deep basin will contribute >3 trillion cubic feet of gas reserves; it may ultimately be a giant field similar in size to the Watonga-Chickasha trend.

The Cyril basin, also known as the Fletcher area, is located in the extreme trough of the Anadarko basin at its southeastern limit. This area was the center of a concentrated deep-drilling play in 1982 (Drisdale, 1982). The area was targeted for gas in the Springer and Goodard sands at depths of 18,000–22,000 ft. Forest Oil Co. discovered gas at East Apache field in the Cyril basin in 1972, and completed the first com-

mercial well in 1974.

The Natural Gas Act of 1978 allowed gas produced below 15,000 ft to be sold at unregulated prices equivalent to 100–110% of No. 2 fuel oil or \$7.60–8.30/mcf and caused a boom in deep drilling for gas. The Springer and Goodard sands at depth failed to provide the reservoirs for the anticipated giant gas field (Drisdale, 1982), and with the collapse of the industry in late 1982 the Cyril basin was left a graveyard of iron.

The "East Clinton-Weatherford Upper Red Fork sand trend" in Blaine, Caddo, and Custer Counties, Oklahoma, discovered in 1979, has developed into a potential major gas field. William A. Clement of Anson Corp., Oklahoma City, Oklahoma, has presented a recent paper (in press) on the field and estimates the current gas reserves at 434 billion cubic feet from 102 wells. Clement's "pink limestone structure map" illustrates the sand trend from its fluvial environment in Blaine, Caddo, and Custer Counties into its delta system located in southwestern Custer, Washita, Beckham, and Roger Mills Counties (Petzet, 1988). This Pennsylvanian Red Fork sand play has been one of the most active drilling plays in the Anadarko basin in recent years.

The "Eakly Britt sand trend" in Caddo, Custer, and Washita Counties, Oklahoma, discovered in 1981, has developed into a potential major gas field, as >50 wells producing from the Springer-Britt sands are estimated to have gas reserves of 910 billion cubic feet. James R. Walker of Dyco Petroleum Corp., Tulsa, Oklahoma, presented his paper on the Eakly trend at the AAPG Midcontinent Meeting in 1985 at Amarillo, Texas. His "Britt structure map" illustrates the productive area trending northwest-southeast for >30 miles. The "Gross Britt sand isopach map" indicates the sand thickness in the productive wells to be a maximum of 50 ft thick (Walker, 1985, and personal communication).

The Berlin gas field in Beckham County, Oklahoma, was discovered in 1977; production is from an Atokan carbonate composed of recycled detrital Arbuckle dolomite. The reservoir was deposited as a shallow marine fan delta and occupies an area of ~41 mi².

Reed Lyday of Meridian Oil, Houston, Texas, has written an excellent paper on the geology of this field (Lyday, 1985); his figure 3 locates the Berlin field north of the Elk City structure in the Anadarko basin. His figure 5, a diagrammatic cross section, illustrates the wash sequences off the Wichita Mountains south of the Elk City structure. Here granite wash overlies dolomite clastic wash, which overlies chert wash. On the north side of the structure the dolomite fan delta is present below the granite washes in the Desmoinesian. The dolomite isopach (Lyday, 1985, fig. 11) indicates a maximum of 80 ft of do-

lomite, using a 50 API gamma-ray unit. Reserves for the field are currently estimated by Lyday (1985) at 242–362 billion cubic feet of gas.

PETROLEUM PRODUCTION SUMMARY

Through 1985, petroleum reservoirs in the greater Anadarko basin produced 82.4 trillion cubic feet of gas and 5.37 billion barrels of oil. Figure 7 illustrates each state's share of these totals. Of this total, the giant Panhandle–Hugoton field (Fig. 8) accounts for 58% of the gas production and 26% of the oil production. With this production excluded, the respective amounts for the states are as follows: Oklahoma, 22.5 trillion cubic feet of gas; Texas Panhandle, 7.3 trillion cubic feet of gas; and Kansas, 4.7 trillion cubic feet of gas. The Texas Panhandle oil production becomes a modest 300 million barrels of oil.

FUTURE POTENTIAL OF THE ANADARKO BASIN

It is obvious now that economics and political policies will dictate the future potential of the Anadarko basin. The deep drilling campaign during the late 1970s and early 1980s has identified that the entire basin contains structural and stratigraphic oil and gas possibilities to depths

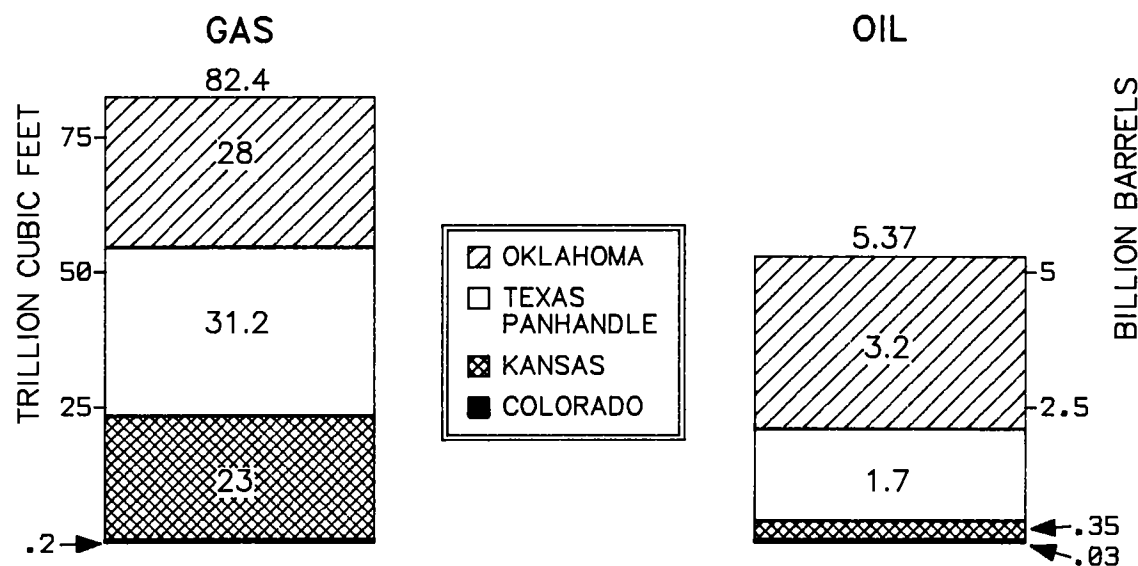
below 25,000 ft. Gas will be the most sought-after prize, and extensions and redrills on increased-density patterns for the lenticular Pennsylvanian sands and Mississippian carbonates will still be the primary reservoirs.

The shelf area of the basin is in a late state of exploration; however, the deep-basin sedimentary section and the mountain-front fault systems still afford opportunities for large stratigraphic and structural traps. The thick sequence of Pennsylvanian sediments and the Mississippian, Devonian, and Cambrian–Ordovician carbonates will provide multiple-reservoir possibilities as our knowledge of the stratigraphy increases by application of seismic data and use of the drill bit.

Reinterpretation of the existing subsurface data and improved seismic coverage will undoubtedly facilitate exploration in the deep basin for years to come. It is hoped that industry, government, and financial institutions will approach it more cautiously in the 1990s than they did during the boom of the late 1970s and early 1980s.

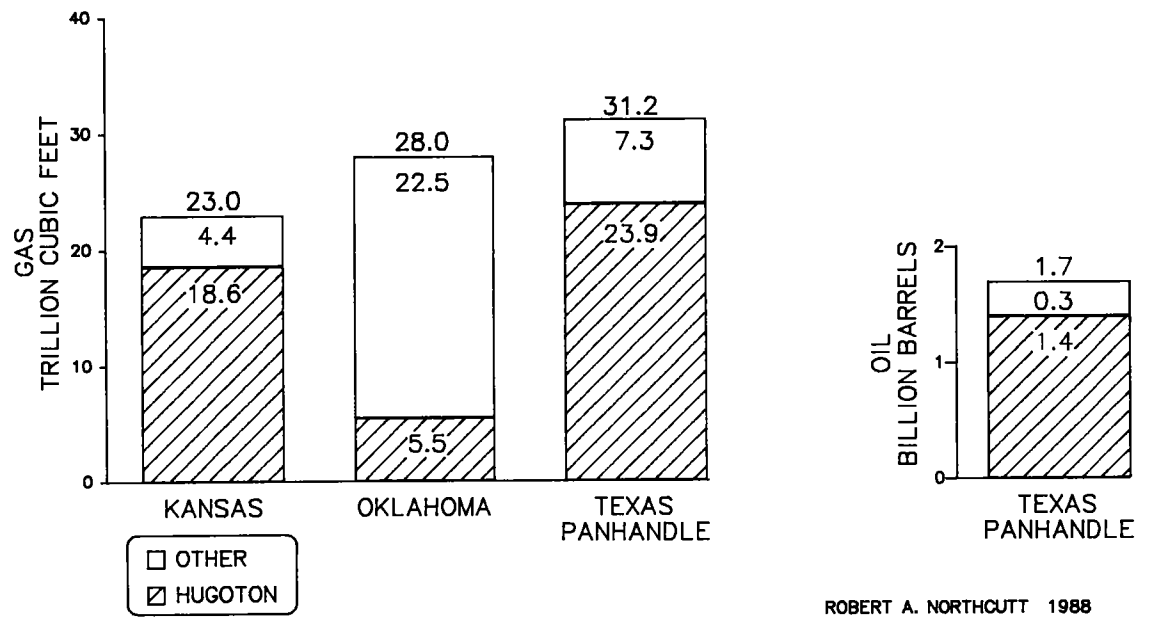
ACKNOWLEDGMENTS

Special thanks are due to Ralph H. Espach, Jr., for his critical review and helpful suggestions; to Dennis F. Smith and William P. Siard for their review and comments of the manuscript; and to Annette Northcutt for her dedicated typing and repeated retyping of our evolving manuscript.



ROBERT A. NORTHCU TT 1988

Figure 7. Oil and gas production, 1917–85, greater Anadarko basin.



ROBERT A. NORTHUTT 1988

Figure 8. Comparison of oil and gas production, 1917-85, greater Anadarko basin with oil and gas production from Hugoton-Panhandle field.

THERMAL MATURITY OF THE ANADARKO BASIN¹

JAMES W. SCHMOKER

U.S. Geological Survey, Denver

Abstract.—Levels of thermal maturity are estimated for Paleozoic strata in five areas of the central Anadarko basin for times between the Paleozoic and the present, and depths of the oil window are plotted as a function of geologic time. Mean surface temperature assumed here for calculating Lopatin's time-temperature index of thermal maturity (TTI) in the central Anadarko basin declines from 80°F (27°C) to 60°F (16°C) from early Paleozoic time to the present. Shallow-water carbonates and lower paleolatitudes suggest warmer climates in the Paleozoic for this area. The geothermal gradient is assumed to equal 4.0°F/100 ft (7.3°C/100 m) in the Late Cambrian and to decay over a 100-m.y. period to the present regional gradient of 1.3°F/100 ft (2.4°C/100 m). Initial basin formation was caused by crustal thinning. Accumulation of thick Pennsylvanian sediments in a foreland-style basin dominated by vertical lithospheric flexure represents a second major period of subsidence. An elevated geothermal gradient during this time is not assumed for TTI calculations, because mathematical models suggest time-invariant heat flows in such basins.

TTI computations based on these assumptions indicate that oil could have been generated in the ancestral Anadarko basin >350 m.y. ago. By the end of the Pennsylvanian, significant volumes of kerogen were in the oil window (and perhaps beyond), and significant volumes have remained in the oil window up to the present day. These circumstances may partially explain the unusual richness of the Anadarko basin as a Paleozoic hydrocarbon province.

INTRODUCTION

A number of models have been put forward for estimating thermal maturity at points in the sedimentary section, and in time, where direct geochemical measurements such as vitrinite reflectance are not available. Lopatin's model, as described and evaluated by Waples (1980), is used here.

Lopatin's time-temperature index of thermal maturity (TTI) is based on the idea that hydrocarbon generation depends on both the temperature and the duration of kerogen heating. The maturity that is accumulated by a given rock unit over a period of time t_1 to t_2 is summed according to the equation

$$TTI = \sum_{i=t_1}^{t_2} 2^{(T_i/10 - 10.5)}, \quad (1)$$

where time is measured in million-year increments, and T_i is the formation temperature (°C) during the i th time increment.

In the study reported here, TTI values for Lower Ordovician to mid-Permian strata in five areas of the central Anadarko basin (Fig. 1) are computed for times between the Paleozoic and the present. From these computed values of ther-

mal maturity, depths of the oil window are estimated as a function of geologic time and plotted, along with sediment-burial curves, for each of the five areas shown in Figure 1.

REGIONAL THERMAL AND BURIAL HISTORIES

Formation temperatures used to compute TTI (equation 1) are derived from surface-temperature, geothermal-gradient, and burial-depth histories. Present-day mean surface temperature in western Oklahoma is ~60°F (16°C). Shallow-water carbonates and paleolatitudes near the Equator suggest a warmer climate in Paleozoic time for the study area. Surface temperatures used here for TTI modeling of the central Anadarko basin decline from 80°F (27°C) to 60°F (16°C) between early Paleozoic time and the present (Schmoker, 1986, fig. 2).

The thermal gradient associated with the early Paleozoic southern Oklahoma aulacogen, of which the present-day Anadarko basin occupies a part, is estimated here from calculations of Feinstein (1981). His model shows a heat pulse due to Late Cambrian rifting that decays over a 100-m.y. pe-

¹This paper is a summary of a more comprehensive report (Schmoker, 1986) prepared for the U.S. Geological Survey's Evolution of Sedimentary Basins Program and published by the Oklahoma Geological Survey.

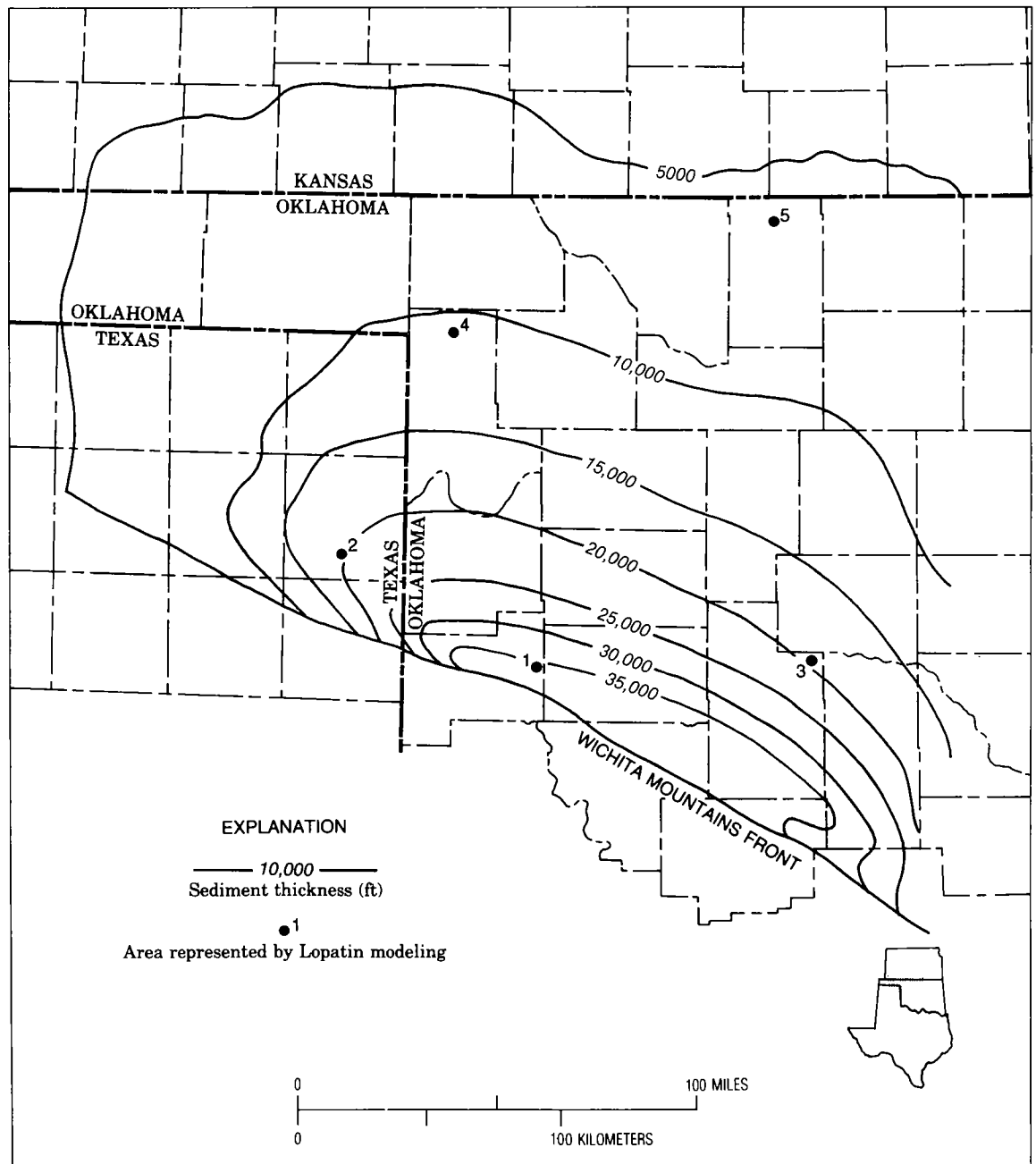


Figure 1. Sediment thickness and areas represented by Lopatin modeling in the central Anadarko basin: 1—Deep-basin area of Beckham and western Washita Counties; 2—Hemphill and Wheeler Counties, Texas; 3—Caddo, Canadian, and Grady Counties; 4—Ellis and Harper Counties; 5—Shelf area of Alfalfa County.

riod, from 4.0°F/100 ft (7.3°C/100 m) during initial crustal thinning, to the present regional geothermal gradient of 1.3°F/100 ft (2.4°C/100 m) (Harrison and others, 1983; Luza and others, 1984).

The present-day Anadarko basin was shaped by a second period of major subsidence during which thick Pennsylvanian sediments accumulated. Although a limited extensional event has been suggested by Garner and Turcotte (1984), a foreland basin dominated by vertical lithospheric flexure is thought here to be more representative of the study area as a whole (e.g., Webster, 1977; Brewer and others, 1983; Gilbert, 1983c). Mathematical models suggest time-invariant heat flows in most foreland basins (Beaumont and others, 1985). Therefore, a constant geothermal gradient equal to that of the present day is used here for TTI modeling of the second period of basin formation.

Decompacted time-depth burial histories were constructed for each of the five areas shown in Figure 1. Stratigraphic horizons span a large range of depths in these areas. The oldest modeled horizon, the top of the Upper Cambrian and Lower Ordovician Arbuckle Group, varies in present depth from ~5,700 ft at the shelf edge (area 5) to ~33,450 ft in the deep part of the basin immediately north of the Wichita Mountains front (area 1).

From past to present, burial histories prepared for TTI modeling reflect moderate subsidence during late stages of the southern Oklahoma aulacogen, rapid subsidence associated with formation of the Anadarko basin, a period of quiescence and slow sediment accumulation between 260 and 60 m.y. ago, and uplift and erosion beginning ~60 m.y. ago and continuing to the present (Schmoker, 1986, fig. 3). Erosion of 2,600 ft is assumed here as an average value for the study area. This value is supported by the projection of plots of vitrinite reflectance versus depth to surface values of $R_o = 0.2\%$ (Dow, 1977).

PRESENT-DAY OIL WINDOW

TTI values calculated for the Paleozoic section of the five areas shown in Figure 1 span seven orders of magnitude. Over this large range, a semi-logarithmic graph of TTI versus present depth describes a straight line, with very little data scatter, represented by the regression equation

$$TTI = 1.38e^{Z/1,970}, \quad (2)$$

where Z is depth in feet. Using equation 2, thermal maturity can be estimated from present depth of burial throughout the study area. Causative factors for this somewhat unexpected but useful relationship were discussed by Schmoker (1986, p. 15).

Comparison to published vitrinite-reflectance (R_o) measurements indicates that the relationship between TTI and R_o in the central Anadarko basin can be expressed as a power function

$$TTI = 351.8 R_o^{4.86}. \quad (3)$$

This calibration is not in close agreement with the generic calibration of Waples (1980, fig. 5), although it does fall within his envelope of data points.

The transition from oil to wet-gas generation is commonly equated to a maturity level of $R_o = 1.3\%$. This level corresponds to $TTI = 1,260$ in the study area and occurs at a present depth of ~13,400 ft. A threshold for hydrocarbon generation of $R_o = 0.5\text{--}0.6\%$ is considered representative of many oil-prone source rocks (Waples, 1985, table 9.5). The threshold for oil generation in the central Anadarko basin corresponds to TTI values between 12 and 29, occurring at present depths of roughly 4,300–6,000 ft.

OIL WINDOW IN THE PAST

The evolution of the oil window through time in the central Anadarko basin, estimated from TTI calculations, is shown in Figure 2. Reliability of this figure undoubtedly decreases as TTI values are projected hundreds of millions of years into the past. Taken as a whole, the oil window migrates upward ~7,500 ft relative to the surface from Pennsylvanian time to the present, and decreases in total thickness from ~10,500 to 9,000 ft.

The envelope defining the oil window (Fig. 2) is subdivided into three segments by discontinuities in slope that correspond to major shifts in basin-subsidence patterns. The oldest segment reflects rapid sedimentation and burial. The middle segment corresponds to gradual subsidence and sediment compaction in a quiescent basin and migrates gradually upward in response to TTI accumulation with the passage of time. The apparent upward migration of the youngest segment is in fact due primarily to erosion and the lowering of the ground surface toward the oil window.

With a single exception, the data points of Figure 2 form a well-defined trend that terminates 330 m.y. before present (latest Mississippian), prior to which most modeled sediments were immature in terms of oil generation. A single data point in Figure 2, circled for emphasis, falls well off the general trend but is not a calculation error. This value represents the top of the Arbuckle Group in area 1 (the most mature modeled horizon) and indicates that oil generation may have occurred in the southern Oklahoma aulacogen—the precursor of the Anadarko basin. The deepest, most mature sediments of the southern

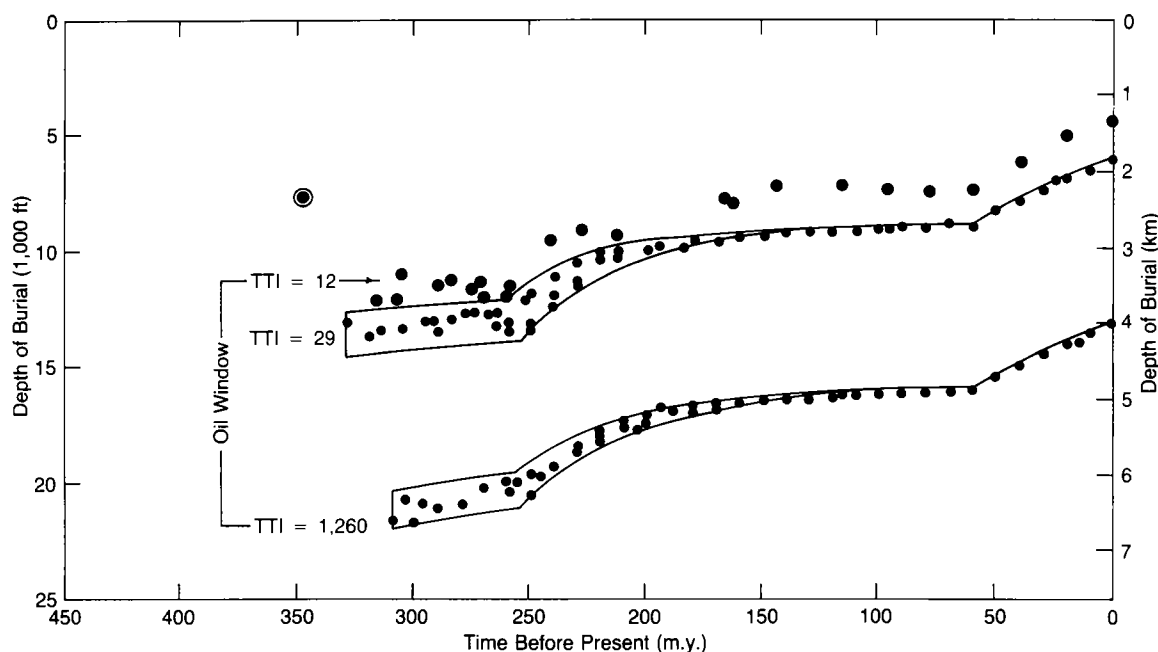


Figure 2. Generalized oil window for Paleozoic rocks of the central Anadarko basin as a function of time before present.

Oklahoma aulacogen lay along the axis of the present-day Wichita Mountains and have been destroyed by uplift and erosion. The "unusual" data point of Figure 2 thus suggests that oil could have been generated >350 m.y. ago in the deepest part of the ancestral Anadarko basin if adequate source rocks were present.

DISCUSSION AND SUMMARY

Figures 3–7 form a largely self-explanatory sequence showing the relationship of representative strata at each of the five locations modeled to the generalized regional oil window of Figure 2. The horizons plotted in these figures provide a framework for interpolation and do not necessarily represent source rocks. Burial reconstructions of the Devonian and Mississippian Woodford Shale at the five studied locations are grouped together in Figure 8 as an example illustrating the relationship throughout the basin of a single formation to the oil window. The Woodford Shale is an important hydrocarbon source rock in the Anadarko basin.

Because significant uncertainties exist in the burial and thermal reconstructions, in the calculation of the oil window, and in the geochemical

specifications of the oil window, the data of Figures 3–8 should be regarded as semiquantitative. Rigorous interpretation of these figures in terms of precise ages and depths is not warranted.

During the period of rapid basin subsidence, burial curves cut sharply across the oil window, and time spent in the zone of oil generation is as short as 20 m.y. (Figs. 3,4,8). During the subsequent period of gradual subsidence, burial curves remain in the oil window much longer. Burial curves and the oil-window envelope are nearly parallel through the period of Tertiary erosion. Within a given formation, the zone of oil generation moves upward and outward toward the shelf with the passage of time.

Hydrocarbons have been generated in an exceptionally long and unbroken history for >350 m.y. in the Anadarko basin. Since Permian time, the basin has been relatively stable. Such conditions favor the generation of large volumes of oil and gas, extensive and diverse migration paths, the widespread distribution of oil and gas throughout the section, and the preservation of petroleum accumulations. These circumstances contribute to the unusual richness of the Anadarko basin as a Paleozoic hydrocarbon province.

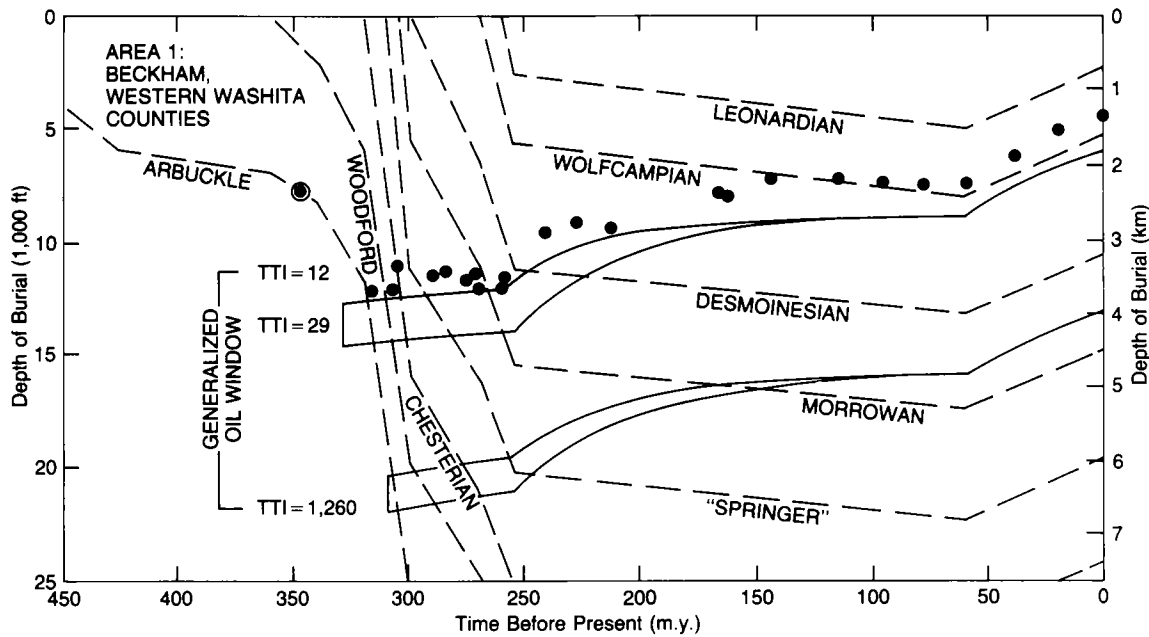


Figure 3. Burial curves for the deep-basin area of Beckham and western Washita Counties, Oklahoma (area 1), superimposed on the regional oil window of Figure 2.

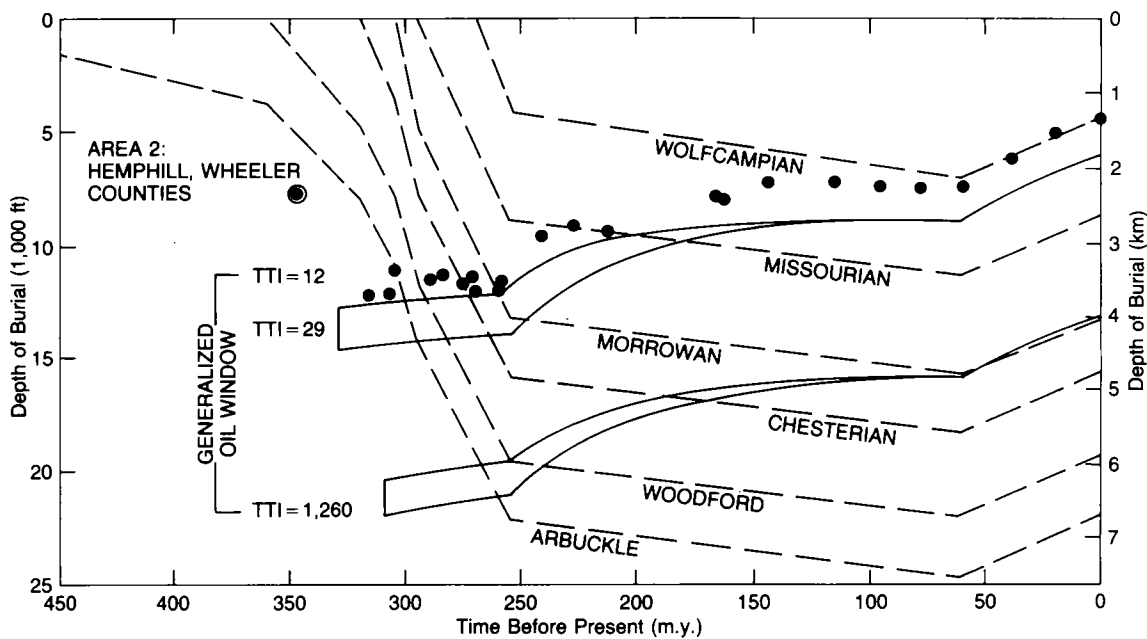


Figure 4. Burial curves for Hemphill and Wheeler Counties, Texas (area 2), superimposed on the regional oil window of Figure 2.

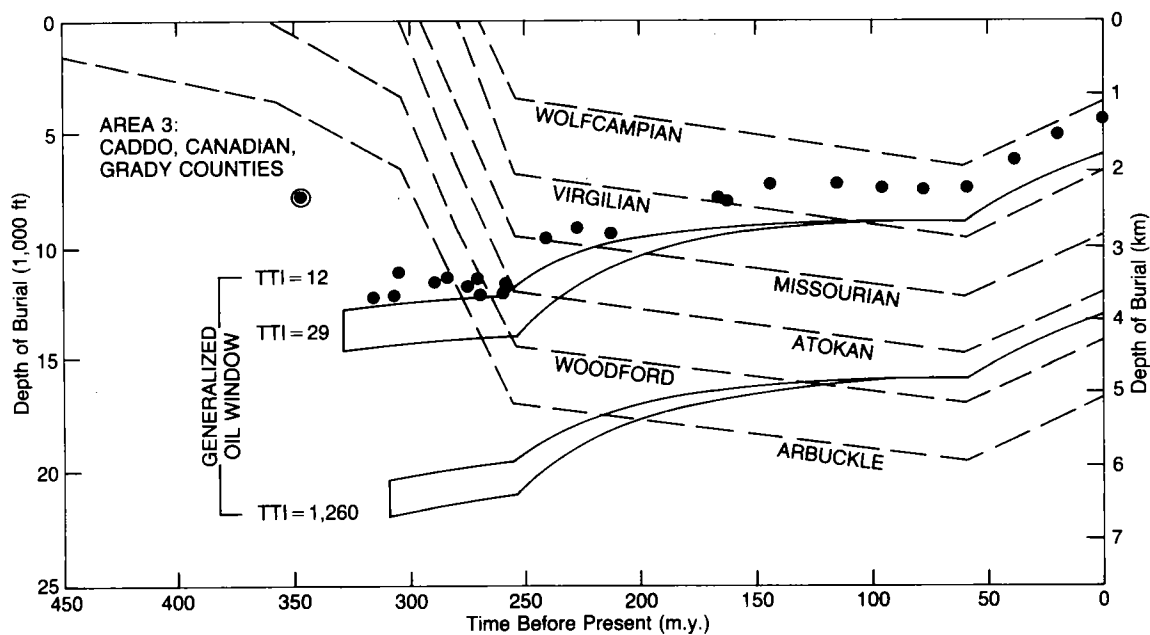


Figure 5. Burial curves for Caddo, Canadian, and Grady Counties, Oklahoma (area 3), superimposed on the regional oil window of Figure 2.

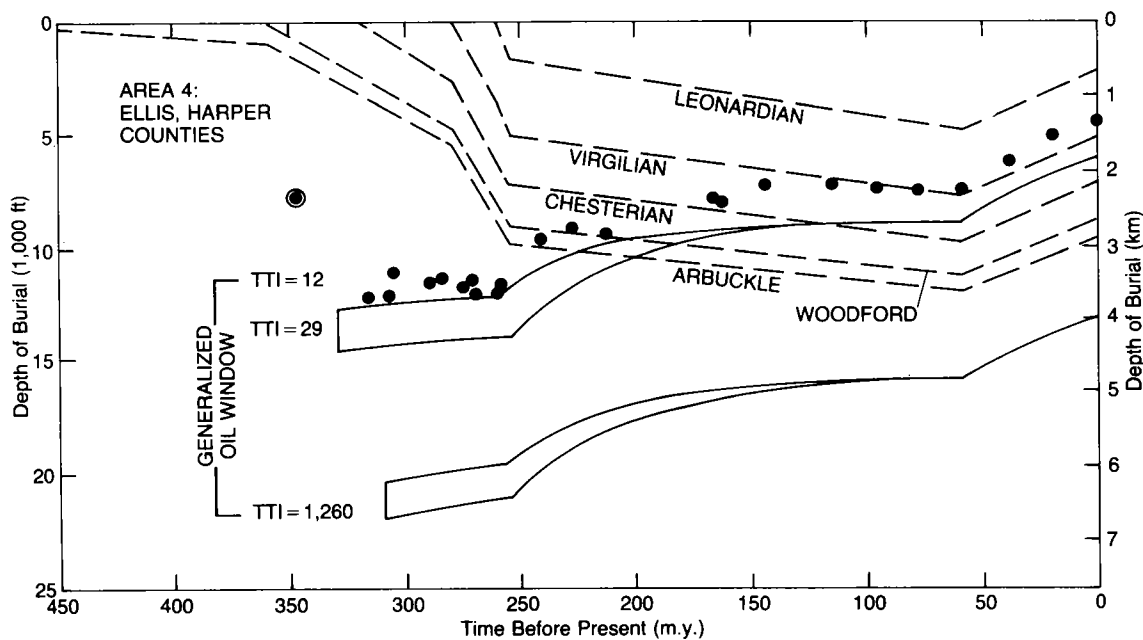


Figure 6. Burial curves for Ellis and Harper Counties, Oklahoma (area 4), superimposed on the regional oil window of Figure 2.

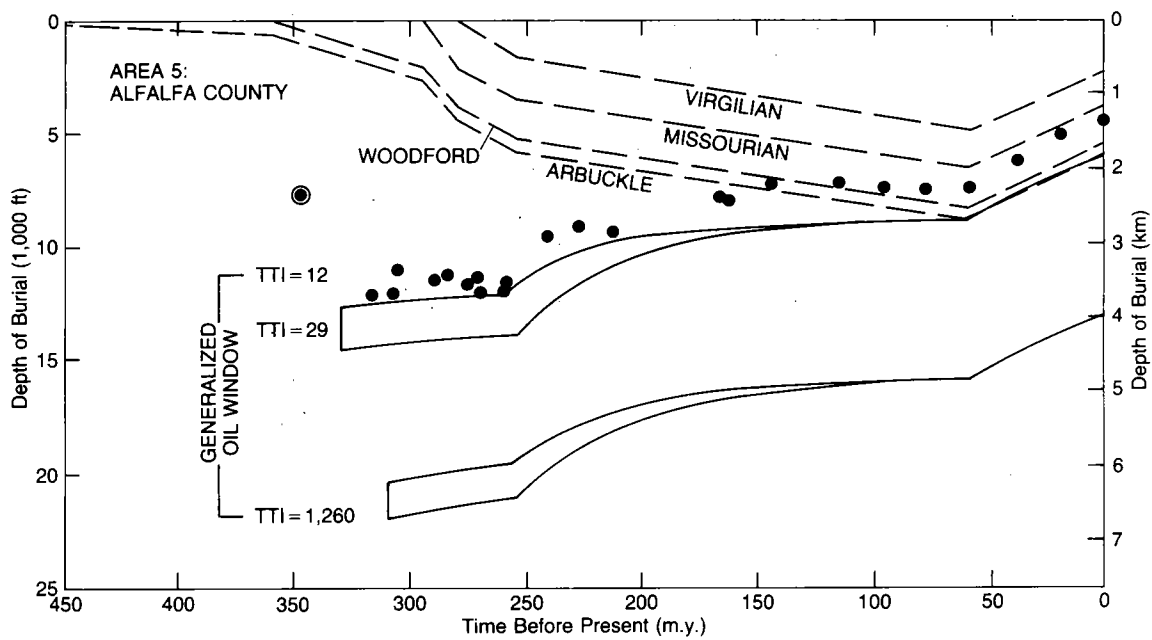


Figure 7. Burial curves for the shelf area of Alfalfa County, Oklahoma (area 5), superimposed on the regional oil window of Figure 2.

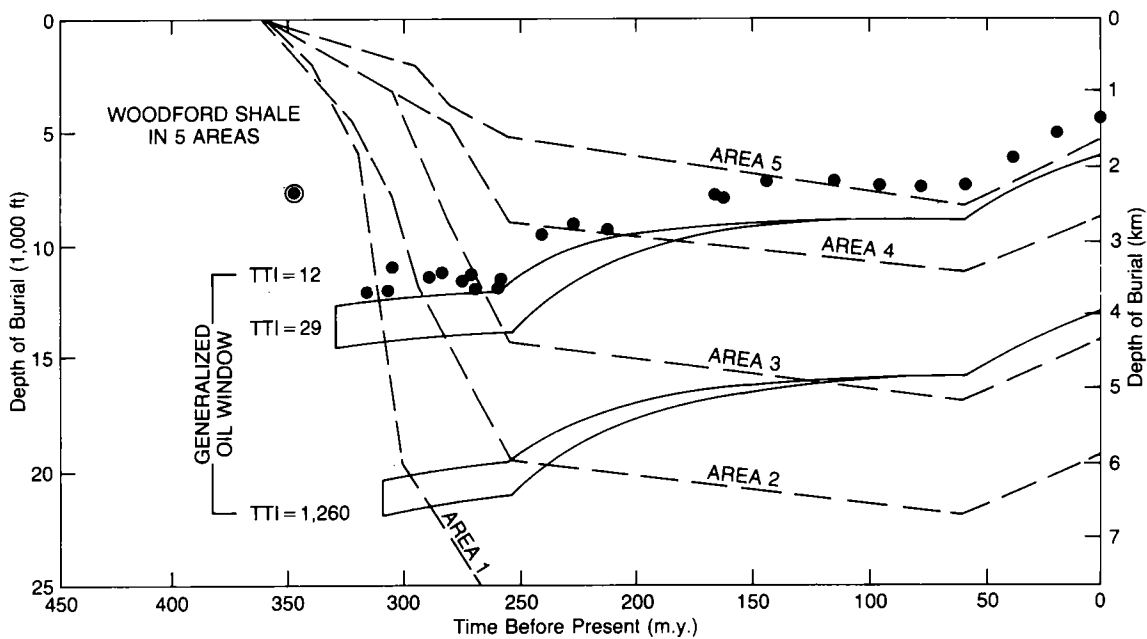


Figure 8. Burial curves for the Woodford Shale in five areas of the central Anadarko basin (Fig. 1), superimposed on the regional oil window of Figure 2.

THERMAL MATURATION OF THE WOODFORD SHALE IN THE ANADARKO BASIN

BRIAN J. CARDOTT

Oklahoma Geological Survey

Abstract.—The Woodford Shale (Upper Devonian–Lower Mississippian) in the Anadarko basin, Oklahoma and Texas, is marginally mature to postmature with respect to the generation of liquid hydrocarbons.

Core material and water-washed well cuttings of the Woodford Shale from 81 wells were examined under reflected white light from whole-rock, dispersed-organic pellets. Thermal maturity was determined by measuring the reflectance in oil immersion (R_o , percent) of low-gray (primary) vitrinite macerals. A minimum of 40 reflectance measurements were recorded for each well. Each well is represented by one or more sample intervals. The Woodford Shale was sampled at depths from 5,060 ft in the northern shelf area, and 3,600 ft in the southeastern part of the basin, to 27,732 ft in the deep Anadarko basin, north of the Wichita frontal fault zone.

Mean random and mean average vitrinite-reflectance (\bar{R}_o) values range from 0.48% in the northern shelf area, 0.42% in the southeastern part of the basin, and 0.47% in the Wichita frontal fault zone, to 4.89% in the deep Anadarko basin. An isorefectance map for the Woodford Shale indicates those areas of the basin where the thermal history of the shale is optimum for generating and preserving liquid hydrocarbons ($\bar{R}_o = 0.5$ –2.0%).

Regional maturation profiles of vitrinite reflectance (\bar{R}_o) versus depth for 80 wells provide a least-squares regression equation that predicts the vitrinite reflectance of the Woodford Shale at most depths in the Anadarko basin and estimates the amount of erosion generalized for the entire basin.

INTRODUCTION

In this paper, thermal maturation refers to the very low-grade metamorphism of sedimentary organic matter. The maturity stages (immature, mature, postmature) refer to the “degree to which hydrocarbon generation has proceeded in a kerogen” (Waples, 1985, p. 211).

The Woodford Shale (Upper Devonian–Lower Mississippian) in the Anadarko basin is a carbonaceous, siliceous, pyritic, dark-gray to black shale. The Woodford Shale was selected for thermal-maturation study because of the following factors:

- 1) The Woodford Shale is considered to be one of the most prolific hydrocarbon source rocks in the Anadarko basin (Webster, 1980; Hatch and others, 1986; Comer and Hinch, 1987; Burruss and Hatch, 1987; Imbus and others, 1987; Jones and others, 1987; Zemmels and others, 1987; Rice and others, 1987; Engel and others, 1988). Hydrocarbon source rocks are characterized by the type, quantity, and thermal maturity of sedimentary organic matter. Hunt (1979, p. 101) stated, “The most important factor in the origin of petroleum is the thermal history of the source rock.”

- 2) The Woodford Shale marks a general boundary between early Paleozoic carbonates and late

Paleozoic clastics (Ham and others, 1973; Hill and Clark, 1980; Kennedy and others, 1982, p. 10–14; Hill, 1984). Thermal maturity based on vitrinite reflectance from black shales is preferred over gray shales, sandstones, and limestones because black shales are more organic-rich, less likely to be oxidized, and more closely approximate the coal benchmark (Jones and others, 1972; Bostick and Foster, 1975; Wenger and Baker, 1987).

- 3) The Woodford Shale is the oldest rock unit in the Anadarko basin that contains woody organic matter, necessary for vitrinite-reflectance analysis (Ham and others, 1973). Hunt (1979, p. 332) stated, “Pre-Silurian rocks contain no vitrinite.”

- 4) The Woodford Shale contains less high-gray (recycled) vitrinite than younger rock units because there were few older sources from which vitrinite could be recycled.

- 5) The Woodford Shale was deposited prior to Pennsylvanian orogenies, thereby recording the thermal history of that period.

- 6) The Woodford Shale extends laterally across the entire Anadarko basin (Amsden, 1975; Johnson and others, 1988, p. 315, pl. 5-H; Hill, 1984).

The region covered in this report includes not only the Anadarko basin as outlined by Johnson (1971), but also the northern shelf area to the

Kansas border on the north, an area east of the Nemaha ridge on the east, and the area bordering the Ardmore basin on the southeast.

Thermal maturation was determined by measuring the reflectance in oil immersion (R_o) of vitrinite from whole-rock sample preparations. Vitrinite reflectance is reported by many to be the best thermal-maturation indicator. The vitrinite-reflectance analysis measures the percentage of white light (resolution of 0.01%) reflected from the vitrinite maceral (modified for shale from American Society for Testing and Materials, 1987, D2798), derived from woody organic matter (woody tissue from the stems, bark, roots, and leaves of vascular plants).

The thermal maturity of the Woodford Shale in the Anadarko basin can be applied: (1) to prediction of oil/gas windows in evaluating the Woodford Shale as a potential hydrocarbon source rock; (2) to understanding the geologic and tectonic history of the Anadarko basin since the Early Mississippian; and (3) to understanding the timing of hydrocarbon generation in and expulsion from the Woodford Shale.

This report updates an earlier report by Cardott and Lambert (1985) which reported the thermal maturity of the Woodford Shale based on vitrinite reflectance of samples from 28 wells in the Oklahoma portion of the Anadarko basin (refer to that report for additional information and interpretations of the vitrinite-reflectance data).

SAMPLING, LABORATORY, AND PETROGRAPHIC METHODS

Core material and water-washed well cuttings of the Woodford Shale from 81 wells, 72 from Oklahoma and 9 from the Texas Panhandle (Appendix), were prepared into whole-rock, dispersed-organic pellets (1–3 mm shale chips embedded in epoxy), polished, and examined under the microscope in reflected white light. Thirteen wells are represented by core material obtained from the Oklahoma Geological Survey Core and Sample Library and from B. J. Cunningham (Amarillo, Texas). Well cuttings were provided from the drilling programs of petroleum companies listed in the Appendix. Well cuttings were washed with water in a 18-mesh sieve (1-mm opening) to remove drilling mud. Well cuttings from deep wells that used an oil-based drilling mud were washed with mild dishwashing detergent.

Whole-rock samples were preferred over kerogen concentrate from acid-digested rock because of the following factors:

1) The Woodford Shale lithology can be identified under the microscope, reducing the possibility of measuring vitrinite reflectance from non-

Woodford lithologies. Well-caving contamination is a common problem when working with well cuttings (Dow and O'Connor, 1982; Bustin and others, 1985, p. 207).

2) The association of organic matter and rock matrix is used in the identification of organic-matter types, as in distinguishing vitrinite macerals from bitumen and pyrobitumen.

3) The Woodford Shale is generally a very organic-rich rock that does not require the concentration of vitrinite for the vitrinite-reflectance analysis.

4) Although abundant liptinite macerals (especially alginite) and bitumen in shale and coal have been found to suppress the reflectance of vitrinite (Hutton and Cook, 1980; Stach and others, 1982, p. 369; Price and Barker, 1985), the effects of acid digestion on vitrinite reflectance have not been fully explained (Stach and others, 1982, p. 369; Dembicki, 1984; Wenger and Baker, 1987).

Thermal maturity was determined by measuring the reflectance in oil immersion (R_o) of first-generation vitrinite macerals. A minimum of 40 reflectance measurements were recorded from the Woodford Shale for each well (Appendix), each sample representing one or more 10-ft sample intervals. The vitrinite-reflectance analysis was performed on a Vickers M17 Research Microscope system adapted for reflected white light in oil immersion (Cargille type B immersion oil with $n_e = 1.5180$), monochromatic green light (546 nm), and total magnification of 500X. Either average reflectance (without a polarizer) or random reflectance (with a polarizer) (Hevia and Virgos, 1977; Juckes and Pitt, 1977; Ting, 1978) were measured on the organic matter (Appendix). "Average" reflectance, as used here, is elsewhere referred to as "random" reflectance (Teichmüller, 1987). Maximum vitrinite reflectance, measured on coals, is not possible on vitrinite phytoclasts dispersed in shale because their small size prohibits stage rotation.

Vitrinite reflectance varies depending on (1) the wavelength of light at which reflectance is measured (standardized at 546 nm); (2) the refractive index of the immersion oil (standardized between 1.515 and 1.519, 1.5180 preferred); (3) the geochemical gelification (vitrinitization) of huminite macerals at reflectances of about 0.4–0.5%; (4) which vitrinite maceral of the vitrinite-maceral group is being measured; (5) the pressure-induced anisotropy of the vitrinite maceral, which produces a range of reflectance values from maximum to minimum in plane-polarized light at reflectance $>1.5\%$; and (6) the orientation of the vitrinite particle. Average reflectance measures all the incident-light vibration directions and gives an average of all values ranging between the maximum and apparent minimum. Random reflectance measures one vibration direction, which can

vary between the maximum and apparent minimum. Ting (1978) gave the same conversion factor for mean average and mean random reflectance in converting to mean maximum reflectance. Random reflectance was preferred in this study (Appendix), as recommended by Hevia and Virgos (1977).

Coal petrologists classify organic matter on the basis of petrography into three maceral groups: liptinite (exinite), vitrinite, and inertinite, each group consisting of several macerals (Stach and others, 1982). Macerals are the microscopically recognizable organic constituents of coal. Organic geochemists classify organic matter on the basis of chemistry into two types: kerogen (defined as organic matter insoluble in organic solvents, such as methylene chloride, chloroform, benzene, methanol-benzene, or hexane) and bitumen (defined as organic matter soluble in organic solvents, generated from the thermal maturation of kerogen) (Barker, 1979, p. 39; Tissot and Welte, 1984). Kerogen is classified into four types: type I is derived from lacustrine algae (e.g., *Botryococcus*) and their marine equivalents (e.g., *Tasmanites*) (equivalent to the coal maceral alginite of the liptinite maceral group); type II is derived from marine phytoplankton, zooplankton, and other microorganisms (bacteria), and terrestrial herbaceous organic matter (partially equivalent petrographically to the liptinite maceral group); type III is derived from woody tissues of terrestrial higher plants (equivalent to the vitrinite maceral group); and type IV (residual) is oxidized or reworked organic matter (equivalent to the inertinite maceral group and high-gray vitrinite macerals) (Tissot and others, 1974; Tissot and Welte, 1984; Ebukanson and Kinghorn, 1985). Bostick (1979) distinguished two types of vitrinite in the determination of thermal maturity by vitrinite reflectance: low-gray vitrinite, which represents the first-generation (primary) vitrinite indigenous to the host rock, and high-gray vitrinite, which is recycled vitrinite redeposited from an older sedimentary rock.

All reflectance measurements used in this study for the determination of thermal maturation by mean vitrinite reflectance are from low-gray vitrinite. Not included in the reported mean-reflectance tabulation were low-gray vitrinite macerals (1) in a light-colored groundmass (interpreted to be non-Woodford), (2) smaller than the fiber-optic measuring probe ($<8\mu\text{m}$, where reflectance is influenced by edge effects), (3) with a radioactive halo, causing a wide range in reflectance, or (4) with rough texture (pitted or otherwise degraded) (Dow and O'Connor, 1982). Other questionable reflectance values—interpreted to be from high-gray vitrinite macerals, bitumen, liptinite macerals, or inertinite macerals—also were not included.

The low-gray vitrinite reflectance values were

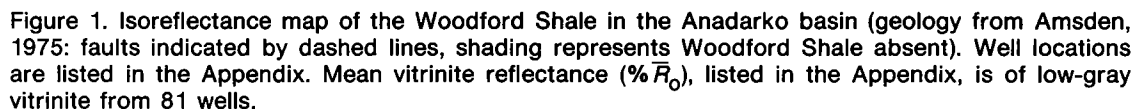
substantiated by other optical thermal-maturity parameters whenever possible: (1) fluorescence color (qualitative fluorescence) of liptinite macerals (*Tasmanites* algal spores; Urban, 1960; Wilson and Urban, 1963; Wilson and Skvarla, 1967; von Almen, 1970) and acritarchs (hystriospheraeids; Urban, 1960; von Almen, 1970; Goodarzi, 1985, p. 73; Crisp and others, 1987) at vitrinite reflectance less than $\sim 1.3\%$; (2) bitumen/pyrobitumen reflectance correlation with vitrinite reflectance (Jacob, 1985); (3) reflectance of inertinite macerals to obtain an upper reflectance limit used to bracket the low-gray vitrinite population (especially when comparing vitrinite with semi-fusinite with bogen structure) (Tissot and Welte, 1984, p. 243; Bustin and others, 1985, p. 37); and (4) elevated reflectance of *Tasmanites* and liptinitic amorphous organic matter (type A amorphous kerogen of Thompson and Dembicki, 1986) beyond the second coalification jump at reflectances greater than $\sim 1.5\%$. Von Almen (1970) reported scolecodonts from the Woodford Shale, which appear similar to vitrinite in reflected white light (Bertrand and Héroux, 1987). Other vitrinite-like organic matter (graptolites, chitinozoans; Goodarzi, 1985; Goodarzi and Norford, 1985; Bertrand and Héroux, 1987) have not been observed in the Woodford Shale.

RESULTS

Organic Petrography Laboratory (OPL) number(s), mean vitrinite reflectance in oil immersion (\bar{R}_o , percent), number of low-gray vitrinite-reflectance measurements per sample, standard error of the mean, and standard deviation are arranged by depth (ft) at top of Woodford Shale in the Appendix. Figure 1 is an isorefectance map showing the location of each well (Appendix) and the corresponding mean vitrinite-reflectance value (Appendix).

DISCUSSION

Hutton and Cook (1980), Price and Barker (1985), and Wenger and Baker (1987) stated that the presence of abundant liptinite macerals (especially alginite, $>10\%$ by volume including minerals) and bitumen in shale and coal suppress the reflectance of the vitrinite maceral by $>0.03\%$. This may be unavoidable in the study of hydrocarbon source rocks, because liptinite macerals, especially alginite, are the source of the oil. Price and Barker (1985, p. 59) indicated that " \bar{R}_o values have been, and are, for the most part, read from exinite-rich sediments examined in organic geochemical studies." The suppression effect on vitrinite reflectance is not unique, as indicated by Price and Barker (1985, p. 73), who wrote that "all maturation indices which are commonly em-



The Woodford Shale is known to contain abundant type A amorphous type II kerogen (partially equivalent to the liptinite [exinite] maceral group) with the balance consisting of type III ker-

ogen (vitrinite) and type I kerogen (*Tasmanites* alginite) (Lewan, 1983; Thompson and Dembicki, 1986; Crossey and others, 1986; Comer and Hinch, 1987; Burwood and others, 1988). Vitrinite reflectance $<1.3\%$ in the Woodford Shale is suspected to be suppressed, although whether it is or not and by how much has not been determined. Vitrinite reflectance of the Woodford Shale $>1.3\%$ is assumed not to be suppressed, because the reflectance of liptinite macerals and bitumen is equal to or exceeds that of vitrinite beyond the second coalification jump at $1.3\% R_o$ (Stach and

others, 1982; Bustin and others, 1985; Jacob, 1985; Teichmüller, 1987). However, Price and Barker (1985, p. 80) indicated that "this suppression extends at least to the R_o range of 4.0% as measured in vitrinite-rich rocks."

The results of the vitrinite-reflectance analysis of the Woodford Shale (Appendix; Fig. 1) will be discussed according to maturation stages modified from those outlined in Table 1 (marginally mature, mature, postmature), owing to similar changes in the physical and chemical properties of vitrinite at each stage and to the types of hydrocarbons generated/preserved at each stage.

Marginally Mature

A hydrocarbon source rock that is marginally mature with respect to the generation of liquid hydrocarbons is expected to have a vitrinite reflectance between 0.35 and 0.6% (Table 1); the range is wide because the onset of oil generation is determined by the type of organic matter (Stach and others, 1982, p. 412; Teichmüller, 1986).

The lowest observed mean vitrinite reflectance of the Woodford Shale in the Anadarko basin was 0.42% (OPL 563, Appendix) at a depth of 6,998 ft. Twenty-nine samples, all from Oklahoma, have a mean vitrinite-reflectance range of 0.42 to 0.6%, ranging in depth from 764 to 9,158 ft (Appendix). The standard error of the mean vitrinite reflectance ranges from 0.01 to 0.02, and standard deviation from 0.045 to 0.157. The samples are from the edges of the basin (Fig. 1).

Two samples are from the Wichita frontal fault zone (OPL 123, 150–153). OPL 123 (R_o 0.48%) is at a present-day depth of 764 ft. The maturity of this sample probably was attained prior to the Wichita orogeny (pre-orogenic), when the Woodford Shale would have been at greater depth (Cardott and Lambert, 1985, 1987). OPL 150–153 (R_o 0.47%) has a present-day depth of 6,150 ft. The maturity probably was set after the Wichita orogeny (post-orogenic). The remaining marginally mature samples are from a broad zone of the shelf areas of the basin on the north, northeast, and east, and from the boundary with the Ardmore basin on the southeast.

The shallowest Woodford Shale sample outside

TABLE 1.—SUMMARY OF HYDROCARBON GENERATION AND PRESERVATION RELATED TO THERMAL MATURATION

Temperature (°C)	Vitrinite reflectance, R_o (%)	Organic stage	Maturity	Hydrocarbon generation
		Diagenesis	Immature	Biogenic methane (marsh gas; early diagenetic methane)
50–65	0.35–0.6	————	————	First oil formation (oil "birth" zone)
	0.6–0.7			Peak oil generation
	0.95			Main phase of oil expulsion
	1.0	Catagenesis	Mature	Peak condensate and wet-gas generation
120–170	1.2			Peak dry-gas generation (thermogenic methane)
	1.3–1.4			Oil floor (oil "death" zone)
	2.0	————	————	Condensate and wet-gas floor
>200	3.0–5.0	Metagenesis	Postmature	Dry-gas preservation limit
		Metamorphism (greenschist facies)		

Source: Cardott and Lambert, 1985.

of the Wichita frontal fault zone is OPL 548 (R_o 0.49%) at a depth of 3,600 ft (Appendix), from the southeastern part of the Anadarko basin. The shallowest samples in the northern shelf areas are OPL 119 (R_o 0.55%, depth 5,060 ft) and OPL 107 (R_o 0.51%, depth 5,130 ft).

The deepest marginally mature Woodford Shale sample from the northern shelf areas is OPL 160 (R_o 0.58%) at a depth of 7,876 ft. Deeper marginally mature Woodford Shale samples are from the eastern and southeastern margins of the basin (Fig. 1). The deepest marginally mature Woodford Shale sample (OPL 740, R_o 0.53%, depth 9,158 ft) is from Garvin County, in the southeastern part of the Anadarko basin.

Clearly, most of the deeper marginally mature Woodford Shale samples are from the southeastern margin of the Anadarko basin. The maturation of the Woodford Shale in this region could have been influenced by geologic factors different from those in the northern shelf areas (lower coalification rate, less erosion, different environment of deposition) or by compositional differences in organic matter (vitrinite type, type and quantity of associated organic matter) (Katz and Liro, 1987; Cardott and Lambert, 1987).

The 0.6% isorefectance contour in Figure 1 is not significantly different from that in the isorefectance map in Cardott and Lambert (1985, fig. 4), with the addition of more marginally mature Woodford Shale samples. The Woodford Shale is marginally mature over a large area of the northern shelf and southeastern margin of the Anadarko basin.

Mature

Mature hydrocarbon source rocks have a range in vitrinite reflectance from 0.6 to 2.0% (Table 1). The zone can be subdivided into two parts: the "oil window," with vitrinite reflectance from 0.6 to 1.3%, and the zone from the oil floor, to the condensate and wet-gas floor, with vitrinite reflectance from 1.3 to 2.0%.

Twenty-five samples, 24 from Oklahoma and 1 from the Texas Panhandle, have a mean vitrinite reflectance of 0.63 to 1.27%, with a depth range from 7,922 to 14,404 ft in Oklahoma, and a depth of 15,614 ft in Texas. There is an overlap of ~1,200 ft between the marginally mature and mature zones. The standard error of the mean vitrinite reflectance ranges from 0.01 to 0.03, and standard deviation from 0.057 to 0.265 (Appendix).

Figure 1 illustrates a northwest-southeast zone in Oklahoma, extending from the north side of the Anadarko basin to the Ardmore basin on the southeast, where vitrinite reflectance ranges from 0.6 to 1.3%. The trend of this zone follows the structure contours of the Woodford Shale

(Cardott and Lambert, 1985, fig. 3). This is not surprising, because Hilt's Law indicates that rank (thermal maturity) increases with increasing depth of burial (Stach and others, 1982). The Woodford Shale is predicted to have generated and preserved oil in this zone, referred to as the "oil window." Woodford Shale samples within the "oil window" from different parts of the Anadarko basin are widely scattered, with no apparent trend according to depth or region (Appendix; Fig. 1), as was the case for the marginally mature samples. The isorefectance contours do not extend into Grady and Stephens Counties in the southeastern part of the Anadarko basin, owing to less well control and a more complicated tectonic history. The single sample from Texas (OPL 701) that falls within the "oil window" may be anomalous, judging from two nearby shallower samples of higher maturity (Appendix).

Fourteen samples, 11 from Oklahoma and 3 from the Texas Panhandle, have a mean vitrinite reflectance from 1.32 to 2.00%, with a depth range from 12,416 to 21,722 ft in Oklahoma and 12,965 to 20,460 ft in Texas (Appendix). There is an overlap of ~5,000 ft between the mature and postmature zones. The standard error of the mean ranges from 0.02 to 0.05, and standard deviation from 0.143 to 0.323 (Appendix). Standard error of the mean and standard deviation (Hunt, 1979, p. 469) increase with increasing vitrinite reflectance, owing to the increasing influence of pressure-induced anisotropy of vitrinite (measured as bireflectance; Stach and others, 1982).

The 1.30–2.00% R_o zone in Figure 1 forms a rim around the deep Anadarko basin, extending from the ancestral Amarillo–Wichita uplift in the Texas Panhandle on the west, along a northwest-southeast trend on the north side of the deep basin, to the Wichita frontal fault zone in Oklahoma on the east. The addition of several Woodford Shale samples from the Texas Panhandle and OPL 386 and 387 in Oklahoma has significantly redefined the location of the 2.0% R_o contour on the west and east sides of the deep basin (cf. Cardott and Lambert, 1985, fig. 4). The Woodford Shale is predicted to have generated and preserved condensate and wet gas in this zone, with the thermal cracking of oil.

Three of the four deepest Woodford Shale samples in the condensate/wet-gas zone (OPL 803, 269, 704) occur in the fault zones north of the ancestral Amarillo–Wichita uplift along the Oklahoma/Texas state line and in the southeastern part of the basin.

Postmature

A hydrocarbon source rock that is postmature with respect to the generation of liquid hydrocar-

bons is predicted to have a vitrinite reflectance ranging from 2.0 to 5.0% (Table 1). The 5.0% R_o value represents the tentative dry-gas preservation limit (Saxby, 1982). Houseknecht and Hathon (1987) indicated methane production from postmature (overmature) rocks with vitrinite reflectance up to 5% R_o in the Arkoma basin of Oklahoma and Arkansas. Dry gas (methane) is the only hydrocarbon preserved in postmature rocks.

Thirteen samples, 8 from Oklahoma and 5 from the Texas Panhandle, have a mean vitrinite reflectance ranging from 2.03 to 4.89%, with a depth range of 16,226 to 27,732 ft in Oklahoma and 16,966 to 22,280 ft in Texas (Appendix). The standard error of the mean vitrinite reflectance ranges from 0.03 to 0.08, and standard deviation from 0.202 to 0.703 (Appendix).

The postmature zone occupies the area of the deep Anadarko basin in Oklahoma and Texas (Fig. 1). The shape of the postmature zone on the isoreference map in Figure 1 is markedly different from that of the isoreference map of the Woodford Shale in Cardott and Lambert (1985, fig. 4), owing to the addition of samples in the Texas Panhandle and OPL 392 in Oklahoma. The 2.0 to 3.5% R_o contours on the west side of the deep basin on the original map were interpreted, lacking other vitrinite-reflectance data, in accord-

ance with the range of mean vitrinite-reflectance values of "2.37 to 2.54% for the interval between 23,830 and 24,065 ft" for the Woodford Shale reported by Katz and others (1982, p. 1150) from the Union of California 1-33 Bruner well (sec. 33, T. 11 N., R. 25 W., Beckham County, Oklahoma). OPL 392 (Appendix; \bar{R}_o 4.05%, depth 23,880 ft) is from the Leede Oil & Gas 1-3 Green well, <2 mi from the Bruner well. The large discrepancy in mean vitrinite-reflectance values for the two wells is due primarily to interpretation of the reflectance values, although the following factors also must be considered:

- 1) Well cuttings were used from both wells. Contamination from well casing is a great problem when working with well cuttings. Katz and others (1982) measured vitrinite reflectance on "isolated vitrinite" (kerogen concentrate), whereas vitrinite reflectance from OPL 392 was measured from whole-rock, dispersed-organic pellets. Although vitrinite reflectance could have been measured from non-Woodford lithology in either well, the possibility of error is greatly reduced by using whole-rock pellets rather than kerogen-concentrate pellets (Stach and others, 1982, p. 363,407; Teichmüller, 1986).

- 2) Cardott and Lambert (1985, p. 1987) cautioned that "Organic matter becomes more homogeneous as aromatization increases during post-

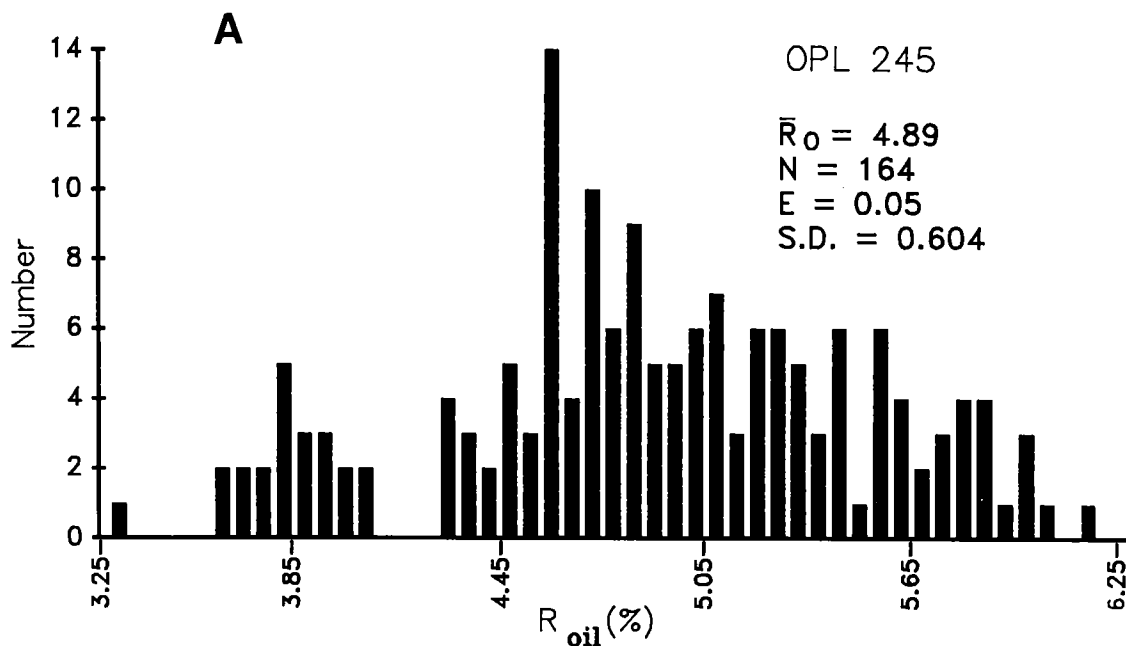


Figure 2. Vitrinite-reflectance histograms of Woodford Shale samples with mean random vitrinite reflectance $>4.0\%$ from the deep Anadarko basin, Oklahoma. Variable frequency and reflectance scales. A—OPL 245, \bar{R}_o 4.89%. B—OPL 392, \bar{R}_o 4.05%. C—OPL 239, \bar{R}_o 4.29%.

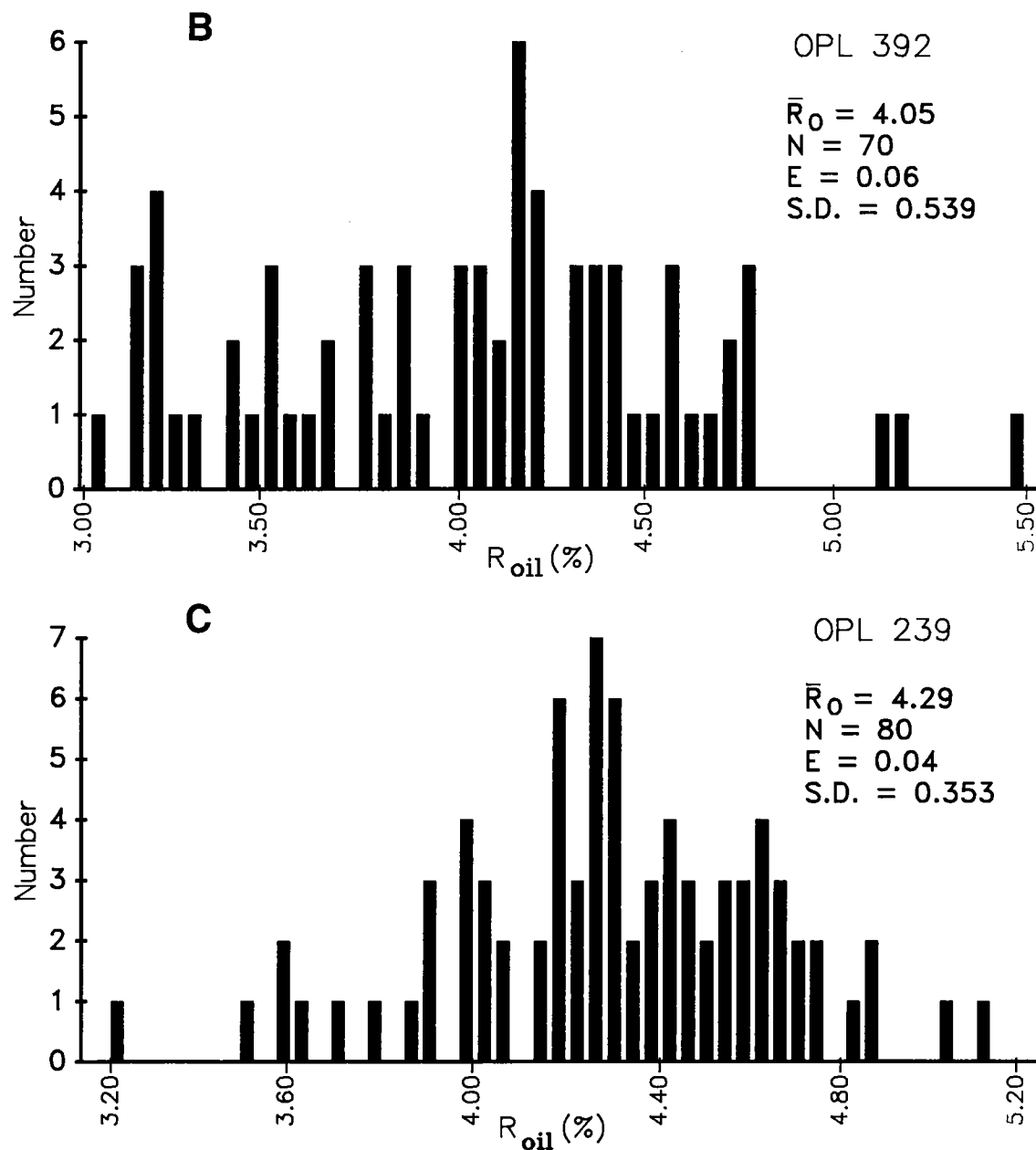


Figure 2. Continued.

maturity with respect to the generation of liquid hydrocarbons (greater than 2% R_0). Low-gray vitrinite and other types of organic matter (lipinite and inertinite macerals, high-gray vitrinite macerals, and pyrobitumen) become less distinct at reflectances $>2\%$ (Tissot and Welte, 1984, p. 243, fig. II.8.10). Structure of phytoclasts is used

to reject non-vitrinite reflectance values of *Tasmanites* (donut shape), inertinite macerals (bogen structure), and pyrobitumen (shape of pore space)—all having high reflectance. Small-sized and rough-textured (pitted, scratched, etched) vitrinite phytoclasts are rejected on the basis of quality. Following these guidelines, the

vitrinite-reflectance population in OPL 392 ranges from 3.06 to 5.47%, with three values >4.77% (Fig. 2B). The 95% confidence interval for the mean is 3.92 to 4.18% R_o . Reflectance values <3.0% represent either small size or rough texture.

3) The anisotropy of vitrinite greatly increases at reflectances >1.5% (Stach and others, 1982; Durand and others, 1986). Random or average vitrinite-reflectance values >2.0% are expected to have a wide range in reflectance values, with associated large standard error of the mean and standard deviation (Hunt, 1979, p. 469). Although maximum reflectance is often recommended for measuring vitrinite reflectance >2.0%, Hevia and Virgos (1977, p. 27) concluded that "For coals (especially anthracites and meta-anthracites), and, in general, for dispersed organic matter in sediments, rank should be measured using the mean random reflectivity of the vitrinite, instead of the mean maximum reflectivity" where mean random reflectivity was determined in plane-polarized light. The significance of measuring average vs. random reflectance has not been determined. Katz and others (1982) did not indicate whether the vitrinite-reflectance values were average or random. Random reflectance was measured in OPL 392. A reflectance histogram should fit a bell-shaped curve of a normal distribution (Gaussian distribution). The relatively narrow range in vitrinite-reflectance values (0.8%), abrupt upper limits, and non-Gaussian shape of reflectance histograms by Katz and others (1982) suggest that they interpreted reflectance values >2.9% to be either high-gray vitrinite, inertinite macerals, *Tasmanites* algal spores, or pyrobitumen. As noted above under the discussion of homogeneity of organic matter, reflectance values <3.0% in OPL 392 were rejected because of small size or rough texture. The reflectance histogram of OPL 392 (Fig. 2B) has a skewness of 0.0948 and a kurtosis of 2.5490. Reflectance histograms for two other samples with mean vitrinite reflectance >4.0% (OPL 245, 239) are illustrated in Figures 2A and 2C for comparison. The standard deviation of OPL 392 (Appendix) is 0.539, higher than predicted by Hunt (1979, p. 469). The regression-predicted reflectance for OPL 392 in the Appendix is 3.98%.

The shape of the western part of the postmature zone for the Woodford Shale in the Anadarko basin is no longer defined by one data point, but is substantiated by five Woodford Shale samples in the Texas Panhandle with mean random vitrinite reflectance from 3.03 to 3.40%, OPL 705 representing split core.

In summary, vitrinite-reflectance values >2.0% are less accurate and more interpretive than lower reflectance values. Interpretations are greatly influenced by sample quality (cuttings vs. core, whole rock vs. kerogen concentrate, small

size and rough texture of vitrinite); microscopic technique (random vs. average reflectance, lack of glass standards with high reflectance); and the physical and chemical properties of organic matter at high maturity (anisotropy of vitrinite, homogeneity).

A thermal anomaly was previously inferred in the deep Anadarko basin (Cardott and Lambert, 1985, 1987), based on the significance of measured mean vitrinite reflectance of 2.5% at 24,065 ft for the Bruner well, and 4.89 and 4.29% at 22,526 and 25,115 ft for OPL 245 and 239. A thermal anomaly is still predicted, based on widely different mean vitrinite-reflectance values at similar depths for OPL 269, 386, 245, 392, 239, and 418 in Oklahoma, and OPL 705, 696, 695, 697, 704, and 703 in the Texas Panhandle (Appendix).

The Woodford Shale is postmature over most of the deep Anadarko basin, and vitrinite-reflectance values >4.0% are inferred over a large area (Fig. 1).

Regression Analysis of Reflectance versus Depth

Vitrinite reflectance of the Woodford Shale can be predicted at most depths in the Anadarko basin and the amount of erosion can be estimated by regression analysis of vitrinite-reflectance-versus-depth data. Dow (1977) illustrated several kerogen-maturation profiles showing increase in vitrinite reflectance with depth in wells. Cardott and Lambert (1985) determined the exponential least-squares regression for mean vitrinite-reflectance values of the Woodford Shale from 28 wells in the Anadarko basin to be

$$R_o = 0.273e^{(0.0001133X)} \quad (1)$$

where X is depth in feet. Schmoker (1986) performed a regression analysis on 83 mean vitrinite-reflectance values versus present depth from the literature from two deep wells (1 Bertha Rogers and 5 Rumberger), Woodford Shale (including the 28 values from Cardott and Lambert, 1985), and uppermost Morrowan shale from the Anadarko basin, with the resultant equation

$$R_o = 0.32e^{(0.0001044X)} \quad (2)$$

where X is depth in feet. The analytical methods used by each investigator in measuring vitrinite reflectance are probably not consistent.

Cardott and Lambert (1987) discussed the advantages of performing a regression analysis on vitrinite reflectance versus depth for geographically separated vitrinite-reflectance values from a single geologic unit. They stated (p. 898) that "The regression analysis tests whether or not there is a relationship between vitrinite reflectance and depth. The goodness-of-fit of the regression equation ($R^2 = 0.918$) suggests that a relationship does exist." They also indicated that

the only assumption in using vitrinite-reflectance profiles as a tool in predicting vitrinite reflectance from present depth is that the present-day depths of the samples are near-maximum. The relationship does not hold in uplifted areas such as the Wichita frontal fault zone.

A linear least-squares regression analysis of vitrinite reflectance versus present depth for 80 wells is illustrated in Figure 3. The depths to the top of the Woodford Shale and the mean vitrinite-reflectance values (R_o) used in the regression analysis are listed in the Appendix. OPL 123

from the Wichita frontal fault zone was excluded from the regression analysis because the sample was not thought to be from near-maximum depth. OPL 123 was uplifted during the Wichita orogeny and acquired its thermal maturity prior to the orogeny. An exponential least-squares regression from a linear/linear plot of reflectance versus depth for 80 wells gives the equation

$$R_o = 0.254e^{(0.0001152X)} \quad (3)$$

where X is depth in feet. The goodness-of-fit (R^2) of regression equation (3) is 0.893. Davis (1986, p. 182) indicated that the goodness-of-fit (R^2) will be near unity if the least-squares regression line is a good estimator of the data. The spread of data about the regression line in Figure 3 is influenced by several factors: (1) geochemical gelification (vitrinitization), which transforms huminite into vitrinite at reflectances $<0.6\%$ (Stach and others, 1982); (2) random experimental error (measuring random and average reflectance, Appendix; assumed linearity of glass standards); (3) interpretation of low-gray vitrinite population; (4) anisotropy of vitrinite broadening reflectance histograms, beginning at R_o 1.0%, with noticeable effect at $R_o >2.0\%$; Dow, 1977; Hunt, 1979, p. 332; (5) suppression of R_o in alginite-rich rocks (>10 vol. % including minerals). Katz and Liro (1987) and Cardott and Lambert (1987) indicated geologic factors that may influence the regression line. Regression-predicted reflectance in the Appendix shows how mean vitrinite reflectance is predicted to increase with depth from regression equation (3). Compare the regression-predicted reflectance values with the measured mean vitrinite-reflectance values.

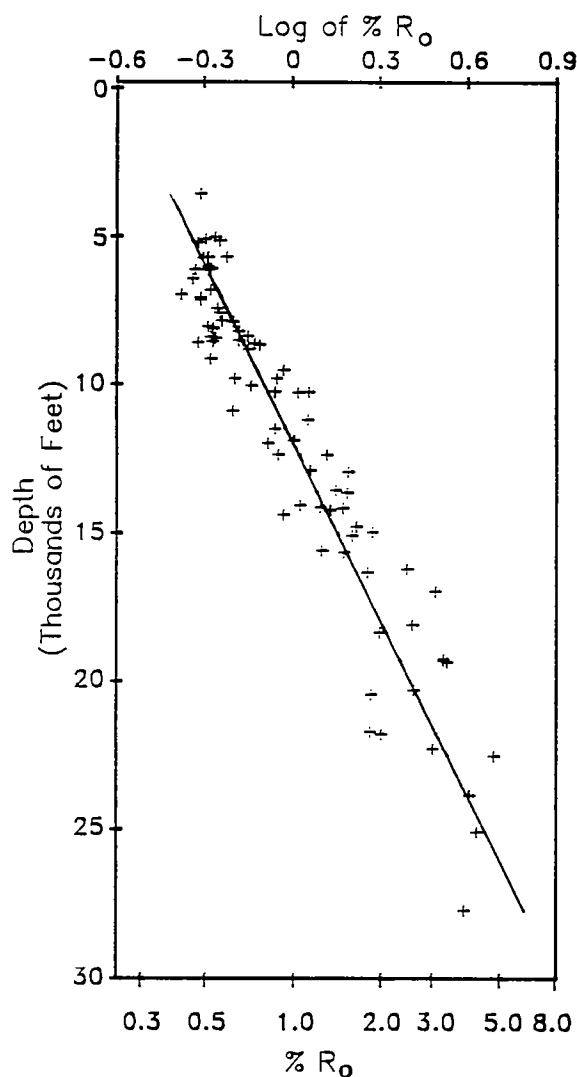


Figure 3. Maturation profile of the Woodford Shale, Anadarko basin, with linear least-squares regression line on semilog plot of mean vitrinite reflectance (R_o) vs. depth from 80 wells.

Hydrocarbon Potential and Erosion Predictions

Based on regression equation (3), the depths of hydrocarbon generation, preservation, and thermal destruction (Table 1) are predicted for the Woodford Shale in Table 2. In contrast, regression equation (2) from Schmoker (1986, p. 15–17) for all potential hydrocarbon source rocks in the central Anadarko basin predicts the following depths: 4,300 ft at R_o 0.5%; 6,000 ft at R_o 0.6%; 13,400 ft at R_o 1.3%; 17,600 ft at R_o 2.0%; and 26,300 ft at R_o 5.0%. Hill and Clark (1980) and Hill (1984) indicated in a paleotemperature profile of the Anadarko basin that the oil window (R_o 0.5–1.3%) occurs approximately from 1,000 to 12,000 ft, and the gas window (R_o 1.3–5.0%) extends approximately from 12,000 to 26,000 ft.

Cardott and Lambert (1985, p. 1994–1995) used regression equation (1) to predict the thermal maturity of the Woodford Shale in several deep petroleum wells. Refer to Cardott and Lambert (1985) for a discussion of several deep wells, the

TABLE 2.—VITRINITE-REFLECTANCE PREDICTIONS
FOR WOODFORD SHALE IN THE ANADARKO BASIN

Vitrinite reflectance R_o (%)	Depth (ft)	Hydrocarbon generation and preservation
0.5–0.7	5,900–8,800	Oil "birth" zone
0.9–1.0	11,000–11,900	Main phase of oil expulsion
1.3–1.4	14,200–14,800	Oil "death" zone
2.0	17,900	Condensate and wet-gas "death" line
5.0	25,900	Tentative dry-gas preservation limit

Based on regression equation (3) of R_o vs. depth (see text).

depths of the Woodford Shale, the predicted vitrinite-reflectance value from regression equation (1), and other published vitrinite-reflectance values for the Woodford Shale. Regression equation (3) can be used to refine the regression-predicted reflectance values.

Of significance is the proximity of OPL 704 in the Texas Panhandle to Chevron's Ruth Ledbetter well (sec. 21, Blk L, J. M. Lindsay Survey, Wheeler County, Texas, ~4 mi north of OPL 704), the deepest gas-producing well in the United States (World Oil, 1988; Oil and Gas Journal, 1988), producing from the Arbuckle Group at a depth of 26,536 ft. The predicted vitrinite reflectance of the Arbuckle Group at 26,536 ft from regression equation (3) is 5.40%, compared to a measured mean vitrinite reflectance of the Woodford Shale in OPL 704 of 1.87% at 20,460 ft (predicted to be 2.68% in the Appendix). Tarafa and others (1988) measured a vitrinite reflectance of 1.47% from air-dried well cuttings of the Woodford Shale in the Ledbetter well at 20,830–20,840 ft. Lack of detailed information on sample preparation and reflectance-analysis procedures precludes direct comparison with the present study. The reported organic carbon value of 6.18% is certainly typical for the Woodford Shale; however, two reported reflectance values from 21,900–21,910 ft (Sylvan) and 23,600–23,610 ft (Arbuckle) are from pre-Silurian strata and could not have been taken from vitrinite. The depths to the top and bottom of the Woodford Shale are 20,795 ft and 20,955 ft (Stephen C. Ruppel, personal communication, 1988). The predicted vitrinite reflectance of the Woodford Shale at 20,795 ft from equation 3 is 2.79%. It is apparent that the Woodford Shale in the Ledbetter and Davidson (OPL 704) wells are

outside the thermal-anomaly zone to the north and east.

The estimated amount of erosion from regression equation (3) at a vitrinite reflectance of 0.2% (the reflectance of protovitrinite when it was deposited) is 2,100 ft (generalized for the entire Anadarko basin). Refer to Cardott and Lambert (1985,1987) and Schmoker (1986) for additional information on estimating the amount of erosion from regional maturation profiles.

CONCLUSIONS

The Woodford Shale (Upper Devonian–Lower Mississippian) in the Anadarko basin, Oklahoma and Texas, is marginally mature to postmature with respect to the generation of liquid hydrocarbons.

Twenty-nine marginally mature (R_o 0.42–0.6%) Oklahoma samples are from depths <9,158 ft from a large area of the shelf on the north and east edge of the basin, the southeast margin transition with the Arbuckle Mountains uplift and Ardmore basin, and the Wichita frontal fault zone.

Twenty-five Woodford Shale samples fall within the "oil window" (R_o 0.63–1.27%). They are from depths of 7,922 to 15,614 ft, closely approximating structure contours in a northwest-southeast trend on the north and east sides of the basin in Oklahoma and western edge of the basin in Texas.

Fourteen samples within the condensate/wet-gas zone (R_o 1.32–2.00%) represent a rim around the deep Anadarko basin at depths from 12,416 to 21,722 ft in Oklahoma and Texas.

Thirteen postmature (R_o 2.03–4.89%) samples

are from the deep Anadarko basin of Oklahoma and Texas at depths of 16,226 to 27,732 ft, with potential for dry-gas preservation.

A regional maturation profile of vitrinite reflectance (R_o) versus depth for 80 wells defined the exponential least-squares regression line by the equation

$$R_o = 0.254e^{(0.0001152X)}$$

where X is depth in feet and the goodness-of-fit (R^2) is 0.893. The regression equation and isoreflectance map are tools to predict the vitrinite reflectance at most depths and corresponding hydrocarbon generation and preservation thresholds of the Woodford Shale in the Anadarko basin.

The amount of erosion, generalized for the entire Anadarko basin, based on a protovitrinite re-

flectance of 0.2%, is 2,100 ft, as estimated from the regression equation.

ACKNOWLEDGMENTS

I thank the many petroleum companies (listed in the Appendix) that provided Woodford Shale samples to the Oklahoma Geological Survey, making this study possible. I thank Stephen C. Ruppel of the Texas Bureau of Economic Geology and Barney J. Cunningham of Amarillo, Texas, for assistance in obtaining the Woodford Shale samples from Texas. I thank Mark Pawlewicz (USGS, Denver) and John Comer (University of Tulsa) for their constructive criticisms of the manuscript.

APPENDIX: SAMPLE INFORMATION, ANALYTICAL DATA, AND STATISTICAL PARAMETERS (ARRANGED BY DEPTH)

OPL No(s).	Operator	Lease	W/C ^a	Location	Depth of Woodford Shale top (ft)	Subsea elevation (ft)	Thickness of Woodford Shale ^d (ft)	Mean vitrinite reflectance in oil, (%) R_o	Number of measurements	Standard error of the mean	Standard deviation	Regression-predicted reflectance
OKLAHOMA												
123 ^b	R. W. Harris	4 Pfenning "Sam"	W	11- 6N-17W	764	+731	?	0.48(a)	75	0.01	0.109	0.28
548	Getty Oil	5 Doak Unit	W	36- 1S- 5W	3,600	-2,347	717	0.49	50	0.01	0.076	0.38
119 ^b	Heston Oil	1-36 Reagan	W	36-15N- 1E	5,060	-4,065	42	0.55(a)	60	0.02	0.126	0.45
107 ^b	Jefferson-Williams	1 Ebert	W	1-22N- 4W	5,130	-3,984	68	0.51(a)	83	0.01	0.088	0.46
114 ^b	Bobby J. Darnell	1 Kindichi	W	14-19N- 2W	5,175	-4,140	60	0.57(a)	75	0.01	0.056	0.46
560	Harper Oil	1-21 Jenkinson	W	21-29N-11W	5,240	-3,951	28	0.48	50	0.01	0.066	0.46
390 ^c	Sinclair O&G	1-31 Ruzek	W	31-26N- 4W	5,722	-4,699	76	0.60	61	0.02	0.157	0.49
784	Alpine O&G	1-6 Stacy	W	6-10N- 2E	5,740	-4,547	112	0.52	60	0.01	0.053	0.49
786	Santa Fe Energy	1-12 Witten	W	12- 7N- 1E	5,752	-4,589	?	0.50	80	0.01	0.088	0.49
555	Jones & Pellow Oil	2-24 Files	W	24- 1S- 6W	6,056	-4,972	137 ^e	0.52	48	0.01	0.078	0.51
586	Anadarko Production	1 Hawkins "A"	C	26-26N-11W	6,110	-4,920	34	0.53	60	0.01	0.063	0.51
150-153 ^b	Jones & Pellow Oil	B-2 Hall	C	36- 7N-13W	6,150	-4,780	NA	0.47	262	0.01	0.109	0.52
587	Calvert Mid-America	2 Bloyd	C	21-27N-15W	6,156	-4,586	53	0.52	50	0.01	0.045	0.52
584	Jones & Pellow Oil	1 Boyd	C	28-12N- 2W	6,468	-5,293	25	0.46	50	0.01	0.047	0.53
801	Alpine O&G	1 Waton	W	32-11N- 2W	6,844	-5,573	64	0.53	50	0.01	0.092	0.56
563	Genesis Energy	1-25 Borquin	W	25- 7N- 2W	6,998	-5,898	71	0.42	50	0.01	0.090	0.57
585	Eason Oil	1 Ruth	C	2-15N- 5W	7,095	-5,958	51	0.49	50	0.01	0.051	0.58
535	Anadarko Production	1-24 McCaskill "C"	W	24- 3N- 3W	7,197	-6,119	205	0.49	49	0.01	0.082	0.58
108 ^b	Clifford Resources	1-22 Doane	W	22-22N- 9W	7,466	-6,123	58	0.56(a)	156	0.01	0.123	0.60
536	Phillips Petroleum	1 McCrory "A"	W	5- 1S- 3W	7,616	-6,684	374	0.57	55	0.01	0.103	0.61
160 ^b	Humble Oil & Refining	1 State Hunton	C	16-18N- 7W	7,876	-6,747	28	0.58	57	0.01	0.089	0.63
108 ^b	Anadarko Production	2 Bane "B"	W	35-23N-15W	7,922	-6,553	37	0.63(a)	269	0.01	0.144	0.63
579	Diamond Shamrock	1-23 Irons	W	23- 7N- 3W	8,072	-6,976	84	0.52	51	0.01	0.072	0.64
133	Texaco	1 Hattie Harrel "C"	W	3- 1N- 5W	8,136	-6,936	?	0.54	40	0.01	0.093	0.65
567	Mack Energy	1 Work	W	28- 4N- 3W	8,151	-7,092	219	0.54	65	0.01	0.096	0.65
113 ^b	Universal Resources	1-24 Eugene	W	24-19N- 9W	8,236	-7,064	25	0.66(a)	120	0.01	0.161	0.66
165-166 ^b	Pan American Petroleum	1 Roetzel Unit "B"	C	13-19N-10W	8,407	-7,237	31	0.71	161	0.01	0.117	0.67

Woodford Shale Thermal Maturation

45

120 ^b	Eason Oil	4 Henderson	W	5-11N- SW	8,424	-7,092	88	0.53(a)	77	0.01	0.116	0.67
549	Eason Oil	1-2 Delliah Hinkle	W	2- 2N- 3W	8,465	-7,303	256	0.55	41	0.01	0.092	0.67
758	Bogert Oil	1-20 Meinders	W	20- 1N- 3W	8,540	-7,506	334	0.66	40	0.01	0.082	0.68
156-157 ^b	Universal Resources	2-16 Damehl	C	16-13N- 6W	8,575	-7,290	83	0.54	94	0.01	0.139	0.68
154-155 ^b	Jones & Pellow Oil	1-10 Robberson	C	10-10N- 5W	8,620	-7,300	104	0.48	129	0.01	0.082	0.69
565	Sydson D'Oro Exploration	1-1 Shields	W	1- 4N- 4W	8,642	-7,660	206	0.75	43	0.01	0.090	0.69
115 ^b	J. Walter Duncan, Jr.	2 Garrett	C	22-17N- 8W	8,698	-7,571	44	0.78(a)	75	0.01	0.069	0.69
804	Heimerich & Payne	1-30 Signa	W	30- 1S- 3W	8,838	-7,762	?	0.71	50	0.02	0.120	0.70
740	Mobil Oil	1 Roberta Miller Unit	W	16- 3N- 3W	9,158	-8,158	206	0.53	40	0.01	0.081	0.73
270	Seneca Oil	2-12 Rehl	W	12-19N-13W	9,540	-7,849	60	0.94	40	0.02	0.150	0.76
110 ^b	Publisher's Petroleum	1 Wilson	W	18-24N-22W	9,822	-7,734	26	0.89(a)	156	0.01	0.185	0.79
787	Western O&G Development	1-7 Craig	W	7- 6N- 3W	9,835	-8,618	139	0.64	50	0.01	0.057	0.79
561	ONEOK Resources	1-1 Hill	W	1- 9N- 6W	10,075	-8,749	103	0.73	40	0.01	0.089	0.81
389 ^c	Phillips Petroleum	1-9 Matti "A"	W	9-16N-10W	10,273	-8,979	98	0.88	72	0.02	0.212	0.83
756	Bogert Oil	1-2 Schreiner	W	2-17N-12W	10,278	-8,658	77	1.15	40	0.02	0.104	0.83
112 ^b	Southland Royalty	1-13, Walters	W	13-19N-15W	10,295	-8,578	51	1.05(a)	60	0.03	0.265	0.83
576	Conoco	1 Ferguson	W	34- 2N- 3W	10,917	-9,908	92	0.63	44	0.01	0.061	0.89
244	TXO Production	1 Heckes	W	8-12N- 8W	11,228	-9,816	180	1.14	40	0.02	0.120	0.93
124 ^b	Gulf Oil	1 Malinka Ring	C	12- 5N- 5W	11,521	-10,361	209	0.88(a)	75	0.01	0.070	0.96
128 ^b	OFT Exploration	1-20 Burgess	W	20-19N-17W	11,925	-10,004	57	1.02(a)	50	0.03	0.198	1.00
243	Arkla Exploration	1 Good	W	15- 6N- 5W	12,008	-10,789	172	0.83	40	0.01	0.081	1.01
569	Amoco Production	1 Dupire	W	4- 4N- 5W	12,386	-11,251	280	0.90	52	0.01	0.085	1.06
246 ^b	Davis Oil	1-28 Ward	W	28-14N-10W	12,416	-10,990	272	1.32	45	0.02	0.143	1.06
241 ^b	May Petroleum	1 Schafer	W	33- 9N- 7W	12,922	-11,694	76	1.16	65	0.02	0.148	1.13
111 ^b	Energy Services	1-26 Hanan	W	26-20N-23W	13,588	-11,088	29	1.42(a)	75	0.02	0.204	1.22
353	Southport Exploration	1-12 Howling Woman	W	12-13N-12W	13,864	-12,078	104	1.55	40	0.04	0.264	1.23
436	H G & G	1-11 Hussey-Reynolds	W	11- 2N- 5W	14,085	-12,909	375	1.07	40	0.03	0.160	1.29
388 ^c	GADSCO	1-6 Kruger	W	6-14N-15W	14,150	-12,371	68	1.26	45	0.02	0.162	1.30
118 ^b	GHK	1-1 Hoffman	C	1-14N-16W	14,186	-12,475	81	1.50(a)	75	0.02	0.147	1.30
116 ^b	Exxon	1 Sabine	W	1-17N-19W	14,257	-12,111	60	1.36(a)	75	0.03	0.249	1.31
570	Amoco Production	1 Woolever	W	18- 2N- 8W	14,404	-13,171	767	0.94	54	0.02	0.122	1.33
394	An-Son	1-25 Frieda	W	25-13N-13W	14,986	-13,375	160	1.89	40	0.04	0.284	1.43
121 ^b	Magnolia Petroleum et al.	1 Smith	W	12-11N-11W	15,105	-13,436	187	1.61(a)	64	0.03	0.222	1.45

OPL No(s)	Operator	Lease	W/C ^a	Location	Depth of Woodford Shale top (ft)	Subsea elevation (ft)	Thickness of Woodford Shale ^d (ft)	Mean vitrinite reflectance f in oil, (%) R_o	Number of measurements	Standard error of the mean	Standard deviation	Regression-predicted reflectance
TEXAS PANHANDLE												
117 ^b	Gulf Oil	1-16 State of OK	W	16-18N-25W	15,672	-13,349	28	1.51(a)	75	0.03	0.283	1.54
271	MCOR O&G	1-29 McKay	W	29-17N-21W	16,226	-14,111	51	2.48	42	0.04	0.264	1.65
803	Helmerich & Payne	3 Cupp "B"	W	21-10N-26W	16,335	-14,243	254	1.82	42	0.05	0.323	1.67
581	Woods Petroleum	2 Switzer	W	32-16N-21W	18,112	-16,115	75	2.59	69	0.04	0.335	2.05
387 ^c	GHK	1-27 Wilbur Hayes	W	27-12N-14W	18,370	-16,563	158	2.00	40	0.04	0.255	2.11
122 ^b	El Paso Exploration	1 Alpha Jones	W	17-9N-22W	20,308	-18,476	630	2.61(a)	225	0.03	0.405	2.64
269	Nortex O&G	1-19 Graham	W	19-3N-7W	21,722	-20,370	191	1.86	40	0.04	0.253	3.10
386 ^c	Forest Oil	1 Bob White Unit	W	16-8N-16W	21,790	-20,196	272	2.03	106	0.05	0.513	3.13
245 ^b	GHK	1-18 Dugger	W	18-13N-20W	22,526	-20,640	152	4.89	164	0.05	0.604	3.40
392	Leede O&G	1-3 Green	W	3-10N-25W	23,880	-21,806	222	4.05	70	0.06	0.539	3.98
239 ^b	GHK	1-2 Harrell	W	2-11N-20W	25,115	-23,255	195	4.29	80	0.04	0.353	4.59
418	GHK	1-1 Robinson	W	1-9N-22W	27,732	-25,744	560	3.88	80	0.08	0.703	6.20
TEXAS PANHANDLE												
694	Humble Oil	1 Miami Cattle	W	37-A 2-H&GN	12,965	-10,165	69	1.56	56	0.02	0.187	1.13
700	Phillips Petroleum	1 Hefley "A"	W	73-M 1-H&GN	14,800	-12,094	70	1.67	42	0.04	0.259	1.40
701	Phillips Petroleum	1 A Horn	W	81-A 5-H&GN	15,614	-12,898	160	1.27	45	0.02	0.134	1.53
705	McCulloch Oil and Statex Petroleum	5 Mathers Ranch	C	165-41 H&TC	16,966	-14,602	9	3.10	60	0.03	0.213	1.79
696	Gulf Oil	1 Puryear	W	22-M 1-H&GN	19,263	-16,743	73	3.30	40	0.05	0.302	2.34
695	Union Oil of CA	1A 90 Hefley	W	90-M 1-H&GN	19,325	-16,728	92	3.29	41	0.05	0.351	2.35
697	Phillips Petroleum	1 Bowers "C"	W	5-Brooks & Burleson	19,368	-16,847	80	3.40	40	0.05	0.307	2.36
704	Chevron Oil	1 Davidson	W	36-A 7-H&GN	20,460	-18,263	74	1.87	40	0.03	0.167	2.68
703	Arkla Exploration	1-31 Reed	W	31-A 3-H&GN	22,280	-19,886	98	3.03	60	0.03	0.202	3.31

^aWell cuttings (W) or core (C).^bData previously published in Cardott and Lambert (1985).^cData discussed in Jones (1984).^dQuestion mark indicates total thickness not penetrated.^eThickness adjusted for dip.^fAll reflectance values were determined as random reflectance measured with plane-polarized white light with the exception of those indicated by "(a)" which indicates average reflectance measured without polarized white light.

CHARACTERIZATION AND ORIGIN OF NATURAL GASES OF THE ANADARKO BASIN

DUDLEY D. RICE, CHARLES N. THRELKELD, AND APRIL K. VULETICH
U.S. Geological Survey, Denver

Abstract.—Natural-gas production in the Anadarko basin is from three geographically separated areas that can be differentiated by age of reservoir and by inferred nature of thermal origin of the gases. In the central basin, nonassociated gases are produced mainly from Upper Mississippian and Pennsylvanian sandstones. Gases become isotopically heavier ($\delta^{13}\text{C}_1$ values range from -49.8 to -33.2 ppt) and chemically drier ($\text{C}_1/\text{C}_{1-5}$ values range from 0.74 to 0.99) with increasing level of thermal maturity. Gas samples are from depths as much as $21,600$ ft. Gases were generated mainly from interbedded shales with type-III kerogen during the mature and postmature stages of hydrocarbon generation. Deviations from the trend are due to mixing and migration of gases generated at different levels of thermal maturity over the past 250 m.y.

In the giant Panhandle-Hugoton field, nonassociated gases are generally produced from Permian carbonates at depths $<3,000$ ft. Gases display little compositional variation ($\delta^{13}\text{C}_1$ values range from -46.4 to -39.9 ppt, $\text{C}_1/\text{C}_{1-5}$ values range from 0.69 to 0.96). Because organic-rich, mature source rocks are not present in the area, gases probably were generated in the central basin from Pennsylvanian or older source rocks during the mature stage of hydrocarbon generation. This implies migration over distances as much as several hundred miles.

In the Sooner trend, associated gases are produced from Silurian, Devonian, and Mississippian carbonates at depths as great as $9,600$ ft and were generated from type-II kerogen during the mature stage of hydrocarbon generation. Associated oil correlates with extracts of the Upper Devonian and Lower Mississippian Woodford Shale. Gases are isotopically lighter ($\delta^{13}\text{C}_1$ values of -47.3 to -40.6 ppt) and chemically wetter ($\text{C}_1/\text{C}_{1-5}$ values of 0.67 to 0.99) than those derived from type-III kerogen at an equivalent level of thermal maturity.

INTRODUCTION

The Anadarko basin, located in western Oklahoma, the northern Texas Panhandle, and southwestern Kansas (Fig. 1), is one of the major hydrocarbon-producing provinces in the United States. Ultimate recovery of natural gas in the basin is estimated to be >110 Tcf (Hill and Clark, 1980). The basin is filled with rocks mainly of Paleozoic age that are as much as $40,000$ ft thick. The basin has a large number of deep exploration wells, and gas production has been established to depths of $\sim 26,000$ ft. Detailed descriptions of the petroleum geology of the basin are given in Adler (1971), Hill and Clark (1980), Kennedy and others (1982), and Rascoe and Adler (1983).

The objectives of this report are to (1) characterize the chemical and isotopic composition of the gases, and (2) discuss their origins and occurrences in relation to source-rock type and thermal maturity.

GEOLOGIC SETTING AND NATURAL-GAS OCCURRENCE

The Anadarko basin is a sedimentary and structural basin bounded on the south by the

Amarillo-Wichita uplift, on the east by the Nemaha ridge, and on the west and north by shelf areas (Fig. 1). The basin is strongly asymmetric, the axis running close to and parallel to the Amarillo-Wichita uplift on the southern margin.

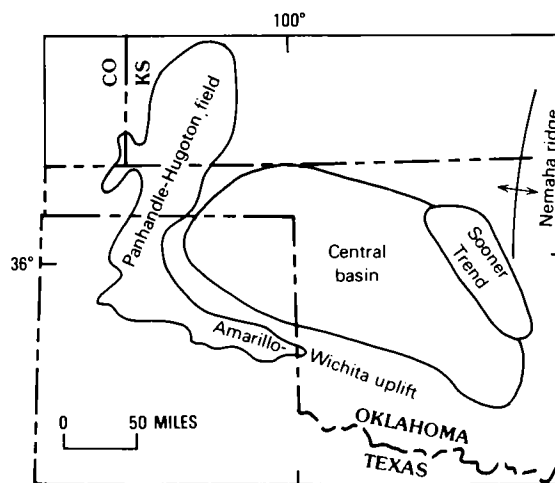


Figure 1. Index map of Anadarko basin showing structural elements and main hydrocarbon-producing areas.

Natural-gas production in the Anadarko basin is primarily from three geographically separated areas—the central basin, Panhandle–Hugoton field, and Sooner trend (Fig. 1). These areas can be differentiated by age of reservoir rock (Fig. 2),

System	Lithology	Producing interval	Hydrocarbon source rock
Permian		Permian (undifferentiated)	Upper and Middle Pennsylvanian
Pennsylvanian		Virgilian	
		Desmoinesian	
		Atokan	
Mississippian		Morrowan	Morrowan
		Springer Formation	Springer Formation
		pre-Chester Mississippian (undifferentiated)	Woodford Shale
Devonian		Hunton Group	Simpson Group
Silurian			
Ordovician		Simpson Group	
Upper Cambrian		Arbuckle Group	

EXPLANATION

	Sandstone		Evaporite
	Shale		Granite wash
	Carbonate		Hiatus

Figure 2. Chart showing Paleozoic producing intervals and hydrocarbon source rocks in the Anadarko basin.

type of trap, and composition and origin of the gases.

In the central basin, hydrocarbon production is mainly nonassociated gas and is established to depths as great as 26,000 ft. In general, gas resources decrease with increasing age of the reservoir. Sandstones of Late Mississippian and Pennsylvanian age are the major reservoirs, and the gas accumulations occur in stratigraphic traps. The Springer and Morrowan producing intervals, with an estimated ultimate recovery of ~14 Tcf (Hill and Clark, 1980), are second in reserves only to the Permian producing interval of the Panhandle–Hugoton field. Smaller reserves of gas are in lower and middle Paleozoic carbonates—such as those of the Arbuckle Group, Simpson Group, Hunton Group, and pre-Chester Mississippian producing intervals (Fig. 2)—and are associated with structural features (Hill and Clark, 1980).

The Panhandle–Hugoton field is the largest gas accumulation in the United States, with estimated recoverable reserves >80 Tcf (Hill and Clark, 1980). The gas occurs primarily in Permian carbonates at depths <3,000 ft. The field is an immense stratigraphic trap caused by the updip facies change from porous carbonates to tight red beds and is enhanced by a downdip hydrodynamic flow (Pippin, 1970).

In the Sooner trend, on the east flank of the basin, production has been established in reservoirs ranging in age from Cambrian to Pennsylvanian. The major part of the production, at depths intermediate between those of the central basin and Panhandle–Hugoton field, is associated gas and oil in fractured Mississippian limestones in a trend parallel to the Nemaha ridge (Fig. 1; Harris, 1975).

THERMAL MATURITY AND SOURCE ROCKS

Using data from different formations and from different locations, Schmoker (1986; this volume) showed a systematic increase in vitrinite reflectance (R_o) and TTI values with increasing depth of burial in the Anadarko basin. Cardott and Lambert (1985) found this same trend with samples from the Upper Devonian and Lower Mississippian Woodford Shale. Schmoker (1986) calculated that the oil-generation window in the central basin extends from depths of ~6,000 to 13,400 ft (R_o 0.6–1.3%). He further estimated that many of the potential source-rock units have been in the thermogenic oil- and gas-generation window almost continuously since late Paleozoic time.

Hatch and others (1986) identified shale intervals of the Middle Ordovician Simpson Group, Upper Devonian and Lower Mississippian Wood-

ford Shale, and Middle and Upper Pennsylvanian as the main oil source rocks in the basin (Fig. 2). Organic-carbon values for thick shales in the Upper Mississippian Springer and Lower Pennsylvanian Morrowan producing intervals range from 0.5 to 3.4%. However, the kerogen is type III, indicating that it is capable of generating mostly gas.

GAS GEOCHEMISTRY AND ORIGIN

Gas samples were collected and analyzed from 81 wells in the central basin, 35 wells in the Panhandle-Hugoton field, and 19 wells in the Sooner trend. The results are summarized in Table 1 and displayed in plots shown in Figures 3 and 4. In the central basin, the samples are arranged in four groups; mostly nonassociated gases from the Upper Mississippian and Pennsylvanian Springer and Morrowan, Atokan and Desmoinesian, and Virgilian producing intervals, and associated gases from the lower Paleozoic (including Upper Cambrian and Lower Ordovician Arbuckle

Group and Middle Ordovician Simpson Group). In the Panhandle-Hugoton field, nonassociated samples are from both the Pennsylvanian and Permian; most samples are from the Permian. In the Sooner trend, gas samples are from reservoirs ranging in age from Ordovician to Pennsylvanian; however, most are associated gases from the Silurian and Devonian Hunton Group and pre-Chester Mississippian carbonates.

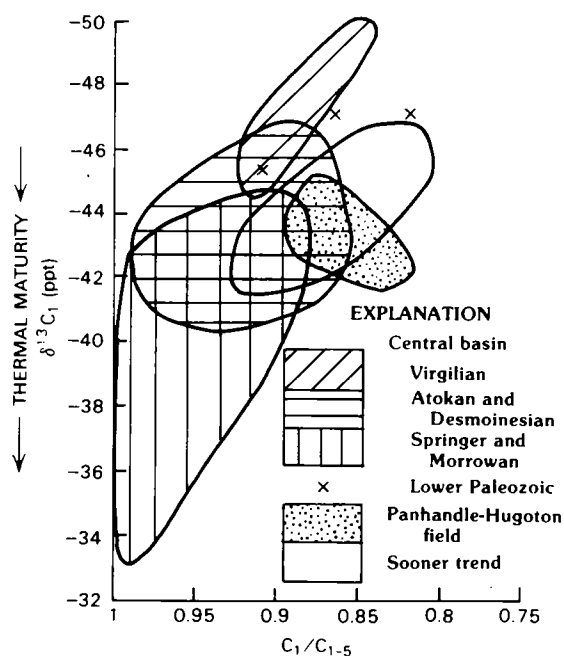


Figure 3. Methane carbon-isotope ratio vs. hydrocarbon composition of natural gases, Anadarko basin. Plot shows fields where samples from the following groups generally cluster: Springer and Morrowan, Atokan and Desmoinesian, and Virgilian producing intervals of the central basin, Panhandle-Hugoton field, and Sooner trend. In addition, three samples from the lower Paleozoic are plotted separately.

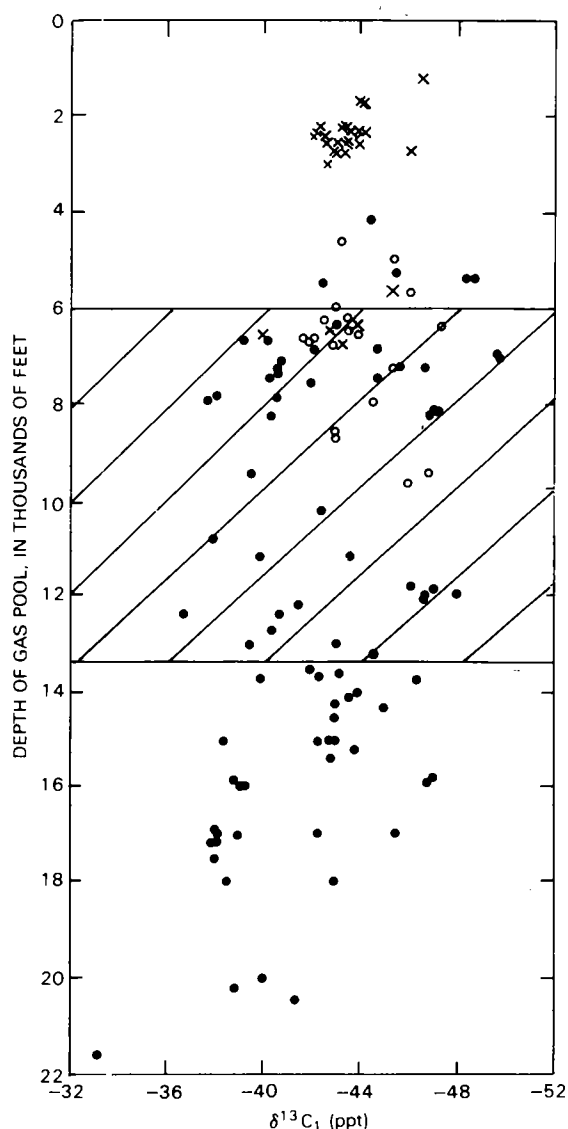


Figure 4. Methane carbon-isotope ratio vs. depth of gas pool, Anadarko basin. Dots represent gas samples from the central basin, Xs the Panhandle-Hugoton field, and circles the Sooner trend. Hatched zone is the oil-generation window according to Schmoker (1986).

TABLE 1.—SUMMARY OF DEPTH OF OCCURRENCE AND CHEMICAL AND ISOTOPIC COMPOSITION OF NATURAL GASES BY AREA IN THE ANADARKO BASIN

No. of wells analyzed	Depth of gas pool (ft)		$\delta^{13}\text{C}_1$ (ppt)		$\text{C}_1/\text{C}_{1-5}$	
	Range	Mean	Range	Mean	Range	Mean
<u>Central basin</u>						
Virgilian						
11	4,124– 8,235	6,534	–49.8 to –42.4	–46.6	0.74–0.91	0.88
Atokan and Desmoinesian						
23	7,212–16,970	12,555	–48.1 to –40.7	–43.9	0.82–0.98	0.93
Springer and Morrowan						
44	6,344–21,614	12,527	–49.2 to –33.2	–39.9	0.89–0.99	0.96
Lower Paleozoic						
3	15,883–16,995	16,273	–47.0 to –45.4	–46.4	0.82–0.91	0.86
<u>Panhandle-Hugoton field</u>						
Permian						
28	1,265– 3,054	2,401	–46.4 to –41.8	–43.3	0.69–0.94	0.85
Pennsylvanian						
7	2,589– 6,752	5,276	–45.2 to –39.9	–42.8	0.85–0.96	0.88
<u>Sooner trend</u>						
Ordovician to Pennsylvanian						
19	4,672– 9,678	6,909	–47.3 to –41.7	–43.9	0.67–0.99	0.87

The chemical and isotopic compositions of all the natural gases in the basin ($\delta^{13}\text{C}_1$ –49.8 to –33.2 ppt; $\text{C}_1/\text{C}_{1-5}$ 0.67 to 0.99) suggest that they are of thermal origin and are the result of thermal cracking processes (Schoell, 1983). They probably were generated during the mature and postmature stages of hydrocarbon generation (Fig. 5), and they become chemically drier and isotopically heavier with increasing level of thermal maturity (Fig. 3). A $\delta^{13}\text{C}_1$ value of about –40 ppt in gases usually corresponds to the bottom of the oil window (Rice, 1983; Schoell, 1983).

Figure 4 shows considerable scatter in the isotopic composition of the gases in the basin with increasing depth of the gas pool. In addition, the expected trend of the gases becoming isotopically heavier with increasing depth or level of thermal maturity is not present. Both of these factors are interpreted to be the result of differences in source-rock type, mixing, and migration. These factors will be elaborated on in the discussion on the three producing areas.

Central Basin

In the central basin, gases from the Upper Mississippian and Pennsylvanian producing intervals

become chemically drier and isotopically heavier with increasing age of the reservoir, as summarized in Table 1. The gases from the Virgilian (mean $\delta^{13}\text{C}_1$ –46.6 ppt; mean $\text{C}_1/\text{C}_{1-5}$ 0.88), and Atokan and Desmoinesian (mean $\delta^{13}\text{C}_1$ –43.9 ppt; mean $\text{C}_1/\text{C}_{1-5}$ 0.93) producing intervals were probably generated during the mature stage of hydrocarbon generation. The gases from the Springer and Morrowan producing intervals (mean $\delta^{13}\text{C}_1$ –39.9 ppt; mean $\text{C}_1/\text{C}_{1-5}$ 0.96) were probably generated during the mature and postmature stages (Fig. 5). This relation is expected, because progressively older producing intervals attained higher levels of thermal maturity. In addition, shales in the Springer and Morrowan producing intervals generally have type-III kerogen, whereas those in the Atokan, Desmoinesian, and Virgilian producing intervals have a mixture of type-II and type-III kerogens.

These Upper Mississippian and Pennsylvanian gases are mainly nonassociated for the following reasons:

1) Source rocks for major Upper Mississippian and Pennsylvanian sandstone reservoirs were generally interbedded shales which contain mainly type-III kerogen that is capable of generating mostly gas.

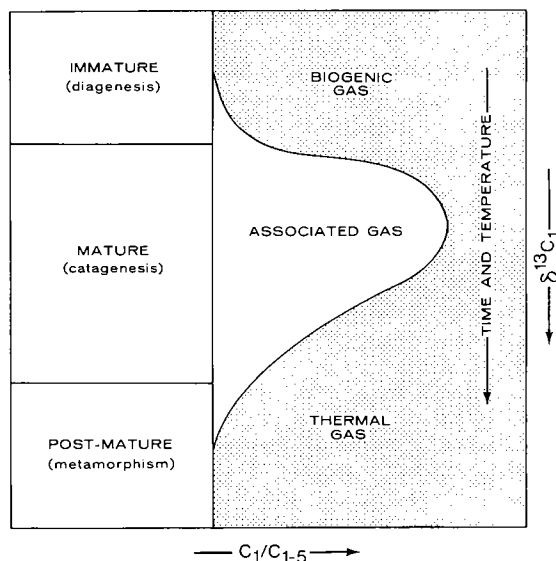


Figure 5. Diagram showing characteristics of natural gas with increasing temperature and time.

2) Hydrocarbons in the Springer and Morrowan producing intervals were mostly generated during the late mature and postmature stages of hydrocarbon generation. Gas is the primary product at these levels, because heavier hydrocarbons, including oil, were destroyed by thermal cracking.

3) Occasionally, the gas cap may have migrated from or been separated from an oil accumulation. This may be true for some of the Atokan, Desmoinesian, and Virgilian accumulations that might have been generated from some type-II kerogen in interbedded shales.

The chemical and isotopic composition of the gas samples from lower Paleozoic reservoir rocks (mean $\delta^{13}\text{C}_1$ -46.4 ppt; mean $\text{C}_1/\text{C}_{1-5}$ 0.86) is similar to that of the Virgilian producing interval (Fig. 3; Table 1). However, gas samples from the lower Paleozoic are associated with oil, occur at greater depths (Table 1), and were probably generated from lower Paleozoic shales with type-II kerogen, such as the Simpson Group (Fig. 2).

As shown in Figure 4, there is a lot of scatter in the isotopic composition of the gas samples in the central basin with increasing depth. A plot of chemical composition vs. depth shows similar scatter. This scatter is attributed to two factors: different types of source rocks, and mixing and migration. First, Rice (1983) showed that gases generated from type-III kerogen are chemically drier and isotopically heavier than those generated from type-II kerogen at equivalent levels of thermal maturity. Although shales with gas-prone type-III kerogen were responsible for generating most of the hydrocarbons, some source rocks with type-II kerogen made contributions because of

the presence of oil accumulations. Second, potential source rocks in the central basin have been in the thermogenic oil- and gas-generation window since late Paleozoic time, and significant quantities of hydrocarbons have been generated since that time. Because natural gas is very mobile and the shale seals are not totally effective, there probably has been considerable mixing and migration, resulting in the scatter illustrated in Figure 4.

Panhandle-Hugoton Field

In the giant Panhandle-Hugoton field, nonassociated gases from both the Pennsylvanian and Permian show little chemical and isotopic variation (mean $\delta^{13}\text{C}_1$ -43.2 ppt; mean $\text{C}_1/\text{C}_{1-5}$ value is 0.86; Fig. 3). Their isotopic composition is comparable to that of the Atokan and Desmoinesian producing intervals in the central basin (Fig. 3); they are interpreted to be thermogenic, and were probably generated during the mature stage of hydrocarbon generation. Except for minor accumulations in the deeper Pennsylvanian reservoirs, the major part of the gas resources occur in Permian reservoirs at depths <3,000 ft (Fig. 4; Table 1), which is above the oil-generation window. Because large volumes of organic-rich, thermally mature source rocks are not present in the area of the Panhandle-Hugoton field, the gases probably were generated from Pennsylvanian and/or older source rocks in the central basin, having migrated as much as several hundred miles. Similar distances have been suggested for oil accumulations in Kansas (Burruss and Hatch, 1987). However, long-range lateral migration is not common for gas accumulations; it probably was made possible in the Panhandle-Hugoton field by good conduits and the regional development of an anhydrite seal.

Based only on the chemical and isotopic composition, it is difficult to determine if the gases were generated from type-II or type-III kerogen. Both types are present in various parts of the Paleozoic section and are thermally mature in the central basin. However, multiple Pennsylvanian and possibly older source rock intervals throughout the basin probably were needed to obtain the quantities of kerogen required to generate the large quantities of gas that have migrated to and were entrapped in the Panhandle-Hugoton field, or lost to the atmosphere in the process.

In addition to the hydrocarbon gases, significant quantities of nitrogen (as much as 40%) and helium (as much as 2%) also occur in the Panhandle-Hugoton field (Moore, 1976). The helium varies in approximate proportion to the nitrogen; higher concentrations of both are reported along faults (Pierce and others, 1964). Pierce and others (1964) postulated a radiogenic origin for the helium because of its close association with

uranium and thorium. Helium-isotope ratios suggest a localized mantle origin for some (P. D. Jenden, personal communication, 1987). The nitrogen probably has either degassed from igneous and metamorphic basement rocks and/or had a mantle origin similar to the helium. In contrast, the hydrocarbon gases had an organic origin and were generated from converted organic matter (kerogen) by thermal degradation and cracking processes. These gases of both organic and inorganic origin occur together in significant quantities because of the excellent, widespread anhydrite seal.

Sooner Trend

In the Sooner trend, dominantly associated gases are produced from Silurian, Devonian, and Mississippian carbonates at depths as great as 9,600 ft. Their isotopic and chemical compositions (mean $\delta^{13}\text{C}_1$ 43.9 ppt; mean $\text{C}_1/\text{C}_{1-5}$ 0.87) suggest that they were probably generated from type-II kerogen during the mature stage of hydrocarbon generation. The organic-rich Woodford Shale occurs in the middle of this productive section and is the likely source. This assumption is confirmed by the fact that many of the oils in the area have been geochemically correlated with the Woodford Shale (J. R. Hatch, personal communication, 1987). The oil and associated gas often occur in the marginally mature part of the section (Fig. 4), which suggests migration from the deeper part of the central basin.

SUMMARY AND CONCLUSIONS

1. The greater Anadarko basin contains major quantities of natural gas that are produced at depths as great as 26,000 ft. The gas samples analyzed for this study become chemically drier ($\text{C}_1/\text{C}_{1-5}$ 0.67 to 0.99) and isotopically heavier ($\delta^{13}\text{C}_1$ -49.8 to -33.2 ppt) with increasing level of thermal maturity; they occur in pools as deep as 21,600 ft. The gases are interpreted to be of thermal origin, and were generated during the mature and postmature stages of hydrocarbon generation.

2. The chemical and isotopic compositions of the gases show considerable scatter with increasing depth of the gas pool. This scatter is attributed to differences in source-rock type and to mixing and migration. Many of the thermogenic gases are in reservoirs above the oil-generation window.

3. Natural-gas production is from three geographically separated areas that can be distinguished by age of reservoir, type of trap, and origin of the gas. In the central basin, mainly non-associated gas is produced from Upper Mississippian and Pennsylvanian sandstones in stratigraphic traps. The gases were generated from interbedded shales with mainly type-III kerogen during the mature and postmature stages of hydrocarbon generation. Scatter in the chemical and isotopic composition of the gases with depth resulted from mixing and migration of the gases that have been generated since late Paleozoic time. In the giant Panhandle-Hugoton field, shallow nonassociated gas produced from Permian carbonates was probably generated during the mature stage of hydrocarbon generation. The gases probably migrated long distances from the central basin, where they were generated from organic-rich, thermally mature source rocks. Associated helium and hydrogen gases have inorganic origins unrelated to the hydrocarbon gases, which were derived from kerogen by thermal cracking processes. In the Sooner trend, the associated gases, produced from fractured Mississippian carbonates below the pre-Pennsylvanian unconformity, were probably generated from type-II kerogen in the Woodford Shale during the mature stage of hydrocarbon generation. Some migration of both oil and gas from deeper in the central basin has probably taken place.

ACKNOWLEDGMENTS

Some of the gas samples in the central basin were analyzed by Global Geochemistry Corp. under Gas Research Institute contract no. 5081-361-0533.

GEOCHEMISTRY OF OILS AND HYDROCARBON SOURCE ROCKS, GREATER ANADARKO BASIN: EVIDENCE FOR MULTIPLE SOURCES OF OILS AND LONG-DISTANCE OIL MIGRATION

R. C. BURRUSS AND J. R. HATCH
U.S. Geological Survey, Denver

Abstract.—Organic geochemical analyses of 104 crude oils and 190 core samples of dark-colored shales from the greater Anadarko basin show three major oil types which generally correlate with reservoir age and source-rock age. Analyses include C_3 – C_{30} whole-oil gas chromatography, C_{10+} saturated-hydrocarbon-fraction gas chromatography, and carbon stable isotopes (ppt relative to PDB) of saturated (sat) and aromatic (arom) hydrocarbon fractions. Three samples from Middle Ordovician Simpson Group reservoirs are “typical” Ordovician oils (type 1), having strong odd-carbon predominance in the C_{13} to C_{19} n-alkanes, containing little or no acyclic isoprenoids, and $\delta^{13}C$ values of –33.9 ppt (sat) and –33.7 ppt (arom). Oils from Silurian to Devonian and Mississippian reservoirs (type 2) show little or no odd-carbon predominance in the n-alkanes, a regular decrease in abundance of n-alkanes with increasing carbon number, pristane/phytane ratios (pr/ph) of 1.1 to 1.5, and $\delta^{13}C$ values of –30.6 ppt (sat) and –30.1 ppt (arom). Oils in Pennsylvanian reservoirs (type 3) have the greatest amounts of C_{15+} hydrocarbons, are isotopically heavy (–27.5 ppt [sat] and –26.4 ppt [arom]), have methyl-cyclohexane as the most abundant hydrocarbon, and have pr/ph values from 2.0 to 0.9.

Oils from the Kansas shelf area of the Anadarko basin are similar to the Anadarko oil types except that they have only traces of toluene and no detectable benzene. The relative abundance of toluene in the C_7 hydrocarbons systematically decreases with distance from the depocenter of the basin. The aromatic compounds are removed by water-washing, and hence could have been lost by contact with progressively greater amounts of formation water during long-distance migration. The lack of thermally mature source rocks in southern and central Kansas supports this hypothesis.

INTRODUCTION

Various aspects of the petroleum geochemistry of the Anadarko basin have been studied over the last 25 years. The Anadarko basin and adjacent shelf areas are a major petroleum-producing province in the Midcontinent of the U.S.A., so that petroleum geochemical studies are not needed to test the resource potential of the basin. However, such studies serve to test the extent and volume of thermally mature source rocks, to establish source-rock/oil correlations, and to examine the timing of generation and the extent of oil and gas migration. This study describes the source-rock potential and geochemical characteristics of a regionally distributed suite of oils from rocks of Cambrian through Permian age. The oil/source-rock correlations and oil compositions are then used to examine the timing and distance of oil migration. A preliminary discussion of this work was presented by Burruss and Hatch (1987).

In this discussion the greater Anadarko basin is considered to comprise the sediments confined by the Amarillo–Wichita uplift on the south, the Sierra Grande uplift–Las Animas arch on the west, the central Kansas uplift–Cambridge arch on the north, and the Nemaha ridge on the east, as dis-

cussed by Davis and Northcutt (this volume). Geologic evidence for timing of oil generation, number of generations of oil, and migration distance is presented by Walters (1958) and Webb (1976). This paper summarizes our geochemical evidence for the number of distinct sources of oil and the extent of migration throughout this broad region of the Midcontinent.

SAMPLES AND ANALYTICAL METHODS

At this writing, we have analyzed 104 oil samples and 190 core samples. The stratigraphic distribution of the samples is shown in Figure 1. Oil samples were obtained from reservoirs ranging in age from Cambrian to Early Permian, and source-rock samples range in age from Middle Ordovician to Late Pennsylvanian. The geographic distribution of oil and rock samples is shown in Figure 2.

The rock samples were characterized for source-rock potential and quality, based on total organic-carbon content, by LECO combustion and by pyrolysis assay with a ROCK-EVAL II instrument, using the methods of Espitalié and

























SYSTEM	SERIES	GROUP	COMMON RESERVOIR NAMES	SAMPLES	
				OIL	SOURCE ROCK
PERMIAN	OCHOAN		OUTCROPPING RED BEDS, W. OKLAHOMA		
	GUADALUPEAN	WHITEHORSE EL RENO			
	LEONARDIAN				
	WOLFCAMPIAN	CHASE COUNCIL GROVE ADMIRE	HUGOTON GAS FIELD		
PENNSYLVANIAN	VIRGILIAN	WAUBAUNSEE TO DOUGLAS			
	MISSOURIAN	LANSING	PERRY SAND		
		KANSAS CITY	COTTAGE GROVE SAND HOGSHOOTER LIMESTONE		
		PLEASANTON			
	DESMOINESIAN	MARMATON	PERU SAND OSWEGO LIMESTONE		
		CHEROKEE	PRUE, REDFORK, BURBANK, BARTLESVILLE, AND BURGESS SANDS		
	ATOKAN	U. DORNICK HILLS	GILCREASE SAND		
	MORROWAN	L. DORNICK HILLS	WAPANUCKA LIMESTONE, PRIMROSE SAND		
	SPRINGERAN		SPRINGER SAND		
MISSISSIPPIAN + DEVONIAN + SILURIAN	CHESTERIAN MERAMECIAN		GODDARD SHALE, CANEY SHALE, SYCAMORE LIMESTONE		
	OSAGEAN KINDERHOOKIAN		BOONE CHERT, MISSISSIPPI CHAT, WOODFORD SHALE, MISENER SAND		
	ORISKANIAN to ALBION	HUNTON			
ORDOVICIAN	CINCINNATIAN TRENTONIAN		SYLVAN SHALE VIOLA LIMESTONE		
	BLACK RIVERIAN CHAZYIAN	SIMPSON	BROMIDE / WILCOX SAND MCLISH SAND OIL CREEK SAND		
	CANADIAN	ARBUCKLE	SILICEOUS LIME		
CAMBRIAN	CROIXIAN	TIMBERED HILLS	REAGAN SAND		
PRECAMBRIAN CRYSTALLINE ROCKS					

Figure 1. Generalized stratigraphic column of Paleozoic rocks in the Anadarko basin, showing common reservoir names and the units from which oil or source-rock samples were obtained. Modified from Landes (1970).

others (1977). Based on the pyrolysis results, samples were selected for Soxhlet extraction with chloroform for 24 hr. Sulfur was removed by refluxing with polished copper metal. The filtered extract was concentrated at room temperature under nitrogen to remove chloroform, then diluted with n-heptane to precipitate asphaltenes. A concentrate of the solution was separated by column chromatography on silica gel, eluting successively with heptane, benzene, and benzene-methanol to collect the saturated-hydrocarbon, aromatic-hydrocarbon, and resin fractions, respectively.

The saturated-hydrocarbon fraction of the rock extract was analyzed by capillary-column gas chromatography. One microliter was injected in a Hewlett-Packard 5880 instrument with an SE54

bonded-phase column, 50 m \times 0.35 mm I.D., temperature programmed from 50 to 320°C at 4°C/min, with a flame-ionization detector (350°C), and injection port at 245°C. Identification of peaks on the resultant chromatograms was based on relative retention times.

All oils were analyzed by whole-oil, capillary-column gas chromatography, using a Hewlett-Packard 5890A instrument with a nonpolar bonded-phase column (HP Ultra 1) 30 m \times 0.20 mm I.D. Analytical conditions were as follows: temperature program from -20 to 300°C at 10°C/min, held at 300°C for 18 min; flame ionization detector (350°C); injection port temperature 300°C; and 0.1 μ L of sample injected and split 150:1. Chromatograms were integrated with a Hewlett-Packard 3392A integrator, and peak

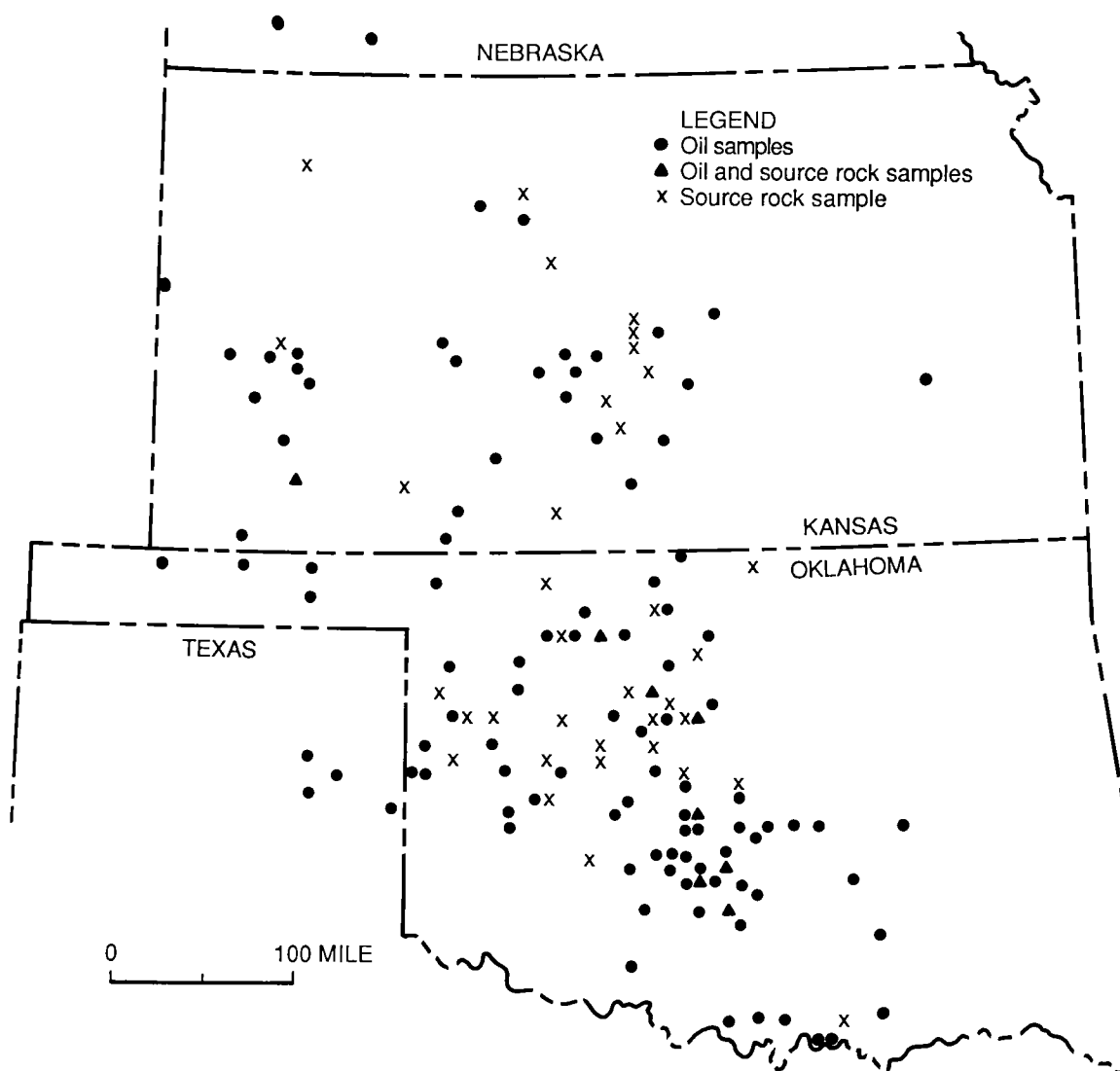


Figure 2. Map of the Anadarko basin, showing the locations of oil and rock samples.

heights and retention times were stored on an HP9816S desktop computer for further processing. Whole-oil chromatograms are subsequently displayed as plots of integrated peak height versus retention time.

Selected oil samples were fractionated into saturated-hydrocarbon, aromatic-hydrocarbon, resin, and asphaltene fractions with a Baker-10 Extraction System (J. T. Baker Chemical Co.), using SPE 3-mL 20- μ filtration, 6-mil silica gel, and 6-mil cyano (CN) columns. Cyclohexane, cyclohexane/benzene (3/1), and chloroform were the elution solvents, using a procedure described in the Baker-10 Extraction System instructions, with modifications described in Anders and others (1987). The saturated-hydrocarbon fraction was further analyzed by capillary-column gas chromatography, using analytical conditions described above for rock extracts.

The carbon stable-isotope ratios of saturated- and aromatic-hydrocarbon fractions of oils and rock extracts were measured with a Finnigan MAT 251 isotope-ratio mass spectrometer, after conversion to carbon dioxide in a high-vacuum combustion, gas-transfer apparatus. Isotopic compositions of carbon dioxide from the samples were directly compared with working reference standards of carbon dioxide, prepared from NBS 19 limestone ($\delta^{13}\text{C} = 1.96$ ppt PDB). All ratios are reported in standard per mil deviation relative to the Pee Dee belemnite standard (PDB):

$$\delta^{13}\text{C ppt} = [(R_{\text{sample}}/R_{\text{standard}}) - 1] \times 10^3,$$

where R is the ratio of ^{13}C to ^{12}C . NBS 21 (graphite) and NBS 22 (whole lube oil) were also analyzed as reference samples.

SOURCE ROCKS

The source-rock potential of 190 core samples of dark-colored shales from Ordovician to Late Pennsylvanian age is shown in Figure 3. Total-organic-carbon (TOC) abundances are shown in Figure 3A as histograms for samples from Pennsylvanian and Mississippian rocks, upper Devonian-Lower Mississippian Woodford Shale, and Ordovician shales. The Woodford Shale and many Pennsylvanian shales are consistently rich in TOC ($>2\%$). Ordovician rocks are generally low in TOC ($<1\%$), although several samples from the shelf in Kansas have TOC values between 1 and 9%. The potential of these rocks for generating hydrocarbons is illustrated in Figure 3B and 3C. Means and ranges of the genetic potential for different stratigraphic intervals (ROCK-EVAL pyrolysis) are shown in Figure 3B. This measurement (total volatile and pyrolyzable hydrocarbons, $S_1 + S_2$) indicates the ability of a rock to generate hydrocarbons. The classification criteria are those of Tissot and Welte (1978, p.

447). The differences among the rock units are similar to those seen in the TOC values. The van Krevelen-type diagram in Figure 3C indicates the type of organic matter present in the rocks. The small number of samples with high hydrogen index values that plot near the curve for type I (algal organic matter) are from Middle Ordovician Simpson Group shales from the Kansas shelf. Woodford Shale and some Pennsylvanian shales plot near the curve for type II (marine organic matter). Most of the low-TOC Ordovician and Pennsylvanian samples plot near the curve for type III (oxygen-rich organic matter).

Using these criteria, the Upper Devonian and Lower Mississippian Woodford Shale and Middle Pennsylvanian marine shales show the best potential to generate hydrocarbons. The Woodford does show some decrease in source-rock potential to the northwest, where it is thinnest stratigraphically and appears to show a facies change consistent with the electric-log observations of Hester and Schmoker (1988, personal communication). The source-rock potentials of most of the samples of Upper Ordovician Sylvan Shale and shaly beds in the Simpson Group are only poor to moderate. This is in part due to the higher levels of thermal maturity of these deeply buried and stratigraphically older units. The source-rock potential of Simpson shale from the shelf area in central Kansas, based on a small number of samples, is good.

Analyses of the solvent extracts of source rocks from localities with similar levels of thermal maturity clearly distinguish three compositions of hydrocarbon products generated by these rocks. Saturated-hydrocarbon distributions from extracts of Simpson Group shales (Fig. 4A) are characterized by strong odd predominance of $n\text{-C}_{16}$ to $n\text{-C}_{18}$ alkanes, with very low abundance of n -alkanes above $n\text{-C}_{18}$ and very low abundance of acyclic isoprenoids. Both saturated- and aromatic-hydrocarbon fractions have values in the range -32 to -29 ppt, although two samples have values of about -27 ppt (Fig. 5A). The origin of this wide range of carbon-isotope values is discussed by Hatch and others (1987).

The extracts of Woodford Shale samples show characteristics common to rocks rich in marine organic matter. The saturated-hydrocarbon distribution (Fig. 4B) shows a regularly decreasing abundance of n -alkanes with increasing carbon number, and little or no odd-carbon predominance. Branched and cyclic isomers have relatively low abundance, with $n\text{-C}_{17}$ /pristane and pristane/phytane ratios of about 5 and 1.5, respectively. The carbon-isotope composition of the saturated- and aromatic-hydrocarbon fractions (Fig. 5A) ranges from -30 to -29 ppt.

Saturated-hydrocarbon distributions of extracts from Pennsylvanian organic-carbon-rich rocks are commonly enriched in higher-molecular-weight n -alkanes compared to the older strati-

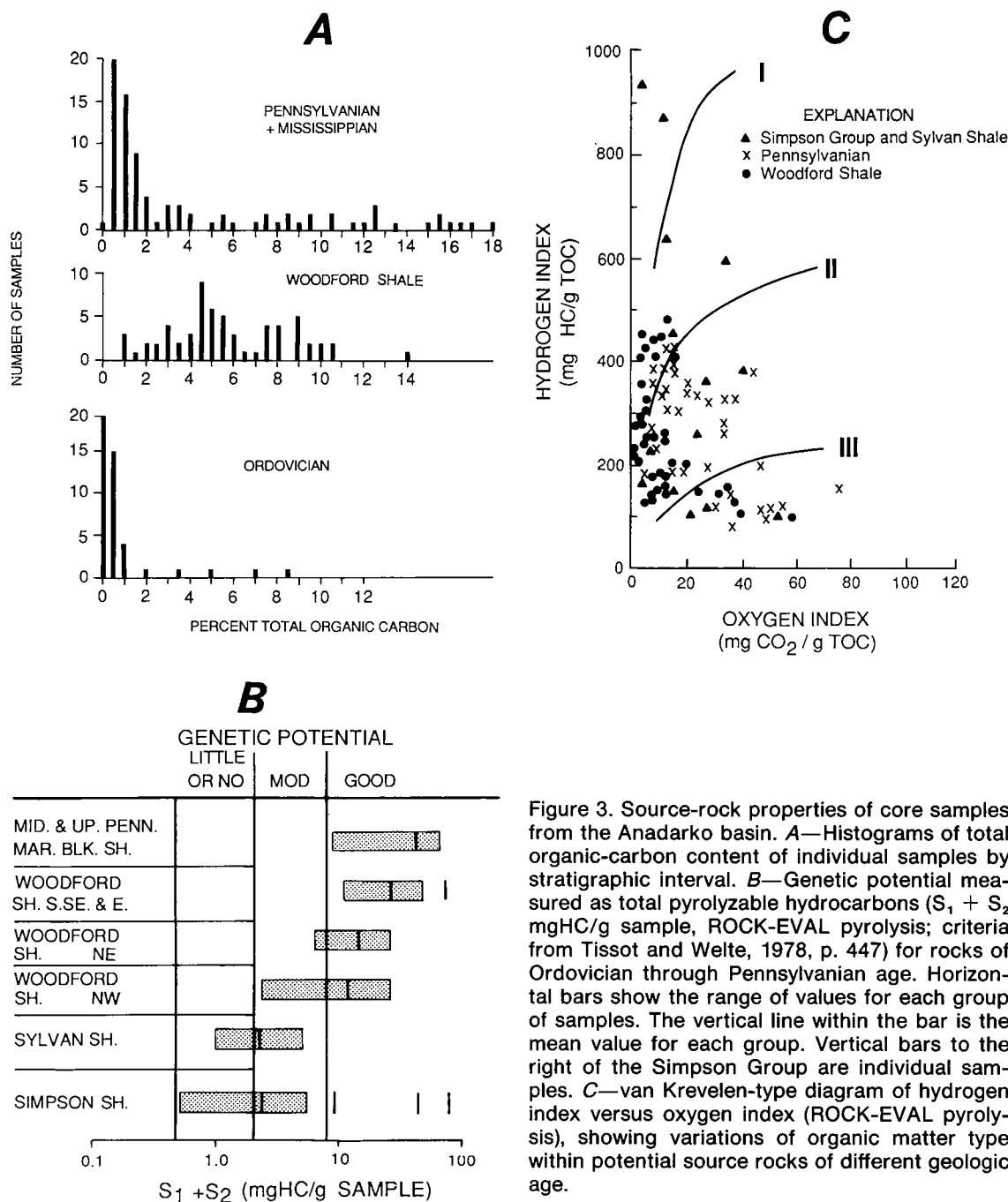


Figure 3. Source-rock properties of core samples from the Anadarko basin. **A**—Histograms of total organic-carbon content of individual samples by stratigraphic interval. **B**—Genetic potential measured as total pyrolyzable hydrocarbons ($S_1 + S_2$ mgHC/g sample, ROCK-EVAL pyrolysis; criteria from Tissot and Welte, 1978, p. 447) for rocks of Ordovician through Pennsylvanian age. Horizontal bars show the range of values for each group of samples. The vertical line within the bar is the mean value for each group. Vertical bars to the right of the Simpson Group are individual samples. **C**—van Krevelen-type diagram of hydrogen index versus oxygen index (ROCK-EVAL pyrolysis), showing variations of organic matter type within potential source rocks of different geologic age.

graphic units (Fig. 4C). The higher-molecular-weight n-alkanes show a slight odd-carbon predominance, and in some samples this distribution of n-alkanes is similar to that of extracts of waxy terrestrial organic matter. Branched and cyclic isomers and acyclic isoprenoids tend to be abun-

dant, with n-C₁₇/pristane and pristane/phytane ratios ranging from 2.0 to 0.7 and from 2.0 to 1.0, respectively. The carbon-isotope composition of these extracts is relatively enriched in ¹³C, values for saturated- and aromatic-hydrocarbon fractions ranging from -29 to -25 ppt (Fig. 5A).

OILS

Gas chromatography of whole-oil samples revealed significant differences in composition of the oils, especially within the gasoline-range (C_4 – C_7) hydrocarbons and in the general distribution of n -alkanes from C_4 – C_{30} . As pointed out by Burruss and Hatch (1987), these differences in com-

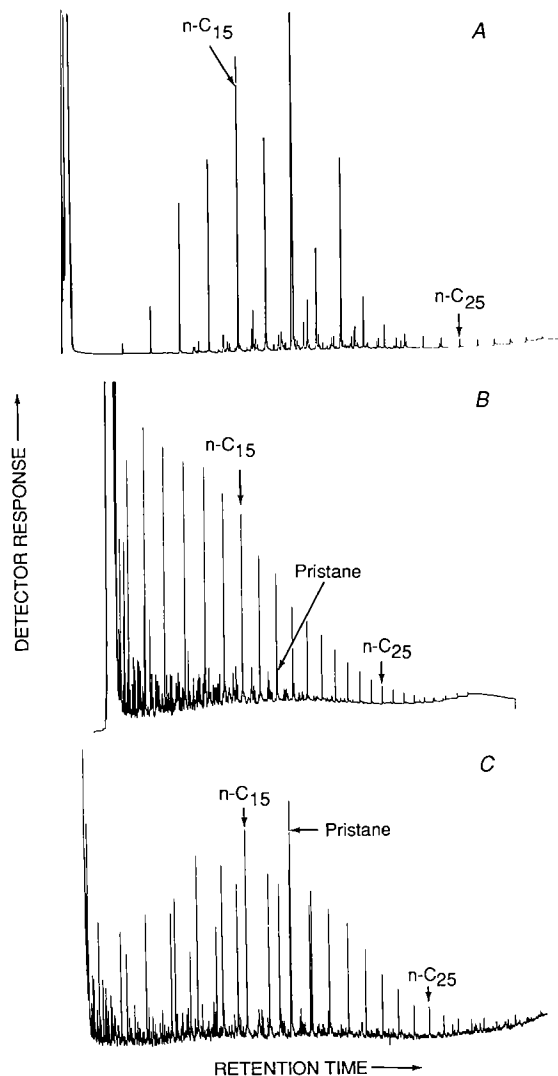


Figure 4. Representative gas chromatograms of saturated-hydrocarbon fractions of solvent extracts of core samples of potential source rocks in the Anadarko basin. A—Extract of Simpson Group shale, Reno County, Kansas. B—Extract of Woodford Shale, Kingfisher County, Oklahoma. C—Extract of a Middle Pennsylvanian shale at the base of the "Big lime," Kingfisher County, Oklahoma.

position occur between oils produced from reservoirs of distinctly different geologic age. Oils produced from reservoirs of a given geologic age (or stratigraphic interval) are compositionally similar.

The most obvious differences in oil compositions are shown in Figures 5B and 6. Oils from Ordovician reservoirs have the characteristics of Ordovician oils throughout the Midcontinent area. These characteristics are a strong odd-carbon predominance from n - C_{13} to n - C_{19} , low abundance of branched and cyclic isomers, and very low abundance to complete absence of pristane and phytane, as shown in Figure 6, type 1. The C_{15+} saturated- and aromatic-hydrocarbon fractions are generally depleted in ^{13}C , with isotopic compositions ranging from -34 to -30 ppt, and one sample as heavy as -28.5 ppt (Fig. 5B). Silurian and Devonian (Hunton Group) and Mississippian reservoirs produce oils characterized by the whole-oil chromatogram in Figure 6, type 2. The n -alkanes show a regularly decreasing abundance with increasing carbon number with no odd-carbon predominance, relatively low abundance of branched and cyclic isomers, pristane/phytane ratio in the range 1.6 to 1.2, and carbon-isotope compositions of saturated- and aromatic-hydrocarbon fractions ranging from -31 to -29 ppt (Fig. 5B). Pennsylvanian reservoirs produce oils of somewhat variable composition. The whole-oil chromatogram in Figure 6, type 3, is a typical example. These oils have an n -alkane distribution that has a relatively high abundance of C_{16+} hydrocarbons, a high abundance of branched and cyclic isomers, pristane/ n - $C_{17} \sim 0.7$, and pristane/phytane ranging from 0.9 to 2.0. The carbon-isotope compositions of the saturated- and aromatic-hydrocarbon fractions range from -30 to -25 ppt (Fig. 5B).

Detailed analysis of the C_7 region of the whole-oil chromatograms reveals significant differences among the oils based on the relative abundance of the isomers of C_7 alkanes and aromatic hydrocarbons. Figure 7 is a ternary plot of n -heptane, methyl-cyclohexane, and the sum of 2-methylhexane and 3-methylhexane. The fields labeled 1,2,3 (Ordovician, Silurian and Devonian plus Mississippian, and Pennsylvanian samples, respectively) contain oils with compositions that fit the "end-member" characteristics discussed above. Almost all oils fall within the region bounded by these end-member compositions, suggesting that many oils are mixtures of the three oil types.

Comparison of the carbon-isotope composition with the C_7 hydrocarbon distribution shows additional evidence of mixing among the oil types. Figure 8 is a crossplot of the abundance of n -heptane versus carbon-isotope composition of the aromatic fraction. Points labeled 1,2,3 are the three end-member oils shown in Figure 6, and the points labeled A,B,C are the oils shown in whole-

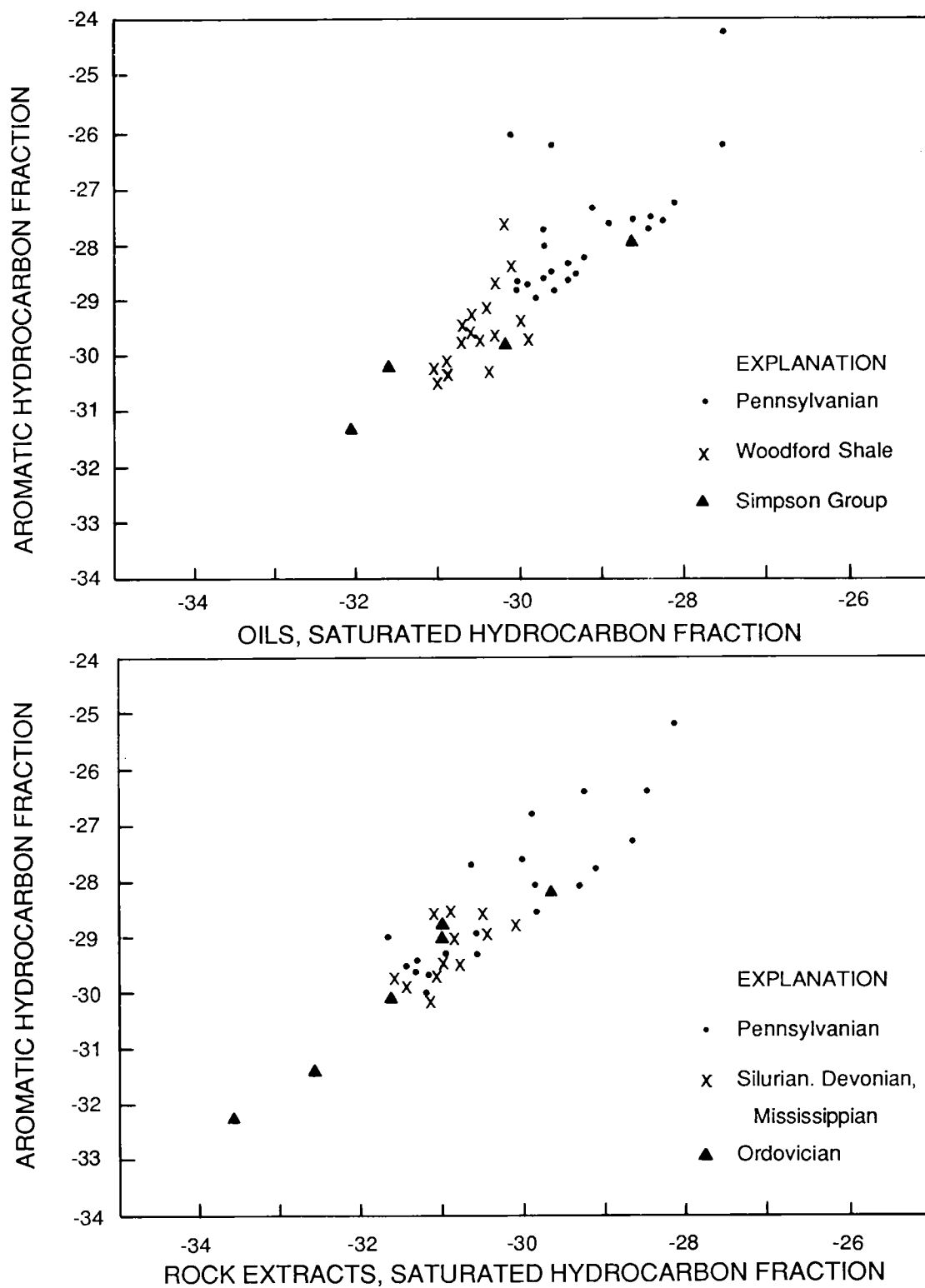


Figure 5. Carbon stable-isotope compositions of saturated- and aromatic-hydrocarbon fractions of rock extracts and crude oils from the Anadarko basin, grouped by geologic age of source-rock sample or reservoir rock.

oil chromatograms in Figure 9. Oils A and B have the characteristics of mixtures of Ordovician oil with Silurian and Devonian oil and Pennsylvanian oil, respectively. Oil C has the characteristics of an oil that is a mixture of all three oil types.

If the aromatic C_7 hydrocarbon, toluene, is included in the analysis of oil types, an unusual feature is observed. The ternary plot in Figure 10 shows that although oil types 1 and 2 are distin-

guished from type 3, many oils that appear to be mixtures are also depleted in toluene, even to the extent that little or no toluene can be detected. This is a feature common in water-washed crude oils (Illich and others, 1981; Bockmeulen and others, 1983; Welte and others, 1982). Where water-washing is due to meteoric-water recharge of aquifers, it is typically accompanied by evidence of biodegradation (Bockmeulen and others, 1983; Welte and others, 1982). Of the 104 oils an-

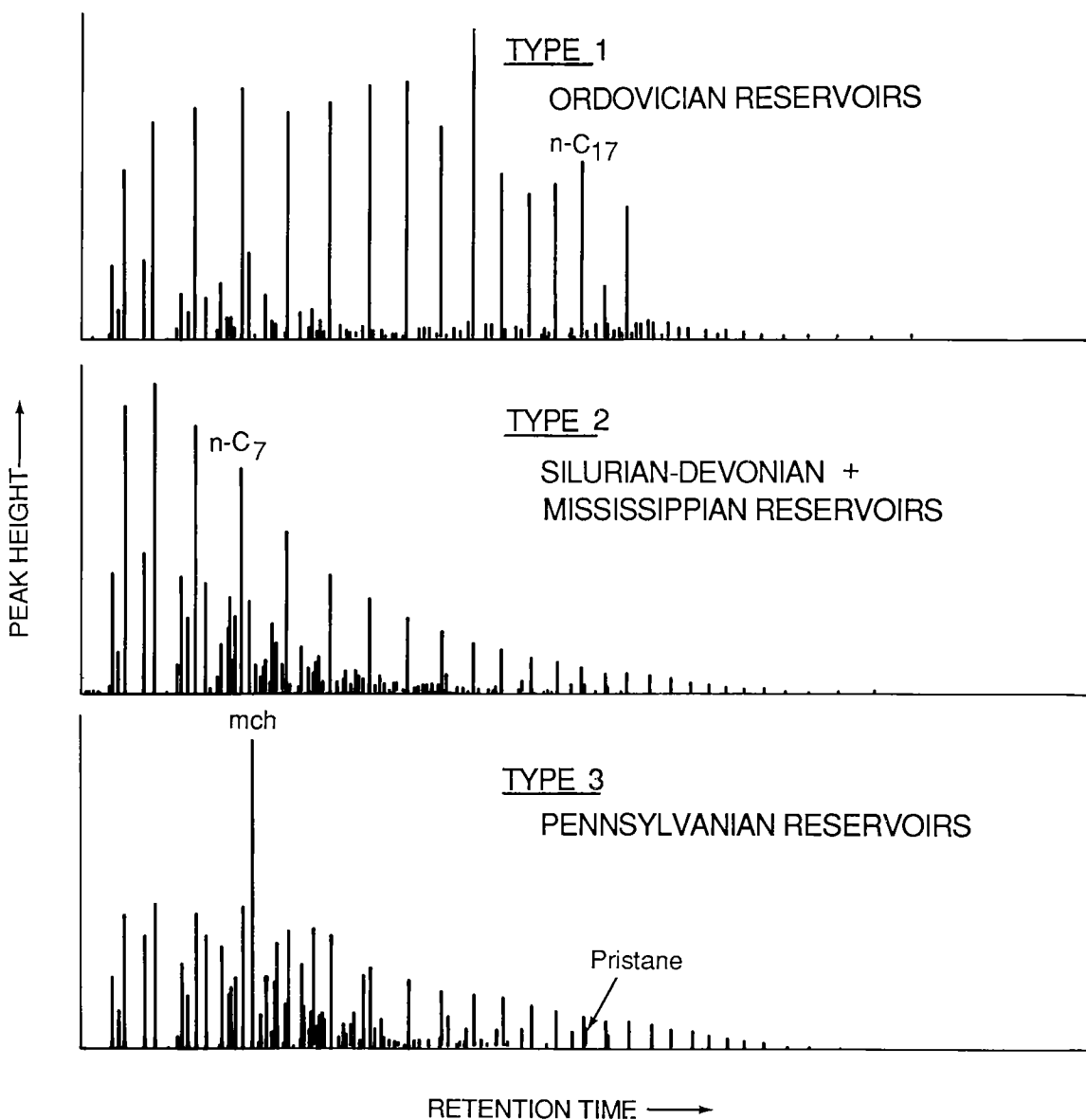


Figure 6. Whole-oil gas chromatograms of representative oil samples from Anadarko basin reservoirs in different stratigraphic intervals, illustrating major differences in hydrocarbon compound distributions.

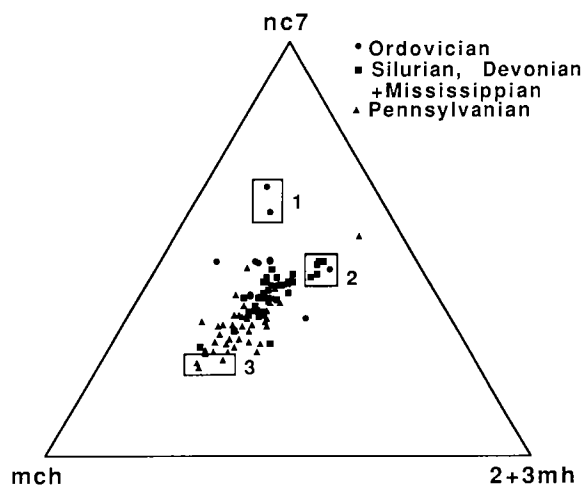


Figure 7. Ternary plot of C_7 gasoline-range hydrocarbon distributions in all Anadarko basin oil samples. Boxes enclose the three end-member oil types (1, Ordovician; 2, Silurian, Devonian, and Mississippian; 3, Pennsylvanian), which are distinguished by the relative abundance of normal, branched, and cyclic C_7 hydrocarbons. Abbreviations: nc7, normal heptane; mch, methylcyclohexane; 2 + 3mh, the sum of 2-methylhexane and 3-methylhexane.

alyzed in this study, only one shows some evidence of biodegradation, although biodegraded oils are known to exist in eastern Oklahoma and Kansas.

DISCUSSION

The geochemical distinctions among the Ordovician to Pennsylvanian source rocks are consistent with the distinctions among the oil types. Analysis of the burial history of the source rocks within the central basin (Schmoker, 1986) indicates that all source rocks become thermally mature for hydrocarbon generation during Middle to Late Pennsylvanian time. Generation and expulsion of hydrocarbons from multiple source rocks at approximately the same time led to mixing of oils in structurally complex traps and traps related to major unconformities.

As sedimentation continued into the Permian, progressive burial of source and reservoir lithologies led to increased levels of thermal maturity, gas generation in the deep basin, and oil generation from source rocks on the shelf. As modeled by Hatch and others (1986) using Schmoker's (1986) analysis of the thermal history of the basin, no source rocks reached maturation levels necessary to generate oil north of a zone stretching from the central Oklahoma-Kansas border through the Hugoton gas field to the Kansas-Colorado border. In order to explain the presence of thermally mature crude oils as far north as the western edge of the Cambridge arch in southwestern Nebraska, we infer long-distance oil migration (Hatch and others, 1986). This inference is consistent with the geologic evidence of Walters (1958) for migration of oils out of the Anadarko basin into traps along the central Kansas uplift.

The geochemical argument for long-distance migration is supported by the observation of the depletion of toluene in many of the oils. If we measure an approximate distance of migration as the radial distance out from the -35,000 ft subsea contour on basement in the Anadarko basin, we can plot toluene content of the oils (as a fraction of n- C_7 , methylcyclohexane, and toluene as shown in Figure 10) versus distance as shown in Figure 11. With the exception of one sample with high toluene from the southern end of the central Kansas uplift (within the Salina basin, and so labeled in Figure 11), there is an obvious trend of decreasing toluene with increasing distance from the depocenter of the Anadarko basin. If the oil samples are separated by stratigraphic interval, as shown in Figure 11, the trend is still apparent. The strongest exceptions are the oils in the Devonian and Mississippian reservoirs. The oils with the highest toluene content occur in reservoirs ~90 mi from the depocenter, near the subcrop erosional edge of the Hunton Group identified by

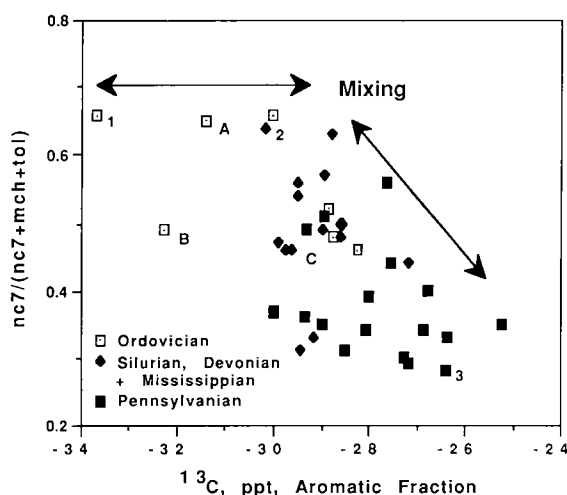


Figure 8. Relationship of gasoline-range composition to carbon-isotope composition of Anadarko basin oils, showing evidence of mixing. Points labeled 1,2,3 are the end-member oils shown in Figure 6. Three mixed oils labeled A,B,C are shown in Figure 9.

Amsden (1975). This is also where the Woodford Shale is presently buried at depths within the oil window, suggesting that these toluene concentrations may be those for a "least-migrated" oil.

The systematic depletion in toluene may be related to migration distance. The low-molecular-weight aromatic hydrocarbons benzene and toluene are the most water-soluble components in crude oils (Price, 1976). As oils migrate farther, they contact progressively larger amounts of formation water into which the water-soluble components will partition. Therefore, water-soluble components should decrease with increasing migration distance. In fact, most oils from reservoirs north of the Oklahoma-Kansas border have no detectable benzene, which has a higher solubility in water than toluene.

There are other possible explanations for some

of our observations. Clayton and others (1987) and Clayton (1988, personal communication) have argued for local generation of oils in Paleozoic reservoirs in southwestern Nebraska. Our analyses of two of the same oil samples reported in Clayton and others (1987) show extreme depletion in toluene, consistent with the evidence for long-distance migration presented in this paper. There is also the possibility that the toluene concentration is related to thermal maturation, implying that the trends versus distance in Figure 11 also reflect depth of burial of the reservoir and source rock. However, the trend of toluene concentration versus depth is not strong, a fact shown by the relatively low concentrations of toluene in the central, deep-basin (migration distances <80 mi) oils from Silurian and Devonian reservoirs and from Pennsylvanian reservoirs.

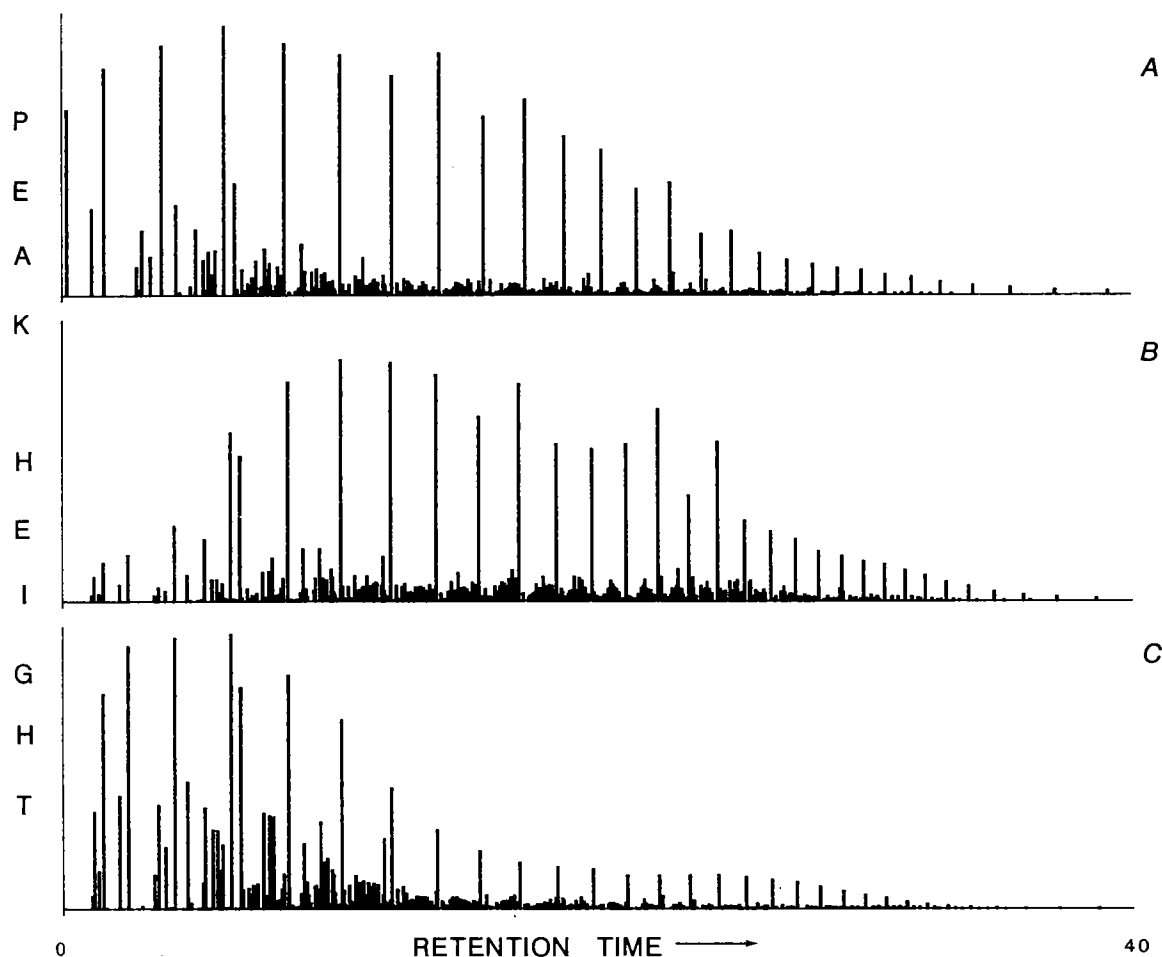


Figure 9. Three mixed oils, labeled A,B,C in Figure 8, shown as whole-oil gas chromatograms.

CONCLUSIONS

Although most of our analyses are routine reconnaissance analyses, we have established several facts in the petroleum geochemistry of source rocks and crude oils in the Anadarko basin. First, organic-rich rocks ranging in age from Ordovician to Pennsylvanian have good source potential and distinctly different geochemical characteristics. Second, there are three distinct compositions of crude oils, distinguished primarily by carbon stable-isotopic compositions and gasoline-range-hydrocarbon compositions. These crude-oil types appear to correlate with extracts of Ordovician, Devonian, and Pennsylvanian source rocks.

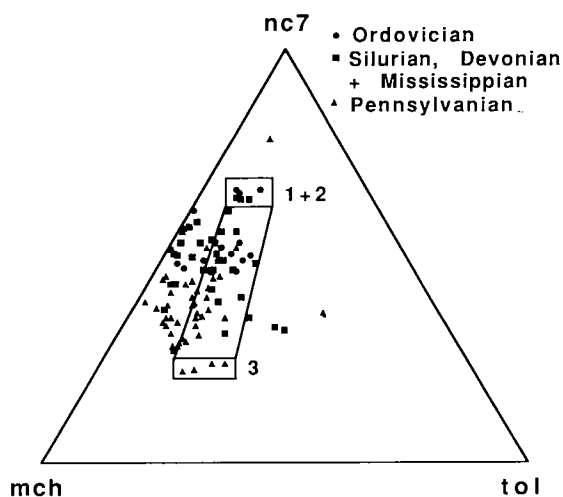


Figure 10. Ternary plot of C_7 gasoline-range hydrocarbons, including the aromatic hydrocarbon toluene, from Anadarko basin oils. Mixing among the three major oil types is evident. Many oil samples show depletion in toluene. Abbreviations: see Figure 7 caption; tol, toluene.

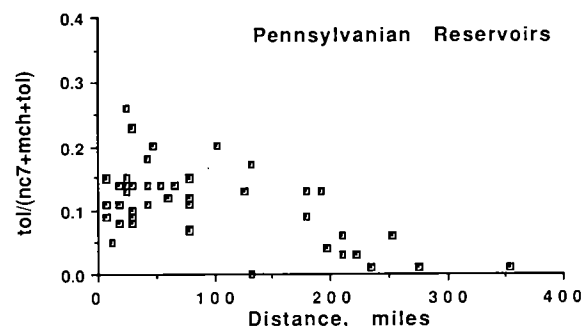
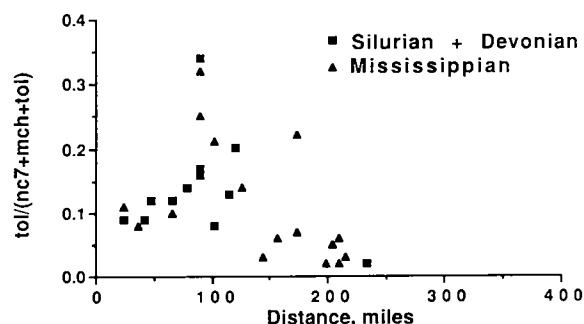
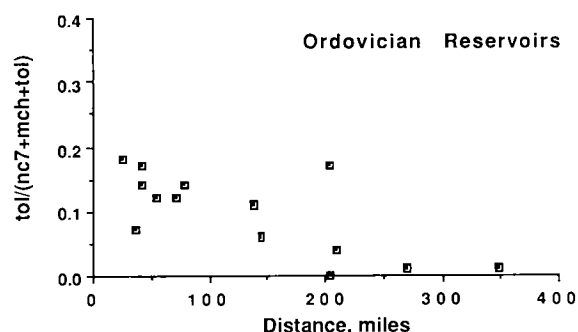
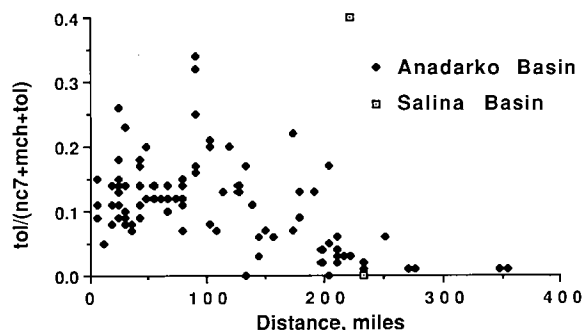


Figure 11. Relationship of the relative abundance of toluene in crude oils (all samples) to distance of the reservoir from the depocenter ($\sim 35,000$ ft subsea contour on basement) of the Anadarko basin. Distance measured as a straight line from the basin center to the sample location. Diagram at top for all samples; other diagrams by stratigraphic interval. The depletion in toluene with increasing distance occurs regardless of geologic age of the reservoir. Abbreviations: see captions for Figures 7 and 10.

Third, lack of thermally mature source rocks on the northwestern shelf and systematic depletion of toluene with distance from the deep basin imply that oils reservoired as far north as the central Kansas uplift and the Cambridge arch in southwestern Nebraska were generated and migrated from source rocks in the Anadarko basin.

ACKNOWLEDGMENTS

This work is supported by the USGS Evolution of Sedimentary Basins Program, in cooperation

with the Oklahoma Geological Survey. Margaret Burchfield, Eldon Cox, and Jane Weber of the Oklahoma Geological Survey provided assistance in obtaining oil samples and core samples, and in performing bitumen fractionations. In addition, we appreciate the assistance of J. L. Clayton, USGS, and S. Jacobson and R. Haack, Chevron USA, in obtaining additional oil samples. Reviews by J. L. Clayton and L. C. Price significantly improved an early draft of this report. Use of commercial trade names in this report does not constitute endorsement by the U.S. Geological Survey.

AN ORGANIC GEOCHEMICAL STUDY OF OILS, SOURCE ROCKS, AND TAR SANDS IN THE ARDMORE AND ANADARKO BASINS

R. P. PHILP, P. J. JONES, L. H. LIN, G. E. MICHAEL, AND C. A. LEWIS

University of Oklahoma

Abstract.—Oils and tar-sand bitumens from the Pauls Valley–Woodford areas of the Anadarko basin have been analyzed to study effects of biodegradation on oils and to determine their possible sources. The tar-sand deposits, located ~1.5 mi south of Woodford, Carter County, Oklahoma, are distributed along the crest of the South Woodford anticline. Sixteen bitumens from the Rod Club Sandstone (Mississippian) were chosen from a single well (Fitzgerald #5) which was cored near the axis of the anticline. Geochemical correlation between the tar-sand bitumen and oils produced in the Pauls Valley area was attempted to determine which of these oils was the source for the tar-sand bitumen. The age of the reservoirs of these oils ranges from Ordovician to Pennsylvanian.

This study has shown that the tar-sand bitumens have been so severely biodegraded that most of the n-alkanes, low-molecular-weight cycloalkanes, isoprenoid alkanes, C_{27} – C_{29} steranes, and light aromatics and sulfur compounds have been removed, and the hopanes and steranes have been extensively altered. The porphyrins from the tar sands were also examined to study possible effects of biodegradation on porphyrins. Previously hypothesized changes in porphyrin structure due to biodegradation have included n-alkyl side-chain cleavages and possible conversion from DPEP-type to ETIO-type porphyrins. The present study showed no observable effects in total porphyrin distributions even at high levels of biodegradation in these tar-sand samples.

INTRODUCTION

Tar sands have been defined by the Interstate Oil Compact Commission (1980) as being any rock, consolidated or unconsolidated, containing crude oil which is too viscous at natural reservoir temperature to be commercially produced by conventional primary recovery techniques. Heavy-oil and tar-sand accumulations are thought to be created by water-washing and bacterial degradation of ordinary crude oils (Winters and Williams, 1969; Bailey and others, 1973; Rubinstein and others, 1977). Water-washing removes the more water-soluble, light hydrocarbons, especially aromatics, whereas biodegradation preferentially removes n-alkanes. Severe degradation can remove isoprenoids, and tetracyclic and pentacyclic terpanoids, making oil–oil correlation and maturity determinations difficult. A knowledge of compositional changes caused by biodegradation is essential for making accurate assessments of genetic relationships among oils, especially severely degraded heavy oils, seeps, and tar-sand bitumens.

In the past two decades, the effect of biodegradation on petroleum composition has been studied extensively. Connan (1984) published a comprehensive review of biodegradation effects on the composition of petroleum in reservoirs. Recently, Philp and Lewis (1987) reviewed the biodegradation effects reported in the literature and summarized them into a table indicating changes that occur with increasing biodegradation.

More than 300 occurrences of heavy oils and bitumen-impregnated rocks have been reported in Oklahoma (Harrison and others, 1981), including 45 tar sands in Carter and Murray Counties. The purpose of the present study is to analyze the chemical composition of a series of tar-sand bitumens from a single well, to study variation of biomarker distributions, hydrocarbons, and porphyrins as a function of biodegradation of the tar-sand bitumens. In the present study 16 tar-sand samples at depths ranging from 16 to 256 ft have been obtained from a tar-sand quarry site in the Ardmore basin, Carter County, Oklahoma (Fig. 1). These samples were cored by the Oklahoma Geological Survey in the Upper Mississippian Rod Club Sandstone within the local structure known as the South Woodford anticline (Harrison and Burchfield, 1984, fig. 2). A detailed description of the study area and regional setting can be found elsewhere (Jones, 1986; Lin, 1987; Michael, 1987). An attempt has been made to correlate the tar-sand bitumen with oils in the Pauls Valley area, at the southeast corner of the Anadarko basin, using biomarkers that survive biodegradation and flash pyrolysis of the asphaltene fraction. It was of particular interest to use the porphyrin distributions for this purpose, because there have been few specific studies on porphyrin distributions in genetically related oils or source rocks. Jones (1986) has already undertaken a study of several oils along with possible source rocks from the Pauls Valley–Hunton uplift area of southern Oklahoma. The same oils and possible source rocks were examined in an at-

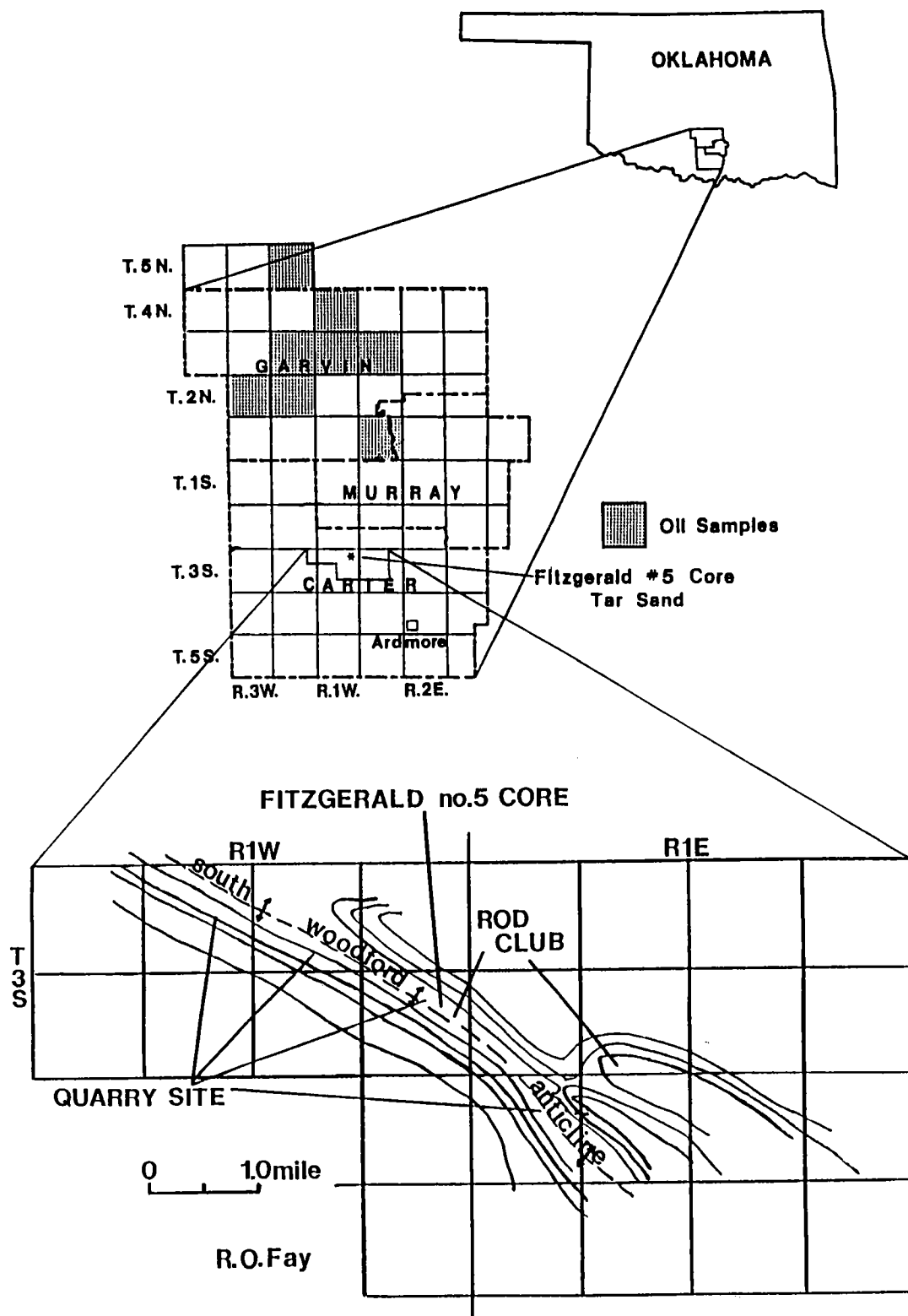


Figure 1. Location of the Fitzgerald #5 well (source of the tar sand samples), drilled in the Upper Mississippian Rod Club Sandstone, within the south Woodford anticline.

tempt to correlate oils and source rocks with the tar-sand extracts from the core.

EXPERIMENTAL PROCEDURE

Hydrocarbon Isolation and Analysis

Tar-sand bitumens (0.3–0.5 g), provided by the Oklahoma Geological Survey, were extracted from the tar sand with dichloromethane. Asphaltenes were removed from bitumens and oils by precipitation with n-pentane for a minimum of 8 hr. The deasphalted bitumen or oil was separated into saturate, aromatic, and NSO fractions by column chromatography, using silica gel (100–200 mesh) and alumina (80–200 mesh). Wherever necessary, molecular sieving was performed to remove n-alkanes from the saturate fraction and to increase the concentration of polycyclic compounds in the sample to improve the detection of biomarkers. Saturate and aromatic fractions were analyzed by gas chromatography, using either a Hewlett-Packard 5890 or Varian 3300 GC with a J & W Scientific DB-5 fused-silica capillary column (30 m \times 0.35 mm, 0.25 μ m film thickness).

Biomarkers present in the saturate and aromatic fractions were determined with a Hewlett-Packard 5890A gas chromatograph equipped with a J & W Scientific DB-5 fused-silica capillary column (ca. 25 m \times 0.25 mm, 0.25 μ m film thickness), interfaced to a Finnigan MAT Model 700 Ion Trap Detector (ITD). Component identification was made by comparison with mass chromatograms of other samples that had been analyzed on the GC-ITD system, and by comparison with previously published data.

Porphyrin Isolation and Analysis

Column chromatography was performed on whole oils, or extracts, to determine the predominant porphyrin metal chelate species present. Chromatography was performed using 100- to 200- μ m-mesh silica and 80- to 200- μ m-mesh alumina activated at 240°C for 3 hr. Vanadyl porphyrins eluted in 10% ethyl acetate/toluene fraction and nickel porphyrins eluted between 10 and 20% toluene/hexane (Barwise and Whitehead, 1979). Identification of separated metal porphyrins was done by visible-spectrum absorption, with diagnostic peaks at 550 nm and 514 nm for nickel, and 570 nm and 531 nm for vanadyl.

Porphyrin Demetallation

Demetallation of porphyrins was performed by a method similar to that of Marriott and others (1984). Thin-layer chromatography (0.25 mm thick 20 cm \times 20 cm silica gel 60 plates, Merck)

was used as a cleanup separation technique prior to high-performance-liquid-chromatography (HPLC) analysis using an Eldex 9600 ternary solvent system and a Rheodyne 7125 injector fitted with a 10- μ L loop. Normal phase chromatography was performed using three 150 mm \times 4.6 mm i.d., 3- μ m silica columns connected in series (Barwise, 1986; Chicarelli and others, 1986). The presence of four diagnostic absorption peaks within the visible spectrum permits identification of demetallated porphyrins, as well as porphyrin type, based upon relative peak heights of the spectrum.

Flash Pyrolysis-GC of Asphaltene

Asphaltenes were dissolved in a small amount of dichloromethane and reprecipitated with n-pentane three times before being subjected to pyrolysis-GC, at a pyrolysis temperature of 600°C, using a CDS (Chemical Data Systems) 122 extended-temperature pyroprobe coupled to a Varian 3300 gas chromatograph. Chromatographic separation was performed with a J & W Scientific DB-5 fused-silica column (30 m \times 0.25 mm, film thickness 1.0 μ m). Carrier-gas flow rate was \sim 1 mL/min, and temperature program was from -25°C (2 min), increased to 300°C at 4°C/min (final temperature held for 30 min). The column effluent was split and monitored by both FID and FPD. All data were collected with Nelson Analytical Chromatography Software Model 2600, running on an IBM PC-XT under PC-DOS #3.6.

RESULTS AND DISCUSSION

Bulk Composition

A ternary diagram of relative weight percentage of saturate, aromatic, and asphaltene plus NSO fractions of oils and tar-sand bitumens is shown in Figure 2. The ordinary oils contain mainly saturated hydrocarbons (71.65–83.19%), while the tar-sand bitumens contain major amounts of aromatic and polar compounds. Fluctuations in the saturate/aromatic ratio for the tar-sand bitumens reflect different rates of bacterial degradation and water-washing for the saturate and aromatic fractions.

Gas Chromatography

The gas chromatograms of the saturate fractions of oils #3, #18, #29, and #30, reservoired in the Oil Creek Formation and thought to be sourced from Woodford shales (Jones, 1986), are shown in Figure 3. The n-alkane concentrations relative to the isoprenoids are much lower in the shallower reservoirs and are indicative of bio-

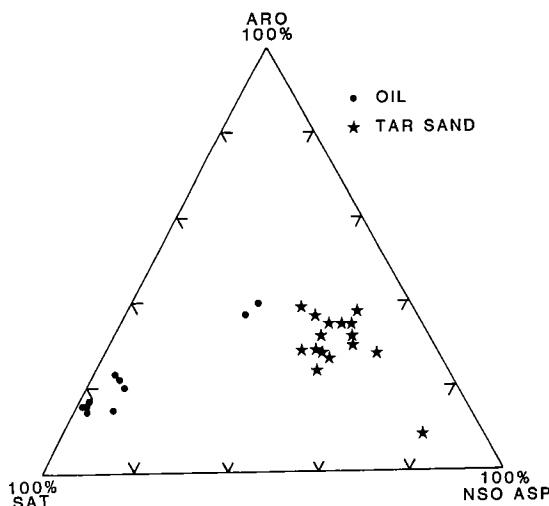


Figure 2. Ternary diagram showing bulk composition of tar-sand bitumens from Fitzgerald #5 well and oils from the Pauls Valley area.

degradation (Winters and Williams, 1969; Bailey and others, 1973).

The tar-sand bitumens are so severely degraded that they contain no n-alkanes or isoprenoids, and only tricyclic and pentacyclic terpenoids could be seen at the end of the large hump of unresolved components. The aromatic fractions also showed severe degradation, such that only a large hump of unresolved components was present along with triaromatic steroid hydrocarbons.

Gas Chromatography-Mass Spectrometry

Steranes

There is a consensus that steranes are degraded far more rapidly than diasteranes (Seifert and Moldowan, 1979; Volkman and others, 1983; Goodwin and others, 1983). Within the steranes, the 20R-5 α (H), 14 α (H), 17 α (H) species are removed faster than their 20S homologs, and the C₂₇ steranes are removed prior to the C₂₈ and C₂₉ species. The *m/z* 217 mass chromatograms (Fig. 4) show that the C₂₇-C₂₉ steranes were removed from the tar sands, and only the C₂₇-C₂₉ rearranged steranes and apparently the C₃₀ steranes have survived biodegradation. The similarity in the distribution of diasteranes and C₃₀ steranes for all of the tar-sand bitumens studied implies that they have a common source. The resistance toward biodegradation of C₃₀ steranes shown in the tar-sand bitumens appears to be useful for correlation studies.

The triaromatic steroid hydrocarbon (*m/z* 231) for the tar-sand bitumen at 204 ft and two oils are shown in Figure 5. The absence of C₂₀ and C₂₁ triaromatic steroid hydrocarbons from the tar sand is assumed to arise from preferential removal during water-washing or biodegradation (Wardroper and others, 1984; Volkman and others, 1984).

The monoaromatic steroid hydrocarbons do not appear to be degraded in these tar-sand bitumens when compared to those of an ordinary oil and, as such, monoaromatic steroid hydrocarbons are more resistant to biodegradation than the triaromatic steroid hydrocarbons, as noticed by Wardroper and others (1984). Biodegradation of aromatic steroid hydrocarbons is not apparent until the C₂₇₋₂₉ steranes, hopanes, and C₂₇₋₂₉ diasteranes have been severely degraded; hence, these compounds are useful for correlation and maturation studies (e.g., Mackenzie, 1984; Seifert and Moldowan, 1978).

Hopanes

The hopane distributions show some differences as a result of varying degrees of biodegradation (Fig. 6), and the sample at 144 ft appears to be one of the least biodegraded in terms of hopane distribution. The preferential removal of 22R hopanes, and the decreasing susceptibility to biodegradation of hopanes in the order C₃₅ > C₃₄ > C₃₃ > C₃₂ > C₃₁ > C₃₀ > C₂₉ has been previously documented by Goodwin and others (1983). The preferential removal of the 22R epimer of C₃₁, C₃₂, C₃₃ hopanes is clearly indicated in the sample at 16 ft (Fig. 6). In this study the susceptibility to biodegradation appears to be partially reversed, and the order is C₃₀ > C₃₁₋₃₃ > C₃₄ and C₃₅ homologs. Moretanes, 17 α (H)-22,29,30-trisnorhopane (T_m), 18 α (H)-22,29,30-trisnorhopane (T_s), and C₂₉ hopane appear to be relatively resistant to biodegradation, as previously reported by Seifert and others (1984). The C₂₄ tetracyclic terpane also appears to be resistant toward biodegradation relative to the hopanes.

The total removal of C₃₀+ hopanes from samples deeper than 240 ft is probably due to an increased contact with ground water. An inspection of the core showed the upper 7-16 ft and the lower 256-270 ft to be composed of grayish-brown to brown sandstone. Most of the intermediate section was composed of dark-brown to black, highly bitumen-saturated sandstone, with a few fractures and light-brown sandstone strings. This implies that the upper and lower parts of the tar sand are more accessible to water and, hence, more severely degraded than the middle section. Since some heavy oil is seeping out along the crest of the South Woodford anticline, heavy oil actively migrating from a reservoir in the vi-

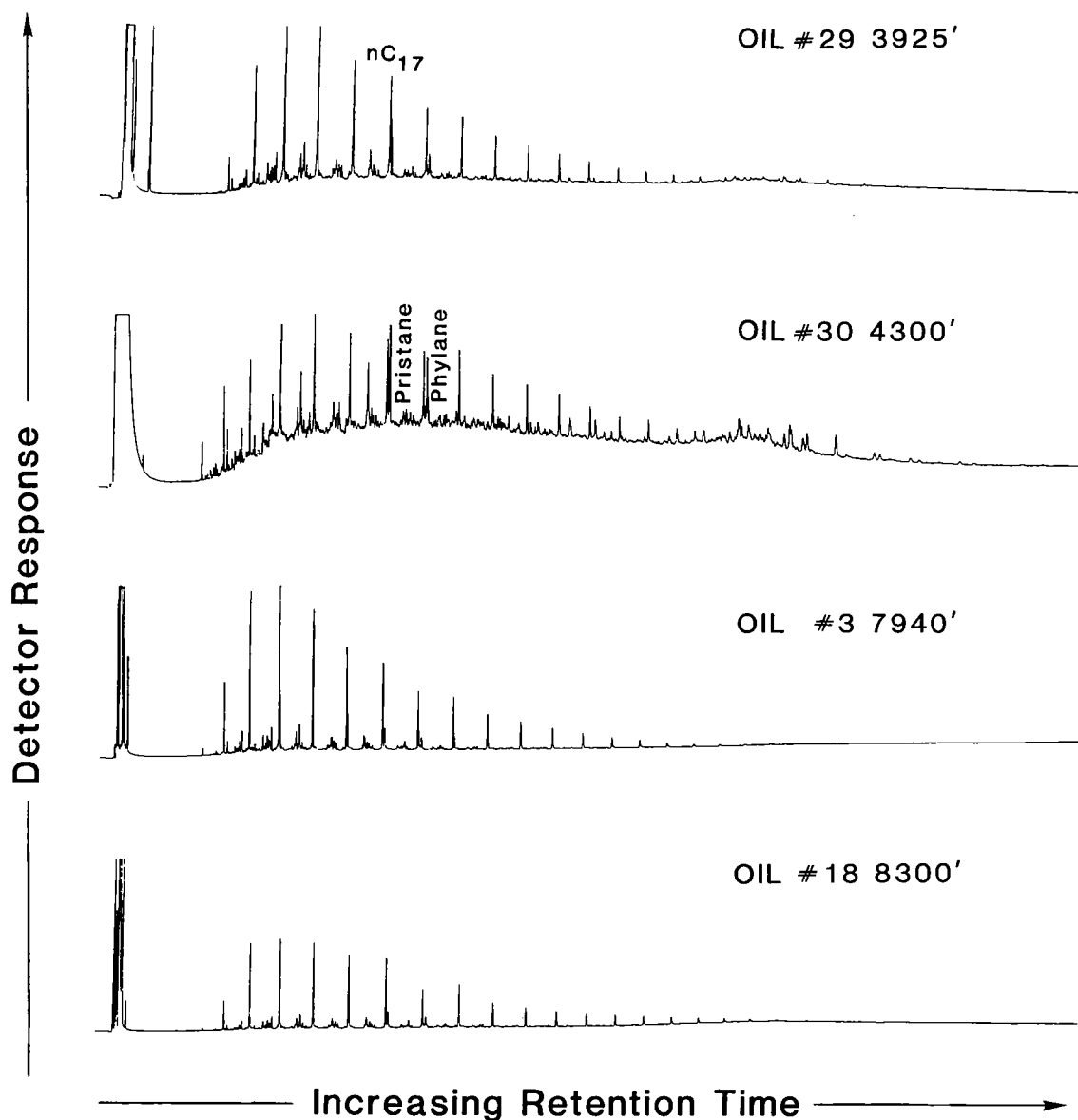


Figure 3. Gas chromatograms showing the distribution of n-alkanes from four of the Oil Creek oils analyzed in this study.

cinity may also be mixing with the tar-sand bitumen and causing changes in the distribution of hopanes.

Porphyryns

To study the effects of biodegradation upon porphyrin distributions, the distinct destruction of certain isomers and the conversion of one group of isomers to that of a different carbon number were monitored. Specifically, conversion

from DPEP-type to ETIO-type porphyrins was monitored by observing the percent DPEP and DPEP-to-ETIO ratio. However, within the error limits set by a standard there were no observable changes in percent DPEP or the DPEP-to-ETIO ratio within the core samples. Ratios of C_{32}/C_{31} and C_{32}/C_{33} DPEP-type porphyrin were measured to look for possible methyl cleavages. The ratio of C_{32}/C_{30} DPEP was measured to look for ethyl cleavages. Based upon ratios measured for extracts of the tar-sand core, there were no observ-

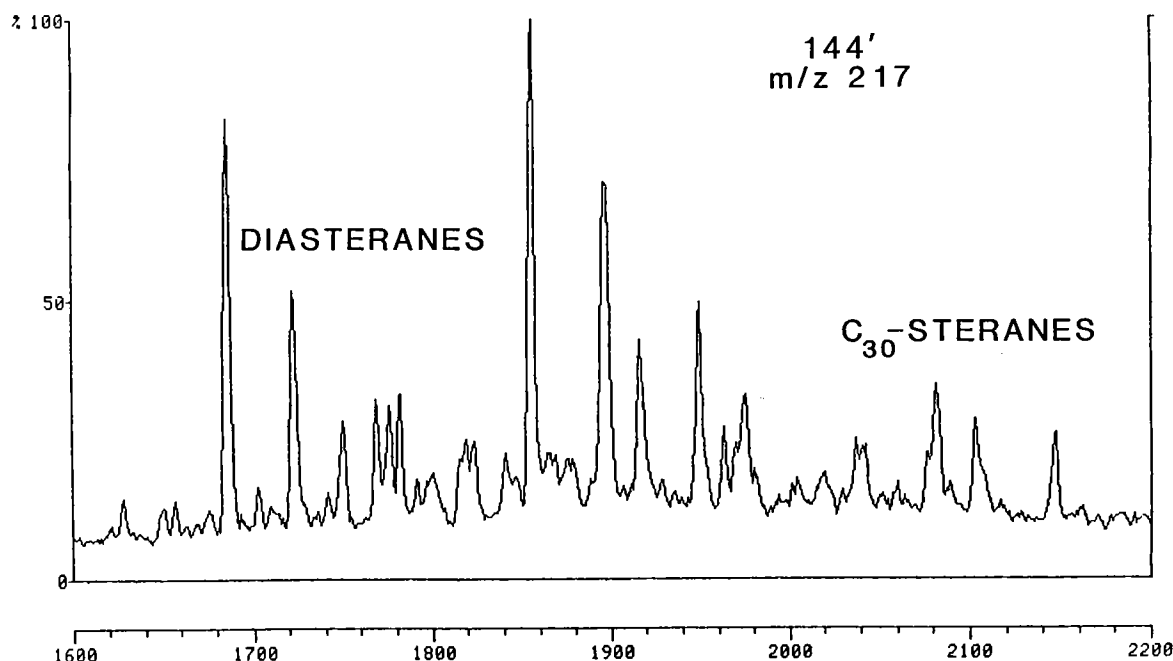


Figure 4. m/z 217 chromatogram, showing that the steranes in the tar sands were severely biodegraded, and only the rearranged steranes and small quantities of the C_{30} steranes remain in the extracts.

able effects upon the porphyrin distributions resulting from biodegradation. The results of this study support previous work by Palmer (1983) and Barwise and Park (1983) which showed no effect of biodegradation on porphyrin distributions.

CORRELATION OF TAR-SAND BITUMEN WITH OIL FROM THE PAULS VALLEY AREA

The oils from the Pauls Valley area previously have been classified into two major groups on the basis of their biomarker distributions (Jones, 1986). In this study only two representative oils, namely Viola oil #20 and Oil Creek oil #29, were used for correlation with the tar-sand bitumen. Oil #29 was chosen not only because it is representative of the majority of oils from the Pauls Valley area, but, more important, because it is of similar maturity to that of the tar-sand bitumen.

The m/z 191 mass chromatograms of oil #20, oil #29, and the tar-sand bitumen from a depth of 204 ft are shown in Figure 7. The chromatograms for oil #29 and the tar-sand bitumen have almost identical tricyclic, tetracyclic, and pentacyclic terpane distributions. Oil #20 differs from the tar-sand bitumen by containing a high concentration of the C_{24} tetracyclic terpane and

an enhanced concentration of the C_{35} hopanes. The distribution of monoaromatic steroid hydrocarbons of oil #20, oil #29, and the tar sand (204 ft) also showed a strong similarity between oil #29 and tar-sand bitumen. Oil #20 has a relatively high concentration of C_{21} and C_{22} monoaromatic steroid hydrocarbons, and a different distribution pattern in C_{27-29} species. The C_{21} and C_{22} monoaromatic steroid hydrocarbons are thought to be more thermally stable than their higher-molecular-weight homologs; thus, oil #20, with the high concentration of C_{21} and C_{22} species, is probably more mature than oil #29 and the tar-sand bitumen. The high maturity of oil #20 is also shown by a lower T_m/T_s value than that of oil #29 (1.17 and 2.10, respectively; Jones, 1986, table 3). The ratio of T_m/T_s decreases with increasing maturity, and has been used as a maturation parameter by Seifert and Moldowan (1978).

The distribution of triaromatic steroid hydrocarbons for oil #20, oil #29, and tar-sand bitumen (204 ft) showed a good similarity between the C_{26-28} distribution for oil #29 and the tar-sand bitumen (Fig. 5). The absence of C_{20} and C_{21} components and the slight decrease in C_{28} 20R with respect to C_{28} 20S indicate that the triaromatic steroid hydrocarbons have been biodegraded, as previously reported by Wardroper and others (1984).

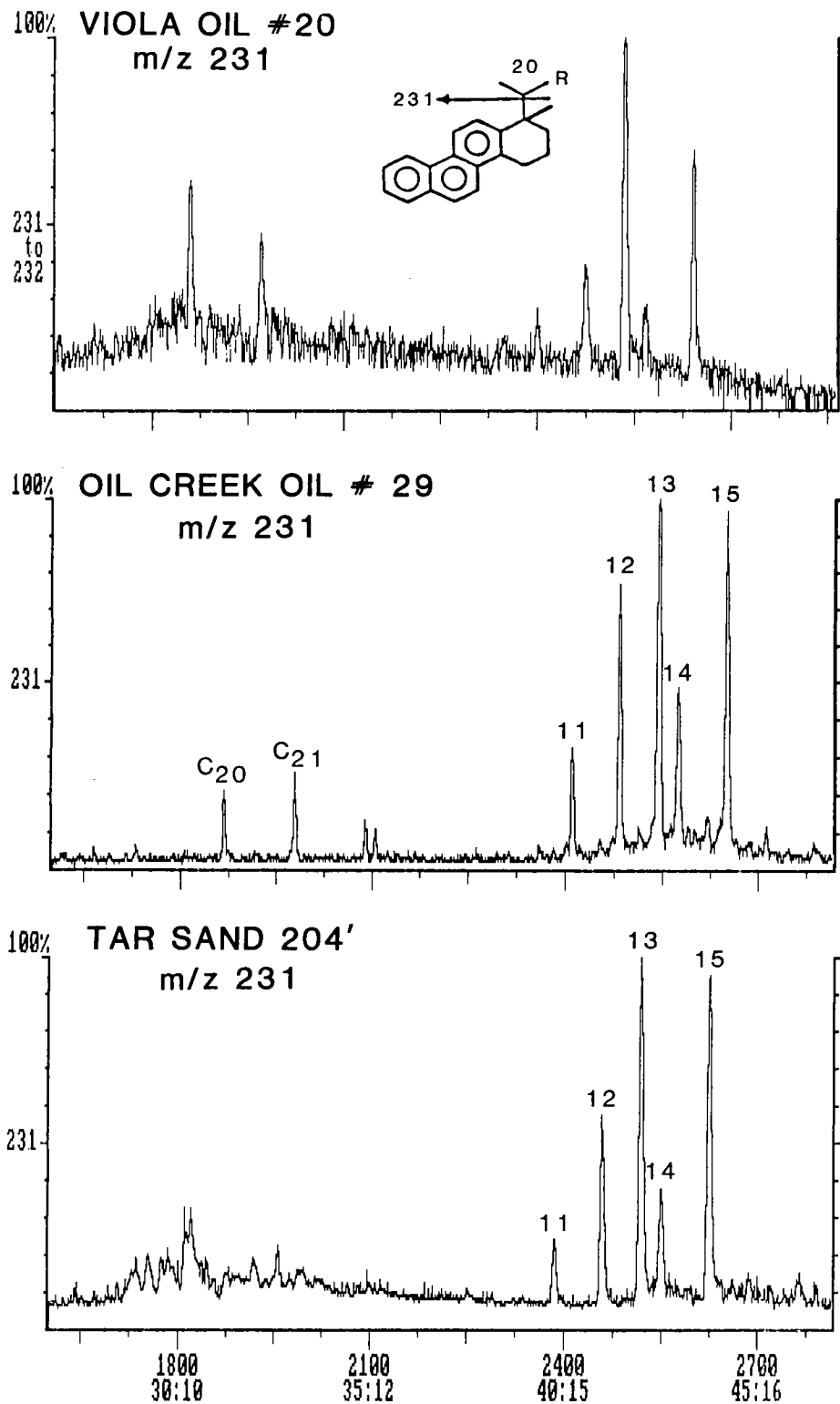


Figure 5. The triaromatic steranes as determined by the ion at m/z 231 were useful for supporting the proposal that the Oil Creek oils and the tar sands were derived from similar sources of organic matter.

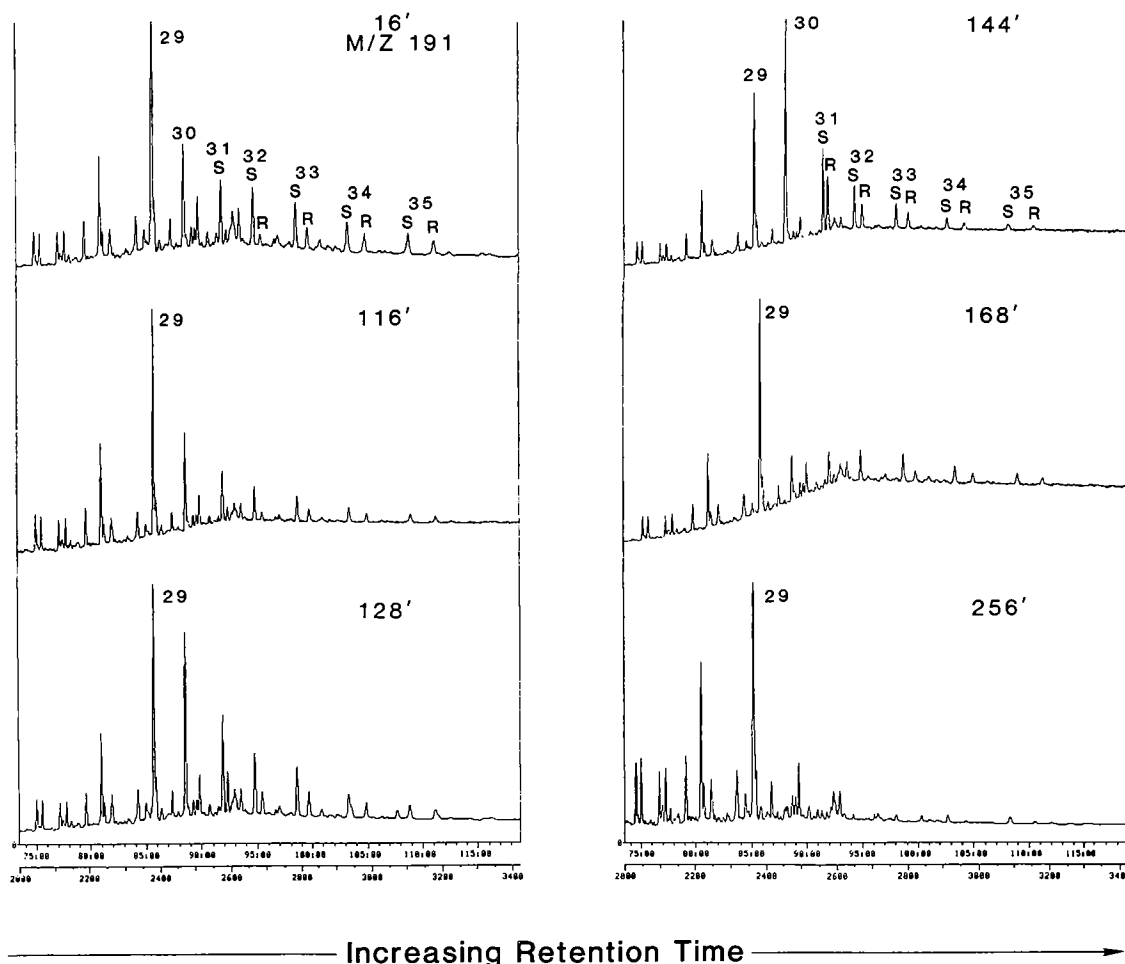


Figure 6. Variations in the extent of biodegradation of the tar-sand bitumens could be evaluated from the hopane distributions determined from the m/z 191 chromatograms, as shown in this diagram for six of the tar sand extracts.

The distributions of diasteranes are very similar in all the analyzed tar-sand bitumens. Since all of the steranes have been removed from the tar-sand bitumen by biodegradation, the m/z 217 mass chromatogram shows only the distribution of diasteranes. Diasteranes are thought to be relatively resistant to biodegradation; hence, they are useful for correlation purposes. The m/z 217 mass chromatograms of nondegraded oils contain both normal and rearranged steranes, making correlation with the tar-sand bitumen difficult. However, we have recently demonstrated the presence of AB ring degraded steranes, and their value for correlation of these tar sands and oils (Jiang and others, 1988).

A plot of percent DPEP versus percent C_{28+29} ETIO series B showed good correlation of these

two maturational parameters for the oils and tar sands. Oil 29 correlates well with the tar sand, as seen from the porphyrin distributions (Fig. 8). Sample 29 (3,925 ft) qualitatively shows the best correlation with the tar-sand extract, with the exception of an increased C_{29} and C_{30} ETIO series A concentration, which is interpreted to be due to slightly increased maturation. The average ETIO series A carbon number for oil 29 is C_{29} and C_{30} for the tar sand. The average carbon number for the ETIO series A decreases upon maturation.

Oil-Source Rock Correlation

Five different formations from Lower Ordovician through Lower Pennsylvanian were sampled as possible source rocks for the oils and tar-sand

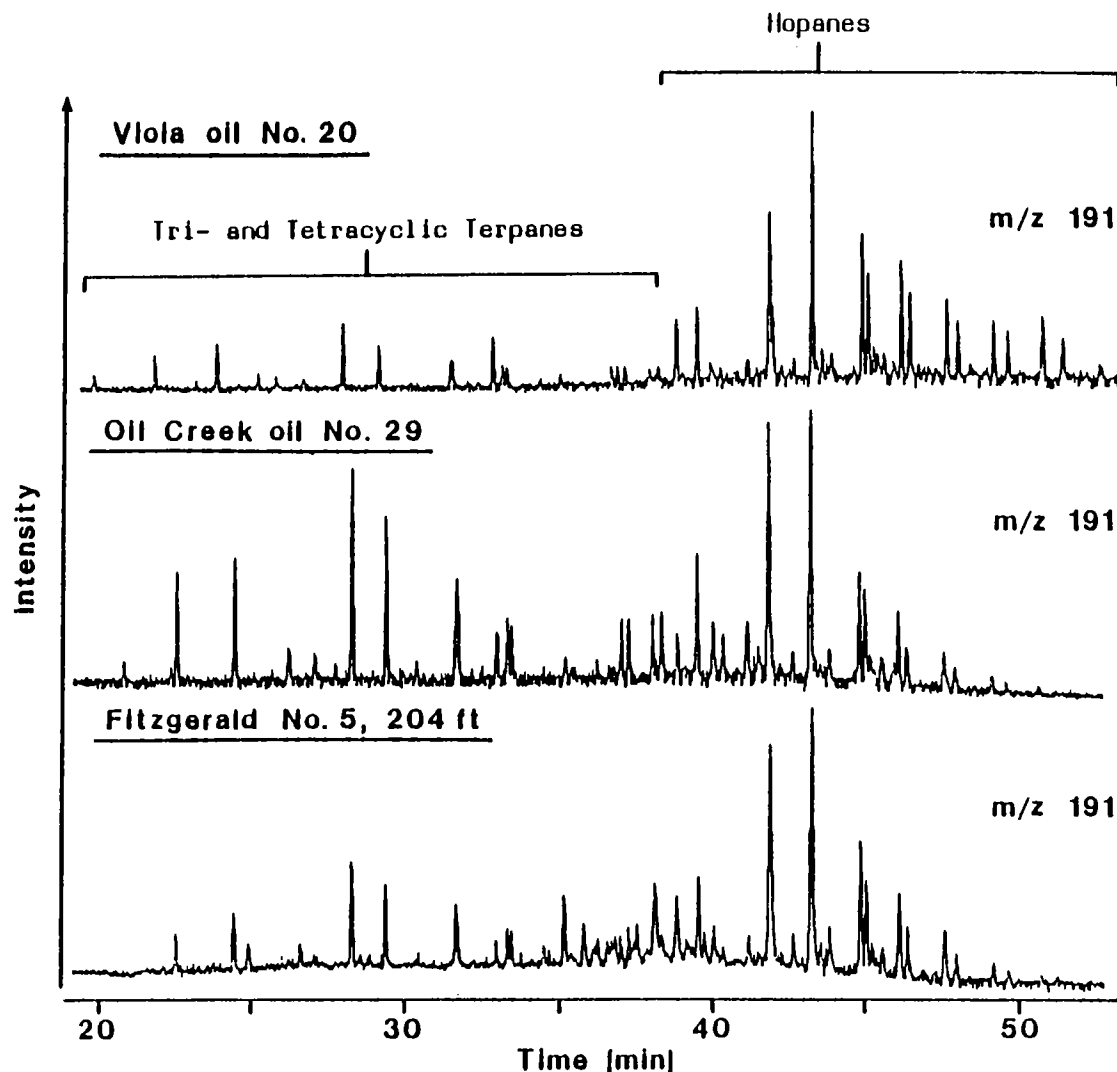


Figure 7. Comparison of the m/z 191 chromatograms for the Viola and Oil Creek oils and the tar-sand bitumen again supported the proposal that the tar sand was related more closely to the Oil Creek oil than to the Viola oil.

bitumens. The porphyrin distribution for the Pennsylvanian Springer shale (7,202 ft) consisted entirely of ETIO-type porphyrins, with a C_{32} ETIO series A predominance. Other possible source rocks which did not correlate with the oils or tar sand were the Viola limestone (8,330 ft) and the Arbuckle limestone (8,796 ft). Based upon other biomarkers, neither sample is considered to have reached maturity levels much beyond that of the Springer shale sample. Both have unique porphyrin distributions, and only ETIO porphyrins are present. The distributions for the Viola, Springer, and Arbuckle units are

definitely different from those for the oils, tar sands, or Woodford Shale, based on the presence of an unknown porphyrin, maturity, and a decrease in total-porphyrin concentration measured qualitatively by absorption spectroscopy. The Woodford Shale extract correlates very well with the tar sand and many of the oils. One diagnostic feature which should be noted is the increased C_{29} ETIO series A which is predominant in the Woodford samples. The same peak is also predominant in many of the oil samples at levels in which the percent DPEP has substantially decreased at what is interpreted as greater matura-

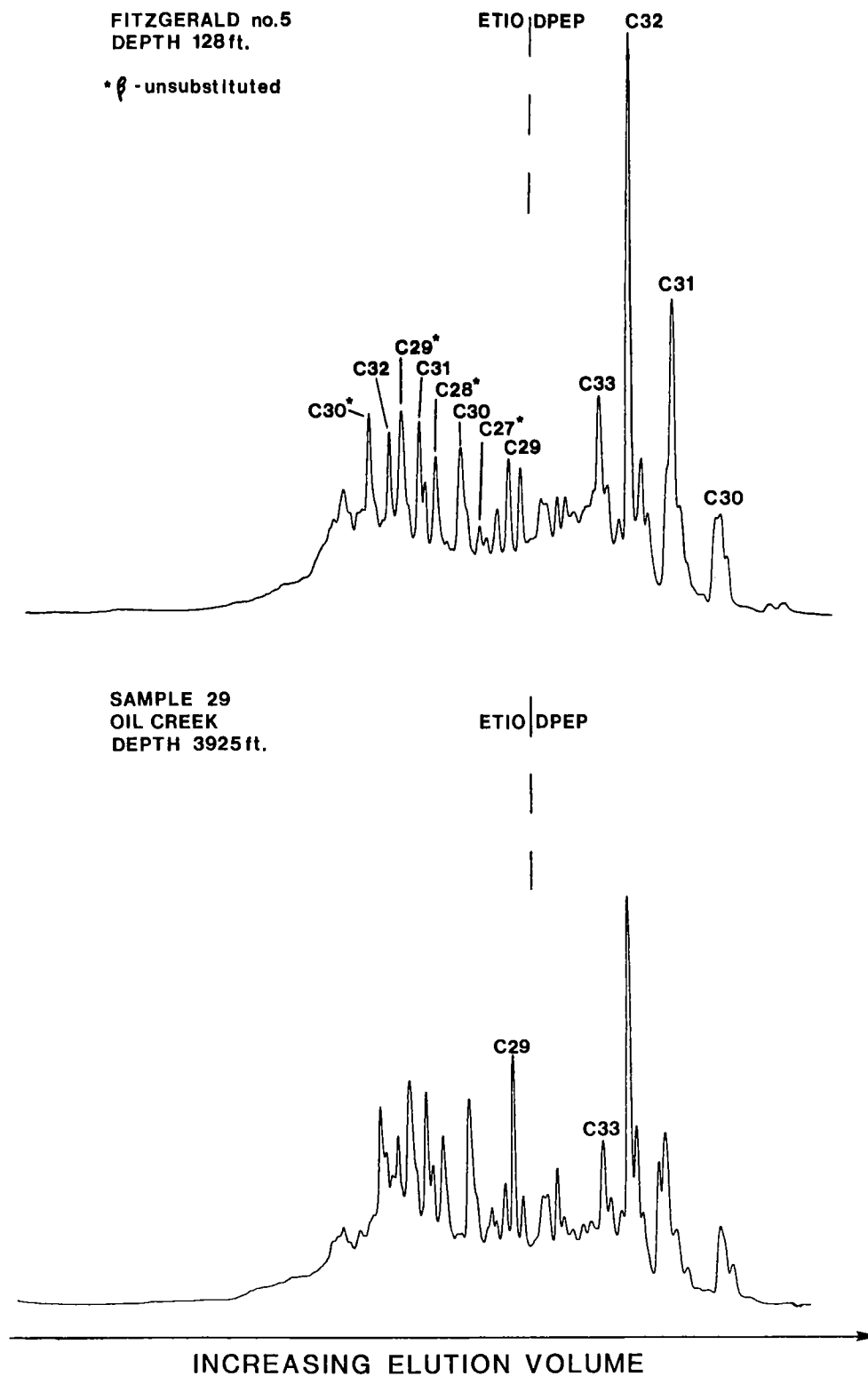


Figure 8. Porphyrin distributions were determined by HPLC, and the resulting chromatograms provided further support to illustrate the relationship between Oil Creek oils and the tar sands.

tion levels. The surface sample of Woodford Shale (Arbuckle Mountains, I-35, exit 42) and samples 8SR (6,571 ft) and 7SR (6,630 ft) probably have generated some hydrocarbons, and the latter may be generating currently, but the major source for the oil is thought to be deeper parts of the basin where the Woodford Shale is more mature.

Pyrolysis-GC

Py-GC of asphaltenes is a useful tool for correlation of biodegraded oils with non-biodegraded oils. This is especially true for severely biodegraded samples where the commonly used biomarkers have been altered or completely removed. Figure 9 shows the asphaltene pyrograms

of Viola oil #20, Oil Creek oil #29, and tar-sand bitumen (204 ft). The pyrograms show a series of doublets consisting of n-alkanes and their corresponding n-alkenes in which the tar-sand bitumen and oil #29 show a good correlation in the distribution of both aliphatic and aromatic hydrocarbons. However, the asphaltene pyrogram of oil #20 shows a distribution dominated by long-chain alkanes extending up to C₃₆, less aromatics, and no detectable pristene. An increase in normal hydrocarbons over isoprenoids, other branched hydrocarbons, and phenolic and aromatic compounds with increasing maturity has been observed in the pyrolysates of kerogens isolated from sediments of increasing maturity (Van de Meent and others, 1980).

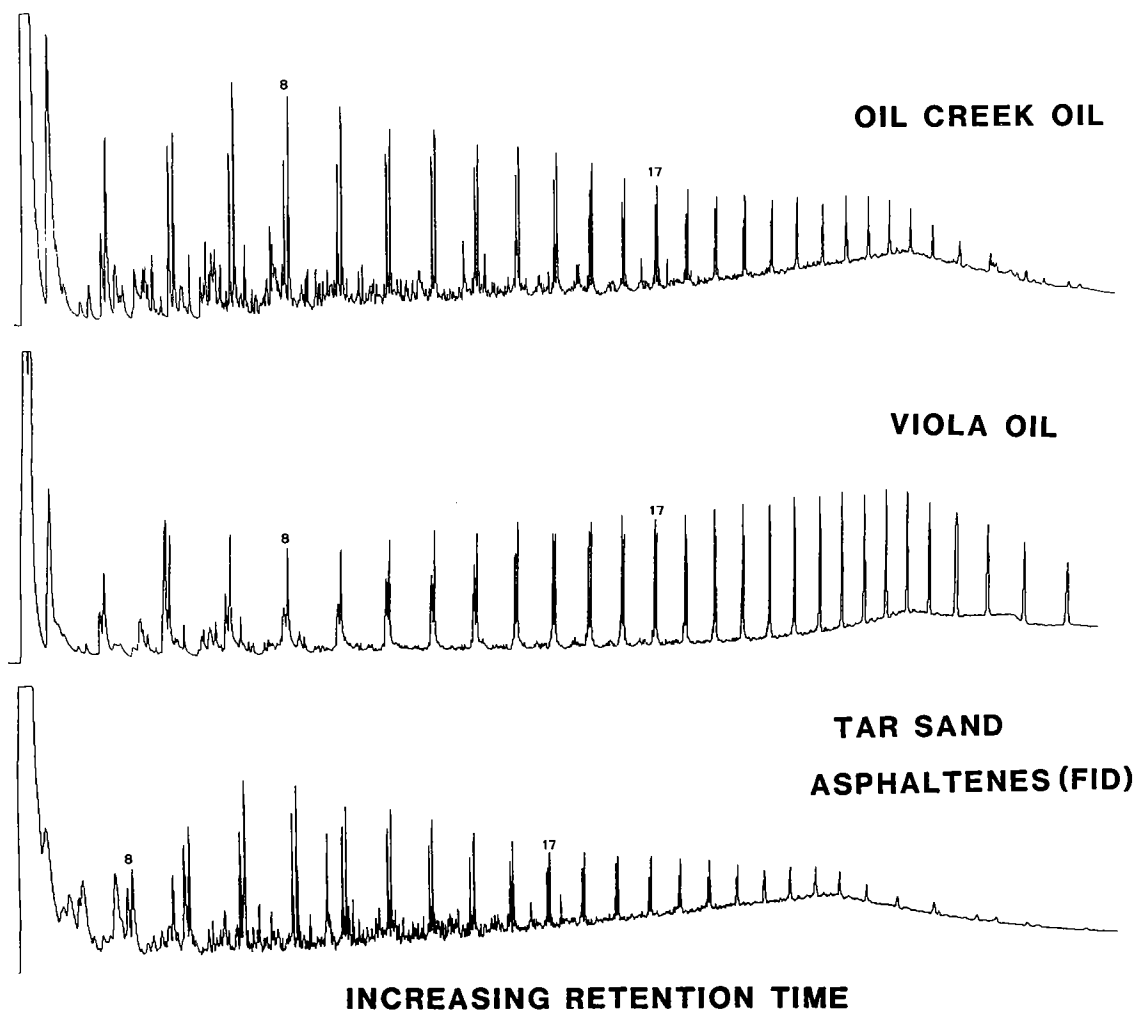


Figure 9. Py-GC of asphaltenes isolated from oils, both degraded and non-degraded, provides another valuable tool for obtaining information on possible correlations between these samples. Note in these chromatograms the similarity between the Oil Creek oil and the tar-sand sample.

CONCLUSIONS

The extent of biodegradation of tar-sand bitumens has been closely examined by GC and GC-MS. The results show that n-alkanes, isoprenoids, naphthalene, alkyl-naphthalenes, phenanthrene, C1-, C2-phenanthrenes, and benzo- and dibenzothiophenes have been removed from the tar-sand bitumens, and only an unresolved complex mixture is shown in the gas chromatograms.

The biomarker distributions in the tar sands are also altered to varying degrees. C₂₇₋₂₉ steranes and C₂₀₋₂₁ triaromatic steroid hydrocarbons are absent, and C_{27-C₂₈}-20R triaromatic steroid hydrocarbons decrease slightly. Hopane degradation with preferential removal of C₃₀₊ hopanes with the 22R configuration was observed. The C₂₉-hopane, T_m, T_s, and moretanes are degraded at a slower rate compared to the C₃₀₊ hopanes. The samples at 144 ft and 204 ft seem intact in terms of hopane distribution, and allow a correlation with oils. The preferential degradation of C_{27-C₂₉} steranes prior to alteration of hopanes can be observed in these two samples. Comparison with the degradation of tar-sand bitumens from the South Sulphur asphalt deposit, in which the degradation of C₃₀₊ hopanes occurred prior to steranes, shows the unpredictability in the relative biodegradation rate of hopanes and steranes. Dias-teranes, C₃₀ steranes, tricyclic terpanes, C₂₄ tetracyclic terpane, and monoaromatic steroid hydro-

carbons appear to be resistant toward biodegradation and are useful for correlation studies. Porphyrins were not observed to be biodegraded, despite high levels of biodegradation, as observed in other biomarkers for the tar sand. Porphyrin distributions are useful for correlation purposes in shallow-reservoir oils which have undergone degradation. Total-demethylated-porphyrin distributions in the present study were not sufficient to establish indisputable correlations, but they could be used in conjunction with information obtained from other biomarkers. The correlation study based on tricyclic terpanes, C₂₄ tetracyclic terpane, hopane, mono- and triaromatic steroid hydrocarbon, porphyrin distributions, and asphaltene pyrolysis-GC shows that the tar-sand bitumen appear to be source-related with oil #29 from the Pauls Valley area, previously proposed to be sourced from the Woodford Shale (Jones, 1986).

ACKNOWLEDGMENTS

The work described in this paper was supported by funds to one of us (RPP) from a number of sources. These include grants from DOE/OBS (#DE-FG05-86ER13412), NSF (EAR #8608820 and #8517312), ACS-PRF (#17775-AC2), and the following oil companies: Union, Texaco, and Mobil.

STRUCTURAL EVOLUTION OF THE SOUTHEASTERN PORTION OF THE ANADARKO BASIN REGION

WILLIAM J. PERRY, JR.

U.S. Geological Survey, Denver

Abstract.—Field investigations in the Lake Classen–Turner Falls, Oklahoma, area of the northern Arbuckle anticline, on the southeastern margin of the Anadarko basin, indicate that transpressional (oblique compressional) deformation of Late Pennsylvanian age dominated the structural development of this area. The Arbuckle anticline is detached along the NW-trending, SW-dipping, left-reverse Arbuckle fault and is thrust obliquely onto the margin of the Tishomingo block to the east. Paleostress analysis of slip lines on mesoscopic faults along the northeastern limb of the Arbuckle anticline, associated in style and geometry with oblique Arbuckle thrusting, indicates compression directed N. 35–60° E.

A seismic line oriented northeast across the northwestern part of the Arbuckle anticline, in Garvin County, Oklahoma, indicates that the anticline may have begun to grow as early as Desmoinesian time. Its final growth took place in Virgilian time, after transpressional (chiefly dip-slip) motion had ceased on the Arbuckle fault northeast and east of Turner Falls. The anticline and underlying Arbuckle thrust probably locked in middle Virgilian time, after which the subsidiary Washita Valley fault developed. The Washita Valley fault probably merges downward and north-westward into the Arbuckle fault.

Locally, as much as 3,000 ft (0.9 km) of up-to-southwest stratigraphic separation has occurred across the steeply SW-dipping to vertical Washita Valley fault. This cannot account for the >14,000 ft (4.3 km) of apparent left-lateral offset of second-order folds across the fault, as the axial planes of these folds dip steeply SW: Dip-slip alone would result in apparent right-lateral separation. Total left-slip is nearly 3 mi (4.8 km), in agreement with the original estimate by W. E. Ham. Development of this fault was synchronous in part with deposition of the middle(?) Virgilian Collings Ranch Conglomerate. This gently warped conglomerate resulted from deep erosion of the structures formed by tight folding and contraction faulting of older rocks during Arbuckle thrusting. Small-scale N- to NW-trending right-slip faults on the north limb of the Arbuckle anticline appear to merge southeastward into the Washita Valley fault zone at an acute angle. These right-slip faults dismember some of the older NW-trending en echelon folds, such as the Russell anticline and the associated northeast limb of the Arbuckle anticline. Subhorizontal slickensides, cross-cutting relationships, and fault-rock character indicate that these faults formed after folding and associated contraction faulting. Several of these faults cut the conglomerate as well. Their orientation with respect to the Washita Valley fault is anomalous: Analogous shear fractures formed in left-slip earthquake-fault zones and in the Riedel experiment are oriented quite differently with respect to the master fault.

West of the Arbuckle anticline, the Arbuckle fault is inferred to continue westward past the town of Marlow, Oklahoma, as a major compartmental or transform fault zone which separates thrust-bounded structures, such as the Velma, Tussey, and Doyle anticlines, from the transpressively shortened structures of the deep Anadarko basin, west of and including the thrust-cored Carter–Knox anticline. This fault zone underwent recurrent motion during Pennsylvanian and Early Permian time as compressive deformation proceeded generally from southwest to northeast on both sides of this zone. Map and cross-sectional relations suggest progressive clockwise rotation (NNE to ENE) of principal compression directions during Pennsylvanian and Early Permian time.

STRUCTURAL IMPRINT ON THE SLICK HILLS, SOUTHERN OKLAHOMA

R. NOWELL DONOVAN

Texas Christian University

W. R. DAVID MARCHINI

Queen's University of Belfast

DAVID A. McCONNELL

Kansas State University

WELDON BEAUCHAMP

Sun Exploration and Production Co., Dallas

DAVID J. SANDERSON

Queen's University of Belfast

INTRODUCTION: SETTING AND SIGNIFICANCE

The Slick Hills are located to the north of the Wichita Mountains and form the first substantial relief south of the Anadarko basin. Morphologically the Hills are bare, rounded, treeless summits with gentle gradients; maximum relief is less than a thousand feet. An alternative name, the Limestone Hills, reflects the underlying geology.

The Hills are exhumed Permian topography, resurrected during recent times from beneath a cover of conglomerates and red beds (Donovan, 1986a). The Leonardian landscape can be envisioned as topographic remnants or inselbergs shedding small fans and talus and slowly disappearing beneath a veneer of their own detritus. The preserved topography is a result of extreme aridity and a consequent lack of chemical weathering. Beneath the unconformity, most of the Slick Hills are built of carbonates assigned to the Cambrian-Ordovician Arbuckle Group (Fig. 1). Smaller areas are formed of the Cambrian Timbered Hills Group, itself underpinned by the Carlton Rhyolite. In the west, four small inliers of the Viola Springs Group form the Sugar Hills.

The Slick Hills occupy an important position in the geological architecture of southern Oklahoma. They are the exposed portion of the frontal fault zone, which juxtaposes the Wichita uplift and the Anadarko basin. At the present level of exhumation they constitute a cameo of the southern Oklahoma aulacogen (Donovan, 1986a). Stripped to its essentials, the history of southern Oklahoma is the record of stress acting upon a

fundamental crustal weakness, trending 120°, which first became active ~1.3 b.y. ago (Denison, 1982). During the Cambrian, rifting along this trend accompanied the initiation of the southern Oklahoma aulacogen as the area became involved in the development of the Proto-Atlantic Ocean. Details of geometrical relationships at this time are still a subject of debate (Condie, 1982; Larson and others, 1985). Tangible record of this period is provided by the bimodal complex of igneous rocks which is best exposed in the Wichita Mountains. Only the structurally highest level of this rift-bounded igneous pile, the Carlton Rhyolite, is exposed in the Slick Hills. On Bally Mountain, Ham and others (1964) measured 3,600 ft in their type section.

In late Cambrian time, following crustal cooling and shrinkage, a marine transgression took place across the craton, including the aulacogen terrain, which at this time comprised a range of low (400 ft) hills of Carlton Rhyolite. The initial record of this transgression consists of conglomerates, quartz-rich sandstones, and shales (the Reagan Formation). These are overlapped by the limestones of the Honey Creek Formation, which in turn pass upward into the platform carbonates of the Arbuckle Group. Along the axis of the aulacogen the latter are as much as 7,000 ft thick, thinning to the northeast and southwest. Within the Arbuckle Group there are subtle hints of basin evolution, as for example at the boundary of the Fort Sill and Signal Mountain Formations (Donovan, 1986a). Nevertheless, the general character of the group is constant: relatively thin-bedded carbonates with no significant shale inter-

FRONTAL FAULT ZONE

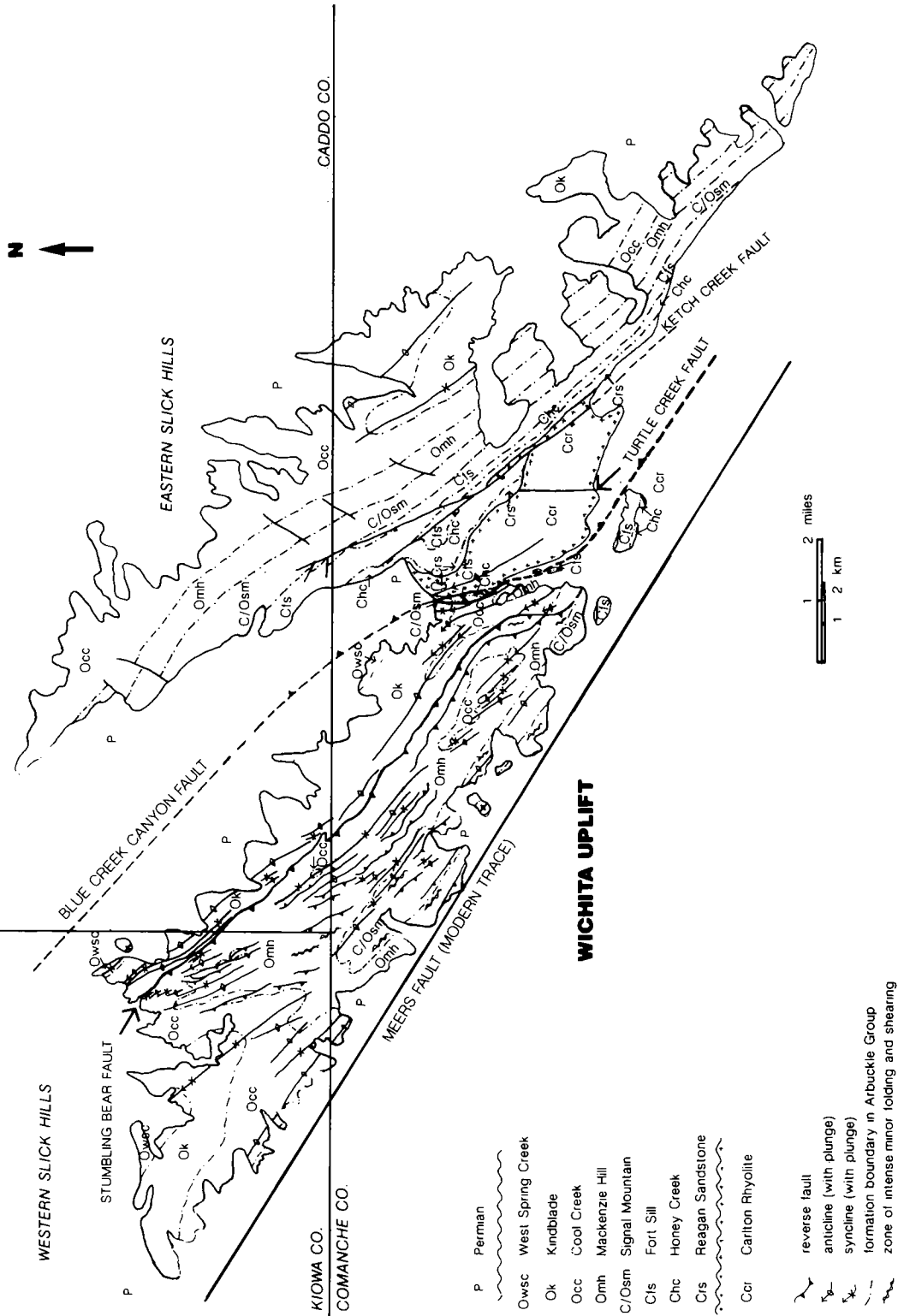


Figure 1. Geological map of the Slick Hills. Simplified from a base map at 6 inches to the mile, and showing only principal structural features and stratigraphic boundaries.

calations. The most consistently thin-bedded section is found in the 1,500-ft thickness of the Signal Mountain and lower Mackenzie Hill Formations. However, individual bed thicknesses >6 ft are very rare throughout the group.

The top part of the West Spring Creek Formation (uppermost unit in the Arbuckle Group) is not exposed in the Slick Hills. Apart from scanty exposures of the Bromide Formation and lower Viola Springs Group (see above), no other rocks older than Leonardian are seen at the surface, although a full and typical Paleozoic section is known in the subsurface.

During the Pennsylvanian and Early Permian, strata in the Slick Hills, in common with the rest of the aulacogen, were deformed during reactivation of the Cambrian rift faults. Timing of this deformation coincides with closure of the Proto-Atlantic Ocean, as recorded by the Ouachita orogene. Much discussion has centered on the basic character of deformation in the aulacogen, in particular on the roles played by compressive and shear stresses. The principal effect of the deformation was to dismember the aulacogen. In part the lower Paleozoic basin was inverted to form such uplifts as the Wichita, Arbuckle, and Criner Hills. Elsewhere the original basin was enhanced to form such spectacular depocenters as the Anadarko and Ardmore basins.

As noted, the Slick Hills occupy the "middle ground" between the Wichita uplift and the Anadarko basin. Structural relief across the zone is enormous: ~10,000 ft across the Meers fault (southern boundary of the frontal fault zone) and >20,000 ft across the Mountain View fault (the northern boundary).

Major deformation ceased by the Leonardian. The Slick Hills were covered by sediments and left in a quiescent state until the present erosion cycle (minor movements on the Meers fault notwithstanding).

The account presented here synthesizes the results of recent mapping of structure in the Slick Hills. Some of this work has already been published (e.g., Babaei, 1980; Donovan, 1982; Beauchamp, 1983; McConnell, 1983; Marchini, 1986; Donovan, 1986a; McCoss and Donovan, 1986; Donovan and others, 1987). Previous work in the area by Harlton (1951, 1963, 1972) established the basic tectonic framework; our work, utilizing remote-sensing data and large-scale mapping (6 in. = 1 mi overall, with enhancement in complex areas), fills in some of the details.

THE TECTONIC FRAMEWORK

The Meers fault juxtaposes the Slick Hills and the Wichita Mountains (Fig. 1); the fault has an impressively linear trace which has been enhanced by Recent movements (Donovan and

others, 1982). There is some ambiguity concerning the subsurface behavior of this fault. In their interpretation of the COCORP data, Brewer and others (1983) suggested a dip of ~40° SW. On the other hand, an analysis of the available magnetic data suggests to R. F. Madole (personal communication) that the fault is more or less vertical in the subsurface. The latter interpretation is supported by the linear character of the fault surface trace.

Although it is everywhere overstepped by Permian rocks and is only known in the subsurface, the Mountain View fault is more clearly understood than the Meers. Both COCORP data and drilling indicate that the structure dips SW at approximately 30–40°.

The Slick Hills are bisected by the Blue Creek Canyon fault, a complex, high-angle, reverse, oblique, left-lateral structure with a SW throw of ~2,000 ft (Donovan, 1982). This sense of throw is the reverse to that of the frontal fault zone as a whole; thus, the structure can be interpreted as an oblique back thrust hosted by the hanging wall of the Mountain View fault. The surface trace of the Blue Creek Canyon fault is sinuous; in general the fault trends ~15° clockwise of the Meers and Mountain View structures (i.e., ~135°), stepping between the two from north of Lawton to Gotebo. However, in the neighborhood of Blue Creek Canyon (the only place the fault is exposed), the structure trends N–S.

To the north and east of the Blue Creek Canyon fault, the eastern Slick Hills display a series of homoclinally dipping rocks, gently folded in places and cut by faults (e.g., the Ketch Creek fault) which do not destroy stratigraphic integrity. In the Western Slick Hills, deformation is far more intense; homotaxial problems cloud precise correlation across some faults. This is particularly the case in the terrain between the Meers and Stumbling Bear structures. The latter is a major reverse fault, trending 120–130°, with a NE throw. Balanced cross sections (Marchini, 1986) suggest that this fault has a staircase geometry characterized more by ramps than flats. Such cross sections have to be treated with caution, as the fault shows abundant evidence of left-lateral shear throughout its trace (McCoss and Donovan, 1986).

THE CAMBRIAN IMPRINT

The Early Cambrian history of the aulacogen was dominated by extensional stress which was accommodated by igneous activity and normal faulting parallel to the aulacogen trend (Gilbert, 1982). Because of Pennsylvanian overprinting, these early faults are difficult to recognize. A convincing case can be made for the Washita Valley fault in the Arbuckle area (R. E. Denison, per-

sonal communication); in the Slick Hills area no such case can be made (although the size and attitude of the Meers fault make it a likely candidate). Nevertheless, a minor Cambrian structural imprint can be determined in the outcrop of the Carlton Rhyolite of the Blue Creek Canyon area. Slight ($\sim 3^\circ$) tilting of the rhyolite preceded deposition of the Reagan Sandstone, while a N-S fracture pattern is more strongly developed in the rhyolite than elsewhere (Donovan and others, 1987). The most important of these fractures is the Turtle Creek fault, a structure which is clearly truncated by the Reagan. Veins associated with the fault suggest that it is a left-lateral structure with a modest throw. Marchini (1986) has suggested that this trend and sense of displacement are compatible with a component of right-lateral transtensive stress during this phase of aulacogen development.

THE PENNSYLVANIAN IMPRINT

The existence of a Cambrian N-S grain within the basement may have had an important influence on the location and trend of faults during Pennsylvanian deformation. Locally the Blue Creek Canyon and Ketch Creek faults (both cutting rhyolite) trend N-S, while interpretations of the subsurface frontal fault zone (e.g., Harlton, 1963) are characterized by significant N- and NW-trending reverse faults. In essence, the frontal fault zone consists of a number of trapezoidal blocks bounded by faults which trend either $\sim 120^\circ$ (the aulacogen trend) or about $150-0^\circ$. Assuming that these faults are all basement-seated (as is certainly the case in the Slick Hills), then it is possible that both trends are inherited from a Cambrian framework.

In the Slick Hills, faults with the greatest throw are the Meers ($\sim 10,000$ ft), Blue Creek Canyon (about 1,700–2,400 ft), and Stumbling Bear (as much as 2,300 ft) (Fig. 1). These faults form a basic framework, defining blocks which are characterized by more or less constant internal strain. Thus, in the eastern Slick Hills shortening is about 7–10%, between the Blue Creek Canyon and Stumbling Bear faults it is $\sim 20\%$, and between the Stumbling Bear and Meers faults it appears to be $\sim 50\%$. These figures are based on deformation within blocks and do not apply to shortening across the frontal fault zone as a whole, much of which is due to reverse movements on the faults themselves.

In the western Slick Hills, much of the strain is taken up in a series of parallel folds whose geometry is influenced by the anisotropy of the thinly bedded Arbuckle carbonates. Most folds exhibit sharply defined hinges and planar limbs; flexural slip faulting is common and as a result folds show variable profiles. One such fold, the Paradox anti-

cline in Blue Creek Canyon (Donovan, 1986a), shows at least 23 major adjustments of profile in 1,800 ft of structural relief. These adjustments involve slight changes in plunge and trend; as a result the fold is clearly compartmentalized.

Clearly no single horizon of décollement exists, although the Signal Mountain and lower Mackenzie Hill Formations (the most thinly bedded parts of the Arbuckle Group) appear to have been particularly susceptible to deformation. In essence, the architecture of the more highly deformed parts of the western Slick Hills consists of stacked, compartmentalized folds generated from various surfaces within the carbonate section. This picture is complicated in the hanging wall of the Stumbling Bear fault by a number of complementary thrusts which mimic the fault and have throws of as much as 1,200 ft. As far as can be determined, most of these thrusts sole in the Signal Mountain–lower Mackenzie Hill section. Any discussion of the level of origin of folds is complicated by the fact that in the Blue Creek Canyon area the Carlton Rhyolite is clearly folded in the axis of the Blue Creek anticline, suggesting that the basal unconformity is not a plane of significant slippage.

More than 100 folds with wavelengths of about 500–2,000 ft have been mapped. Most folds are asymmetric and verge NE; some folds have limbs which are overturned by as much as 30° . Where folds are particularly tight, axial-plane pressure-solution cleavage is developed in fold hinges; spacing of this cleavage varies from 1 mm to 5 cm. Three regions of differing fold trend have been recognized:

- 1) Within approximately half a mile of the Meers fault, fold axes trend subparallel to the fault;
- 2) In most parts of the Hills, fold axes trend $10-30^\circ$ clockwise of the fault; in this area some en echelon arrays, most of which are left-handed, are developed;
- 3) In the Blue Creek Canyon area, N-S folds, plunging consistently N, are developed adjacent to the anomalously trending section of the Blue Creek Canyon fault.

Shear zones are a consistent feature of the more intensely deformed part of the Slick Hills. They are typically 2–3 ft across and display en echelon sigmoidal arrays of subvertical solution surfaces (McCoss and Donovan, 1986). The zones are characteristic of major fault traces and are also locally developed along the vertical limbs of tight folds. Preliminary work suggests that the shears are preferentially developed in fine-grained limestones with a relatively high siliciclastic content. Where subparallel to the Meers trend, the sigmoids show a left-lateral sense of shear. Rare zones trending $\sim 20^\circ$ show right-lateral shear.

Discussion of Pennsylvanian Deformation

The character of Pennsylvanian deformation in the southern Oklahoma aulacogen is the subject of considerable debate between those who favor basement-involved thrusting as the primary deformation style (e.g., Ham and others, 1964; Denison, 1982; Brown, 1984) and those who favor left-lateral strike slip (e.g., Wickham and others, 1976; Budnick, 1983). Considerable NE-SW compression, causing shortening across the frontal fault zone, can be inferred from the geometry of both major faults and folds. Transport to the northeast can be inferred both from the relatively small-scale structures in the Slick Hills and from subsurface data (Brewer and others, 1983).

Evidence for left-lateral strike-slip motion is more equivocal, as few convincing piercement points have as yet been identified. Nevertheless, several lines of evidence suggest a component of left-lateral shear: (1) en echelon fold arrays; (2) folds oriented clockwise to the principal (Meers) fault; (3) left-lateral shear zones.

The orientations of folds and shear belts have been analyzed by McCoss and Donovan (1986), using a geometric technique developed by McCoss (1986). They show that displacement vectors for both folds and shears are oriented at $\sim 45^\circ$ to the Meers fault (i.e., $\sim 075^\circ$), suggesting that left-lateral oblique slip (convergent wrench) has taken place on the major faults which bound the aulacogen. These authors also suggest that a minor development of left-lateral faults in the terrain between the Stumbling Bear and Meers faults (oriented $\sim 075^\circ$) can be interpreted as Riedel shears accommodating extension parallel to the aulacogen trend.

The deformation patterns described above suggest that Pennsylvanian deformation in the Slick Hills (and by inference the frontal fault zone) was a response to left-lateral transpressive stress (Fig. 2). Transpression has been modeled by Sanderson and Marchini (1984); predictions from their model which can be tested successfully in the Slick Hills include:

- 1) En echelon folds oriented at low angles of obliquity to principal bounding faults;
- 2) Riedel fractures oriented at relatively high angles to bounding faults;
- 3) Extension fractures oriented at a high angle (but not orthogonal) to major bounding faults; such fractures, oriented $030\text{--}050^\circ$, have been documented by Donovan and others (1987);
- 4) Impressive crustal thickening and vertical uplift have taken place within the frontal fault zone; the importance of a compressive component in the deformation of the Slick Hills is highlighted by oblique back-thrust movement on the Blue Creek Canyon fault; such thickening is not a consequence of simple wrench-type simple shear

(e.g., Wilcox and others, 1973).

5) Minor gentle folds developed on the shallow-dipping limbs of major folds are obliquely oriented clockwise to the trend of the major structure; Sanderson and Marchini (1984) suggested that in such cases the major fold formed first and was subsequently rotated counterclockwise and tightened; assuming constant incremental strain, the newly formed minor folds then developed on flat-lying surfaces at angles similar to the original trend of the major fold.

The tests discussed above can be applied throughout most of the Slick Hills. However, two regions (noted above) require special attention. Close to the anomalously trending (i.e., N-S) section of the Blue Creek Canyon fault, folds trend a few degrees west of north (Fig. 1). We interpret this anomalous area as a compressive bend, oriented at a high angle to the strike-slip component of deformation. Sanderson and Marchini (1984) have suggested that transpression at such bends produces folds at a high angle to the regional trend, in a zone marked by local crustal thickening. In the present case, part of the increased strain in the area is taken up by oblique reverse faulting on both the Blue Creek Canyon and Stumbling Bear faults, some by folding (which involves the Carlton Rhyolite), and part by a considerable amount of pressure-solution cleavage. As noted previously, it is possible that this compressive bend is an expression of an underlying basement framework inherited from Cambrian deformation.

A second area of interest involves the southernmost part of the Hills, where fold trends are almost parallel to the Meers fault. The classic interpretation of this relationship (e.g., Harding, 1976) is that folds in this area have been subject to left-lateral frictional drag, rotating into near parallelism with the fault. Although some folds do appear to have rotated (see above), we have not uncovered evidence to support rotation of this magnitude. An alternative explanation is that the folds in this area formed in a more-compressive regime than that encountered elsewhere. In an analysis of stress adjacent to the San Andreas fault, Mount and Suppe (1987) have suggested that at present this fault is a near-frictionless surface and that consequently the regional transpressive plate motion has decoupled into a low-stress strike-slip component and a high-stress compressive component. As a result, folds and thrusts parallel the fault. The difficulty with this interpretation in the Slick Hills lies in demonstrating that the Meers fault was a frictionless surface. A third explanation is that the subparallelism is a complex boundary effect in which the juxtaposition of the rigid, mechanically homogeneous igneous basement and the highly anisotropic sedimentary sequence resulted in a degree of forced folding in the carbonates.

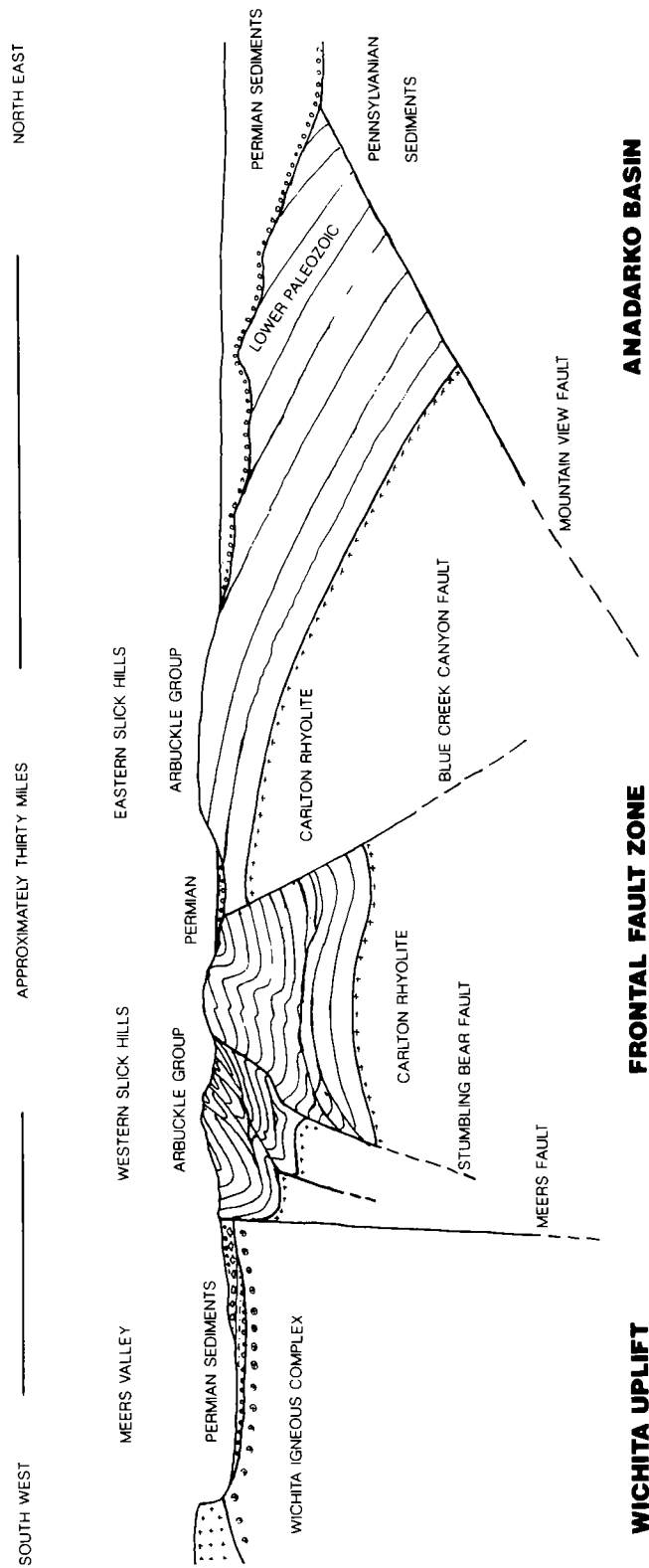


Figure 2. Schematic cross section across the frontal fault zone, showing the relationship between the Slick Hills and adjacent terrain. Not to scale, vertical exaggeration considerable.

THE PERMIAN IMPRINT

One of the difficulties encountered in analyzing the structural imprint in the Slick Hills is in timing of the deformation. As far as we have been able to ascertain, the deformation has a consistent style. Locally, a relative sequencing of events can be determined (e.g., both the Blue Creek Canyon and Stumbling Bear faults cut adjacent folds); absolute timing is not possible. What is clear is that by Leonardian time the Slick Hills had attained their present position relative to surrounding terrains and were exposed to weathering processes.

The evolution of the Permian Meers Valley has been discussed by Bridges (1985), Collins (1985), and Donovan (1986a). Most of the valley is filled with alluvial detritus: conglomerates, sandstones, and shales; however, adjacent to the Meers fault, breccias containing house-size boulders of carbonate are interbedded with pebble conglomerates of similar composition. It is easiest to account for these "megabreccias" by assuming that they are scarp-related detritus produced when the Meers fault reactivated in Leonardian time with a reversed sense of throw (i.e., down to the southwest). The obvious interpretation is that fault movement at this time was normal and perhaps due to stress release; however, many of the clasts found in the megabreccias are derived from the Kindblade Formation (second from top of the six formations of the Arbuckle Group). At the present time, the nearest exposures of this formation are either north of the present watershed of the Slick Hills (itself an inherited Permian feature) or 3 mi northwest along the Meers fault trace. The latter outcrop is the most obvious source for the boulders; it follows that a considerable component of left-lateral motion may have accompanied the Permian movements of the Meers fault.

CONCLUSIONS

The Slick Hills are an exhumed Permian range which constitutes the exposed portion of the frontal fault zone between the Wichita uplift and the Anadarko basin. The Hills, which are built mostly of lower Paleozoic thinly bedded carbonates, bear the imprint of three periods of tectonic deformation:

- 1) A light Cambrian imprint of N-S fractures and small left-lateral faults;

- 2) Comprehensive Pennsylvanian deformation compartmentalized into areas of approximately constant strain by basement-involved framework faults, including the Mountain View, Blue Creek Canyon, Stumbling Bear, and Meers faults; greatest strain is seen between the Blue Creek Canyon and Meers faults, and is manifest as parallel-style folds (more than 100 have been mapped), reverse faults (which sole within the carbonates), and zones of left-lateral shear fabric. Our analysis of the geometric relationships among these structures leads us to suggest that the area was subjected to left-lateral transpression;

- 3) Since early Permian time, the area has been relatively quiescent; breccias containing large (house-size) boulders in the Meers Valley are believed to record rejuvenation of the Meers fault during the Leonardian; this down-to-the-southwest rejuvenation reversed the previous sense of displacement of the fault; modern movements have continued in this mode.

ACKNOWLEDGMENTS

It is a pleasure to acknowledge the continuing support of the Oklahoma Geological Survey throughout the course of this study. R.N.D. is grateful for support from Sun Co. and the Moncrief family. W.R.D.M. appreciates support from N.E.R.C. (United Kingdom).

CONSTRAINTS ON MAGNITUDE AND SENSE OF SLIP ACROSS THE NORTHERN MARGIN OF THE WICHITA UPLIFT, SOUTHWEST OKLAHOMA

DAVID A. McCONNELL
Kansas State University

ABSTRACT.—The magnitude and sense of slip across the northern margin of the Wichita uplift is evaluated by (1) analyzing the suite of structures within the frontal fault zone which separates the uplift from the adjoining Anadarko basin, and (2) palinspastically restoring pre-Mississippian thickness trends between the basin and the frontal fault zone to estimate the magnitude and sense of offset across the uplift-bounding faults.

Deformation within the frontal fault zone is dominated by structural styles similar to those associated with basement-involved shortened terranes, such as the Laramide foreland deformation of the Rocky Mountains. Palinspastic restoration of isopach patterns between the hanging wall (frontal fault zone) and footwall (Anadarko basin) of the Mountain View fault, and restoration of slip on basement faults, provide ratios of left-slip:reverse-slip ranging from 3:1 to 1.4:1.

INTRODUCTION

The Wichita uplift and Anadarko basin are elements within the Ancestral Rocky Mountains (Lee, 1918; Ver Wiebe, 1930), which formed during Carboniferous intraplate deformation of southwestern North America. Recently, there have been differing interpretations of the relative magnitude of lateral and reverse components of slip along the uplift-bounding faults during the Carboniferous deformation (e.g., Kluth and Cooney, 1981; Budnik, 1986). It is necessary to understand the kinematic evolution of individual uplifts within the Ancestral Rocky Mountains in order to understand the evolution of the whole province. This paper focuses upon the magnitude and sense of offset across the northern margin of the Wichita uplift.

In order to determine the relative significance of lateral and vertical offsets, I will (1) describe the structures mapped along 60 mi of the northern boundary of the Wichita uplift, and compare structural styles with those of typical strike-slip and reverse dip-slip terranes, and (2) palinspastically restore the thickness trends across the uplift-bounding faults to place limits on the magnitude and sense of slip between uplift and basin.

The subsurface geology presented herein is based on analysis of data from ~1,500 wells (Fig. 1; McConnell, 1987; McConnell, in prep.). Most (>80%) of this information came directly from the interpretation of well logs; the remainder of the data were taken from well-completion cards (scout tickets). As the density of drilling varies throughout the study area, the description of the structure emphasizes the southeastern part of the

area where well control yields most information on deformation of the sedimentary section.

REGIONAL SETTING OF THE WICHITA UPLIFT

The bimodal suite of igneous rocks which crop out in the Wichita Mountains (Fig. 2, wm) represents the only Cambrian igneous rocks within the southern Midcontinent (Ham and others, 1964; Gilbert, 1982). Deformed lower Paleozoic sedimentary rocks crop out in a series of outlying hills (Slick Hills) to the north of the Wichita Mountains (Fig. 2, sh). These hills have been exhumed from beneath a veneer of post-orogenic Permian sediments which cover >90% of the study area.

The subsurface distribution of Paleozoic stratigraphic units within the Anadarko basin has been discussed by Huffman (1959), Statler (1965), Panhandle Geological Society (1969), Amsden (1975), and Hill (1984). However, few workers (Jordan, 1962) have considered the relative distribution of these units within the frontal fault zone, which separates the Wichita uplift from the basin (Fig. 2).

The Wichita uplift is asymmetric in profile, with a maximum structural relief (change of elevation) of ~7.5 mi between the basement rocks which crop out in the mountains and equivalent rocks in the deepest portion of the Anadarko basin. Relief is an order of magnitude less across the Burch-Waurika-Muenster fault system, which separates the uplift from the Palo Duro (Hardeman) basin to the south (Ham and others, 1964).

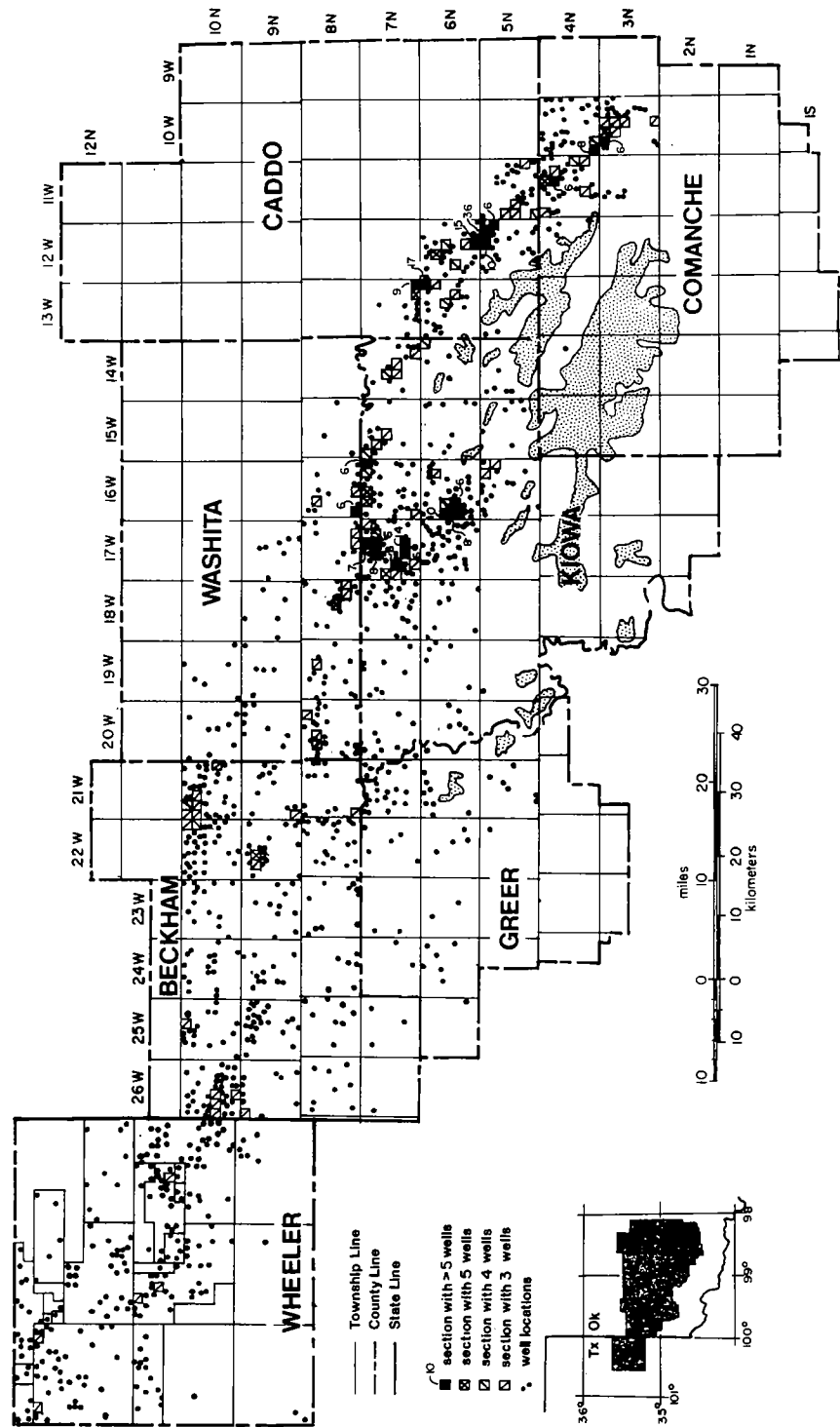
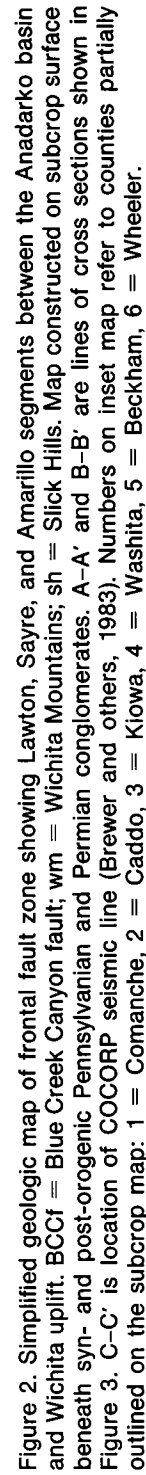


Figure 1. Distribution and density of well control within the area of study. Stippled pattern represents lower Paleozoic outcrop.



A COCORP seismic line across the northern boundary of the Wichita uplift showed a 30–40° SW-dipping fault with reverse separation, which was traced to a depth of 12–15 mi (Brewer and others, 1983). Takken (1968) obtained slightly steeper dips (40–55°) for a shallow (<1 mi deep) portion of the same fault. Within the Wichita Mountains, McLean and Stearns (1986) attributed fracture patterns observed in Cambrian granites to a Carboniferous left-lateral strike-slip regime. Gilbert (1982) showed that several of the boundaries between igneous units, previously mapped as faults (cf. Miser, 1954), are actually non-faulted contacts, and that sheet-like granite sills were deformed into large-wavelength (5-mi), low-amplitude (<300 ft) folds about NW-trending (290°) axes.

DESCRIPTION OF MAP-SCALE STRUCTURES

The Wichita Mountains and the Slick Hills represent portions of two distinct structural elements within southwest Oklahoma: (1) a structurally coherent, uplifted block of basement rocks, and (2) deformed Upper Cambrian–Upper Mississippian sedimentary rocks overlying basement fault blocks. The Wichita Mountains are the outcropping portion of the uplifted basement block. The Cambrian igneous rocks of these mountains are separated by the Meers fault from the deformed Cambrian–Ordovician carbonates of the Arbuckle Group in the Slick Hills. NE-verging folds and thrusts of the Slick Hills (Marchini, 1986; McConnell and others, 1986) are the most extensively exposed structures within the predominantly subsurface frontal fault zone, which is divisible into three parts along strike (Fig. 2). The Lawton segment is the southeastern part of the frontal fault zone, and the only segment in which lower Paleozoic sedimentary and basement rocks crop out at the surface. An upper Paleozoic unconformity lies approximately at sea level and separates Permian units from the underlying deformed pre-Pennsylvanian section. Fewer than 30 wells have drilled into lower Paleozoic sedimentary rocks in the Sayre (central) segment of the frontal fault zone. The unconformity lies 1.2–2 mi below sea level, beneath Middle Pennsylvanian clastic rocks. The Amarillo segment is the northwestern part of the frontal fault zone, and is located almost entirely within the Texas Panhandle. An erosional surface ~2.5 mi below sea level separates Lower Pennsylvanian rocks from deformed Ordovician–Mississippian units.

Only the structures within the Lawton segment will be discussed herein. Similar features are present, though less thoroughly investigated by

drilling, in the Sayre and Amarillo segments (McConnell, 1987).

Lawton Segment

The northern boundary of the frontal fault zone is represented by the Mountain View fault system, and the southern boundary by the Meers fault (Fig. 2). The combination of field and subsurface data within the Lawton segment of the frontal fault zone provides an opportunity to analyze structures in more detail than would be possible solely from subsurface mapping.

Within the Slick Hills, the Blue Creek Canyon fault (Fig. 2, BCCf) can be traced along strike for >25 mi, bisecting the Slick Hills and juxtaposing Cambrian basement rocks (Carlton Rhyolite) of the eastern Slick Hills against Cambrian–Ordovician sedimentary rocks (Timbered Hills and Arbuckle Groups) to the west. The sedimentary rocks constitute a thick, layered sequence of micritic limestones. Flow layering within the rhyolite parallels bedding in the gently dipping limestones of the eastern Slick Hills (Ham and others, 1964).

The western Slick Hills are structurally complex in comparison with the homoclinal dips recorded for most of the eastern Slick Hills (Marchini, 1986). Trains of NE-verging folds and thrusts exhibit a subparallel alignment with the Meers fault and Blue Creek Canyon fault (McConnell and others, 1986). Individual folds can be traced as far as 3.8 mi within the western Slick Hills and have a parallel-fold geometry with planar limbs and narrow hinge zones.

Northwest of the Slick Hills, in sec. 3, T. 6 N., R. 14 W., the Wagner and Brown #1 Traub well drilled through a NE-dipping panel of Arbuckle Group rocks and penetrated >2.5 mi of basement rocks in the hanging wall before passing again into carbonates (Arbuckle Group?) in the footwall (Fig. 3A). Thirty-four wells have been drilled through the fault plane and are interpreted to indicate a consistent SSW dip of 40° for the fault (Figs. 3A,4). Wells which penetrated the footwall at shallow elevations (<1.25 mi below sea level) encountered overturned and folded Upper Mississippian–Lower Pennsylvanian shales and sandstones (Fig. 3A; Takken, 1968). There is little control on the character of deformation in the footwall of the Mountain View fault (Fig. 3A). However, regardless of present footwall configurations, the top of basement must be restorable to the structural level of equivalent rocks in the adjacent basin; thus, total reverse separation across the Mountain View fault is ~8 mi in the line of cross section A–A' (Figs. 2,3A).

Southeast of the Traub well, in sec. 19, T. 5 N., R. 11 W., the Exxon #1 Apache well drilled through a thick section of Arbuckle Group lime-

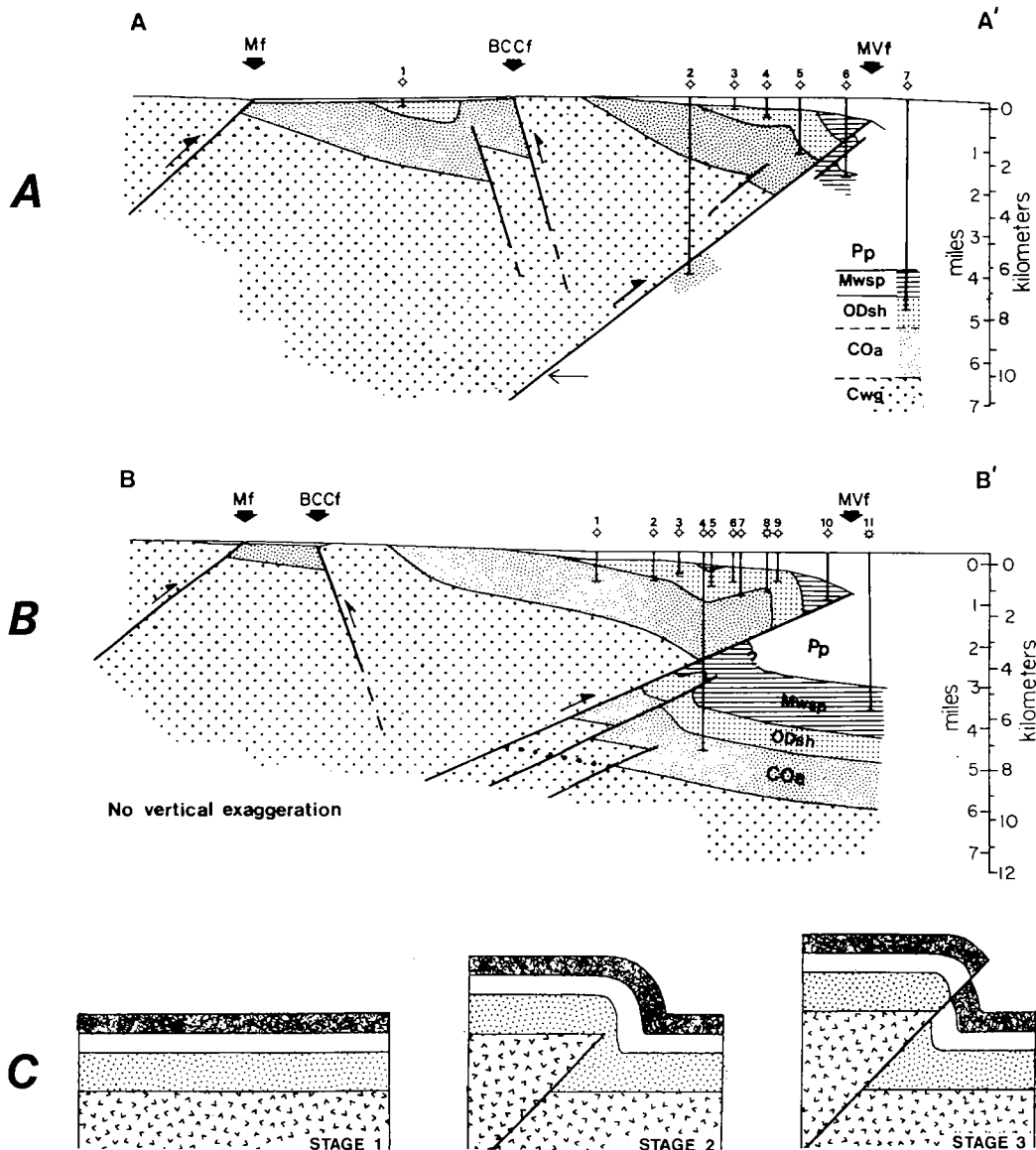


Figure 3. Cross sections through the Lawton segment of the frontal fault zone (lines of sections shown on Fig. 2). MVf = Mountain View fault system; BCCf = Blue Creek Canyon fault; Mf = Meers fault. Stratigraphic abbreviations as shown in Figure 2, plus Cwg = Cambrian igneous rocks, Pp = Pennsylvanian-Permian). A—Arrow in footwall indicates approximate position of the footwall cutoff for the top of basement after footwall units are restored to subhorizontal configuration; reverse slip component for fault estimated as length of fault between basement cutoffs in hanging wall and footwall. Wells used to construct cross section: 1 = Pope and Rainey #1 Rushton; 2 = Wagner and Brown #1 Traub; 3 = Thermodyne #2 Pahpotamah; 4 = Amerada #1 Mitchell; 5 = Conoco #1 Giles; 6 = Sohio #1

Morrow; 7 = Forest #1 Tahpoodle. B—Wells used to construct cross section: 1 = Skelly #1 Moore; 2 = Sun #1 Hiers; 3 = Sun #1 Imach; 4 = Exxon #1 Apache; 5 = Western Division Industries #1 Tarrant; 6 = Lubell #1 Asepermy; 7 = Reed #1 Yellowfish; 8 = Core #1 Takewa; 9 = Texaco #1 Strat; 10 = Rock Island #1 Reiss; 11 = Samson #1 Mindemann. C—Line drawing illustrating proposed evolution of uplift. Stage 1, prior to deformation; stage 2, initial slip on basement faults, folding of sedimentary rocks to form a monocline; stage 3, fold in sedimentary rocks is cut by mountain-flank thrust, continued shortening in both basement and sedimentary rocks accommodated by displacement on uplift-bounding faults.

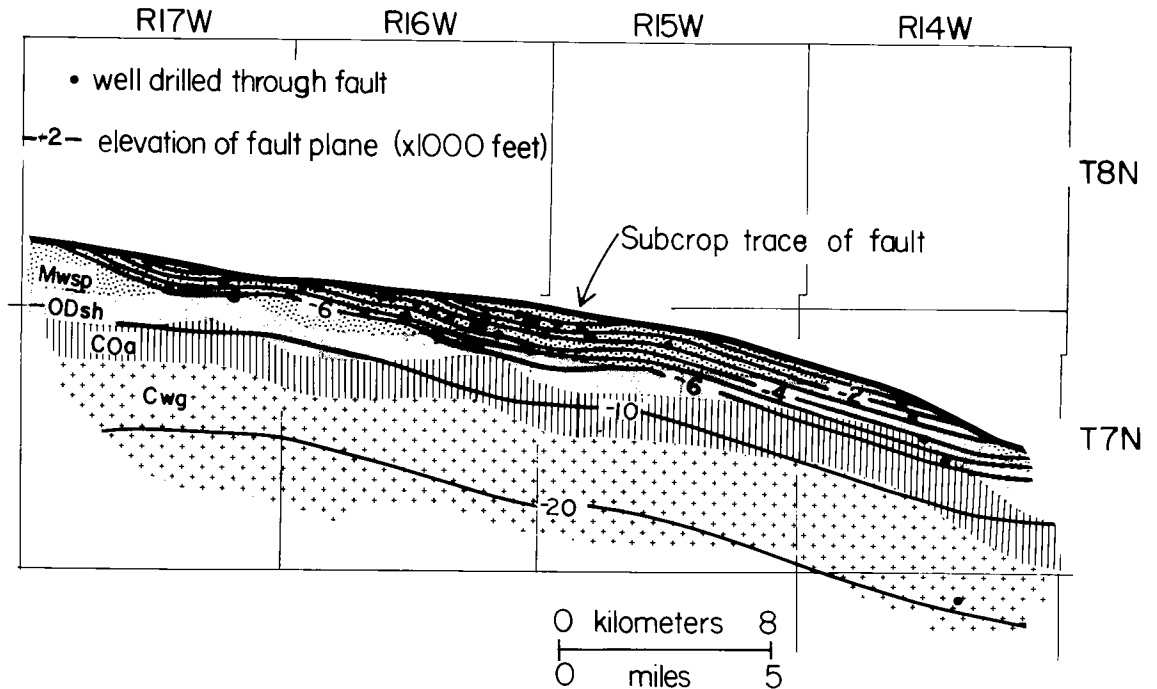


Figure 4. Structure-contour and subcrop map on Mountain View fault. Subcrop map represents hanging-wall cutoffs on the fault plane. For location, see Figure 2. Stratigraphic abbreviations as in Figures 2 and 3.

stones and crossed a major frontal fault into folded and faulted Ordovician–Mississippian units (Fig. 3B). A fold pair is defined in the hanging wall of the Mountain View fault system (Figs. 2,3B). These asymmetric folds show a NE vergence and a NW plunge. Wells penetrating the most basinward limb of the anticline drilled through panels of sedimentary rocks which show apparent thickening of as much as 600% due to the effects of a steep NE dip. The frontal structures represent a minimum total reverse separation on basement faults of 4.4 mi in cross section (Fig. 3B).

INTERPRETATION OF MAPPED STRUCTURES

Structural assemblages often can be used to gain insight into the tectonic evolution of a region (Harding and Lowell, 1979). However, the structures alone cannot give an indication of the absolute magnitude of displacements within a zone of deformation such as the frontal fault zone. Given the contrasting tectonic hypotheses for intraplate deformation, the thrust-like character of the northern margin of the Wichita uplift (Brewer

and others, 1983) can be used to argue for (1) reverse dip-slip, basement-involved thrusting similar to that of the Wind River uplift, Wyoming (Smithson and others, 1978); (2) oblique-slip as either reverse left-slip (Marchini, 1986) or left-handed reverse-slip (McConnell and others, 1986); or (3) a combination of separate episodes of left-slip and reverse dip-slip faulting (Brewer and others, 1983).

Major strike-slip systems commonly possess an associated suite of structures which include echelon folds, Riedel shear arrays, secondary normal and thrust faults, and a through-going, linear–curvilinear fault trace (Wilcox and others, 1973; Christie-Blick and Biddle, 1985). Some of these structural features are shared by shortened terranes, the principal difference being the alignment of folds and secondary faults relative to the primary (master) fault. Within strike-slip regimes, folds and faults normally are oriented oblique (30°) to the primary fault, whereas secondary folds and faults parallel the primary fault within a reverse-slip regime (Harding and Lowell, 1979).

Deformation within the Lawton segment of the frontal fault zone is characterized by (1) asymmetric, NE-verging folds along the basinward margin of the frontal fault zone (Figs. 2,3); (2)

structural thickening of sedimentary rocks in the hinges of these anticlines due to thrusting (McConnell and others, 1986; McConnell, 1987); (3) steepened and/or overturned panels of sedimentary rocks marking the transition from the frontal fault zone to the basin (Fig. 3); and (4) S- to SW-dipping, basement-involved faults with reverse separations (Figs. 3,4).

Both the consistent steepening of dips and the presence of folds which parallel the leading edge of the frontal fault zone have been interpreted to indicate that the sedimentary section initially formed an unbroken monoclinical fold over faulted steps in basement (Fig. 3C). The fold was subsequently breached by mountain-flank thrusts which propagated upward from the basement faults (McConnell and others, 1986). Similar deformation sequences have been proposed for the interaction of basement rocks and sedimentary rocks in the Rocky Mountain foreland (Berg, 1962; Schmidt and Garihan, 1983).

An interpretation of a COCORP seismic-reflection line across the Sayre segment (Fig. 2, line C-C'; Brewer and others, 1983) yields a basement fault geometry similar to that described here for the frontal faults of the Lawton segment.

The folds, steeply overturned panels of sedimentary rocks, and reverse separations on basement-involved faults can all be interpreted as evidence that the frontal fault zone represents a zone of shortening of the upper crust between the Wichita uplift and the Anadarko basin. In contrast, there are few structures recognized within the frontal fault zone which can be used as *a priori* evidence for left-slip on the frontal faults. However, the obvious component of reverse-slip on the uplift-bounding faults (Fig. 3) may mask components of strike-slip within the frontal fault zone. In the following section, I summarize previous interpretations of lateral offsets associated with the Wichita uplift, and undertake a palinspastic restoration of thickness trends between the frontal fault zone and basin to investigate the significance of strike-slip offsets across the leading edge of the frontal fault zone.

CARBONIFEROUS TECTONISM OF THE WICHITA AND AMARILLO UPLIFTS

Regional Deformation in Southern Oklahoma and the Texas Panhandle

Several authors have suggested that the formation of the Wichita uplift was related to lateral displacements along the preexisting (Early Cambrian) trend of the southern Oklahoma aulacogen. These interpretations have been based upon (1) analogy with slip on faults within the

Arbuckle Mountains to the southeast (Wickham, 1978a; Budnik, 1986; see also Tanner, 1967; Booth, 1981; Brown, 1984); (2) examination of structural patterns observed within the frontal fault zone (Evans, 1979) and Wichita Mountains (McLean and Stearns, 1986); (3) plate-tectonic models for the development of the Gulf of Mexico (Pindell, 1985) and the Ouachita orogen (Viele, 1986); and (4) palinspastic reconstructions of isopachs and erosional patterns across the Amarillo uplift (Budnik, 1986).

Map patterns of mesoscopic structures adjoining the Washita Valley fault in the Arbuckle Mountains (Booth, 1981) have been interpreted to indicate left-lateral displacement on the fault. Tanner (1967) and Brown (1984) have offered alternative explanations for the offset of Simpson Group isopach patterns across the fault, by left-slip and by reverse-slip, respectively. Although the sedimentary and basement rocks involved in the Arbuckle and Wichita uplifts are similar, their tectonic settings, relative to the Ouachita foreland, vary significantly. The Arbuckle Mountains are located near the margin of the foreland, at a change in trend of the Ouachita orogen, whereas the Wichita Mountains are located farther into the foreland. Caution must therefore be exercised in drawing analogies between these areas with respect to character of deformation.

Fracture orientations within the granites of the Wichita Mountains were interpreted by McLean and Stearns (1986) to represent the response of the granitic sills to a Carboniferous left-lateral shear couple. Fracture maxima at 275° and 360° define a suborthogonal array which McLean and Stearns (1986) interpreted as Y- and X-shears (Bartlett and others, 1981) from a typical Riedel shear array.

Pindell (1985) highlighted NW-trending fault arrays on the northern boundary of the Wichita uplift and interpreted these patterns to suggest that the uplift experienced Carboniferous *right-lateral* offsets, as an element within a tectonic collage bounding the southern margin of the North American continent. However, Pindell did not present any evidence in support of this conclusion. Evans (1979) interpreted structural assemblages within the frontal fault zone as indicative of left-slip along NW-trending faults within the frontal fault zone. Viele (1986) proposed a model which would place a major (95-mi) left-lateral offset along the southern margin of the Wichita uplift. A geometric requirement of this model would be a N-S-trending zone of crustal stretching located at the western end of the Wichita-Amarillo uplift. Viele (1986) suggested that the depositional basins of the Ancestral Rocky Mountains may have represented this zone of extension.

Budnik (1986) presented evidence for Carbon-

iferous left-lateral slip along the Wichita megashear, which he recognized as a NW-trending lineament extending from southern Oklahoma to Utah. Budnik's analysis was based upon the palinspastic restoration of Arbuckle Group isopachs and a pre-Mississippian erosion surface across the Amarillo uplift. He interpreted offsets in these patterns between the Palo Duro and Anadarko basins to be the result as much as 95 mi of left-lateral displacement along the megashear, but he did not specify how much displacement was accommodated along individual fault systems. The frontal fault zone would represent the most northerly element of the Wichita megashear in Texas and Oklahoma.

Although most of the authors cited above shared the view that left-slip took place along the bounding faults of the Wichita uplift, the magnitude of the slip component between the uplift and the Anadarko basin has remained unresolved.

Palinspastic Restoration of the Hunton Group, Southwest Oklahoma

Isopach maps have been constructed for several Paleozoic units within the Anadarko basin (Huffman, 1959; Statler, 1965; Panhandle Geological Society, 1969; Hill, 1984), but none of these included data available from the frontal fault zone. Amsden (1975) analyzed cores and samples of Hunton Group (Late Ordovician-Devonian) rocks from nine wells within the frontal fault zone, but noted that the thicknesses in these wells are inaccurate due to structural complications. The distribution and thickness of the Hunton Group is constrained in the Anadarko basin (Amsden, 1975), whereas stratigraphically lower units have seldom been penetrated in the deeper portion of the basin adjoining the frontal fault zone. The thickness of the Hunton Group varies from 200–1,600 ft along strike within both the basin and the frontal fault zone (Fig. 4). The complete thickness of the Hunton Group is penetrated by more than 200 wells within the frontal fault zone; many of these wells were drilled in the Apache field (T. 5–6 N., R. 12 W.; Fig. 1). More than 100 additional wells drilled through a partial (minimum) thickness. Overlying Mississippian strata were originally distributed on a broad carbonate shelf (Craig and others, 1979) and exhibit less-substantial thickness changes along strike than the Hunton Group. Also, fewer complete sections of these Mississippian units are preserved within the frontal fault zone.

Thicknesses of the Hunton Group in wells within the Oklahoma portion of the Anadarko basin were taken from Amsden (1975) and augmented with some recent (post-1975) wells. Hunton thicknesses within the frontal fault zone and

the Texas Panhandle were determined for this study (Fig. 5). Drilled thicknesses have been corrected for the influence of dip and structural repetition to yield true thicknesses. Prior to palinspastic restoration, a broad correlation of thicknesses is observed between the basin and the frontal fault zone (Fig. 5). The Hunton Group is >1,000 ft thick between R. 13 W. and R. 26 W. in the frontal fault zone, and between R. 15 W. and R. 26 W. in the basin.

Palinspastic restorations require that the offset along the uplift-bounding faults be removed in order to juxtapose correlative patterns within the basin and frontal fault zone at a comparable structural level. The first step in the palinspastic restoration of the Hunton Group isopach patterns is the removal of the slip across the frontal faults which cut the sedimentary section. The second step is the removal of the remaining reverse separation on the basement faults, this separation being represented within the sedimentary section by folding.

Crowell (1959, p. 2653) defined slip on a fault as "the relative displacement of formerly adjacent (piercing) points on opposite sides of a fault." Piercing points are recognized where lines such as isopachs intersect a fault surface. Fault dip, and the elevation and location of piercing points in the hanging wall and footwall, must be known to completely define fault slip.

The dip of the Mountain View fault between R. 14 W. and R. 17 W. is defined by drilling as 40° SSW (Fig. 4). The Hunton Group dips gently (<2°) S within the Anadarko basin adjoining the frontal fault zone (Fig. 6), but reverses dip direction beneath the frontal faults as Hunton Group rocks must intersect the Mountain View fault above the elevation of the Arbuckle Group (Fig. 3A). A line of intersection between the top of the Hunton Group in the footwall and the plane of the Mountain View fault can be defined at an elevation of –16,000 to –17,000 ft (Fig. 6). Footwall piercing points for the 900- to 1,200-ft Hunton Group isopachs are projected to intersect the fault surface along this line. Piercing points in the hanging wall must lie along the mapped fault trace in T. 7 N., R. 14–15 W. at elevations of –500 to –6,000 ft (Fig. 4). Fault slip is represented by a line joining equivalent piercing points in the hanging wall and footwall (Fig. 7).

Variables involved in the calculation of fault slip are fault dip, the elevation of the Hunton Group in the frontal fault zone and basin, and the trend of the Hunton Group isopachs (Figs. 4–6). Using well control, the first two parameters can be constrained to fall within relatively narrow limits (Figs. 4,6); however, subtle variations in the trends chosen for the isopachs may alter the relative magnitudes of the left- and reverse-slip components of fault slip (Figs. 5,7). The trends of Hunton Group isopachs within the eastern part

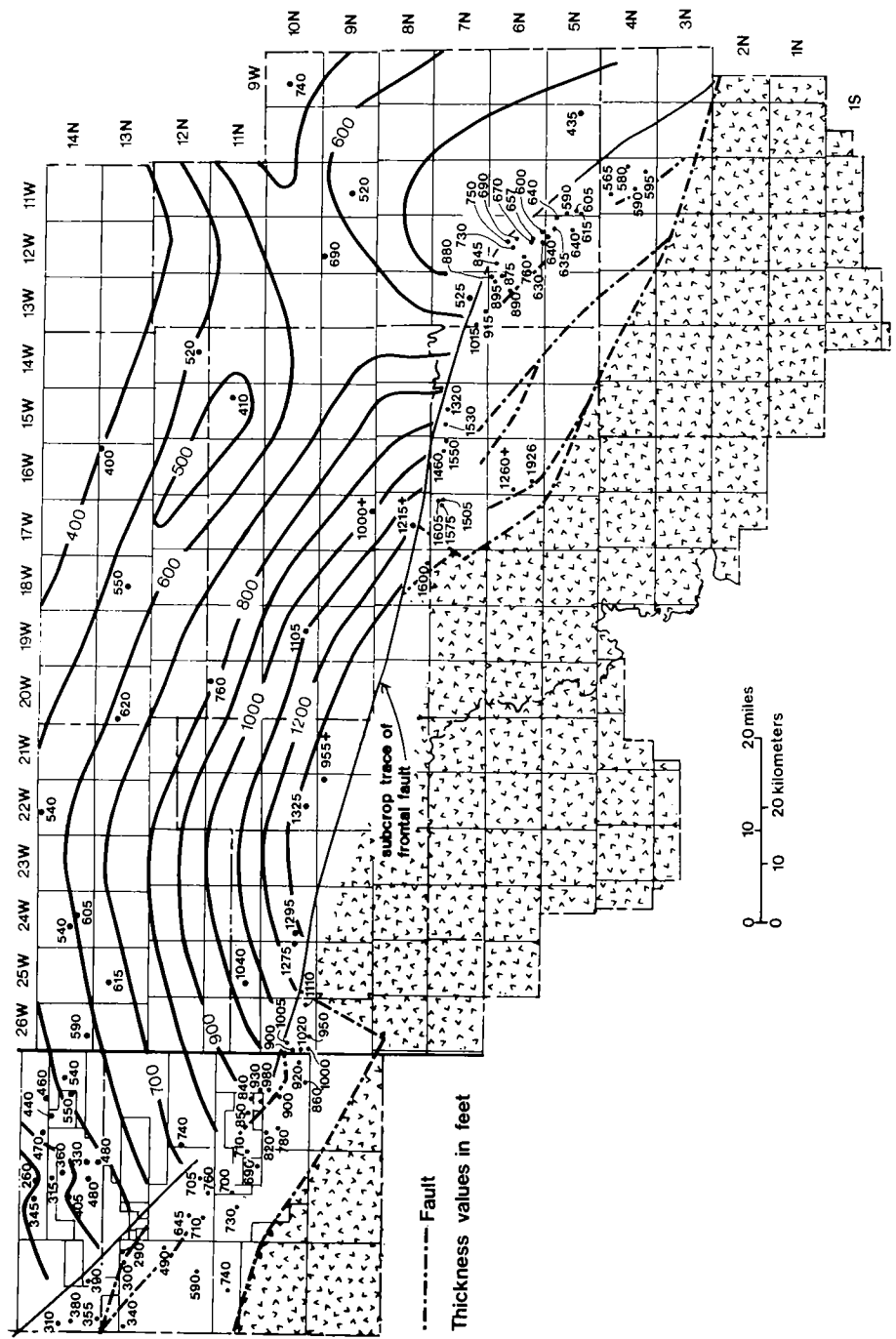


Figure 5. Isopach map of the Hunton Group in the Anadarko basin, and distribution of representative thicknesses of the Hunton in the frontal fault zone. Thicknesses have been corrected for the effects of dip and structural repetition. A majority of the thicknesses recorded from the Anadarko basin in Oklahoma were taken from Amsden (1975). Pattern in southern half of figure corresponds to the Wichita uplift.

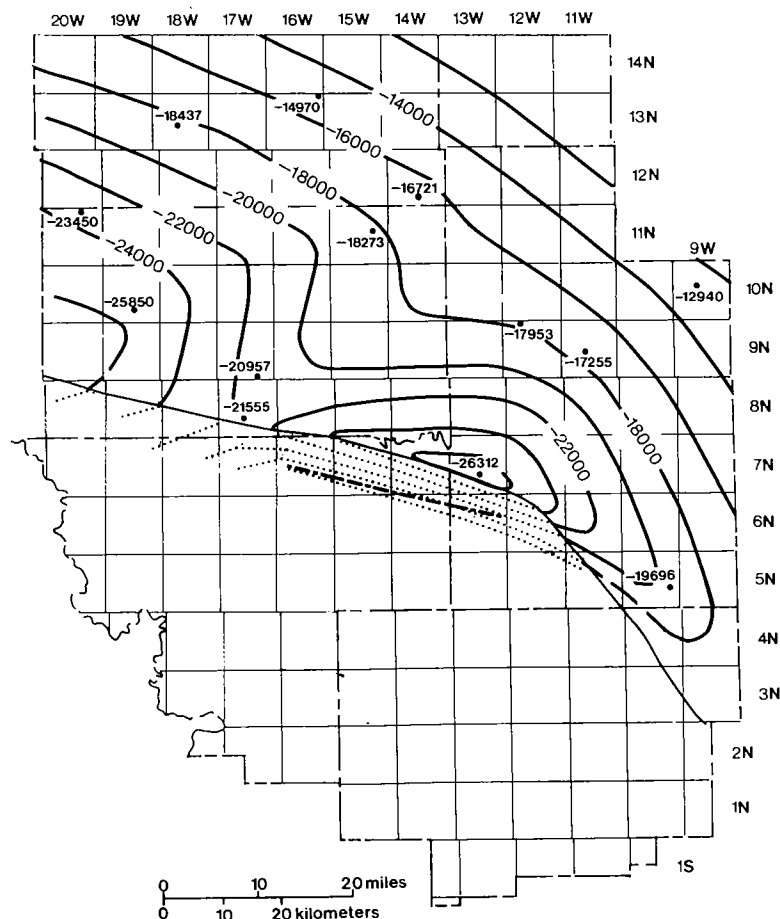


Figure 6. Structure contour map on top of the Hunton Group within the eastern Anadarko basin. Elevations in feet; structure contours shown as dotted lines where they lie below the Mountain View fault plane. Dashed line represents the intersection of the fault with the top of the Hunton Group.

of the deep Anadarko basin are primarily controlled by information taken from four wells (Forest #1 Tahpoodle, sec. 27, T. 7 N., R. 13 W.; PCX Corporation #1 Koper, sec. 28, T. 8 N., R. 17 W.; Phillips #1-A Wesner, sec. 35, T. 9 N., R. 17 W.; Lone Star #1 Rogers, sec. 27, T. 10 N., R. 19 W.). The #1 Koper and #1-A Wesner wells did not penetrate a complete thickness of the Hunton Group, but sample descriptions (#1-A Wesner; Amsden, 1975) and log signatures (#1 Koper) are interpreted to indicate that both wells reached the Chimney Hill Subgroup, the basal unit of the Hunton Group (Amsden, 1975). Consequently, the thicknesses in these wells are regarded as minima (Figs. 4,7A). Increasing these values would alter the trend of the isopachs and shift the footwall piercing points to the east (Fig. 7B), thus yielding a lower value for the lateral component of slip. Regardless of which configuration is chosen, the slip on the fault was oblique

(reverse left-slip). The relative magnitudes of the left- and reverse-slip components range from 3:1 (14.5:4.5 mi; Fig. 7A) to 2:1 (9.5:4.5 mi; Fig. 7B), and in both cases slip was ENE (080-090°).

The sedimentary section is restored to an intermediate structural configuration by the restoration of fault displacements in the Hunton Group (Fig. 3C, stage 2). Slip on the Mountain View fault system is therefore considered in two parts: (1) slip which offset the Hunton Group (stage 3); and (2) an initial episode of slip on the basement faults, which resulted in folding of the Hunton Group strata (stage 2). To completely determine the magnitude of slip across the frontal fault zone, the total slip on the basement faults must be removed to restore the sedimentary section to its presumed initial configuration (Fig. 3C, stage 1). An initial reverse-slip component of 2.2 mi is estimated for the Mountain View fault. This is calculated by subtracting the component of re-

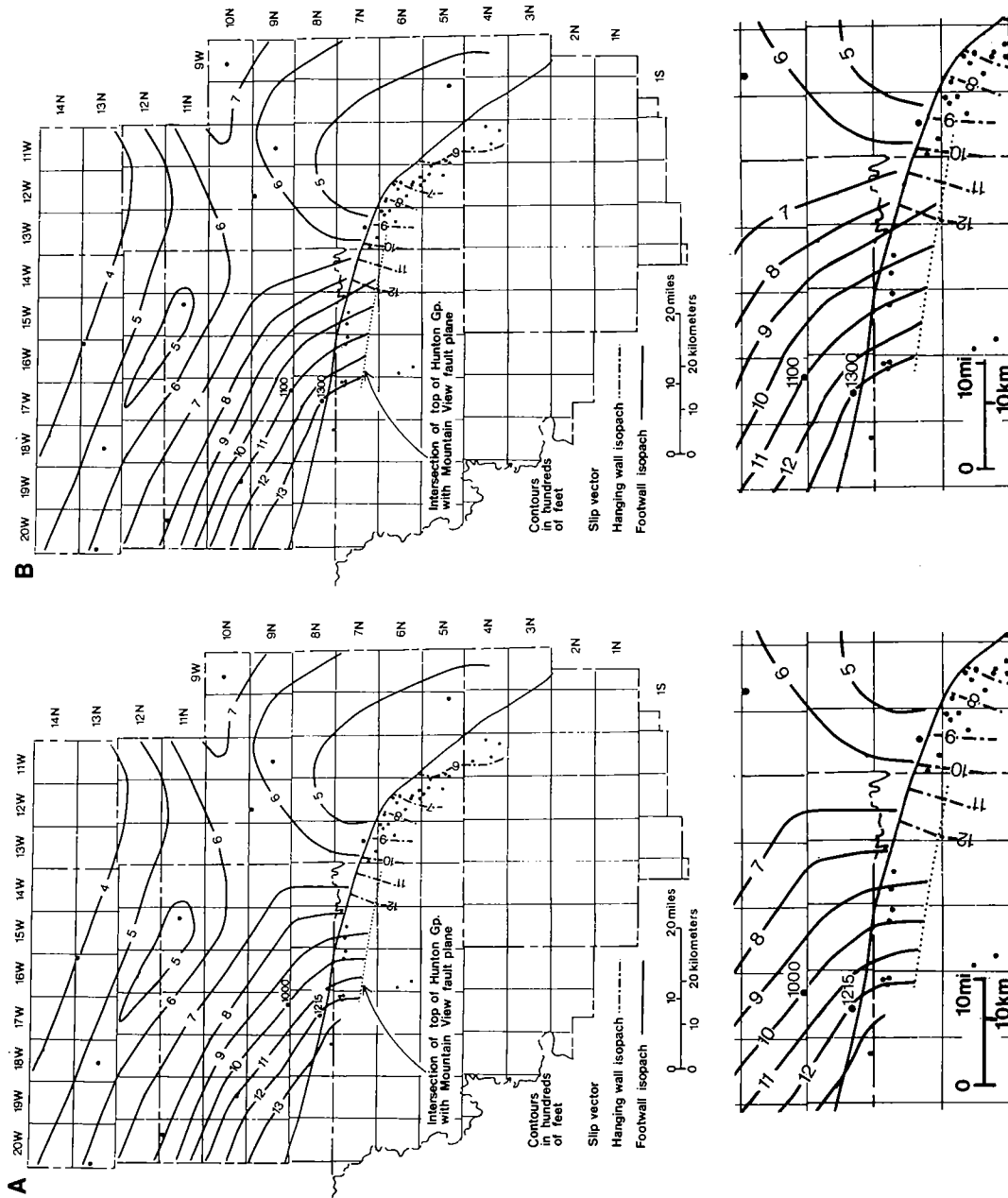


Figure 7. Slip vectors indicating sense of offset of isopachs in footwall and hanging wall of the Mountain View fault. A—Isopachs in basin constructed from minimum thickness values for #1-A Wesner and #1 Koper wells. B—Isopachs in basin constructed from greater estimated thicknesses for the same wells (see text for discussion). Rectangular boxes outlined by heavy lines in A and B are shown at larger scale below.

verse-slip represented by the offset of the Hunton Group (4.5 mi) from the reverse separation measured between the hanging wall and (projected) footwall cutoffs for the top of basement on cross section A-A' (Fig. 3A).

The remaining slip on the basement faults was removed assuming three different slip ratios: (1) a left-slip:reverse-slip ratio of 3:1 (Fig. 7A), (2) a left-slip:reverse-slip ratio of 2:1 (Fig. 7B), and (3) solely reverse-slip. Each ratio is representative of a different kinematic model for the initial evolution of the uplift. This yields left-slip components of 6.6 mi, 4.4 mi, or 0 mi, respectively, for the three slip ratios.

DISCUSSION

The magnitude of the component of left-slip across the Mountain View fault is dependent upon the choice of isopach pattern and upon the interpretation of the initial kinematic evolution of the frontal fault zone. The maximum calculated left-slip is 21 mi, and the minimum is 9.5 mi. The magnitude of the reverse-slip component does not change much with variations in isopach trends, and is independent of the interpretation of the kinematic development of monoclinial folds. Total reverse slip is ~6.7 mi; therefore, the possible range for the ratio of left-slip:reverse-slip is 3:1 to 1.4:1.

Thus, a significant component of left-slip can be documented across the leading edge of the frontal fault zone, and this must be reconciled with the observation that few of the structures which are considered typical of strike-slip environments (Wilcox and others, 1973) can be recognized in the frontal fault zone. A possible explanation is that there were two separate episodes of displacement on the uplift-bounding faults. During the first episode, reverse-slip was dominant, whereas during the second episode left-slip took place. Folds and secondary thrust and normal faults typically form in sedimentary rocks prior to the development of a through-going strike-slip fault (Wilcox and others, 1973). The sequential development of these structures may have been prevented if the sedimentary rocks were breached by a reverse-slip fault which then was reactivated as a left-slip fault.

Although there is a recognizable component of left-slip associated with the evolution of the fron-

tal fault zone, the amount of slip is an order of magnitude less than that proposed by Budnik (1986) for the Wichita megashear. It is noted that Budnik (1986) did not restrict lateral offsets to fault zones on the northern margin of the Wichita and Amarillo uplifts, but simply attributed separations to displacement within the megashear. However, the northern margin of the Wichita uplift is the most significant Carboniferous structural discontinuity within the Ancestral Rocky Mountains; as such, it would be expected to reflect the regional deformation style. If there is an alternative site of left-slip within the Wichita megashear, the most probable location is along the southern margin of the uplift, as inferred by Viele (1986). There are no published attempts to measure the sense and magnitude of slip across this margin.

CONCLUSIONS

The following points are summarized from this study:

- 1) Structures within the frontal fault zone are typical of those associated with a basement-involved shortened terrane. The structural assemblage consists of (i) asymmetric folds along the leading edge of the frontal fault zone; (ii) steepened to overturned panels of sedimentary rocks marking the transition from the frontal fault zone to the basin; (iii) S- to SW-dipping, basement-involved reverse faults.

- 2) Palinspastic restorations of the Late Ordovician-Devonian Hunton Group are used to infer ENE-directed oblique-slip on the Mountain View fault system. The oblique-slip can be broken down into components of left-slip (9-21 mi) and reverse-slip (6.7 mi).

- 3) The left-slip component is an order of magnitude smaller than that proposed in some previous models of Carboniferous intraplate deformation within Texas and Oklahoma (Budnik, 1986).

ACKNOWLEDGMENTS

Discussions with R. Nowell Donovan and M. Charles Gilbert have fueled my interest in the tectonic evolution of southwestern Oklahoma and have helped to define some of the problems discussed herein.

HORIZONTAL STRESSES FROM WELL-BORE BREAKOUTS AND LITHOLOGIES ASSOCIATED WITH THEIR FORMATION, OKLAHOMA AND TEXAS PANHANDLE

RICHARD L. DART

U.S. Geological Survey, Denver

Abstract.—Orientations of crustal stresses are inferred from stress-induced well-bore breakouts in three areas in the south-central United States: the eastern part of the Anadarko basin in central Oklahoma, the Marietta basin in south-central Oklahoma, and the Bravo dome area of the central Texas Panhandle. Inferred directions of maximum horizontal principal stress (SH_{max}) are ENE for the eastern Anadarko basin, and NE for the Marietta basin and the Bravo dome area.

For the Bravo dome area, the magnitudes of the three principal stresses (S_1 , S_2 , S_3) are known from existing hydraulic-fracturing (hydrofrac) measurements, and a normal-faulting stress regime ($S_V > SH_{max} > SH_{min}$) is implied. For the eastern Anadarko basin and the Marietta basin, the magnitudes of the principal stresses are not known. Because Quaternary left-lateral oblique slip on the Meers fault in south-central Oklahoma suggests strike-slip ($SH_{max} > S_V > SH_{min}$) and reverse faulting ($SH_{max} > SH_{min} > S_V$), the study region is inferred to be a possible transition zone between areas of extensional and compressional stresses.

Breakout data from the eastern Anadarko basin yield a single consistent SH_{max} orientation. Data from the Marietta basin and the Bravo dome area have bimodal-orthogonal distributions consisting of breakouts and orthogonal sets of well-bore enlargement orientations. Orthogonal trends in the data are probably related to drilling-induced hydraulic fracturing of the well bore, or to preexisting natural fractures or joint sets intersecting the well bore. On the dipmeter log, breakouts and fracture enlargements have elliptical cross sections of similar size and shape. Orthogonally oriented well-bore enlargements are differentiated by comparing their long-axis orientations with directions of known or inferred horizontal stress.

Dispersion, or data scatter, among enlargement orientations (bimodal data sets) increases the standard deviations for many well data sets from the Marietta basin and the Bravo dome area. In these two areas, some dispersion may reflect variation in stress conditions across fault-bounded blocks and the orientations of fractures or joints within these blocks.

Although breakouts and fracture enlargements formed in all parts of the thick sequences of sedimentary rocks logged, they occurred primarily in limestone, shale, and dolomitic rocks, reflecting the abundance of these rock types in the study areas.

INTRODUCTION

Numerous borehole field studies (Cox, 1970; Bell and Gough, 1979,1982; Gough and Bell, 1981,1982; Hickman and others, 1985; Plumb and Hickman, 1985; Teufel, 1985; Zoback and others, 1985) and theoretical and laboratory studies simulating borehole stress conditions (Mastin, 1984; Haimson and Herrick, 1985; Zoback and others, 1985) have shown well-bore breakouts to be (1) stress-induced spall zones that typically elongate vertically within the well bore; (2) the result of compressional shear failure of the well bore, associated with unequal horizontal compressive stresses about the well bore; (3) elliptical in cross section; and (4) aligned in the direction of minimum horizontal compressive stress (SH_{min}). The idea that breakouts reflect local in situ stress conditions is supported by the agreement among stress directions inferred from

breakouts and stress orientations from studies using other types of stress data, i.e., earthquake focal mechanisms, hydrofrac measurements, and geologic indicators of stress (Gough and Bell, 1981,1982; Hickman and others, 1985; Plumb and Hickman, 1985; Dart and Zoback, in press).

Breakout-data analysis is an important tool in understanding present-day stress conditions in areas where more-detailed stress measurements may not have been made. An understanding of in situ stress conditions is essential in evaluating seismic hazard, recent crustal deformation, and the potential for slip on existing faults. In the petroleum industry, knowledge of borehole stress conditions can be critical in the engineering and design of the drilling operation and hydrofrac treatment (Dart and Zoback, in press).

The three areas of interest (the eastern Anadarko basin, the Marietta basin, and the Bravo dome area) were selected for study on the basis of

data availability, their proximity to the Anadarko basin, and their involvement in the structural and tectonic evolution of Oklahoma and the Texas Panhandle. This paper offers a more-detailed analysis of data presented in earlier reports (Dart, 1987; Dart and Zoback, 1987).

GEOLOGIC SETTING

Located on the boundary between the Great Plains and Central Lowlands physiographic provinces, the study region (Fig. 1) is an area of deep sedimentary basins filled with thick sequences of Paleozoic marine rocks, separated by uplifted basement structures of Cambrian and Precambrian igneous and metamorphic rocks (Jordan, 1967; Johnson and others, 1972; Johnson and Denison, 1973; Johnson and others, 1984). The primary WNW structural trend of basins and basement highs, extending across southern Oklahoma into the Texas Panhandle, developed throughout the Paleozoic Era during periods of basement faulting, igneous intrusion, basin subsidence, and orogenic deformation (Ham and others, 1964; Hoffman and others, 1974; Wickham, 1978a; Perry, in press). The stratigraphic history of the region appears to be dominated by episodes of carbonate and shale deposition attributed to eustatic fluctuations and intervals of clastic deposition associated with subareal erosion of uplifted areas.

The eastern Anadarko basin underlies most of central Oklahoma (Figs. 1,2). The study area is bounded on the south by the Amarillo-Wichita uplift, the Marietta and Ardmore basins, and the Arbuckle uplift, and on the east by the Nemaha ridge. The frontal fault system forms a reverse-faulted zone of detachment separating the Anadarko basin on the north from the Amarillo-Wichita uplift (Gilbert, 1983c; Perry, in press). The deepest part of the basin occurs along this boundary, where an accumulation of >40,000 ft of Paleozoic sediments forms the most complete Paleozoic section in the Midcontinent structural province (Adler, 1971). This Cambrian to Permian section is composed of two major rock types: Cambrian to Mississippian carbonates, and shales unconformably overlain by Pennsylvanian to Permian clastic sediments (Petroleum Information Corp., 1982). The lower part of this section was formed during a period of shallow marine deposition and rapid basin subsidence (Feinstein, 1981); the upper part of the section was deposited in response to the erosion of the Amarillo-Wichita and Criner uplifts south and east of the basin (Moore, 1979). Faulting along the eastern and southern boundaries of the basin occurred during formation of the Amarillo-Wichita uplift and in response to compressional tectonics associated with uplift of the Ouachita

Mountains and Nemaha ridge (Fig. 1; Gilbert and Donovan, 1982; Burchett and others, 1985). Ramelli and others (1987) and Luza and others (1987) have documented Quaternary reactivation of movement on the Meers fault, as well as possible recent movement on other WNW-trending faults within the frontal fault system in southern Oklahoma.

The Marietta basin in Oklahoma (Figs. 1,3), at the eastern end of the Amarillo-Wichita uplift, is within the southern Oklahoma aulacogen. This NW-trending synclinal structure is bounded on the northeast by the Criner uplift and on the southwest by the Waurika-Muenster uplift. The early depositional history of this area, predating the formation of the Marietta syncline, involves deposition of a thick sequence of Cambrian to Ordovician carbonates overlain by Upper Ordovician through Lower Mississippian limestone, sandstone, and shale formations (Henry, 1968).

The Wichita orogeny in Late Mississippian to early Atokan time and the Arbuckle orogeny in early Desmoinesian to early Virgilian time were significant events in the structural and depositional histories of the Marietta basin. Formation of the Criner and Muenster-Waurika uplifts and the faulting and folding associated with initial development of the Marietta syncline accompanied the Wichita orogeny (Tomlinson and McBee, 1959).

Early syncline development is possibly associated with the deformation of the southern Oklahoma aulacogen (Wickham, 1978a). Significant deposition within the syncline did not begin until Middle Pennsylvanian, Desmoinesian time. The Marietta syncline was little affected by the tectonics of the Arbuckle orogeny. During this period of orogenic activity, the Criner uplift acted as a structural barrier to SW compressional stresses and to associated crustal shortening and faulting; however, at the close of the Pennsylvanian, Virgilian and Permian sediments were eroded from the Arbuckle Mountains and deposited over the area. Basin subsidence associated with sediment loading continued into post-Permian time (Frederickson and Redman, 1965).

Located within the larger Permian basin, the Bravo dome (Figs. 1,4) is a Late Mississippian to Early Pennsylvanian tectonic feature positioned between the Dalhart and Palo Duro basins (Budnik and Smith, 1982). Formation of the Bravo dome coincided with development of the Amarillo-Wichita uplift. By mid-Permian time, deposition of carbonate and clastic (granitic wash) sediments in response to Late Mississippian to Early Pennsylvanian tectonism completely covered structural features like the Bravo dome, and filled the smaller basins in the region (McGookey and Goldstein, 1982). Within this part of the Texas Panhandle a sequence of Per-

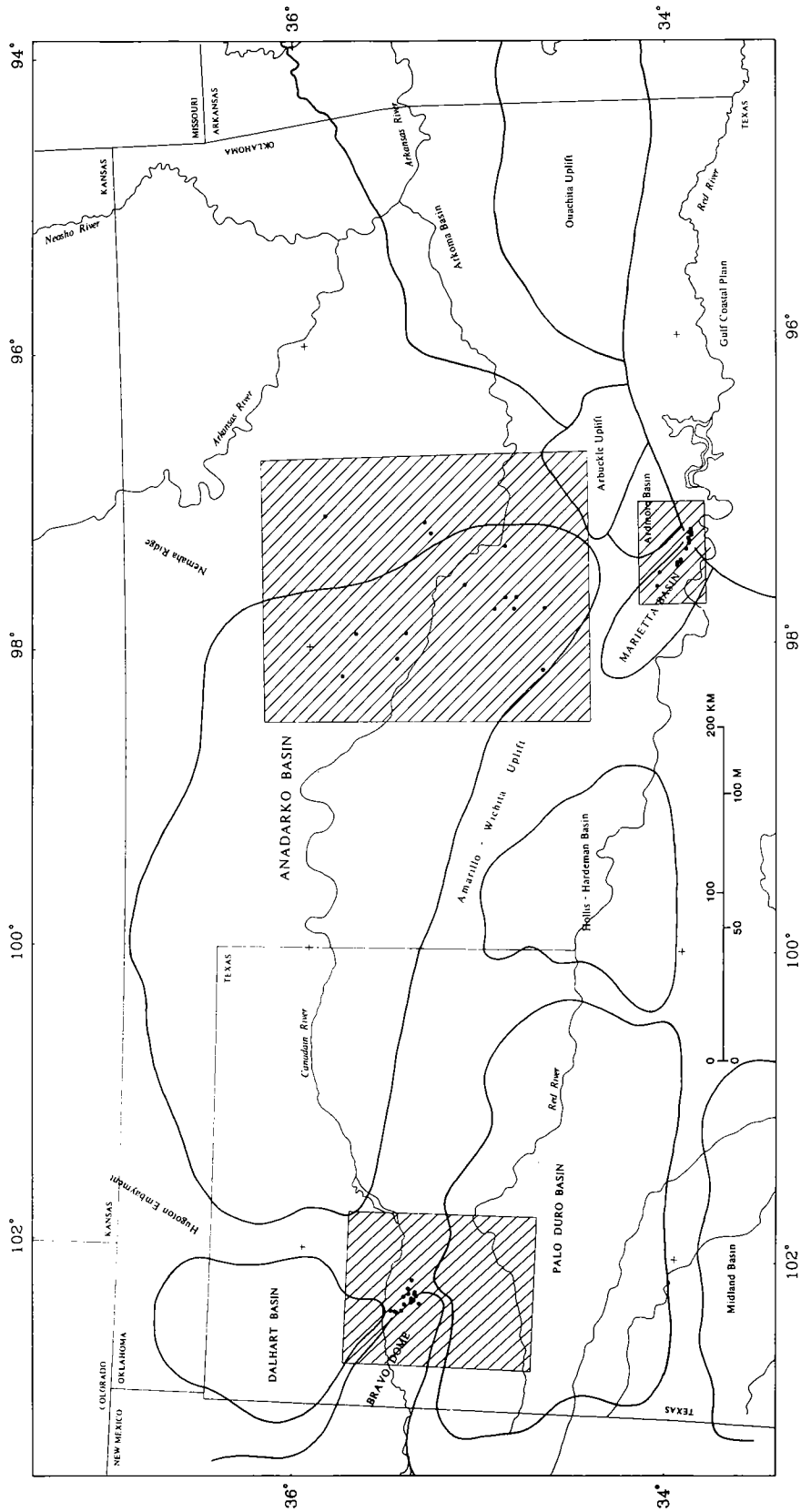
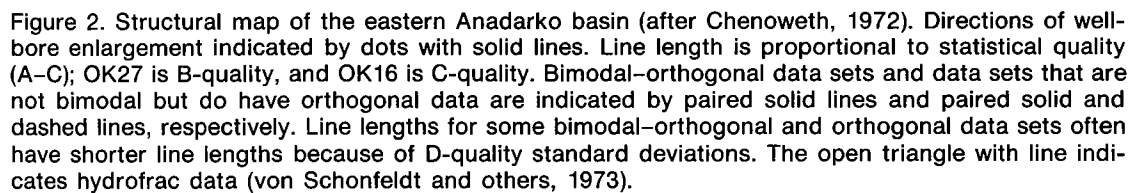


Figure 1. Generalized structure map of Oklahoma and the Texas Panhandle showing location of study areas (boxes with diagonal lines) and wells used (solid dots). Outlines and locations of basins and uplifts after Nicholson (1960); Johnson and others, (1972); Morris (1974); Haley (1976); and Petroleum Information Corp. (1983).



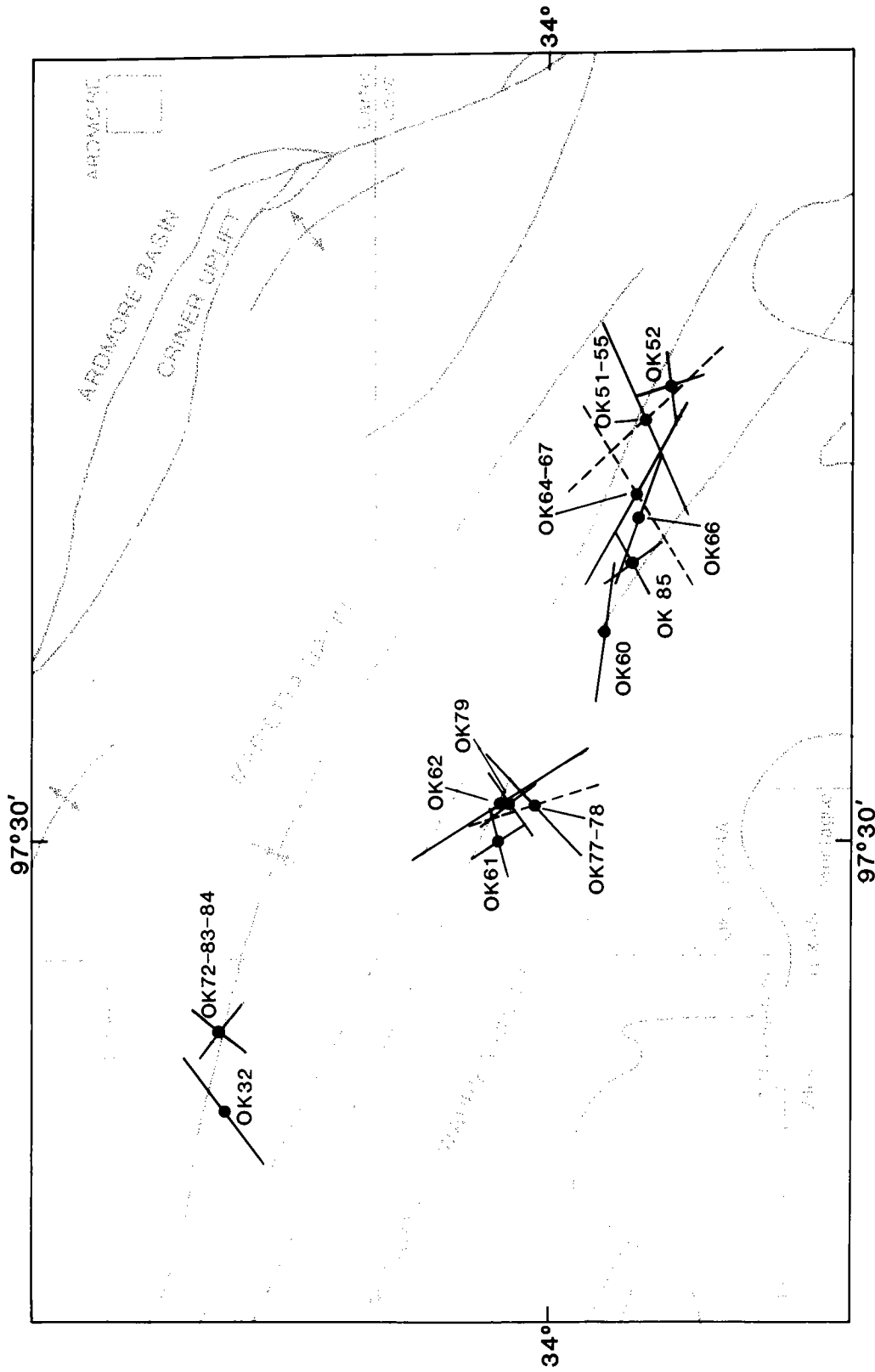


Figure 3. Structural map of the Marietta basin (after Chenoweth, 1972), showing directions of well-bore enlargements (see Fig. 2 for explanation). OK62 is B-quality and OK32 is C-quality.

mian salt-bearing formations, interbedded with marine mudstone, siltstone, anhydrite, and dolomite, covers the Bravo dome (Presley, 1980). This overlying sedimentary accumulation is cut by a series of NW-striking, high-angle faults that define basement structures (Fig. 4; Dutton and others, 1982). The most prominent of these is the Potter County fault, separating the Bravo dome

from the Dalhart basin. Basement faults associated with the Paleozoic tectonism of the Amarillo-Wichita uplift are probably reverse faults (Dutton and others, 1982). Fault-related deformation of the late Tertiary Ogallala Formation indicates Cenozoic fault movement in the Texas Panhandle (Budnik, 1987).

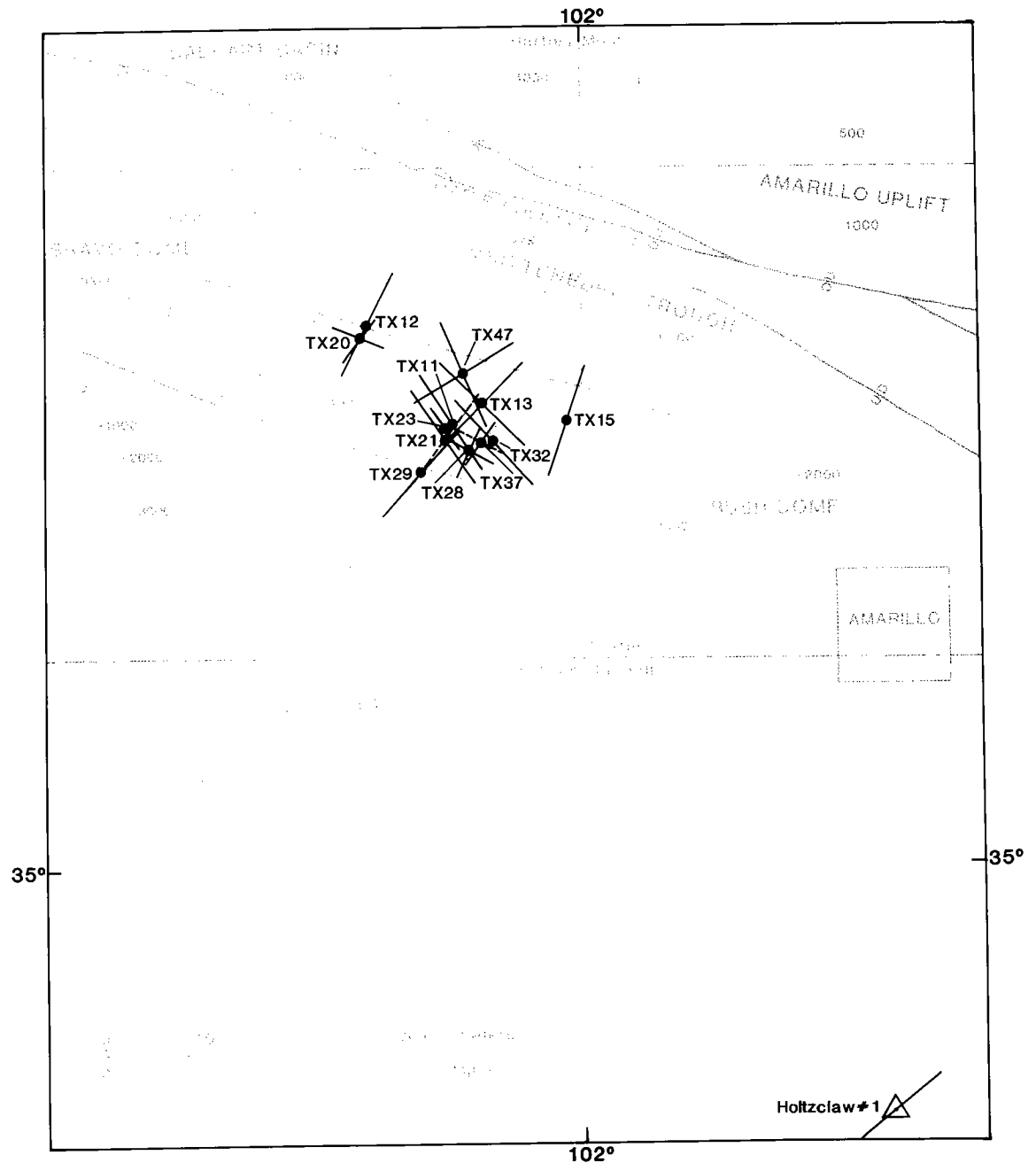


Figure 4. Structural map of the Bravo dome area (after McGookey and Goldstein, 1982), showing directions of well-bore enlargement (see Fig. 2 for explanation). TX12 is C-quality.

WELL-BORE ENLARGEMENT DATA

Well-bore enlargement data are the measured long-axis orientations of stress-related elliptical features observed on standard petroleum-industry four-arm, high-resolution dipmeter and fracture-identification well logs. Breakout-stress studies are economical because of the existence and availability of well-log data from exploration companies, log libraries, or data suppliers like the Petroleum Information Corp.

The two types of well-bore enlargements important to this study are (1) stress-induced breakouts associated with shear failure of the well bore; and (2) orthogonally oriented, stress-related-fracture borehole enlargements likely associated with either drilling-induced hydraulic fracturing of the well bore, or favorably oriented preexisting fractures or closely spaced joint sets intersecting the well bore (Fig. 5; Dart and Zoback, in press). Fracture enlargements should orient in the direction of SH_{max} , perpendicular to the trend of breakouts in the same well, hence creating an orthogonal-bimodal distribution of enlargement orientations. Borehole enlargements due to preexisting fractures reflect the trend of these preexisting fractures. Whether hydrostatically induced or preexisting, fractures appear to aid in the formation of stress-related, elliptically shaped well-bore enlargements.

Statistically, well-bore enlargement data sets are treated as axially symmetric, circular-normal distributions of two-dimensional vectors (Batschelet, 1965; Dart, 1987). Standard statistical calculations for mean direction, mean deviation, and standard deviation are performed, and the results are displayed as rose diagrams of data sets (Figs. 6–8); to avoid biased interpretations of inferred stress orientations by the analyst or the reader, rose-diagram plots are proportional to pedal area, not pedal length (Werner, 1976).

In the three studied areas, borehole data from 46 selected wells consisting of 40 well data sets (Tables 2–4) were analyzed. Only well data sets with statistical qualities of C or better (Table 1; M. L. Zoback, personal communication, 1987), bimodal-orthogonal, and orthogonal data sets were used in the statistical calculations of study-area data composites (Figs. 6–8; Tables 2–4). Well locations and the calculated mean orientations of the data are plotted in Figures 2–4.

Plotted well data sets (Figs. 2–4) consist of four or more well-bore enlargement orientations. Bimodal-orthogonal data sets have orthogonal modes of relatively equal numbers of well-bore enlargement orientations, whereas orthogonal data sets usually have only one well-bore enlargement orientation orthogonal to a preferred (primary) mode of the data. Mean orientations of both modes of bimodal-orthogonal data sets

TABLE 1.—QUALITY CRITERIA FOR
BREAKOUT DATA

Data-set quality	Number of breakouts	Standard deviation
A	≥ 10	$\leq 12^\circ$
B	≥ 6	$> 12^\circ, \leq 20^\circ$
C	≥ 4	$> 20^\circ, \leq 25^\circ$
D	< 4	$> 25^\circ, \leq 30^\circ$
VP	—	$> 30^\circ$

Note: A breakout data set is considered VP (very poor) if its standard deviation is $> 30^\circ$, regardless of the number of breakouts measured. From M. L. Zoback, personal communication, 1987.

(Figs. 2–4) are plotted as solid lines. Preferred modes and orthogonal trends in orthogonal data sets are plotted as solid and dashed lines, respectively.

The 16 well-data sets in the eastern Anadarko basin study area formed a consistent NNW trend of the breakout data. Bimodal data sets did not occur, and only 3 of the 16 data sets had minor orthogonal ENE trends (Fig. 2; Table 2). Clearly, stress-related fracture well-bore enlargements rarely occurred in the eastern Anadarko basin study area.

Common in the Marietta basin and the Bravo dome area are bimodal-orthogonal and orthogonal data sets and well-data sets consisting entirely of inferred fracture well-bore enlargements (Figs. 3,4). In the Marietta basin, 1 of the 12 well-data sets consisted of NW-oriented breakout data, 5 well-data sets consisted of ENE to NE-oriented inferred fracture enlargements, 6 data sets were bimodal-orthogonal, and 3 of the 12 data sets were orthogonal by definition (Table 3). A similar situation was observed in the Bravo dome area data, where the 12 data sets displayed equal numbers of breakout, inferred-fracture, and bimodal-orthogonal data sets (Table 4). Two of the 12 data sets were orthogonal by definition.

LITHOLOGIES OF ENLARGEMENT FORMATION

Both breakouts and fracture enlargements most often developed in limestone, dolomite, and shale formations (Table 5; Fig. 9). This seems indicative of the predominance of carbonates and shales in the Paleozoic stratigraphy throughout the study region (Hills and Kottlowski, 1983; Mankin, 1983).

In the eastern Anadarko basin, 62% of the breakouts and 80% of the fracture well-bore en-

TABLE 2.—BOREHOLE DATA FROM THE EASTERN ANADARKO BASIN

Well Name	County	Lat.	Long.	Ground Level (ft)	Well Depth (ft)	Logged/Interval (ft)	Date Interval (ft)	Feet	Number	Log Quality	Statistical Quality	Standard Error	Angular Deviation	Stations	Comments
Comp.	—	—	—	—	—	—	—	4887	84	—	—	2.1	18	348	Basin composite
OK4	Grady	34.887	-97.737	1064	13273	11213-13219	11192-13205	170	4	Good	C	8.5	17	344	
OK5	Grady	34.930	-97.668	1155	13390	8824-13374	11658-12666	45	4	Fair	C	4.8	10	344	
OK9	Canadian	35.485	-97.906	1342	12546	10036-12536	10086-14035	38	4	V. Good	C	10.8	22	350	
OK11	McClain	35.141	-97.585	1210	9891	5777-9871	6811-8541	389	8	Good	C	7.6	22	328	
OK15	Grady	34.985	-97.739	1070	13073	10415-13031	11641-12803	232	5	Fair	C	0.3	4	340	Orthogonal
OK16	Grady	35.216	-97.881	1242	12204	10544-12154	10990-11861	135	4	Good	C	7.0	14	327	
OK17	McClain	34.928	-97.337	1115	7894	5813-7863	5847-6673	169	4	Good	D	6.7	12	341	Orthogonal
OK18	Grady	34.872	-97.667	1003	12408	9278-12398	10078-11898	189	4	Fair	C	1.1	2	339	
OK22	Grady	34.729	-97.732	1229	10059	3649-10059	3991-6318	525	9	Good	B	0.3	7	5	Orthogonal
OK27	Kingsfisher	35.749	-97.910	1091	8771	6091-8795	6091-8217	225	6	V. Good	B	7.5	6	14	
OK36	Logan	35.905	-97.146	902	4185	2161-4100	2446-3911	437	7	Good	B	4.8	13	346	
OK38	Cleveland	35.346	-97.182	1205	5073	3033-5066	3133-4811	229	4	Poor	C	8.5	17	334	
OK40	Cleveland	35.319	-97.246	1086	5522	3521-5521	3762-5186	375	4	Fair	C	5.2	10	338	
OK100	Comanche	34.725	-98.240	1206	8978	1182-6832	3202-6727	579	5	Fair	C	10.4	23	34	
OK102-108	Canadian	35.659	-97.731	1250	6904	4934-6902	5084-6707	793	5	Poor-Good	D	5.4	1	358	Orthogonal
OK105	Canadian	36.530	-99.052	1394	11491	9401-11488	10223-11362	357	7	Good	B	3	7	2	

Depths are in feet below sea level unless otherwise stated.

Dashes indicate no data available.

Feet and number refer to the totals of vertical feet and number of individual well-bore enlargements

TABLE 3.—BOREHOLE DATA FROM THE MARIETTA BASIN

Well Name	County	Lat.	Long.	Ground Level (ft)	Well Depth (ft)	Logged/Interval (ft)	Data Interval (ft)	Feet	Number	Log Quality	Statistical Quality	Standard Error	Angular Deviation	Strata	Comments
Comp.	—	—	—	—	—	—	—	2404	66	—	—	3.3	20	311	Basins composite
OK 32	Jefferson	34.135	-97.626	816	6871	4471-6464	5987-6592	216	4	Good	C	9.9	20	64	
OK 51-55	Love	33.962	-97.281	730	9934	5386-9933	5726-9592	183	7	Poor-Fair	C	0.8	10	340	Orthogonal
OK 52	Love	33.949	-97.266	918	10547	8911-10516	8939-10211	116	4	Fair	D	8.8	12	341	Bimodal/Orthogonal
OK 60	Love	33.976	-97.387	930	8123	5054-8100	5776-7908	115	4	Poor	C	10.1	20	278	
OK 61	Love	34.023	-97.492	855	8028	6028-9771	7214-7894	106	6	Good	D	7.0	10	328	Bimodal/Orthogonal
OK 62	Love	34.022	-97.476	840	7708	5690-7799	5818-7619	421	10	Good	B	5.5	18	323	
OK 64-67	Love	33.963	-97.320	785	9123	6900-9126	6228-8776	286	7	Good-Fair	B	0.8	12	289	Orthogonal
OK 66	Love	33.956	-97.331	845	8799	6739-8798	8337-8635	162	4	Poor	C	5.7	11	289	
OK 72-83-84	Jefferson	34.137	-97.595	839	7999	5789-7998	7049-7798	312	5	Fair-Fair	D	1.4	2	310	Bimodal/Orthogonal
OK 77-78	Love	34.004	-97.474	913	7819	5774-7796	7072-7698	163	6	Fair-Good	C	8.9	22	343	Orthogonal
OK 79	Love	34.022	-97.476	876	7760	5708-7745	6508-7654	173	5	Good	D	3.5	5	323	Bimodal/Orthogonal
OK 85	Love	33.960	-97.352	954	8399	6333-8383	6833-8189	151	4	Fair	D	3.5	5	323	Bimodal/Orthogonal

Depths are in feet below sea level unless otherwise stated.

Dashes indicate no data available.

Feet and number refer to the totals of vertical feet and number of individual well-bore enlargements

TABLE 4.—BOREHOLE DATA FROM THE BRAVO DOME AREA

Well Name	County	Lat.	Long.	Ground Level (ft)	Well Depth (ft)	Logged/ Interval (ft)	Data Interval (ft)	Feet	Number	Log Quality	Statistical Quality	Standard Error	Angular Deviation	Sum	Comments
Comp.	---	---	---	---	---	---	---	1851	66	---	---	2.9	17	319	Area composite
TX 11	Oldham	35.370	-102.306	4020	4202	2192-4198	2322-3244	184	8	Good	C	8.8	25	328	
TX 12	Oldham	35.465	-102.372	3279	4857	2861-4864	3446-4393	360	7	Fair	C	8.1	22	27	
TX 13	Oldham	35.379	-102.260	3615	4475	2469-4469	2788-3655	229	7	Fair	C	2.1	4	314	Bimodal/Orthogonal
TX 15	Oldham	35.390	-102.163	3257	2781	1438-2779	2291-2611	166	4	Good	C	10	19	19	
TX 20	Oldham	35.443	-102.379	3500	4757	2740-4747	3110-3747	85	4	Good	D	1.8	2	293	Bimodal/Orthogonal
TX 21	Oldham	35.355	-102.301	3706	3733	2883-3583	3031-3305	95	4	Fair	C	0.9	8	327	Orthogonal
TX 23	Oldham	35.388	-102.331	3715	4076	2075-4075	2340-3157	55	4	Good	C	5.9	12	326	
TX 28	Oldham	35.328	-102.368	3575	4064	1965-4063	2428-4019	128	6	Fair	D	3.6	6	302	Bimodal/Orthogonal
TX 29	Oldham	35.297	-102.335	3542	3235	1232-3232	1233-1744	128	4	Fair	C	12	23	37	
TX 32	Oldham	35.371	-102.213	3539	3750	1650-3739	2453-3100	53	4	Fair	C	9.4	19	317	
TX 37	Oldham	35.366	-102.237	3590	3596	400-3618	826-2786	129	4	Fair	D	3.9	1	300	Orthogonal
TX 47	Oldham	35.404	-102.330	3451	6887	837-6839	1227-5691	239	10	Good	C	3.8	9	336	Bimodal/Orthogonal

Depths are in feet below sea level unless otherwise stated.

Dashes indicate no data available.

Feet and number refer to the totals of vertical feet and number of individual well-bore enlargements

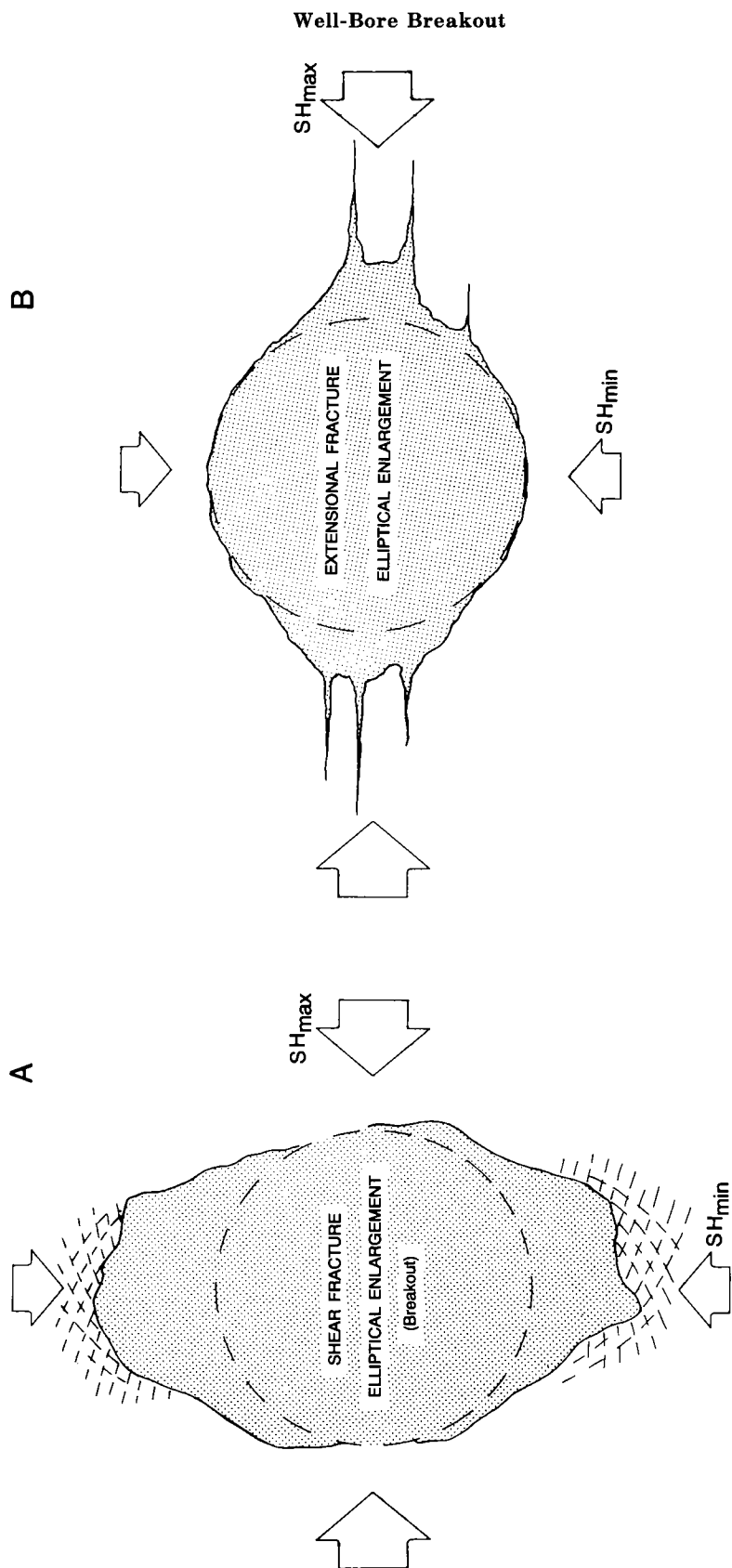


Figure 5. Cross-sectional schematics of well bores with original borehole shape (dashed line) and enlarged borehole shape (solid line). Breakout (A) and fracture (B) elliptical well-bore enlargements are shown.

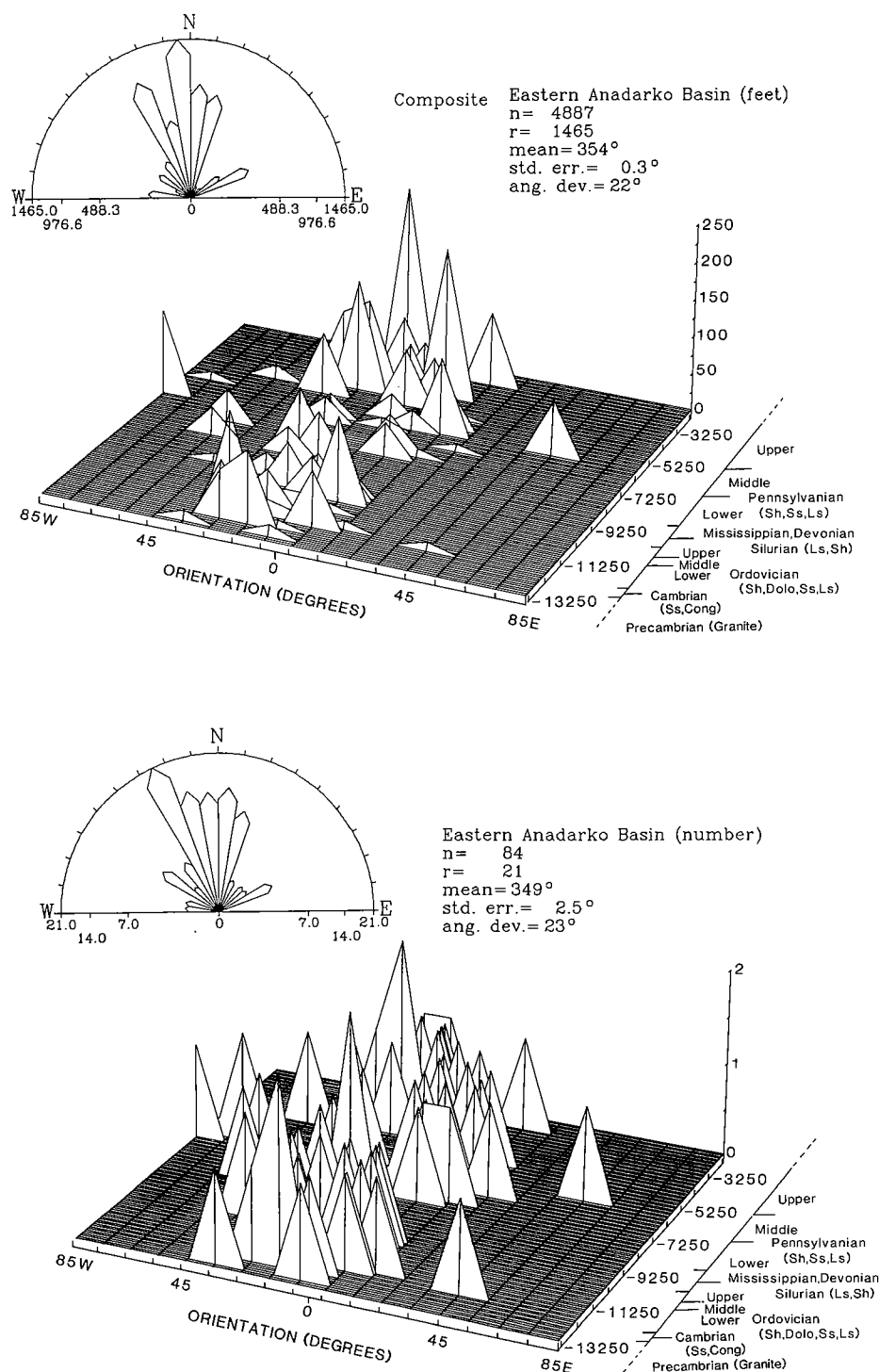


Figure 6. Three-dimensional histograms and frequency rose diagrams for the eastern Anadarko basin. Shown are the distributions of well-bore enlargements with azimuth versus depth (subsea) versus frequency of occurrence (feet or number). See text for explanation of statistical values shown. Depth increments are in 1,000-ft intervals. Approximate stratigraphic contacts are Upper and Middle Pennsylvanian at 5,500 ft, Middle and Lower Pennsylvanian at 7,000 ft, Lower Pennsylvanian and Mississippian etc. at 9,000 ft, Mississippian and Upper Ordovician at 10,200 ft, Upper and Middle Ordovician at 10,700 ft, Middle and Lower Ordovician at 11,200 ft, Lower Ordovician and Cambrian at 12,500 ft, and Cambrian and Precambrian at 13,000 ft.

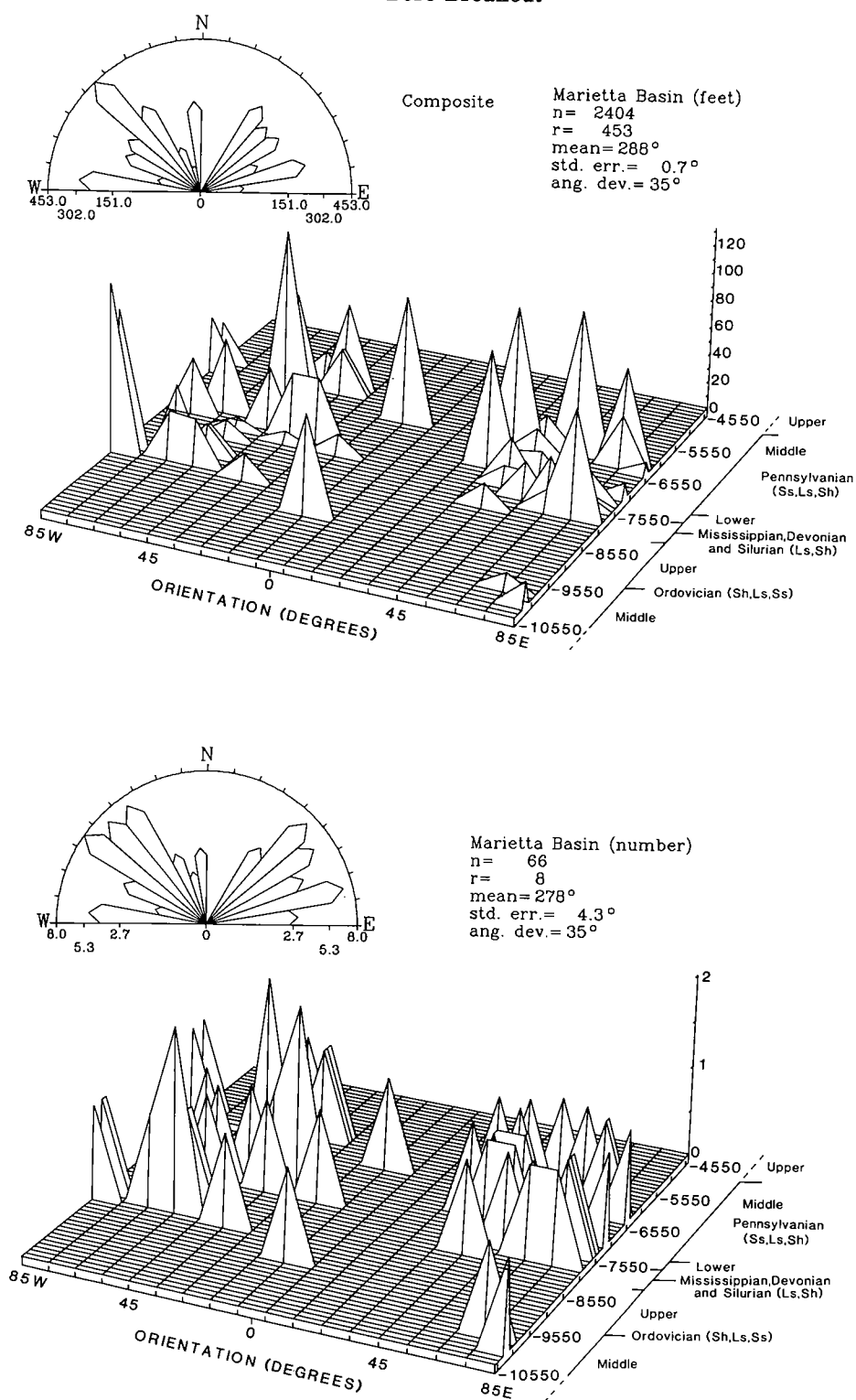


Figure 7. Three-dimensional histograms and frequency rose diagrams for the Marietta basin. Depth increments are in 500-ft intervals (see Fig. 6 for explanation). Approximate stratigraphic contacts are Upper and Middle Pennsylvanian at 5,000 ft, Middle and Lower Pennsylvanian at 7,500 ft, Lower Pennsylvanian and Mississippian etc. at 7,700 ft, Mississippian and Upper Ordovician at 8,300 ft, and Upper and Middle Ordovician at 9,000 ft.

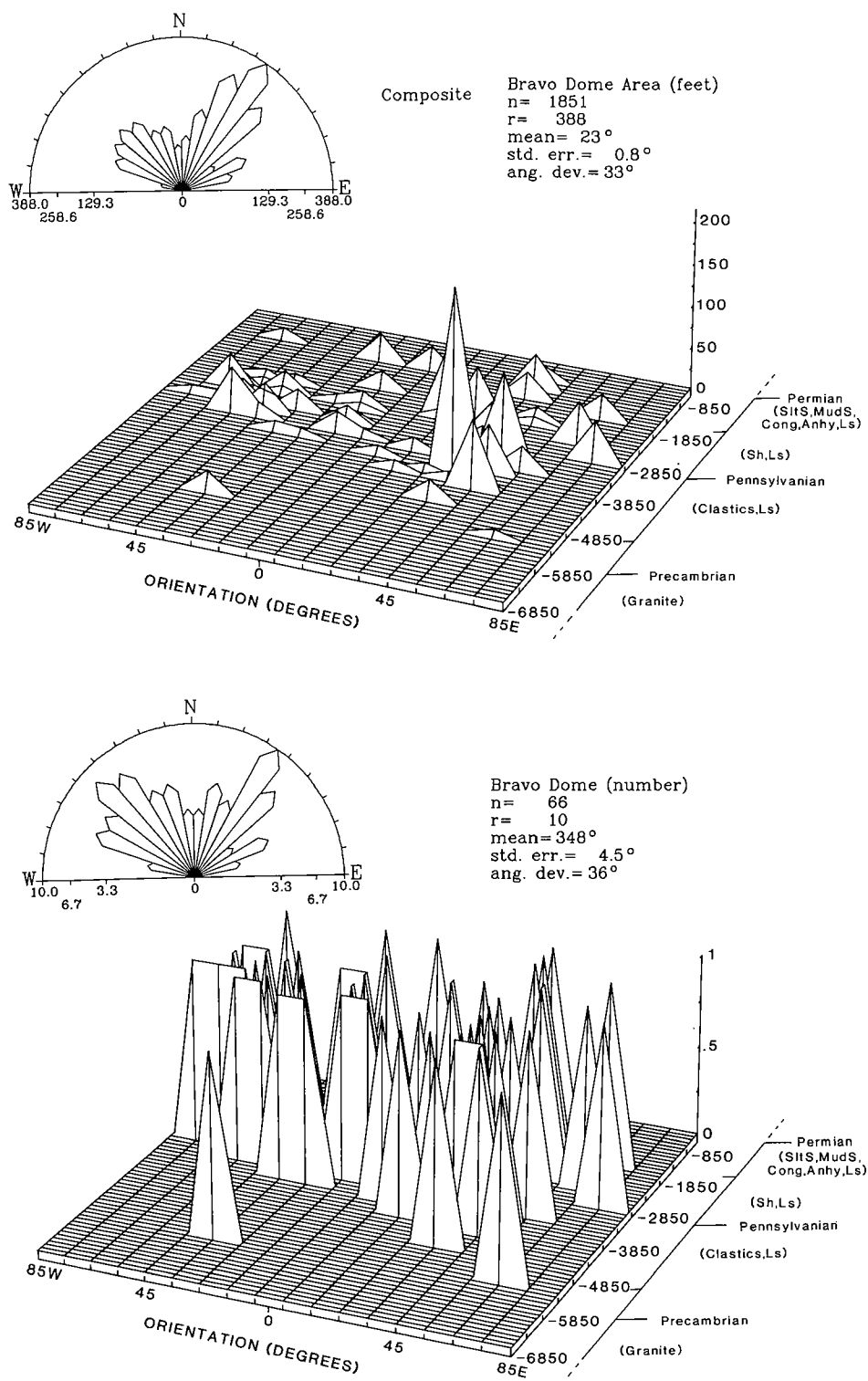


Figure 8. Three-dimensional histograms and frequency rose diagrams for the Bravo dome area (see Fig. 6 for explanation). Clastics are granite wash. Depth increments are in 500-ft intervals. Approximate stratigraphic contacts are Permian and Pennsylvanian at 1,700 ft, Pennsylvanian and Precambrian at 5,000 ft.

Well-Bore Breakout

111

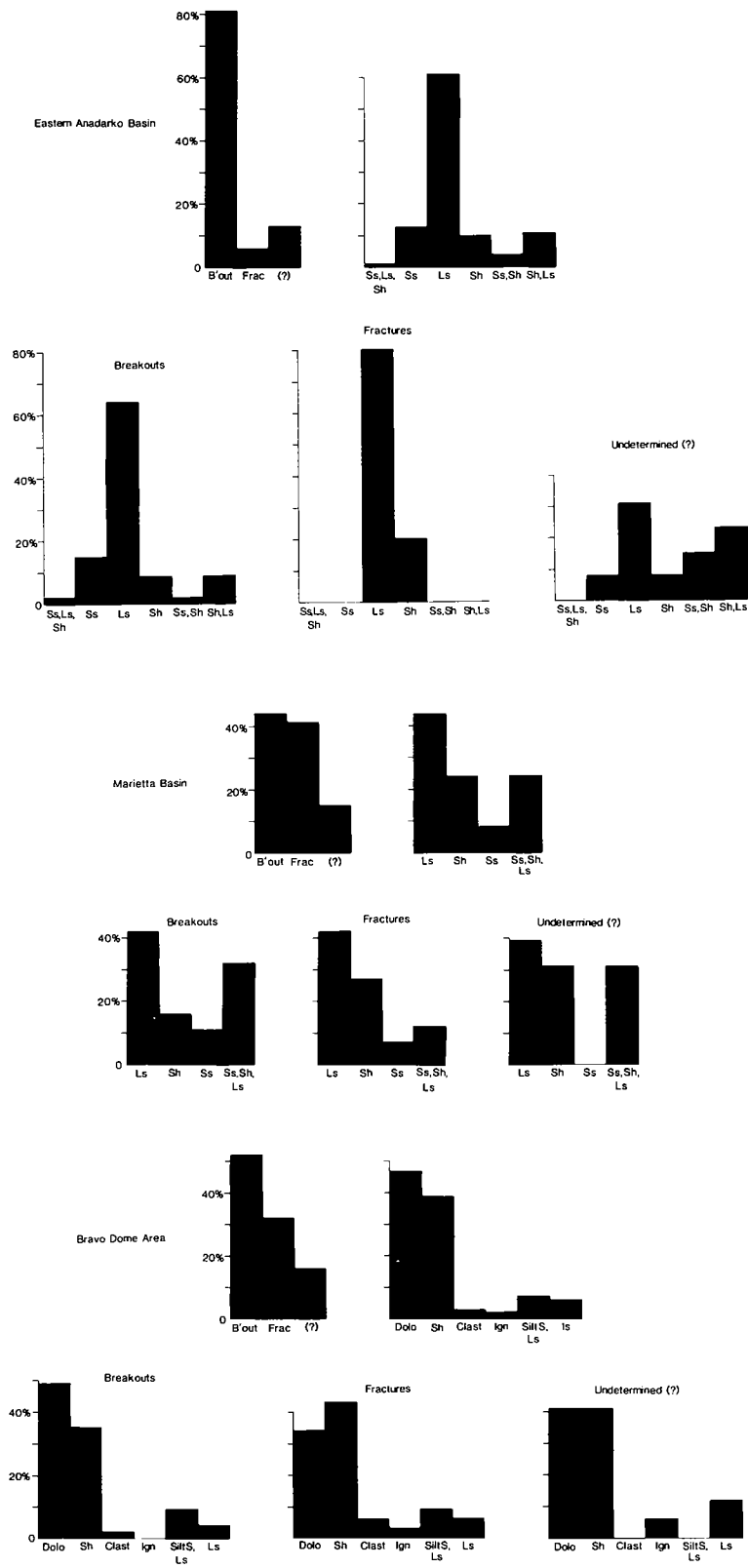


Figure 9. Bar graphs of well-bore enlargement type (breakout, fracture, or undetermined type) and lithologies of enlargement occurrence. Bars are percentages of the total data set for each study area.

TABLE 5.—STRATIGRAPHIC SECTIONS OF LOGGED FORMATIONS AND WELL-BORE ENLARGEMENT OCCURRENCE

System	Series	East Anadarko basin		Marietta basin		Bravo Dome area	
		Lithologic unit		Lithologic unit		Lithologic unit	
Permian	Leonardian					Clear Fork Gp. Tubb sandstone "Red Cave Fm." (MDS) "Panhandle limestone" (B1) "Brown dolomite" (B22,F11,*3) Permian? (B4)	
	Wolfcampian						
Pennsylvanian	Virgilian	Pawauska Fm. (LS) "Endicott sand" "Lovell sand" "Tonkawa sand" Hoxbar Gp. Dewey limestone Avant limestone Mbr. (B5) "Checkerboard sand" (B6) "Cleveland sand" (B1) Hogshooter limestone (B2) "Layton sand" "Wade sand" Confederate limestone (B2)			Cisco Gp. (SH,F4,*)		
	Missourian			Hoxbar Gp. Daube limestone Anadarche limestone "Hewitt lignite" "Palatine shale" Confederate limestone (B1) "Chubbee sand"		Canyon Gp. "Pennsylvanian shale" (B6,F6,*2) "Missourian shale" (B1) "Canyon Granite Wash" "Upper Granite Wash" (B1,F2) "Massive Granite Wash" "Granite Wash"	
	Desmoinesian						
		Deese Gp. (B5,F2) "Hart sand" (B1) "Big Lime" (B1) "Oswego lime" Cherokee Gp. "Prue sand" (F1) Vedigris limestone "Skinner sand" "Pink lime" "Osborne sand" (B1) "Red Fork sand" Inola limestone "Bartlesville sand" "Gibson sand" Atoka Fm. (SH,LS,B1)		Deese Gp. (LS,SS,SH,B7,*2) "Detrital zone" "Lower Deese" (coal) "Maroon shale" (B2,F2) "Pennsylvanian sand" "Sanders" (Lower Deese Gp. ?; SS,SH,B3,F1)		Strawn limestone "Granite Wash"	
	Atokan						Dornick Hills Gp. (SH,SS,LS,

Morrowan	Novi limestone Morrow Gp. (SH,LS) Primrose sandstone Springer Gp. (SH) Upper Norton sandstone Cunningham sandstone Britt sandstone	CONG,B3,F5, * 1) "Pennsylvanian detrital zone"
Mississippian	Chesterian Caney shale "Chester limestone" (B1) "Manning zone" (LS,SH) Meramecian "Meramec limestone" "Mississippi limestone" (* 1) Mayes limestone- Sycamore limestone	Mayes limestone Sycamore limestone
Devonian	Upper Lower Woodford shale "Misener sandstone" Hunton Gp. (LS,B2) Bois d'Arc limestone (B4)	Woodford shale (F1) Hunton Gp. (LS,SH)
Silurian	Lower Chimneyhill limestone (B2)	
Ordovician	Upper Middle Lower Sylvan shale (B3,F2,* 1) "Sylvan dolomite" Viola limestone (B15,* 1) Simpson Gp. Bromide Fm. (SS,LS,B6) Tulip Creek Fm. (SS,B2) McLish Fm. (SS,B3) Oil Creek Fm. (DOLO,LS,SH,SS,B3) Joins Fm. (DOLO,LS) Arbuckle Gp. (LS,B2)	Sylvan shale Viola limestone (B11,F14,* 3) Simpson Gp. (B2,F4) Bromide Fm. (LS,SS,B1,F2) McLish Fm. Birdseye limestone Mbr. (F1) "Green shale" (Oil Creek Fm. ?;F1)
Cambrian	Upper Timbered Hills Gp. Reagan sandstone (SH, CONG,B2)	
Precambrian	Granite	Granite (F1,* 1)

Notes: Well-bore enlargement type and frequency of occurrence: breakout (B#), fracture (F#), uncertain (* #). Quotation marks indicate informal names. Permian? indicates undifferentiated Wolfcampian clastic and limestone formations. Stratigraphic nomenclature follows usage of Jordan (1957), Bradfield (1968), Adler (1971), Preston and others (1982), McGookey and Goldstein (1982), AAPG (1983a,b), Petroleum Information Corp. well scout-cards of formation tops.

largements developed in limestone. Smaller percentages occurred in sandstone and shale formations (Table 5; Fig. 9). In the Marietta basin, 43% of both breakout and fracture well-bore enlargements occurred in limestone (Fig. 9). Also, 30% of the breakouts developed in sandstone, shale, and limestone beds, and 27% of the fracture enlargements occurred in shale formations (Fig. 9). In the Bravo dome area, 49% of the breakouts and 34% of the fracture well-bore enlargements developed in dolomite, whereas 35% of the breakouts and 43% of the fracture enlargements occurred in shale (Fig. 9).

Stress-induced breakouts and stress-related fracture well-bore enlargements are less likely the result of rock-type preference and more probably a function of the abundance of carbonate and shales in the stratigraphic section and the existing *in situ* stresses. That is, the stress conditions necessary to initiate well-bore enlargement appear to be present within the dominant sedimentary lithologies logged.

FRACTURE ENLARGEMENTS AND DATA SCATTER

Orthogonal trends in bimodal data sets associated with breakout and fracture well-bore enlargement orientations contribute significantly to increased standard deviations for individual well-data sets and to the appearance of dispersion or data scatter data composites for the Marietta basin and Bravo Dome area (Figs. 6–8).

In the present study, breakout and fracture well-bore enlargements are differentiated by comparing their enlargement orientations with known directions of SH_{max} from hydrofrac measurements (Figs. 2,4; Table 6). It is inferred from the data that breakouts in the study areas are NNW- to NW-oriented well-bore enlargements.

Comparison of conductivity values associated with long and short enlargement axes (short/long axis conductivity ratios) has been suggested as a possible method of distinguishing between breakout and fracture well-bore enlargements (Blümling, 1986). This conductivity method should work well only when the formation in which the enlargement has formed is of low porosity; that is, favorably oriented preexisting vertical fractures or drilling-induced hydraulic fractures associated with fracture well-bore enlargements may create a more direct path for induced current, and thus higher conductivity values (D. G. Davis, personal communication, 1988) than the current path associated with the curvilinear shear failure of breakout well-bore enlargement formation (Dart and Zoback, *in press*). In highly fractured or porous rock, a directed current should tend to be dispersed, resulting in lower conductivity values, thus making differentiation of enlargement type difficult. With this method, detailed infor-

mation concerning the lithologies and porosities of the logged rocks would be necessary. However, greater accuracy in distinguishing between types of well-bore enlargements may be achieved with digitized dipmeter well logs, which would afford the analyst a greater sampling frequency of conductivity data.

In the areas studied, fracture and joint patterns observed at the surface and at depth agree with orientation trends in well-bore enlargement data. A study of subsurface fractures in the "Mississippi Lime" and the Devonian and Silurian Hutton Limestone (9,055–9,331 ft below ground surface) of Kingfisher County in the eastern Anadarko basin study area (Fig. 2) revealed a bimodal pattern of vertical natural fractures (Brevetti and others, 1984). Observed were a primary N–S trend and a secondary E–W trend. These fractures occurred within the depth interval for breakout occurrence. The mean orientations of both fracture trends were subparallel to the mean orientations of breakouts and to the minor set of orthogonally oriented, inferred-fracture well-bore enlargements.

In the Slick Hills area of Oklahoma, adjacent to and north of the Meers fault in the southwest corner of the eastern Anadarko basin study area (Fig. 2) and ~70 km northwest of the Marietta basin, Wilhelm and Morgan (1986) observed a bimodal pattern of geographic lineaments oriented between N. 30–60° W. and N. 40–50° E. These well-constrained lineament patterns are thought to be associated with NW-striking left-lateral and high-angle thrust faults and with NE-striking right-lateral faults (Wilhelm and Morgan, 1986). This bimodal pattern of fault-related lineaments agrees with the mean orientations of breakouts and orthogonal, inferred fracture well-bore enlargements from Marietta basin wells (Fig. 3).

In the Bravo dome area of the Texas Panhandle (Fig. 4), as in the Marietta basin study area, surface and subsurface fractures form bimodal trends that were oriented roughly WNW and NE (Gustavson and Budnik, 1985; Gustavson and Finley, 1985). Although the bimodal trends of these fractures were somewhat random, agreement does exist between the bimodal trends of subsurface near-vertical fractures (Gustavson and Budnik, 1985) observed in the Stone and Webster Holtzclaw #1 well (Fig. 4) and NW- and NE-oriented well-bore enlargements in the Bravo dome area.

In all three study areas, the mean orientations of breakouts and inferred-fracture well-bore enlargements approximate the bimodal orientations of observed natural fractures within or adjacent to these areas. This finding tends to support the idea of a genetic relationship between the formation of some well-bore enlargements and preexisting vertical fractures.

TABLE 6.—IN SITU STRESS MEASUREMENTS FROM HYDROFRACTURE AND OVERCORING STUDIES IN THE SOUTH-CENTRAL UNITED STATES

Study type	Location	Rock type	Depth from ground surface (ft)	S _v (psi)	SH _{min} (psi)	SH _{max} (psi)	SH _{max} (direction)
HF ^a	Kingfisher Co., Okla., eastern Anadarko basin	N.D.	N.D.	N.D.	N.D.	N.D.	N. 65° E.
OC ^b	Johnston Co., Okla., Arbuckle uplift	Granite	4.5	0	519	1,075	N. 94° E.
HF ^c	Randall Co., Texas, Palo Duro basin	Siltstone	1,854	1,835	1,110	1,260	N. 30° E.
"	"	Anhydrite	2,334	2,335	N.D.	N.D.	N. 40° E.
"	"	Salt	2,434	2,780	2,915	N.D.	N. 60° E.
"	"	"	2,585	2,950	3,500	N.D.	N. 60° E.
"	"	Limestone	2,794	2,810	1,940	2,650	N. 45° E.

Abbreviations: HF, hydrofrac; OC, overcoring.

^aFrom von Schonfeldt and others (1973).

^bFrom Hooker and Johnson (1969).

^cFrom Borjeson and Lamb (1987).

Studies have shown drilling-induced hydraulic fracturing to be related to an increase in hydrostatic pressure within the well bore, or to a decrease in rock tensile strength (Ellis and Swolfs, 1983; Stock and others, 1985). Unfortunately, association of hydraulic fracturing with the formation of inferred fracture well-bore enlargements could not be verified for the study areas, due to the unavailability of detailed drilling records of pumping pressures and fluid weights. However, changes in relative conductivity on dipmeter logs did show the coincidence of well-bore enlargements with formation or bedding boundaries.

A possible mechanism for the development of fracture enlargements of either type involves the "chipping out" of the well bore during the drilling process (D. G. Davis, personal communication, 1988). By this means, the well bore is enlarged elliptically in an area weakened by drilling-induced hydraulic fractures or by favorably oriented, open, preexisting vertical natural fractures or joint sets intersecting the borehole. The process of fracture-related enlargement may be aided by the erosional effects of circulating drilling fluid and drill-string wear.

Due to the difference in horizontal stress concentration about the borehole, favorably oriented,

preexisting vertical fractures intersecting the well bore should remain open, thus increasing the possibility of mechanical well-bore enlargement. A possible example of this process is given by Gustavson and Budnik (1985) in their discussion of the preferred NE orientation of fracture-related solution features in the Permian salt-bearing stratigraphy of the Texas Panhandle and NE-oriented hydraulic fractures induced in the Stone and Webster Holtzclaw #1 well (Fig. 4). Gustavson and Budnik postulated that the dissolution of salt-bearing formations was more rapid in the direction of SH_{max} along NE-oriented fractures.

Fractures intersecting the well bore do not always develop well-bore enlargements. Eighty-four fractures from six Marietta basin wells, based on conductive anomalies seen on fracture identification logs (The Anchutz Corp., unpublished data, 1987), rarely developed well-bore enlargements. These 84 fractures, having a mean azimuth of N. 42° E. and occurring primarily in the Upper Ordovician Viola Limestone, were compared with 35 NE-oriented well-bore enlargements from 13 additional wells in the same basin. The 35 enlargements inferred to be fracture-related were often, but not always, accompanied by fracture-conductivity anomalies; they occurred primarily in

limestone and shale formations, and had an average orientation of N. 65° E. The 27° difference in average orientation between these two groups of data may be due in part to variation in natural fracture orientation, spacing, and dip, or to the variation between present-day and paleostress orientations.

Preexisting fractures intersecting the borehole at azimuths parallel or subparallel to the SH_{min} direction may also contribute to the development of stress-induced breakouts. This appears to be the case for at least one well-bore enlargement in the eastern Anadarko basin (well OK16; Fig. 2). The enlargement was associated with a conductivity anomaly indicative of fracturing but oriented in the direction inferred for breakouts. This situation is not interpreted to be a 90° rotation of the stress field but rather stress-induced breakout formation within an interval of the well bore weakened by preexisting vertical fracturing or jointing.

Another factor contributing to the formation of fracture well-bore enlargements in the study areas could be an increase in the difference in horizontal stress magnitudes associated with gravitational loading, rock properties, and bedding thickness (Amadei and others, 1988). Amadei and others (1988) proposed a model of gravity-induced variation in stress magnitudes in anisotropic, stratified rock masses by treating layered strata as finite mechanical units. Their model predicts that induced components of horizontal stress can vary in magnitude between rock units, becoming less or greater than the vertical stress.

Formation of randomly oriented well-bore enlargement associated with lower confining pressures at shallow depths (Dart, 1987; Springer, 1987) can generally be ruled out as a contributor to data scatter because near-surface (<1,000-ft subsea) well-bore enlargements were often washed out and enlarged in both orthogonal directions. Therefore, they were not considered reliable data.

Small differences in horizontal-stress magnitudes (Springer, 1987), as measured in the Stone and Webster Holtzclaw #1 well (Fig. 4), may have contributed to dispersion among enlargement orientations (Table 6) in the Bravo dome area. Without in situ measurements of horizontal stress magnitudes, this evaluation for the eastern Anadarko and Marietta basins could not be made.

The observed randomness in enlargement orientations inferred to be associated with fracturing of the well bore in the area studied is not thought to be related to a large horizontal-stress ratio and variation in borehole shape (Morin and others, in press). Large horizontal stress differences were not observed in the Stone and Webster Holtzclaw #1 well, and the study region (Fig. 1) is relatively aseismic (Stone and Webster Engi-

neering Corp., 1983), suggesting a small difference in horizontal stresses regionally.

INFERRED STRESS DIRECTIONS AND RELATIVE STRESS MAGNITUDES

Directions of SH_{max} calculated from measurements (Table 6) agree with the directions of SH_{max} inferred from breakout data (Table 7) in the study region. The average direction of SH_{max} inferred from hydrofrac measurements for the region (Fig. 1) is N. 50° E., and the average direction of SH_{max} inferred from breakout data for the three study areas is N. 56° E.

The relative magnitudes of S_1 , S_2 , and S_3 within the study region may be evaluated from available hydrofrac data, evidence of recent faulting, and the frequency of breakout occurrence with depth. Measured values of S_V , SH_{min} , and SH_{max} from hydrofrac measurements exist for one well within the study region (Fig. 2; Table 6). The relationship of principal stress magnitudes from the Stone and Webster Holtzclaw well #1 (Fig. 4), located 80 km southeast of the Bravo dome area in the Palo Duro basin, is

$$S_1 > S_2 > S_3, \text{ or } S_V > SH_{max} > SH_{min}, \\ \text{or } S_V > S_{NE} > S_{NW}.$$

The ratio of S_V to SH_{max} is 1.19 and the ratio of SH_{max} to SH_{min} is 1.28 for siltstone and limestone formations (Table 6). Stresses measured for intervening salt formations (Table 6) deviate from this stress relationship. Because salt is an elasto-plastic rock, stresses measured in salt formations are not considered reliable indicators of the regional stress field (Borjeson and Lamb, 1987).

In the Arbuckle uplift (Fig. 1), the surface overcoring stress measurements (Table 6) are an unreliable indication of stress conditions within the region because of the domed igneous structure of the uplift (H. S. Swolfs, personal communication, 1988). Breakout stress data agree only generally with stress directions calculated from overcoring measurements in this area.

Stress-magnitude calculations using mini-frac (Swolfs, personal communication, 1988) and leak-off test data (Ervine and Bell, 1987) were not possible for the study areas, because these types of borehole-pressure test data were not available from petroleum-industry sources.

Initiation of shear-failure spalling and rate of breakout development appear to be controlled by the horizontal-stress difference about the well bore and by confining strength of the rock (Martin, 1984; Haimson and Herrick, 1985; Zoback and others, 1985). A rough evaluation of relative horizontal stress differences may be inferred by

TABLE 7.—INFERRED STRESS DIRECTIONS FROM WELL-BORE ENLARGEMENTS

Location	Primary rock type in which enlargements occur	Enlargement depth interval (ft subsea)	SH _{max} from breakout data	Azimuth of fracture enlargement
Eastern Anadarko basin	Limestone and shale	−2,446 to −13,205	N. 78° E.	N. 51° E.
Marietta basin	Limestone and shale	−5,726 to −10,499	N. 41° E.	N. 65° E.
Bravo Dome area	Dolomite and shale	−924 to −6,516	N. 49° E.	N. 37° E.

examining the frequency of breakout occurrence with depth. Assuming the fracture gradient (Society of Professional Well Log Analysts, 1984) and the magnitudes of S_1 , S_2 , and S_3 all increase at their respective rates with depth, the following conditions are likely true: (1) when breakouts do not occur or are random in orientation, $SH_{max} \approx SH_{min}$; (2) when breakouts do occur, $SH_{max}/SH_{min} > 1$ (Zoback and others, 1985); (3) when the frequency of breakout occurrence increases with depth, the horizontal-stress difference increases with depth (since the fracture gradient is also assumed to be increasing with depth, but at a slower rate); (4) when the frequency of breakout occurrence remains about the same with depth, the horizontal-stress difference probably remains constant; and (5) when the frequency of breakout occurrence decreases with depth, the horizontal-stress difference decreases with depth or increases at a slower rate than the increase in the fracture gradient. Thus, breakout occurrence and the extent of breakout development in any given area are likely associated with the rates at which in situ stresses change with depth.

In a seismically active area where S_1 is horizontal, such as the New Madrid area of the Mississippi Embayment (Zoback and Zoback, 1981), stress-induced well-bore enlargements from two wells (Dart, 1987) appear to be of greater vertical length and have distinct characteristic traces (as seen on the dipmeter log). In contrast, a relatively aseismic area like the Palo Duro basin (Stone and Webster Engineering Corp., 1983), where S_1 is vertical and where in the near surface S_2 may not be significantly greater than S_3 (Table 6; Borjeson and Lamb, 1987), well-bore enlargements in nearby wells (Bravo dome area), on the average, have the appearance of shorter vertical lengths, and their trace character as seen on the dipmeter log appears less well defined (log quality on Table 4). When comparing well-bore enlargements from areas having different levels of seismic activity with similar sedimentary litholo-

gies, as seems to be the case with the New Madrid seismic zone and the Bravo dome area, well-bore enlargement length and frequency of occurrence may be largely a function of the horizontal-stress difference.

Figures 6, 7, and 8 illustrate the relationship of well-bore enlargement vertical length and frequency of occurrence to depth. For the eastern Anadarko basin data (Fig. 6), frequency of breakout occurrence (number) does not appear to decrease with depth for the logged interval (~3,000 to ~13,000 ft). However, there does seem to be a decrease in breakout length (feet) with depth (Fig. 6). This decrease is expected, given the longer time during which breakouts can develop in the upper part of the borehole and the longer exposure time to drill-string wear. Although the marked decrease in breakout occurrence between ~6,000 and ~9,000 ft depth (Fig. 6) cannot be accounted for, it may be a result of an increase in rock tensile strength or a decrease in the ratio of horizontal stresses within this interval of Middle and Lower Pennsylvanian Desmoinesian, Atokan-Morrowan, and Springerian formations.

In the Marietta basin (Fig. 7), both breakouts and fracture well-bore enlargements appear to occur at approximately the same frequency with depth. The fact that they seem to terminate at ~9,000 ft may be related to the small number of wells (3) with logged intervals extending below this depth. In the Marietta basin data, scatter among breakout orientations contrasts with the tight grouping of NE-oriented fracture-related well-bore enlargements. This contrast may be a function of the ratios of principal stresses in situ. A decrease in the ratio of horizontal stresses in the Marietta basin may contribute to scatter among breakout orientations, whereas an increase in the ratio of S_v to SH_{max} may contribute to drilling-induced hydraulic fracturing of the well-bore and formation of fracture enlargements. In normal-faulting stress regimes where S_1 is vertical, drilling-induced hydraulic fracturing is more

likely to occur than in compressive stress regimes where S_1 is horizontal (Healy and others, 1984; Stock and others, 1985).

Breakout and fracture well-bore enlargements occur with depth at approximately the same frequency (number) in the Bravo dome area data (Fig. 8). Fracture enlargements have longer vertical lengths (feet) than breakouts and, as in the Marietta basin data, appear to form a tighter grouping of NE orientations than NW-oriented breakout enlargements (Fig. 8). Neither breakouts nor fracture well-bore enlargements occur below 5,750 ft. Only 1 of the 12 well-data sets had a logged interval extending below this depth. In the logging interval above 5,750 ft, both breakout and fracture well-bore enlargement development does appear to decrease with depth. Very few well-bore enlargements of either type occur within the 1,500-ft interval from 4,250 to 7,500 ft (Fig. 8). This apparent decrease in well-bore enlargement development below 4,250 ft may indicate changing stress ratios ($S_V/S_{H_{max}}$ and $S_{H_{max}}/S_{H_{min}}$) with depth. The tight grouping of well-developed fracture enlargements in the Bravo dome area data may be indicative of a normal-faulting stress regime. Hydrofrac measurements of S_1 , S_2 , and S_3 from the Stone and Webster Holtzclaw #1 well in the northern Palo Duro basin (Fig. 4) confirm this part of the Texas Panhandle (Fig. 1) to be a normal-faulting stress regime.

Several important observations can be made concerning the state of stress within the study region:

1) Strike-slip and reverse-fault movement on the Meers fault (Fig. 2) and possible displacement on other WNW-oriented faults in the Wichita frontal fault system of southern Oklahoma are inconsistent with a normal-faulting stress regime indicated for the Texas Panhandle.

2) The hydrofrac measurements in the Stone and Webster Holtzclaw #1 well (Fig. 4; Table 6) were made at shallow depths (1,854–2,794 ft below ground surface). The ratios $S_V/S_{H_{max}}$ and $S_{H_{max}}/S_{H_{min}}$ are close to 1.0. The difference between $S_{H_{max}}$ and $S_{H_{min}}$ appears to increase while the difference between S_V and $S_{H_{max}}$ appears to decrease with depth. This would indicate that the ratios of stresses may be different at depth than in the near surface.

3) The Bravo dome and northern Palo Duro basin areas lie on or very near the boundary between the southern Great Plains and Midcontinent stress provinces. The state of stress for these two provinces is interpreted as being opposite (Zoback and Zoback, 1980). The southern Great Plains stress province is a region of extensional tectonics with $S_{H_{min}} = S_{NNE}$, whereas the Midcontinent stress province is a region of compressional tectonics with $S_{H_{max}} = S_{NE}$ (Zoback and Zoback, 1980). Therefore, near-surface stress

conditions in the Bravo dome area may deviate from those found farther east within the Midcontinent stress province.

4) In view of the hydrofrac data (Table 6) and the apparent recent strike-slip and reverse movement on the Meers fault (Ramelli and others, 1987; Luza and others, 1987; Madole, 1988), a transitional stress regime is inferred for the study region, changing from normal faulting ($S_V > S_{H_{max}} > S_{H_{min}}$ or $S_V > S_{NE} > S_{NW}$) in the Texas Panhandle to strike-slip ($S_{H_{max}} > S_V > S_{H_{min}}$ or $S_{NE} > S_V > S_{NW}$) and reverse faulting ($S_{H_{max}} > S_{H_{min}} > S_V$ or $S_{NE} > S_{NW} > S_V$) in Oklahoma.

Given such a limited stress-magnitude data base (Tables 6,7), speculation on the relative magnitudes of vertical or horizontal stresses within the study region is problematic.

TRANSPRESSIONAL (OBLIQUE COMPRESSIONAL) STRESSES AND FAULT-BOUNDED BLOCKS

Much of the data from the Marietta basin and the Bravo dome area is bimodal (Figs. 2–4,7,8,10), unlike the eastern Anadarko basin, where bimodal sets of enlargement orientations are less common (Figs. 2,6,10). This dramatic increase in the number of bimodal-orthogonal data sets in the Marietta basin and the Bravo dome area appears to be indicative of the fracture history and a possible local change in stress conditions relating to mapped subparallel surface faults in the Marietta basin (Fig. 3) and mapped subparallel basement faults in the Bravo dome area (Fig. 4). Well locations in the eastern Anadarko basin (Fig. 2) are distributed over a broad area and generally do not appear to be located between subparallel faults.

Preexisting fractures in an array of orientations may exist within blocks bounded by subparallel faults. The area between or above subparallel discontinuities may likely have experienced an intense fracturing history resulting in sets of favorably oriented fractures or joints, increasing the likelihood of fracture well-bore enlargement.

Where fracture enlargements have formed in response to drilling-induced hydraulic fracturing, an increase in the occurrence of inferred-fracture enlargements may reflect local changes in the regional stress field. Drilling-induced hydraulic fracturing is more likely to develop in a normal-faulting stress regime (Healy and others, 1984; Stock and others, 1985). An apparent extensional (normal) faulting stress regime in the Marietta basin study area, as suggested by the occurrence of fracture well-bore enlargements, may be a local stress anomaly in an otherwise compressional stress regime. Rogers (1984) and Hempton and Neher (1986) described structural settings where

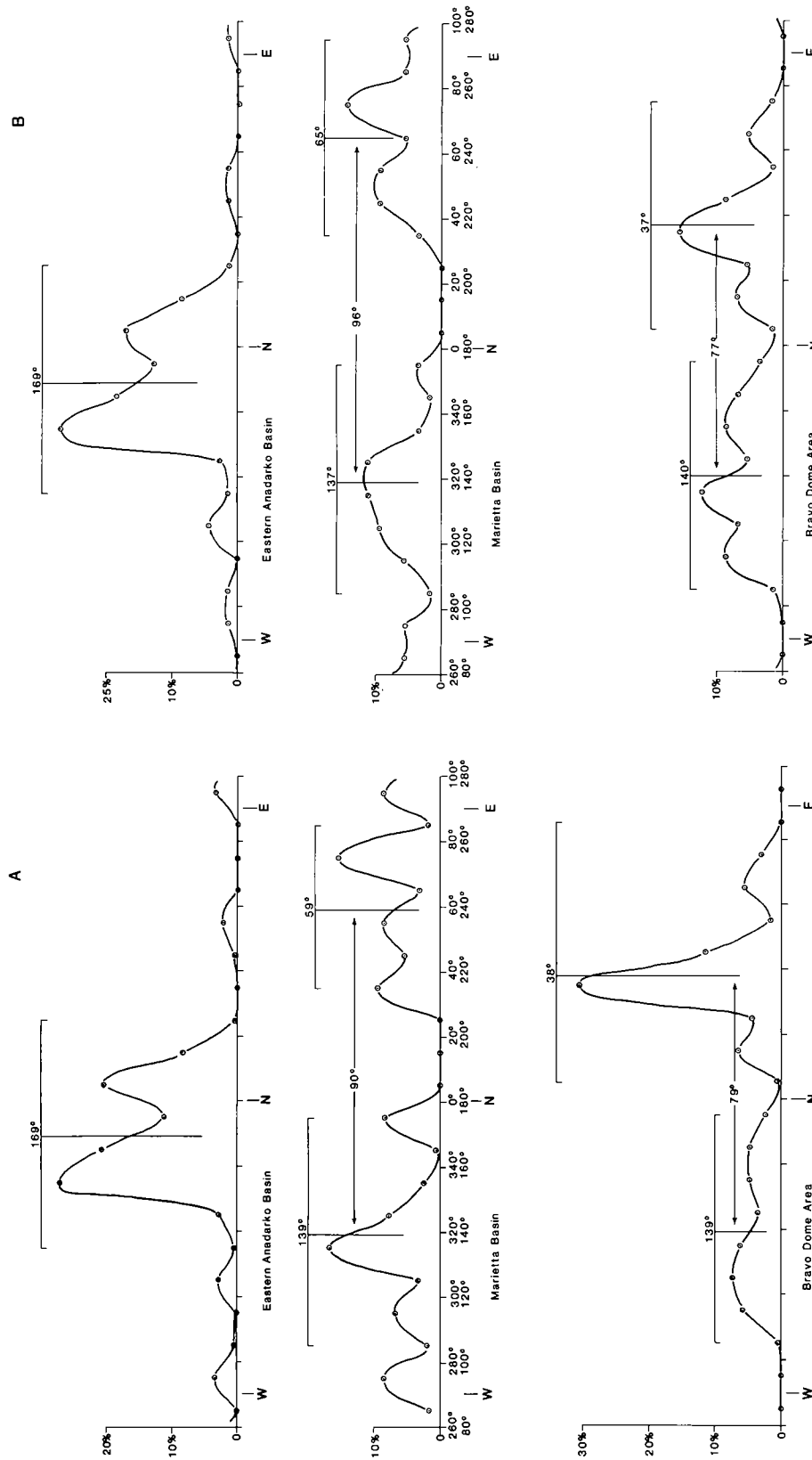


Figure 10. Histogram plots of well-bore-enlargement data illustrating the bimodal-orthogonal distribution of enlargement orientations from the Marietta basin and the Bravo dome area. Only data from wells with A through C statistical qualities or with bimodal-orthogonal distributions were used (Tables 1–4). Plot groups are vertical feet of well bore for a given azimuth (A) and cumulative number of individual well-bore enlargements for a given azimuth (B). Plots are a function of the percentage of the data used, either feet or number.

extensional and compressional stresses develop between and near the ends of left-stepping and right-stepping en echelon strike-slip faults in response to regional horizontal compression oblique (transpressional) to their strike. Subparallel faults in the Marietta basin and Bravo dome area are not en echelon by definition; however, these two areas appear to structurally resemble the areas described by Rogers (1984) and Hempton and Neher (1986). This apparent similarity of structural settings and horizontal-stress orientations suggests the possibility that extensional stress conditions (normal-faulting regime) might exist within blocks bounded by WNW-trending subparallel faults where SH_{max} is oblique to their strike.

A comparison of the calculated orientations of SH_{max} from breakout data (Table 7) shows a 37° difference between the eastern Anadarko and Marietta basins and a 29° difference between the eastern Anadarko basin and the Bravo dome area. SH_{max} orientations calculated for the Marietta basin and the Bravo dome area differ by only 8° . The similarities of these two differences (37° and 29°) may correlate with the apparent similarities in structural settings of the Marietta basin and the Bravo dome area, and with the possible local variation in horizontal stresses associated with the orientation of SH_{max} and WNW-trending subparallel faults.

CONCLUSIONS

From well-bore breakout data, SH_{max} is inferred to be $N. 78^\circ E.$ for the eastern Anadarko basin, $N. 41^\circ E.$ for the Marietta basin, and $N. 49^\circ E.$ for the Bravo dome area.

Bimodal sets of well-bore-enlargement data are interpreted as consisting of a NNW to NW mode of stress-induced breakouts and a ENE to NE mode of stress-related fracture enlargements.

Fracture well-bore enlargements are likely associated with drilling-induced hydraulic fracturing of the well bore, or with preexisting vertical fractures or closely spaced joint sets intersecting the well bore.

The occurrence of breakouts and fracture well-

bore enlargements does not seem to be dependent on sedimentary rock type.

The stress regime for the study region appears to be transitional from normal faulting at shallow depths in the Bravo dome area of the Texas Panhandle to strike-slip and reverse faulting in Oklahoma.

Bimodal-orthogonal data sets of well-bore-elongation orientations may be more likely to develop in wells located in areas bounded by subparallel faults striking oblique to the SH_{max} direction (transpressional stress).

An extensional (normal-faulting) stress regime in the Marietta basin may be a local fault-related stress anomaly.

ACKNOWLEDGMENTS

I would like to thank the following individuals and companies for the generous assistance in acquiring much of the data needed for this study: David Walker (Baker and Taylor, Drilling Co., Amarillo); Mark Ramsey and E. G. Kerns (Cities Service Oil and Gas Corp., Oklahoma City); Bill Osten (Phillips Petroleum Co., Oklahoma City); T. A. Deines, Stephen O'Niell, and P. L. Clymer (Marathon Oil Co., Midland, Texas); J. A. Norton (Consolidated Oil and Gas, Inc., Denver); Greg Riepl (States Petroleum, Inc., Irving, Texas); D. J. Wechsler, Daniel Hanson, and M. D. Wittstrom (Chevron, U.S.A., Inc., Oklahoma City); Jackie Ritchey and Bill Clement (AnSon Gas Corp., Oklahoma City); Ted Price (Samedan Oil Corp., Oklahoma City); S. A. Maier (The Anchutz Corp., Oklahoma City); Phil Schrenier and A. R. Dowell (Texaco, U.S.A., Denver); and Tom Verolust (Mustang Production Co., Oklahoma City).

Conversations with D. G. Davis of the Colorado School of Mines and W. J. Perry, Jr., S. H. Frezon, M. L. Zoback, and H. S. Swolfs of the U.S. Geological Survey were very helpful in clarifying a number of important points. I am indebted to W. J. Perry, Jr., H. S. Swolfs, and M. L. Zoback for their critical reviews of the text.

Also, I would like to thank Eleanor M. Omdahl, U.S. Geological Survey, Denver, for editing and patiently correcting the manuscript.

NEOTECTONICS AND SEISMICITY OF THE ANADARKO BASIN

KENNETH V. LUZA

Oklahoma Geological Survey

Abstract.—Recent mapping in southwestern Oklahoma has identified a prominent scarp in Permian rocks and Quaternary alluvium along a 26-km-long segment of the Meers fault. Quaternary stratigraphic relationships and ^{14}C age dates constrain the age for the last movement of the Meers fault between 2,000 and 1,000 yr B.P. The Meers fault is part of a complex system of NW-trending faults that form the boundary between the Amarillo–Wichita uplift and the Anadarko basin. This fault system, generally referred to as the Wichita frontal fault system, extends ~475 km across southern Oklahoma and part of the Texas Panhandle. No historic or recent earthquake activity is known to have occurred along the exposed portion of the Meers fault. Furthermore, only a very few earthquakes are known to have occurred along the Wichita frontal fault system.

More than 370 locatable earthquakes have occurred in the Anadarko basin. The record of felt earthquakes dates back only to 1897, and instrumental recordings were begun in December 1961. Prior to 1962, only 40 earthquakes were known to have occurred in the Anadarko basin—30 in Oklahoma and 10 in Texas. More than half of these events occurred in Canadian County, Oklahoma. All the earthquakes in Oklahoma and Texas were located either from historical accounts or from seismograph stations outside the State. In late 1961, two seismograph stations were installed in Oklahoma. One (WMO) was located in the Wichita Mountains, and the other (TUL) near Tulsa. From 1962 to 1976, 16 earthquakes were reported felt. In 1976, a program was begun to install seven semipermanent and three radio-telemetry seismograph stations in Oklahoma. These additional seismograph stations have greatly improved accuracy of earthquake detection and location in the State of Oklahoma, as well as in the adjacent states.

From 1977 to 1987, more than 320 additional earthquakes were located in the Anadarko basin, mostly of magnitudes <2.5 . However, 22 earthquakes were reported felt. A majority of the Anadarko-basin earthquakes occur on the eastern margin of the basin along a 40-km-wide, 135-km-long zone that extends from Canadian County to the south edge of Garvin County. A few earthquakes have occurred in the shelf and deep portions of the basin.

INTRODUCTION

The Anadarko basin and surrounding region are generally characterized as a stable area having relatively low seismic activity (King, 1951). Recent investigations in southwestern Oklahoma document Holocene movement on part of the Meers fault (Gilbert, 1983a,b; Donovan and others, 1983; Ramelli and Slemmons, 1986; Madole, 1986,1988; Crone and Luza, 1986; Luza and others, 1987). The Meers fault is part of a complex system of NW-trending faults that form the boundary between the Amarillo–Wichita uplift and the Anadarko basin. Geomorphic relationships and the offset of Pleistocene and Holocene deposits provide the evidence for recent movement on the Meers fault.

A seismograph station near Tulsa (TUL) has continuously monitored earthquake activity in the State since 1961. In 1976, the U.S. Nuclear Regulatory Commission initiated a number of cooperative programs with state geological surveys and/or universities to study areas of anomalously high seismicity east of the Rocky Mountains

(Luza, 1978). One of the program objectives was to correlate earthquake activity with tectonic structures. A statewide network of seismograph stations was installed in Oklahoma to achieve this program objective. The network, which became fully operational in 1977, is principally responsible for the location of more than 320 additional earthquakes in the Anadarko basin since the network became operational.

GEOLOGIC SETTING

The Anadarko basin is a NW-trending, asymmetrical, sedimentary and structural basin of Paleozoic age in western Oklahoma and the north Texas Panhandle (Fig. 1). It is flanked on the west by the Cimarron arch, on the south by the Amarillo–Wichita uplift, on the east by the Nemaha uplift, and on the north by the northern shelf. One of the deepest sedimentary basins in the North American craton, the Anadarko basin has more than 11 km of sedimentary rocks in the deepest part (Rowland, 1974a,b). The division be-

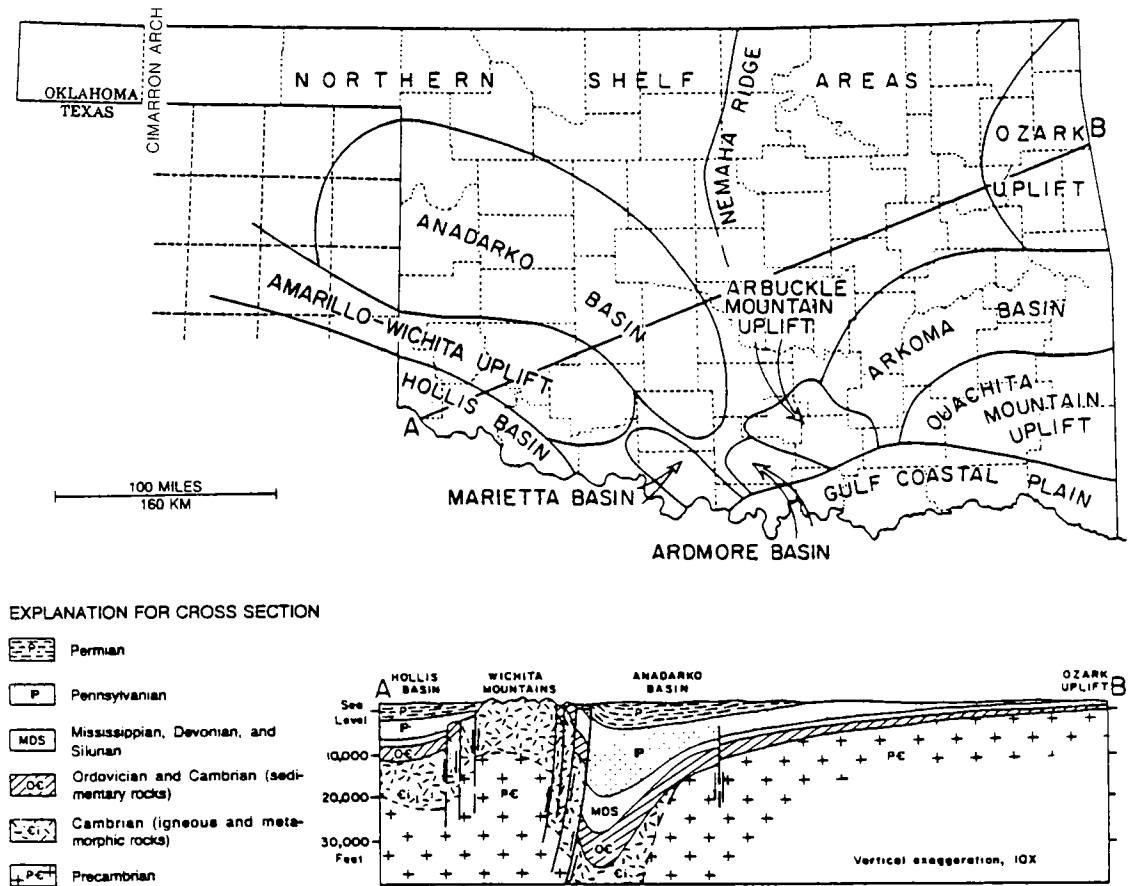


Figure 1. Major geologic and tectonic provinces of Oklahoma (after Johnson and others, 1971). Cross section shows thick Paleozoic sedimentary rocks in the Anadarko basin, and the Wichita frontal fault system, which separates the Wichita Mountains from the Anadarko basin.

tween the deep Anadarko basin and the shelf areas was arbitrarily established at about the -4,500-m basement contour (Petroleum Information Corporation, 1982). The Anadarko basin, which encompasses that area within the -1,500-m basement contour, embraces an area of ~90,650 km² (~35,000 mi²) in western Oklahoma, the north Texas Panhandle, and southwestern Kansas (Fig. 2).

The Anadarko basin evolved into a site of sediment accumulation as a consequence of faulting and subsidence along the ancient continental margin in Early and Middle Cambrian time. Ham and others (1964) grouped the Paleozoic sediments that accumulated in this region from the Late Cambrian through the Permian into four major intervals. The dominant lithologies of these intervals are as follows: (1) Late Cambrian–Early Devonian marine carbonates; (2) Late Devonian–Mississippian dark shales; (3) Pennsylvanian

dark shales, sandstones, thin marine limestones, and conglomerates; and (4) Permian red shales, sandstones, conglomerates, and evaporites. In part, the sedimentation patterns were controlled by the uplift of the Amarillo–Wichita Mountains. Uplift began in the Late Mississippian or Early Pennsylvanian and lasted through the Pennsylvanian (possibly into the Early Permian).

A complex system of NW-trending faults forms the boundary between the Amarillo–Wichita Mountains and the Anadarko basin. This fault system, generally referred to as the Wichita frontal fault system, extends for ~475 km across southern Oklahoma and part of the Texas Panhandle (Harlton, 1963, 1972; Ham and others, 1964). The Mountain View fault, Duncan–Criner fault, Cordell fault, and Meers fault are the major segments that comprise the Wichita frontal fault system (Fig. 3). The frontal fault system is dominated by moderately to steeply dipping reverse

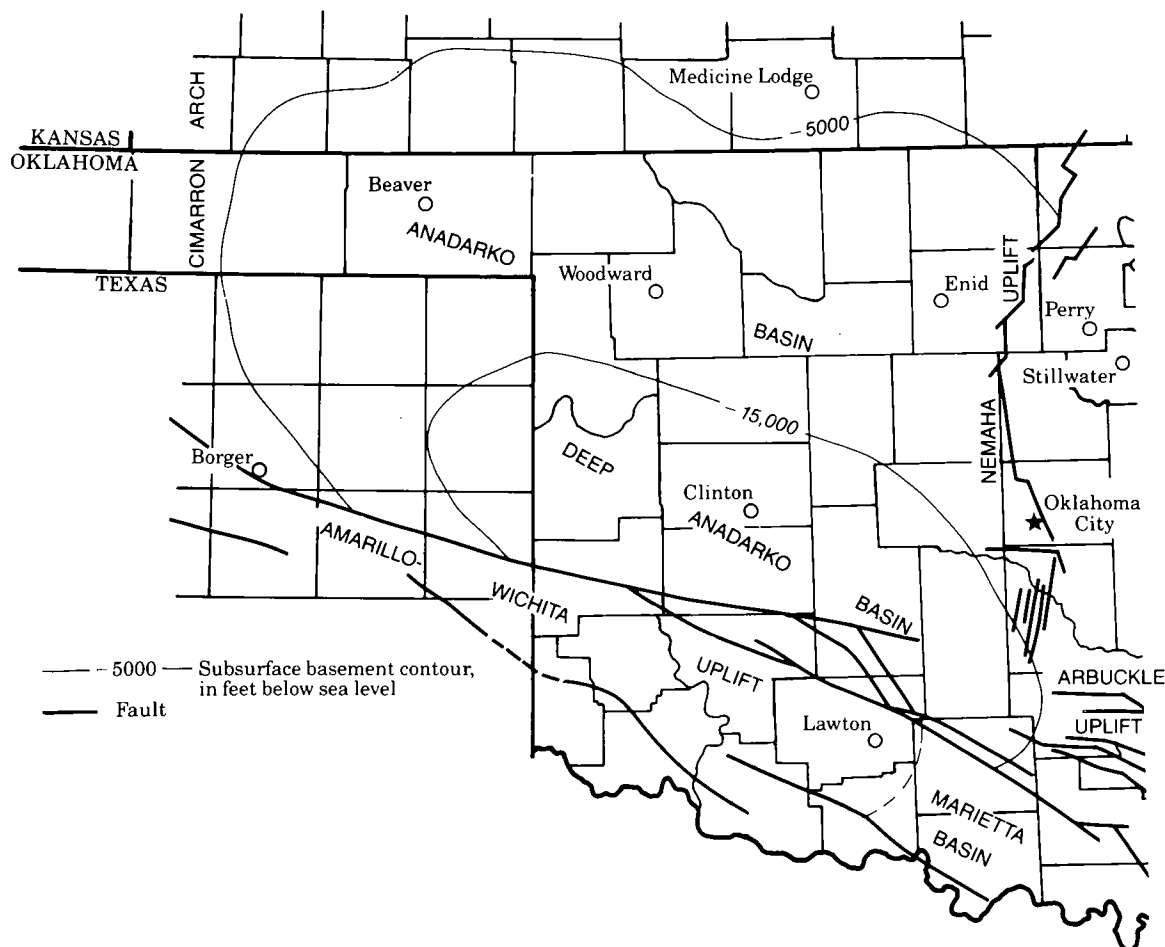


Figure 2. Major structural features bordering the Anadarko basin. The Anadarko basin is defined as the area within the -5,000-ft subsurface basement contour, and the division between the deep Anadarko basin and the shelf areas is the -15,000-ft subsurface basement contour (modified from Petroleum Information Corporation, 1982).

faults which have a combined net vertical displacement of >9 km (Ham and others, 1964). Of these faults, the Meers has the greatest net throw, ~ 6.4 km.

HOLOCENE MOVEMENT ON THE MEERS FAULT

Harlton (1951) originally named the Meers fault the Thomas fault for exposures in T. 4 N., R. 13-14 W., on the George Thomas Ranch. The fault trace forms a continuous, straight line that offsets Permian sediments (Figs. 3,4). This fault is, in part, responsible for the large structural offset between the Wichita Mountains to the south

and the Cambrian-Ordovician rock exposures on the north (Harlton, 1951, 1963).

On the Geologic Map of Oklahoma, Miser (1954) renamed the Thomas fault the Meers Valley fault. Ham and others (1964) and Havens (1977) dropped the word "Valley" from the fault name. Today, the commonly accepted name for Harlton's Thomas fault is the Meers fault.

The Meers fault trends N. 60° W. and displaces Permian conglomerate and shale for a distance of at least 26 km, from near the Comanche-Kiowa county boundary to East Cache Creek. At the northwest end of the fault trace, the fault displaces limestone-pebble conglomerates (Post Oak), whereas at the southeast end sandstones and calcrete-bearing shales of the Hennessey are

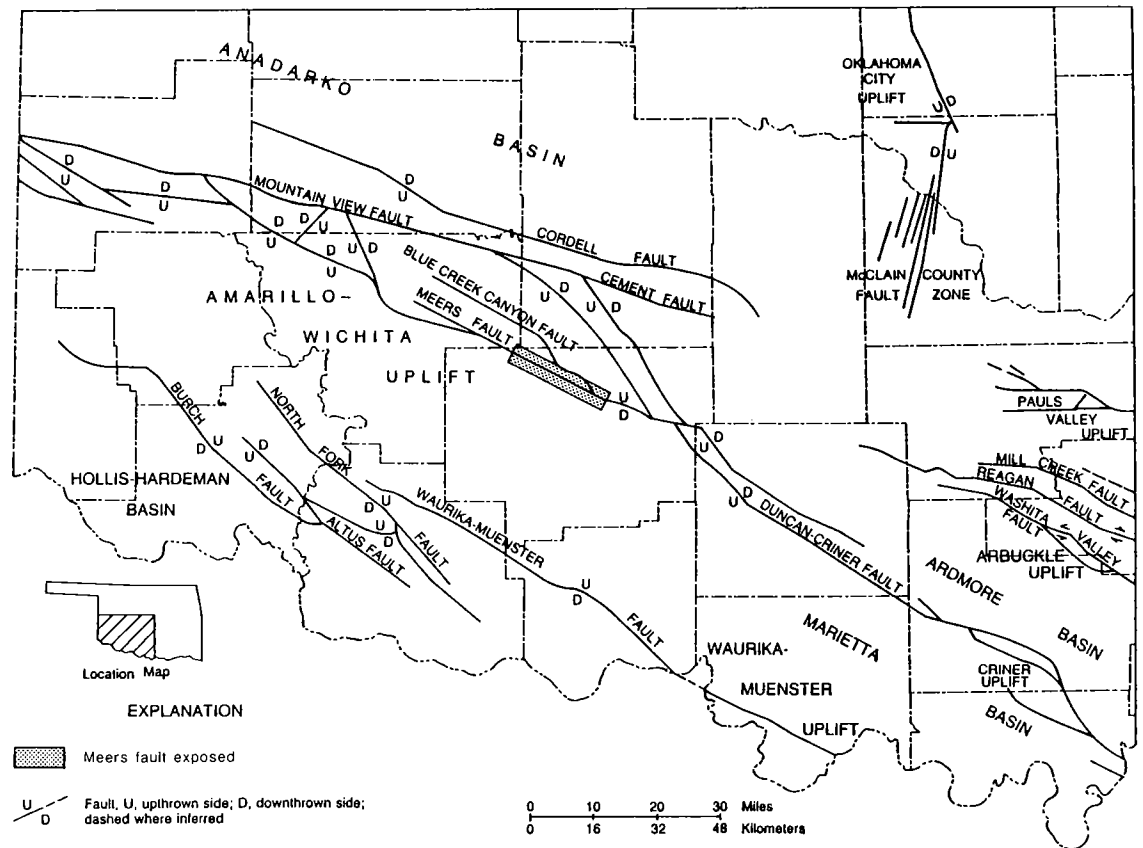


Figure 3. Major structural features in southwestern Oklahoma. Compiled from Ham and others (1964) and Harlton (1951, 1963, 1972).

displaced. The topographic expression of the fault is consistently down-to-the-south; the highest scarps are 3–5 m high along the central part, ~5 km southeast of State Highway 58 in sec. 33, T. 4 N., R. 12 W. Harlton (1963) extended the fault from the outcrop northwestward into the subsurface toward the Texas–Oklahoma state line and southeastward to the intersection with the Criner uplift.

The topographic scarp was initially interpreted as a fault-line scarp. The date of the last movement was thought to be Permian and related to the last adjustment between the Anadarko basin on the north and the Wichita uplift on the south.

Moody and Hill (1956) briefly noted that the Meers fault (Thomas fault) offsets Quaternary alluvium, and that the fault scarp is recent. This observation was generally overlooked until Gilbert (1983a,b) presented convincing evidence to support Quaternary movement on the Meers fault. Gilbert (1983a,b), Donovan and others

(1983), and Tilford and Westen (1984,1985) presented geomorphic evidence for recent movement. Their arguments are strongly supported by the continuity of the fault trace across Paleozoic rocks and Quaternary alluvium. Other evidence supports recent movement. For example, streams flowing normal to the fault scarp have incised channels into bedrock on the upthrown side of the fault and deposited recent alluvial fans on the downthrown side. In addition, Quaternary deposits exposed in a stream cut in sec. 2, T. 3 N., R. 12 W. are clearly offset by the fault.

Recent mapping by Madole (1986,1988) identified six fluvial allostratigraphic units in the vicinity of the Meers fault (Figs. 5,6). The units range in age from late Holocene to middle Pleistocene. Five units are believed to have regional distribution and the sixth unit, fault related fan alluvium, occurs in only close proximity to the fault. Quaternary stratigraphic relationships and ^{14}C age dates demonstrate that the last movement on



Figure 4. Aerial view (looking north) of the Meers fault displacing Post Oak Conglomerate on the Kimbell Ranch (secs. 15, 16, T. 4 N., R. 13 W.). Photograph by D. B. Slemmons, 1983.

the Meers fault was during the late Holocene. The last movement postdates the Browns Creek Alluvium, 13,000–14,000 yr B.P., and predates the East Cache Alluvium, 800–100 yr B.P. The topographic offset caused by faulting produced local stream incision on the upthrown side and deposition of sheetwash and fan alluvium on the downthrown side. Three ^{14}C age dates from material buried by fan alluvium indicate that faulting and deposition of fan alluvium probably occurred between 1,400 and 1,100 yr B.P.

The regional and local Quaternary stratigraphic relationships served as a guide for the location of two trench sites across the fault (Figs. 6–8). Trench one was excavated in the lower Holocene alluvium (Browns Creek Alluvium), and trench two was excavated in unnamed gravels thought to be upper Pleistocene. The two trenches provided important information about the age and characteristics of deformation associated with the Meers fault scarp (Figs. 9,10). In both trenches, the dominant mode of deformation is warping and flexing of the alluvium. Brittle deformation expressed as discrete faults accounts for about one-tenth to one-quarter of the total deformation. The difference in the amount of brittle deformation appears to be related to the degree of induration of the sediments at each site.

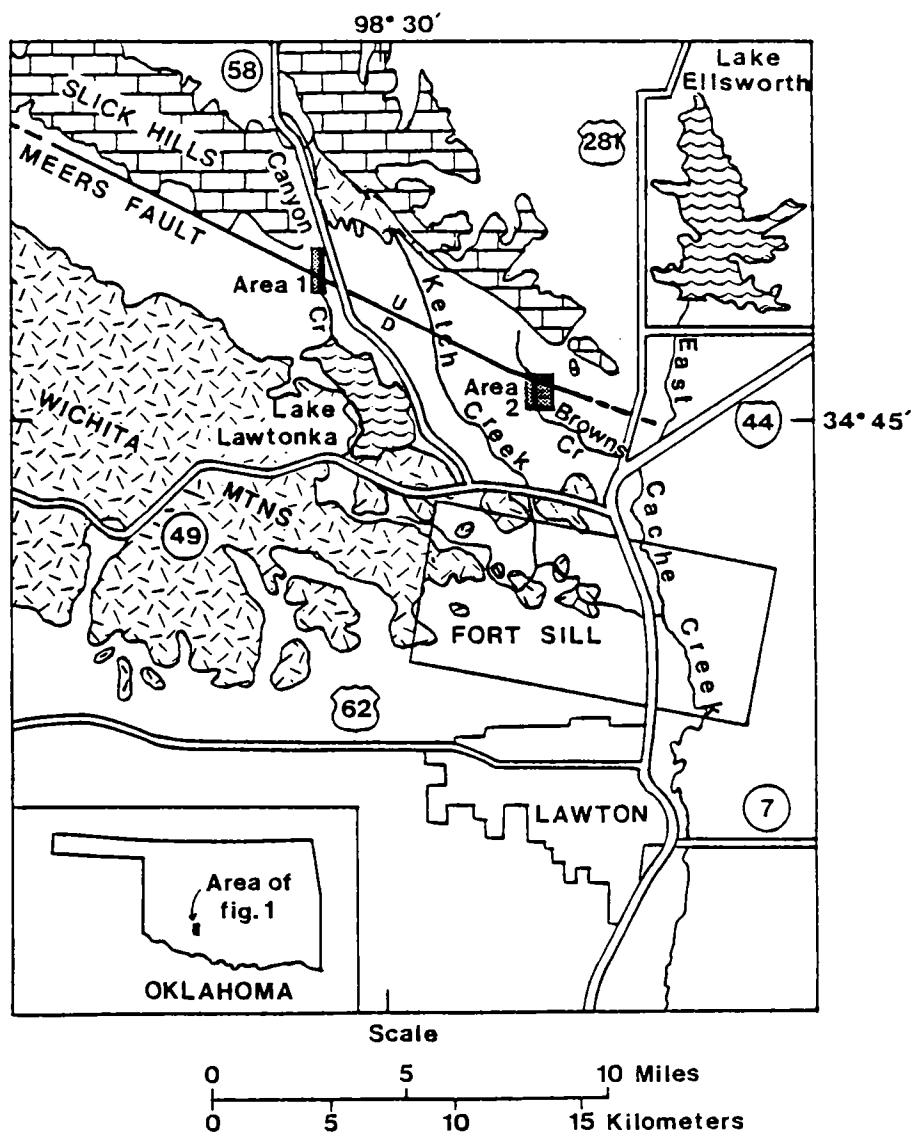
The surface faulting that formed the scarp in the vicinity of the trenches occurred during the late Holocene. The ^{14}C age dates on samples from the trenches suggest that the scarp formed about 1,700–1,300 yr ago. The age of the faulting from

trenching studies is consistent with the age determined from regional Quaternary stratigraphic studies.

The stratigraphy in the trenches and scarp profiles suggests that the net tectonic throw at both trench sites is ~ 3 m. A majority of the deformation took place in the vertical direction. The similar amounts of throw and the stratigraphy at each site suggest that the alluvium exposed in each trench was deformed by one surface-faulting event. If this interpretation is correct, major surface faulting has occurred only once since deposition of the gravel in trench two. Although their age is poorly constrained, these gravels are thought to be middle to late Pleistocene in age. This implies a lengthy recurrence interval (tens of thousands of years) for surface faulting on this part of the Meers fault. This conclusion assumes that the motion on the fault is consistent during succeeding events; however, the amount of vertical and lateral slip was difficult to detect in the gravels in trench two, and an undetected event in the gravels would reduce the inferred recurrence interval.

EARTHQUAKE DETECTION AND SEISMICITY IN THE ANADARKO BASIN

Prior to about 1950, the few seismographs that operated in states adjacent to Oklahoma were not



EXPLANATION




- | | |
|-------------------------------------------------------------------------------------|---------------------------------------------------------------------------------------|
|  |  |
| Rocks of Permian age, undifferentiated | Rocks of Late Cambrian and Early Ordovician age, Timbered Hills and Arbuckle Groups |
|  | |
| Rocks of Middle Cambrian age, Wichita Mountain Igneous Complex | |

Figure 5. Generalized bedrock geologic map of the region, showing the location of the Meers fault and the two study areas of Madole. Trench sites are in area 1.

YEARS (10 ³)	EPOCHS AND THEIR SUBDIVISIONS		ALLUVIAL UNITS
0	HOLOCENE	Late	East Cache Alluvium
5		Middle	
7.5		Early	
10	QUATERNARY PLEISTOCENE		Browns Creek Alluvium
		Late	
130			Kimbell Ranch Alluvium
		Middle	Porter Hill Alluvium
790			Lake Lawtonka Alluvium
		Early	
1700			

Figure 6. Subdivisions of Quaternary time and the estimated ages of alluvial units along the Meers fault (Madole, 1986-88).

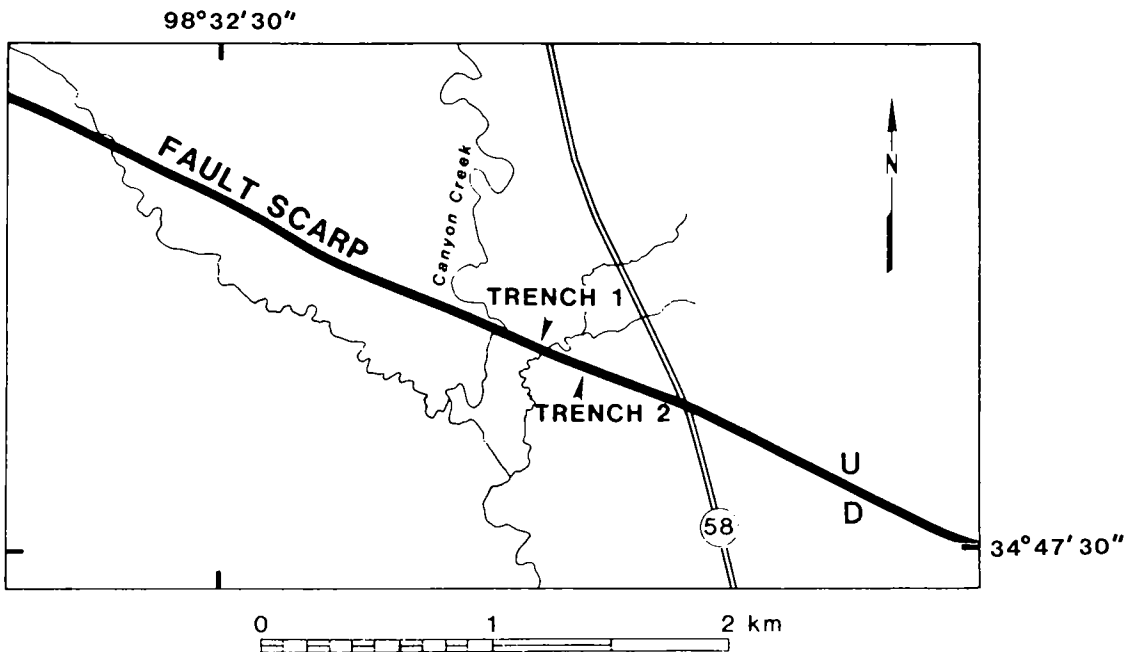


Figure 7. Locations of trenches across the Meers fault, Comanche County, Oklahoma.

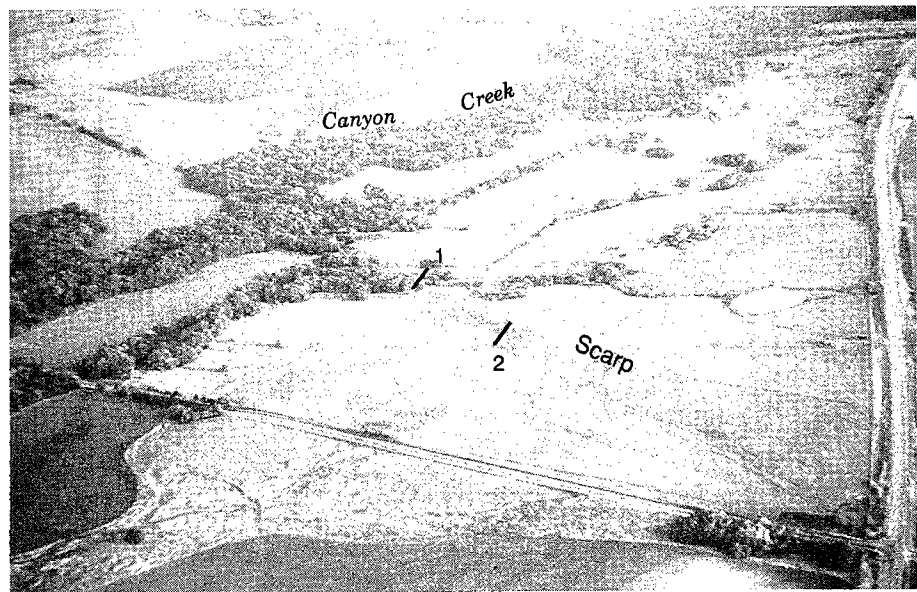


Figure 8. Aerial view of the Meers fault and trench locations. State Highway 58 on the right. Numbered lines are trenches as labeled in Figure 7. Photograph by D. B. Slemmons, 1983.

sensitive enough to detect most earthquakes occurring in the State. Only written records of humans having felt earthquakes were available. These records were usually in local newspapers only. Some of the larger felt earthquakes were listed in the "Seismological Notes" column of the bimonthly *Bulletin* of the Seismological Society of America. A more complete earthquake listing was begun about 1929, in the annual publication *United States Earthquakes*.

Seismographs were first operated in Oklahoma in 1961 at the Jersey Production Research Company's (now Exxon) Leonard Earth Sciences Observatory in southern Tulsa County, and at the U.S. Air Force Advanced Research Projects Agency's Wichita Mountains Seismological Observatory in Comanche County. The Leonard Earth Sciences Observatory was designated by the abbreviation TUL from 1961 up to and including its current operation as the Oklahoma Geological Survey's Oklahoma Geophysical Observatory. The Air Force installation in Comanche County, designated by the abbreviation WMO, was designed and operated primarily to detect and distinguish between distance earthquakes and distant underground nuclear tests. WMO closed in 1971 after several years of sharply curtailed activity. Both WMO and TUL seismographs made excellent recordings of P waves from distant earthquakes, but they par-

tially filtered out high-frequency waves characteristic of nearby earthquakes.

In the early 1970s, TUL became the established source of information to the seismological community for Oklahoma earthquakes and some earthquakes of nearby areas. The Observatory became one of 50 agencies throughout the world that report epicenters directly to the International Seismological Centre in Newbury, England, for publication in its monthly bulletin and semi-annual catalog. In 1975 the Observatory began officially to furnish the National Oceanic and Atmospheric Administration (NOAA), and subsequently the U.S. Geological Survey, with data on earthquakes felt in Oklahoma for the annual publication *United States Earthquakes*.

The University of Oklahoma Earth Sciences Observatory, the Oklahoma Geological Survey, and the U.S. Nuclear Regulatory Commission started a cooperative program in 1976 to study seismicity of the Nemaha uplift and other areas of Oklahoma. The Observatory staff began a program to computerize the accumulated earthquake catalog, which included a compilation of earthquake information from published and unpublished reports, the data being held on magnetic tape for complete or selected printing as needed.

Prior to 1962, all earthquakes in the Anadarko basin were located either from historical accounts or from seismograph stations outside the region.

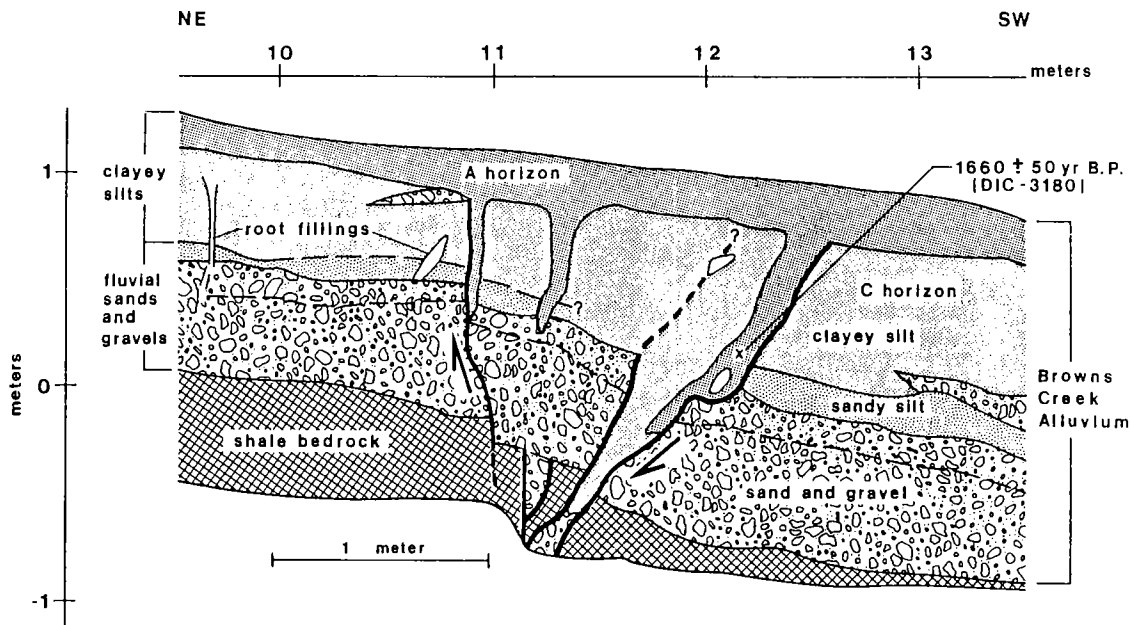


Figure 9. Part of the trench 1 log, showing stratigraphic relations near the main fault and locations of ^{14}C age sample. Heavy lines are faults and edges of cracks that could be recognized by abrupt changes in the stratigraphy, dashed where inferred; arrows show general sense of displacement across the main fault zone. Fine lines are stratigraphic contacts, dashed where subtle. (From Crone and Luza, 1986.)

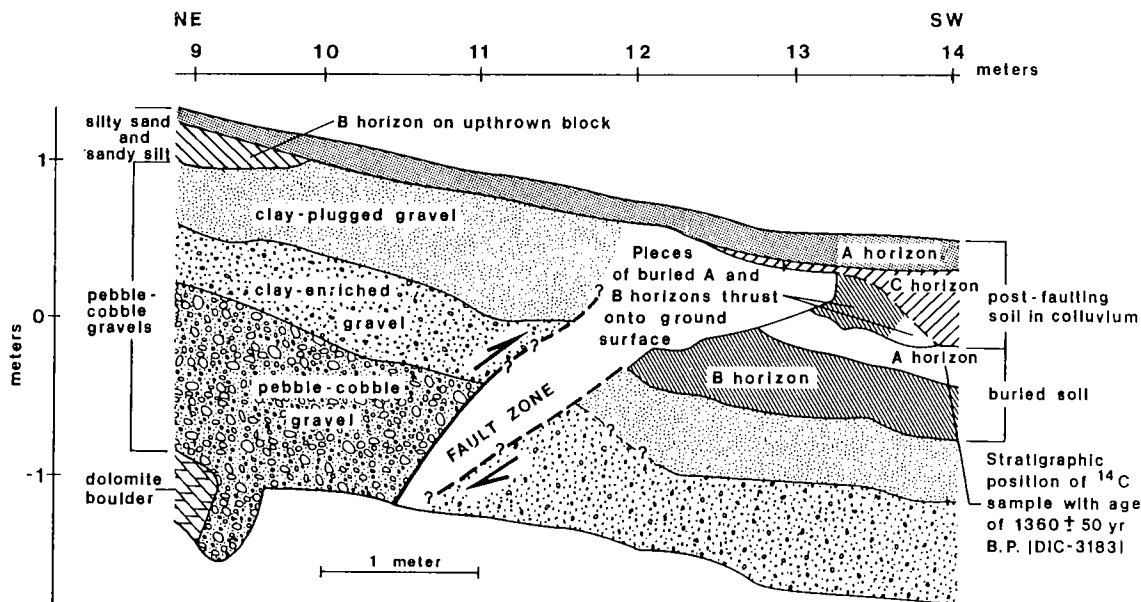


Figure 10. Part of trench 2 log, showing stratigraphic relations near the main fault zone. Heavy lines are faults that could be recognized by abrupt changes in the stratigraphy (dashed where inferred); arrows show general sense of displacement across the main fault zone. Fine lines are stratigraphic contacts (dashed where subtle). (From Crone and Luza, 1986.)

Therefore, the epicentral locations are based on data that may vary greatly in accuracy. During this time, 40 earthquakes were known to exist in the Anadarko basin—30 in Oklahoma and 10 in Texas (Fig. 11). More than half of these events took place in Canadian County, the largest known Oklahoma earthquake, magnitude 5.5(mb), occurring near El Reno on April 9, 1952. This earthquake was felt in Des Moines, Iowa, and Austin, Texas, and the felt area was $\sim 362,000 \text{ km}^2$ ($\sim 140,000 \text{ mi}^2$).

From 1961 to 1972, seismographs at stations WMO and TUL provided excellent records of distant earthquakes. However, most local earthquakes went unrecorded because of the poor high-frequency-response characteristics of the seismographs. In 1973, station TUL began to re-

cord high-frequency seismograms. This greatly increased the capability to detect small earthquakes and to discriminate earthquakes from quarry blasts. However, the location of earthquakes depended either on finding felt reports and/or on having clear first-motion directions and horizontal-amplitude measurements made from the seismic records. From 1962 to 1976, 16 earthquakes, 14 in Oklahoma and 2 in Texas, were located in the Anadarko basin (Fig. 11). Ten of the 16 earthquakes were reported felt (Fig. 12).

In 1976, a program was begun in cooperation with the U.S. Nuclear Regulatory Commission to install at least seven semipermanent and three radio-telemetry seismograph stations in Oklahoma (Fig. 13). These additional seismograph stations have tremendously improved earthquake

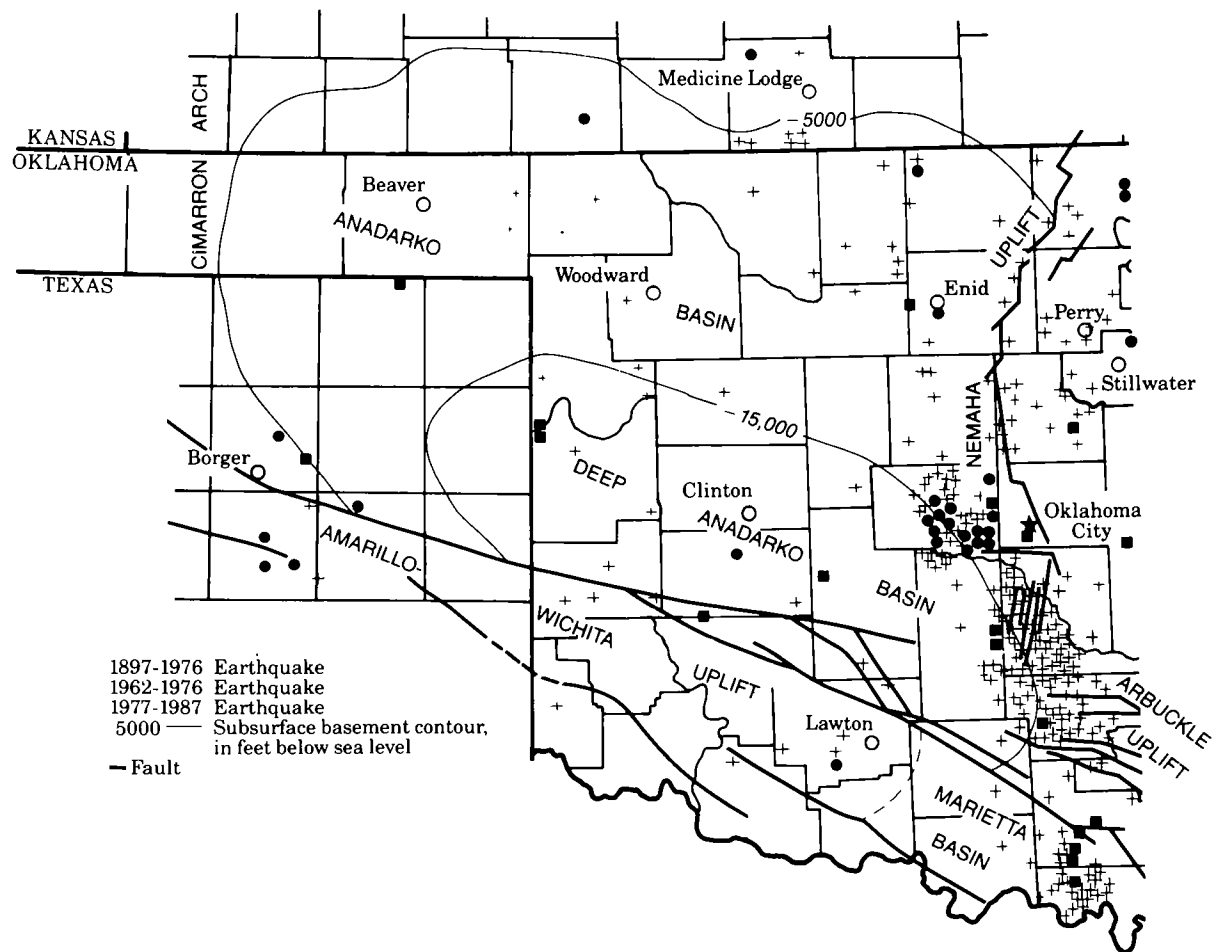


Figure 11. Distribution of earthquakes by time interval within and adjacent to the Anadarko basin (Lawson and others, 1979; Lawson and Luza, 1980-88; Steeples, 1984; U.S. Department of Energy, 1986; Reagor and others, 1982; Stover and others, 1981a,b).

detection and location accuracy in Oklahoma and adjacent areas. This is reflected by the large increase in locatable Oklahoma earthquakes. From 1977 to 1986, more than 320 additional earthquakes were located in the Anadarko basin (Fig. 11), mostly of magnitudes <2.5 . However, 22 earthquakes were reported felt (Fig. 12).

DISCUSSION

More than 370 locatable earthquake events have taken place in the Anadarko basin since 1897. The earthquake data show at least two seismic trends worthy of discussion.

One trend is in north-central Oklahoma. There appears to be a 40-km-wide, 145-km-long earth-

quake zone that extends northeastward from near El Reno (Canadian County) toward Perry (Noble County) (Fig. 11). Most of the earthquakes within this zone have occurred in the vicinity of the El Reno–Mustang area, which has been the site of numerous earthquakes since 1908. The correlation of historical and recent earthquake activity with known structural features remains unclear. The El Reno–Perry trend appears to cut diagonally across the Nemaha uplift at an angle of $\sim 30^\circ$. The southern end of this trend appears to be more active than the middle and northern parts. Both the recent and the historical earthquake data seem to support this observation.

The second trend is situated between Canadian County and the south edge of Garvin County. A majority of the Anadarko-basin earthquakes have

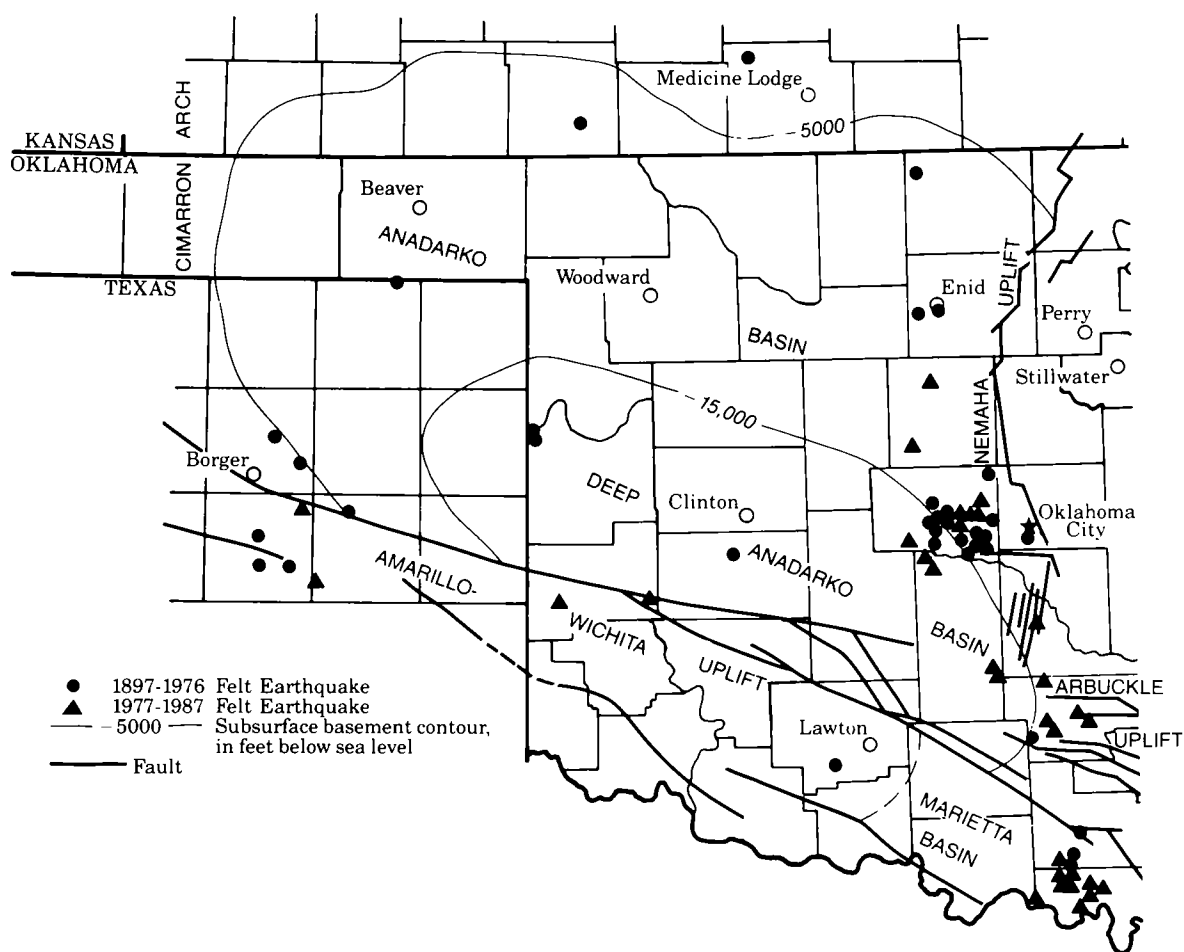


Figure 12. Distribution of felt earthquakes within and adjacent to the Anadarko basin during 1897–1987 (Lawson and others, 1979; Steeples, 1984; U.S. Department of Energy, 1986; Reagor and others, 1982; Stover and others, 1981a,b; Lawson and Luza, 1980–83, 1985, 1986, 1988).

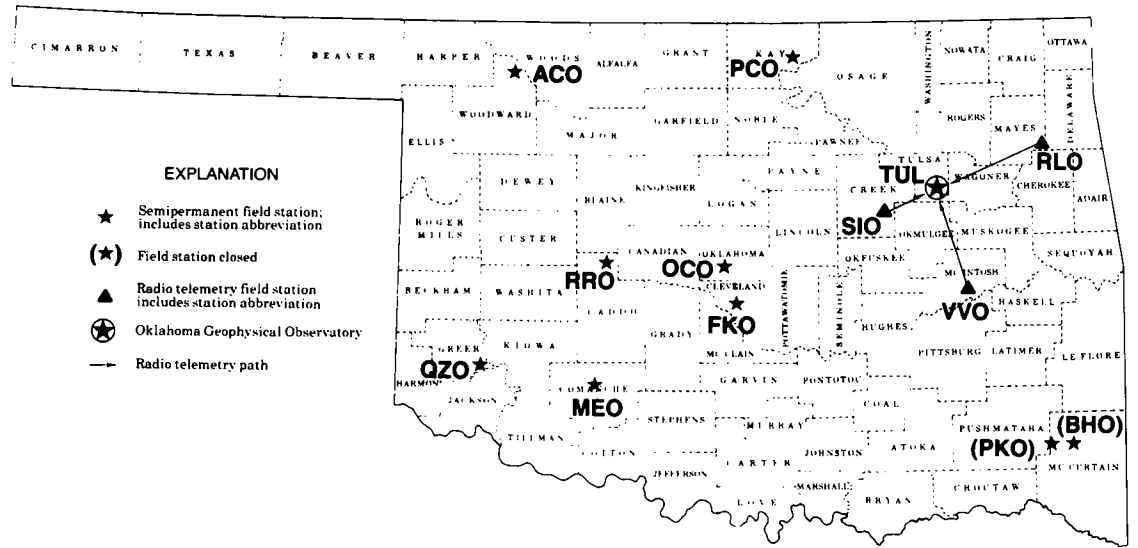


Figure 13. Active seismograph stations in Oklahoma.

occurred within this 40-km-wide, 135-km-long zone. More than 90% of the earthquakes within this zone have taken place since 1977 (Fig. 11). The trend closely parallels the McClain County fault zone, which is ~40 km wide and ~60 km long. Perhaps this highly complex fault zone, which contains numerous subparallel faults, is the southernmost extension of the Nemaha uplift.

A few earthquakes have occurred in the shelf and deep portions of the basin. The Amarillo–Wichita uplift and associated fault zone are seis-

mically very quiet. The Amarillo–Wichita uplift consists of older layered gabbros overlain by granite sheets. The uplifted area may behave more rigidly than the surrounding region. Thus, along the frontal fault system stress may build up to levels higher than in the more seismically active areas (Donovan and others, 1983). When the stress along the frontal fault system has been relieved by a large earthquake (as along the Meers fault), this region may experience very low seismic activity for a considerable time.

ANADARKO BASIN CONODONT STUDIES

JOHN E. REPETSKI

U.S. Geological Survey, Reston

Abstract.—Preliminary analysis of early Paleozoic conodonts from the subsurface within and adjacent to the Anadarko basin demonstrates their utility in stratigraphic and thermal evolution studies in the basin. More than 100 samples from 30 drill holes produced conodonts that can be correlated with faunas known from rock sequences exposed along the southern flanks of the basin. For the Middle Ordovician to Devonian, extant biozonations and/or recent published literature based on Oklahoma surface sections allow good biostratigraphic correlation into the subsurface and often allow testing of physical correlations. In contrast, conodonts from the Arbuckle Group (Lower to Middle Ordovician) are less well known. Faunas from the upper half of the group are documented only in unpublished theses, and published faunas are in need of restudy and revision. However, this limited information, along with work in progress in Oklahoma and data from carbonate platform facies elsewhere in North America, still permit correlations into the subsurface with the promise of increasingly improved resolution.

Down-hole and regional conodont color alteration index (CAI) values demonstrate consistent patterns within and adjacent to the basin. The relationships of CAI values to present burial depths are as follows: (1) CAI 1 to 1½, 0 to ~10,000 ft; (2) CAI 2, ~10,800 to at least 12,000 ft; (3) CAI 2½, ~11,600 to 17,000 ft; and (4) CAI 3, 15,000 to at least 19,500 ft. A potential pitfall encountered in thermally indexing the meager populations of conodont elements that often are recovered from small samples of core or cuttings is that some of the conodonts may be anomalously darkened. Such darkening can result from post-mortem, pre-burial biogenic degradation of their contained organic matter at the seawater/sediment interface. Care must be taken to index consistently the least-altered elements in these "mixed-color" samples.

DIAGENESIS OF HYDROCARBON-BEARING ROCKS IN THE MIDDLE ORDOVICIAN SIMPSON GROUP, SOUTHEASTERN ANADARKO BASIN, OKLAHOMA

JANET K. PITMAN

U.S. Geological Survey, Reston

ROBERT C. BURRUSS

U.S. Geological Survey, Denver

Abstract.—Quartzarenites and subarkoses in the Middle Ordovician Simpson Group in the Gulf Costello No. 1 and Sunray-DX Parker No. 1 Mazur wells, southeastern Anadarko basin, have undergone a complex diagenetic and petroleum-migration history. During early burial, petroleum migrated locally through sandstones; patches of bitumen in calcite and bitumen-lined quartz overgrowths containing oil-bearing inclusions reflect the introduction of petroleum-bearing fluids at shallow depths. Stable-isotope data reveal that early calcite precipitated at near-surface temperatures from fluids dominated by marine carbon. At moderate to deep burial, calcite dissolution, followed by ferroan-dolomite and clay-mineral precipitation, occurred at about the same time as the rocks reached levels of thermal maturity sufficient for the generation of hydrocarbons. Maximum paleotemperatures during deep burial are estimated from maturation models to have reached 250°F in the Costello well and 300°F in the Mazur well. Maturation-derived temperatures in the Costello well are consistent with preliminary homogenization temperatures (210–250°F) for oil inclusions along microscopic healed fractures that formed during deep burial, thus supporting an Early to Middle Pennsylvanian timing for the generation and migration of late-stage hydrocarbons. The early petroleum phase, emplaced while the rocks were at shallow burial depths, migrated from mature source rocks deeper in the basin.

INTRODUCTION

Hydrocarbons in the Middle Ordovician Simpson Group, southeastern Anadarko Basin, occur in fine- to medium-grained quartzarenites that have undergone a complex depositional and diagenetic history. Our studies show that reservoir rocks in the Simpson were affected by extensive diagenetic modification during early burial, and were subjected to at least two stages of hydrocarbon migration. Maturation modeling and preliminary fluid-inclusion geothermometry establish the relative timing of individual diagenetic events and discrete petroleum-migration episodes with respect to the burial history of the Simpson.

Cores of the Simpson Group from the Sunray-DX Parker No. 1 Mazur well (sec. 1, T. 3 N., R. 5 W.) and from the Gulf Oil Co., Costello No. 1 well (sec. 14, T. 5 N., R. 5 W.) in the southeast part of the basin (Fig. 1) were selected for petrographic and geochemical study. Hydrocarbon shows were encountered in the Mazur well, and oil was tested in the Bromide Formation of the Simpson Group in the Costello well. Core material from both wells shows oil staining in porous sandstones and along fracture surfaces.

METHODS

Core of the Simpson Group were taken from the Mazur well at 15,000–17,000 ft, and from the Costello well at 11,000–12,000 ft; individual sandstones were selected for mineralogic and geochemical analysis. More than 150 thin sections were studied petrographically (300 counts per section) in order to identify the primary and secondary mineral phases and their paragenetic relations. Each section was impregnated with blue epoxy to identify pores, stained with both cobaltinitrite to determine the presence of K-feldspar, and stained with combined potassium ferricyanide and alizarin-red S to distinguish ferroan from nonferroan carbonate.

Stable-isotope analysis was performed on representative samples of end-member carbonate to determine their carbon- and oxygen-isotope compositions. Individual analyses were determined by reacting carbonate with phosphoric acid and analyzing the evolved CO₂ gas. The results are reported in per mil relative to the PDB (Pee Dee Belemnite Chicago) standard.

Fluid inclusions containing oil were identified by fluorescence microscopy using long-wave ultra-

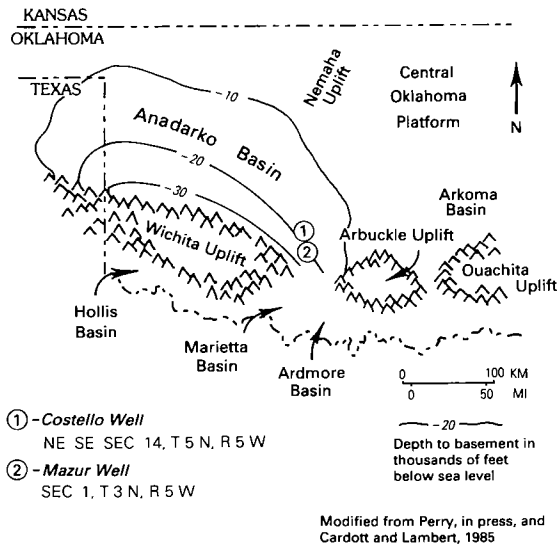


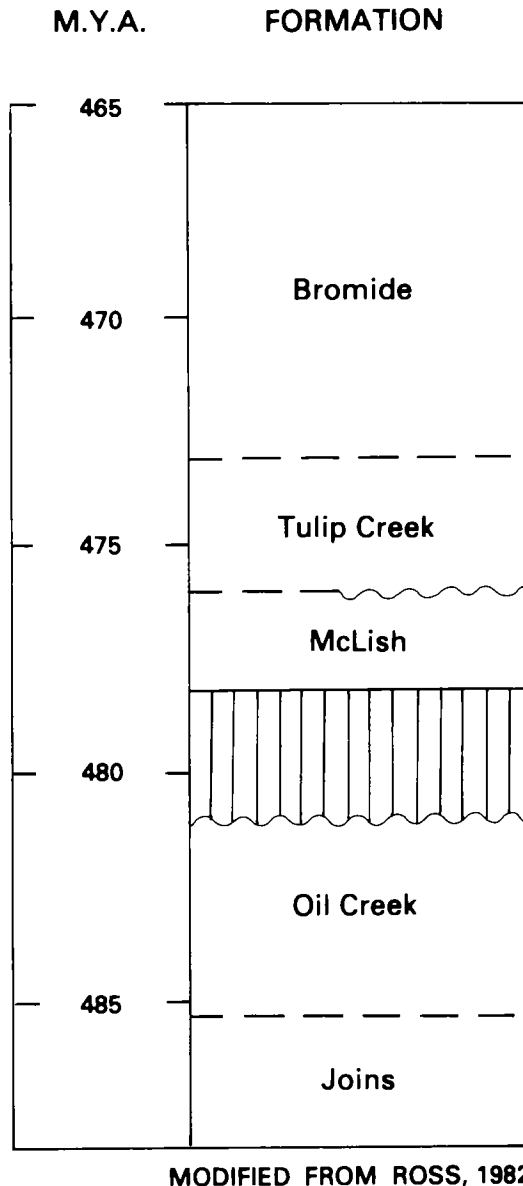
Figure 1. Map of the Anadarko Basin, showing location of the Gulf Costello and Sunray-DX Mazur wells.

violet (UV, 365 nm) illumination with techniques described by Burruss (1981) and Burruss and others (1985). Preliminary homogenization temperatures were made on fragments of thin sections, using the USGS gas-flow stage for heating/cooling microscopy, and using the methods described in Hollister and others (1981).

GEOLOGIC SETTING

The Simpson Group in the southeastern Anadarko basin comprises a thick sequence of sediment deposited in a shallow marine environment in the southern Oklahoma aulacogen during the Middle Ordovician. Rocks preserved in the Simpson represent a westward-thinning clastic wedge that records marine transgressive-regressive cycles associated with sea-level fluctuations. In the area of study, the Simpson Group attains a thickness of ~1,500 ft. This thick sequence of sediment reflects deformation contemporaneous with rapid sedimentation in an actively subsiding basin. Deposition and subsidence continued through Pennsylvanian time as the Simpson underwent progressive burial beneath younger Paleozoic rock. At maximum burial, the Simpson in the Costello well was at a depth of ~14,000 ft, and in the Mazur well it was at a depth of ~18,000 ft. Stratigraphic reconstruction and vitrinite-reflectance studies (Schmoker, 1986) reveal that 2,000–5,000 ft of sediment may have been removed by erosion late in the burial history.

The Simpson Group has been subdivided into five formations, which are, in descending order, the Bromide, Tulip Creek, McLish, Oil Creek, and Joins (Decker and Merritt, 1931; Fig. 2); the Joins was not sampled for this study. In the two study wells, each formation consists of a lower sandstone lithofacies and an upper mudstone-siltstone-limestone lithofacies (Flores and Keighin, personal communication, 1987; Pitman and Wiggs, unpublished data, 1987). Based on



MODIFIED FROM ROSS, 1982

Figure 2. Stratigraphic column showing formations of Middle Ordovician Simpson Group.

the distribution of lithologies, sedimentary structures, and biologic constituents, the cored rocks represent sedimentation in shallow marine shoreface and tidal-flat environments.

MINERALOGY

In the study wells, sandstones in the Simpson Group, except in the McLish Formation, are dominantly fine- to medium-grained quartzarenites that contain >90% detrital quartz. Rare feldspar grains, accessory minerals, and fossil fragments occur locally. The upper part of the McLish consists of fine-grained, subarkosic sandstones containing detrital quartz, potassium feldspar, and small amounts of chert (Weber, 1987). The relative proportions of framework-grain types are illustrated in Figure 3 and are summarized on Table 1.

Detrital Grains

The dominant framework grain in Simpson sandstones is quartz, averaging ~65% of the whole rock. Quartz occurs as rounded, monocrystalline grains that are often pitted or fractured and display undulatory extinction. In some sandstones, the surfaces of quartz grains are coated with a thin film of bitumen.

Feldspar is an important constituent (1–2%) in the McLish Formation, but is virtually absent in

the other units. Feldspar is dominantly a potassium-rich variety, comprising small, subangular to subrounded grains of orthoclase, perthite, and microcline whose size and shape approximate those of nearby quartz grains. Subequal amounts of plagioclase are present locally in some sandstones. Varying degrees of alteration characterize individual grains. Some grains are fresh and unaltered, whereas others show preferential replacement by carbonate, partial dissolution, or alteration to clay.

Rock fragments are generally absent in Simpson sandstones, except in the McLish, where small, rounded grains of fine-crystalline chert are present. Many chert grains have undergone partial dissolution or have been deformed between framework grains to form a pseudomatrix.

Depositional matrix, introduced by burrowing organisms, constitutes ~5% of the whole rock. X-ray-diffraction analysis reveals that most of this material is composed of well-ordered illite and chlorite, although in the Costello well some allogenic clay is composed of mixed-layer illite-smectite. In areas where matrix is widespread it has been replaced by euhedral rhombs of ferroan dolomite or shows the effects of partial dissolution.

Various amounts of collophane, zircon, and tourmaline are present in some sandstones. Fragments of bryozoans, conodonts, brachiopods, echinoderms, trilobites, and ostracodes are locally abundant, particularly in the Bromide and Oil Creek Formations.

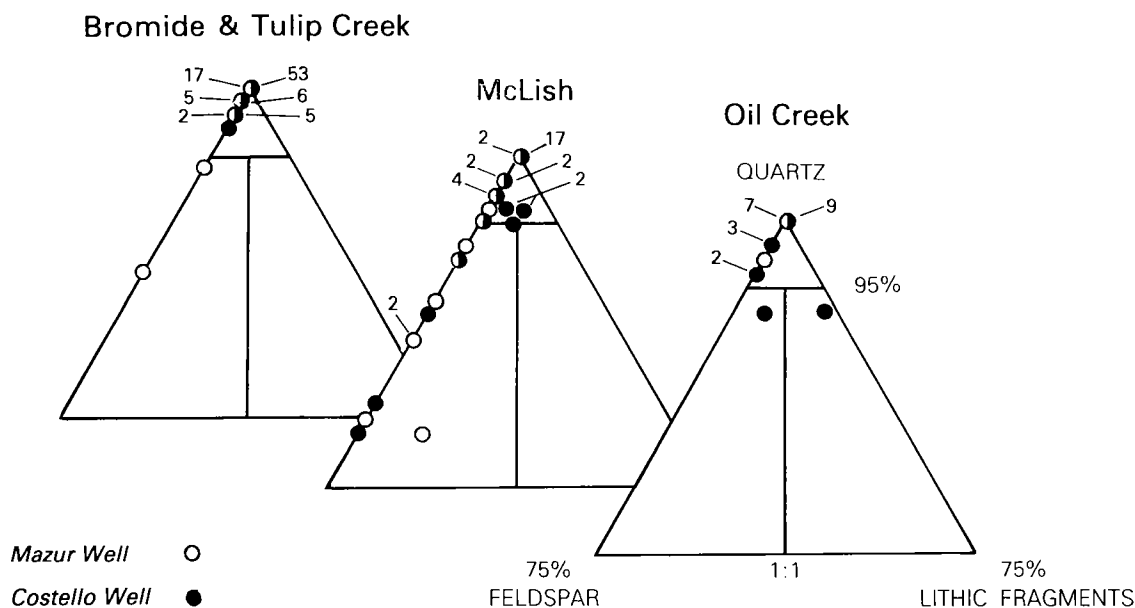


Figure 3. Ternary diagram showing framework-grain composition for formations of the Simpson Group.

TABLE 1.—SUMMARY OF MEAN MODAL VALUES AND STANDARD DEVIATIONS
(IN PARENTHESES) FOR SANDSTONES IN THE SIMPSON GROUP

Formation	Quartz	Feldspar	Matrix	Rock fragments	Secondary quartz	Authigenic carbonate	Other
<u>Costello Well</u>							
Bromide	72.35 (9.11)	0.22 (0.66)	4.37 (8.63)	0.22 (0.79)	9.24 (7.71)	6.96 (10.20)	6.20 (4.95)
Tulip Creek	75.00 (9.54)	0.29 (0.56)	0.10 (0.30)	--	8.14 (6.17)	7.29 (11.72)	8.57 (6.34)
McLish	53.72 (13.74)	1.86 (3.79)	5.72 (9.83)	0.10 (0.31)	8.66 (6.82)	18.83 (12.88)	10.17 (5.08)
Oil Creek	65.56 (14.25)	0.81 (1.11)	7.63 (9.86)	0.38 (1.26)	2.94 (4.04)	19.81 (15.36)	2.06 (2.11)
<u>Mazur Well</u>							
Bromide	64.31 (11.92)	0.23 (0.83)	6.54 (8.72)	--	4.92 (6.87)	20.23 (12.77)	2.46 (2.50)
Tulip Creek	72.08 (19.66)	0.58 (0.51)	1.25 (2.83)	--	6.75 (9.84)	13.25 (18.70)	5.08 (3.20)
McLish	52.24 (13.21)	3.59 (3.22)	5.65 (5.01)	0.12 (0.49)	7.71 (8.72)	25.59 (15.76)	4.65 (2.74)
Oil Creek	69.00 (17.17)	0.13 (0.35)	3.25 (6.11)	--	5.25 (5.20)	18.18 (18.26)	2.63 (2.26)

Authigenic Constituents

Simpson sandstones have been modified by a variety of authigenic mineral cements. The dominant pore-fill cement in both wells is secondary quartz, distributed as syntaxial quartz overgrowths. Typically, it averages ~7% of the whole rock (Table 1). Quartz cement is most widespread in quartzarenites that are texturally mature and contain little detrital matrix, early carbonate cement, or evidence of early-migrated hydrocarbons. Authigenic quartz often is absent or poorly developed in immature feldspathic sandstones and quartzarenites which contain significant amounts of allogenic clay or carbonate cement. In the Costello well, quartz overgrowths in the Bromide Formation often are incompletely developed, and coated with a thin film of bitumen. Where the overgrowths are not intergrown, they form open, triangular, primary pores.

Authigenic carbonate in sandstones varies

widely in abundance both within and between formations (Table 1). It ranges from about 5 to 25% in the Bromide, from 10 to 13% in the Tulip Creek, from 22 to 24% in the McLish, and from 18 to 25% in the Oil Creek. Petrographic analysis reveals an iron-rich and iron-poor carbonate assemblage that is complex both in its mineralogic composition and in its distribution. No distinct carbonate trends related to burial depth were evident in either well. Nonferroan calcite, the most abundant carbonate phase, occurs as an anhedral to subhedral, poikilotopic, pore-fill cement that may contain patches of bitumen. This variety of calcite often is associated with fossiliferous debris. Framework grains enclosed by nonferroan calcite typically show rare grain-to-grain contact and little quartz-overgrowth cement. Ferroan calcite may partly to completely replace nonferroan calcite and fossil fragments. In areas where ferroan calcite is abundant, it forms an optically continuous, coarsely crystalline cement; like nonferroan calcite, it contains inclusions of bitumen.

Sandstones displaying secondary porosity often show evidence of calcite dissolution. The most common features indicating secondary porosity are embayed margins of quartz grains and grain overgrowths, pores containing remnants of calcite cement, and discrete patches of calcite. Some feldspar grains in the McLish Formation show the effects of dissolution along cleavage planes; however, replacement calcite was not observed in any of these grains, suggesting that they may have dissolved in situ.

The most common type of dolomite in Simpson sandstones occurs as coarse, euhedral crystals that are zoned with respect to their iron content. Individual rhombs typically display well-developed crystal faces with no evidence of prior dissolution; in many samples they are associated with patches of clay or bitumen. Where rhombic dolomite is widespread, it usually replaces matrix material and early calcite cement. It also may occur as small isolated crystals along granulation bands and stylolite seams. Rhombic dolomite is poorly developed in sandstones where there has been extensive quartz cementation.

X-ray-diffraction analysis reveals a clay-mineral assemblage in the Costello well consisting of varying proportions of mixed-layer illite-smectite, small amounts of kaolinite, and moderate to large amounts of well-crystallized illite and chlorite (V. Colton-Bradley, personal communication, 1987). This clay assemblage is distinct from that reported from the Mazur well, which is composed predominantly of well-ordered illite (Pollastro, personal communication, 1986). Together, these authigenic phyllosilicates form a dense network in some pores.

Other Features

Fractures filled with bitumen or rare calcite occur locally in some sandstone beds in addition to stylolites with seams consisting of insoluble residue, heavy minerals, or bitumen. Both features cut all authigenic mineral cements.

FLUID INCLUSIONS

Fluorescence microscopy reveals that Simpson sandstones may contain fluid inclusions in detrital mineral grains, in authigenic mineral phases, and along microfractures. In the Mazur and Costello wells, there are numerous inclusions in individual quartz grains that are similar to inclusions described by Burruss (1981). Typically, these inclusions are nonfluorescent. One-phase inclusions are CO_2 -rich; two-phase inclusions are aqueous; and three-phase inclusions are CO_2 - H_2O rich—characteristic of metamorphic and igneous rocks.

In sandstones from the Costello well, sparse

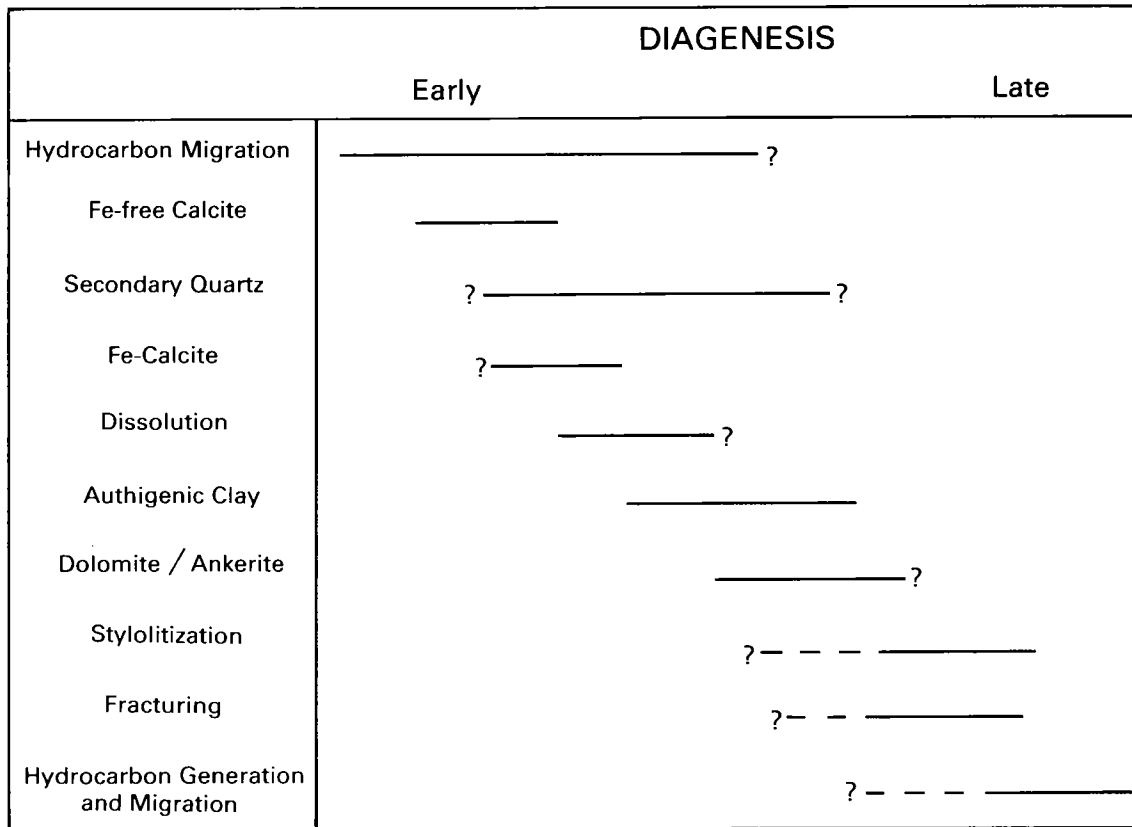
fluid inclusions are associated with discrete authigenic mineral cements. Individual inclusions may be trapped along dust rims on detrital quartz grains, or randomly distributed within syntaxial quartz overgrowths. Likewise, they may occur along dust rims separating detrital feldspar cores from authigenic overgrowths, although these inclusions are rare, because feldspar is generally uncommon in Simpson sandstones. Fluid inclusions in authigenic carbonate minerals were not identified; however, the thin sections used for fluorescence microscopy were etched and stained to differentiate ferroan from nonferroan carbonate, which may have destroyed any inclusions. Thus, the occurrence of inclusions in authigenic carbonate is uncertain and requires further study.

Fluorescence analysis shows that some sandstones in the Costello well locally contain linear trains of fluid inclusions along healed microfractures that crosscut detrital mineral grains and authigenic mineral cements. Where stylolites are present, the microfractures commonly are oriented perpendicular to the stylolite seam, although a few samples with fractures transecting partly dissolved quartz grains are oriented parallel to stylolite seams.

The most common fluid inclusions trapped in authigenic cements and along microfractures are two-phase, composed of fluorescent liquid petroleum and vapor. Less commonly, microfractures comprising oil-bearing inclusions also contain nonfluorescent, two-phase aqueous liquid and vapor inclusions and, very rarely, three-phase inclusions containing petroleum liquid, aqueous liquid, and vapor. These three inclusion types also occur along dust rims of detrital quartz grains in both the Mazur and Costello wells. In the Costello well, petroleum inclusions on dust rims and trapped within secondary quartz overgrowths may contain a rare dark-brown phase that appears to be similar to bitumen or "oil stain" that may have precipitated from the petroleum liquid after it was trapped in the inclusion. Fluorescent organic matter within mineral cements other than that in inclusions was not observed.

DIAGENESIS

Sandstones in the Mazur and Costello wells have undergone a complex diagenetic history punctuated by two episodes of hydrocarbon migration (Fig. 4). The major events include (1) early hydrocarbon migration; (2) precipitation of nonferroan calcite, followed by secondary quartz; (3) development of ferroan calcite; (4) dissolution of calcite; (5) formation of authigenic clay; (6) crystallization of zoned Fe-bearing dolomite; (7) development of fractures and stylolites; and (8) late-stage hydrocarbon migration. The markedly similar diagenetic sequence in these moderately



to deeply buried sandstones indicates that most postdepositional alteration took place early in the burial history, before the rocks reached maximum burial.

Pervasive quartz cementation in Simpson sandstones generally occurred at shallow to moderate burial depths, before significant hydrocarbon migration but after the precipitation of calcite. In sandstones where incompletely developed quartz overgrowths lined with bitumen create open primary pores, and overgrowths contain petroleum inclusions, the accumulation of oil apparently was sufficient to have inhibited the further growth of quartz, thus preserving the sandstones from complete alteration. Several sources may have contributed to the large volume of secondary quartz preserved in most sandstones. A significant amount of quartz cement could have formed during early burial if silica-saturated ground water mixed with sea water in sands while they were porous and permeable. Another source of silica may have been clay-mineral reactions that oc-

Carbonate Development

The complex carbonate assemblage observed in Simpson sandstones reflects the chemical and isotopic composition of pore fluids that evolved during burial. The earliest carbonate mineral, nonferroan calcite, formed early in the burial history at shallow depths, before grain compaction or development of quartz overgrowths. This early carbonate phase was followed by precipitation of ferroan calcite later in the burial history. Re-worked fossil fragments in sandstones and nearby

beds of limestone were sources of ions for calcite crystallization. Both varieties of calcite were subjected to a period of dissolution late in the burial history, possibly caused by carbonic acids that were released in response to the maturation of hydrocarbons. Waters derived from compaction of interbedded shales, or fluids that migrated from deeper in the basin, also may have been responsible for some carbonate dissolution. Zoned ferroan dolomite, the last carbonate phase to form in sandstones, acquired most of its magnesium and iron from illitic matrix, which is almost completely replaced. Some magnesium also may have been supplied to solution by shale-dewatering or released during the smectite-to-illite conversion.

The isotopic composition of discrete carbonate phases in the Simpson Group is shown in Figure 5. Carbon compositions for calcite and dolomite (about 0 to -5‰) are in the range commonly associated with marine carbonate, with no evidence for a significant influx of organic carbon from plant material or mature kerogen. The oxygen compositions for carbonate (about -3 to -9‰) show significant scatter but no isotopic trend with increased burial depth. Compositional variations in oxygen, on the order of 6‰, most likely reflect the combined effects of temperature during diagenesis and pore waters whose chemical and isotopic composition evolved during burial.

Because much of the carbonate precipitated at relatively shallow burial depths, the original isotopic composition of fluids buried with the sediments likely approximated that of sea water.

HYDROCARBONS

Petrographic studies and fluid-inclusion analysis combined with maturation modeling reveal two episodes of hydrocarbon migration in Simpson sandstones in the Mazur and Costello wells—one in the early Paleozoic, when the rocks were at shallow depths, and the other late in the Paleozoic, when the rocks had attained their maximum burial depth and paleotemperature. The earliest stage is represented by solid bitumen and fluorescent oil inclusions associated with authigenic mineral cements. Tiny blebs and masses of pyrite also may be associated with the bitumen. Bitumen locally fills primary pores, forms a thin film on partly developed quartz overgrowths, and in rare cases is trapped at the dust rim between a quartz grain and grain overgrowth. Discrete oil-bearing inclusions occur along the dust rim and are trapped within secondary-quartz overgrowths. This early petroleum-migration event is also represented by patches of bitumen that occur locally in pore-fill and replacement carbonate, although discrete fluid in-

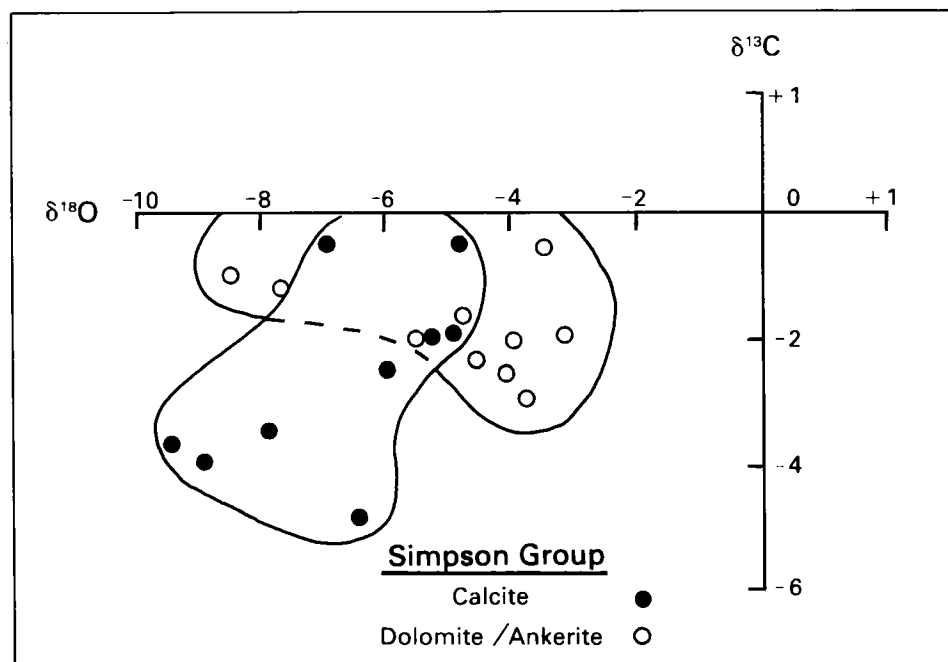


Figure 5. Crossplot of carbon and oxygen isotope compositions for end-member carbonate in the Simpson Group.

clusions were not observed. Textural relations between bitumen and mineral cements indicate that this petroleum phase migrated early in the burial history, when the rocks were at shallow burial depths, and before they had been affected by mechanical compaction or postdepositional alteration.

A second petroleum-migration event occurred late in the burial history. In the Costello well, fractures and stylolites filled with bitumen and healed microfractures containing oil-bearing inclusions cut all authigenic mineral phases, indicating that they formed during deep burial. By extrapolation, the bitumen coating fracture surfaces and forming a residue along stylolite seams, and oil inclusions along microfractures, represent a petroleum phase that was deposited at about the same time under the same burial conditions.

The burial and thermal history for the Simpson Group in the Mazur and Costello wells is depicted on a time-temperature diagram (Fig. 6) modified from Schmoker (1986). Superimposed on the burial curves is the progression of the oil-window through time. Based on the estimated

maximum overburden thickness and temperature gradient ($1.3^{\circ}\text{F}/100\text{ ft}$) shown in the model, Simpson strata in the southeastern part of the basin attained levels of thermal maturity sufficient for hydrocarbon generation in the Early Pennsylvanian, when the rocks were close to their maximum burial depth and temperature. The association of bitumen and petroleum inclusions with fractures and stylolites, and the hydrocarbon-generation history, suggest that late-stage oil migration in the Simpson in the study area likely was contemporaneous with active petroleum generation during the Pennsylvanian; however, it is uncertain whether the petroleum was sourced locally, or whether it migrated from organic-rich rocks elsewhere in the basin. It is evident from the model that Ordovician source rocks in the southeastern part of the basin were thermally immature before the Pennsylvanian, and thus could not have generated the oil phase that migrated early in the burial history when the rocks were at shallow burial depths. Therefore, these hydrocarbons must have migrated from mature Ordovician source rocks deeper in the basin. The deep-

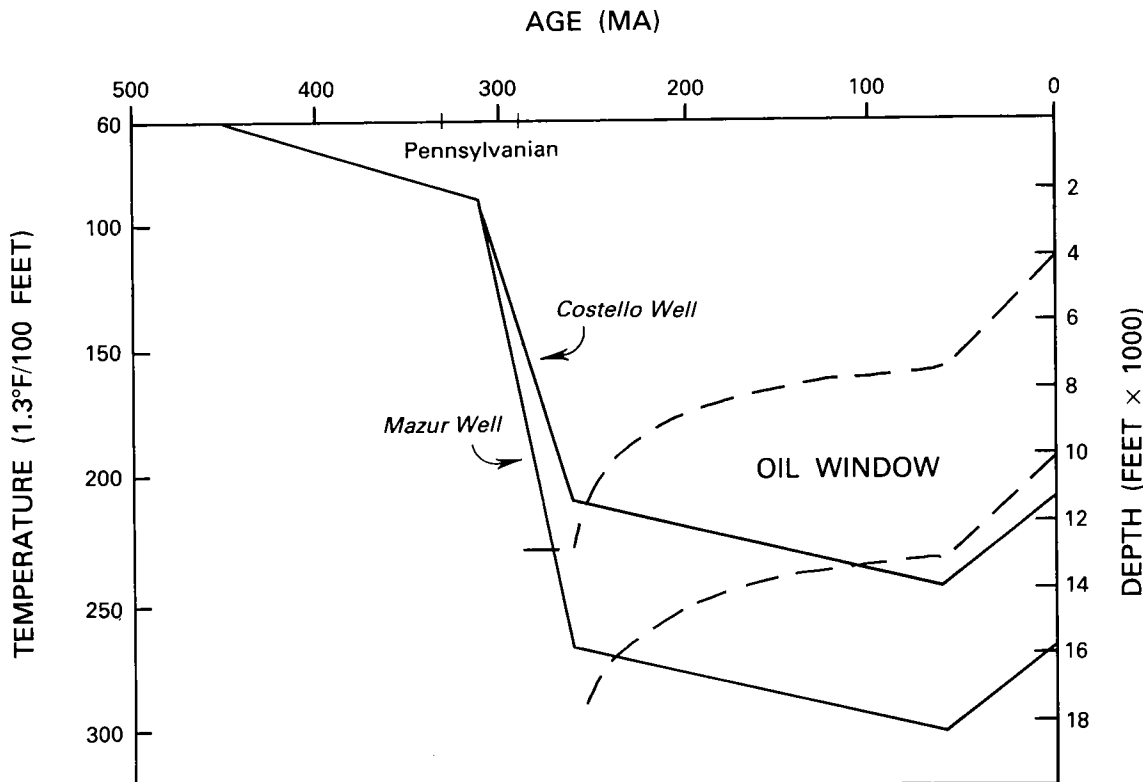


Figure 6. Modified time-temperature diagram, showing the reconstructed burial and thermal history of the Simpson Group in the Mazur and Costello wells. Individual burial curves represent the top of the Simpson Group. Dashed lines depict zone of hydrocarbon generation.

est part of the basin was along the axis of the Wichita Mountains—now uplifted and eroded.

During maximum burial and active hydrocarbon generation, the maturation model indicates that paleotemperatures reached 250°F in the Costello well and 300°F in the Mazur well, assuming that the present geothermal gradient did not vary significantly through time. The maturation-derived peak burial temperatures for the Costello well are consistent with homogenization temperatures of petroleum inclusions along microfractures, which range from 210 to 250°F. These temperature data support an Early to Middle Pennsylvanian timing for late-stage petroleum migration in the Simpson Group in the

southeastern part of the basin. Moreover, they indicate that diagenetic alteration in the Simpson was essentially complete by the time the rocks were close to maximum burial in the Pennsylvanian.

ACKNOWLEDGMENTS

The Oklahoma Geological Survey kindly provided core material from the Costello and Mazur wells. This study was funded by the U.S. Geological Survey Evolution of Sedimentary Basins Program.

DEPOSITIONAL AND POST-DEPOSITIONAL HISTORY OF MIDDLE PALEOZOIC (LATE ORDOVICIAN THROUGH EARLY DEVONIAN) STRATA IN THE ANCESTRAL ANADARKO BASIN

THOMAS W. AMSDEN

Oklahoma Geological Survey

The Anadarko basin is a S-dipping and thickening sedimentary basin whose present configuration is controlled largely by the late Paleozoic Wichita fault zone and the Ouachita thrust plate (Figs. 1,2). The basin-thickening produces a reasonably well-defined depocenter trending NW-SE and located in the approximate position of the Wichita fault zone (Amsden, 1975, panels 5,6). This thickening of the sediments is believed to be the result of an increased rate of subsidence rather than to an increase in water depth. Middle Paleozoic deposition occurred mainly in warm, shallow, carbonate seas supporting a rich invertebrate fauna (Amsden, 1960,1975), interrupted at

times by an influx of fine detritus (Fig. 2) derived mainly from a southeastern source (Amsden, 1969,1975,1980,1981; Amsden and others, 1980). An excellent example of the latter is the Henryhouse-*Kirkidium* biofacies, which extends from the Arbuckle Mountains outcrop area across a considerable part of the Anadarko basin (Fig. 3; Amsden, 1969,1975,1981). Deposition was interrupted by areas of moderate uplift, generally accompanied by little or no faulting, and exposing the sea floor to subareal erosion and dissolution. A number of such uplifts are present, but the two largest are the pre-Frisco-Sallisaw (Fig. 4) and the pre-Woodford (Fig. 5). The general trend of

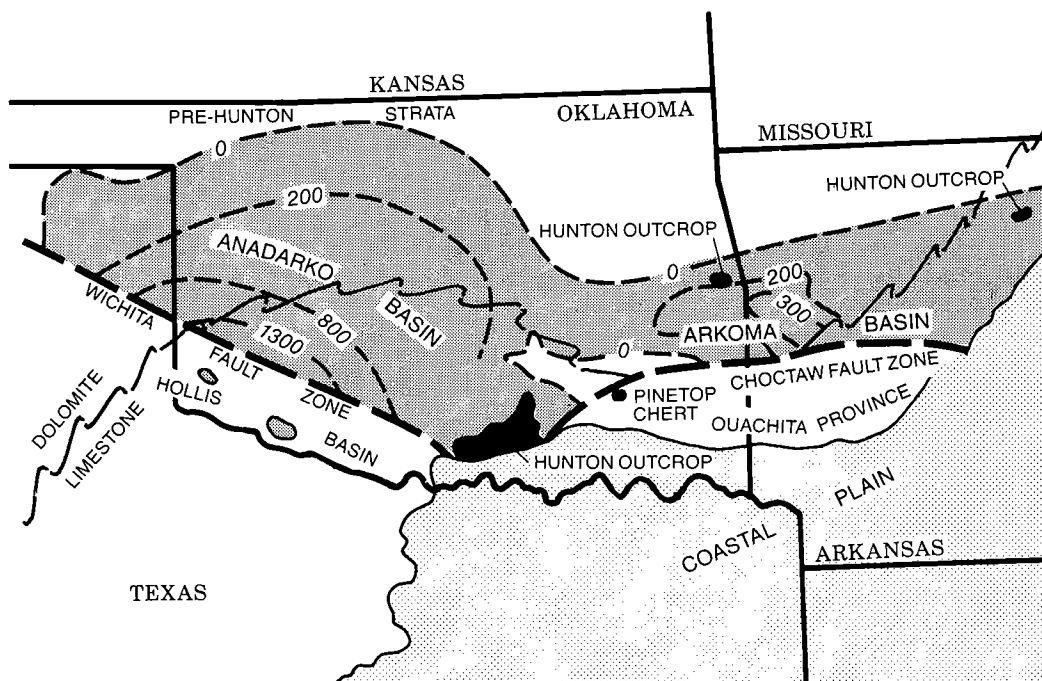


Figure 1. Pre-Woodford subcrop map showing the Anadarko and Arkoma basins. Isopach lines on the top of the Hunton Group.

DEVONIAN	MISSISSIPPIAN – UPPER DEVONIAN		WOODFORD SHALE	
	MIDDLE DEVONIAN		MISENER	
	LOWER	SAWKILLIAN	SALLISAW FORMATION	
		DEERPARKIAN	FRISCO FORMATION	
		HELDERBERGIAN	BOIS D'ARC FM.	
	UPPER	HUNTON GROUP	HARAGAN FM.	
			HENRYHOUSE FORMATION	
			KIRKIDUM BIOFACIES	
			CLARITA – ST. CLAIR FMS.	
			PRICES FALLS MEMBER	
SILURIAN	UPPER	PRIDOLIAN – LUDLOVIAN	COCHRANE – BLACKGUM FMS.	
		WENLOCKIAN		
	LOWER	LLANDOVERIAN C		
		LLANDOVERIAN A, B		
	UPPER	HIRNANTIAN	KEEL FORMATION	
		RICHMONDIAN	SYLVAN SHALE	
ORDOVICIAN	UPPER	MAYSVILLIAN	WELLING FM.	
			VIOLA GROUP	
	MID.		VIOLA SPRINGS FM.	

Figure 2. Stratigraphic section discussed in this report. Shaded formations are those containing moderate to heavy amounts of fine-silt- and clay-sized terrigenous detritus.

these uplifts is NW–SE, roughly paralleling faulting in the ancestral aulacogen and the Wichita fault zone (Amsden, 1980, p. 48,57).

Late Ordovician, Silurian, and Early Devonian strata with similar lithofacies–biofacies characteristics can be traced over a wide area in the southern Midcontinent region, indicating the presence of a large, shallow, epicontinental carbonate basin, or series of interconnected basins (Fig. 6). Remnants of these strata are preserved in the subsurface of Kansas, and a generally complete sequence of Late Ordovician through Early Devonian carbonate strata can be identified in the Anadarko basin, Arbuckle Mountains–Criner Hills outcrop area, and Arkoma basin, and in the outcrops of north-central Arkansas and along the Mississippi River in Missouri and Illinois (Amsden, 1960,1968,1974,1980; Amsden and Rowland, 1965; Amsden and Barrick, 1986,1988). Similar strata are exposed in the Tennessee Valley (Amsden, 1949), as erosional remnants in the central Texas uplift (Barnes and others, 1947), and in the Permian basin (Wilson and Majewske, 1960; Wright, 1979; J. Barrick, personal communication, 1988).

A reasonably well-defined limestone/dolomite boundary extends across this region, separating a dolomite province lying to the north and west

from a limestone province lying to the south and east (Fig. 6). This dolomitization, which affects post-Welling to pre-Frisco strata (all of pre-Deerparkian age; Fig. 2), has been traced from the Anadarko basin east to the Mississippi River, and a lithofacies map prepared by me some years ago (Amsden, 1955) shows the continuation of the limestone/dolomite boundary across the northeastern United States. Wright (1979, fig. 10) showed a dolomite/limestone facies boundary across the Permian basin of West Texas (dolomite on the west, limestone on the east). Berry and Boucot (1970), in their monograph on the Silurian strata of North America, included a map dividing the North American continent into an interior dolomite facies bordered by an outer limestone facies. The limestone/dolomite boundary shown on Figure 6 of the present report is in reasonable accord with this boundary as shown on their map of North America. This is not the place to discuss the problems concerned with Silurian dolomitization in the Midcontinent region of the United States, other than to note that it represents a magnificacies of impressive dimensions.

The present brief report is a summary of a more detailed bulletin now in preparation on the middle Paleozoic history of the Anadarko basin.

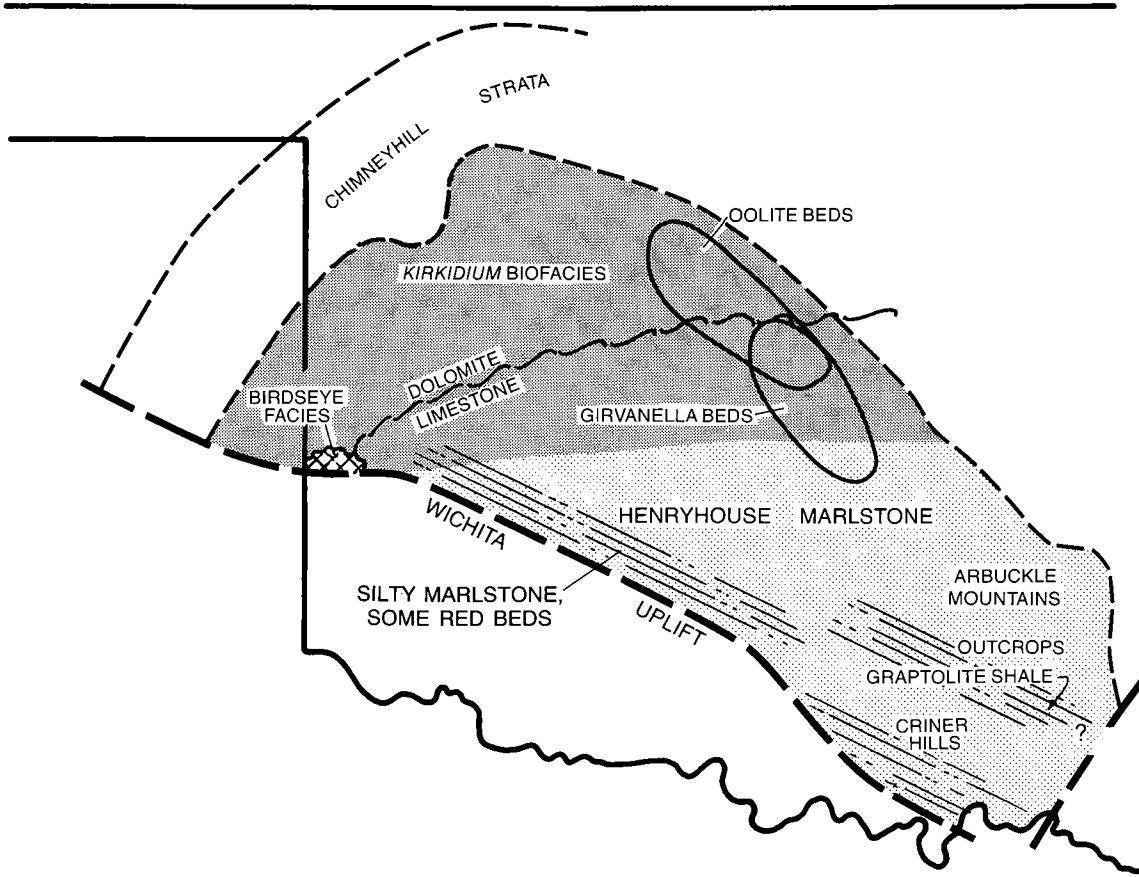


Figure 3. Distribution of the Henryhouse-marlstone-Kirkidium biofacies.

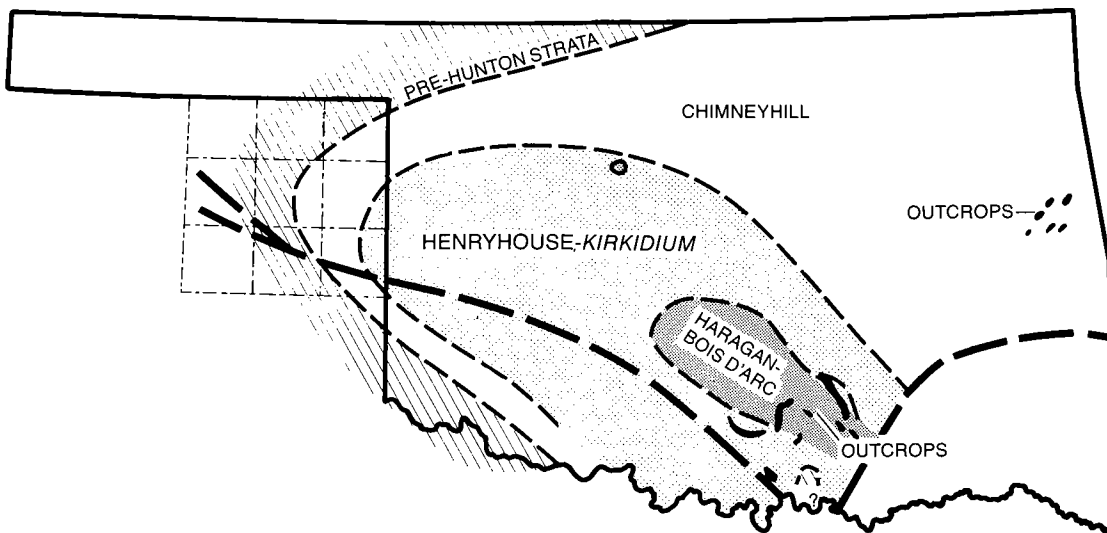


Figure 4. Pre-Frisco-Sallisaw subcrop map.

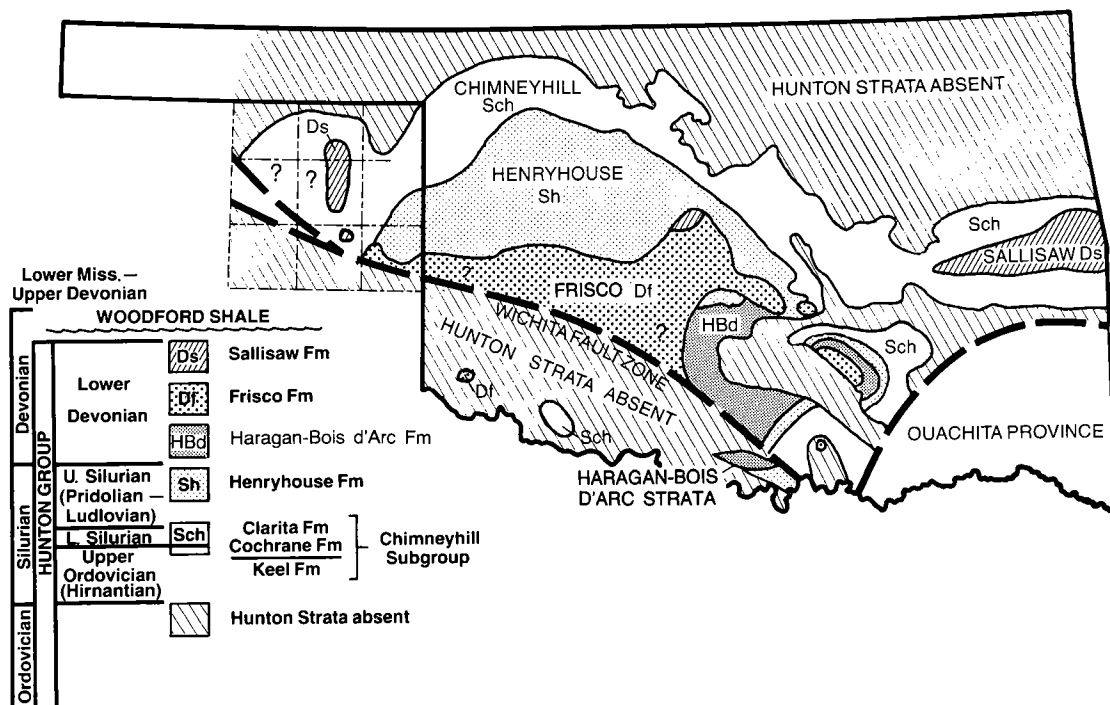


Figure 5. Pre-Woodford subcrop map.

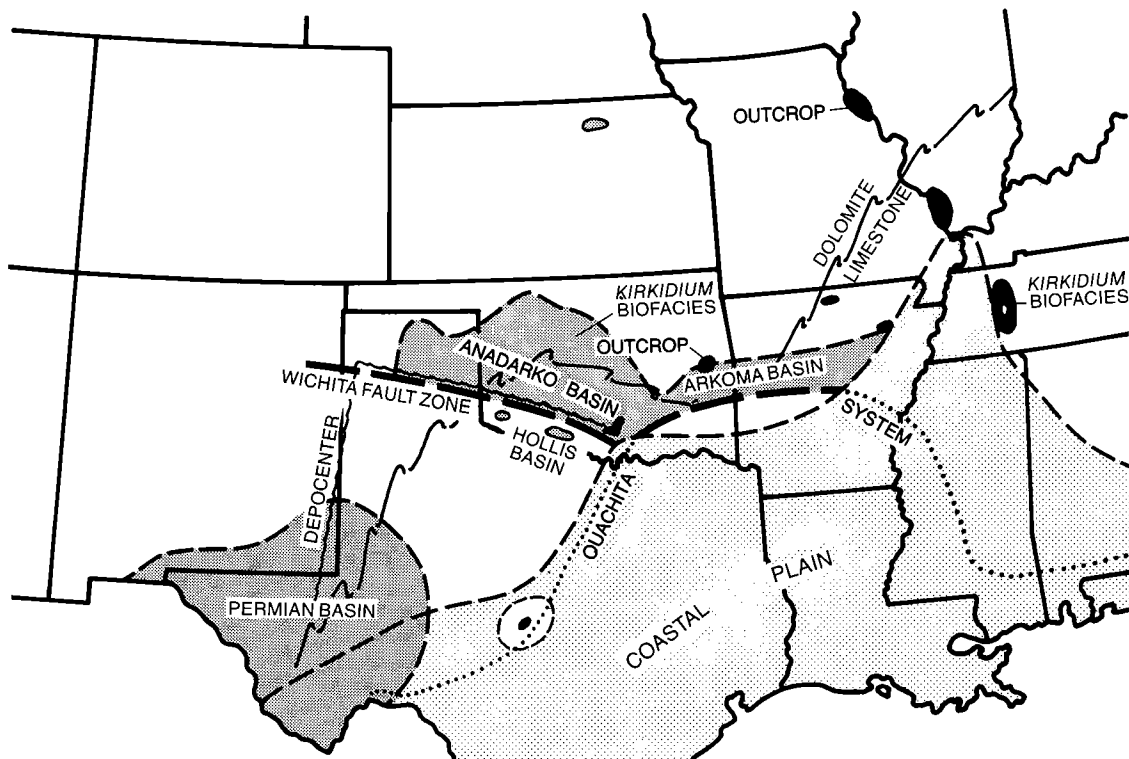


Figure 6. Inferred distribution of middle Paleozoic strata in the ancestral Anadarko basin.

DEPOSITIONAL FACIES, PETROFACIES, AND DIAGENESIS OF SILICICLASTICS OF MORROW AND SPRINGER ROCKS, ANADARKO BASIN, OKLAHOMA

C. WILLIAM KEIGHIN AND ROMEO M. FLORES

U.S. Geological Survey, Denver

Abstract.—Investigations of 6,500 ft of core and ~100 thin-sectioned core samples from 30 drill holes from the Oklahoma Panhandle to the southeast part of the Anadarko basin, Oklahoma, have led to the recognition of three depositional facies of the Springer and Morrow Formations of Mississippian and Pennsylvanian age, as recognized by geologists working in the subsurface of the Midcontinent region. Lithofacies include (1) fluvial-influenced coastal (FIC), (2) tidal-influenced nearshore (TINS), and (3) mixed, which shows mixed tidal and non-tidal marine influence (MT/NTM). The FIC facies is restricted to down-hole depths of 4,400–8,000 ft; the TINS facies is recognized only between down-hole depths of 4,000 and 18,000 ft. Thin-section study of sandstone indicates that quartz arenite is the most common rock type in both the FIC and TINS facies. Subarkose is present, but not common, in the FIC facies. Sublitharenite is moderately common in the TINS facies. Calcite skeletal fragments, mainly of brachiopods and crinoids, are more abundant in the FIC facies than in the TINS facies. The mixed facies includes quartz arenite, subarkose, and sublitharenite. Iron-bearing carbonate cements are observed in rocks of all three depositional facies. Porosity is typically <10%, and has been reduced by compaction and redistribution of silica, as well as by iron-bearing carbonate cements. Clay cements are less common, but are locally important. Loss of porosity due to mechanical compaction is significant in some samples from depths >12,000 ft. Thin films of bitumen have inhibited the effects of diagenesis in some samples. Fractures are identified in core samples, but are rare in thin sections. Porosity is due primarily to dissolution of glauconite, clays or clayey matrix, and some framework grains, but many dissolution pores are partly or completely filled with various clays, and only microporosity remains.

INTRODUCTION

As part of a cooperative program between the Oklahoma Geological Survey and the U.S. Geological Survey on the Evolution of Sedimentary Basins, this report focuses on one of the most productive stratigraphic intervals in the Anadarko basin. This interval consists of the Springer and Morrow units of Mississippian and Pennsylvanian age, respectively, which are, in the entire Midcontinent, second only to the Hugoton–Panhandle field in natural gas reserves (Hill and Clark, 1980). Production ranges from depths of ~4,500 ft in the Panhandle to ~17,000 ft in the deeper, southeast part of the Anadarko basin. The core holes on which this investigation is based are shown in Figure 1; a list of the core holes is given in the Appendix.

The Anadarko basin, which contains as much as 40,000 ft of Paleozoic sedimentary rocks, is generally bounded by the Wichita uplift on the southwest, and by the Nemaha Ridge on the northeast (Fig. 2). The boundary between the Wichita uplift and the Anadarko basin sediments is strongly faulted (Evans, 1979; Perry, in press). Within this 40,000-ft interval, the Springer–Morrow interval ranges in thickness from zero (in the

up-dip, Panhandle portion of the basin) to >6,000 ft in the deepest, southeast portion of the basin (Simon and others, 1977). The Springer–Morrow is a siliciclastic sequence consisting mostly of interbedded sandstones, siltstones, and shales. Minor amounts of carbonates and coals are interbedded with the siliciclastics in the deep and shallow parts of the basin, respectively. The lower part of the interval is bounded by the Mississippian (Chesterian) limestone, and the upper part is bounded by the Atokan Thirteen Finger limestone.

The Morrow–Springer interval is, in general, considered to be a product of marine and marginal marine deposition (Busch, 1959; Kasino and Davies, 1979; Simon and others, 1977; Al-Shaieb and Walker, 1986). The marine portion of the sequence is mostly in the southeast (deeper) part of the basin, and the marginal marine part is found in the northwest (Panhandle) part of the basin. In the southeast part of the basin, Busch (1959) interpreted NW-trending lower Morrow sandstones as beach deposits. Simon and others (1977) suggested that the same sandstones are offshore bars reworked from deltaic deposits by longshore currents. Khaiwka (1972) and Shelby (1980) suggested deposition of the Morrow sand-

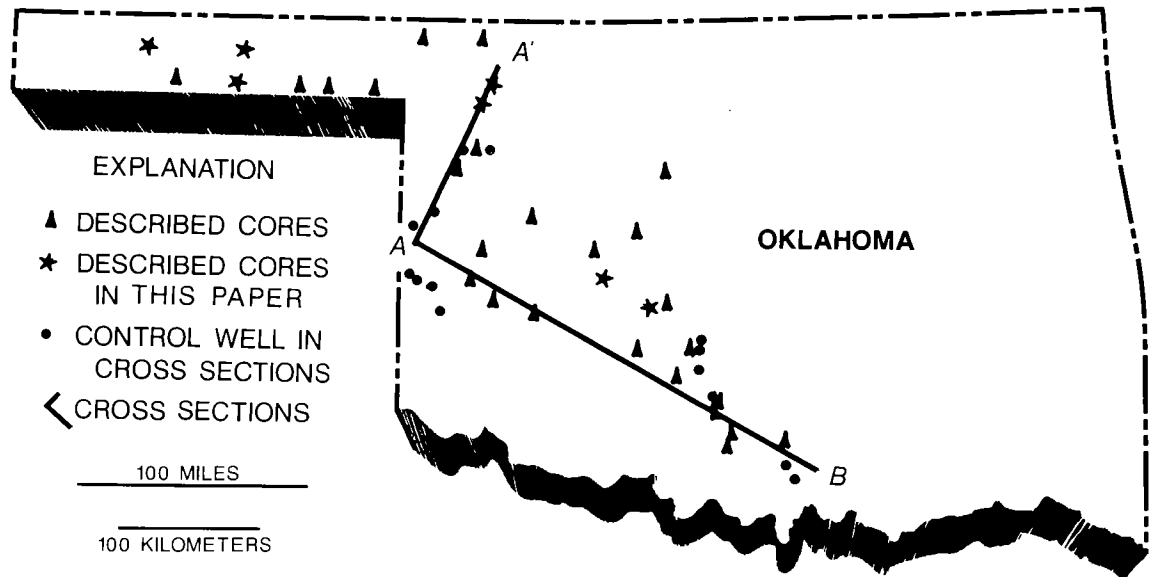
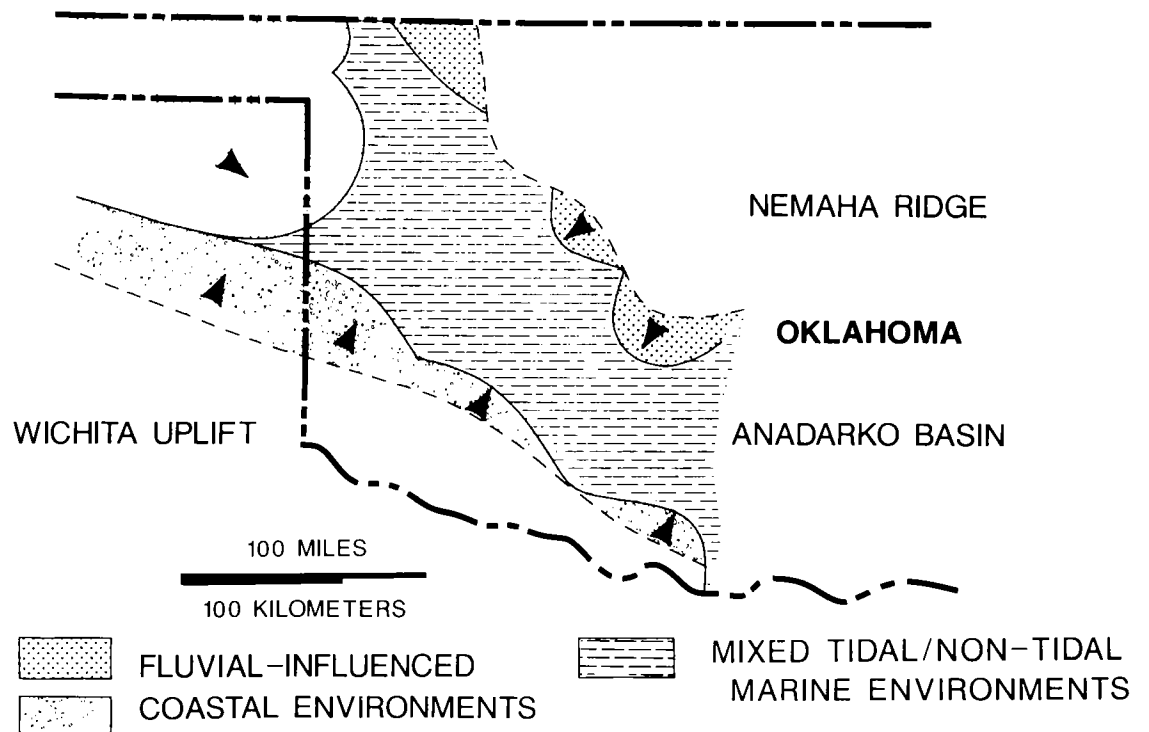


Figure 1. Location of core holes on which this investigation is based, and the lines of cross sections shown in Figure 3A,B.



MODIFIED FROM MOORE (1979) AND
AL-SHAIEB AND WALKER (1986)

Figure 2. General outline of the Anadarko basin, and major depositional environments in which Morrow sediments were deposited.

stones in deltaic environments. Al-Shaieb and Walker (1986) described these deltaic environments as tide-dominated and fan deltas. The tide-dominated deltas are associated with tidal ridge/shoal deposits, offshore bars, and tidal-flat deposits. In the northwest (Panhandle) part of the basin, Kasino and Davies (1979) suggested that the Morrow sandstones were deposited in estuarine deltas and tidal-flat environments.

The stratigraphic distribution of the Morrow sands in the southern and northeast parts of the basin—including sandy siltstones, silty sandstones, and medium-grained and conglomeratic sandstones—is shown in Figure 3. In general, the Morrow sands are found in the upper part of the studied interval. Although the individual units are typically thin, as much as 350 ft of Morrow sands is found in the upper part of the interval. In the lower part of the interval, as much as 200 ft of sands occurs. Because of their past history of production and their economic potential, these sands were studied for depositional facies in relation to their petrofacies and diagenesis.

DEPOSITIONAL FACIES

The depositional facies of the Morrow sandstones and associated sedimentary rocks are determined from vertical facies profiles or sequences, described from as much as 6,500 ft of core from 30 drill holes. Rock types of the facies sequences were described for their lithology, color, gross mineralogy, nature of contacts, vertical change in texture, sequence of sedimentary structures, biogenic sedimentary structures, and body-fossil content. On the basis of these criteria of facies recognition, three major lithofacies sequences were established: (1) fluvial-influenced coastal (FIC), (2) tidal-influenced nearshore (TINS), and (3) mixed tidal and non-tidal marine-influenced (MT/NTM) facies sequences.

FIC Facies Sequences

The FIC facies sequences identified in drill-hole cores are restricted to down-hole depths of approximately 4,400–8,000 ft in the northwest (Panhandle) part of the Anadarko basin. Figures 4–6 show FIC facies sequences exemplified by cores from three drill holes. The facies sequences—which consist of interbedded sandstones, siltstones, mudstones, coals, carbonaceous shales, and limestones—display a variety of facies types that include (1) distributary-channel/overbank, interdistributary-bay, and swamp facies types; (2) crevasse-splay, interdistributary-bay, and marsh facies types; and (3) crevasse-splay, swamp, overbank, bay, and swamp facies types.

The distributary-channel/overbank facies type

(Fig. 4) is a generally fining-upward (fine- to medium-grained), feldspathic sandstone that has an erosional base marked by shale-clast conglomerate. The sandstone is cross-bedded, ranging from 6 to 8 in. thick. The upper part of the sandstone consists of breccia/mud-matrix conglomeratic sandstone with an erosional base, which in turn grades upward into silty sandstone interbedded with siltstone and shale. This fine-grained sequence is ripple-laminated (discontinuous, wavy laminations), with ripples defined by coaly organic laminae. “Coffee grounds” and plant fragments also are common, and a few bioturbations are present. The sandstone is underlain by shale that contains plant fragments, vertical-burrow trace fossils, and a few chitinous-brachiopod fragments.

The shale is interpreted to be an interdistributary-bay deposit. The shale is in turn underlain by a coal bed deposited in a swamp environment.

Figures 5 and 6 show the succession of the crevasse-splay, overbank, interdistributary-bay, and marsh/swamp facies types. The crevasse-splay facies consists of a fine-grained, ripple-laminated, feldspathic sandstone with a sharp base. The ripple-laminated units are ~2.5 ft thick. The upper part of the sandstone is unconformably overlain by coarse-grained to granular, feldspathic sandstone with low-angle cross-beds representing a crevasse-channel deposit. The crevasse-splay/channel-sandstone complex is underlain and overlain by mudstones, shales, and siltstones that contain abundant plant fragments and chitinous- (*Lingula*) and calcareous-brachiopod shells. The middle part of the mudstone/shale interval in the upper part of the facies sequence contains coaly laminae, coaly silty shale, and ferruginous root casts interpreted to be marsh deposits. The mudstone/shale interval probably represents interdistributary-bay deposits. Facies illustrated in Figure 6 are similar to the facies sequence in Figure 5, except for the presence of limestone (wackestone), representing carbonate precipitation in the bay, and coal, reflecting peat accumulation in a swamp.

Environmental Interpretation

The facies types recognized from the FIC facies sequences show characteristics of modern and Carboniferous delta-plain deposits (Coleman, 1976; Ferm, 1970; Wanless and others, 1970). However, the abundant fossiliferous horizons and carbonate units suggest that saline waters encroached upon the delta plain, either by marine transgression or by local subsidence resulting from differential compaction of sediments. The presence of both chitinous and calcareous brachiopods indicates the influence of brackish and saline waters, respectively, on the delta plain. The

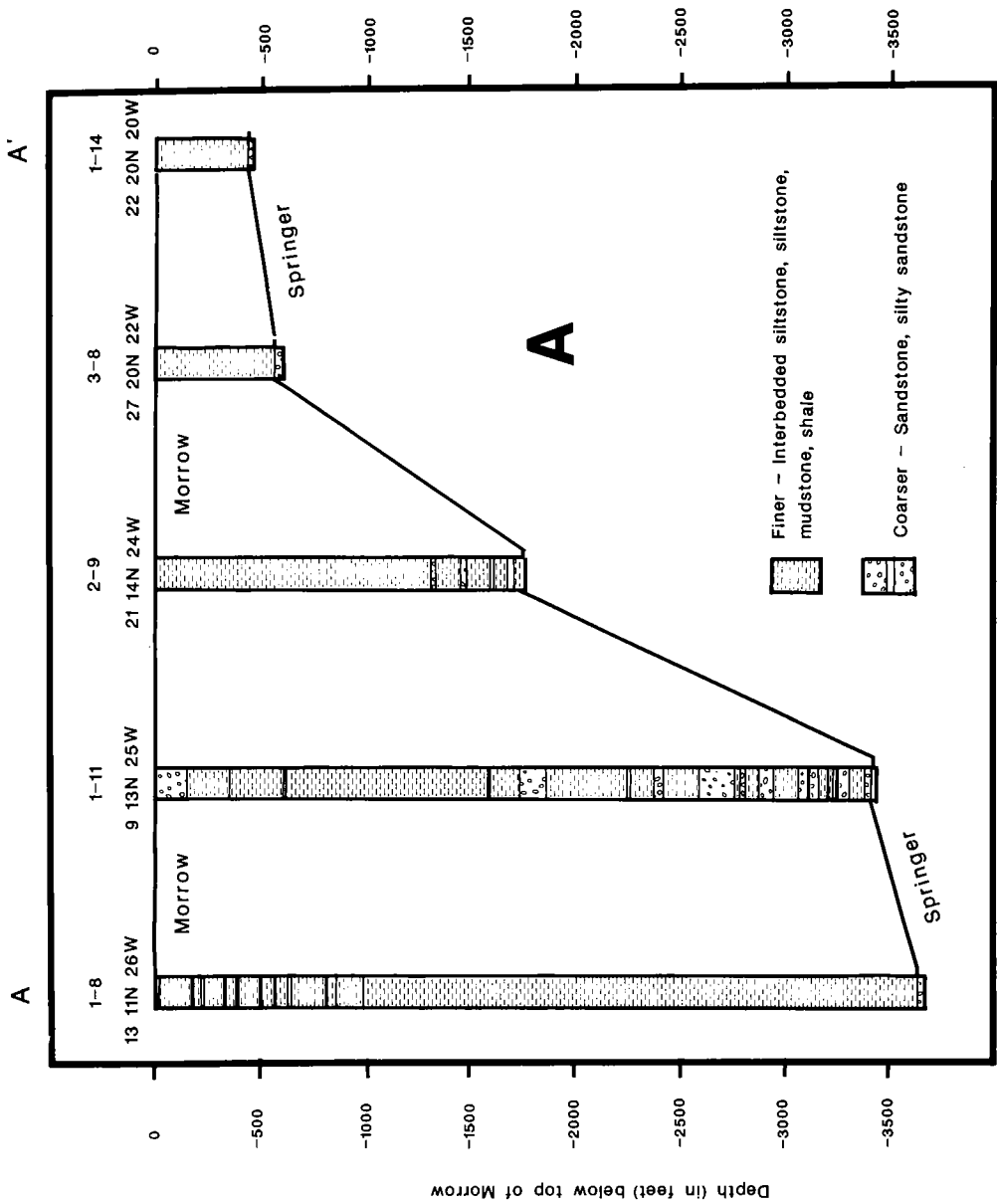


Figure 3. Stratigraphic cross sections A-A' (A) and A-B (B), based on well logs from drill holes located in Figure 1, showing general distribution of coarser and finer sediments. Data were processed by Molnia according to the procedure described by Molnia and others (1988).

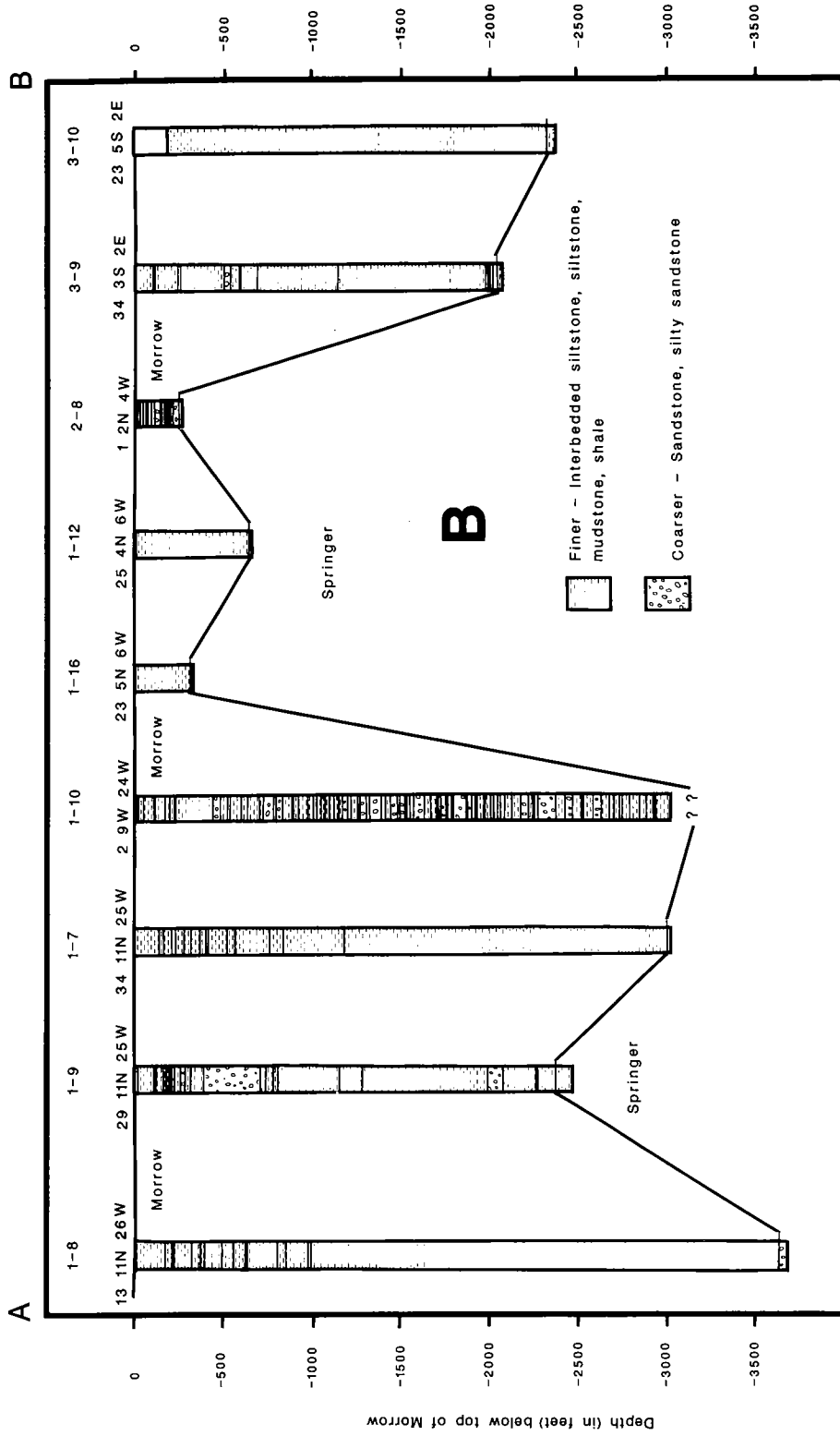
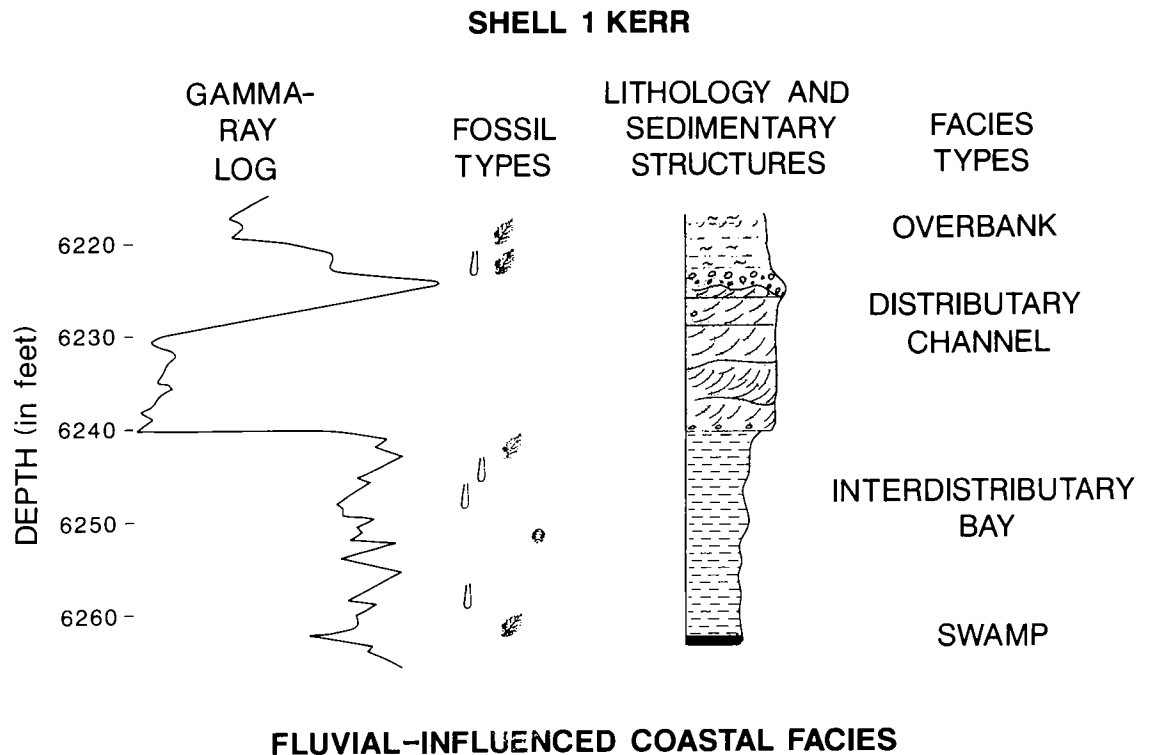


Figure 3. Continued.



EXPLANATION

	SANDSTONE		PLANT FRAGMENTS
	SILTSTONE		CALCAREOUS BRACHIOPODS
	SHALE		CHITINOUS BRACHIOPODS
	MUDSTONE		CRINOIDS
	CARBONACEOUS SHALE		CORALS
	COAL		BURROWS
	LIMESTONE		ROOTMARKS
	CONGLOMERATE		MUDCRACKS
	IRONSTONE		
	CROSS-LAMINATIONS		PARALLEL LAMINATIONS
	RIPPLE LAMINATIONS		DISH STRUCTURES

Figure 4. Features associated with the distributary-channel/overbank and interdistributary-bay/swamp facies types in the FIC facies; Shell 1 Kerr drill hole, sec. 6, T. 4 N., R. 17 ECM.

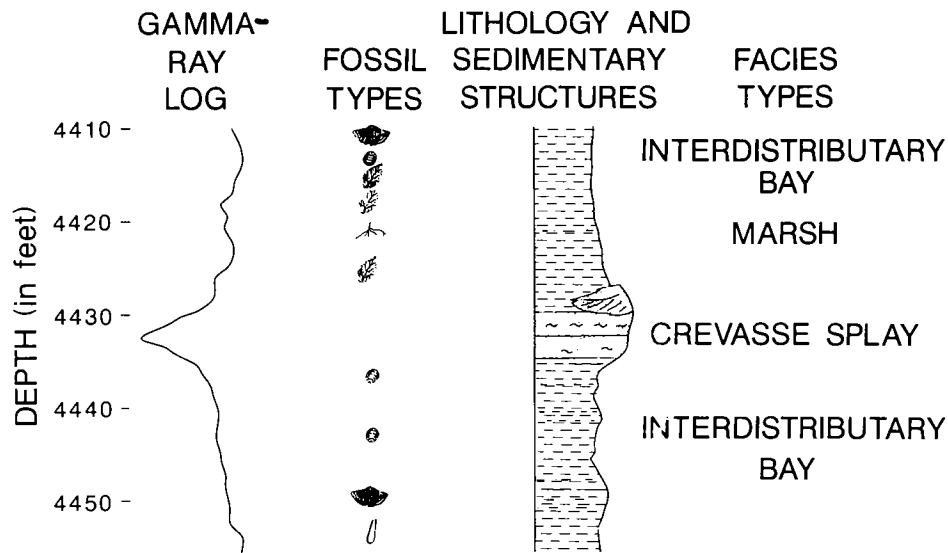
GULF 1 KELLY**FLUVIAL-INFLUENCED COASTAL FACIES**

Figure 5. Lower-delta facies types within the FIC facies, as described from the Gulf 1 Kelly drill hole, sec. 1, T. 4 N., R. 10 ECM. Symbols as in Figure 4.

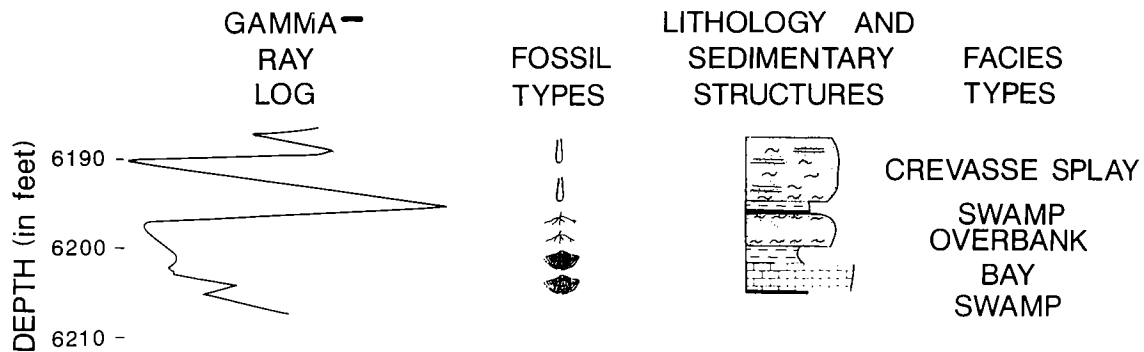
SOUTHLAND ROYALTY 1-31 DAISY**FLUVIAL-INFLUENCED COASTAL FACIES**

Figure 6. Crevasse-splay, overbank, bay, and swamp facies types in the FIC facies, Southland Royalty 1-31 Daisy drill hole, sec. 31, T. 2 N., R. 17 ECM. Symbols as in Figure 4.

occurrence of brackish and marine waters on the delta plain suggests deposition in the lower part of the delta plain. This interpretation is consistent with the occurrence of distributary-channel and crevasse-splay facies types, as well as development of only a few, thin coal beds. Thus, the Morrow sandstones were deposited in a lower-delta plain that was probably fed by fluvial systems that drained the northwest embayment of the Anadarko basin.

TINS and MT/NTM Facies Sequences

The TINS and MT/NTM facies sequences were identified from drill-hole cores restricted to down-hole depths of approximately 4,000–18,000 ft in the northwest (shallow) and southeast (deeper) parts of the Anadarko basin, respectively. The facies types described in the TINS facies sequence (Fig. 7) include (1) channel/subtidal-bar/lagoon, and (2) clastic-dominated shallow-marine and carbonate-dominated shallow-marine facies.

TINS Facies Sequences

The intertidal facies type (Fig. 7) of the TINS facies sequences consists of rhythmically alternating zones of red and green, fine-grained, quartzose sandstones. These sandstones are interbedded with mudstones and siltstones; the mudstones show mud-crack structures. The sandstones exhibit a variety of ripple laminations, from flaser, discontinuous/wavy, to lenticular (both connected and single) bedding. These ripple laminations are frequently destroyed by vertical and horizontal trace-fossil burrows.

The tidal-channel facies type (Fig. 7), which underlies the intertidal facies type, is composed of stacked, quartzose, coarsening-upward (fine- to medium-grained), thin to thick (4–13 ft), sharp-to erosional-based sandstones. The basal contacts of these sandstones are marked by ironstone and shale clasts (rip-up clasts), as well as by coal spars. The sandstones are cross-bedded, with a few ripple laminations in the upper part. Root marks lined with carbonaceous films were found on top of two of these coarsening-upward sandstones. Fragments of calcareous brachiopods and crinoid stems occur in the sandstone as lag deposits. Vertical bioturbations are common in the upper parts of these sandstones, particularly in the transition into the overlying intertidal facies type.

The subtidal facies type (Fig. 7) consists of shale with a few silty lenses that are ripple-laminated (lenticular, single sets). Where the silty lenses do not exhibit ripple laminations, the sedi-

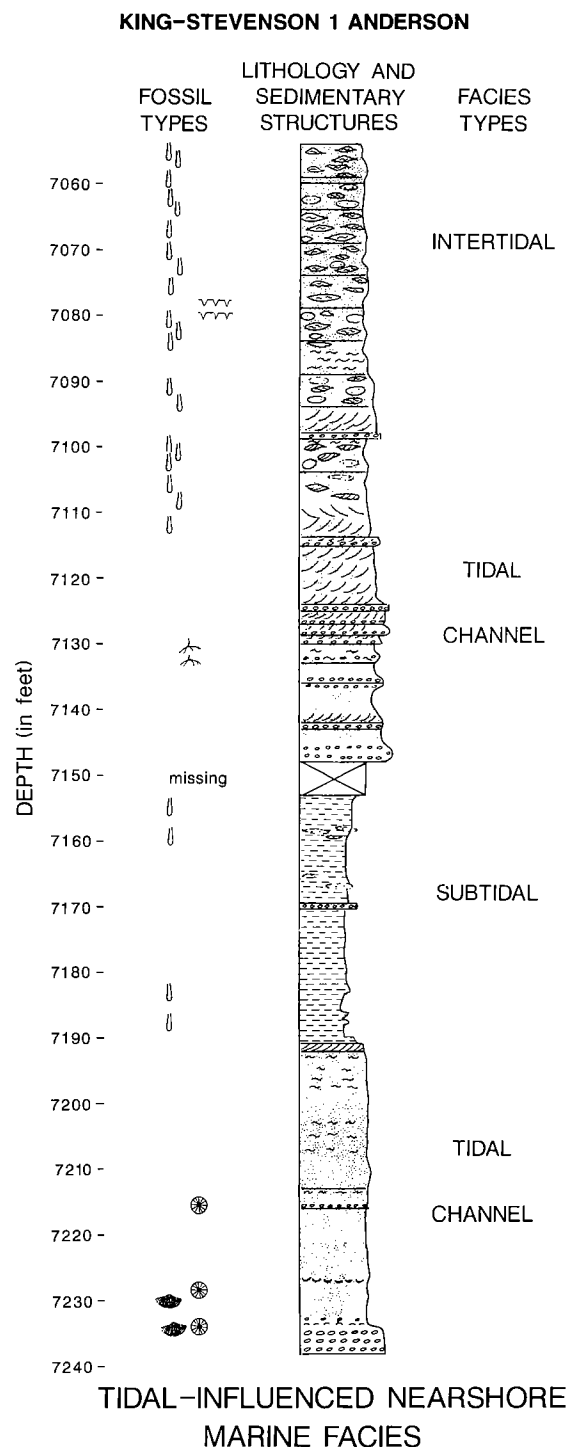


Figure 7. Tidal-channel, intertidal, and subtidal facies types within the TINS facies, King-Stevenson 1 Anderson drill hole, sec. 26, T. 25 N., R. 20 W. Symbols as in Figure 4.

mentary structures are destroyed by vertical trace-fossil burrows. The shale contains horizons of horizontal trace-fossil burrows. The shale also consists of a sharp-based, sandy conglomerate of ironstone and shale clasts.

Environmental Interpretation

The TINS facies sequence represents deposits in tidal-influenced environments ranging from the upper part of the intertidal zone to below wave base, or subtidal (Kumar and Sanders, 1974; Knight and Dalrymple, 1975; Owenshine, 1975). The variegated sandstones formed in the intertidal zone where oxidation and reduction of iron occurred in response to sea-level fluctuations. Subaerial exposure in the intertidal zone is indicated by mud cracks. The ripple laminations in the intertidal facies types occur during pulsatory current flow and slackwater deposition (Reineck and Singh, 1980). Dissection of the intertidal zone by tidal channels is indicated by the stacked, coarsening-upward sandstones. Deposition below tidal and wave-base level in the subtidal environment is indicated by the bioturbated shale.

MT/NTM Facies Sequence

The channel, subtidal, and lagoonal facies types of the MT/NTM facies sequences consist of coarsening-upward intervals. The subtidal-bar facies type (Fig. 8) is composed of interbedded shale and very fine-grained, quartzose sandstone in the lower part, and a very fine- to fine-grained, quartzose sandstone in the upper part. The interbedded shale and sandstone are rippled (wavy- and flaser-bedded) and bioturbated horizontally and vertically by trace fossils. A few ironstone lenses are present. The upper sandstone has a sharp base marked by ironstone clasts, and contains ripple laminations and convolutions. This rock type represents a channel facies type scoured into the subtidal-bar facies type. The sandstone grades upward into interbedded burrowed silty sandstone, sandy shale, and black, papery, carbonaceous shale which probably reflect deposition in a lagoon. This lagoonal facies type is in turn overlain by a coarsening-upward subtidal-bar facies type. This succession of facies types is underlain and overlain by a subtidal facies type consisting of burrowed shale and rippled silty lenses and silty sandstone very similar to TINS facies sequences.

The shallow-marine facies types of the MT/NTM facies sequences (Fig. 9) consist of interbedded mudstones, siltstones, and sandstones (clastic-dominated shallow-marine) and interbedded limestones, sandstones, siltstones, and mudstones (carbonate-dominated shallow-marine). The clastic-dominated shallow-marine facies type

includes a siltstone-rich interval consisting of rippled and burrowed siltstones with siderite nodules and layers; it is interbedded with silty, burrowed mudstones and sharp-based, fine-grained, quartzose, rippled and cross-bedded sandstones. The carbonate-dominated facies type is composed of fossiliferous limestones (wackestones) interbedded with lithofacies similar to those of the clastic-dominated shallow-marine facies types. The fossils occur in several horizons, and consist of fragments or whole shells of calcareous brachiopods, crinoid stems, and horn corals. Ironstone and siderite layers and nodules are present throughout the limestones.

Environmental Interpretation

The facies types of the MT/NTM facies sequences reflect a mixed clastic/carbonate shallow-marine environment or open-shelf platform typical of Carboniferous deposits (Brown, 1969; Heckel, 1980). The sandstones of the clastic-dominated facies type probably represent "sand ridges" deposited by bottom currents. The limestones of the carbonate-dominated facies type probably were deposited on carbonate platforms removed from heavy clastic influx. Thus, we suggest that the carbonate platforms were probably found in the outer part of the shelf, compared to the belt of "sand ridges," found in the shallower or inner part of the shelf.

PETROFACIES/DIAGENESIS

Although the examined cores represent diverse facies, and the samples examined in thin section and with the scanning electron microscope were from depths ranging of approximately 4,000–18,000 ft below the surface, evidence of diagenetic modifications is seen in almost all samples. A significant, if not major, fraction of the porosity present in the clastic rocks is secondary (Al-Shaieb and Walker, 1986; Haiduk, 1987; McBride and others, 1987). Diagenesis, through mechanical compaction as well as chemical cementation, also played an important role in the reduction of porosity and permeability. Physical compaction is indicated by deformation of labile rock fragments and glauconite, and by small-scale stylolites. Compaction is seen throughout the depth range of the examined samples. However, chemical diagenesis is more significant in influencing the reservoir properties of the clastic units. Porosity was reduced, sometimes almost completely, through cementation by carbonate minerals, especially iron-bearing carbonates; the distribution of carbonate cements is highly variable. Silica, in the form of overgrowths on detrital quartz grains, is also present as a cement in some samples; the distribution of this cementing agent is also variable, even within a single thin section.

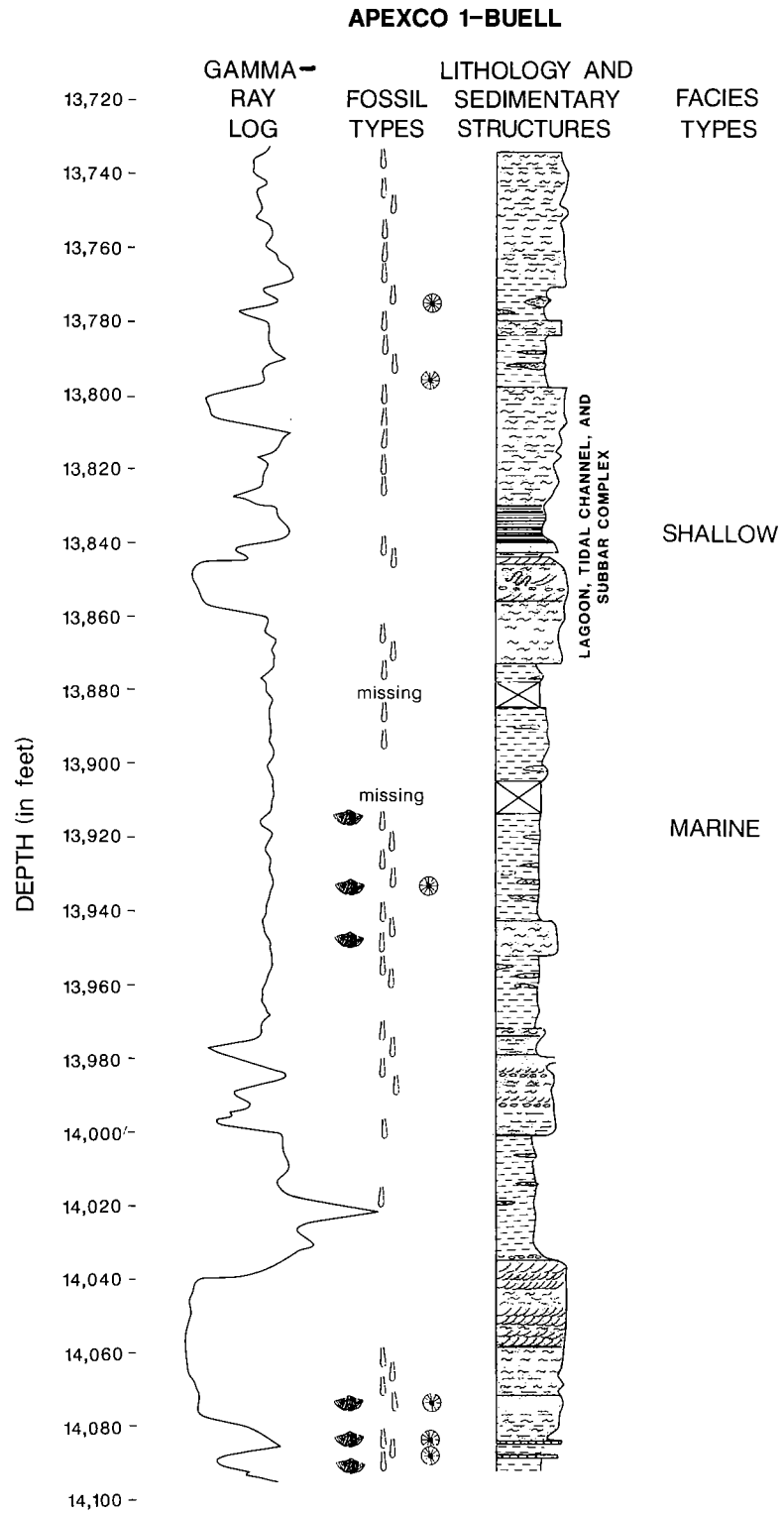


Figure 8. Lagoon/subtidal-bar facies types within the MT/NTM facies, Apexco 1 Buell drill hole, sec. 10, T. 11 N., R. 12 W. Symbols as in Figure 4.

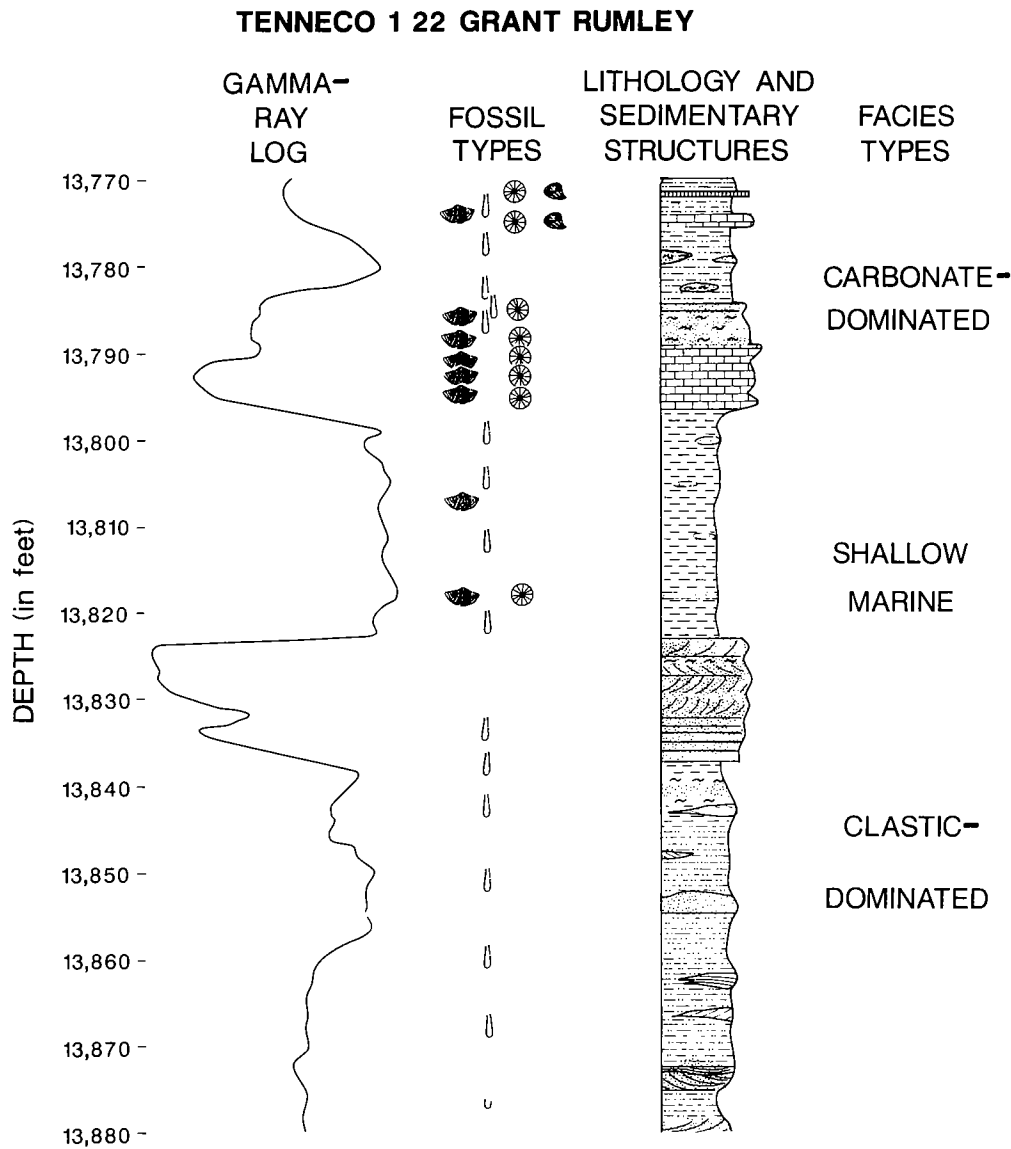


Figure 9. Shallow-marine facies (carbonate- and clastic-dominated) within the MT/NTM facies, Tenneco 1 22 Grant Rumley drill hole, sec. 22, T. 9 N., R. 9 W. Symbols as in Figure 4.

FIC Facies

Variations in grain size and visible porosity—which includes both macro- and micro-porosity—within a short vertical distance are illustrated in Figures 10A and 11A. There are also variations in the types and distribution of cementing agents, which include silica (overgrowths on detrital quartz grains) and iron-bearing and iron-free carbonate minerals. Authigenic pore-filling kaolinite is seen, but in very minor quantities.

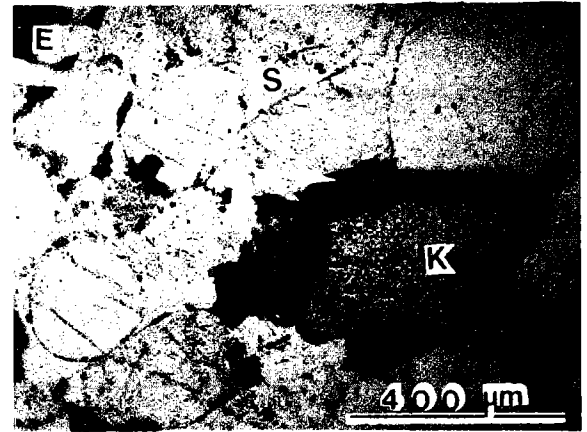
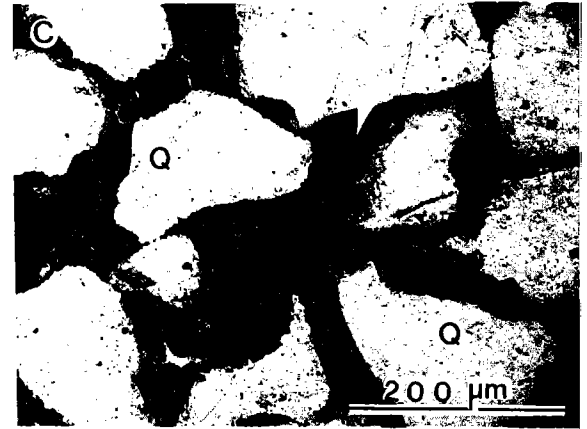
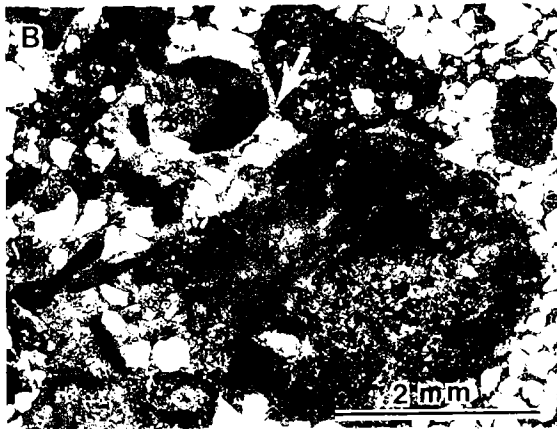
Green glauconite (Fig. 11B), which is irregularly distributed, has been affected both by physical compaction and by chemical alteration (partial dissolution, replacement by clay minerals).

TINS Facies

Some features of samples collected from the King-Stevenson 1 Anderson core hole (sec. 26, T. 25 N., R. 20 W.) from depths of approximately 7,100–7,230 ft are shown in Figure 11C–E.



Figure 10. Photomicrographs of thin sections illustrating petrographic variations, and some effects of diagenesis. *A*—Microlaminated sublitharenite and organic-rich siltstone from FIC facies; Petro-Lewis 2-8 Cates drill hole, sec. 8, T. 1 N., R. 23 ECM, depth 7,776 ft; crossed polars. *B*—Fe-bearing carbonate (arrow) forms tight cement in fossiliferous sandy limestone, MT/NTM facies; Apache 1 Baker drill hole, sec. 24, T. 23 N., R. 21 W., depth 7,834 ft. *C*—Quartz arenite very tightly cemented by Fe-bearing carbonate cement (mottled; arrow); floating texture of detrital quartz grains (Q) indicates early cementation; MT/NTM facies; Michigan-Wisconsin 1 Raab, sec. 32, T. 15 N., R. 17 W., depth 12,748 ft. *D*—Fine-grained quartz arenite, tightly cemented by overgrowths of authigenic silica on grains of detrital quartz; very thin fracture (arrow) is filled with authigenic clay; MT/NTM facies; Michigan-Wisconsin 1 Raab, depth 12,749 ft; crossed polars. *E*—Remnant of leached phosphatic fragment (arrow; colophonane?) lines pore now almost completely filled with kaolinite (K); quartz arenite composing this sample is typically tightly cemented by overgrowths of authigenic silica (S); MT/NTM facies; Michigan-Wisconsin 1 Raab, depth 12,763 ft.



Glauconite pellets are irregularly distributed; the pellets are common in some samples, but not observed in other samples. Glauconite grains illustrate the effects of both physical and chemical diagenesis, and in some cases have been largely removed by dissolution, forming secondary porosity. Kaolinite was not identified in these samples, but minor quantities of authigenic chlorite are present. Granular siderite and/or ankerite are distributed throughout the sample suite, and high concentrations of these carbonates occur as laminae in some samples. In addition to compacted ductile grains, evidence of post-depositional compaction is illustrated by small-scale stylolites.

MT/NTM Facies

The distribution of cementing agents within a single core is as variable as in the FIC facies; this is illustrated in Figures 10C–E and 11F. Similar variations, both in distribution of cements and in types of diagenetic reactions, are observed between cores, regardless of the depth of the studied samples (Figs. 10B–E, 11F).

CONCLUSIONS

The FIC and TINS lithofacies are present in the northwest (Panhandle and nearby) part of the Anadarko basin. These lithofacies consist mainly of lower-delta-plain deposits. Associated with these lithofacies are tidal and intertidal lithofacies. The influence of tides and brackish water in this part of the basin suggests that the northwest part of the Anadarko basin was an embayment strongly affected by sea-level fluctua-

tions. The MT/NTM lithofacies are present in the southeast (deeper) part of the basin, and consist mainly of clastic- and carbonate-dominated shallow-marine deposits. These lithofacies reflect an open-shelf platform in which the clastic-dominated facies types were deposited as “sand ridges” on the inner part of the shelf, and the carbonate-dominated facies types were deposited as “carbonate platforms” on the outer part of the shelf. Although it is possible to differentiate the Morrow sandstones according to their facies characteristics, it is more difficult to clearly distinguish them on the basis of their petrofacies and diagenetic properties. Cementation—most commonly by iron-bearing and iron-free carbonates, as well as by silica overgrowths—occurs irregularly throughout the investigated sample suite. Compaction is seen throughout the entire studied depth range, and has served to reduce porosity in many samples. In addition to compaction of labile grains (especially glauconite), stylolites, from micro- to macro-scale, span the entire investigated depth range. The most consistent, and probably most significant, diagenetic modification of the studied sandstones is the introduction of secondary porosity by dissolution of glauconite, rock fragments, and, to a lesser degree, detrital framework grains.

ACKNOWLEDGMENTS

We wish to acknowledge the assistance of the Oklahoma Geological Survey, Charles J. Mankin, Director, in providing access to the examined cores, and Eldon Cox and Walter Esry in the Oklahoma Geological Survey Core and Sample Library, for their generous help.

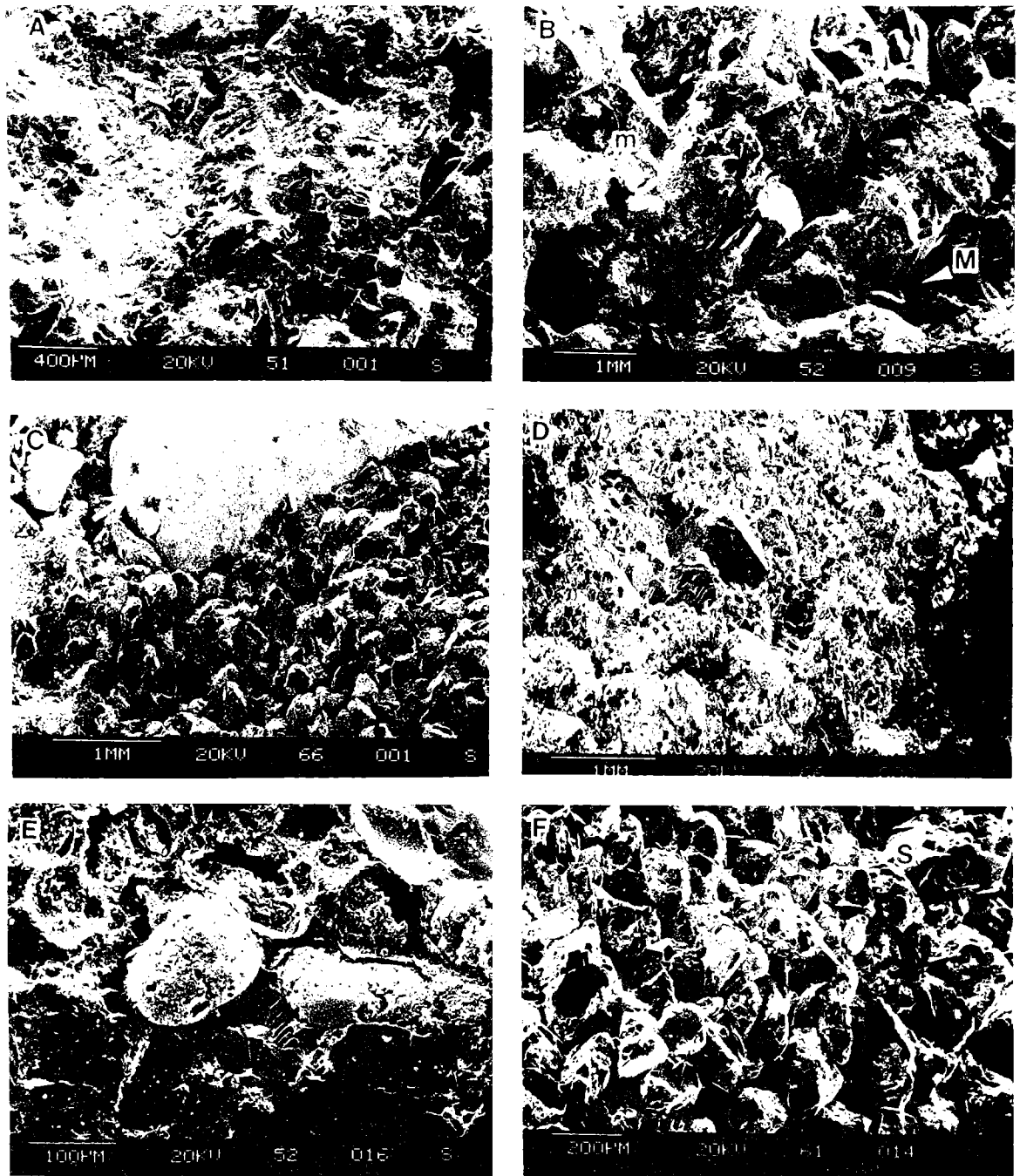


Figure 11. Scanning electron microscope photographs illustrating variability of grain size, cementation, porosity, and leaching in samples from different examined facies. *A*—Scattered detrital framework grains and compacted rock fragments (now pseudomatrix), tightly cemented by carbonate cement; only microporosity is present; FIC facies; Shell 1 Kerr, sec. 6, T. 4 N., R. 17 ECM, depth 6,220 ft. *B*—Coarse sand showing

both intergranular (macro-, M) and intragranular (micro-, m) porosity; microporosity is due to partial leaching of rock fragments and growth of authigenic clays; sample as in *A*, depth 6,225 ft. *C*—Fossil fragments (arrows) surrounded by medium-sized quartz grains and clay-rich rock fragments; intergranular pores appear to be interconnected, and essentially free from cements; TINS facies; King-Stevenson 1 Anderson, sec. (continued on opposite page)

APPENDIX:
List of drill holes from which cores were described,
or from which geophysical logs were digitized for
construction of the cross sections shown in Figure 3A,B

Core holes

Sec.	Twp.	Range	Well name	Unit*	Depth range of cored interval
1	4N	10ECM	Gulf 1 Kelly	Morrow	4,410-4,740
6	4N	17ECM	Shell 1-6 Kerr	Morrow	6,217-6,574
31	2N	17ECM	Southland Royalty 1-31 Daisy	Morrow	6,187-6,204
8	1N	23ECM	Petro-Lewis 2-8 Cates	Morrow	7,730-7,786
13	1N	21ECM	King-Stevenson 1 Weader	Morrow	7,890-7,978
5	1N	26ECM	Huber 1 Towle	Morrow	8,431-8,480
25	28N	21W	Apache 1 Huenergarot	Morrow/Chester	5,652-5,670
26	25N	20W	King-Stephenson 1 Anderson	Morrow	7,054-7,236
24	23N	21W	Apache 1 Geneva Baker	Morrow	7,746-7,840
33	20N	21W	Odessa Natural Gas 1 Milstead	Morrow	10,306-10,476
18	18N	22W	Sarkeys 1-18 Miller	Morrow	11,712-11,770
32	15N	17W	Michigan-Wisconsin Pipeline 1 Raab	Morrow/Spgr.	12,727-12,898
26	14N	10W	Edwin Cox 1 Miller	Morrow	10,152-10,200
3	12N	21W	Petro Consultants 1-3 Weatherly	Morrow	17,947-17,994
3	12N	21W	Petro Consultants 1 Weatherly	Springer	18,894-19,010
12	12N	13W	Mustang Production Co. Meacham 1-12	Cunningham	13,362-13,398
10	11N	12W	Apexco 1 Buell A	Springer	13,736-14,103
7	10N	21W	Trigg Paul King 1-7	Morrow	15,863-15,888
28	9N	20W	Phillips 1 Celson	Cunningham	18,227-18,236
20	8N	17W	Horco & Mobile [Humble] 1 Anne Schmidt	Morrow	16,302-17,271
22	9N	9W	Tenneco 1-22 Grant Rumley	Morrow/Spgr.	13,575-13,890
36	5N	11W	Texaco 1 Carr	Springer	16,067-16,111
35	5N	10W	Kerr-McGee 1 Tentanque	Springer	18,076-18,111
23	5N	6W	Humble 1 Patterson	Springer	11,904-12,078
8	3N	7W	Chevron 1 Berta B Lay	Springer	16,625-16,663
7	1N	4W	Gulf 1 Graham	Springer	6,302-7,551
1	1S	4W	Atlantic Refining 1 Markham	Springer	4,802-5,324
17	2S	3W	Atlantic Refining 1 Walker-Voorhees	Springer	4,988-5,007
8	3S	2E	Gulf 1 Coffee	Springer	4,050-4,100
16	3S	3W	Humble 1 Wm. Woodruff	Springer	10,323-10,440

Wells from which geophysical logs were digitized for construction of Figure 3A,B

Cross-section well number	Sec.	Twp.	Range	Well name
1-7	34	11N	25W	Mesa 2-34 Cox
1-8	13	11N	26W	Exxon Rhome Nix 1
1-9	29	11N	25W	Mesa Tipton 29
1-10	2	9N	24W	Conoco Phillips 2-1
1-11	9	13W	25W	El Paso Natural Gas Pierce 1
1-12	25	4N	6W	Marshall Oil Co. 1 Jenkins
1-14	22	20N	20W	Magnolia Oil Co. J. C. Borden 1A
1-16	23	5N	6W	Humble 1 D. B. Patterson
2-8	1	2N	4W	Roy Furr and AM
2-9	21	14N	24W	Inexco Oil Co. Lovell 1
3-8	27	20N	22W	Pan Am 1 Goff Oil Chance Shaham 1
3-9	34	3S	2E	Getty Otey 1-34
3-10	23	5S	2E	Coquina Oil Co. State Park 1

*As listed in the Oklahoma Geological Survey core-collection catalog.

26, T. 25 N., R. 20 W., depth 7,095 ft. D—Aggregate of rounded, medium-sized to coarse grains which are aggregates of silt- and clay-sized authigenic quartz, authigenic clays, and detrital material; only microporosity is present; sample and facies as in C; depth 7,221 ft. E—Thin layer containing a high concentration of rounded glauconite pellets; pellets contain micropores, but most of this sample is tightly ce-

mented; sample and facies as in C; depth 7,071 ft. F—Fine-grained quartz arenite in which intergranular porosity exists even though overgrowths (S) of authigenic silica are common; intragranular microporosity is due to partial leaching of rock fragments and formation of authigenic clays; there is little evidence of compaction in this sample; MT/NTM facies; Humble 1 Patterson, sec. 23, T. 5 N., R. 6 W., depth 11,946 ft.

QUANTITATIVE PETROGRAPHIC ANALYSIS OF DESMOINESIAN SANDSTONES FROM OKLAHOMA

THADDEUS S. DYMAN

U.S. Geological Survey, Denver

Abstract.—Desmoinesian sandstones from the northern Oklahoma platform and the Anadarko, Arkoma, and Ardmore basins record a complex interaction between mid-Pennsylvanian source-area tectonism and cyclic sedimentation patterns associated with numerous transgressions and regressions. Framework-grain summaries for 50 thin sections from sandstones of the Krebs, Cabaniss, and Marmaton Groups and their surface and subsurface equivalents were subjected to multivariate statistical analyses to establish regional compositional trends for provenance analysis.

R-mode cluster and correspondence analyses were used to determine the contributing effect (total variance) of key framework grains. Fragments of monocrystalline and polycrystalline quartz; potassium and plagioclase feldspar; chert; and metamorphic, limestone, and mudstone-sandstone rock fragments contribute most to the variation in the grain population. *Q*-mode cluster and correspondence analyses were used to identify four petrofacies and establish the range of compositional variation in Desmoinesian sandstones. Petrofacies I is rich in monocrystalline quartz (78–98%); mica and rock fragments are rare. Petrofacies II is also rich in monocrystalline quartz (60–84%) and averages 12% total rock fragments. Petrofacies III and IV are compositionally heterogeneous and contain variable percentages of monocrystalline and polycrystalline quartz, potassium feldspar, mica, chert, and metamorphic and sedimentary rock fragments.

Quantitative analyses indicate that Desmoinesian sandstones were derived from sedimentary, igneous, and metamorphic source areas. Sandstones of petrofacies I and II occur mostly in the lower Desmoinesian and are widely distributed, although they are most abundant in eastern and central Oklahoma; sandstones of petrofacies III and IV are widely distributed and occur primarily in the middle and upper Desmoinesian. The range of compositional variation and the distribution of petrofacies are related to paleotectonics and basin development, sediment recycling, and varying depositional environments.

INTRODUCTION

The present-day geologic framework of Oklahoma and the entire southern Midcontinent region is related directly to Pennsylvanian paleotectonic development (Fig. 1). Source-area variability and multiple marine transgressions and regressions have resulted in abrupt facies changes and complex depositional cycles. Many published studies have reconstructed Pennsylvanian paleogeography using stratigraphic and sedimentologic data within these depositional cycles, but detailed petrologic studies are rare. Published compositional data for sandstones are generally limited to field or core rock descriptions and are not detailed enough for provenance studies. Quantitative analysis of existing data is difficult.

Desmoinesian sandstones in Oklahoma record a complex interaction between source-area tectonism, regional transgression, and sediment recycling. These sandstones are readily identifiable in both outcrop and core and exhibit much compositional heterogeneity. Studies of compositional variations in these sandstones may aid in paleogeographic reconstruction and stratigraphic correlation, especially where nomenclature is confus-

ing. These studies may be valuable because of the significant oil and gas potential of Desmoinesian strata in Oklahoma.

A quantitative petrographic analysis of Desmoinesian sandstones was conducted in order to (1) define sandstone petrofacies for regional correlation and determine which framework grains contribute most to variations in sandstone composition; (2) describe lateral and vertical variations in source area to better understand the sedimentary-tectonic framework of the Desmoinesian in the region; and (3) determine the usefulness of statistical analyses in petrographic studies. The most important goal of this study was simply to define the range of compositional variation in sandstones in order to better understand the distribution of sandstone petrofacies. The petrographic data base exhibited much variation, and because variations in the sample population were difficult to define subjectively, a statistical approach was undertaken.

This study is preliminary and is intended to establish a base for future quantitative petrographic studies. The compositional range of Desmoinesian sandstones may be expanded in the future as more sandstones are analyzed. Ad-

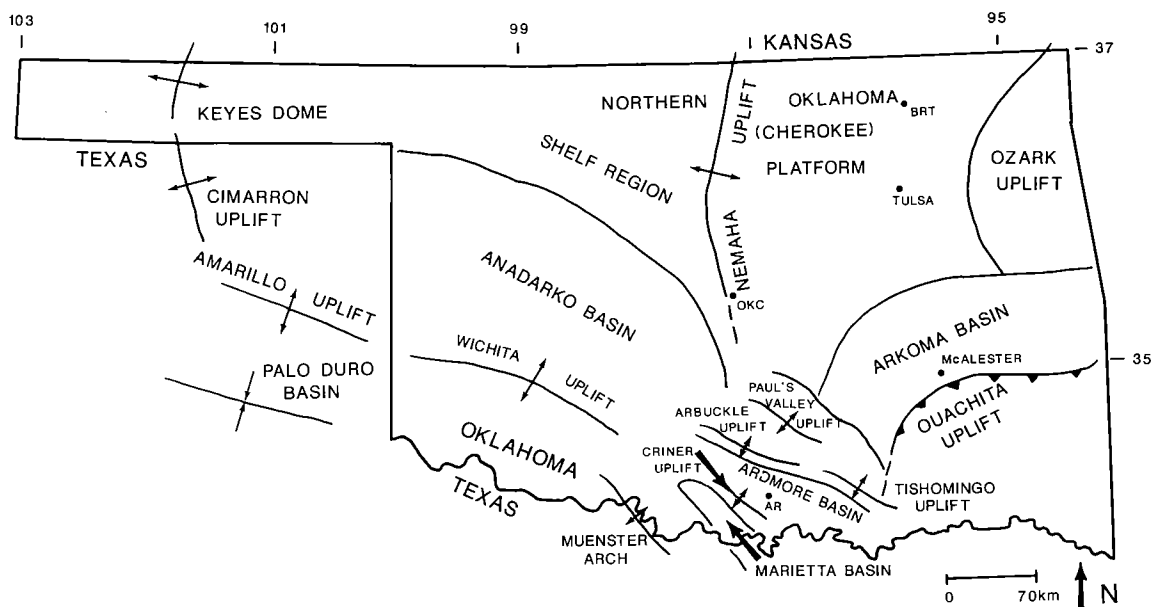


Figure 1. Major Pennsylvanian structural features of Oklahoma. Data from Branson (1962), Johnson (1971), Frezon and Dixon (1975), and Krumme (1981). OKC = Oklahoma City; AR = Ardmore; BRT = Bartlesville.

ditional sandstones must be compositionally and sedimentologically analyzed before a thorough understanding of Pennsylvanian paleogeography is attained. Any final provenance determination should be based on stratigraphic, sedimentologic, and petrologic data.

Core samples were obtained from the Oklahoma Geological Survey Core and Sample Library. This report has been prepared for the U.S. Geological Survey's Evolution of Sedimentary Basins Program.

REGIONAL GEOLOGY

The geography of Oklahoma and the surrounding region during the Pennsylvanian was strongly affected by the Ouachita orogeny, the result of a collision of North America with South America and Africa (Kluth and Coney, 1981). Regional structural elements active during the Pennsylvanian are shown in Figure 1. The Amarillo–Wichita–Criner uplift was a prominent structural feature during most of the Pennsylvanian and extended for >300 mi from the Texas Panhandle southeastward into southern Oklahoma. The Muenster arch is a southern extension of the Wichita–Criner trend, but is separated from the Criner uplift by the Marietta basin (Frezon and Dixon, 1975). The Cimarron uplift and Keyes dome form a northward extension of the Amarillo uplift in the Oklahoma Panhandle.

The Nemaha uplift is a prominent subsurface structural feature that trends from south of Oklahoma City northward for >400 mi into Nebraska (Luza, 1978). The axis of this feature represents the highest part of a more extensive Early Pennsylvanian positive area often referred to as the Nemaha highlands.

The Anadarko basin is bordered by the Nemaha uplift on the northeast, the central Kansas shelf on the north, and the Amarillo–Wichita–Criner trend on the south. It is one of the deepest cratonic basins in North America and contains ~40,000 ft of Cambrian through Permian sedimentary rocks along its southern margin. More than 20,000 ft of stratigraphic separation exists along the Wichita megashear in southwestern Oklahoma (Evans, 1979).

During Desmoinesian time, the southern part of the Ouachita geosyncline in southeastern Oklahoma was uplifted by thrusting and folding, and a prominent positive feature known as the Ouachita uplift developed. The northern part of the geosyncline and a shelf region to the north retained a basin configuration, referred to as the Arkoma basin (Branson, 1962). The Arbuckle and Pauls Valley uplifts were positive elements in south-central Oklahoma during Desmoinesian and Missourian time. The Ardmore basin contains nearly 20,000 ft of Upper Mississippian and Pennsylvanian strata and is separated from the Anadarko basin by local uplifts (Jacobson, 1959).

The Ozark uplift in northeastern Oklahoma

and Missouri is an earlier Paleozoic structural feature that was rejuvenated during the mid-Pennsylvanian at approximately the same time as the Ouachita uplift (Branson, 1962; Frezon and Dixon, 1975).

REGIONAL STRATIGRAPHY AND SEDIMENTOLOGY

Stratigraphic names for outcrop and core samples of sandstones were taken from published reports and summaries prepared by well-site geologists. Stratigraphic nomenclature in Oklahoma is confusing in part because of facies differences between platform and basin and in part because of historic differences in surface and subsurface nomenclature (Krumme, 1981). Figure 2 illustrates Desmoinesian sandstone nomenclature for the state, compiled from Jordan (1957), Tomlinson and McBee (1959), Branson (1962), Frezon and

Dixon (1975), Ebanks (1979), Krumme (1981), and Sutherland (1982). Limestone and shale units not addressed in this report have been omitted from the figure. Informal subsurface stratigraphic names also have been omitted from Figure 2 because of the uncertainty of precisely correlating them with surface units.

Desmoinesian formations have been divided into three groups, which are, from oldest to youngest, the Krebs, Cabaniss, and Marmaton (Krumme, 1981). These groups and their stratigraphic equivalents are bounded by unconformities and are found throughout Oklahoma. In the Ardmore and eastern Anadarko basins, equivalent strata are included in the Deese Formation. In western Oklahoma, the Krebs and Cabaniss Groups are informally referred to as the Cherokee Group or are left as undivided Desmoinesian strata (Frezon and Dixon, 1975). The term Cherokee Group is generally not accepted in Oklahoma (Ebanks, 1979).

The oldest Desmoinesian formation in central and eastern Oklahoma, the Hartshorne Sandstone, rests unconformably on older Pennsylvanian or pre-Pennsylvanian strata. The overlying McAlester Formation is predominantly shale, but contains one regionally persistent sandstone referred to as the Warner Sandstone Member and its informal subsurface equivalent, the Booch sandstone. The Savanna Formation unconformably overlies the McAlester Formation in the Arkoma basin and contains many discontinuous sandstone and coal beds. The base of the overlying Boggy Formation is drawn at the base of the Bluejacket Sandstone Member and its informal subsurface equivalent, the Bartlesville sandstone (Branson, 1962). Informal subsurface sandstone equivalents of the upper part of the Boggy (Taft Sandstone Member) include the Red Fork and Burbank sandstones.

The Thurman Sandstone unconformably overlies shales in the upper Boggy in southern Oklahoma, but is absent on the northern Oklahoma platform. The overlying Senora Formation is laterally persistent but lithologically variable. The Chelsea Sandstone Member is locally present in eastern Oklahoma. The Skinner sandstone is an informal subsurface equivalent of the Senora Formation (Krumme, 1981).

The upper Desmoinesian Marmaton Group is composed primarily of shales, sandstones, and limestones. In the Arkoma basin, the Calvin Sandstone forms the base of the group, but is replaced by the Fort Scott Limestone on the northern Oklahoma platform. The informal Peru sandstone may represent a lateral shelf equivalent of the Calvin. The overlying Peru sandstone is part of the Labette Shale (Krumme, 1981). Sandstones in the upper Marmaton Group, such as the informal Cleveland sandstone, are interbedded with shales and are often discontinuous.

SERIES	GROUP	FORMATION AND MEMBER
DESMOINESIAN	MARMATON	Upper Marmaton Gp. sandstones Labette Shale Calvin Sandstone
	CABANISS	Senora Formation Chelsea Sandstone Member Thurman Sandstone
	KREBS	Boggy Formation Taft Sandstone Member Bluejacket Sandstone Member Savanna Formation McAlester Formation Warner Sandstone Member Hartshorne Sandstone

Figure 2. Generalized stratigraphic section of Desmoinesian sandstone strata in the Arkoma basin and central Oklahoma platform. Data from Jordan (1957), Tomlinson and McBee (1959), Branson (1962), Frezon and Dixon (1975), Ebanks (1979), Krumme (1981), and Sutherland (1982). Because of the discontinuous nature of Pennsylvanian sandstones and the difficulty of correlating surface with subsurface units, informal subsurface names have been excluded from the chart. The chart is incomplete, because only stratigraphic units addressed in this report are included. The Deese Formation of south-central Oklahoma includes strata equivalent to the three groups presented here.

Desmoinesian sandstones were deposited in fluvial, deltaic, and marine depositional environments associated with the Early Pennsylvanian northward transgression. During the early Desmoinesian, fluvial, deltaic, and shallow marine depositional environments dominated the northern Oklahoma shelf, whereas deeper-water marine environments dominated the southern Anadarko and Ardmore basins. With a presumed southward shift in provenance (Krumme, 1981), marine carbonate shelf sedimentation dominated northern Oklahoma during the late Desmoinesian. Coarse-grained alluvial sediments were deposited along the margins of uplifts. Because of local source-area influence and sea-level changes, paleoenvironments may have varied from these regional trends. Most of the sandstones analyzed in this report were deposited in deltaic and shallow marine environments. Compositional variations are considered to be due primarily to different source areas; however, compositional modification due to changing depositional environments cannot be totally discounted until a thorough provenance study has been completed.

METHOD OF STUDY

The study includes both core and outcrop samples on the northern Oklahoma platform, both east and west of the Nemaha uplift, and in the Anadarko, Arkoma, and Ardmore basins in both western and southeastern Oklahoma (Figs. 1,3).

Fifty medium-grained sandstone samples were cut, thin-sectioned, stained for potassium feldspar, and point-counted using >300 point counts per slide. Quartz grains were examined for extinction patterns, inclusions, and overgrowths (Folk, 1968). Accessory minerals such as micas, hornblende, garnet, and zircon were identified as present or absent. Compositional variations due to differences in weathering between surface and subsurface samples were not addressed in the statistical analysis; these variations are considered minor in this population of sandstones.

Locations and composition data for all samples in this study can be found in Dyman (1987). Data were aggregated according to methods presented in Dickinson and Suczek (1979).

STATISTICAL ANALYSIS OF COMPOSITIONAL DATA

R-mode correspondence analysis was applied to determine the contributing effect (percentage of total variance) of each framework-grain type (variables). Based on their contributing effect, variables were aggregated into genetic groups. *Q*-mode cluster analysis and correspondence analysis were applied to determine sample relationships and the range of compositional variation. Samples were then aggregated into petrofacies groups to analyze stratigraphic and geographic variations in sandstone composition.

Correspondence analysis is a form of factor

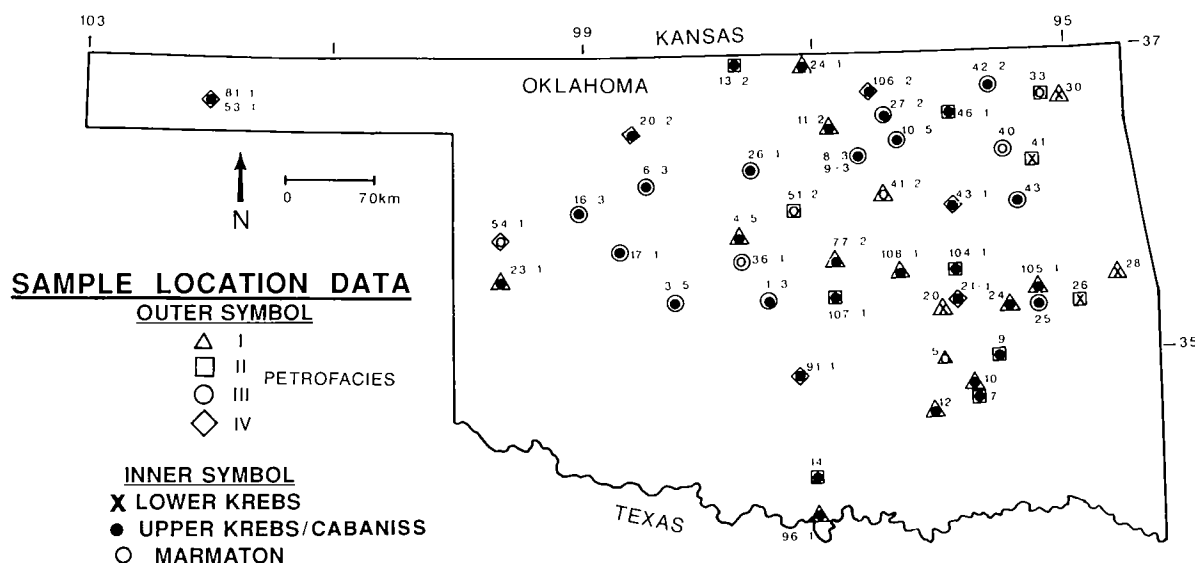


Figure 3. Sample-location and sample-identification map (see text). Dyman (1987) contains detailed location and compositional data for all samples used in this study.

analysis that combines the results of both *Q*- and *R*-mode studies and reduces variable-scaling problems. Correspondence analysis reduces the problem of *N*-dimensional space (many variables) by projecting combinations of original variables on a new set of axes (eigenvectors) defining new hypothetical variables called factors (David and others, 1977). Variable contribution on the new set of axes is based on variance. Data standardization to reduce problems induced by varying magnitude is not required. Data are transformed into conditional probabilities by dividing each data element by the sum of all elements.

Output from correspondence analysis includes (1) relative and absolute factor-variable contribution matrices that define the relative or absolute contribution of each original variable (as a percent) to each new factor (variables important in distinguishing all samples together); (2) a factor-score data matrix that contains factor-score loadings (variables important in distinguishing each sample from other samples); and (3) factor-score maps (plots), created from the factor-score matrix, which graphically display sample similarity in factor space. Lines are drawn on each plot to illustrate how each numbered variable contributes to differences among samples. The lines pass through a portion of factor space defined by their *R*-mode loadings. The lines represent the strength and direction according to which the different variables affect the sample population (David and others, 1974). The lines intersect at a point representing the average composition of the sandstones. The proximity of a group of sample points near a variable line (or lines) illustrates the similarity of samples and the variable (or variables) responsible for the similarity. Closely spaced sample points on one factor-score plot (for example, a plot of factors 1 and 2) may not occur together on a plot of different factors (for example, factors 3 and 4), because of the difference of variable contribution to different factors.

Cluster analysis is a multivariate classification method by which relatively homogeneous groups are defined by assigning samples to a group based on their similarity. A dendrogram defining all of the groups is created by the computer program (Davis, 1973, 1986). In hierarchical clustering, the most-similar samples are joined in a cluster which then successively joins with other clusters until all samples are included in the dendrogram. Modal analyses for Desmoinesian sandstones were first standardized using the variable-mean deviation to ensure that each variable was weighted equally.

The program of Davis (1973) for weighted pair-group clustering was used with the *r*-correlation coefficient in this study. Cluster dendrograms produced with distance coefficients may include well-defined cluster groups even if some samples are very unlike other samples. In this study, clus-

ter dendrograms were generated separately with distance and *r*-correlation coefficients, and the two methods provided similar results.

In the method of weighted pair-group clustering, correlation matrices of samples are calculated, and samples with high correlations are extracted. In subsequent steps, similarity matrices are recomputed, treating clustered elements as a single element. Each new cluster member is given equal weight with the existing cluster; thus, late cluster arrivals carry more weight than do earlier arrivals.

Several alternative clustering methods are available (Davis, 1986), and the best clustering method may be determined by the specific data set. Davis (1986) suggested that the weighted pair-group method provides the best results, but that researchers should compare different methods. In this study, the results from cluster analysis were corroborated by correspondence analysis.

***R*-Mode Analysis**

Table 1 represents the absolute variable-factor contribution matrix for the 10 framework-grain types analyzed in this study. Sandstone, siltstone, and mudstone grains were combined for the statistical analysis (mudstone-sandstone in Table 1). Dark-gray to brown, siliceous and calcareous mudstones and shales were the most abundant of the three types. In some cases it was difficult to differentiate between weakly foliated metamorphic grains and shale grains. Together, the first four factors contribute 85% to the variation in the total sample of framework grains.

Factor 1 is controlled primarily by the high loading for potassium feldspar due to the two samples from the Cherokee Group in the Oklahoma Panhandle (samples 53-1, 81-1). The high loading for limestone in factor 3 is due to limestone-rich samples from northern and southern Oklahoma (samples 20-2, 91-1). Samples rich in variables with high loadings for factor 2 are widely distributed in Oklahoma, in part because of the many grain types contributing to factor 2. Factors 3 and 4 are controlled primarily by chert and lithic grains from middle and upper Desmoinesian samples.

When the correspondence analysis was rerun without the samples rich in potassium feldspar and limestone, cumulative variation was distributed proportionally, according to the relative importance of the remaining variables. Monocrystalline and polycrystalline quartz, mudstone-sandstone, and metamorphic grains contributed more to each factor.

Quartz, chert, potassium and plagioclase feldspar, and limestone, mudstone-sandstone, and metamorphic grains contribute most to variation in this population of Desmoinesian sandstones.

TABLE 1.—ABSOLUTE VARIABLE-FACTOR CONTRIBUTION MATRIX
(FIRST 4 FACTORS) AND CUMULATIVE PERCENT CONTRIBUTION
FOR ORIGINAL FRAMEWORK- GRAIN VARIABLES

Grain type	Factor			
	1	2	3	4
monocrystalline quartz	1.2	22.4	2.9	0.1
polycrystalline quartz	0.8	16.4	2.3	2.0
chert	0.1	10.4	1.5	17.6
plagioclase	2.9	10.8	1.6	0.1
potassium feldspar	92.0	0.3	0.6	1.2
mudstone-sandstone	0.2	4.2	7.9	28.8
limestone	0.7	19.1	76.1	0.4
volcanic	0.1	0.2	0.1	4.9
metamorphic	1.7	15.0	5.0	42.8
mica	0.2	0.9	1.6	2.1
Cumulative Percent Contribution	41	60	77	85

Q-Mode Analysis

Four petrofacies groups were identified for 50 sandstone samples, using cluster analysis. Figure 4 illustrates the weighted pair-group dendrogram and petrofacies groups, using all 10 original framework variables. Petrofacies subdivision based on clustering procedures is somewhat arbitrary, especially when cluster groups join at low levels of similarity. Additional cluster groups could be defined, depending on the level of compositional similarity we wish to establish in the sample population. Table 2 summarizes the characteristics of each petrofacies defined in this study. Petrofacies differences are based on compositional variations in framework grains. Quartz extinction patterns and the presence or absence of accessory minerals do not significantly vary among samples and were not used to differentiate sandstones.

The geographic distribution of petrofacies for lower, middle, and upper Desmoinesian sandstones is presented in Figure 3. For the purpose of this study, lower Desmoinesian includes only the lower part of the Krebs (Hartshorne Sandstone, and Warner Sandstone Member of the McAlester Formation); middle Desmoinesian includes the upper part of the Krebs (Savanna and Boggy sandstones) and Cabaniss Groups; and upper Desmoinesian includes sandstones in the Marmaton Group. This subdivision is arbitrary

and is used only to address gross compositional variations in Desmoinesian strata. The three-group breakdown also alleviates some of the problems of correlating informal subsurface with surface nomenclature. Future studies with more samples could define additional or different stratigraphic groups.

Petrofacies I

Petrofacies I is subdivided into two petrofacies subgroups and is rich in monocrystalline quartz (mean 84%; Fig. 5). Subgroup A contains an average of 88% monocrystalline quartz, whereas subgroup B contains 80%. Polycrystalline quartz averages only 5% for petrofacies I. Lithic grains are rare or absent in subgroup A, but reach a maximum of 14% for subgroup B (sample 11-2, Red Fork sandstone, northern Oklahoma; Fig. 3). Metamorphic grains are more abundant than sedimentary grains for both subgroups, but are most abundant in subgroup B. Feldspar is rare or absent in both subgroups.

Petrofacies I is widely distributed throughout the study area, especially along a north-trending belt in part coinciding with the axis of the Nemaha uplift. Stratigraphically, all three groups of Desmoinesian age are represented in petrofacies I, but most samples are from the lower and middle Desmoinesian. No relationship appears to exist between stratigraphic group assignment and

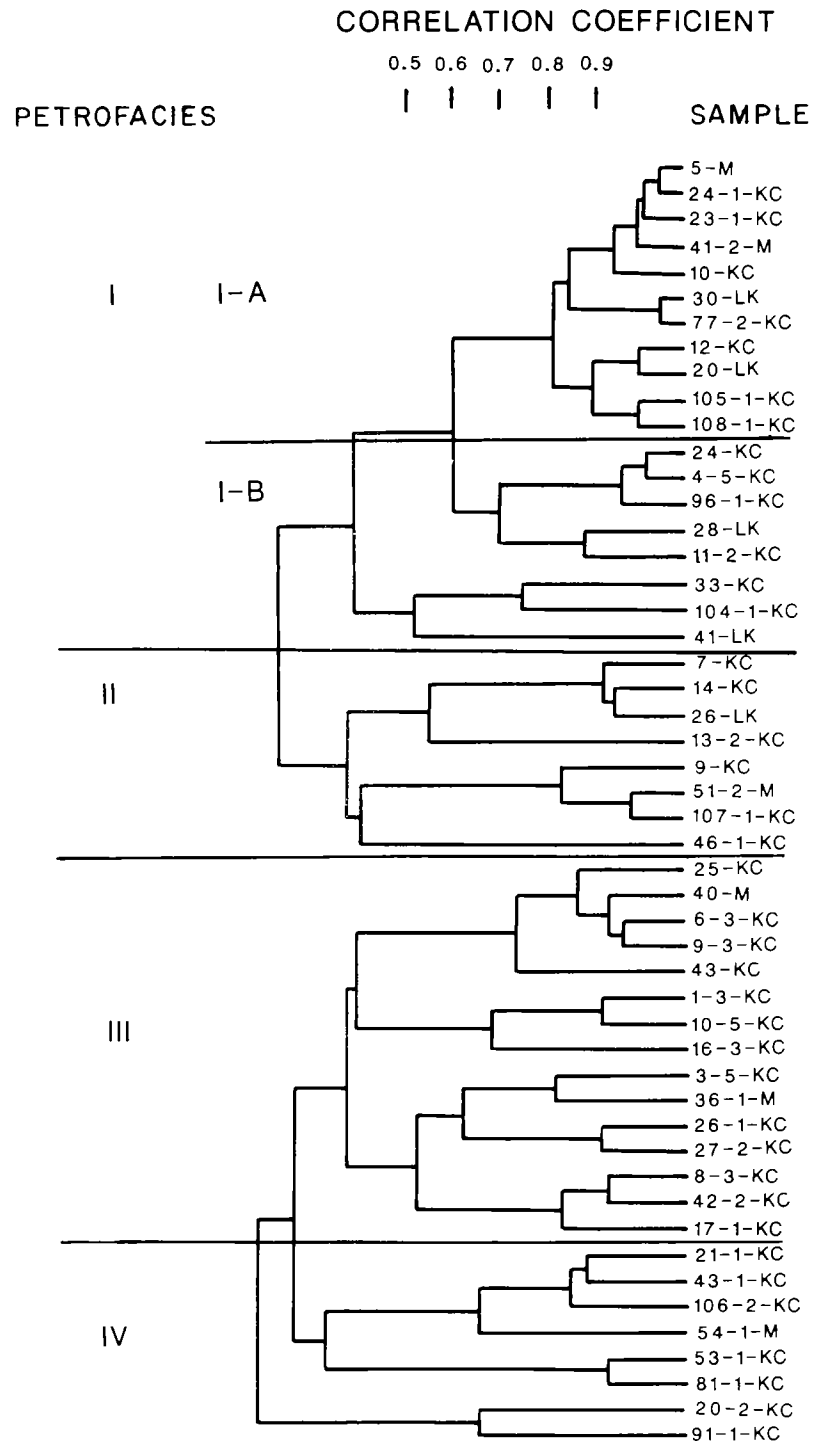


Figure 4. Weighted pair-group average (WPGA) dendrogram of framework grains for Des Moinesian sandstones. See Dyman (1987) for detailed sample locations and identification. Petrofacies I and II are rich in monocrystalline quartz and contain rare rock fragments, whereas petrofacies III and IV are compositionally heterogeneous and contain variable amounts of all constituents. See Table 2 for detailed petrofacies description.

TABLE 2.—PETROFACIES SUMMARY FOR DESMOINESIAN SANDSTONES IN THIS STUDY

Petrofacies	Framework grains, point counts (%)		Distribution and comments
	Mean	Range	
I (N = 19)	Qm = 84 Qp = 5 Lt = 4 F = 1	78–98 1–9 1–14 0–3	Samples widely distributed throughout Oklahoma. Generally found in lower Desmoinesian Krebs Group. Two Cabaniss Group samples (05, 41-2). Two subgroups defined (I-A, I-B). Subgroup A contains a mean of 88% Qm; subgroup B contains a mean of 80% Qm. Straight to slightly undulose quartz extinction. Trace of zircon and tourmaline.
II (N = 8)	Qm = 75 Qp = 10 Lt = 12 F = 2	60–84 3–15 2–24	Distributed throughout the Desmoinesian and absent only from the western part of the study area. Straight to slightly undulose quartz extinction. Trace of zircon, tourmaline, and hornblende.
III (N = 15)	Qm = 60 Qp = 13 Lt = 21 F = 4	49–74 7–22 11–37 0–8	Compositionally heterogeneous group restricted to middle and upper Desmoinesian samples, distributed throughout study area. Highest MRF content in sample population (mean 9%). Contains sample 36-1 with 5% mica and sample 17-1 with 8% plagioclase. Variable quartz extinction. Trace of zircon, tourmaline, and hornblende.
IV (N = 8)	Qm = 65 Qp = 7 Lt = 16 F = 12	45–85 0–20 7–28 1–36	Compositionally heterogeneous upper Desmoinesian group, widely distributed throughout study area. Group includes 2 feldspar-rich samples (53-1, 81-1) from the Oklahoma Panhandle and 2 limestone-rich samples (20-2, 91-1) from the north and south margins of the study area. Variable quartz extinction. Trace of zircon, tourmaline, and hornblende.

Note: Qm = monocrystalline quartz; Qp = polycrystalline quartz; Lt = total lithic grains; F = total feldspar; N = number of samples in each group; MRF = metamorphic rock fragments.

geographic distribution. Both upper Desmoinesian petrofacies I samples (sample 05, Senora Formation, and sample 41-2, Peru sandstone; Fig. 3) are in subgroup A and average >90% total quartz.

Petrofacies II

Compared to petrofacies I, petrofacies II contains less monocrystalline quartz (mean 75%), more chert (mean 8%), and more polycrystalline quartz (mean 10%) (Fig. 6). Petrofacies II is more heterogeneous in composition than petrofacies I, averaging 12% total lithic grains (including chert) and 2% feldspar. Sample 46-1 (Bartlesville sandstone) is not representative of petrofacies II (Fig. 4), containing only 70% total quartz; its presence in petrofacies II is probably an artifact of the clustering method.

Petrofacies-II samples are found throughout the Desmoinesian in all but the westernmost por-

tion of the study area. Petrofacies II is intermediate in composition between quartz-rich petrofacies I and quartz-poor petrofacies III and IV.

Petrofacies III

Petrofacies III is compositionally heterogeneous and generally contains <70% monocrystalline quartz (mean 60%), although values range from 49 to 74% (Fig. 7). Polycrystalline quartz ranges from 7 to 22% and averages 13%. Petrofacies III is lithic-rich (mean 21%), and metamorphic grains are the most abundant (mean 9%). Sandstones range from those with abundant metamorphic and polycrystalline quartz grains (samples 40, Senora Formation, and 6-3, Red Fork sandstone) to those with abundant chert and metamorphic grains (samples 26-1, Red Fork sandstone, and 42-2, Bartlesville sandstone). Some samples contain abundant plagioclase (sample 17-1, Red Fork sandstone, 8%), or mica



Figure 5. Petrofacies I sandstone: Red Fork sandstone, Gulf Oil Co. No. 1 Sheik, sec. 25, T. 28 N., R. 1 E.; sample 24-1, 3,605 ft; quartzarenite; 3 mm across.

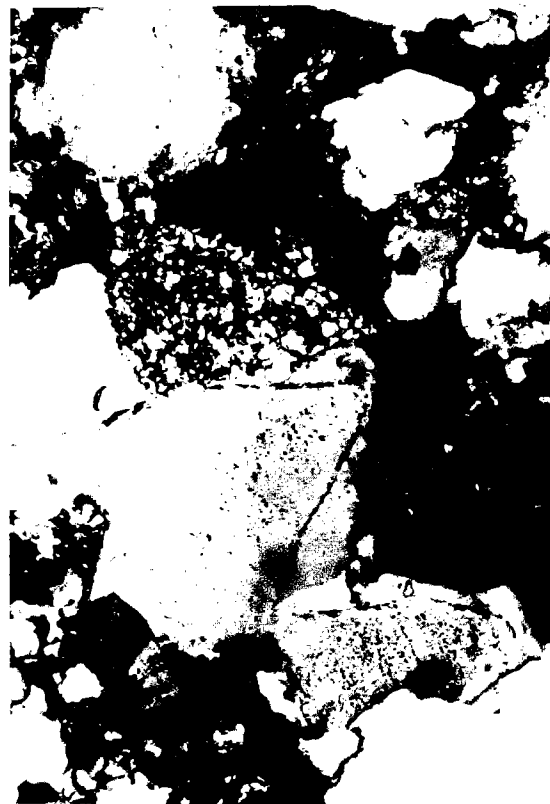


Figure 6. Petrofacies II sandstone: Red Fork sandstone, Indian Wells No. 4-24 Hajek, sec. 24, T. 28 N., R. 5 W.; sample 13-2, 4,681 ft; litharenite; 3 mm across.

(sample 36-1, Prue sandstone, 5%). Many compositionally intermediate forms exist.

Petrofacies-III samples are found throughout the study area, but are restricted to the middle and upper Desmoinesian. Samples from petrofacies III and IV together form lithic-rich concentrations in eastern and western Oklahoma (Fig. 3). Metamorphic-rich petrofacies-III samples are abundant in the northwest, central, and eastern portions of Oklahoma.

Petrofacies IV

Petrofacies IV is also compositionally heterogeneous, because cluster groups join at low levels of similarity. Petrofacies IV contains samples with 45–85% monocrystalline quartz (mean 65%). Polycrystalline quartz varies from 0 to 20% and averages 7%. Samples range from those with abundant potassium feldspar from the Oklahoma Panhandle (samples 53-1 and 81-1, Cherokee Group; Fig. 8) to those with abundant limestone

grains from the northern and southern portions of the study area (samples 20-2, Red Fork sandstone, and 91-1, Deese Formation; Fig. 9). Petrofacies-IV samples are generally feldspar- and lithic-rich, and sedimentary-rock grains are more abundant than metamorphic-rock grains. Several plagioclase-bearing samples (sample 20-2, Red Fork sandstone, 5%) occur in petrofacies IV. Many compositionally intermediate forms exist.

Petrofacies-IV samples are widely distributed in Oklahoma, but are restricted to middle and upper Desmoinesian strata.

Factor-Score Maps

The relative importance of each grain type in differentiating between sandstone samples cannot be graphically presented using cluster diagrams. Correspondence analysis factor-score maps were generated in order to (1) corroborate the petrofacies subdivision identified by cluster analysis (recognition of the four petrofacies on the factor-



Figure 7. Petrofacies III sandstone: Burbank sandstone, Oliphant No. 1 Henry, sec. 27, T. 24 N., R. 7 E.; sample 27-2, 2,630 ft; litharenite; 3 mm across.



Figure 8. Petrofacies IV sandstone: Red Fork sandstone, Texaco No. 1 Hartley, sec. 33, T. 3 N., R. 10 E.; sample 81-1, 4,535 ft; subarkose; 3 mm across.

score maps); (2) observe sample distribution in factor space (relating the samples compositionally, establishing the range in compositional variation, identifying provenance); and (3) identify variable influence for factor-score groupings (effect of each variable on each sample). Figures 10 through 12 are factor-score maps for the first four factors, incorporating the 10 framework-grain types used in the cluster analysis.

Figure 10 is the factor-score map for factors 1 and 2. Sixty percent of the sample-population variance—contributed mostly by potassium feldspar, quartz, plagioclase, chert, and limestone and metamorphic grains—is represented by the first two factors (Table 1). The cluster of points in the lower left part of the diagram represents monocrystalline-quartz-rich (variable 1) samples, predominantly from petrofacies I and II (samples 5, 10, and 41-2). Monocrystalline-quartz-rich samples in the lower portion of the lower left also tend to contain metamorphic grains (sample 28, Warner Sandstone Member; variable 9), whereas

samples in the upper portion of the left tend to contain more potassium-feldspar grains (e.g., sample 43-1, Bartlesville sandstone; variable 5).

The scattered array of points at the right and top of the figure represents quartz-poor samples of petrofacies III and IV from the middle and upper Desmoinesian. Samples 53-1 and 81-1 at the top of the diagram are the potassium-feldspar samples from the Cherokee Group in the Oklahoma Panhandle; sample 46-1 (Bartlesville sandstone; variable 8) is the only sample containing volcanic grains; sample 26-1 (Red Fork sandstone) represents monocrystalline-quartz-poor, polycrystalline-quartz-rich (variable 2) samples of petrofacies III and IV. The distribution of most points is gradational, and intermediate forms exist between clusters of samples.

Figure 11 is the factor-score map for factors 3 and 4, which together contribute ~25% to the total variation in the sample population. This plot emphasizes sample differences due to the distribution of chert, mudstone-sandstone,

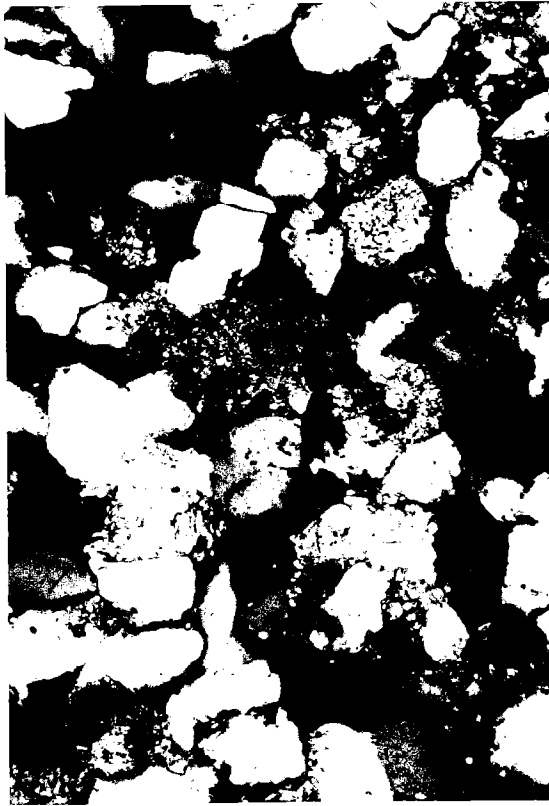


Figure 9. Petrofacies IV sandstone: Deese Formation, Buck-Leben No. 1 Harmon, sec. 8, T. 4 N., R. 1 W.; sample 91-1, 5,467 ft; litharenite; 3 mm across.

monocrystalline and polycrystalline quartz, and limestone and metamorphic grains. This plot is similar to Figure 10 because the quartz-rich and quartz-poor petrofacies and samples rich in potassium feldspar and limestone can be recognized. Because monocrystalline and polycrystalline quartz have lower loadings for factors 3 and 4, sample points are more centrally located on Figure 11, and their lines are short.

The factor-score plot for factors 2 and 4 (Fig. 12) reveals a greater spread of sample points because these two factors are not dominated by a single variable (for example, limestone or potassium feldspar), but contain higher loadings for several variables. Samples rich in metamorphic grains (samples 40, 6-3; variable 9) are well identified at the top of the figure because of the high loading for variable 9 in factor 4. The greater spread in monocrystalline-quartz-rich samples (petrofacies I and II) is due to minor variations in the contribution of chert, lithic, and feldspar grains.

Sample-distribution patterns in factor space

based on other combinations of factors (e.g., factors 2 and 3) provide the same relationships presented here. The four petrofacies previously defined using cluster analysis can be recognized using the correspondence-analysis method. However, the variation in composition of sandstone samples based on the influence of each grain type is best illustrated using the correspondence-analysis factor-score maps. The compositional limits defined for each plot represent the known compositional limits for Desmoinesian sandstones in this study.

PALEOGEOGRAPHIC IMPLICATIONS

Quantitative analyses in this study indicate that Desmoinesian sandstones were derived from sedimentary, metamorphic, and granitic source areas (craton, orogenic belt, and batholith, respectively). Compositional trends from these quantitative analyses include the following:

1) There is a slight upward increase in compositional heterogeneity from early to late Desmoinesian, but some exceptions exist. The lower Desmoinesian Warner Sandstone Member and Hartshorne Sandstone are the most quartz-rich, but contain slightly less quartz westward in eastern Oklahoma. There is a change upward stratigraphically in eastern Oklahoma from Atokan predominantly marine shelf sandstones, to Desmoinesian predominantly deltaic sandstones (O'Donnell, 1983). The central Oklahoma quartz-rich (petrofacies I) belt coincides in part with the Nemaha uplift. Adkison (1972) identified a north-trending sandstone-rich belt within the Ordovician Simpson Group in south-central Kansas. The north-trending quartz-rich belt may have its source in these areas of quartz-rich Simpson Group sandstone; however, a thorough basin analysis should be conducted in order to fully define this trend.

2) Total lithic content is greatest (petrofacies III and IV) in two broadly defined north-trending belts in western and eastern Oklahoma. The total average lithic content of Desmoinesian sandstones is greatest in northern Oklahoma, suggesting that available lithic detritus from southern sources may have been trapped in the deeper parts of the Anadarko, Ardmore, and McAlester basins. However, Hare (1970) recognized schistose metamorphic fragments and shale fragments in the Thurman Sandstone and identified a Ouachita source for the Thurman Sandstone in Hughes and Coal Counties (southeast Oklahoma). Jacobson (1959) identified sedlitharenites rich in shale fragments in the Desmoinesian Deese Formation in the Ardmore basin, and attributed these to unroofing of shales of the Mississippian and Pennsylvanian Springer Formation from the

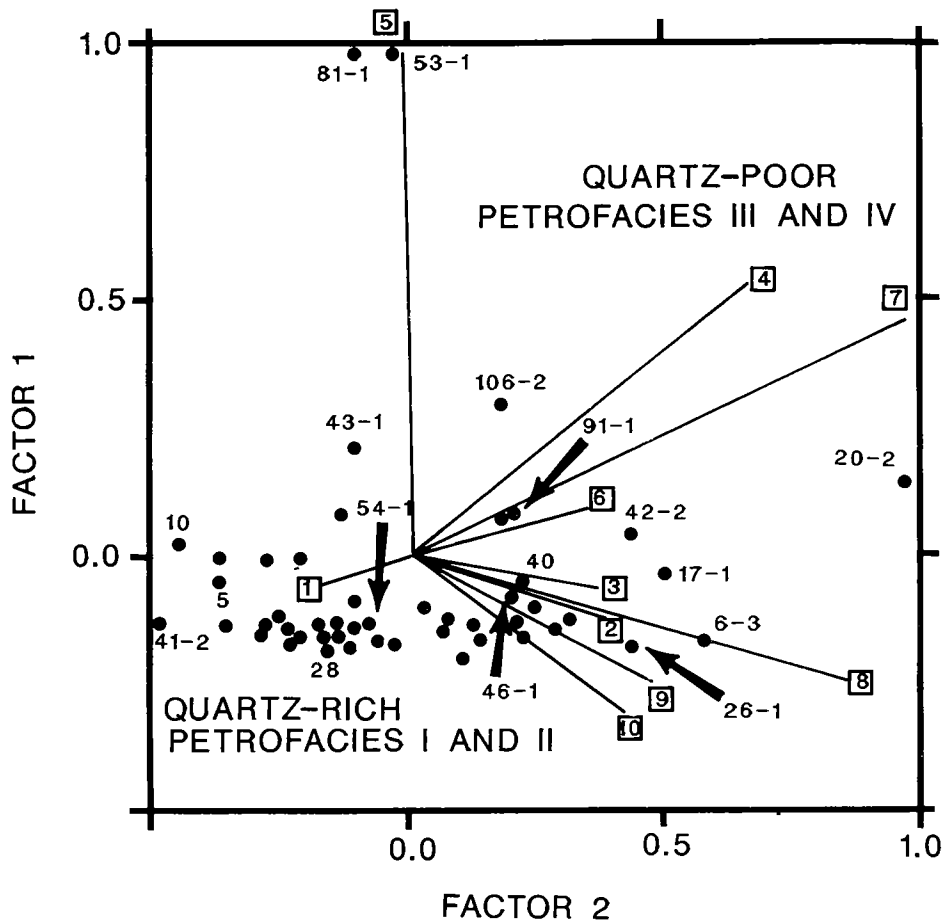


Figure 10. Correspondence-analysis factor-score map, factors 1 and 2. Variable number represent variable contribution in factor space. Refer to Figure 3 for sample location and identification. Variable numbers represented by lines on plot as follows: (1) monocristalline quartz, (2) polycrystalline quartz, (3) chert, (4) plagioclase, (5) potassium feldspar, (6) sandstone, (7) limestone, (8) volcanic, (9) metamorphic, (10) mica. Refer to Table 1 for factor loadings.

Arbuckle uplift. No change in the early to late Desmoinesian distribution of lithic grains was identified in this study.

3) Sandstones rich in limestone detritus are concentrated in two zones, one in northern and one in southern Oklahoma. Unroofing of lower Paleozoic carbonate terranes may have been greater in the Wichita-Criner and Arbuckle regions during the middle Desmoinesian (Tomlinson and McBee, 1959). Dunham (1955) identified limestone conglomerates and cherty, quartzose, and calcareous sandstones in the Deese Formation in the northern part of Murray County in southern Oklahoma. The northern-Oklahoma sample may be related to lower Paleozoic carbonate source areas of the Nemaha and central Kansas uplifts. Additional samples must be analyzed

before the influence of local limestone sources can be fully established.

4) Areas rich in polycrystalline quartz coincide in part with areas rich in monocristalline quartz and areas rich in total lithic grains, but the relationship to provenance is not clear. Problems may exist in assigning polycrystalline grains to either sedimentary lithic grains or quartz.

5) The two arkosic sandstones from the Oklahoma Panhandle are related to western uplifts of the Ancestral Rocky Mountains. Precambrian granitic basement rocks of the Arbuckle and eastern Wichita-Criner uplifts were not a sediment source during the Desmoinesian. Feldspar-bearing samples in northeastern Oklahoma are probably related to cratonic source areas to the north and east.

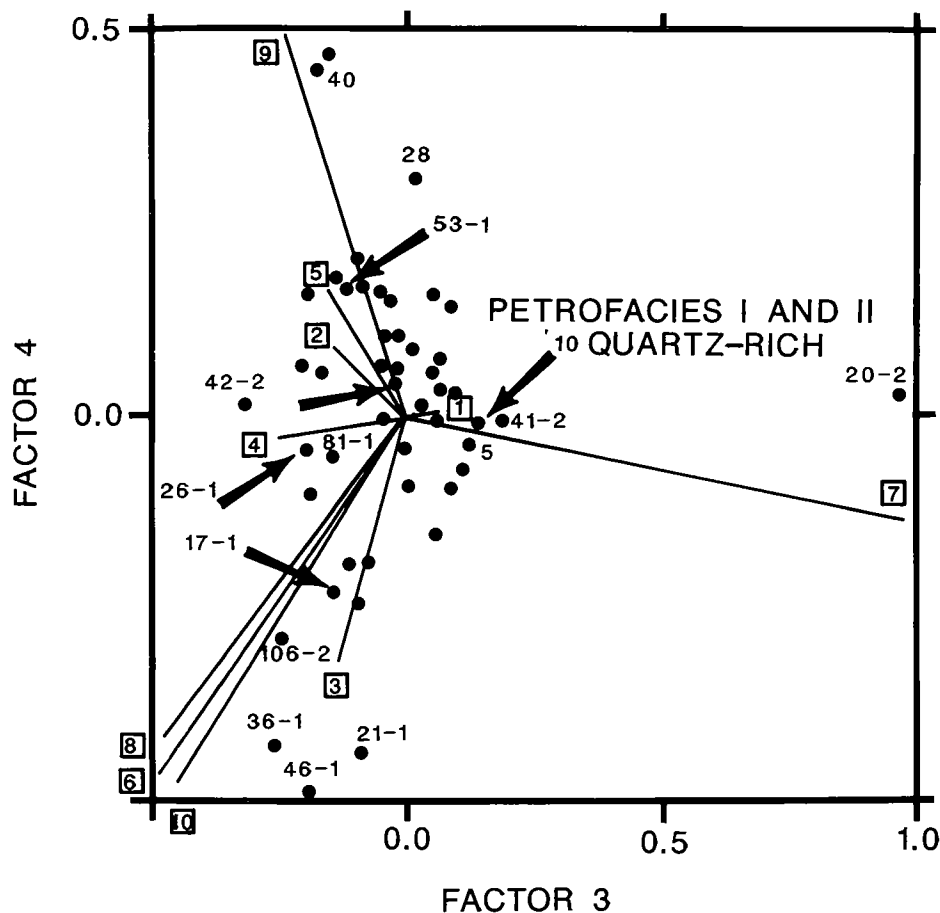


Figure 11. Correspondence-analysis factor-score map, factors 3 and 4. Variable numbers represent variable contribution in factor space. Refer to Figure 3 for sample location and identification. Variable numbers represented by lines on plot as follows: (1) monocrystalline quartz, (2) polycrystalline quartz, (3) chert, (4) plagioclase, (5) potassium feldspar, (6) mudstone-sandstone, (7) limestone, (8) volcanic, (9) metamorphic, (10) mica. Refer to Table 1 for factor loadings.

SUMMARY

Correspondence and cluster analyses are very useful in understanding compositional variation and establishing petrofacies in highly variable sample populations such as the one used in this study.

R-mode correspondence analysis indicates that the relative proportions of monocrystalline and polycrystalline quartz, chert, potassium and plagioclase feldspar, and limestone, metamorphic, and mudstone-sandstone grains best characterize Desmoinesian sandstones in the population of samples studied here. Mica and volcanic grains, however, are not important in differentiating sandstones.

Q-mode cluster and correspondence analysis indicate that lower Desmoinesian sandstones

(Krebs Group) are relatively homogeneous and rich in monocrystalline quartz, with rare rock fragments (petrofacies I and II). Basal Desmoinesian quartz-rich sandstones are restricted to eastern Oklahoma. Middle to upper Desmoinesian sandstones (Cabaniss and Marmaton Groups) are compositionally heterogeneous (petrofacies III and IV) and are widely distributed throughout the state. Desmoinesian sandstones exhibit a slight upward increase in compositional heterogeneity. Source areas include the craton, foreland blocks of the Ancestral Rocky Mountains, and the orogenic terranes of southern Oklahoma. The broad, north-trending, quartz-rich belt of the Desmoinesian coincides in part with the Nemaha trend and may have been derived from sandstone-rich beds within the Simpson Group.

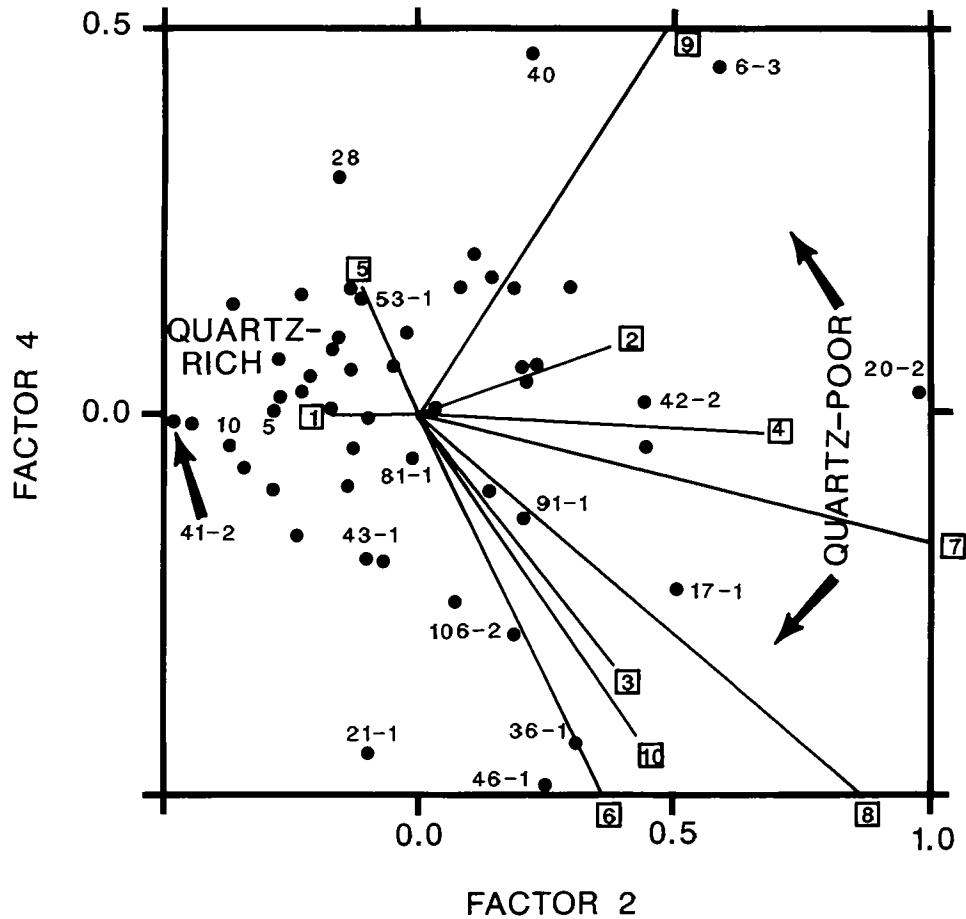


Figure 12. Correspondence-analysis factor-score map, factors 2 and 4. Variable numbers represent variable contribution in factor space. Refer to Figure 3 for sample location and identification. Variable numbers represented by lines on plot as follows: (1) monocrystalline quartz, (2) polycrystalline quartz, (3) chert, (4) plagioclase, (5) potassium feldspar, (6) mudstone-sandstone, (7) limestone, (8) volcanic, (9) metamorphic, (10) mica. Refer to Table 1 for factor loadings.

PALEOHYDROLOGY OF THE ANADARKO BASIN, CENTRAL UNITED STATES

DONALD G. JORGENSEN

U.S. Geological Survey, Lawrence, Kansas

Abstract.—Geohydrologic systems in the Anadarko basin in the central United States are controlled by topography, climate, geologic structures, and aquifer hydraulic properties, all of which are the result of past geologic and hydrologic processes, including tectonics and diagenesis.

From Late Cambrian through Middle Ordovician time, a generally transgressive but cyclic sea covered the area. The first deposits were permeable sand, followed by calcareous mud. During periods of sea transgression, burial diagenesis decreased porosity and permeability. During periods of sea recession, uplift diagenesis increased porosity and permeability, especially in exposed rocks. During most of Silurian and Devonian time, the sea receded; increased porosity and permeability resulted from uplift diagenesis. However, at the end of the Devonian and during the Early Mississippian, very slightly permeable clay, which now is a regional confining unit, was deposited in a mostly euxinic sea. Later during Mississippian time, calcareous muds, which became limestone, were deposited in and adjacent to the Anadarko basin and underwent burial diagenesis.

During Pennsylvanian time, rapid sedimentation accompanied rapid subsidence in the Anadarko basin. A geopressure zone probably resulted when sediments with little permeability trapped depositional water in Lower Pennsylvanian sands. Burial diagenesis included compaction and thermal alteration of deeply buried organic material, which released carbon dioxide, water, and hydrocarbons. By Middle Pennsylvanian time, the sea had submerged most of the central United States, including the Ozarks, as tectonic activity reached its maximum.

During Late Pennsylvanian and Early Permian time, the Ouachita uplift had been formed and was higher than the Ozarks. Uplift was accompanied by a regional upward tilt toward the Ouachita-Ozarks area; the sea receded westward, depositing large quantities of calcareous mud and clay, and precipitating evaporitic material in the restricted-circulation environment. By the end of Permian time, >20,000 ft of Pennsylvanian and Permian sediments had been deposited in the Anadarko basin. These thick sediments caused rapid and extreme burial diagenesis, including alteration of organic material. During Permian time in the Ozarks area, development of the Ozark Plateaus aquifer system commenced in the permeable Cambrian-Mississippian rocks near the St. Francois Mountains as the Pennsylvanian confining material was removed. Since Permian time, uplift diagenesis has been more active than burial diagenesis in the Anadarko basin. Synopsis of paleohydrologic interpretation indicates that Cambrian-Mississippian rocks in the Anadarko basin should be relatively impermeable, except for local secondary permeability, because rocks in the basin have undergone little uplift diagenesis.

INTRODUCTION

The purpose of this paper is to present information about the Anadarko basin gained from an investigation of paleohydrology. The paleohydrologic investigation provided information concerning hydraulic properties of rocks, water chemistry, and flow systems. The information also has implications about petroleum and epigenetic mineralization, but they are not the focus of this report.

The paleohydrologic approach is similar in many ways to a basin analysis, the most notable exception being that the geohydrologic flow system is bounded by hydrologic boundaries that are not necessarily basin boundaries. The paleohydrologic approach generally includes consideration of historical geology, with special emphasis

on plate tectonics, meteorology, and ground-water hydrology. Paleohydrologic investigations on a regional scale rely greatly on paleogeographic information. The interpretations of Bambach and others (1980) of "pre-Pangaea" and the interpretations of Dietz and Holden (1970) were used in interpreting the global paleogeography. Also, interpretations reported in various U.S. Geological Survey reports were relied upon for interpretations on a continental scale. Interpretations of depth of burial largely are based on thickness maps of lithostratigraphic units. Specifically, the reports on the Mississippian System (Craig and Varnes, 1979), Pennsylvanian System (McKee, Crosby, and others, 1975), Permian System (McKee, Oriel, and others, 1967b), Triassic System (McKee, Oriel, and others, 1959), and Jurassic System (McKee, Oriel, and others, 1956)

were relied upon heavily.

This paper presents some of the information obtained for the Central Midwest Regional Aquifer-System Analysis (CMRASA). CMRASA was one project of the national RASA program of the U.S. Geological Survey (Sun, 1986). Detailed information from the CMRASA is reported in the chapters (reports) of U.S. Geological Survey Professional Paper 1414, as well as in technical journals, proceedings of symposia, and numerous other reports. Detailed paleohydrologic information, including information on the Anadarko basin, and area-wide correlation of aquifers and formations are reported in Chapter B (Jorgensen and others, in press).

PALEOHYDROLOGY

The Anadarko basin lies within the stable interior of the North American continent. The basin is not in itself a distinct hydrologic system; however, its southern boundary is a hydrologic boundary of a hydrologic study area (CMRASA study area) that is considerably larger than the basin. The hydrologic study area and the basin are shown in Figure 1. The origin of the hydrologic flow systems will be discriminated by the paleohydrology.

Since Cambrian time, most of the study area has undergone relatively gentle deformation, involving upwarp and downwarp of the Earth's

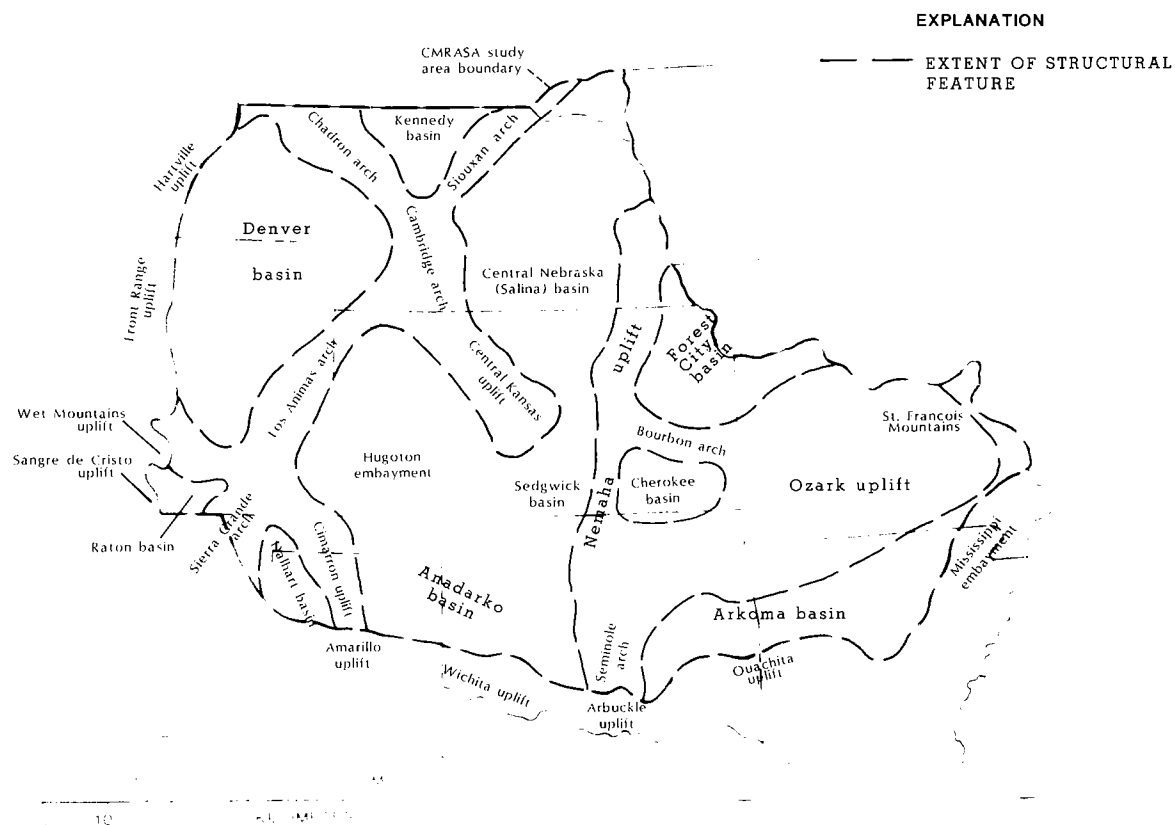


Figure 1. Major structural features of the central United States.

crust over large areas. Structurally, the study area has been dominated by broad basins and arches (Fig. 1). Accordingly, most folding of sedimentary rocks has been subtle, and few major fault zones of regional significance occur. However, along the south and west margins of the study area, strong crustal deformation by mountain-building forces has resulted in intense faulting along the Arbuckle, Wichita, and Amarillo uplifts, forming nearly impermeable boundaries (Fig. 2), because the water-bearing units were completely or almost completely offset. Faults along the west margin are also hydrologic boundaries at most locations, because the permeable layers have been offset. Most faults in the interior of the study area are not hydrologic boundaries, because permeable layers on each side of the fault are not completely offset.

Precambrian rocks, which underlie the strati-

graphic section of interest, consist mainly of igneous and metamorphic rocks of various types that together form a basement confining unit. Deep burial of these rocks at most locations has precluded detailed knowledge of their nature. The general nature and structure of the Precambrian rocks throughout most of the study area has been mapped by Sims (1985). Along the southern boundary in Oklahoma, the basement includes extrusive rhyolite or intrusive granite of Early to Middle Cambrian age (Ham and others, 1964).

Information concerning faults and fractures in the oldest rocks, such as the Precambrian, is of special importance, because they mark weak zones that were sometimes reactivated at various intervals during subsequent geologic time. Orientation of fractures, faults, and anticlines also indicates something about the direction of tectonic stresses.

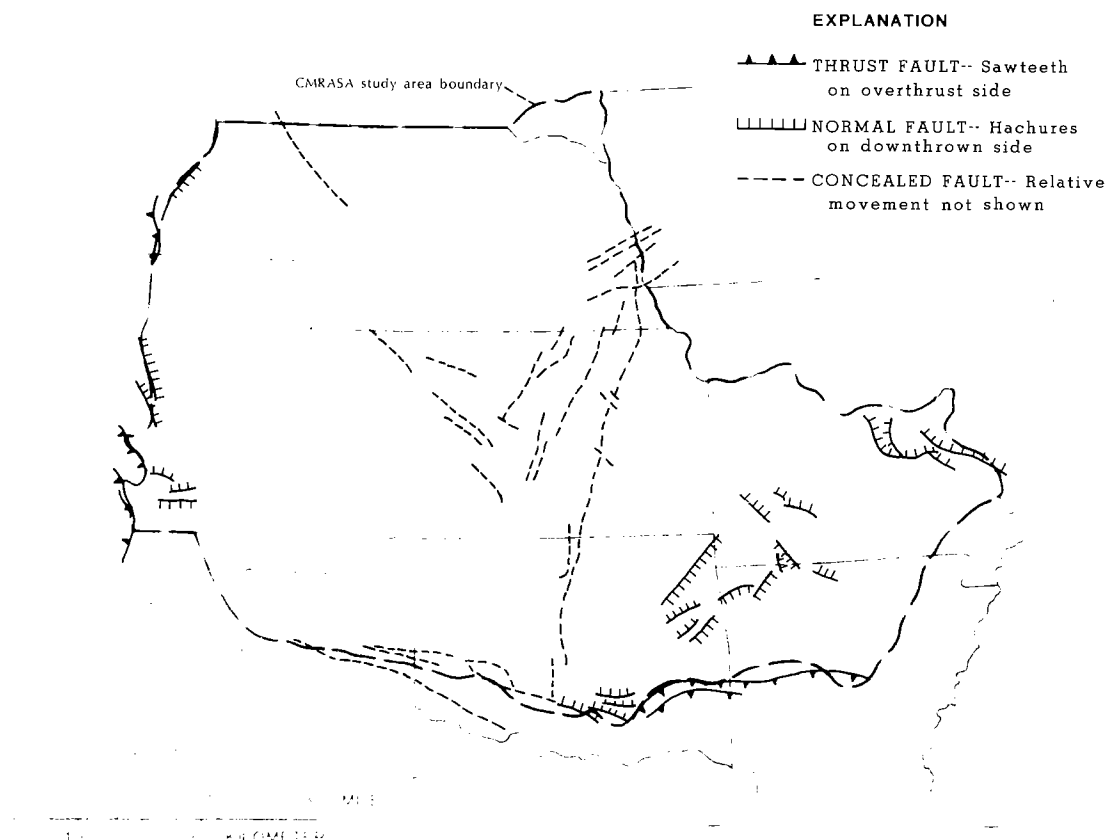


Figure 2. Major fault zones in the central United States.

Large Precambrian faults were oriented in the present NW-SE direction. The boundary between metamorphic and igneous Precambrian rocks in the region has the same alignment (Warner, 1980, p. 14); Warner further concluded that the central United States was moderately mobile during the Precambrian.

Dake (1930, p. 194) stated that the Ozark uplift during the Precambrian, formed a large landmass which consisted of rhyolite lava and ash, along with granite porphyry, and basic dikes. He further stated that the landmass, nearly 2,000 ft high, was deeply eroded and faulted by Cambrian time. Precambrian faulting was also reported by Bridge (1930, p. 135). The core of the St. Francois Mountains is an epizonal granite batholith emplaced 1,500 m.y. ago and is part of a broad, largely subsurface belt of silicic igneous rocks of similar age, which extends at least from Michigan

through Oklahoma (Sides, 1978, p. 2). Lineaments of the Precambrian rocks mapped by Hayes (1962) are aligned N. 50° W. and N. 65° E. El-Etr (1967, p. 1) reported that the greatest density of lineaments is associated with the St. Francois Mountains.

Yarger (1982, p. 179) concluded from magnetic evidence that in Kansas block faulting and possible dike intrusions, which are normally associated with continental rifting, exist along the central Midcontinent rift (also termed the North American geophysical anomaly). It is not known why the rift (Fig. 3), which is of rather limited width, did not further develop.

The ancestral Nemaha uplift is identified as a Precambrian structure. A Precambrian basin may have existed in southern Oklahoma. Recent seismic investigations imply that >20,000 ft of Precambrian sedimentary rocks underlie the Wichita

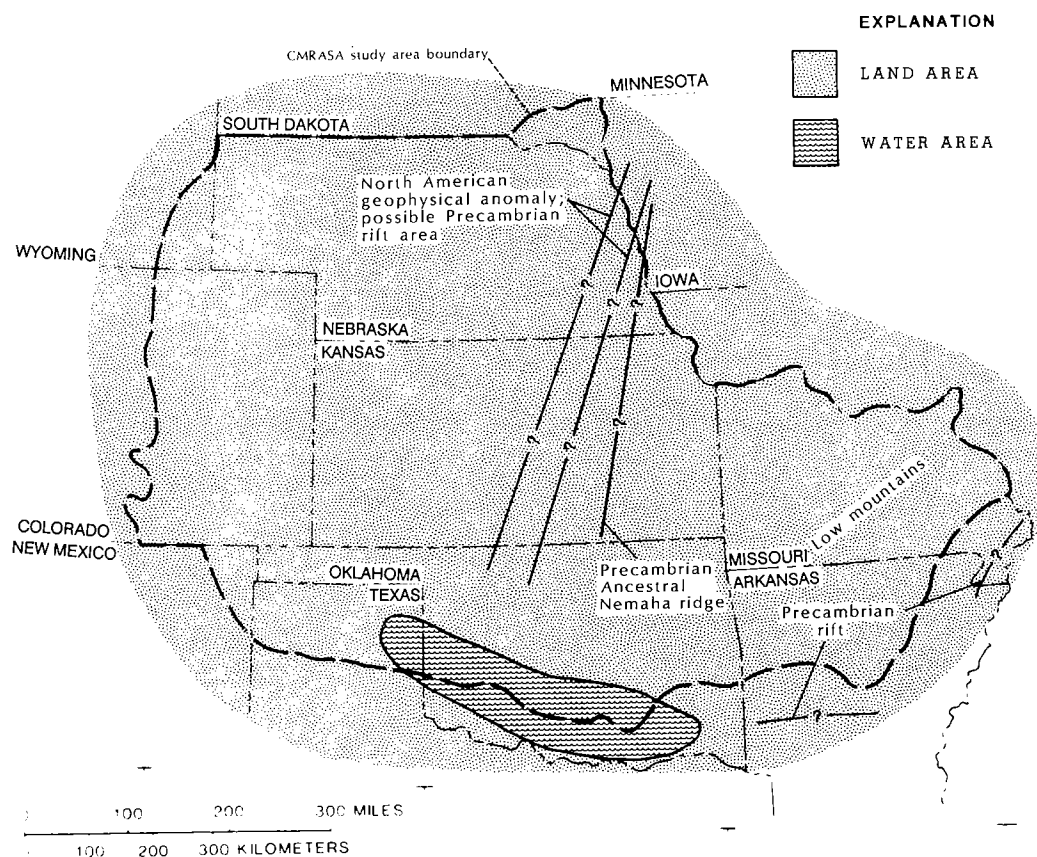


Figure 3. Early Cambrian features in the central United States.

Mountains (Brewer, 1982, fig. 26). Rifts along the present Arkoma basin and along the northern end of the Mississippi alluvial plain, which mark the subsurface Mississippi embayment, are believed to be late Precambrian (Houseknecht and Matthews, 1985; Schwalb, 1982). The faults and fractures in the indurated Precambrian rocks were paths for ground-water flow and limited dissolution. Fractures created anisotropic permeability. This alignment of faults, fractures, and other lineaments fluctuated somewhat during Paleozoic time, but the general trends of approximately N. 35° E. and N. 55° W. would persist.

The top of the basement surface represents a major unconformity (resulting from a long period of erosion or nondeposition). Permeable broken or weathered rock on the basement surface, sometimes termed "granite wash," forms a permeable zone at many locations.

From the beginning of Cambrian time through Middle Cambrian, the central United States was above sea level, Precambrian rocks were being eroded (Fig. 3), and no mountains existed. The climate was probably warm and wet. During the Late Cambrian, the area, except for the Transcontinental arch and small islands (Fig. 4), was inundated by a normal marine sea. The first deposits were permeable near-shore sands, parent material of the Lamotte and Reagan Sandstones. In some areas, calcareous muds were deposited along with the sands. Thickest sediments were deposited in a subsiding basin that extended from central Oklahoma through central Arkansas. Advances of the sea were interrupted by periods of sea recession. During the periods of sea recession, uplift diagenesis, including lithification of calcareous mud to limestone and sand to sandstone occurred. (Calcareous muds are typically

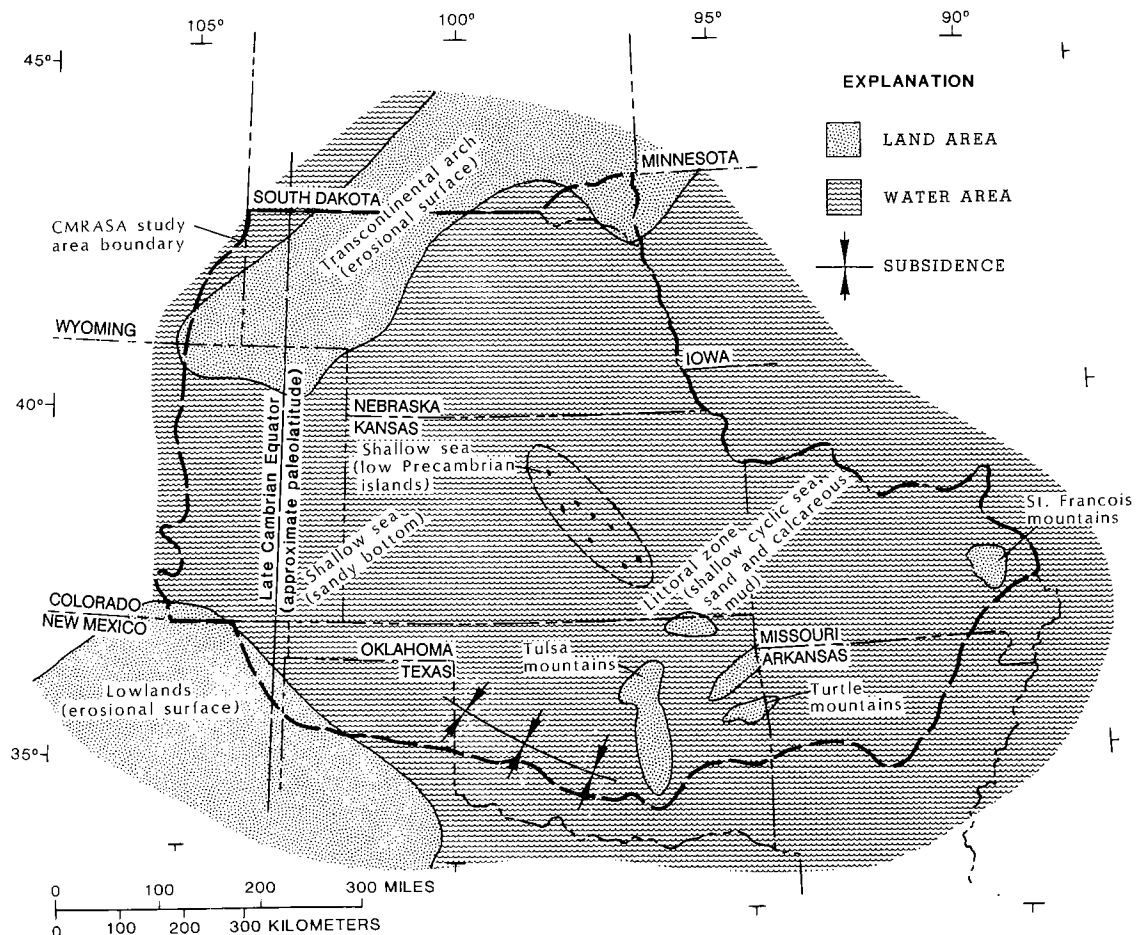


Figure 4. Late Cambrian features in the central United States.

lithified near shore above sea level or near shore below sea level.) Saline water deposited with the deposited sediments probably was flushed from the mantle of Cambrian and subjacent rocks during periods of sea recession. Erosion removed overburden load and caused extensional fracturing (fracturing resulting from relaxation of a principal stress). The fracturing created secondary porosity, but, more important, created permeable paths along which dissolution, especially of calcareous material, occurred. At some locations, especially near coastlines, rocks containing saline water were in contact with fresh ground water from the landmasses. At these locations, dissolution and dolomitization were likely (dolomitization is believed not to be atypical when fresh waters rich in magnesium and calcium mix with marine waters; these mixing zones typically are near shore).

During Ordovician time, the Oklahoma–Arkansas basin continued to subside, and the Ozark uplift began. Climate likely was warm and humid, because the area was near the Equator and no high mountains were near. Calcareous mud was the dominant shallow-water sediment. Sediment accumulated to thicknesses >6,000 ft, and burial diagenesis ensued in these areas. Compaction of the sediments squeezed water from the rock as primary porosity was reduced. Pressure dissolution and recrystallization in pore spaces occurred in consolidated rocks, especially carbonate rocks. At depths $\geq 5,000$ ft, assuming a normal geothermal gradient, thermal diagenesis of organic material and clay minerals at a slow to moderate rate could be expected. (Thermal diagenesis of organic material results in the production of CO_2 , water, and hydrocarbons. Thermal diagenesis of clay results in liberation of water, and alteration of smectite to illite. These processes collectively generate pressure and generally create fluids rich in CO_2 . The fluids, in turn, dissolve selected carbonate and silicious materials along their pathway, thus selectively increasing secondary porosity and permeability.)

Most Ordovician sediments adjacent to the Ozark uplift were near-shore calcareous muds, largely algal lime. As during Late Cambrian time, the sea was cyclic. Calcareous muds were lithified to limestone, especially during periods of sea recession, and dolomitization occurred near coastlines. Erosion removed sediments from the land area (Fig. 5) and decreased stress, which resulted in extensional fracturing, creating paths for dissolution of carbonate and other rock materials, especially by near-surface ground water of meteoric origin, near coastlines. Most processes greatly increased porosity and permeability.

Nearly the entire study area—except for southern Oklahoma, northern Arkansas, and the present Salina basin—was uplifted during the Silu-

rian and Devonian, and uplift diagenesis was dominant. Exposed rocks on the extensive warm and wet lowlands were severely eroded. Large quantities of pre-Silurian rock were removed, which resulted in unloading and extensional fracturing. Regional flow systems of ground water of meteoric origin developed, flushing formation waters from the Cambrian and Ordovician rocks. Near-surface dissolution of carbonate material greatly increased the permeability of the exposed rocks.

At the end of the Devonian or possibly during the very early Mississippian, the warm, transgressing equatorial sea probably submerged the area, exclusive of the Transcontinental arch. Subsidence and regional tilt occurred as the remnant ocean off Laurasia was being subducted below Gondwana. Sand was deposited near shore, and extensive clays were deposited offshore. The extensive and only slightly permeable clay layers restricted fluid flow from the underlying carbonate rocks to the overlying sediments.

The most important characteristic of the Mississippian Period was active tectonism that initiated large structural features, which henceforth were to affect geology and hydrology. These features include the Colorado–Wyoming uplift, Anadarko basin, Nemaha uplift (ridge), and Arkoma basin (Ouachita trough). Calcareous sediments were deposited in the shallow equatorial sea over the Upper Devonian and Lower Mississippian clay layers until Late Mississippian time.

Late Mississippian time was generally characterized by cyclic but dominantly recessive seas, and by the end of the Mississippian only the deeper parts of the Anadarko basin were submerged (Fig. 6). Thermal diagenesis continued in these basins. Elsewhere, lithification, erosion, fracturing, and dissolution occurred. Permeable karst topography developed in the uplifted areas of Colorado and the Ozarks.

Pennsylvanian climate was wet and warm because the area was astride the Equator. The Pennsylvanian sea was cyclic, but generally advancing, and by early Middle Pennsylvanian time it had covered the Ozarks. During Pennsylvanian time, large compressive stresses continued to develop, primarily N and S. The stresses developed as Laurasia and Gondwana continued to collide. These stresses were relieved by downwarping, faulting, and folding. The east-central part of the study area remained at or above sea level. Most uplifts—including the Front Range, Apishapa–Sierra Grande, Criner, Amarillo, Wichita, and Arbuckle—occurred in a wide, arcuate belt along the west and southern boundaries of the study area. Other uplifts included the Ouachita, Ozark, Nemaha, and Cambridge–Central Kansas (Figs. 7,8).

Subsidence was mostly in the Ouachita trough

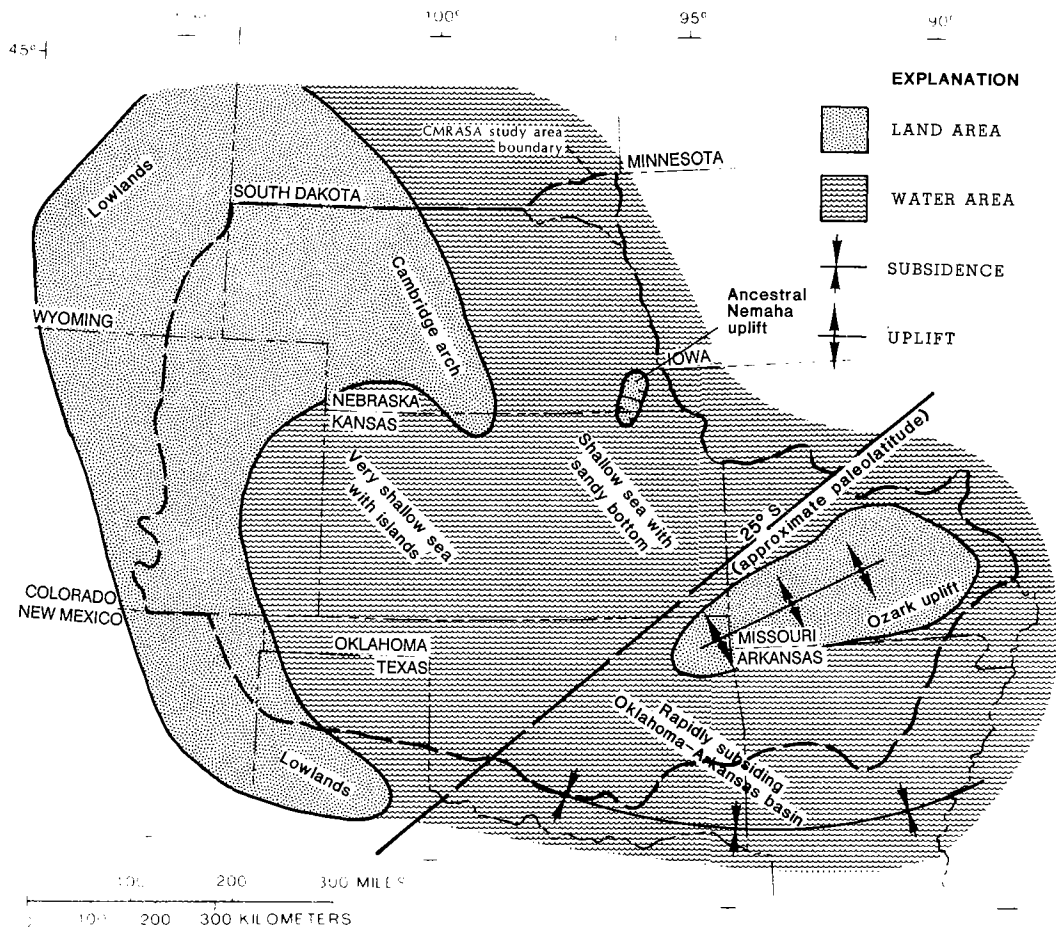


Figure 5. Middle Ordovician features in the central United States.

(Arkoma basin, a foreland basin) and the Anadarko basin (a shear basin). The Anadarko basin is similar to a foreland basin, and the Ouachita uplift is a collision feature associated with the Arkoma basin. Volcanism, which is typically associated with a subduction complex, is not known to be associated with the Ouachita uplift nor with the Amarillo, Wichita, and Arbuckle uplifts adjacent to the Anadarko basin. Modern prototypes of foreland basins have normal geothermal gradients. The geothermal gradient of a modern subduction complex not associated with volcanism is not known.

Most Pennsylvanian sediments associated with cyclic seas were clay, sand, and calcareous mud. In the eastern part of the study area, a large volume of organic material accumulated, especially during the Middle Pennsylvanian. Rapid sedimentation of clay and sand in the Anadarko ba-

sin likely trapped depositional water, creating a geopressure zone in the Lower Pennsylvanian sediments. Pre-Pennsylvanian rocks were buried to depth >10,000 ft, where thermal diagenesis would be rapid and nearly complete. The deep burial reduced primary porosity, but secondary porosity and permeability were increased in selected strata. Adjacent to the Front Range and the Amarillo-Wichita-Criner uplifts, permeable arkosic sediment was deposited in a band a few tens of miles wide. The arkose facies grades laterally to clay. Fresh ground water from the adjacent uplifts moved through the arkose deposits, but probably not into the adjacent deep-basin deposits. By the end of the Pennsylvanian, the Ouachita uplift had developed and was higher than the Ozarks, and the entire Ozarks-Ouachita area was above sea level (Fig. 8).

The Permian was a time of reduced tectonic

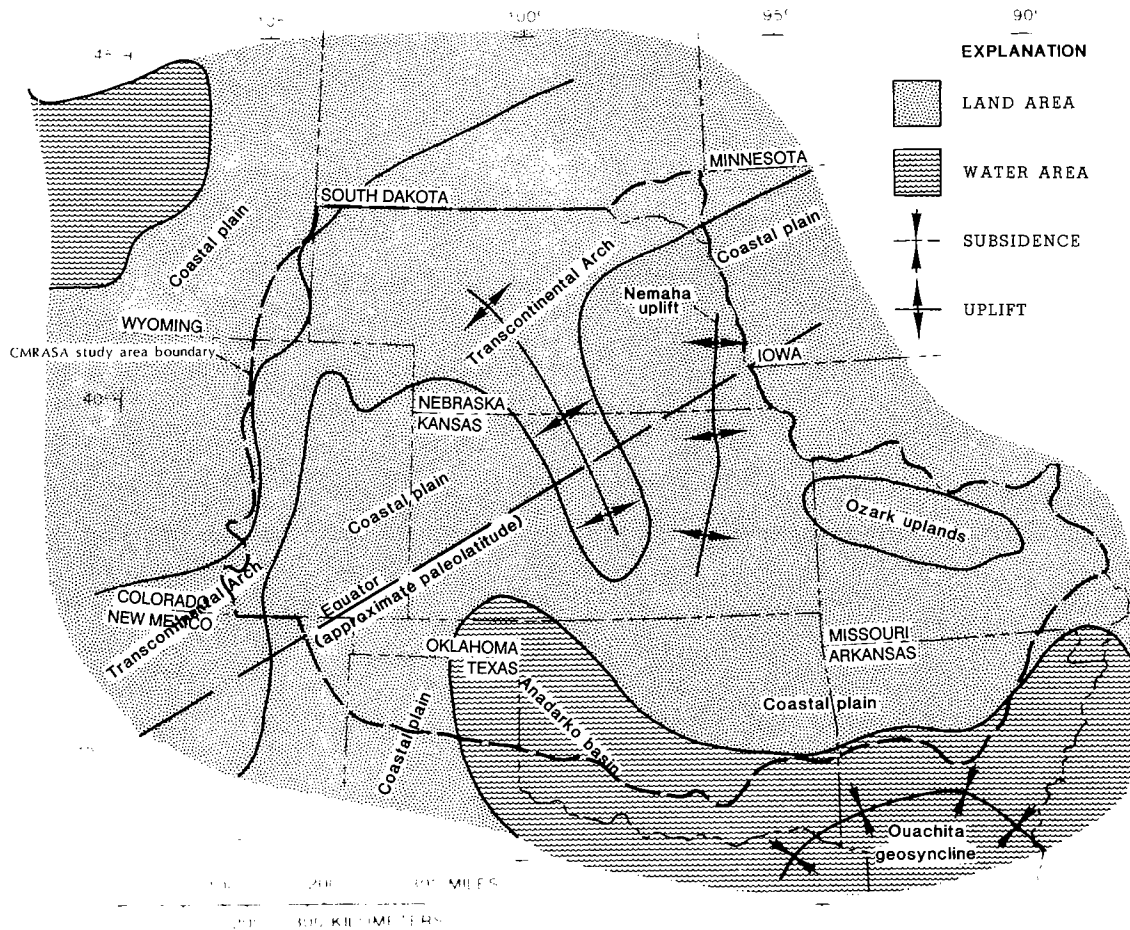


Figure 6. Latest Mississippian features in the central United States.

activity compared to the Pennsylvanian. The Early Permian sea, similar to the Late Pennsylvanian sea, was cyclic with alternate recessions and transgressions. During the Early Permian (Leonardian and earlier), regional tilting upward to the east, associated with the Ouachita and Appalachian orogeny, closed the seaway across the Ozarks. These mountains between Laurasia and Gondwana were high enough to disrupt the subtropical easterly winds, creating an intense rain shadow. The climate was dry and hot on the Laurasia side (central United States), and wet on the Gondwana side (eastern United States). The closing of the seaway restricted circulation and resulted in extensive evaporite precipitation over most of the central United States, except on the flanks of the Ozark and Ouachita uplifts. In addition to regional tilting, uplift of the Ozarks continued. Major fracturing of the pre-Pennsyl-

vanian carbonate rocks in the Ozark area occurred as the result of tensional stresses associated with uplift, and later by extension caused by erosional unloading. The Ouachita Mountains were eroding or subsiding at a very rapid rate and, by the end of Early Permian, little relief remained.

Tectonic activity in Colorado continued from Pennsylvanian into Permian time. Arkosic sediments continued to be deposited along the Front Range, Apishapa, and Sierra Grande uplifts. In Oklahoma, the Anadarko basin continued to subside, and the Wichita uplift continued. Detritus from the Wichita uplift was a dominant source of sediment in the subsiding Anadarko basin. Increase of pressure in the geopressure zone due to thermal pressuring with burial likely occurred.

The sea retreated to the west during the Late Permian, as the study area continued to be tilted

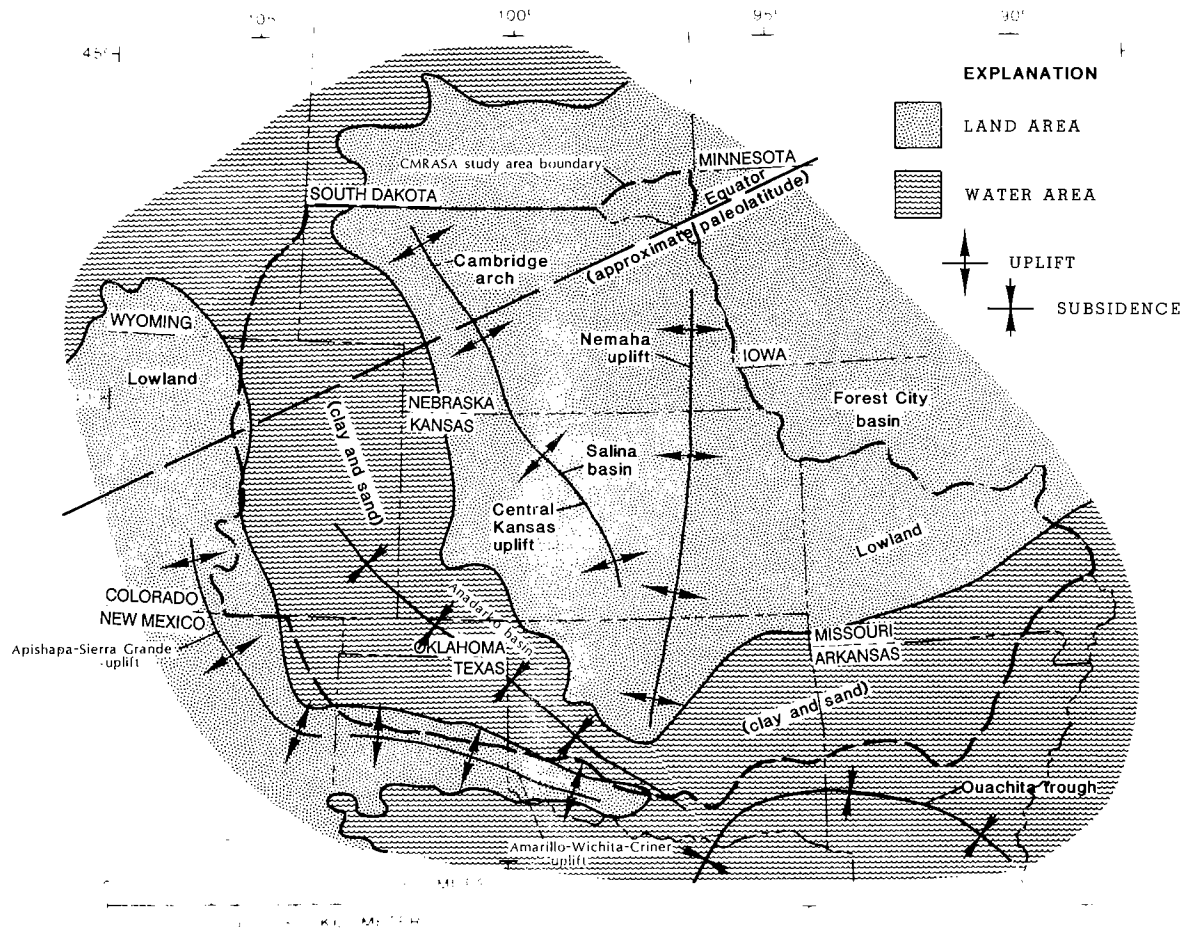


Figure 7. Early Pennsylvanian features in the central United States.

upward to the east. At the end of Permian time, >20,000 ft of Pennsylvanian and Permian sedimentary rocks—mostly shale, sandstone, limestone, and evaporites—had collected in the Anadarko basin. The sandstone layers are relatively permeable in comparison to the evaporite and shale layers. The areally extensive shale and evaporite layers restricted flow to and from the subjacent pre-Pennsylvanian rocks. It is not known whether the Pascola arch in southeastern Missouri and northwestern Tennessee, reported as a post-Early Permian uplift by Bethke (1986), was associated with the regional tilting of the Permian in the Ozarks area.

At the end of the Permian, confining units of Pennsylvanian shale around the St. Francois Mountains in the Ozarks area were being eroded. As the shale and other rocks were removed from the higher elevations, a regional flow system de-

veloped in the highly fractured and permeable rocks of Cambrian–Mississippian age. Permeability of the exposed carbonate rocks increased largely as the result of weathering and near-surface dissolution. The extent of the Ozarks flow system was controlled by topography and by the extent of the overlying confining shales.

Deposition during the Early Triassic occurred only in northwestern Colorado and western Nebraska. Red clay, calcareous mud, and dolomite were deposited in the sea with restricted circulation. As during the Late Permian, the central Colorado uplifts were being rapidly eroded, and sediments were deposited in the freshwater lake in the Dockum basin in southeastern Colorado and the Texas and Oklahoma Panhandles. It is probable that regional stress changed from compressive to tensional during Triassic time, a precursor to the movement of the North American

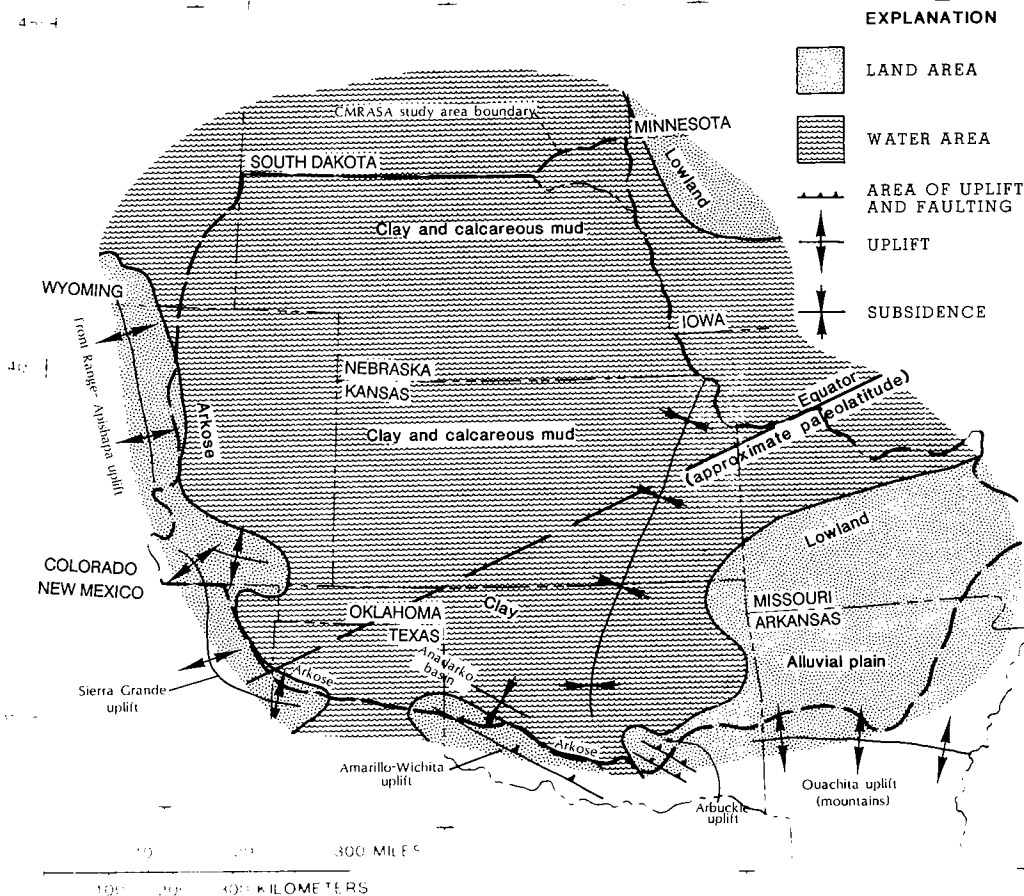


Figure 8. Late Pennsylvanian features in the central United States.

plate away from Pangaea. In general during the Triassic, land areas within the central United States area had little relief and were not significant source areas of sediment. The removal of the slightly and very slightly permeable Pennsylvanian and Permian rocks on the Ozark uplift increased the extent of the Ozarks flow system.

Most of the study area was above sea level during the Jurassic; however, the sea in which clay and sand were being deposited existed in the western part of the area. Subsidence along the Mississippi embayment was such that the Jurassic sea encroached into the new lowland. It is not known if subsidence in the Mississippi embayment was a product of the breakup of Pangaea. The Ozarks flow system continued to expand as it did during the Triassic. At the end of the Jurassic, the sea receded, and the entire study area was above sea level.

At the beginning of the Cretaceous, most of the study area was above sea level and undergoing erosion. The erosion was ended by a rapid transgression of the Cretaceous sea from both north and south. Moderately permeable, fine-grained sand and intercalated clay were deposited on alluvial plains or in near-shore estuaries by the advancing sea. As the sea continued to advance, clay replaced sand as the dominant sediment. This very slightly permeable clay, which today forms the Kiowa Shale and equivalents, restricted vertical flow to permeable sand below. Maximum extent of the Kiowa sea is unknown; however, it is likely that the sea covered the entire study area, with the exception of part of the Siouxan arch and Ozark uplift. Clay deposition was ended by a recession of the sea, which in part was the result of an Early Cretaceous regional uplift of the eastern part of the study area. The Pascola

uplift in the Bootheel area of Missouri may have been contemporaneous with the regional uplift.

A period of erosion ensued, which was interrupted by a second Early Cretaceous sea advance. Sediments of the initial transgression were permeable near-shore sand (parent material of the Dakota Sandstone), followed by clay. Maximum extent of the sea is not known, except that it extended beyond the present extent of the Dakota Sandstone and may have covered most of the western part of the study area. Burial diagenesis occurred from the late Early Cretaceous through most of the Late Cretaceous.

During most of Late Cretaceous time, clay was the dominant sediment. Maximum sedimentation was in the Denver basin, where 3,000–8,000 ft accumulated. The burial reduced primary porosity and permeability; however, thermal diagenesis may have selectively increased permeability locally in the buried Lower Cretaceous sandstones.

Near the end of the Cretaceous, the Laramide orogeny resulted in uplift in many areas, such as the Front Range. The Laramide orogeny, with NNE compression, was caused by the collision of the Farallon plate and the North American plate. Back-arc basins formed to the east of the Rocky Mountains (a collision arc). Thermal gradients exceeding normal were likely in the back-arc basins, such as the Denver basin, and thermal gradients $>3.5^{\circ}\text{F}/100\text{ ft}$ were likely in parts of the Front Range and Rocky Mountains. At the end of the Cretaceous, the sea receded northward, as the western part of the study area again was tilted upward.

The Laramide orogeny continued into Tertiary time, as evidenced by mountain-building in central Colorado and Wyoming. Extensive erosion of the uplifts resulted in deposition of widespread, thick, permeable alluvial material (parent material of the Ogallala Formation) on the plains. The deposition further enhanced burial diagenesis in the Denver and Anadarko basins and the western part of the study area. Except beneath the deeper part of the Anadarko and Denver basins, a west-to-east regional flow was started in the Lower Cretaceous sandstones and in the underlying Cambrian–Mississippian rocks, because the regional tilt was now downward to the east.

In the eastern part of the study area, erosion continued to remove Pennsylvanian and Permian rocks from the Ozarks, further extending the Ozarks flow system that was continuing to develop in the Cambrian–Mississippian rocks (Ozark Plateaus aquifer system).

With time, the Laramide mountain-building ended, and the rock stresses in the study area changed from compression to tension. Thereafter, erosion of alluvial materials on the plains exceeded deposition of detritus from the mountains. Thicknesses of the Tertiary material re-

moved may have exceeded 2,000 ft.

Unloading by the removal of eroded Cenozoic sediments over the Denver basin has resulted in the expansion of the rock mass and reduction of pore pressure; this ended outward movement of water in the basin, and initiated an inward movement of water toward the center of the basin as the pore pressure in the rocks was reduced (Ottman, 1984). In rocks having slight hydraulic conductivities, pore pressure became less than hydrostatic, and “underpressuring” resulted. Similarly, in the Anadarko basin, erosion of Cenozoic rocks has reduced pore pressure in the buried rocks. This may be the mechanism that has created subhydrostatic pressure in most Middle and Upper Pennsylvanian and Permian rocks over much of the central United States, including the Anadarko basin. The unloading reduced the extent of the geopressure zone.

At the end of Tertiary time, the sea retreated north to the Williston basin in North Dakota, and also south of the Ouachita folded area in Arkansas and southeastern Oklahoma. The Equator may have been located along a line from southern Texas to southern Florida. Extensive forests grew in the subtropical climate. Drainage patterns similar to the present ones were established, and organic material was abundant.

The Quaternary was marked by episodes of extensive glaciation interspersed with much warmer interglacial periods. Although glaciation directly affected only the northeast edge of the study area, climatic changes affected the entire study area. The advances and retreats of the glaciers were accompanied by a concomitant lowering and raising of sea level. The change in sea level directly affected near-surface water levels in rocks near shore, and also the base level of erosion. These changes altered pore pressure in the subsurface. The glaciers also altered regional topography and, in turn, direction of ground-water flow. Cyclic loading and unloading by the ice affected stress distribution and probably caused some additional fracturing of competent rocks. The unglaciated area within the area of study underwent erosion.

PRESENT GEOHYDROLOGIC SYSTEM

Regional aquifer systems and regional aquifers (Fig. 9) in the central United States are the Ozark Plateaus aquifer system, Western Interior Plains aquifer system, Great Plains aquifer system, and the High Plains aquifer.

The High Plains aquifer extends from South Dakota to north Texas and consists of the Ogallala Formation and hydrologically connected permeable Quaternary deposits. The present water-

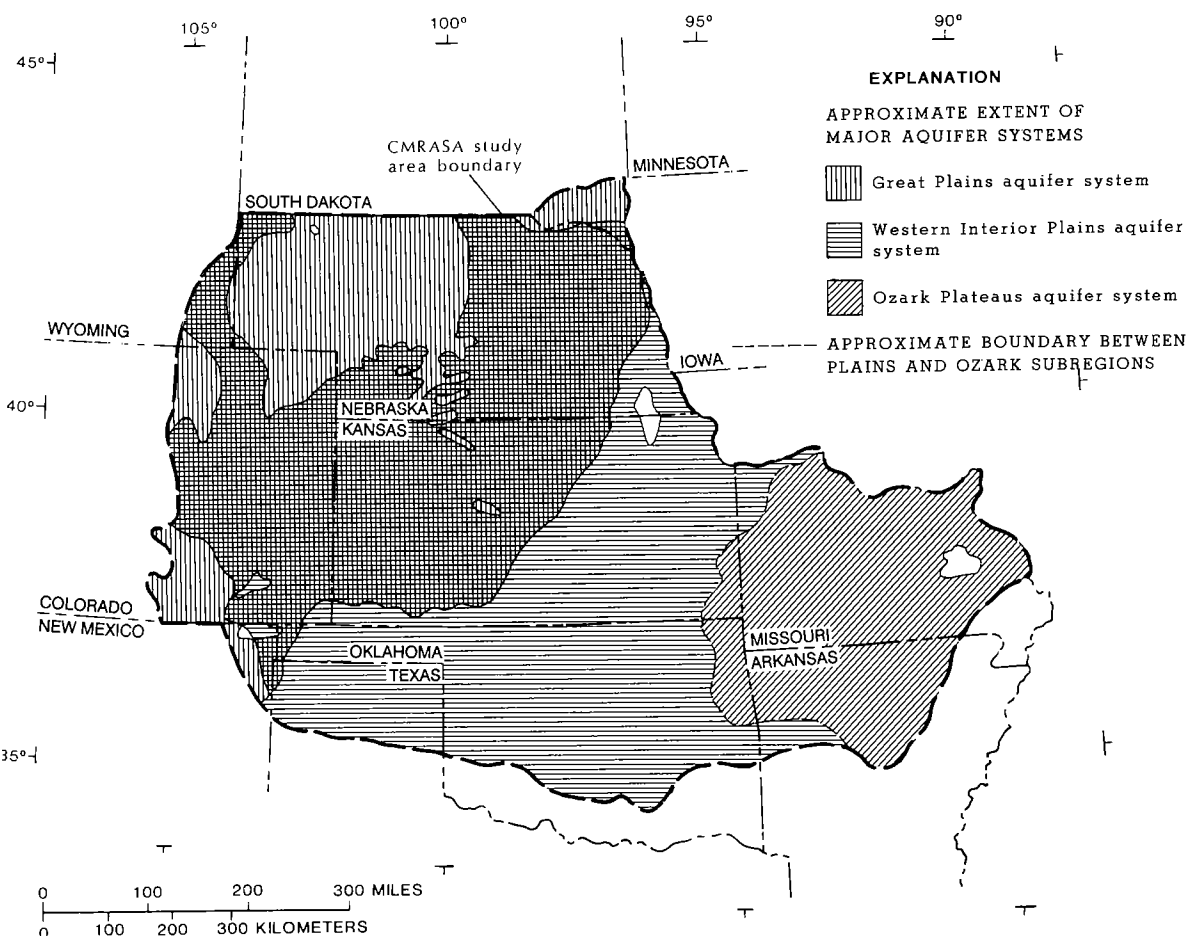


Figure 9. Extent of major aquifers.

bearing Ogallala Formation is an erosional remnant of a much more extensive Tertiary deposit. (Presently, thickness of the Ogallala ranges from near zero to 1,000 ft, 100–200 ft being typical.) The Ogallala is immediately underlain by Cretaceous and older rocks except in west-central Nebraska, where it overlies older undifferentiated Tertiary material (Weeks and Gutentag, 1981).

The Ozark Plateaus aquifer system, which is the important freshwater aquifer system of the Ozark Plateaus (termed Ozark subregion in Figure 10), consists of the St. Francois aquifer, the Ozark aquifer, the Springfield Plateau aquifer, and confining units.

In general, ground water in the Ozark subregion flows outward from high-water-table elevations associated with high land surface toward the Missouri River, Mississippi River, Mississippi embayment, and the broad lowland that is

roughly coincidental with the Central Lowland. The aquifer system is composed mostly of water-bearing dolostone, limestone, and sandstone of Cambrian Ordovician and Mississippian age. Because the area has experienced several episodes of uplift diagenesis and has been above sea level nearly continuously since Ordovician time, except during part of the Pennsylvanian, the rocks are well fractured and solutioned and have well-developed anisotropic permeability. The western extent of the flow system is partly controlled by the thickness of the eroded edge of the Pennsylvanian shales and limestones that form a confining system (Fig. 11). On the west, the Ozark Plateaus aquifer system grades into the transition zone, where water from the Ozark Plateaus aquifer system meets saline water of the Western Interior Plains aquifer system. The transition zone is approximately discriminated by the extent of

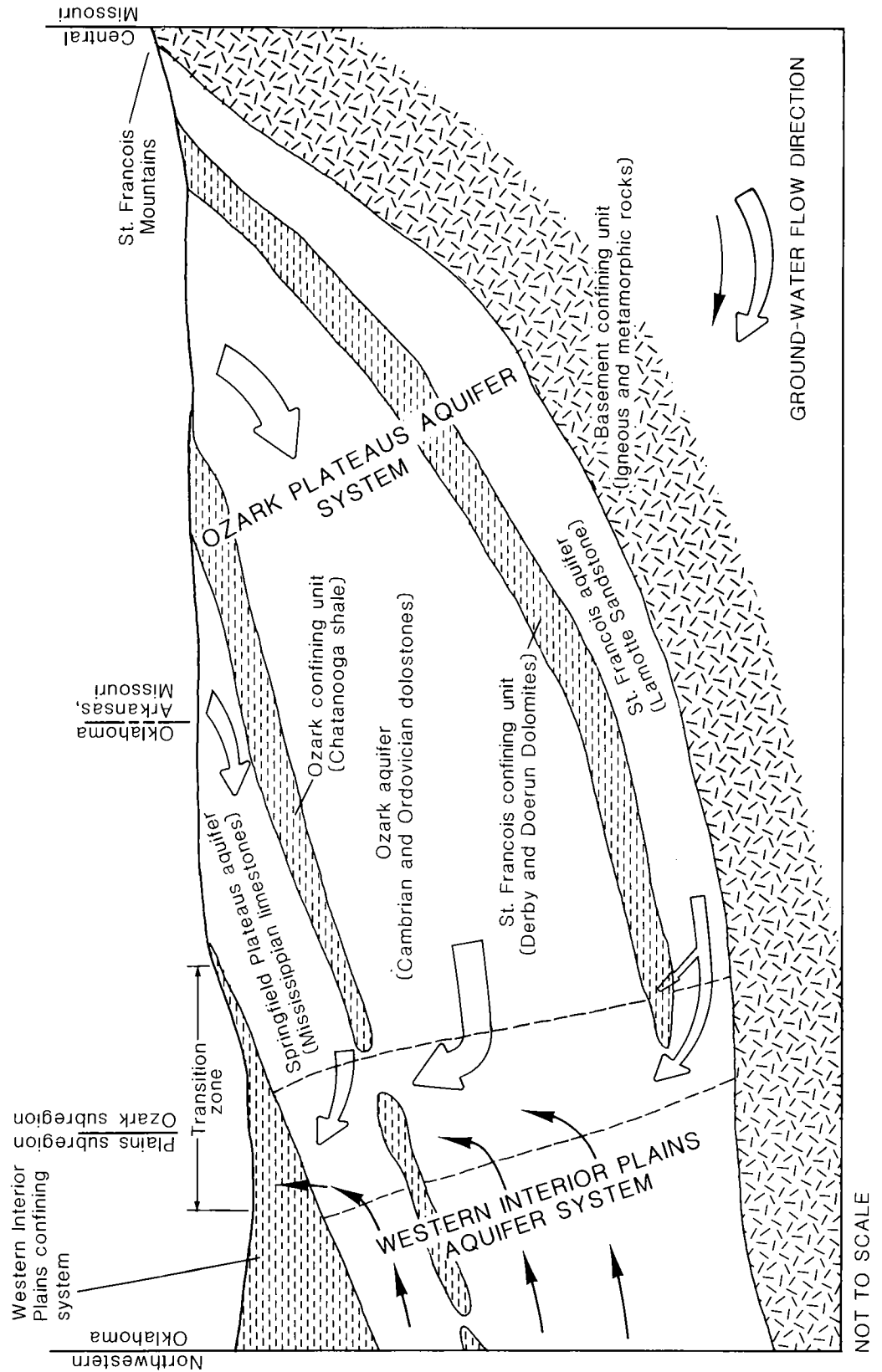


Figure 10. Aquifers in the transition zone.

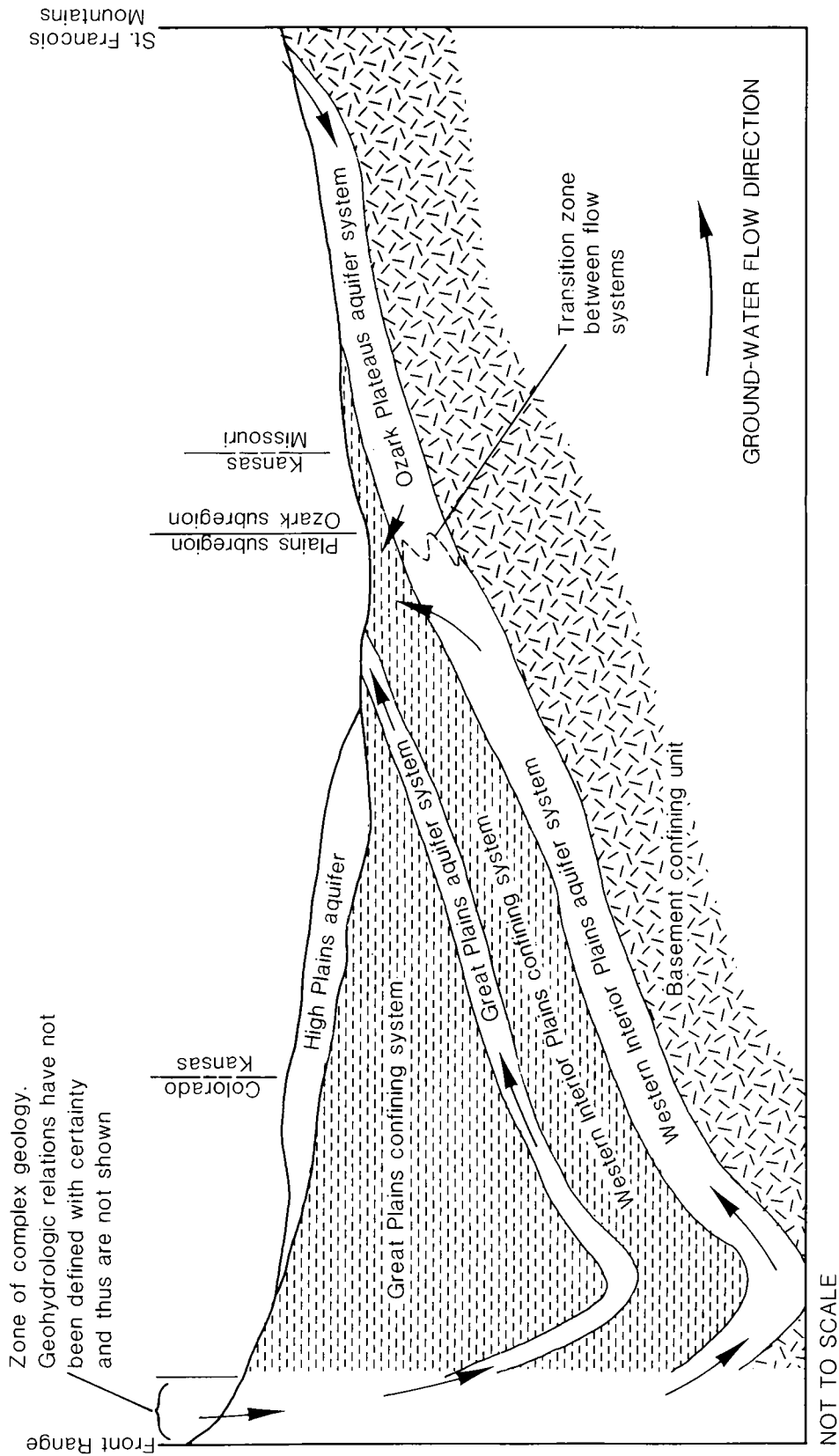


Figure 11. Major geohydrologic units in the Plains and Ozark subregions.

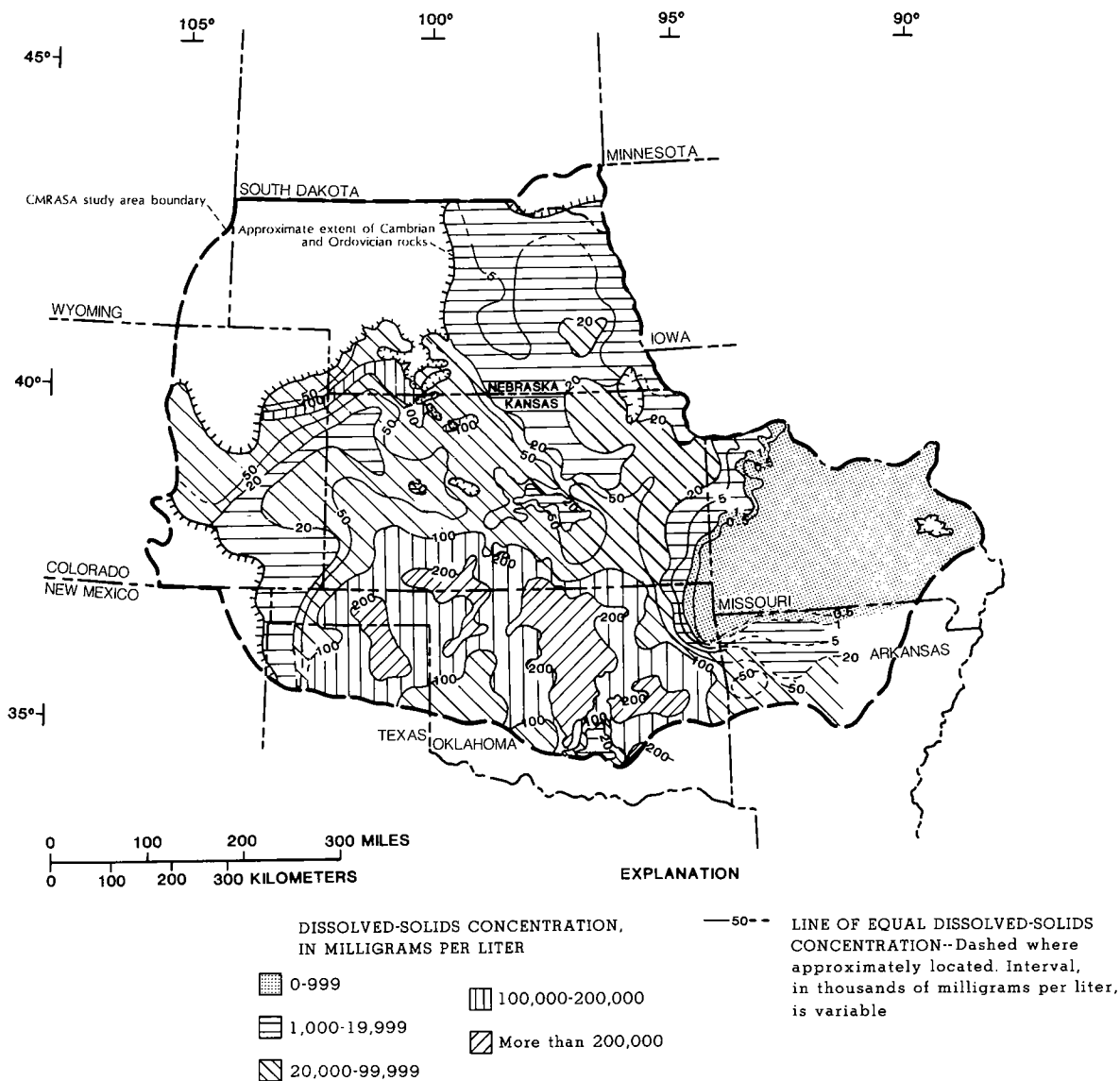


Figure 12. Dissolved-solids concentrations in water from Cambrian and Ordovician rocks.

the water that contains <1,000 mg/L dissolved solids (Fig. 12).

The Western Interior Plains aquifer system is located in the western part of the Interior Plains Physiographic Division, for which it is named. The aquifer system includes Cambrian-Mississippian dolostone, limestone, and sandstone. The aquifer system contains saline water and brines, several areas having dissolved-solids concentrations >200,000 mg/L (Fig. 12). Direction of water flow in the aquifer system mostly is topographically controlled, except in the Anadarko basin. In

general, flow is southeast from Nebraska and from the west across Colorado and Kansas toward the transition zone. Flow is very slow, especially in the Anadarko basin, where a trivial amount of water flows outward from the geopressure zone in the overlying Early Pennsylvanian sandstone and shales (Fig. 13; 4,000-ft closed contour in north Texas and western Oklahoma).

Permeability data for the Western Interior Plains aquifer system are scarce, because no water wells are available. The only data are from drill-stem tests conducted in oil and gas reser-



underwent uplift during most of the Silurian and Devonian. Area 5 is an area where the rocks have never been exposed since deposition and thus have experienced very little uplift diagenesis. Area 6, which includes the Anadarko and Arkoma basins, is similar to area 5, except that these areas have undergone extreme burial diagenesis. Continued presence of the geopressure to the present time is proof of very slight permeability of the deeply buried rocks of the Anadarko basin. (Signor and others, in preparation, report that model analysis of the aquifer systems of the central United States indicates that the relative distribution of permeability shown in Figure 14 is appropriate.)

The brines within the Western Interior Plains aquifer system are of unknown origin. They are not solely depositional water, because they exist in some areas that have at certain times been above

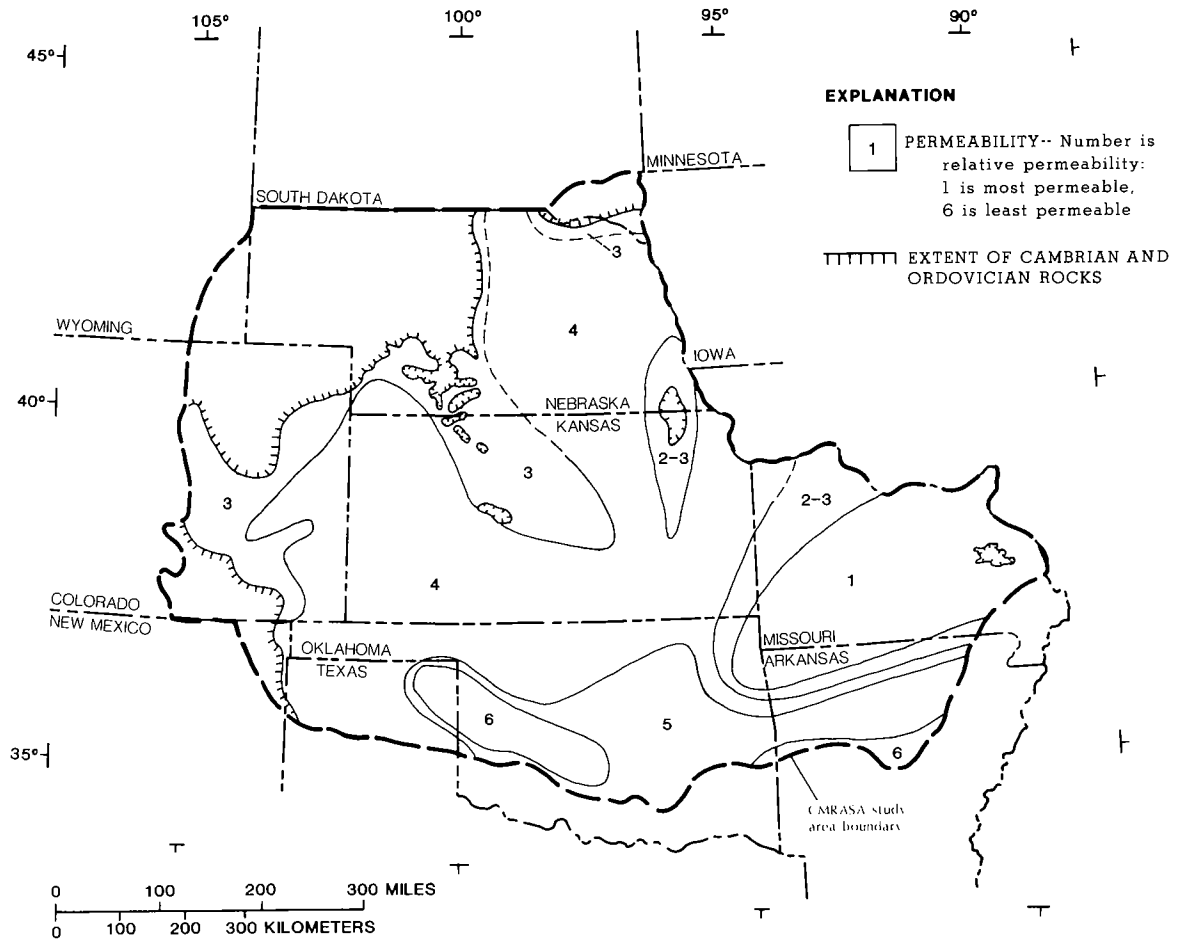


Figure 14. Relative permeability of Cambrian and Ordovician rocks.

sea level, as during the Devonian; thus, depositional water likely was flushed with fresh ground water. Other possible origins include a solution of dissolved evaporites, an evaporative brine, or a filtration brine. The present regional flow system (from west to east) has existed since the Laramide orogeny; thus, the brines are believed to be older than 65 m.y. For some time before the Permian, the flow direction was probably from east to west.

SUMMARY

This paleohydrologic analysis of the central United States, including the Anadarko basin, is an example of how the paleohydrologic approach can produce information about the extent of ground-water flow systems, the hydrologic

properties of their aquifers, and the chemistry of the contained water. The present geohydrologic system is controlled by topography, geologic structures, climate, and hydraulic properties. All of these conditions are the result of past hydrologic and geologic processes.

The hydrologic study area, which includes the Anadarko basin, is in the central United States. The area extends from the foothills of the Rocky Mountains in Colorado to the Missouri and Mississippi Rivers in eastern Nebraska and Missouri, and from South Dakota to the Ouachita, Arbuckle, and Wichita Mountains of Arkansas and Oklahoma.

From the end of the Precambrian to Late Cambrian time, the study area was above sea level, and an uneven erosional surface had developed. The crystalline rock was fractured by the resultant stresses from large compressive forces, and

NW-SE and NE-SW lineaments were formed. This alignment remained, with some deviation, throughout Paleozoic time.

From Late Cambrian through Middle Ordovician time, a transgressive but cyclic sea covered the area. The first deposits were mostly permeable sand, followed by slightly permeable, calcareous muds of aragonite and algal lime. During periods of uplift and/or sea-level recession, uplift diagenesis occurred, greatly increasing porosity and intrinsic permeability. (Uplift diagenesis, which includes erosion of exposed rocks, typically results in extensional fracturing, dissolution of minerals in rocks along fractures, and probable dolomitization of limestone near coasts where fresh ground water and saline water mix.)

During most of Silurian and Devonian time, most of the area was above sea level. Uplift diagenesis greatly increased the porosity and intrinsic permeability of the rocks. During the Late Devonian and Early Mississippian, a transgressive and euxinic sea covered most of the area, and very slightly permeable clay was deposited, subsequently restricting flow to and from the underlying rocks.

Calcareous mud, which was lithified to permeable limestone, was the dominant sediment during much of the Mississippian. Tectonic activity increased, as evidenced by uplifts, such as the Colorado-Wyoming and the Nemaha. Subsiding basins, such as the Arkoma and the Anadarko, received large quantities of sediment that covered the older rocks, causing burial diagenesis. (Processes of burial diagenesis typically include compaction, compression, thermal alteration of organic material, thermal alteration of clay, pressure dissolution at grain contacts, and recrystallization in pores.) In general, the burial diagenesis reduced primary porosity and permeability. However, CO₂-rich solutions, products of thermal alteration of organic material, affected increased secondary porosity and permeability by selective dissolution of carbonate minerals within the rock section.

Tectonic activity reached its maximum during Pennsylvanian time and decreased through the

Permian. Uplifts—which include the Front Range, Apishapa, Criner, Amarillo, Wichita, Arbuckle, Ozark, Nemaha, Cambridge-Central Kansas, and Ouachita—were active. The Arkoma and Anadarko basins continued to subside and received >20,000 ft of sediments at some locations. The dominant sediment was clay, with lesser amounts of calcareous mud, sand, and evaporites. During the Permian, a regional tilt upward to the east developed; the sea receded, and regional ground-water flow from east to west commenced over much of the area. In the Ozarks area, a small ground-water flow system developed around the St. Francois Mountains.

During Triassic and Jurassic time, the eastern part of the study area was above sea level, and uplift diagenesis was active. However, during the Early Cretaceous, a transgressive but cyclic sea deposited permeable sand and clay over the western and central parts of the study area. During the Late Cretaceous, clay was deposited in thick layers, and burial diagenesis prevailed over most of the area, including the Denver basin. At the end of the Cretaceous and into the Tertiary, major uplifts, such as the Front Range, occurred as part of the Laramide orogeny. Uplifts in the west accompanied the regional tilting of the study area downward to the east. Regional ground-water flow from west to east started in the Lower Cretaceous sandstone and in pre-Pennsylvanian rocks; this flow continues today. The ground-water flow system near the St. Francois Mountains, which started during the Permian, continued to expand as Pennsylvanian and Permian rocks were removed by erosion. Collation of geohydrologic information indicates that among Cambrian-Mississippian rocks in the central United States the rocks in the Ozark uplift are the most permeable, and that rocks on the Nemaha and Central Kansas uplifts are permeable. Rocks on the basin platforms are less permeable. Rocks in the Anadarko basin are the least permeable, because these rocks have experienced little or no uplift diagenesis since the deposition of the parent sediments.

MINERALOGIC AND TEXTURAL RELATIONS IN DEEPLY BURIED ROCKS OF THE SIMPSON GROUP (MIDDLE ORDOVICIAN)—IMPLICATIONS IN DIAGENESIS AND PETROLEUM GEOLOGY

RICHARD M. POLLASTRO

U.S. Geological Survey, Denver

Abstract.—The mineral composition and petrography of sandstones, shales, carbonates, and intermediate lithologies were determined on 112 core samples of the Middle Ordovician Simpson Group in the Sunray DX Parker No. 1 Mazur well, Grady County, Oklahoma. Core was recovered from present depths of about 15,900–17,200 ft and included all or parts of the Bromide, Tulip Creek, McLish, Oil Creek, and Joins Formations.

The bulk-rock mineral composition of Simpson Group rocks is diverse. The mean weighted composition of 50 sandstone samples is 66% quartz, 14% clay, and 18% carbonate, as determined by X-ray powder diffraction (XRD). Some sandstones from the Oil Creek and Tulip Creek Formations contain as much as 96% quartz. These quartz-rich sandstones were cemented early by silica. Feldspar averages 2%; some sandstones from the McLish Formation contain as much as 15% feldspar. Potassium feldspar is commonly more abundant than plagioclase; potassium feldspar overgrowths are found in some of the sandstones.

Most of the shales are clay-rich and quartz-poor, averaging about 85% clay minerals, 7% quartz, and 3% feldspar, by weight, as determined by XRD. Carbonate, fluorapatite, and pyrite are present in variable amounts. Such high clay/quartz ratios are not characteristic of shales and suggest that silica has been expelled by diagenetic processes during burial.

The main clay mineral in the Simpson Group at these depths is illite, although iron-rich chlorite is locally concentrated in sandstones. Illite typically makes up >90 wt. % of the clay minerals in sandstones and >95 wt. % of those in shale and carbonate. Total clay content, determined from XRD, correlates closely with total gamma-ray intensity from geophysical logs, because illite is the primary potassium-bearing phase in these deeply buried rocks. Therefore, the gamma-ray log is a good indicator of “shaliness” in potential Simpson reservoirs at similar depths.

Much of the carbonate was introduced into the sandstones during burial as calcite, dolomite, or ankerite cement. Early iron-free calcite is commonly replaced by iron-bearing calcite, dolomite, or ankerite. Sandstones and carbonate rocks also contain rhombic dolomite. Many of the dolomite rhombs contain overgrowths of ferroan dolomite or ankerite, as evidenced by staining. Ankerite cementation is later and less selective than earlier dolomite and commonly replaces earlier carbonate or silica cements. Dolomite commonly replaces detrital clay and calcite. Spatial and textural relations suggest that the conversion of smectite to illite contributed, in part, to the formation of dolomite and ankerite cements.

Scanning electron microscopy reveals that much of the diagenetic illite occurs as tabular fibers in pores or as pseudomorphic intergrowths after smectite. Most chlorite in sandstones is authigenic and occurs as a pore-lining cement or as a pseudomorphic replacement after kaolinite.

Secondary porosity, formed mainly from the dissolution of intergranular carbonate cements, is best developed in sandstones from the Oil Creek and Tulip Creek Formations.

INTRODUCTION

This study describes the mineralogy and textural character of deeply buried rocks of the Simpson Group sampled from core in the deep Anadarko basin, and discusses and illustrates how diagenesis has modified the original mineralogy and has determined, in part, the present mineral and textural relations. Although all lithologies were analyzed, this study focuses on the mineralogy and diagenesis of sandstones and shales, with a particular emphasis on the clay minerals in these rocks.

The diagenesis of sandstones, shales, and carbonates has received considerable interest during the past few decades. Of particular interest are studies that relate effects of diagenesis on reservoir quality and the source-rock potential of organic-rich rocks. Combined, these studies in mineralogy, petrography, and inorganic/organic diagenesis can aid in determining the timing of both the generation and migration of hydrocarbons (Scholle and Schluger, 1979; McDonald and Surdam, 1984; Gautier, 1986).

The mineralogy and texture of sedimentary rocks provide a physical and chemical history of

both depositional and diagenetic (post-depositional) environments. The initial mineralogy and texture of a potential reservoir rock have a strong influence on the rock's diagenetic history. Therefore, a good understanding of diagenetic history and porosity distribution requires reconstruction of the original detrital materials (Hayes, 1979). It has been well documented from case-history studies that potential reservoir rocks that have been deeply buried commonly undergo several cementation and dissolution events. Petrographic data reported by Weber (1987) indicate that although a large number of sandstone samples from the McLish Formation in the Mazur well are quartz arenites originally containing >95% detrital quartz by volume, they presently contain as much as 45% authigenic constituents.

Clay minerals can provide information on the geologic framework and diagenetic history of sedimentary rocks and basins. They can be used as compositional, directional, and distance indicators relative to source terrains (Carson and Arcaro, 1983), as well as environmental indicators during deposition and burial history (Weaver, 1979; Hower, 1981). In some cases, systematic changes in clay minerals of sedimentary rocks occurring with progressive burial depth in a basin can allow prediction of the thermal history for the basin and, therefore, the thermal history of hydrocarbon source beds (Hoffman and Hower, 1979; Weaver, 1979; Burtner and Warner, 1986; Pollastro and Scholle, 1986; Pollastro and Barker, 1986; Schoonmaker and others, 1986; Pollastro and Schmoker, 1988, this volume; Scotchman, 1987).

Potential hydrocarbon reservoirs in clastic rocks rarely escape the introduction of clay minerals during deposition and/or diagenesis. Identification of clays combined with recognition of the nature of occurrence can be extremely useful in the production and recovery of hydrocarbons (Almon and Davies, 1981). In addition, the use of borehole geophysical tools, particularly the natural gamma-ray log, has been useful in providing information on mineralogical relations and variations in sedimentary-rock reservoirs (Fertl and others, 1982; Fertl, 1984). However, interpretations of these logs are best made by direct comparison with laboratory measurements.

GEOLOGIC SETTING AND STRATIGRAPHY

The Anadarko basin of western Oklahoma, southwestern Kansas, and northern Texas Panhandle is one of the deepest Paleozoic basins in North America (Fig. 1). In the deepest part of the basin, sediments are ~40,000 ft thick. The Anadarko basin contains numerous productive intervals from both clastic and carbonate rocks.

Thick, dark shales of Devonian to Early Mississippian and Pennsylvanian age are the primary hydrocarbon source beds for these reservoirs (Adler, 1971).

The Anadarko basin is a markedly asymmetrical basin with its steep limb and axis adjacent to, and parallel with, the NW-trending Amarillo-Wichita uplift that borders the basin on the south; to the north were relatively stable shelf areas. The principal tectonic elements of the basin were formed during the Wichita orogeny from the late Morrowan through early Desmoinesian (Rascoe and Adler, 1983). As a result of concurrent growth and erosion of the Amarillo-Wichita Mountains from the Early Pennsylvanian to the Early Permian, pre-Pennsylvanian rocks were eroded, and the sediments were deposited in the basin as a terrigenous clastic wedge. The Arbuckle Mountains to the southeast were not formed until the Late Pennsylvanian. The thermal history of the Anadarko basin has been described in detail by Schmoker (1986).

The Simpson Group consists of five formations, as first proposed by Decker and Merritt (1931), including all rocks from the top of the Arbuckle Group to the base of the Viola Formation (Fig. 2). The five formations, in ascending stratigraphic order, are the Joins, Oil Creek, McLish, Tulip Creek, and Bromide Formations. The Simpson Group comprises sandstones, shales, and carbonates, most of which were deposited in relatively shallow marine environments (Longman, 1976; Lewis, 1982). Regional paleogeography and detailed lithofacies maps of the Simpson Group have been published by Schramm (1964).

METHODOLOGY

General

Approximately 120 samples of sandstone, shale, and carbonate were obtained from core of the Sunray DX Parker No. 1 Mazur well, Grady County, Oklahoma (sec. 1, T. 3 N., R. 5 W.). The cored intervals were recovered at a present depth range of about 15,900–17,200 ft, including parts or all of each of the five formations of the Simpson Group (Fig. 2).

The analytical approach was twofold. The first phase of the analysis involved the qualitative and quantitative X-ray powder diffraction (XRD) mineralogy of the bulk-rock and clay mineralogy of the <2- μ m fraction; the <0.25- μ m fraction was also examined for expandable clay phases. Most samples contained carbonate; therefore, to avoid flocculation during separation of the clay-size fractions, all carbonate was removed by acid dissolution.

The second phase of the analysis was to visually examine the rock and determine the textural,

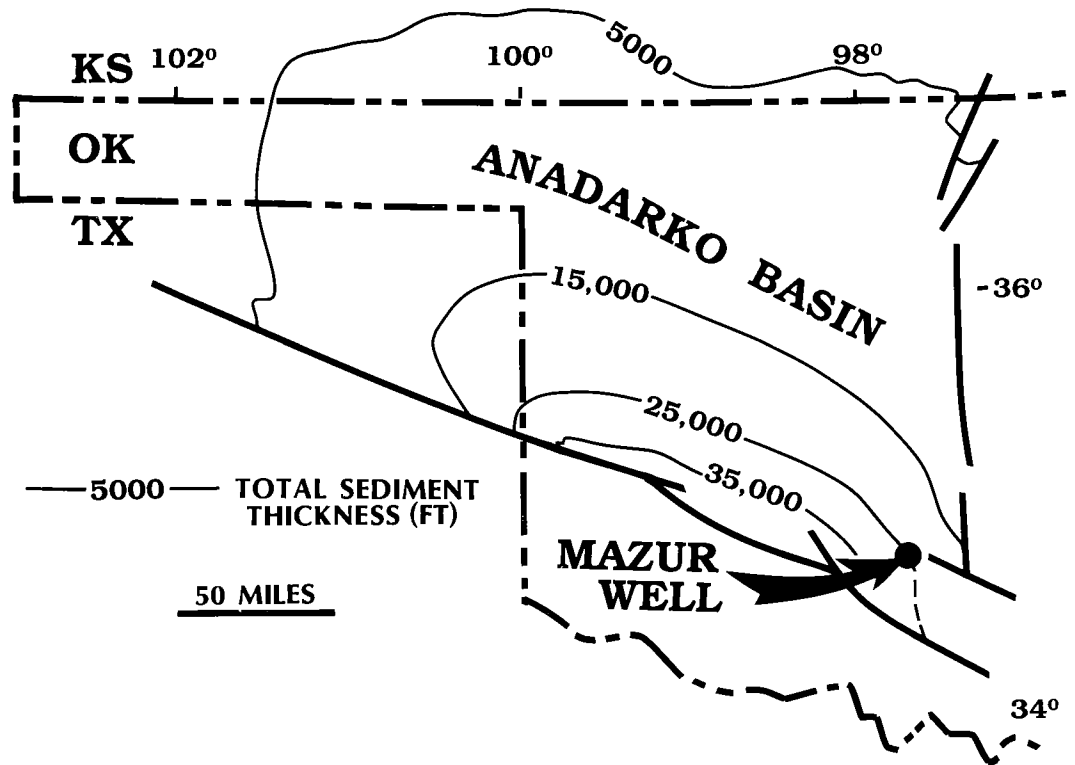


Figure 1. Map showing greater Anadarko basin, sediment thickness, and general location of Sunray DX Parker No. 1 Mazur well.

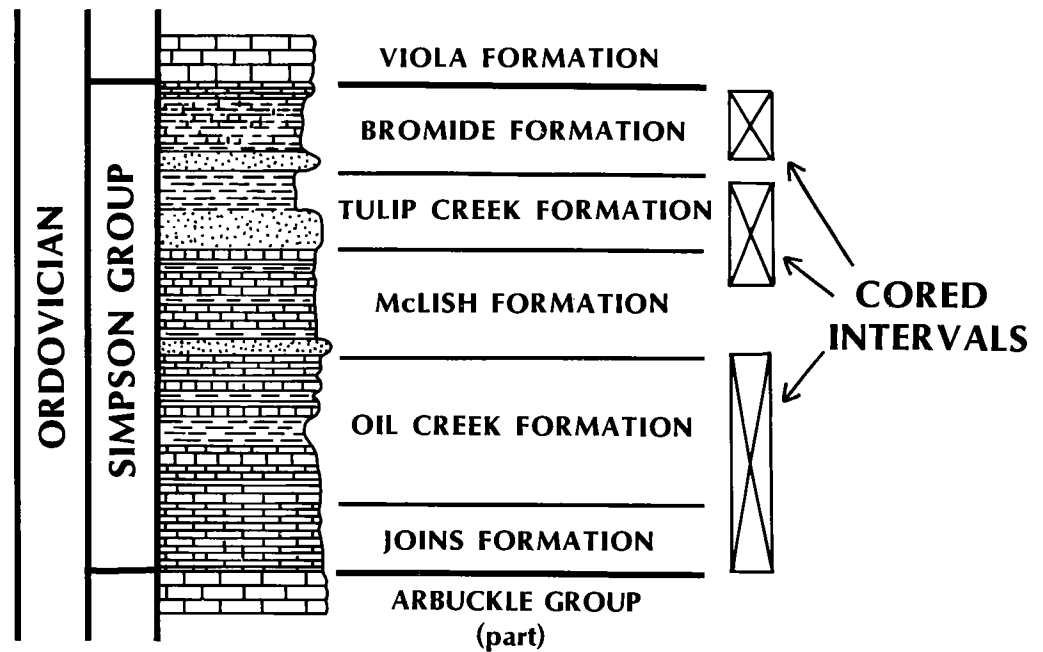


Figure 2. Stratigraphic section of Simpson Group rocks (modified from Johnson and others, 1984), showing cored intervals studied in the Sunray DX Parker No. 1 Mazur well.

diagenetic, and genetic relations through petrographic methods. This was done using thin sections and scanning electron microscopy (SEM).

Analytical

Plugs 1 in. (2.5 cm) in diameter were taken from cores for each lithology. Half of each plug was prepared for XRD analysis; the adjacent half was used for thin section and SEM.

Samples for XRD were washed and scrubbed to remove surficial contaminants, dried, and then ground to <35 mesh. Each sample was then split into two portions, using a Jones splitter, for (1) whole-rock XRD, and (2) carbonate dissolution and clay-mineral analysis. Carbonate was dissolved in 1N HCl, and the residue was filtered and washed immediately after effervescence stopped, so as to minimize solution of non-carbonate minerals (Pollastro, 1977). The insoluble residue was dried overnight at 65°C. The weight percent of the residue and/or carbonate was then determined. A small portion of the residue was spot-checked for undissolved carbonate with 6N HCl. For this study, carbonate rocks are defined as those containing 50 wt. % or more carbonate minerals. Similarly, quartz sandstones are defined as those samples containing 50% or more quartz, and shale as those containing 50% or more clay minerals, as determined from XRD.

Qualitative and semiquantitative estimates of the minerals in whole rock were made through XRD analysis of randomly oriented powders that were ground to a maximum grain size of 44 μm (<325 mesh), packed from the back side into aluminum specimen holders. A fine, random texture was imparted onto the surface to be irradiated, in order to further disrupt any preferred orientation created while mounting the sample (see Schultz, 1978). Semiquantitative weight percent values for total clay (phyllosilicates) and other minerals or mineral groups were calculated by comparison with several prepared mixtures of minerals with similar XRD characteristics by the procedures outlined by Schultz (1964) and Hoffman (1976), with those modifications described by Pollastro (1985). The semiquantitative relative weight percent values calculated for total carbonate minerals by XRD were then compared with those determined by chemical dissolution.

Oriented clay aggregates of the <2- μm and <0.25- μm (equivalent spherical diameter) fractions were prepared by a modified filter-membrane-peel technique (Pollastro, 1982) similar to that described by Drever (1973). Semiquantitative XRD analyses of the clay-size fractions were made by the method of Schultz (1964), with some modification (see Pollastro, 1985). Composition and ordering of interstratified illite/smectite (I/S) clay were determined on oriented, ethylene-glycol-saturated specimens of both the <2- μm and

<0.25- μm fractions, and by the methods of Reynolds and Hower (1970) and Reynolds (1980).

Thin sections were impregnated with blue epoxy to aid in recognizing porosity. Each section was then stained with potassium ferrocyanide and alizarin red, for the identification of carbonate phases (Dickson, 1966), and with potassium cobaltinitrite to distinguish potassium feldspars from plagioclase. SEM samples of freshly fractured rock chips were air-dusted, mounted on aluminum stubs, and coated with $\sim 100\text{\AA}$ of gold/palladium.

RESULTS AND DISCUSSION

Bulk-Rock Mineralogy

The bulk-rock composition for all samples analyzed is summarized in Figure 3; this ternary diagram for displaying mineralogical data from XRD is proposed here. The three end members of the diagram, quartz, total clay, and total carbonate, are the three major components in the studied rocks and represent here the pure end-member lithologies, quartz sandstone, shale, and carbonate, respectively. Figure 3 shows that the mineralogical composition of Simpson Group rocks from the Mazur well is diverse; these rocks range in composition from very pure end-member lithologies to "mixed" lithologies having intermediate compositions.

Table 1 lists the average and range in composition for shale and sandstone of the Simpson Group from the Mazur well. Again, the three basic components of these rocks are quartz, clay, and carbonate. Shales are unusually clay-rich and quartz-poor—particularly shales from the Bromide, Tulip Creek, and upper part of the McLish—to a present depth of 16,400 ft (interval 1 in Table 1). These shales average 84% clay, 7% quartz, <3% carbonate, $\sim 4\%$ feldspar, and 2% pyrite, by weight, as determined from XRD (Table 1). However, below this depth (interval 2), the Simpson Group shales are much richer in carbonate and quartz, averaging 62% clay, 15% quartz, and 13% carbonate; average feldspar and pyrite contents are about 6% and 4% respectively (Table 1).

No good mineralogical data were found in the literature for shallowly buried Paleozoic shales in the Anadarko basin; therefore, the Mazur core data are compared to the mineralogical data of Schultz and others (1980) for Upper Cretaceous shale and bentonite (Table 2). Although the data used for comparison are from the Upper Cretaceous Pierre Shale, it represents compositions derived mainly from freshly derived volcanic material. In contrast, a shale sourced mainly from reworked older rocks should typically contain more quartz and less clay.

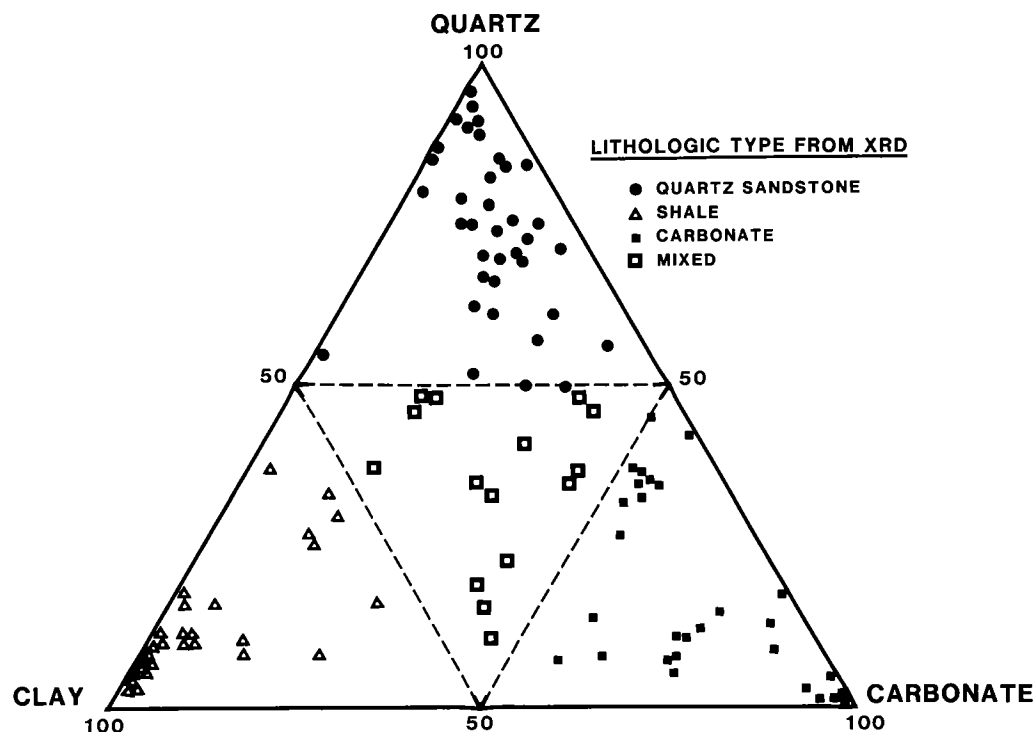


Figure 3. Ternary diagram showing mineral composition and lithologic type for samples of the Simpson Group in the Mazur well. Data in weight percent of bulk rock, determined by X-ray powder diffraction analysis.

Such high-clay and low-quartz values for the Simpson Group suggest that these shales are either products of altered volcanic ash falls, similar to the marine shale and bentonite of the Pierre Shale, or that the composition of Simpson shales has been modified under deep burial conditions (that is, a significant amount of silica has been removed or transferred from shales to adjacent lithologies). Similar high clay/quartz ratios are characteristic of bentonites or tonsteins (Schultz and others, 1980; Pollastro and Martinez, 1985; Precht and Pollastro, 1985; Pollastro and Pillmore, 1987). There is no evidence to support extensive volcanism as a source for most or all of the shales during Simpson deposition; therefore, it is suggested here that silica has been removed from these shales during deep burial diagenesis.

However, this interpretation introduces problems in balancing the silica budget in the adjacent sandstones or other lithologies analyzed. The question concerning silica budgets has also been addressed by Boles and Franks (1979a) and Houseknecht (1988), among others. Although there is no petrographic evidence for extensive late silica cementation in adjacent sandstones in the Mazur well, silica expelled from shales may

have been transported updip, providing a source for much earlier cements in shallow reservoirs. This interpretation has also been suggested by Houseknecht (1988) for sandstones of the Bromide and other formations.

The bulk XRD mineralogical composition of 50 sandstone samples from the Simpson Group in the Mazur well is also summarized in Table 1. Sandstones average 66% quartz, by weight, with some from the Oil Creek and Tulip Creek Formations containing as much as 96% quartz. All sandstone samples, other than a few nearly pure ones, contained appreciable clay and carbonate, averaging 14 and 18 wt. %, respectively. Feldspar content averages ~2 wt. %, and pyrite <1%. The bulk XRD data for samples from the McLish Formation are in close agreement with petrographic data reported by Weber (1987) from thin-section analysis.

Origin of Mineral Phases in Sandstones

The origin of the mineral components in the studied sandstones is summarized in Table 3, as interpreted from thin-section and SEM analyses. Many of the mineral components of the Simpson

TABLE 1.—RANGE AND MEAN COMPOSITION FOR 36 SAMPLES OF SHALE AND 50 SAMPLES OF SANDSTONE FROM THE PARKER NO. 1, SUNRAY DX MAZUR WELL, GRADY COUNTY, OKLAHOMA

	Shale				Sandstone	
	Interval 1 Range	Mean	Interval 2 Range	Mean	Range	Mean
Quartz	2-11	7	3-33	15	50-96	66
Clay	58-92	84	41-78	62	2-35	14
Carbonate	0-21	3	0-42	13	0-48	18
Feldspar	0-7	4	0-27	6	0-15	2
Pyrite	0-14	3	1-20	4	0-3	<1

Notes: Analysis determined by X-ray powder diffraction, expressed in weight percent of bulk rock. Shale interval 1 refers to Bromide, Tulip Creek, and upper McLish Formations to core depth of 16,400 ft; interval 2 includes Simpson Group shales sampled between 16,400 and 17,400 ft.

TABLE 2.—AVERAGE MINERALOGIC COMPOSITION OF SIMPSON GROUP SHALES FROM THE MAZUR WELL (DETERMINED BY XRD) VERSUS THAT OF TYPICAL SHALE AND BENTONITE BEDS. VALUES IN WEIGHT PERCENT OF BULK ROCK.

	Simpson Group shales (Mazur well)	Typical shale* marine	Typical shale* nonmarine	Typical bentonite bed**
Quartz	11	22	25	2
Clay	74	68	61	83
Carbonate	7	2	7	3
Feldspar	4	5	7	4
Other	3	3	minor	minor

*Data from Schultz and others (1980) for 366 samples of "ordinary shale" of the Pierre Shale and equivalent rocks.

**Data from Schultz and others (1980) for 119 samples of marine bentonite of the Pierre Shale and equivalent rocks.

Group shales and carbonates from the Mazur well have origins similar to those described for the sandstones.

General interpretations of the origin of the mineral phases in the sandstones, as listed in Table 3, are as follows: quartz occurs as detrital framework grains and syntaxial quartz-overgrowth cement; calcite occurs both as detrital limestone fragments and as authigenic cement; dolomite, ferroan dolomite, and ankerite are present as authigenic cements and/or replacement phases; clay minerals (illite and chlorite) are detrital as clay matrix or clay clasts in sandstones and as authigenic cements or replacement phases; detrital potassium feldspar grains occasionally have syntaxial overgrowths (Fig. 4A); plagioclase was observed only as detrital framework grains; phosphate minerals occur as detrital collophane

TABLE 3.—MINERALS PRESENT IN SANDSTONES OF THE SIMPSON GROUP FROM THE MAZUR WELL, AND THEIR INTERPRETED ORIGIN(S)

Mineral phase	Detrital	Diagenetic
Quartz	Yes	Yes
Calcite	Yes	Yes
Dolomite	?	Yes
Ankerite	No	Yes
Illite	Yes	Yes
Chlorite	Some	Yes
Kaolinite	?	Yes
Potassium feldspar	Yes	Yes
Plagioclase	Yes	No
Phosphate	Collophane	Fluorapatite
Pyrite	No	Yes

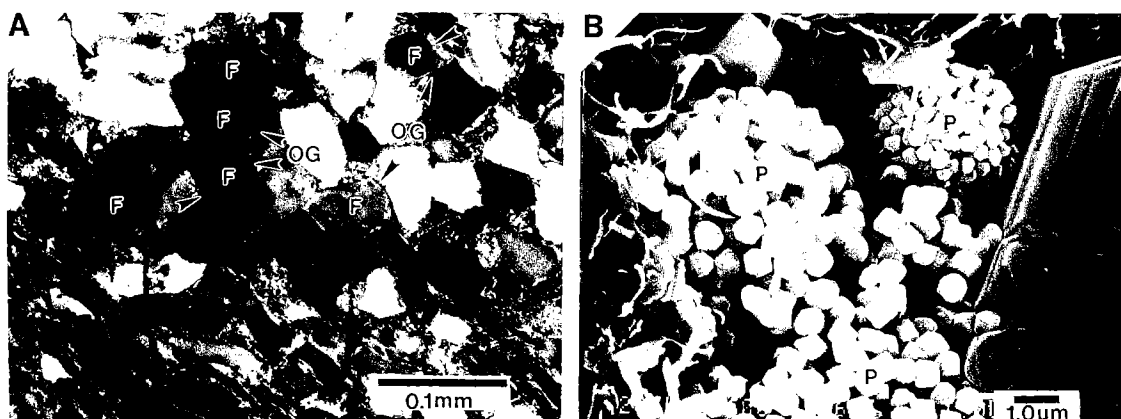


Figure 4. A—Thin section photomicrograph of sandstone from McLish Formation showing detrital potassium feldspar (F) grains with overgrowth (OG) cement. B—Scanning electron micrograph of framboidal pyrite (P) and other authigenic minerals in pore of sandstone.

fossil fragments, but some amorphous collophane is diagenetically aggraded to crystalline fluorapatite. Finally, early framboidal pyrite (Fig. 4B) and late octahedral pyrite are common diagenetic phases in all lithologies. These relations and observations will be demonstrated from photomicrographs in a later section.

Clay Mineralogy

General Composition

The clay mineralogy of sandstones and shales from the Mazur well is summarized in Table 4. Carbonate rocks have a clay-mineral assemblage similar to that of shales. The dominant clay mineral in the Simpson Group at these depths is illite, with local concentrations of iron-rich chlorite in sandstones. Trace amounts of kaolinite were found in few shale samples above 16,000 ft; there was a distinct absence of kaolinite in all other samples. Illite is defined here as both a discrete 10Å phase and an apparent regularly interstratified I/S phase from XRD profiles after glycol saturation (Fig. 5). Following the concept of fundamental particles and interparticle diffraction (Nadeau and others, 1984a,b,1985), ordered I/S is defined here as "thin" illite crystals 20–50Å in thickness. All I/S in rocks of the Simpson Group from the Mazur well was ordered ($R > 1$), as defined by XRD profiles; therefore, all I/S clay was calculated as illite.

The mean clay-mineral composition of Simpson Group shale and carbonate rocks from the Mazur well is 96 relative weight percent illite and 4% chlorite, as determined by XRD (Table 4). Little chlorite is present in shales, perhaps representing a detrital signal; shales containing higher concentrations of chlorite (as much as 11%) were

sampled adjacent to sandstones containing abundant authigenic chlorite.

Sandstones average 85% illite and 15% chlorite. However, local concentrations of iron-rich chlorite in sandstones may account for as much as 82% of the clay minerals. In contrast, many sandstones contain no chlorite. Illite and chlorite are interpreted here as both detrital and authigenic components of sandstones, as will be further discussed in the following section.

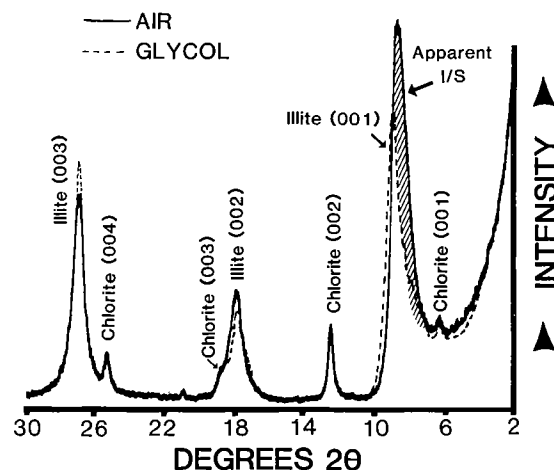


Figure 5. Typical X-ray powder diffraction profiles of oriented, <2-µm fraction of Simpson Group rocks from Mazur well, showing discrete illite, chlorite, and apparent mixed-layer illite/smectite (I/S) basal (001) reflections. Apparent I/S defined by diagonal pattern. CuK-alpha radiation.

TABLE 4.—AVERAGE CLAY-MINERAL COMPOSITION AND RANGE FOR 62 SAMPLES OF SHALE AND CARBONATE AND 50 SAMPLES OF SANDSTONE FROM THE SIMPSON GROUP IN THE MAZUR WELL. VALUES IN RELATIVE WEIGHT PERCENT OF CLAY MINERALS FROM <2- μ M FRACTION

	Shale and Carbonate Mean	Range	Sandstone Mean	Range
Illite (Illite + I/S)	96	88–100	85	18–100
Iron chlorite	4	0– 11	15	0– 82
Kaolinite	trace	—	trace	—

Note: I/S = ordered illite/smectite.

al Diagenesis

The present clay mineralogy of the Simpson Group in the Mazur well is largely a result of deep burial diagenesis and is consistent with an assemblage wherein burial temperatures exceeded 150°C (Hoffman and Hower, 1979), as evidenced by XRD and SEM analyses. The major clay-mineral reaction that occurs during the progressive burial of sedimentary rocks is the conversion of smectite to illite (Hower, 1981). This reaction has been illustrated by Pollastro (1985, p. 273, fig. 8). I will refer to the smectite-to-illite reaction throughout the remaining portions of this paper and discuss how this reaction may have played a role in influencing the present mineral composition of the rocks studied.

Smectite, contained in the sediments or rocks at near-surface or shallow-burial conditions, is converted to illite under increased temperature and pressure due to burial depth (Hower and others, 1976). Boles and Franks (1979a) and Pollastro (1983, 1985) proposed that the reaction involves the dissolution of smectite, conserving aluminum and potassium, and the precipitation of illite. Calcium, silica, iron, and magnesium are released from smectite in the reaction. These authors suggested that these elemental reaction products combine to form, at least in part, authigenic mineral phases in pores or fractures of deeply buried rocks. Typical phases that may form include dolomite, fine-grained quartz or quartz-overgrowth cement, chlorite, and illite cement or overgrowths (Boles and Franks, 1979a; McHargue and Price, 1982; Pollastro, 1985). However, in open systems, these elements may leave the system completely and not necessarily result in immediate authigenic minerals.

XRD profiles interpreted in accordance with the interparticle diffraction concept indicate that no true smectite is present in the Simpson Group

rocks from the Mazur well. Morphological evidence from SEM observations suggests that earlier smectite-bearing clay present in these rocks has been converted to illite. This is evidenced by textures similar to those described by Pollastro (1985) from SEM analysis, where intergrowths and overgrowths of tabular fibers of illite are superimposed within or on a honeycomb or "cornflake" morphology. Such textures suggest that an earlier smectite-rich clay was recrystallized during diagenesis and converted to a present illite composition.

Sandstones from the Mazur well commonly contain authigenic illitic clay cements. Many of these cements were precipitated as illite late in the burial history. However, some of the cement was probably once smectitic and later converted to illite under relatively deep burial conditions. Figure 6A shows a scanning electron micrograph of a clay cement in a sandstone of the Bromide Formation at ~16,000 ft. The overall texture of the clay cement is a honeycomb or "cornflake" morphology. Such a morphology is typical of smectite. High magnification SEM images of the cement (Fig. 6B) show that the honeycombs or cornflake-like platelets have a finer intergrowth fabric of interwoven tabular fibers that is characteristic of illite. It is proposed here that illite is a pseudomorphic intergrowth after smectite. In addition, superimposed on the edges of the honeycombs are subsequent overgrowths of tabular illite fibers (Fig. 6A,B).

Similar textures were observed in shales of the Simpson Group from the Mazur well. The scanning electron micrograph of Figure 6C shows an overall fabric typical of shale where detrital clay particles are oriented parallel to bedding. Closer examination of these particles reveals that the clay particles also have a finer intergrowth texture consisting of tabular fibers (Fig. 6D), sug-

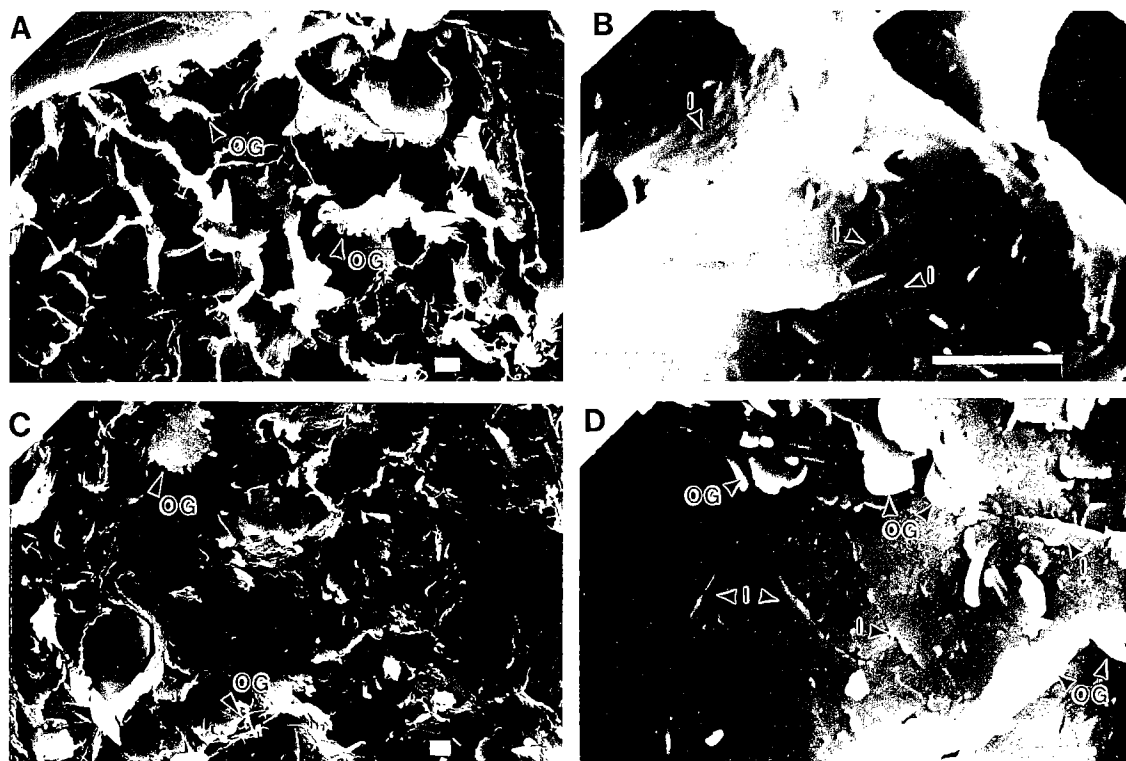


Figure 6. Scanning electron micrographs. *A*—Illitic cement with “cornflake” habit and illite overgrowths (OG) in sandstones. *B*—Higher magnification of cement in *A*, showing intergrowths of tabular fibers of illite (I). *C*—Shale fabric, showing some illite overgrowths (OG). *D*—Higher magnification of shale in *C*, showing illite intergrowths (I) and overgrowths (OG). Scale bars equal 1.0 μm .

gesting recrystallization of a smectite-rich precursor to the present illite composition.

Iron-rich chlorite is the dominant clay mineral in six of the Simpson Group sandstone samples, and a minor component in most. Diagenetic iron-rich chlorite in the sandstones occurs in two forms. Most commonly it occurs as a pore-lining clay cement precipitated directly from pore fluids (Fig. 7A). Pore-lining chlorite cement is found coating framework grains. Chlorite of this type occurs as characteristic pseudo-hexagonal or ragged-edged, thin, clay plates forming an overall “house of cards” or rosette structure (Fig. 7A). The second type of occurrence is as a pseudomorphic replacement after earlier, pore-filling, vermicular kaolinite (Figs. 7B,8A). Chemical analysis of the chlorite pseudomorphs was confirmed by energy-dispersive X-ray analysis.

Typically, the precipitation of kaolinite from pore fluids occurs during or immediately following carbonate dissolution (Loucks and others, 1979; Lindquist, 1978; Boles, 1982). Based on the spatial and textural relations observed here, and the common paragenetic sequences reported for

sandstones, kaolinite was probably precipitated as a pore-filling clay as an earlier pore-filling carbonate (calcite?) cement was being dissolved. Kaolinite was later replaced by, or converted to, iron-chlorite during maximum burial where temperatures exceeded 150°C (Hoffman and Hower, 1979).

In summary, mineralogic and textural evidence suggests that the present clay-mineral assemblage of Simpson Group rocks from the Mazur well, consisting of illite and chlorite, is largely a result of deep-burial diagenesis.

Paragenesis

Figure 9 shows the paragenesis for all diagenetic stages observed and interpreted for sandstones of the Simpson Group in the Mazur well; however, this does not mean that these events have occurred in all sandstone samples. Many of the diagenetic stages interpreted here are similar to those reported by Weber (1987) and Pitman and Burruss (this volume); however, several additional diagenetic stages are identified, and in this

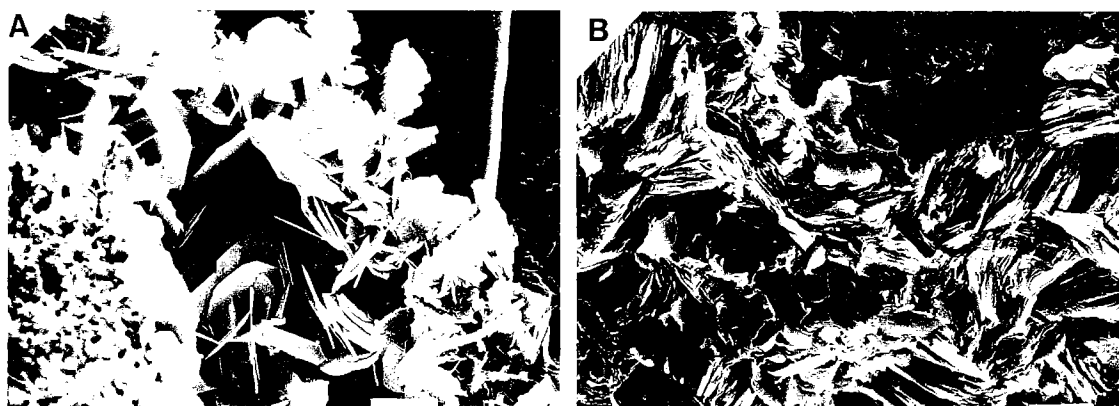


Figure 7. Scanning electron micrographs. *A*—Pore-lining iron chlorite cement in sandstone. *B*—Pseudomorphs of iron chlorite after kaolinite as pore-filling booklets and vermicules in sandstone. Scale bars equal 10 μm .

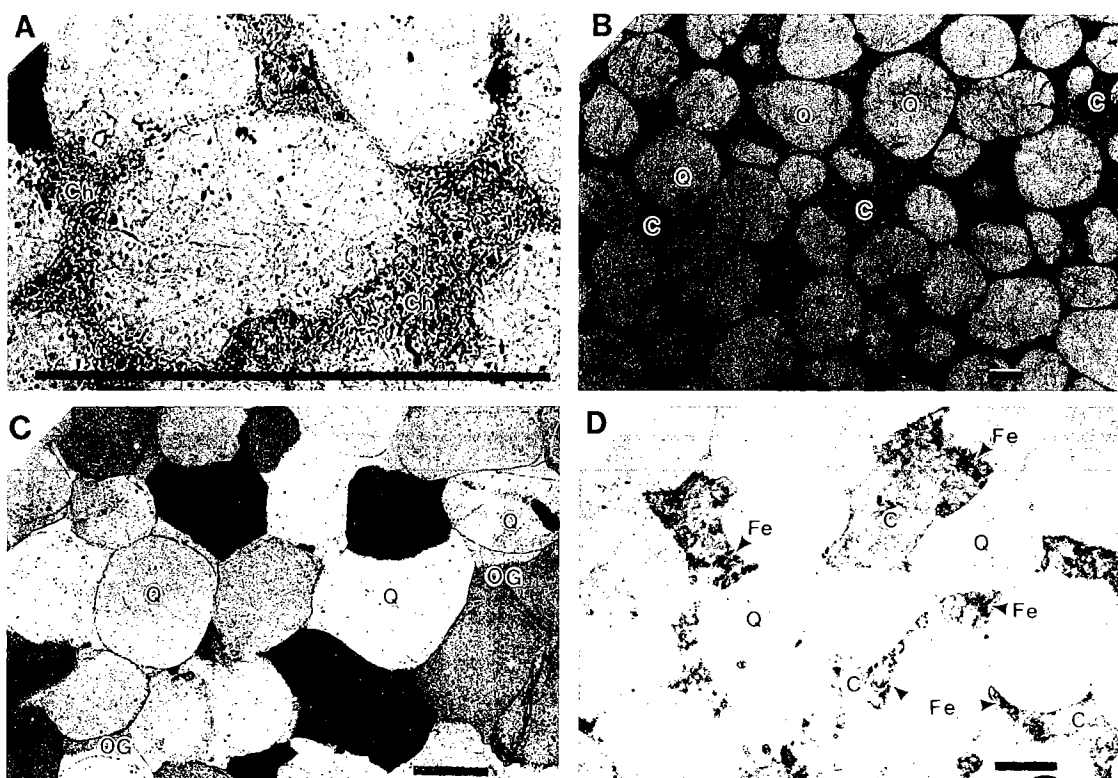


Figure 8. Thin section photomicrographs. *A*—Pore-filling pseudomorphs of chlorite (Ch) after kaolinite. *B*—Quartz (Q) grains “floating” in iron-free calcite (C) cement; note high “minus-cement” porosity. *C*—Quartz-rich sandstone, showing quartz grains (Q) with extensive, early quartz-overgrowth (OG) cement. *D*—Sandstone containing iron-free calcite (C) replaced by darker-stained iron-bearing calcite (Fe) cement. Scale bars equal 0.2 μm .

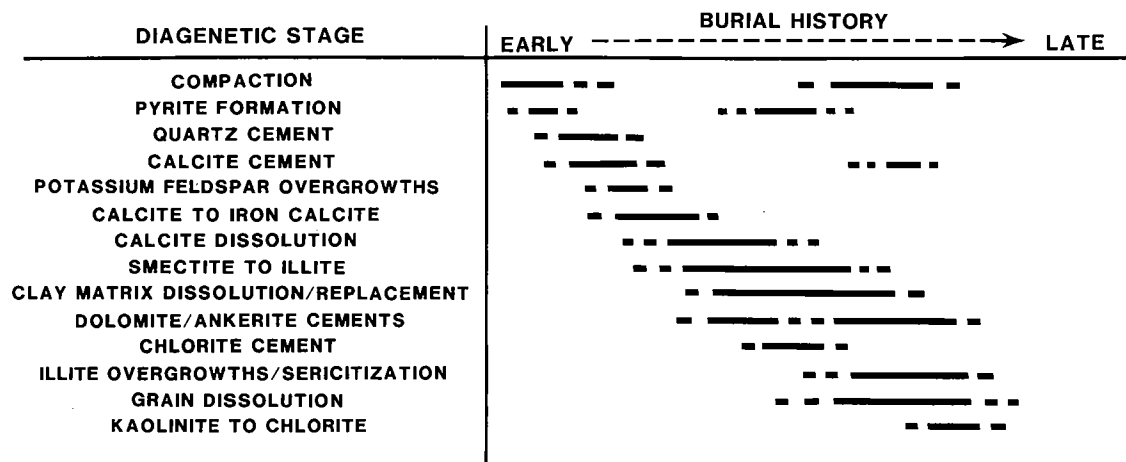


Figure 9. Paragenetic sequence relative to burial history interpreted for sandstones of the Simpson Group in the Sunray DX Parker No. 1 Mazur well.

paper there is much greater emphasis on clay-mineral reactions and their role in sandstone diagenesis.

Early diagenesis is characterized by some compaction, formation of framboidal pyrite (Fig. 4B), and early cementation by iron-free calcite or quartz. Early cementation of calcite (Fig. 8B) and quartz (Fig. 8C) is evidenced by few grain-to-grain contacts of the well-rounded quartz grains, where the grains appear "floating" in the cement. The high "minus-cement" porosity also suggests that cementation occurred before significant primary porosity was lost due to compaction.

Diagenetic stages during intermediate burial include the conversion of smectite to illite, replacement or conversion of iron-free calcite to iron-bearing calcite, dissolution of calcite cements and clay matrix, and formation of dolomite and potassium-feldspar cements. Early iron-free calcites are commonly replaced by iron-bearing calcite, as evidenced by stained thin sections (Fig. 8D). These intergranular calcite cements are commonly dissolved, creating secondary porosity and some late compaction. In some sandstone samples from the McLish Formation that contain abundant potassium feldspar grains, potassium feldspar overgrowths were developed (Fig. 4A).

The onset of illitization of smectite occurs during intermediate stages of burial, when temperatures approach 60°C (Hoffman and Hower, 1979). The smectite-to-illite reaction is probably nearly complete when burial temperatures reach ~110°C, and there is a distinct absence (or disappearance in well profiles) of the 17Å glycol phase on XRD profiles (Pollastro and Barker, 1986). Octahedral pyrite and pore-lining chlorite cement are also precipitated during intermediate stages of burial.

Latest stages of diagenesis include illite growth/overgrowth (sericitization), formation of ferroan dolomite and ankerite, some quartz cement, and conversion of kaolinite to chlorite. With increased burial and temperature >110°C, the mean particle size of illite crystals increases (Nadeau, 1985; Eberl and others, 1987; Pollastro, 1985, in press). This illite growth process is also referred to as sericitization (Eberl and others, 1987; Pollastro, in press).

Evolution of Dolomite and Ankerite

Authigenic dolomite, both ferroan and nonferroan, and ankerite occur as isolated rhombs to extensive cements throughout the entire section of Simpson Group rocks in the Mazur core. The evolution of dolomite cements is similar to the evolution of ferroan calcite cements where iron-bearing dolomite or ankerite evolves from or replaces earlier iron-free dolomite. This order of genesis is best displayed by stained thin sections, where darker-stained overgrowths of ankerite encase rhombs of earlier, clear, iron-free dolomite (Fig. 10A).

There is a consistent relation where rhombs of dolomite are proximally and texturally associated with clay and calcite. The dolomite commonly replaces detrital clay matrix (Figs. 10B, 11A). At high magnification, SEM reveals individual clay particles engulfed by the most recent stages of dolomite crystal growth (Fig. 11B). The dolomite replaces earlier calcite cement (Fig. 10C), or replaces calcite in limestone (Fig. 10D).

Dolomite cementation is followed by cementation or replacement by ankerite. Ankerite cementation is typically more extensive. Ankerite

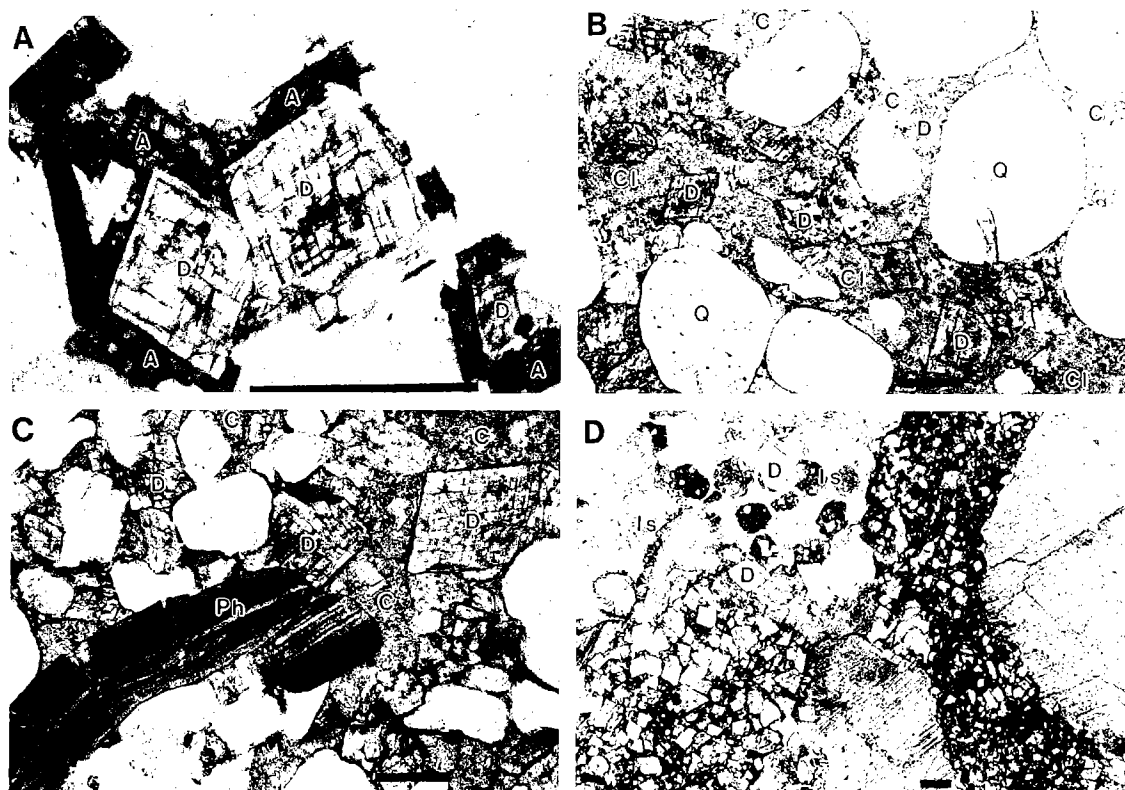


Figure 10. Thin section photomicrographs. *A*—Dolomite (D) rhombs with darker-stained ankerite (A) overgrowths in sandstone. *B*—Dolomite (D) replacing clay (Cl) and calcite (C) cement in sandstone. *C*—Dolomite (D) replacing calcite (C) cement in sandstone; Ph, phosphate fossil fragment. *D*—Dolomite (D) replacing calcite in limestone (Is). Scale bars equal 0.2 mm.

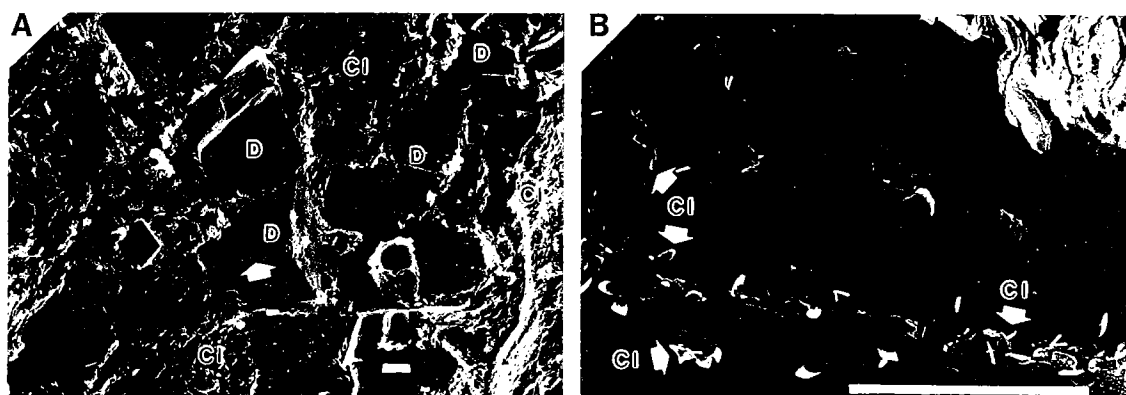


Figure 11. Scanning electron micrographs. *A*—Dolomite (D) replacing detrital clay (Cl) in sandstone; arrow indicates area shown in *B*. *B*—Higher magnification of area from *A*, showing dolomite replacing individual particles of clay (Cl). Scale bars equal 10 μm.

automorphically replaces earlier detrital clay, and calcite or quartz cements. Ankerite also replaces quartz framework grains in sandstones (Fig. 12A).

It is suggested here that some of the late dolomite and ankerite cements in the rocks of the Simpson Group were formed from the conversion of smectite to illite. Several investigators have suggested that the release of calcium, magnesium, and iron from the smectite-to-illite reaction produces dolomite and other authigenic mineral phases in sedimentary rocks during deep-burial diagenesis (Boles and Franks, 1979a; McHargue and Price, 1982; Pollastro, 1985). The consistent spatial and textural relations of dolomite, clay, and calcite, and the absence of smectite, determined from XRD profiles, support the concept that clay-mineral diagenesis may have played a role in the formation of late dolomite and ankerite.

The formation of dolomite from clay is diagrammed in Figure 13. Calcium, iron, and magnesium are released during the conversion of

smectite to illite. As smectite is converted to illite, smectite is dissolved and illite is precipitated (Pollastro, 1985; Nadeau, 1985). Calcium, magnesium, and iron probably nucleate dolomite within the clay matrix of sandstones, and dolomite grows in part at the expense of the clay. Much of the calcium for dolomite formation is probably derived from the dissolution of local calcite cement. This reaction mechanism is thought to have formed some of the dolomite; however, it cannot explain the extensive cementation by ankerite.

Reservoir Characteristics

Porosity in Sandstones

All porosity revealed from thin-section analysis is secondary (dissolution) porosity and is best developed in the sandstones of the Tulip Creek and Oil Creek Formations. Secondary porosity in these sandstones is mostly intergranular. Some

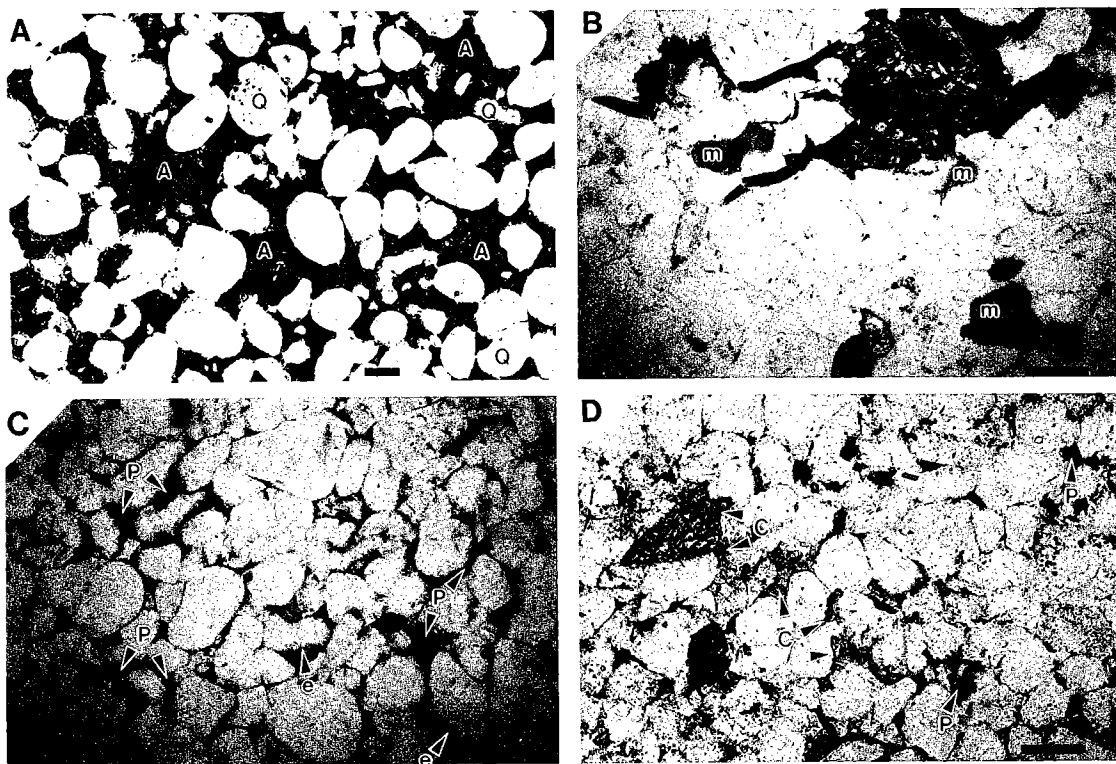


Figure 12. Thin-section photomicrographs. A—Ankerite (A) cement partly to completely replacing quartz (Q) framework grains and earlier intergranular cement(s) in sandstone. B—Moldic porosity (m) in sandstone. C—Secondary intergranular porosity (P) from the removal of calcite, as evidenced by etched grains (e). D—Remnants of calcite (C) cement in quartz sandstone showing secondary porosity (P). Scale bars equal 0.2 mm.

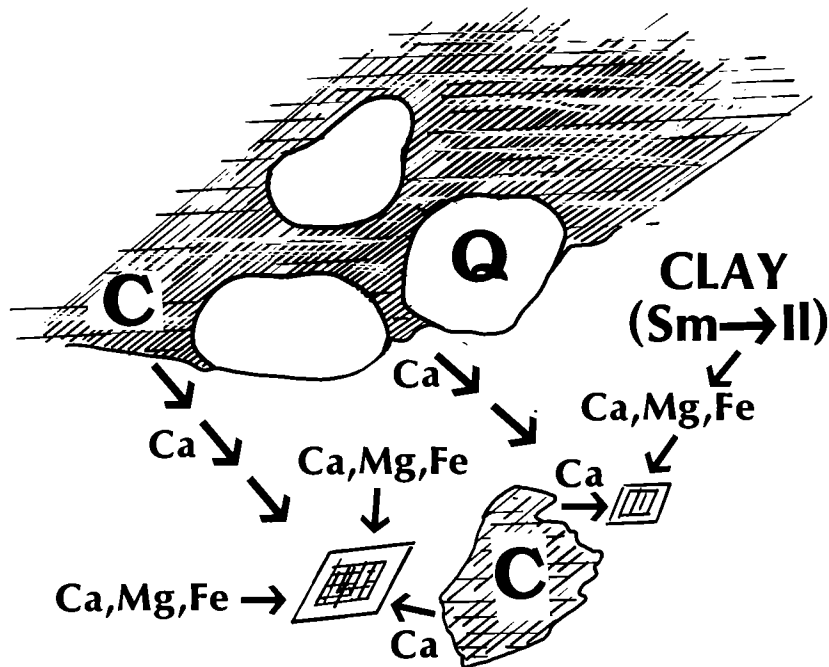


Figure 13. Diagrammatic interpretation of the formation and evolution of dolomite/ankerite from the conversion of smectite (Sm) to illite (Il) associated with detrital clay (CLAY) and calcite (C) cement in deeply buried sandstones and carbonate rocks of the Simpson Group, Mazur well. Elements exchanged in the reaction include calcium, magnesium, and iron.

intragranular (moldic) porosity from the dissolution of framework grains is also present in few sandstones (Fig. 12B).

Secondary intergranular porosity in sandstones of the Simpson Group sampled from the Mazur well was from the dissolution of earlier calcite and ferroan-calcite cements. Evidence for this interpretation is provided by irregular and etched surfaces of framework grains (Fig. 12C), indicative of earlier calcite removal, and small remnants of calcite cement found in some of the thin sections (Fig. 12D). There is also evidence for late physical and chemical recompaction of the sandstone after removal of the calcite. This is indicated by areas containing remnants of calcite cement having greater "minus-cement" porosity (Fig. 12D).

Clay Content Versus Gamma-Ray Log

The response of the total gamma-ray log measured in the Mazur well is a good indicator of clay content or "shaliness" in potential Simpson Group reservoirs at this depth, because of a general lack of potassium feldspar and a clay-mineral assemblage in these rocks consisting mainly of potassium-bearing illite. This is demonstrated by

the excellent agreement between total clay content, determined from XRD, plotted on a point-to-point log versus the continuous total gamma log (Fig. 14). After initial calibration of the XRD data to the gamma-ray log, total gamma response can be used to determine clay content in similar deeply buried Simpson Group reservoirs.

SUMMARY

The rocks of the Simpson Group from the Mazur well consist of quartz sandstones, shales, carbonates, and a variety of mixed lithologies. Although the bulk-rock mineral composition of the Simpson Group from the Mazur well is diverse, clay minerals are restricted to illite and chlorite, because of deep burial conditions. Diagenesis has significantly modified the original textures and mineralogic composition of most deeply buried Simpson samples. Many of the sandstones have undergone extensive cementation by carbonates and silicates. Several mineral phases in these sandstones have undergone multiple stages of dissolution and/or replacement. Shales are clay-rich and quartz-poor, suggesting that some silica was removed during progressive burial.

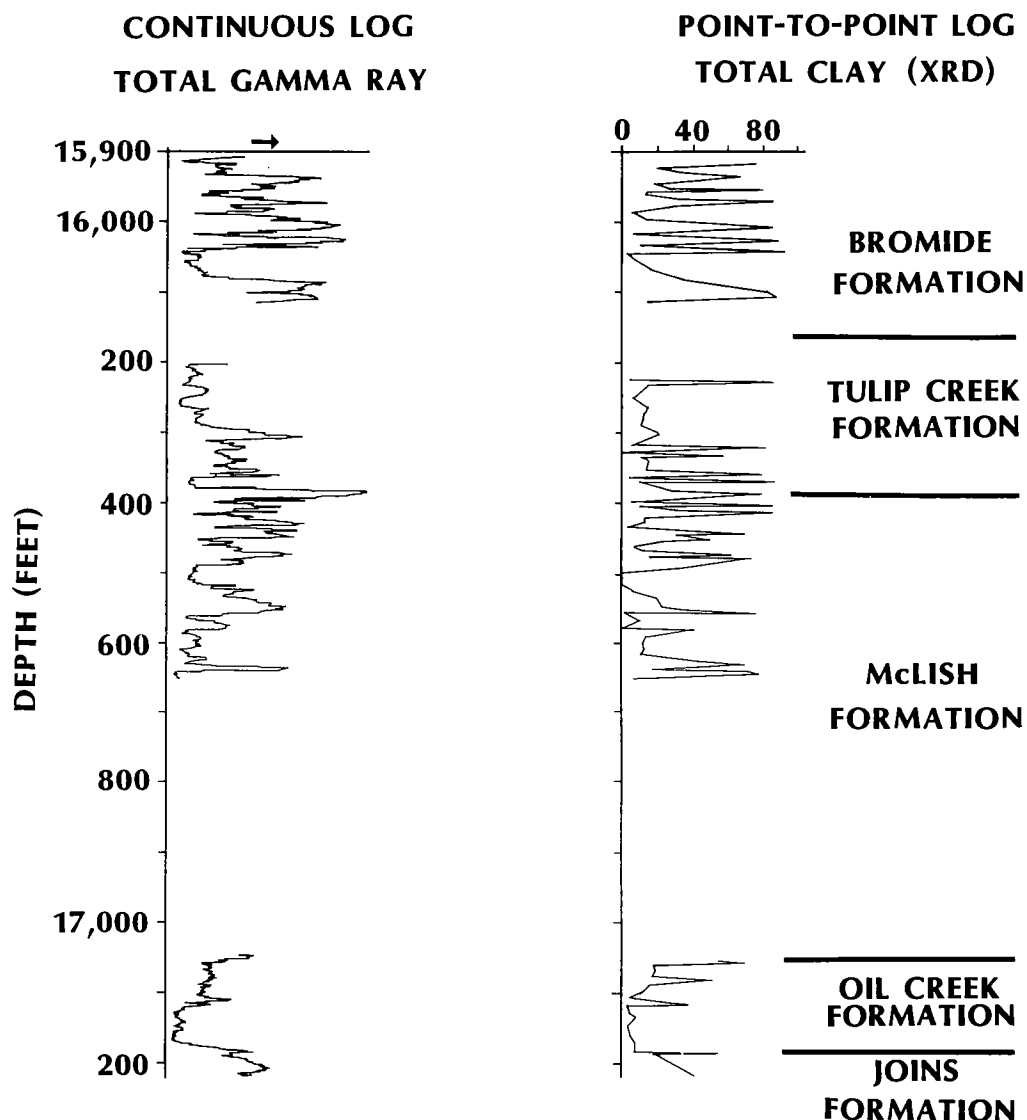


Figure 14. Continuous total gamma-ray log response versus point-to-point log plot of total clay content, in weight percent from X-ray powder diffraction (XRD), from cored intervals of the Simpson Group, Mazur well.

Secondary porosity is best developed in sandstones from the Tulip Creek and Oil Creek Formations, resulting from dissolution of earlier calcite cements. Potential Simpson reservoirs at depths >15,000 ft can probably be evaluated for clay content using the gamma-ray log, because illite is the primary potassium-bearing phase.

ACKNOWLEDGMENTS

I would like to thank C. J. Schenk and T. S. Dyman for their critical reviews and stimulating discussions. The manuscript has benefited greatly from these processes.

SULFIDE MINERALIZATION AND MAGNETIZATION, CEMENT OIL FIELD, OKLAHOMA

RICHARD L. REYNOLDS, NEIL S. FISHMAN, MICHAEL W. WEBRING,
RICHARD B. WANTY, AND MARTIN B. GOLDBABER
U.S. Geological Survey, Denver

Abstract.—Geochemical, petrographic, and rock-magnetic studies were undertaken to investigate possible sources for reported positive aeromagnetic anomalies over the Cement oil field, Oklahoma. Ferrimagnetic pyrrhotite (monoclinic, Fe_7S_8), intergrown with more-abundant, nonmagnetic pyrite (FeS_2), is present in well-cutting, core, and quarry samples at Cement, and it is the only identified source of possible enhanced magnetization in rocks over the field. Magnetite, found only in well cuttings from Cement, is contamination from drilling. Magnetite was considered previously by others to be the source of magnetic anomalies at Cement.

Several observations indicate that the sulfide minerals formed as a result of hydrocarbon seepage. The pyrrhotite is confined to beds above oil and gas reservoirs. These beds, which lack detrital organic matter, contain higher sulfide and lower sulfate S (1.7 and 0.1 wt. %, respectively) than correlative beds off the field (0.2 and 1.1 wt. %, respectively). In the Cement field, isotopic ratios of sulfide S show a systematic decrease upward through the Permian section from positive (heavy) values (maximum, +12% at 610–760 m depth) to negative (light) values (–1 to –11% at 32–230 m; –26 to –30% at the surface). The geochemical results, together with time-temperature data derived from burial curves, limit the major sources for sulfide in the Fe–S minerals. Isotopically heavy sulfide was generated either by abiologic mechanisms at temperatures $>90^\circ\text{C}$ in hydrocarbon reservoirs beneath Permian strata, or by bacterial sulfate reduction at temperatures $<60^\circ\text{C}$ in the lower parts of the Permian section. In the latter case, bacterial sulfate reduction would have occurred under sulfate-limited conditions to produce isotopically heavy sulfides. Isotopically light sulfide that is dominant toward the surface is attributed to bacterial reduction of sulfate which was present in unlimited abundance relative to the microbial capacity for reduction. The bacterial sulfide in Permian rocks is related to the petroleum reservoirs at depth through the use of leaking hydrocarbons, or associated compounds, as food sources by the sulfate-reducing microbes.

Magnetic forward modeling techniques were used to assess whether pyrrhotite in the Permian strata could contribute to the observed aeromagnetic anomalies at Cement. A geometric model was constructed of six bodies having different shapes and magnetizations, based on geology and on the petrologic and geochemical results, and supplemented by rock-magnetic measurements of shallow core and outcrop samples. The rock column through which hydrocarbons passed was divided into three sulfide-bearing zones on the basis of pyrrhotite content, and it was capped by a weakly magnetic, 30-m-thick zone that contains ferric oxide minerals formed mainly from oxidized pyrite. Red beds unaffected by sulfidization, and a zone of rock depleted in hematite but lacking sulfide, were modeled as weakly magnetic bodies surrounding the sulfidic zones.

The synthetic magnetic signatures are controlled mainly by pyrrhotite-bearing bodies at depths of 200–500 m that lie above two anticlinal domes in Pennsylvanian beds. The magnetizations of these bodies are estimated from (1) petrographic estimates of pyrrhotite content relative to pyrite contents; (2) content of sulfide sulfur determined from chemical analysis; and (3) magnetic susceptibility values of monoclinic pyrrhotite. Total magnetization of the bodies of highest pyrrhotite content ranges from about 3×10^{-3} to 56×10^{-3} amp/m in the present field direction, yielding calculated magnetic anomalies (at 120-m altitude) having amplitudes <1 nT to ~ 6 nT, respectively, and wavelengths of ~ 4 km. The synthetic magnetic profiles are dissimilar to the observed total-field profiles, which are characterized by anomalies having amplitudes as much as 60 nT and by short wavelengths (typically <1 km). We attribute the short-wavelength features in the observed total magnetic field mainly to culture, such as buried well casings. At Cement, the observed magnetic signals caused by culture would mostly, if not entirely, mask any contribution from rock magnetism in the Permian strata.

Our results demonstrate that pyrrhotite, formed by hydrocarbon reactions and within a range of concentrations estimated at Cement, is capable of causing subtle magnetic anomalies in sedimentary rocks. Numerous assumptions, however, were made in estimation of magnetizations of Permian rocks at Cement; moreover, the observed total magnetic fields over the Cement field are apparently dominated by cultural features. For these reasons, the results should not be taken to indicate or to imply that aeromagnetic anomalies related to hydrocarbon seepage have been documented at Cement oil field.

NATURAL RESOURCES INFORMATION SYSTEM (NRIS) OF OKLAHOMA: ANADARKO BASIN DATA

MARY K. GRASMICK

Geological Information Systems,
University of Oklahoma

Abstract.—A great need exists for more-accurate, detailed information on the natural resources of Oklahoma, both for technical uses such as exploration and research and for public information and policy uses. In response to this need, the Oklahoma Geological Survey has undertaken efforts to develop the Natural Resources Information System of Oklahoma, a compilation of publicly available data on the State's resources. Oil and gas resources have provided one initial thrust for these efforts, with several data bases under development to record oil- and gas-related information. A well-history file is being developed, based on completion reports, with supplemental data from sources such as scout tickets and well logs. Production data are being maintained at the lease, field, and county levels. Other data in the system include lease and field locations, formations, and field-history information.

From NRIS, needed data are available for Anadarko basin research. Sample applications are provided as illustrations of the information available to the research community through NRIS.

INTRODUCTION: THE NEED FOR INFORMATION

In late 1985, the Oklahoma Geological Survey defined a goal of developing an integrated system of computerized information on the geological resources of the State. This effort, called the Natural Resources Information System (NRIS) of Oklahoma, was undertaken in response to the need for more-accurate, detailed, and accessible information on the State's nonbiological resources. Initial emphasis for the system has been placed on computerizing information relating to the oil, gas, and coal resources of the State.

Oil and natural gas have been economically important resources for Oklahoma since statehood in 1907. In fact, petroleum production began prior to statehood, with the completion of the No. 1 Nellie Johnstone in 1897. Thus, petroleum has been of primary interest to the Survey since its inception, and it is a major thrust in the development of NRIS. The remainder of this paper describes the oil and gas subsystems of NRIS which currently are under development, and provides information regarding the availability of these data to the public, particularly as related to investigations in the Anadarko basin area of Oklahoma.

In the work the Survey has done over the years, several key areas have been defined that repeatedly would have benefited from a computerized information source. These information needs provided the foundation upon which the oil and gas subsystems of NRIS were formulated.

For example, the Survey is commonly involved in research on the geological characteristics of various areas in the State, based on in-depth information from all of the oil and gas wells drilled in the area. Historically, that information has been contained in scattered documents and libraries, accessible only through extensive manual searches. Definition of the boundaries of oil and gas fields in Oklahoma has been possible only through manual efforts to reconcile producing records with known field boundaries, so the "official" definitions of field boundaries have been determined frequently to be out of date and erroneous. The ability to allocate oil and gas production to specified fields, and to specific formations, is fundamental to the geological understanding of hydrocarbon occurrence and distribution.

OGS researchers are called upon to perform a variety of geological investigations, most of which have been completed in the past through extensive manual efforts; the development of NRIS will greatly improve the timeliness and comprehensiveness of these investigations. This need for information exists throughout various sectors of the society. Public policy benefits from an informed decision base; private industry needs information to further its efforts in exploration and development. NRIS data will be accessible for fundamental research as well as applied investigations. As a state agency, OGS has a responsibility to make the results of its efforts available to all interested parties, and therefore has attempted to consider as many needs as practical in the design of the system.

THE DEVELOPMENT OF NRIS TO MEET THOSE NEEDS

NRIS was designed in response to this identified need for data from a diverse public. Machine-readable data are being compiled from publicly available information on the State's natural resources. Because credibility of the contained information is the priority consideration, the primary goal for NRIS is to build a system with the highest possible data quality, even though quality-assurance measures do increase costs.

The system has been designed to be relatively simple to understand and manipulate by a variety of users for a multitude of applications. Subsets of the data can be downloaded to the personal-computer level for specific applications. With the expected use of the data by Survey staff, students, faculty, and the public, new applications should be fairly easy to develop by individuals unfamiliar with the system. User routines and documentation are being developed to facilitate these activities.

In some respects, NRIS can be thought of as an evolutionary system; it is expected that future design changes will be relatively routine, based on the addition of new hardware or software capabilities, new data accessibility, or new ideas about information needs.

NRIS SYSTEM OVERVIEW

Figure 1 is a schematic for the oil and gas portions of NRIS. There are actually two major subsystems within NRIS for oil and gas data: the Oil and Gas Well History Subsystem and the Oil and Gas Production (OGP) Subsystem. Within the production subsystem, files are being developed to maintain data on oil and gas leases, fields, and county production.

Oil and Gas Well History Subsystem

The well-history files are designed to provide historic "snapshots" of information on oil and gas wells. Most of the data are based on information reported during the drilling of wells: geological and engineering data on well completions, formations, initial production tests, well logs, cores, and samples. Approximately 800 data items have been defined for the well-history data; a sample record is provided in the Appendix.

Between 300,000 and 350,000 wells have been drilled in Oklahoma; drilling completion reports (called Form 1002A) are on file for about 250,000–275,000 of these wells. These completion reports are the foundation for the well-history information within NRIS.

Supplemental well-history data are available throughout the State in libraries of scout tickets, well logs, and core and drilling samples. A primary goal in computerizing these supplemental data is to provide references for the existence of cores, samples, and well logs in various libraries, and thereby reduce the effort required to determine if there are samples available for wells being researched. These data are being added to the well subsystem in a variety of ways. Some sources are being computerized through parallel activities, and then merged with the 1002A records to complete the well-history information; other sources are only available through special manual research. Given the cost to complete the manual research, these data are being collected through special projects that focus on specific regions in the State.

This subsystem is not designed to compete with existing commercial sources of well-history information; its primary function is to bring together all publicly available sources of information on any particular well.

Oil and Gas Production Subsystem

Since 1983, the Oklahoma Tax Commission has released to the Survey computerized production data from tax reports on oil and gas leases; these data have provided one of the foundations for the OGP Subsystem. Each month, a tape is released of reported production for all oil and gas leases (or subleases) in the State.

The Lease Master File of the OGP Subsystem primarily is based on the Tax Commission data. Data items on this file include monthly production totals, producing formations, and locations (county and township, range, section, and quarter-quarter section).

The formation names reported to the Tax Commission provide a starting point for determining production by formation; however, these names require both editorial and geological standardization before they can be used in this manner. Through NRIS, the Oklahoma Geological Survey is developing a "formations editing" system that will result in a significant improvement in the availability of formation production data for Oklahoma.

The Field Master File of the OGP Subsystem is designed to store information on all current and historical oil and gas fields within Oklahoma. Data items on the field file include monthly production totals, locations (county and township, range, section, and quarter-quarter section), and historical data regarding changes in field designations due to field consolidations. Plans are to add cumulative production totals, discovery well, and abandonment data to the file in the coming year.

The Oklahoma Nomenclature Committee of

the Midcontinent Oil and Gas Association is responsible for designating the official oil and gas field names and outlines within Oklahoma. Over the last several years, the OGS has begun working more closely with the Nomenclature Committee, individual staff members serving either on the Committee or in an advisory capacity for the Committee decisions. The results of the Committee's work are released in a set of "Blue Sheets" that is the foundation for NRIS field-location and history data. About 3,000 fields are currently designated as "official" (or potentially producing) by the Nomenclature Committee; another 3,000 names have been "discontinued" but are availa-

ble through historical records. All of these fields are maintained on the Field Master File.

Field production data are developed through a process of matching lease records to fields (based on STR and quarter-section locations), and by summing the lease production records for each field to get field totals. The Energy Information Administration of the U.S. Department of Energy assigns field codes to all domestic oil and gas fields as a means to standardize field identifications throughout government and industry; within NRIS this DOE/EIA field code is recorded for each field, and on those lease records that have been identified with each field.

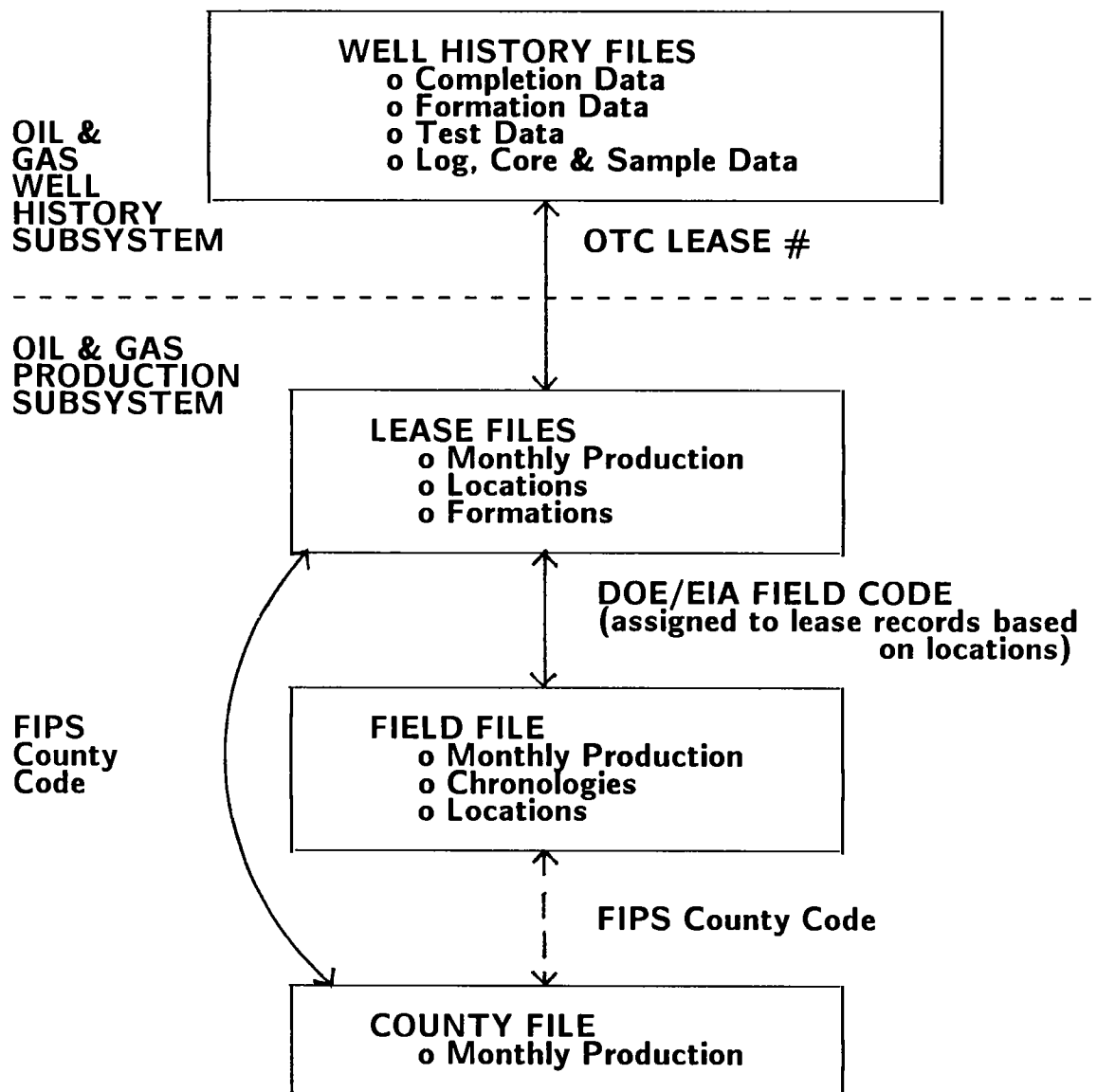


Figure 1. Natural Resources Information System, Oil and Gas Subsystems.

The County Master File is designed to store monthly production totals by county. This information can be obtained by aggregating production from other files; however, it is information used with such frequency that it is maintained separately to facilitate these applications.

Linking the Oil and Gas Files

Through various key data items, records from all of the files can be linked for use in particular applications or analyses. The Oklahoma Tax Commission Lease Number is maintained on records on the Well History files, as well as the Lease Master files, so that information can be aggregated for all wells within a particular lease. The DOE/EIA Field Code is used as the key identifier on the Field Master File, and also is assigned to lease records; by extension, the field code also can be linked back to well records associated with assigned leases. County codes, as specified by the Federal Information Processing Standard (FIPS 6-3), are maintained on all records on all files, to simplify analyses by county.

SAMPLE ANALYSES: ANADARKO BASIN DATA

A paper presented in this conference by K. S. Johnson provides an overview of the geology of the Anadarko basin; Davis and Northcutt provide an overview of the petroleum development of the region; other papers presented in this conference provide detailed information on structural style, depositional lithologies, diagenetic histories, and other aspects of the geology of various parts of

the Anadarko basin. The goal of this paper is to provide information about the availability of data for the Anadarko basin, rather than provide explanations of the geology or petroleum history. As a way of providing some ideas regarding the potential applications for the NRIS data, sample analyses based on data from the Anadarko basin area have been included. Ellis County was chosen as the target area for these analyses.

Figures 2 and 3 are based on data from the Well History Subsystem. Wells from T. 24 N., the northernmost township in Ellis County, were selected for these applications. There are 240 completion reports on file for wells in this area, with drilling dates back to 1950. Figure 2 presents the number of wells drilled and completed as producers versus the number of dry wells, for each decade since 1950. In Figure 3, the total number of wells drilled during each decade is presented separately for each of the four ranges (R. 23-26 W.) in T. 24 N. of Ellis County.

Figure 4 is an application based on data from the Oil and Gas Production Subsystem. For Ellis County, the total monthly nonassociated gas production is plotted for each month from January 1983 through December 1987. For comparative purposes, the monthly production totals within Ellis County for three separate fields also are plotted: the Gage field, the Higgins South field, and the Mocane-Laverne gas area.

PROJECTED DATA AVAILABILITY

A goal for the NRIS system is to make these data available to the public in an easily usable form. Standardized reports now being produced will be available through the Oklahoma Geologi-

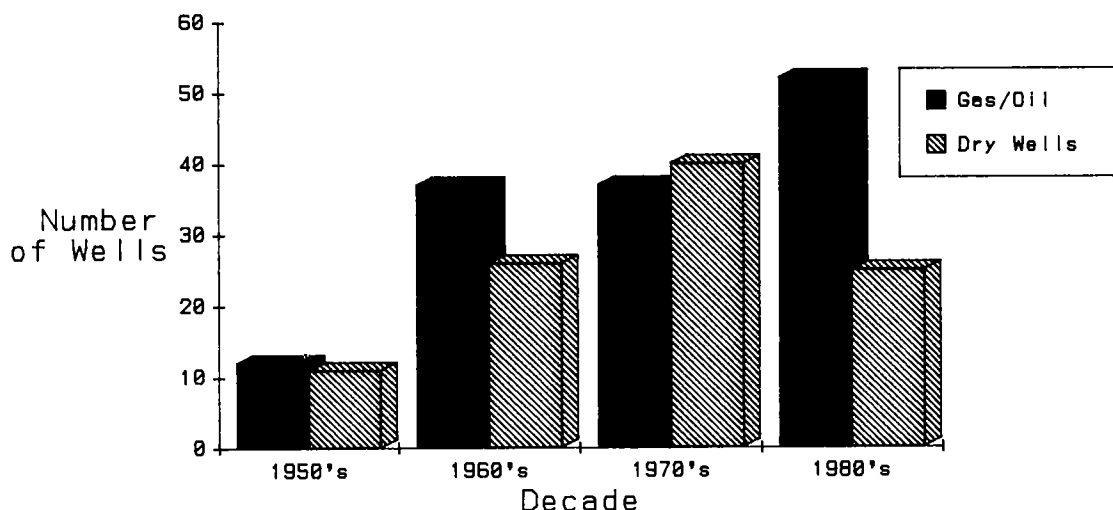


Figure 2. Gas/oil versus dry wells by decade drilled, Ellis County, T. 24 N.

cal Survey—such as reports of production by field or county, or reports of all data available on wells in specified geographic areas. Machine-readable copies of data subsets are available on diskettes, as well as mainframe magnetic tapes, and specialized data requests can be filled on a consultation basis.

The efforts to build the Well History Subsystem are in process, and are being approached on a regional basis. Over 30,000 records for the Ouachita Mountains and Arkoma basin areas in southeastern Oklahoma are now on file, and in early 1988 efforts were begun on records for the

Anadarko basin area. It is expected that processing for the entire State will take three to seven more years, depending on funding levels.

System-development efforts for the Lease and Field Master files are currently in process. The production updating system is essentially in place, and the formations editing routines are under development. It is expected that some of these data will be available for public distribution this summer. The County system is now completed and available on request. More specific information regarding these data can be obtained by contacting the Oklahoma Geological Survey.

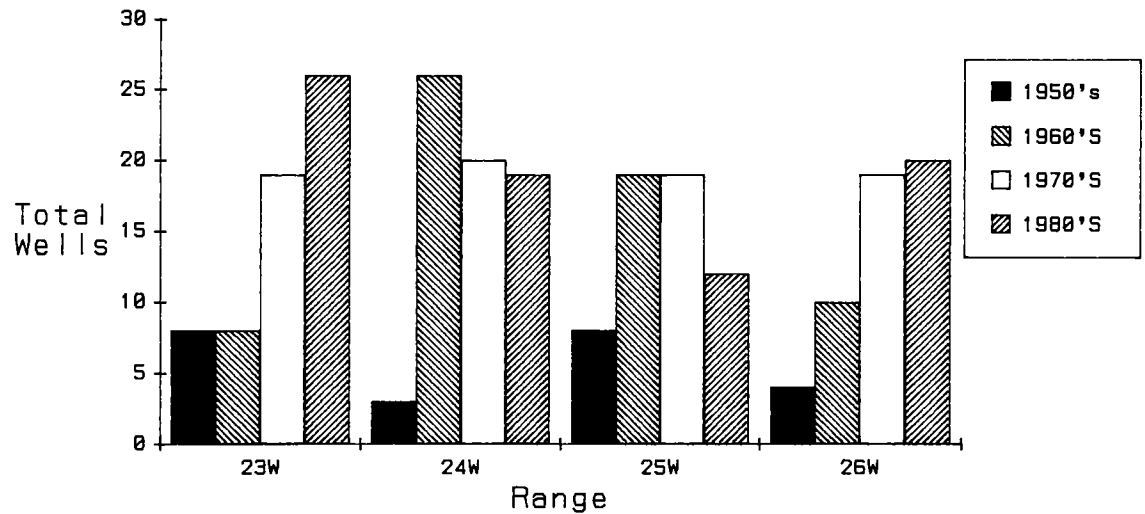


Figure 3. Total wells drilled by decade, Ellis County, T. 24 N.

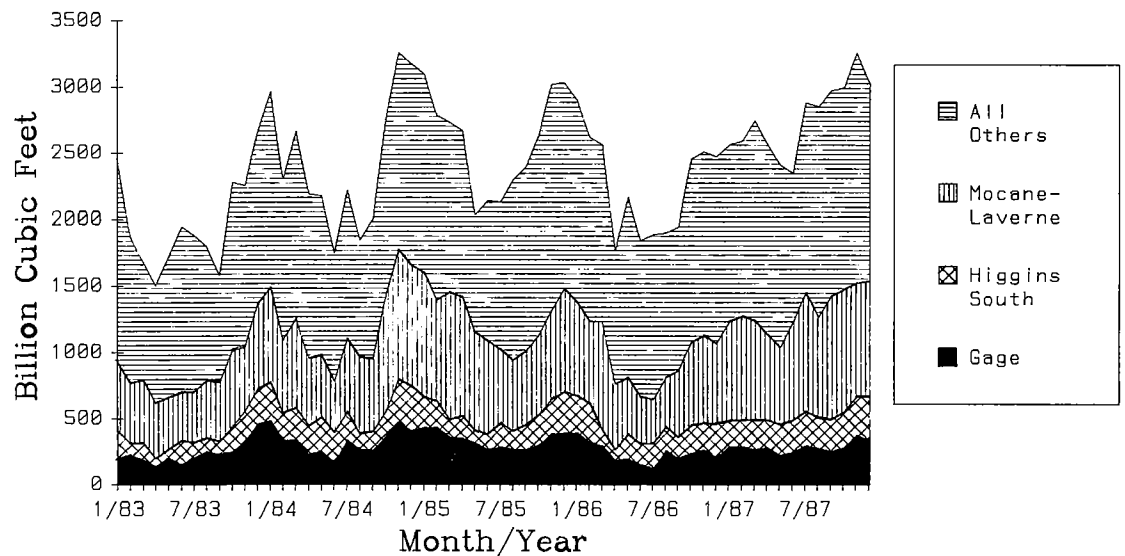


Figure 4. Nonassociated gas production, Ellis County.

APPENDIX:

OKLAHOMA WELL HISTORY FILE
SAMPLE RECORD

WELL IDENTIFICATION SECTION

OGS IDENTIFICATION NUMBER - 033844
API WELL NUMBER - 04521502
OTC / OCC OPERATOR ID NUMBER - 02930
CORPORATION COMMISSION FORM ID NUMBER - 87000068
FORM TYPE - 1002A 85
DATE FORM RECEIVED - 1986 12 16
DATE FORM SIGNED - 1986 12 08
BATCH NUMBER - 0307850308
FORM KEYED ON - 1988 03 09

LOCATION SECTION

STATE POSTAL CODE - OK
COUNTY NAME - ELLIS
COUNTY CODE - 045
SECTION - 02 TOWNSHIP - 24N RANGE - 24W
QUARTER SECTION - C W 1/2 NW 1/4
OPERATOR NAME - JOHN H HILL
OPERATOR ADDRESS - 17400 DALLAS PKWY SUITE 210
DALLAS
TX 75252
OPERATOR PHONE NUMBER - (214) 931-7331
FARM NAME - CROOKS
WELL NUMBER - 1-A
DRILLING STARTED - 1986 03 05
DRILLING FINISHED - 1986 03 12
DATE OF FIRST PRODUCTION - 1986 11 02
COMPLETION DATE - 1986 07 07
DISTANCE FROM SL OF 1/4 SECTION (FT.) - 1320
DISTANCE FROM WL OF 1/4 SECTION (FT.) - 660
ELEVATION OF DERRICK FLOOR (FT.) - 2162.4
ELEVATION OF GROUND (FT.) - 2151.9

WELL COMPLETION TYPE

MULTIPLE ZONE COMPLETION

LOCATION EXCEPTION INFORMATION

LOCATION EXCEPTION
LOCATION EXCEPTION ORDER NUMBER - 294283, 297418, 2938
PENALTY - 25%

OIL OR GAS ZONES SECTION

ZONE NAME	FROM	TO
01 OSWEGO	6455	6465
02 MORROW	7434	7481

CASING & CEMENT INFORMATION SECTION

01 CASING SET / CEMENT (LINE 1)
CASING SET TYPE - SURFACE
CASING SET SIZE (INCHES) - 8 5/8
CASING SET WEIGHT (LBS/FT.) - 24
CASING SET GRADE - J-55
CASING SET FEET - 1210
CASING TEST PSI - 3000
CEMENT SACKS - 610
CEMENT FILLUP - 1210
CEMENT TOP - 0

02 CASING SET / CEMENT (LINE 2)
CASING SET TYPE - PRODUCTION
CASING SET SIZE (INCHES) - 5 1/2
CASING SET WEIGHT (LBS/FT.) - 15.5, 17
CASING SET GRADE - J-55
CASING SET FEET - 7615
CASING TEST PSI - 3000
CEMENT SACKS - 410
CEMENT TOP - 4900

PACKERS SET SECTION

	DEPTH (FT.)	MAKE
01	7360	BAKER

COMPLETION & TEST DATA BY PRODUCING FORMATION SECTION

01 PRODUCING FORMATION NAME - OSWEGO
SPACING & SPACING ORDER NO. - 293689 640 ACRES
CLASSIFICATION GAS
PERFORATED INTERVALS - 6455-6465
FORMATION ACIDIZED? - YES, 15% HCL/5000
FORMATION FRACTURED TREATED? - YES, 40000 GALS

INITIAL TEST DATA
TEST DATE - 1986 11 25
OIL - BBL. / DAY - 0
GAS - MCF / DAY - 178
WATER - BBL. / DAY - 0
EXTRACTION TYPE (PUMPING / FLOWING) - FLOWING
INITIAL SHUT-IN PRESSURE - 1650
CHOKE SIZE (INCHES) - 20/64
FLOW TUBING PRESSURE - 277

02 PRODUCING FORMATION NAME - MORROW
SPACING & SPACING ORDER NO. - 40718 640 ACRES
CLASSIFICATION GAS
PERFORATED INTERVALS - 7434-7481
FORMATION ACIDIZED? - YES, 15% HCL/1500
FORMATION FRACTURED TREATED? - YES, 40000 GALS

INITIAL TEST DATA

TEST DATE - 1986 11 25
OIL - BBL. / DAY - 0
GAS - MCF / DAY - 1065
WATER - BBL. / DAY - 5.7
EXTRACTION TYPE (PUMPING / FLOWING) - FLOWING
INITIAL SHUT-IN PRESSURE - 1550
CHOKE SIZE (INCHES) - 20/64
FLOW TUBING PRESSURE - 653

PRODUCTION DEPTHS SECTION

TOTAL DEPTH OF WELL - 7750

FORMATION RECORD SECTION**FORMATION NAMES AND DEPTHS**

01 FORMATION - HOOVER
TOP DEPTH - 4252
BOTTOM DEPTH - 4320
02 FORMATION - TORONTO
TOP DEPTH - 5290
BOTTOM DEPTH - 5366
03 FORMATION - TONKAWA
TOP DEPTH - 5548
BOTTOM DEPTH - 5568
04 FORMATION - HOGSHOOTER
TOP DEPTH - 6340
BOTTOM DEPTH - 6400
05 FORMATION - OSWEGO
TOP DEPTH - 6450
BOTTOM DEPTH - 6546
06 FORMATION - MORROW SHALE
TOP DEPTH - 7250
BOTTOM DEPTH - 7430
07 FORMATION - MORROW SAND
TOP DEPTH - 7430
BOTTOM DEPTH - 7560
08 FORMATION - CHESTER LIME
TOP DEPTH - 7560

ADDITIONAL INFORMATION ON FORM

ELECTRICAL SURVEY WAS RUN -
DATE OF LAST ELECTRICAL SURVEY LOG - 1986 03 12
TRUE VERTICAL DEPTH - 7747

COMMENTS AND REMARKS SECTION

SOURCE OF SUPPLEMENTARY INFORMATION - 01
CODING REMARKS - ALL: DUAL COMPLETION WITH THE MORROW
THRU TUBING AND THE OSWEGO THRU ANNULUS

PART II

ABSTRACTS AND SHORT REPORTS RELATED TO POSTER PRESENTATIONS

ANADARKO BASIN HISTORY FROM STRATIGRAPHIC RESPONSE PATTERNS

GLENN S. VISHER

Geological Services and Ventures, Inc., Tulsa

Abstract.—An analysis of the Anadarko basin in southwestern Oklahoma illustrates the interrelation of tectonic and depositional controls. Seismic data to five seconds, regional gravity data, and deep wells to >31,000 ft provide a data base that is useful in interpreting basin and deposition history.

Early Paleozoic history, Cambrian to upper Mississippian, reflects shelf carbonate deposition. Subsequent history, as indicated by seismic sections, shows the development of a wrench-faulted basin subsiding faster than sedimentary infilling. The principal periods of basin subsidence occurred during periods of onlap unconformity development, at the base of the Springer, at the Mississippian–Pennsylvanian boundary, and at the Atokan–Desmoinesian boundary. Basin-center subsidence, from the Upper Mississippian to the Desmoinesian, was >6,000 ft. Shelf deposition was replaced by deep-basin, low-density, submarine-fan deposits. Subsidence then continued, but with the reestablishment of shelf sedimentary sequences.

Gravity data indicate a negative anomaly, suggesting low-density sedimentary fill in the basin center, and/or changes in lithosphere density in the basin area. This response pattern is consistent with subsidence and the development of a sediment-starved topographic basin. Subsidence was produced by the interaction of low-density sedimentary sequences and “driving” subsidence associated with both positive and negative flower structures marginal to the basin axis.

Sea-level changes and the response of subsidence to basin sedimentation patterns, basin topography, and sediment density were interactive with “tectonic” controls.

INTRODUCTION

One of the principal problems facing geodynamicists today is understanding the causality of basin subsidence. Thermal expansion and cooling has been modeled to account for basin subsidence, but histories and events do not conform to simple patterns of cooling. Cratonic-margin basins, reflecting crustal extension, fit this model better than cratonic basins. Extensional basins have a history reflecting driving subsidence in early stages, slowing rates of subsidence producing basin fill, and patterns of unconformities that reflect the history of shelf progradation and basin fill (Roberts and Caston, 1975). Extensional basins—for example, the North Sea, the Sirte basin, and basins on broad cratonic shelves—partially reflect this history. However, unconformity patterns in most cases are coincident with worldwide eustatic sea-level falls, and do not exclusively reflect local cooling histories.

Cratonic epeiric seas and foreland basins rarely follow such a history. Unconformities are correlative in time to eustatic sea-level falls, and do not fit cooling histories, tectonic events, or local depositional and topographic patterns. Interpreting tectonic, sea-level, thermal-conductivity, and sedimentary response patterns requires an examination of the basin depositional history.

ANADARKO BASIN DEPOSITIONAL HISTORY

Stratigraphic Controls

The Anadarko basin illustrates these relationships (Fig. 1). It contains the deepest wells drilled into a sedimentary basin (the deepest of these >31,000 ft); detailed gravity, seismic, and heat-flow information is available; and many cored wells provide specific information on depositional history.

Basement structure shows the Anadarko basin to be a faulted foreland basin. Bounding faults on the southwest are locally high-angle reverse faults, with some thrusting. The marginal structural high is a strong gravity anomaly on regional Bouguer gravity maps. The structure of the Cement field is a classic example of a positive “flower” structure (Harding and others, 1983).

A stratigraphic cross section illustrates deposition on a lower Paleozoic marginal shelf, on the southern margin of the North American craton (Fig. 2). Additional data from wells south of this section indicate the transition from carbonates into deeper-water shales. Minor thickening of all stratigraphic intervals occurred across the marginal shelf in all units up to the Upper Mississip-

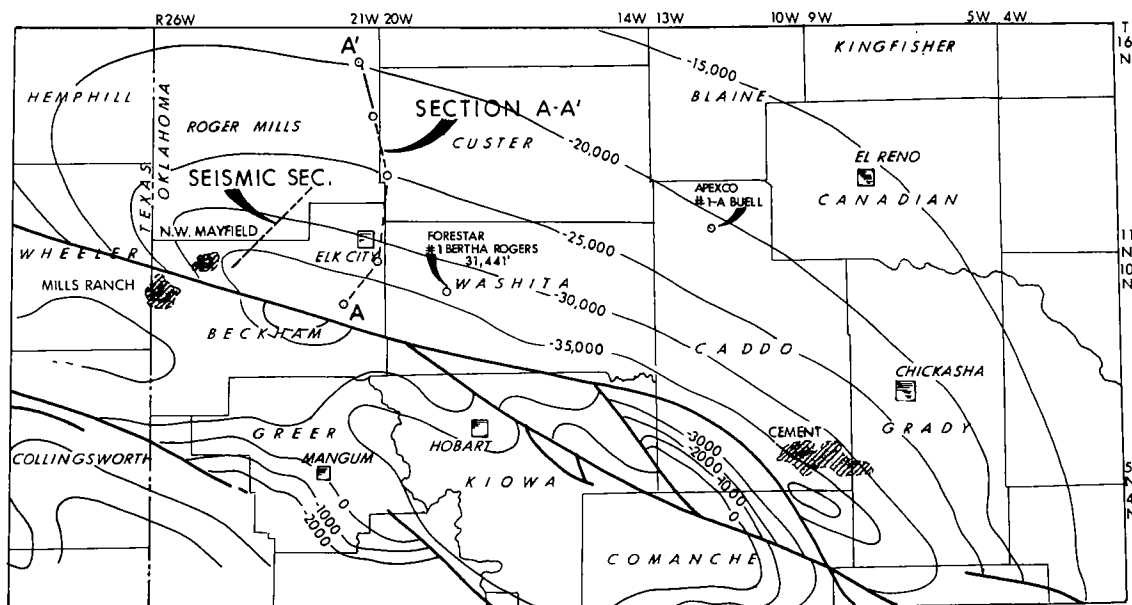


Figure 1. Structure-contour map of the basement surface in the deep Anadarko basin. Elevations in feet below sea level. Section A-A' is shown in Figure 2. Key wells and fields are indicated. Supporting data were derived from the seismic line marked on this map.

pian Chester limestone marker. A worldwide eustatic sea-level fall occurred after deposition of the Chester limestone marker, and stratigraphic units onlap this unconformity. Caney and Goddard shales are present to the south of this section in both wells and outcrop. Goddard equivalents, possibly correlatives of the lower Springer, are present in deeper wells in the Anadarko basin (Fig. 3).

History and Deposition

More than 2,000 ft of onlap occurs in the lower Springer from the basin center (Fig. 2). Springer clastics underlie a thick Morrow shale interval, which can be interpreted as deeper-water fan deposits (Fig. 3). Core study of the upper Springer, Cunningham sandstone in the Apexco #1-A Buell (sec. 10, T. 11 N., R. 12 W.) indicates a submarine-fan origin (Tassone and Visser, 1978). Morrow sandstones above the Pennsylvanian-Mississippian unconformity also underlie thick Morrow shales, and are interpreted as probable submarine-fan deposits (Fig. 2).

More than 6,000 ft of basin subsidence and fill is reflected by these units. This is far more than the onlap resulting from the worldwide eustatic sea-level rise across the Chester and basal Pennsylvanian unconformities. The driving subsidence during this period of worldwide eustatic sea-level

rise must be more than coincidental. It is the thesis of this paper that a starved basin developed due to the relatively slow rate of sediment supply, and low-density-shale deposition led to a crustal density anomaly.

Structural History

Many structural geologists suggest that the Anadarko basin is an aulacogen (Wickham, 1978b), and some suggest strike-slip movement on both the north and south boundaries of the basin (Donovan, this volume). The continued uplift of the southern flank of the basin may be an effect of thermal anomalies developed by the Chesterian and lower Pennsylvanian depositional history. Uplift of the Wichita-Amarillo structural trend at the continental margin, due to this thermal anomaly, may have produced a spreading center, the strike-slip movement on faults bounding the basin, and the continuing subsidence of the Anadarko basin foredeep. The Wichita-Amarillo trend continued to rise from the late Morrowan through the Wolfcampian, and developed >15,000 ft of chert and granite wash in fan-deltas (Fig. 2), resulting in continuing subsidence of the Anadarko basin foredeep. High heat flow has been maintained in the Wichita Mountains granitic crust; the deeper Anadarko basin is characterized by high temperatures due to low-den-

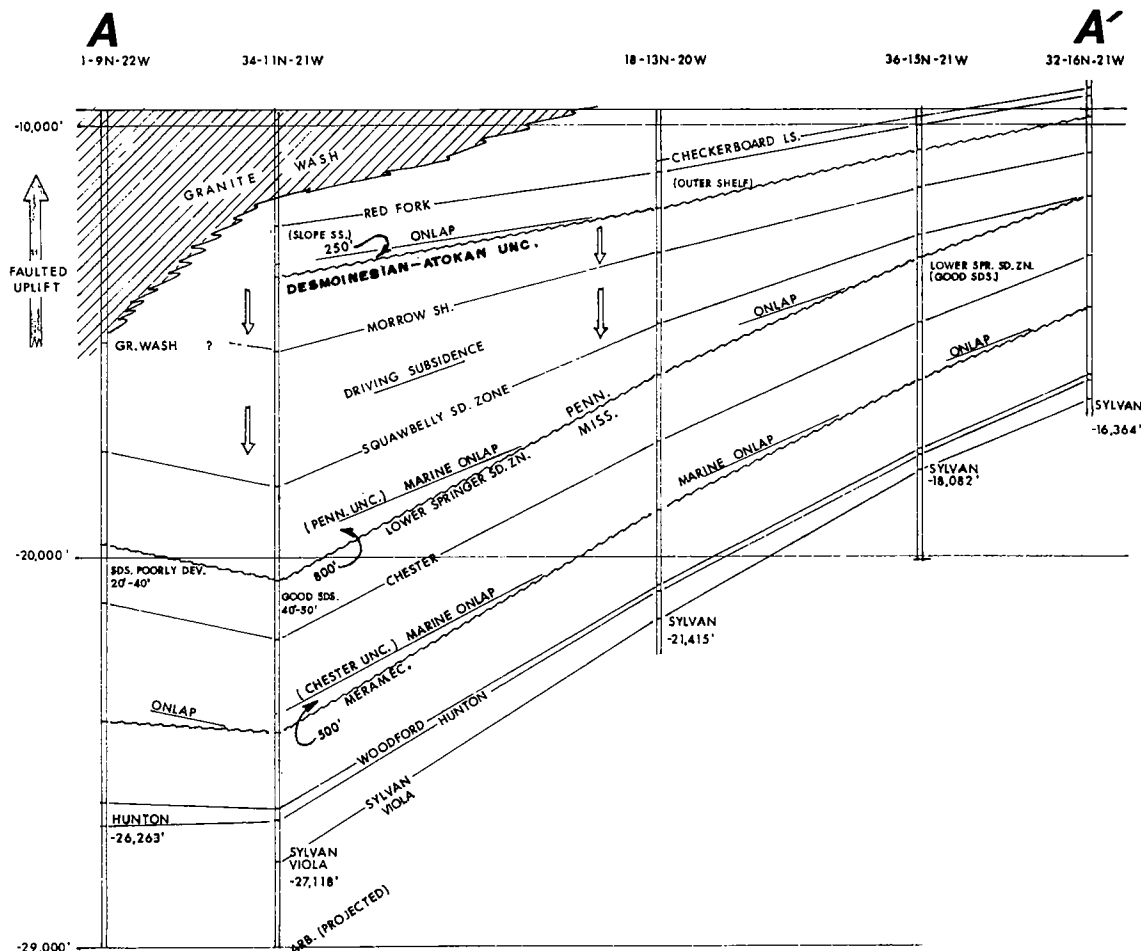


Figure 2. Structural cross section showing patterns of time-rock correlation, unconformities, and onlap. Uplift and the hinge zone are indicated by arrows. Line of cross section shown in Figure 1.

sity and low-thermal-conductivity shales; and the positive gravity anomaly in the Wichita-Amarillo uplift contrasts with the negative anomaly in the Anadarko basin.

DISCUSSION

Controls for cratonic spreading centers have been poorly understood. They may be inferred from regionally gravity data, and subsequent

analysis of fracture patterns, lineaments, and cratonic strike-slip fault movements may provide insight into the structural history of cratonic basins. Uplifts marginal to cratonic basins appear to be closely related to basin depositional histories, and—as has been amply demonstrated by many basin studies—structural and depositional histories are causally interrelated. The new *twist* outlined here is that the depositional history controls the structure rather than the structure controlling the depositional history.

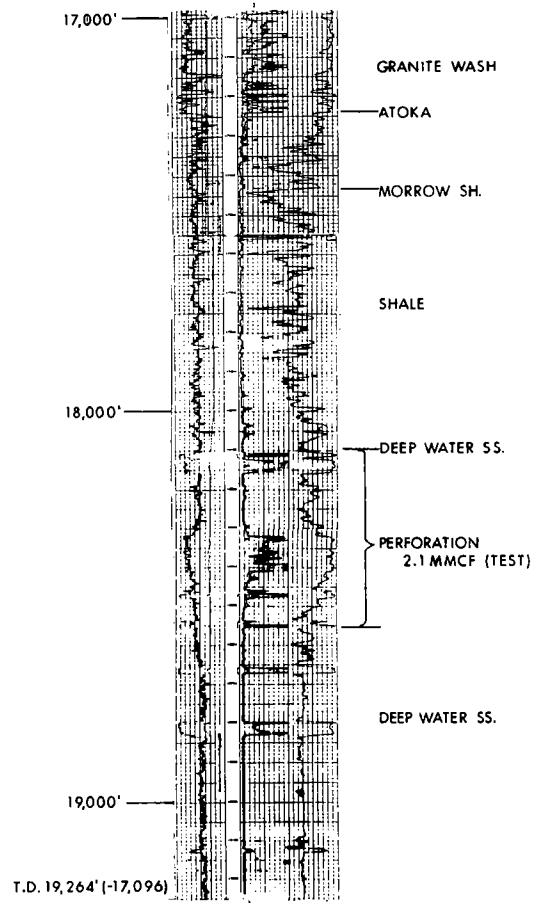


Figure 3. Key well showing deep-basin sub-marine-fan depositional units.

REGIONAL GRAVITY OF THE ANADARKO BASIN AREA AND A MORE DETAILED LOOK AT THE WICHITA FRONTAL FAULT ZONE

S. L. ROBBINS AND MERIDEE JONES-CECIL

U.S. Geological Survey, Denver

G. R. KELLER, JR.

University of Texas, El Paso

We presented poster displays on gravity surveys in and around the Anadarko basin at the Anadarko Basin Workshop in Norman, Oklahoma, on April 5–6, 1988. These displays, not reproduced in the present paper, were the following:

- 1) In color, an isostatic residual-anomaly gravity map of the Anadarko basin and surrounding areas at a scale of 1:1,000,000 (lat. 33°–39°45' N., long. 95°–103° W.);
- 2) In color, a complete Bouguer-anomaly gravity map of the same area and scale as 1;
- 3) A black-line complete Bouguer-anomaly gravity map with station locations on a cultural base of the same area and scale as 1;
- 4) In color, a complete Bouguer-anomaly gravity map of the Lawton and Anadarko 30' × 60' Quadrangles, Oklahoma, at a scale of 1:250,000;
- 5) A black-line complete Bouguer-anomaly gravity map with station locations on a topographic base of the same area and scale as 4;
- 6) In color, an isostatic residual-anomaly gravity map of the same area and scale as 4;
- 7) Two gravity profiles across the Meers fault, northwest of Lawton, Oklahoma, in which observed values include complete Bouguer reductions and isostatic compensation, station spacings ~100 ft apart within 0.5 mi of the fault;
- 8) Two gravity profiles using Bouguer and isostatically reduced data along the north-south COCORP seismic lines 2 and 6 (Brewer and others, 1984), station spacing 1 mi.

Data from >4,000 gravity stations from the Defense Mapping Agency and >8,000 stations from the University of Texas at El Paso were used in the compilation of the gravity maps. In addition, 379 stations from Barrett (1980) and Santiago (1979) were used. Gravity data along the profiles and an additional 77 regional stations were collected by the first two authors in May 1987, using a LaCoste and Romberg gravity meter. (Use of brand names in this report is for descriptive purposes only and does not necessarily constitute endorsement by the U.S. Geological Survey.) The gravity values are based on the

IGSN-1971 datum (Morelli, 1974), and the data were reduced using the GRS-1967 formulas (International Association of Geodesy, 1971), with an assumed average crustal density of 2.67 g/cm³. The terrain effect, out to a distance of 167 km from each station, was removed for most stations using a computer program based on Plouff (1977). The terrain effect for the stations established by Robbins and Jones-Cecil was removed by manually making corrections to a distance of 0.59 km and using the computer program from there out to 167 km. Isostatic corrections were made using a computer program by Simpson and others (1983), assuming an Airy-Heiskanen compensation model. The parameters used for this model were as follows: (1) density of the topographic load, 2.67 g/cm³, (2) depth of the root below sea level, 30 km, and (3) density contrast at depth, +0.4 g/cm³. The color maps of the displays were generated by gridding the data using a computer program by Webring (1981) and plotting the gridded data using Godson's (1980) COLOR program. The black-line gravity maps were contoured using the program "Interactive Surface Modeling" by Dynamic Graphics, Inc. The gravity profiles were plotted using a program by Saltus and Blakely (1983).

Displays 1, 2, and 3 are intended for publication as a U.S. Geological Survey Geophysical Investigations GP-series map.

In comparing the complete Bouguer gravity map (display 2) with the isostatic residual anomaly gravity map (display 1), the most obvious difference is the removal of the decreasing gradient to the west, as seen in display 2. In addition, the isostatic correction enhances a large gravity low over the Ouachita Mountains.

The most prominent features on the maps are gravity highs over the Amarillo-Wichita and Arbuckle uplifts. These highs are similar in magnitude to the highs over the southern end of the Midcontinent gravity high (northern Kansas, northeast corner of these maps). There is a NNE-trending, 25–30 mgal gravity high just east of long. 99°, beginning just north of the Wichita-up-

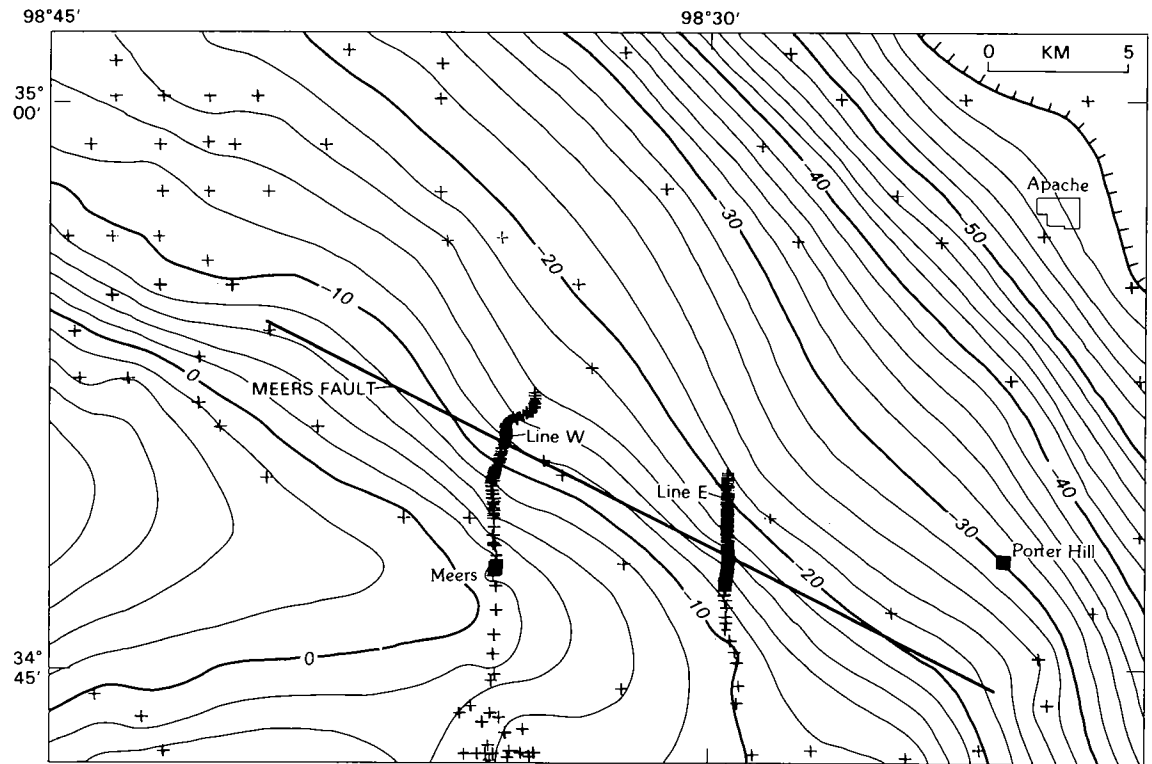


Figure 1 (above and opposite). Complete Bouguer gravity map in the area of the Meers fault northwest of Lawton, Oklahoma, with two Bouguer and isostatic gravity profiles. Contour interval 2 mgal; + = gravity station.

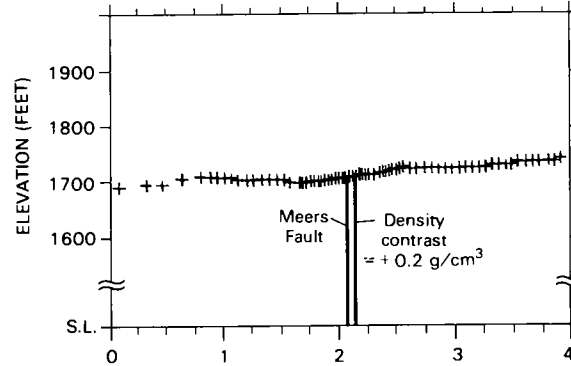
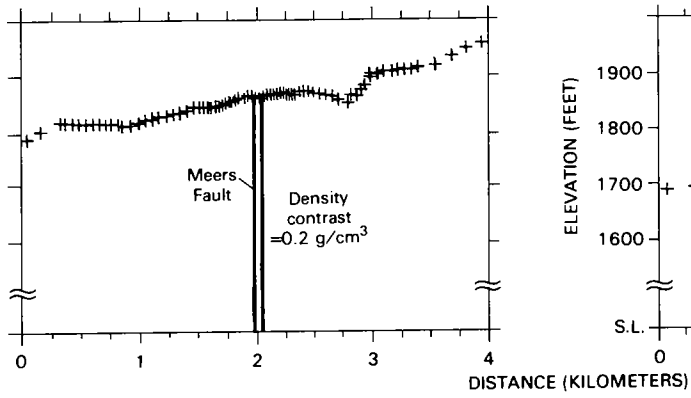
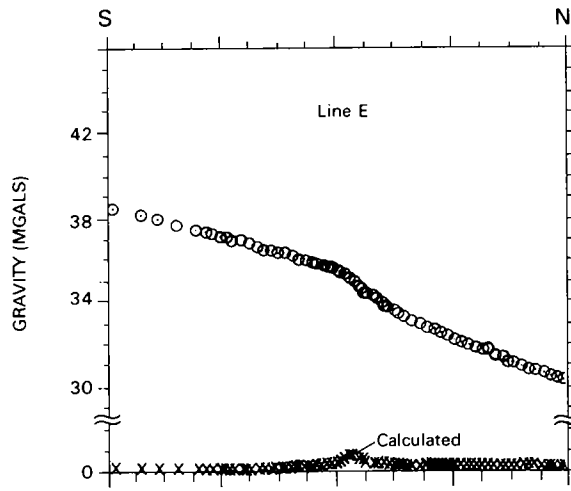
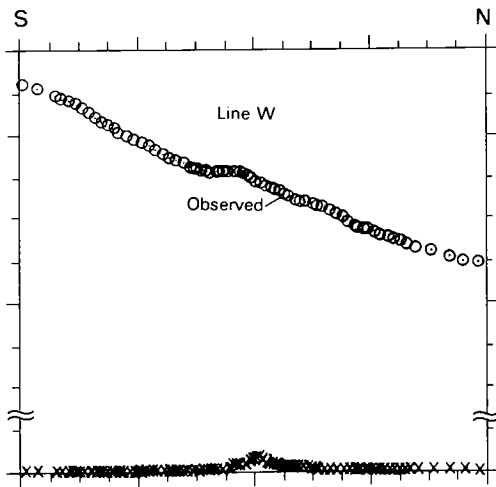
lift gravity high (a little north of lat. 35°). This high is over a deep part of the Anadarko basin, about one degree of longitude west of the Nemaha uplift. This high is more or less on line with the southern end of the Midcontinent high, and may be caused by very deeply buried, high-density volcanic rocks. Such rocks are associated with the Midcontinent high in the Great Lakes region. There are not enough gravity stations in southern Kansas to confirm this connection. The gravity low over the Anadarko basin, as shown on the isostatic residual map (display 1), is similar in magnitude to the lows over the Hollis and Harde-man basins, suggesting an association between them.

One of the prominent features on displays 4, 5, and 6 is a steep gravity gradient which decreases to the northeast away from the Wichita uplift. In the area near the Meers fault, the Wichita uplift gravity high is at its widest, and the gravity gradient on the north side of the uplift is the gentlest. In this area, the gradient changes trend from NE on the east to almost N on the west.

Just north of this direction change, the NNE-trending, 25–30 mgal gravity high begins. The surface geology under this gravity gradient is very complex, including both thrust and strike-slip faults that trend in several directions, and surface outcrops of highly disturbed lower Paleozoic rocks.

The gravity profile along COCORP seismic line 6 (display 8; Brewer and others, 1984) and the aeromagnetic data discussed by Jones-Cecil and Crone (this volume) suggest that a buried gab-broic(?) body may be present in the area of the gentler gravity gradient north of the Meers fault.

Figure 1 of the present report shows 4-km segments of the two gravity profiles centered over the Meers fault (display 7). On both profiles there is a sharp positive gravity anomaly of ~ 1 mgal centered roughly over the fault. This anomaly can be approximated by a 70-m-wide, dike-like zone along the fault, extending vertically down to sea level, with a density increase of $+0.2$ g/cm³.



CONSTRAINTS ON THE ANADARKO BASIN-WICHITA UPLIFT BOUNDARY INTERPRETED FROM AEROMAGNETIC DATA

MERIDEE JONES-CECIL AND ANTHONY J. CRONE
U.S. Geological Survey, Denver

Modeling and interpretation of aeromagnetic data across the transition between the Anadarko basin and the Wichita uplift in the vicinity of the scarp on the Meers fault (Fig. 1) constrains structural relationships and lithologic contrasts at this boundary. We digitized aeromagnetic data from the map based on a detailed survey flown in 1954 (U.S. Geological Survey, 1975). The flight lines for this survey were oriented east-west, spaced 0.25 mi apart, and flown 500 ft above the ground. The digitized data were gridded using a minimum-curvature gridding program (MINC; Webring, 1981) and plotted as a color-shaded relief map using an unpublished program written by M. W. Webring. The color-shaded relief map was shown in the Anadarko Basin Workshop poster session. Figure 2 is a generalized contour map made from the digitized data, using the unpublished program CONTOUR3, written by R. H. Bracken, R. H. Godson, and M. W. Webring.

The main structure between the Anadarko basin and the Wichita uplift is the Wichita frontal fault system, which extends NW-SE for >300 km across southwestern Oklahoma (Harlton, 1963). The Meers fault (Meers Valley fault of Harlton) is one of the major faults in this system, and recent studies have demonstrated Holocene movement on at least a 26-km-long segment of this fault (Ramelli and Slemmons, 1986). Our study examines the relationships between the Meers fault as mapped at the surface and buried structures in the upper crust. Interpretation of the aeromagnetic data establishes important constraints on the subsurface location and dip of the Meers fault.

As previously pointed out by Purucker (1986), the Meers fault is expressed as a well-defined NNW-trending boundary between the high-amplitude, short-wavelength aeromagnetic signature of igneous rocks in the Wichita uplift to the southwest and the low-amplitude, long-wavelength signature of the rocks to the northeast. As mapped by Ramelli and Slemmons (1986), the continuous surface scarp extends southeast of point *a* to approximately point *d* as shown in Figure 1. The aeromagnetic data suggest that the fault continues northwest of point *a* and breaks into three or more splays. At point *b* (Fig. 1), the splays cut through a lobe of rock with a magnetic signature similar to that of the igneous rocks of

the Wichita Mountains. Farther northwest (near point *c*), the sharp contrast in the magnetic signature across the fault diminishes where the continuation of the fault is inferred from drill data (Harlton, 1963). In this area, the magnetic data suggest that the fault curves to a more northerly trend, and a subsidiary, more westerly trending branch enters the block of the Wichita uplift. Near the southeast end of the scarp (point *d*), the aeromagnetic expression is subdued (Fig. 2) because a very magnetic body merges with the Wichita uplift from the north-northwest. This magnetic body is expressed on the surface as outcrops of Carlton Rhyolite. The aeromagnetic map suggests that the exposed rhyolite is the tip of a large body of high-susceptibility rock with magnetic properties similar to those of the highly magnetic rocks in the Wichita uplift.

Magnetic models along lines A-A' and B-B' (Fig. 2), determined using the SAKI modeling program (Webring, 1985), yield a two-dimensional, depth-versus-length picture of the magnetic relationships across the boundary between the Anadarko basin and the Wichita uplift (Figs. 3 and 4). As with any generalized linear inversion, solutions are non-unique but do provide constraints on permissible variations in the shape and susceptibility of rock bodies along the profiles. We started with simple geologic models, using a generalized geologic map and schematic cross section of the Wichita uplift (Gilbert, 1982), a near-vertical Meers fault (Harlton, 1963), and a moderately SW-dipping Mountain View fault (Brewer and others, 1983). We used susceptibility values of various rock types in the range of values determined by Ku and others (1967), and from our measurements of 24 samples of Cambrian, Ordovician, and Permian sedimentary rocks and three samples of the igneous rocks.

The initial models fit the data quite well, with a few noteworthy exceptions. The areal extent and high susceptibility of the magnetic body beneath the Carlton Rhyolite north of the Meers fault was unexpected. The Stanolind 1 Perdasofpy well, located close to profile B-B' on the basinward flank of the magnetic body, penetrated granite at a depth of 1.7 km and basalts and spilites at a depth of 2.7 km. In our model, however, the top of the magnetic body is ~2 km deep where the 1 Perdasofpy well projects onto the

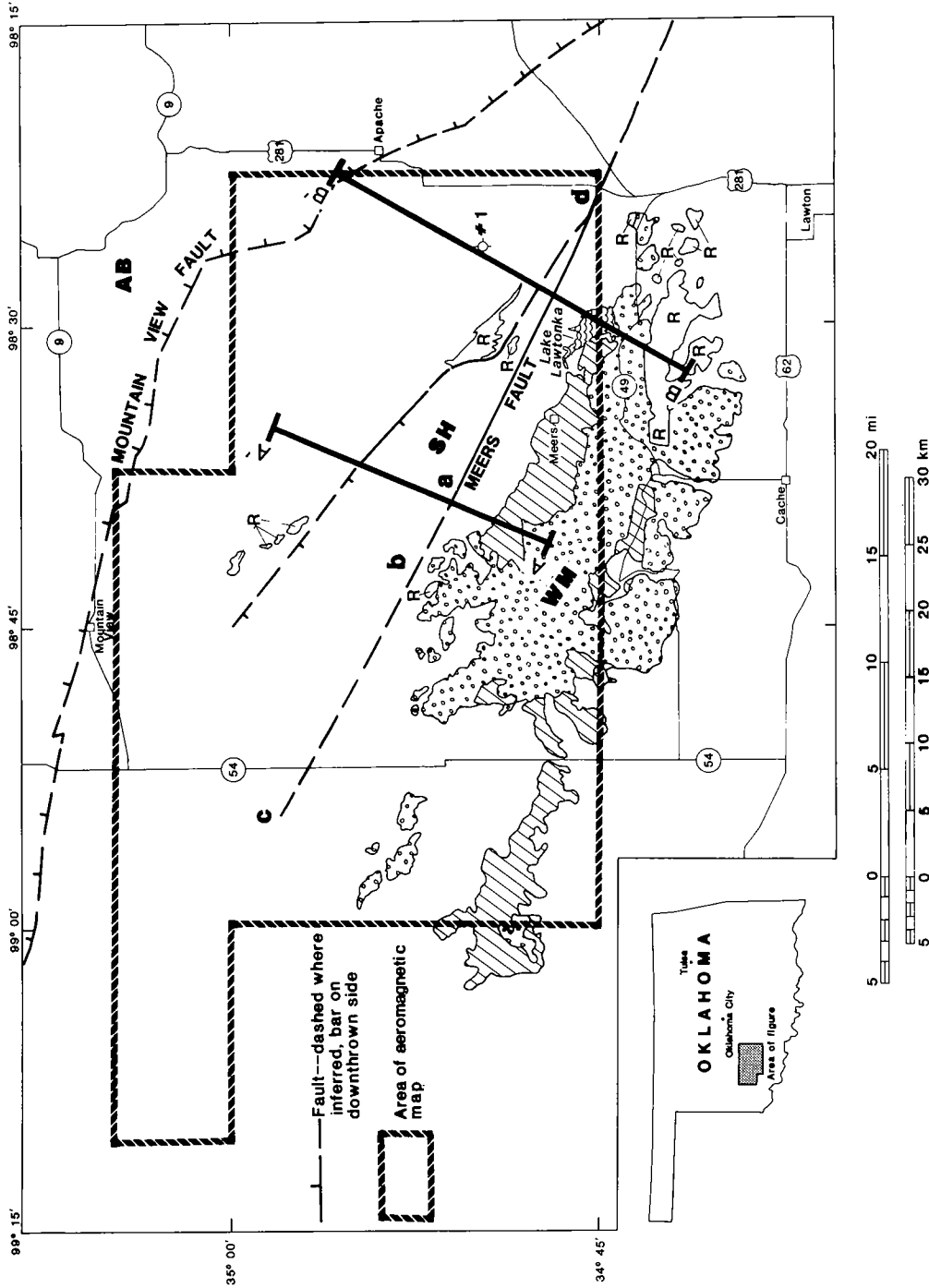


Figure 1. Generalized structural and igneous geologic map of study area (after Havens, 1977; Carr and Bergman, 1976; and Harlton, 1963). Diagonally ruled areas = Raggedy Mountain Gabbro Group; stippled areas = Wichita Granite Group; R = selected outcrops of Carlton Rhyolite. #1 is location of the Stanolind 1 Perdasofpy well. SH = Slick Hills (Cambrian and Ordovician sedimentary rocks); WM = Wichita Mountains; AB = Anadarko basin. Points a, b, c, and d are referred to in text. Aeromagnetic data along A-A' and B-B' are modeled in Figures 3 and 4. Late Paleozoic vertical displacement on the Meers fault was down-to-the-north; Holocene displacement was down-to-the-south.

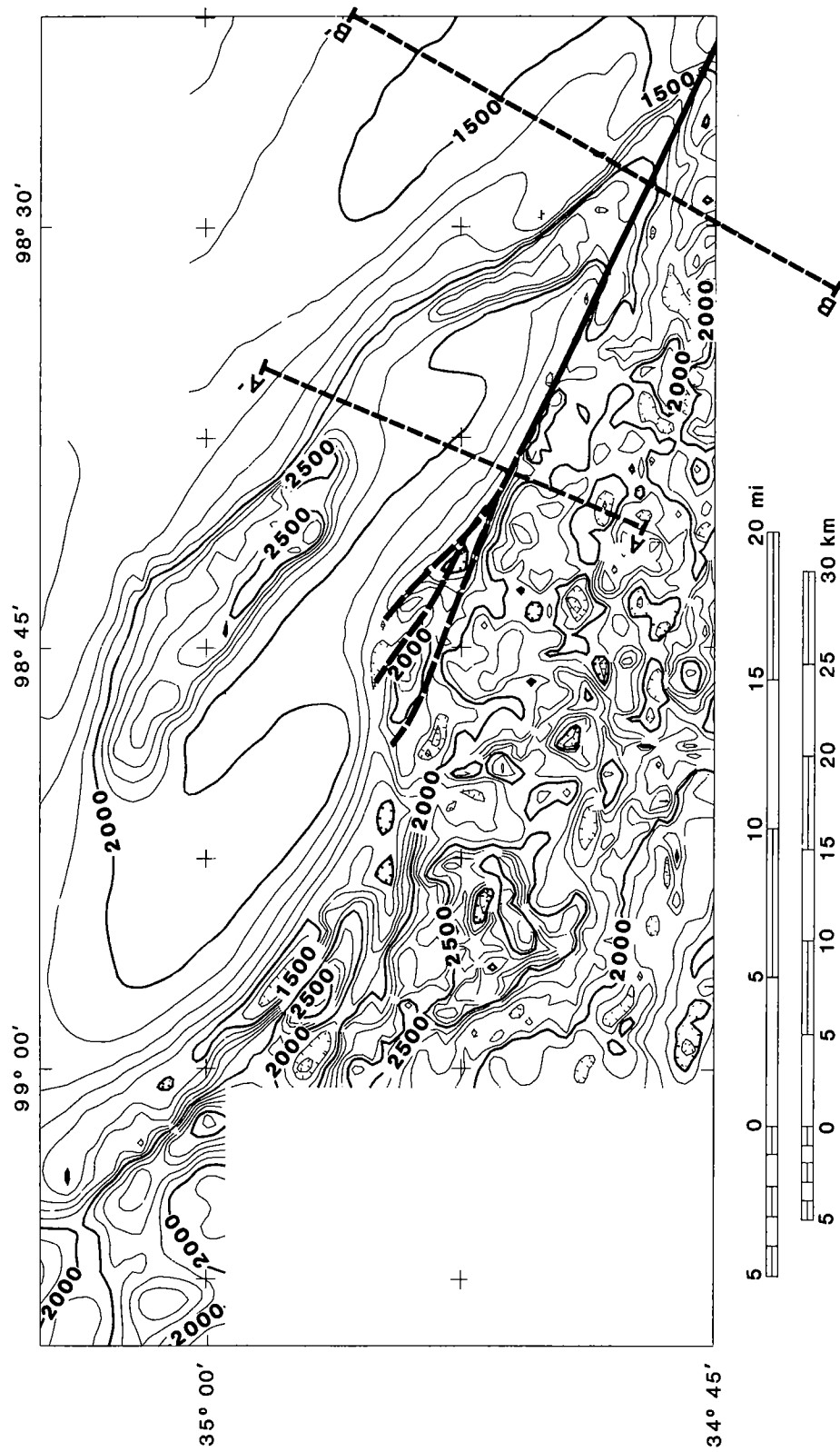


Figure 2. Generalized contour map of aeromagnetic data. Contour interval 100 nTesla. Holocene rupture of Meers fault shown as solid line. Interpreted northwest subsurface extension of surface rupture shown as long dashes. Profiles A-A' and B-B' are modeled in Figures 3 and 4.

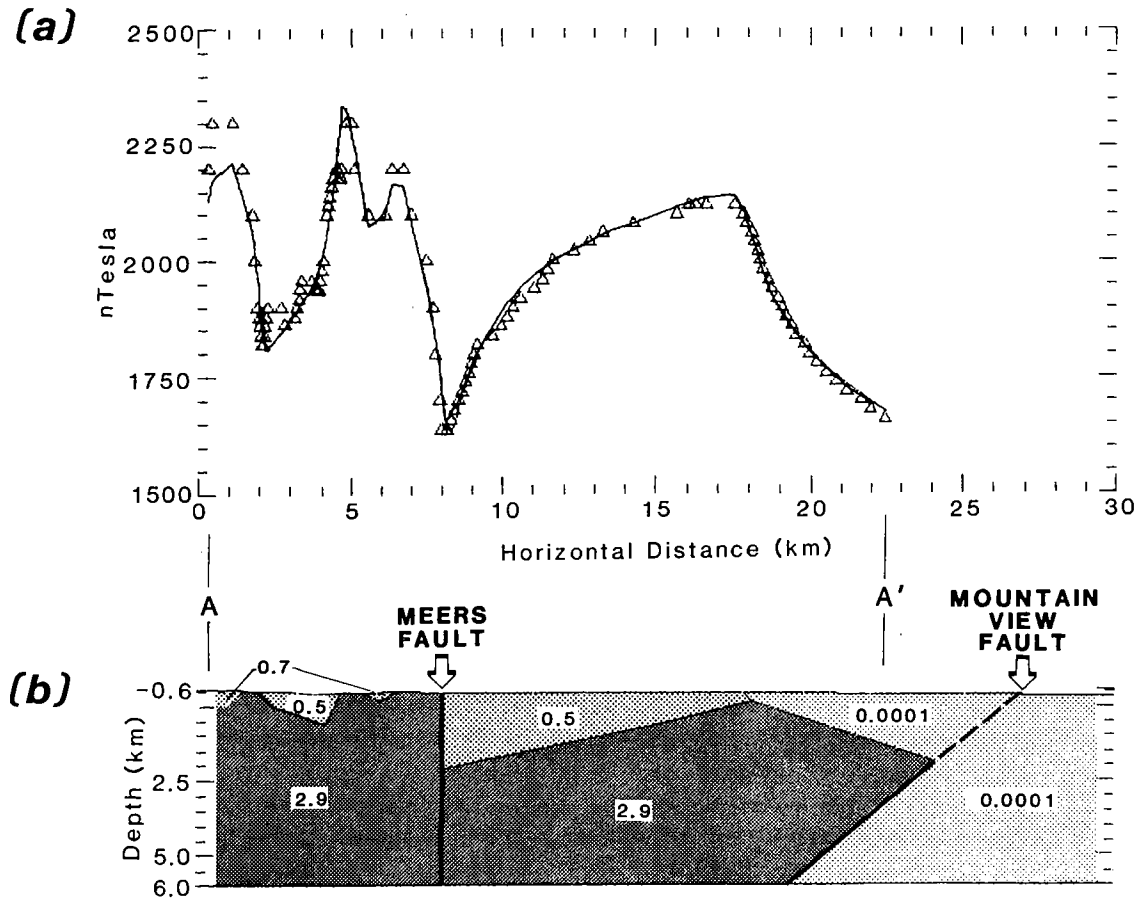


Figure 3. *A*—Plot of observed magnetic values (triangles) and curve calculated for model along profile A-A'. *B*—Cross section of model along profile A-A'. Numbers in bodies are susceptibilities in SI units $\times 10^{-2}$. Dark stippling indicates bodies with susceptibilities in the range of highly magnetic, mafic rocks. Lighter stippling and susceptibilities of 0.5 to 0.7×10^{-2} SI indicate probable granitic or rhyolitic rocks. All susceptibilities $< 0.001 \times 10^{-2}$ SI are effectively nonmagnetic sedimentary rocks. Horizontal and vertical scales equal; negative depths indicate elevation above sea level.

line of the profile (Figs. 1 and 4). The aeromagnetic map and the two profiles show that the configuration of the magnetic body north of the Meers fault changes along the trend of the fault. In profile A-A' (Fig. 3), the top of the body is ~ 2 km deep and does not rise close to the surface for ~ 10 km to the northeast. In profile B-B' (Fig. 4), the magnetic body is close to the surface directly northeast of the Meers fault. For the most part, the susceptibilities in our models closely correspond to measured susceptibilities. However, the susceptibility of the more-magnetic part of the Wichita uplift, and of the buried magnetic body northeast of the Meers fault, must be $\sim 2.9 \times 10^{-2}$ SI units or greater to fit the observed data. This susceptibility is at the high end of the range of observed values (Ku and others, 1967).

After fitting the observed data with geologically

acceptable models, we then perturbed the models to examine the effects of changing fault geometries. We modeled both a moderately (45°) N- and S-dipping Meers fault, but both perturbations fit the data poorly, especially for profile A-A', where the susceptibility contrast is very large. The results constrain the Meers fault to a near-vertical dip. In addition, we examined the effect of changing the attitude of the Mountain View fault, another major fault in the frontal fault system. In profile A-A' the magnetic data permit very little change in the location or dip of the Mountain View fault. In profile B-B' the data allow more variability, but they still require a moderate southerly dip on the Mountain View fault.

We varied the susceptibilities of different bodies to test the effect on the models. In profile

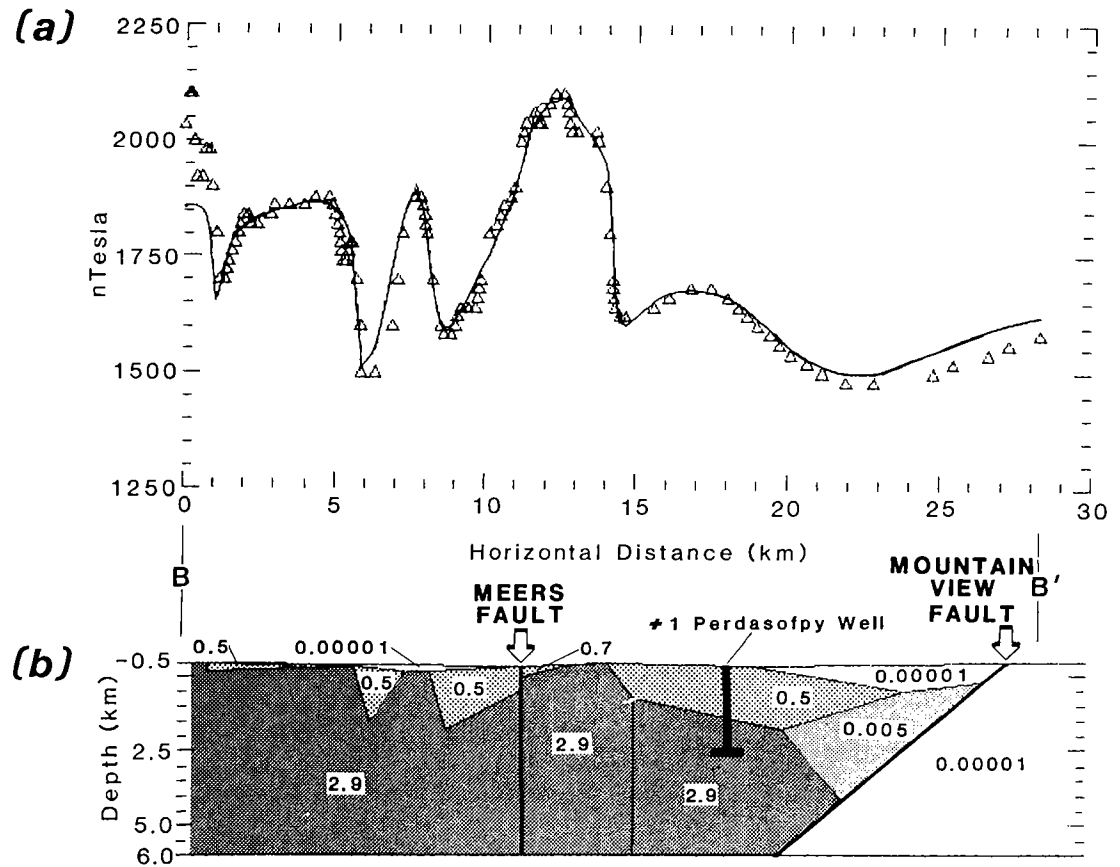


Figure 4. A—Plot of observed magnetic values (triangles) and curve calculated for model along profile B-B'. B—Cross section of model along profile B-B'. Numbers shown in bodies are susceptibilities in SI units $\times 10^{-2}$. Dark stippling indicates bodies with susceptibilities in the range of highly magnetic, mafic rocks. Lighter stippling and susceptibilities of 0.5 to 0.7×10^{-2} SI indicate probable granitic or rhyolitic rocks. Susceptibilities of $\sim 0.005 \times 10^{-2}$ SI are in the upper range of susceptibilities measured from samples of Cambrian, Ordovician, and Permian sedimentary rocks from the area. All susceptibilities $< 0.001 \times 10^{-2}$ SI are effectively nonmagnetic sedimentary rocks. Stanolind 1 Perdasofpy well projected onto plane of cross section. Horizontal and vertical scales equal; negative depths indicate elevation above sea level.

A-A', we initially modeled the material above the highly magnetic body immediately northeast of the Meers fault with a susceptibility in the range of rhyolite (0.5×10^{-2} SI). Reducing this susceptibility to the range of the Cambrian-Ordovician sedimentary rocks (0.001×10^{-2} SI) had a minimal effect on the model. Thus, the material overlying the highly magnetic body in the vicinity of the Slick Hills could be either sedimentary rock, rhyolite or—most likely—some of each.

Future studies will combine gravity data with our models, incorporate additional well information, and constrain relations by using seismic-reflection data. These combined sources of information will improve constraints on interpretations of structural relations within the Wichita frontal fault system. Nevertheless, these preliminary

models and interpretations of the aeromagnetic data provide valuable new insights into the geometries and lithologies of rocks within the fault system. The aeromagnetic data indicate the presence of a large magnetic body basinward of part of the Meers fault. The northwestern termination of Holocene surface rupture as mapped by Ramelli and Slemmons (1986) may be controlled by the fault breaking into multiple splays. The splays enter an aberrant, basinward lobe of probable igneous material. Whether the lobe is the cause or the effect of the splaying is not clear, but it seems likely that the lobe affects the geometry and behavior of this part of the fault. Our models of the aeromagnetic data require a near-vertical Meers fault and a moderately SW-dipping Mountain View fault.

GENETIC-SEQUENCE STRATIGRAPHY OF THE UPPER DESMOINESIAN OSWEGO LIMESTONE ALONG THE NORTHERN SHELF MARGIN OF THE ANADARKO BASIN, WEST-CENTRAL OKLAHOMA

TIMOTHY P. DERSTINE

Southern Methodist University

Abstract.—A detailed-sequence stratigraphic study was conducted for the Oswego limestone, an upper Desmoinesian (Pennsylvanian) hydrocarbon reservoir along the Putnam trend in Dewey and Custer Counties, Oklahoma, in the vicinity of the northern shelf break of the Anadarko basin. Descriptions of nine cores, detailed correlations of 160 well-logs, and facies maps of Oswego limestone, supplemented by seismic data along dip profile, were used to define three stratigraphic sequences and their associated depositional facies (Fig. 1). These distinctive lithofacies include: (1) shelf wackestone-packstones, (2) phylloid-algal-mound deposits, (3) fringing grainstone-packstones, (4) basin/basin-margin shales and mudstones, (5) shelf mudstone/shales, (6) spicular carbonates, and (7) calcareous terrigenous clastics. The limestone and related sedimentary facies form three stratigraphic sequences bounded by conformities whose correlative unconformities must be present in the depositional up-dip, landward position. Each stratigraphic sequence contains a Lowstand Systems Tract (LST), an overlying Highstand Systems Tract (HST), and a condensed section (shale/mudstone facies), identified on the gamma-ray logs as radioactive kicks that can be correlated between wells (Fig. 2).

The well-defined stratigraphic sequences—determined from detailed well-log correlations that consider genetic units—illustrate the evolution of these carbonate and local clastic deposits along Oswego shelf-to-basin profiles as a consequence of sea-level oscillations and slow subsidence. Repeated successions of shelf wackestone-packstones, phylloid-algal-mound deposits with fringing grainstone-packstones and scattered spicular carbonates, and basin shales are the depositional facies that make up the Lowstand Systems Tract. The LST is capped by a thin shale that reflects an episode of rapid relative sea-level rise and flooding of the Oswego carbonate shelf. This episode represents the time of deposition of the condensed section and the Highstand Systems Tract. The black shales/mudstones deposited during this rapid flooding event form a problematic downlapping unit, because terrigenous sediment evidently was supplied from both the Oklahoma-Kansas area to the north and the Wichita-Amarillo high to the south. The HST is very thin, if present at all, within the sequences. Deposits in the HST are thin mud drapes found above the condensed section that indicate drowning or backstepping of carbonate sources.

The Putnam trend within the study area produces oil and gas from the phylloid-algal-mound (bank) deposits that formed at the shelf margin. These algal-mound deposits contain vuggy and moldic porosity and are bound by tightly calcite-cemented facies. To the north, the mounds are bounded by the wackestone-packstones of shelf facies, and to the south by the fringing grainstone-packstones that formed on the seaward margin in relatively high-energy environments. The algal-mound deposits with sufficient porosity and permeability for oil and gas production are contained almost exclusively in the LST.

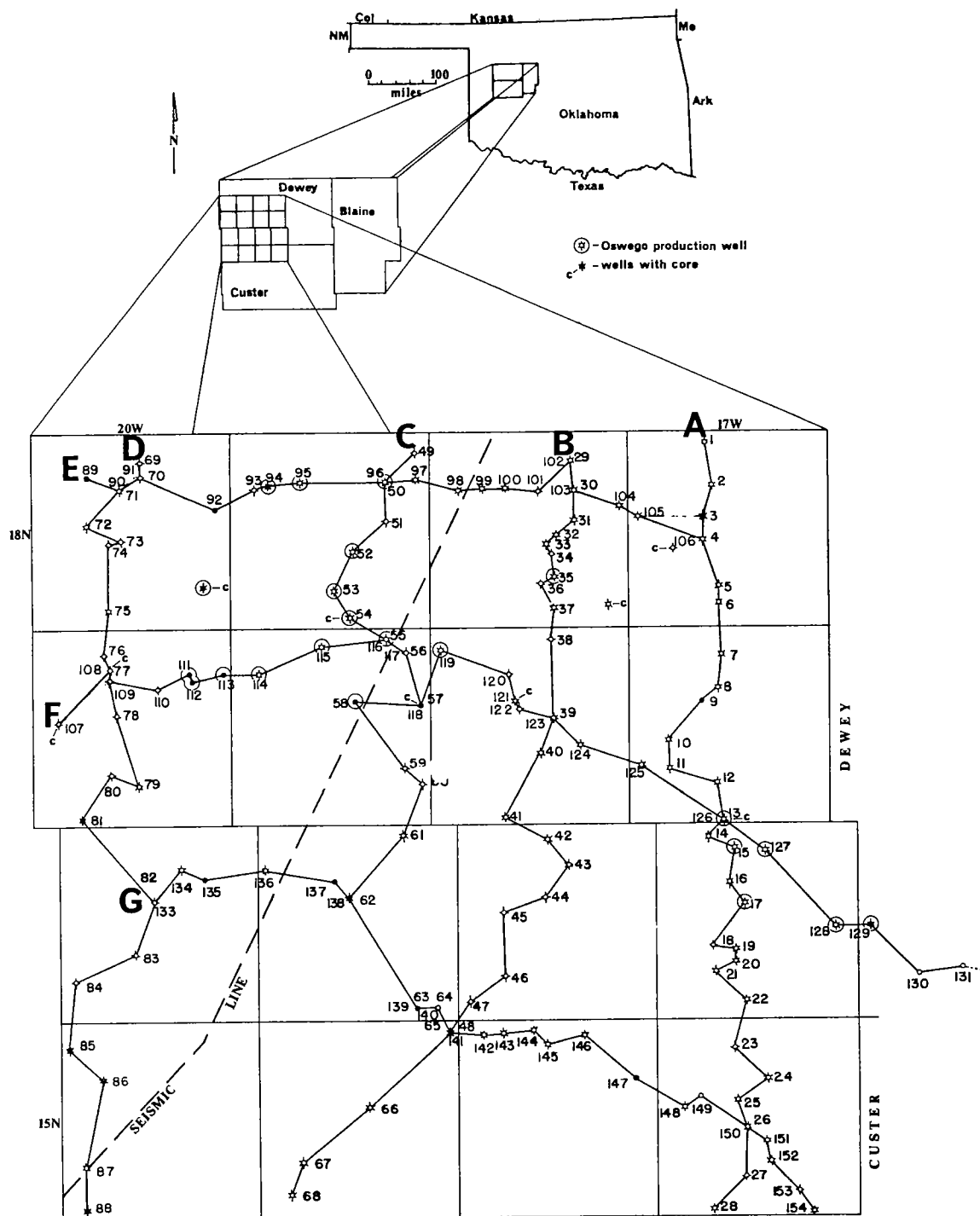


Figure 1. Location of study area showing distribution of well logs, core, and seismic line.

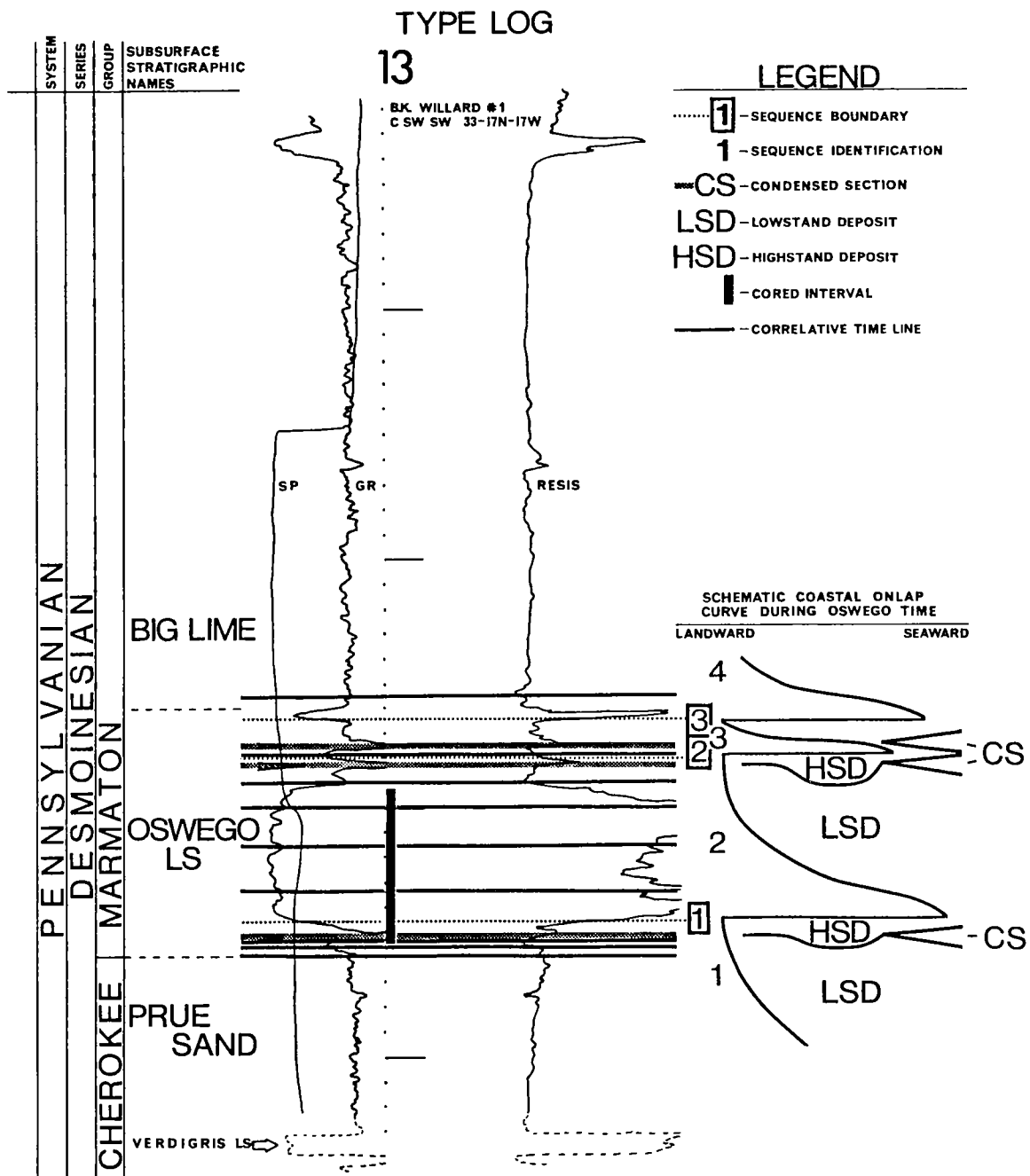


Figure 2. Type log for the Oswego limestone, showing the subsurface nomenclature of Desmoinesian strata in the Anadarko basin. A schematic coastal onlap curve and sequence stratigraphic subdivisions are given for the Oswego study interval. The Oswego is defined by three principal stratigraphic sequences separated by sequence boundaries.

ANALYSIS OF SEDIMENTARY FACIES AND PETROFACIES OF LOWER MORROWAN-UPPER CHESTERIAN SANDSTONES, ANADARKO BASIN, OKLAHOMA

C. WILLIAM KEIGHIN AND ROMEO M. FLORES

U.S. Geological Survey, Denver

Three major lithofacies have been identified within the Morrow (Pennsylvanian) and Springer (Pennsylvanian–Mississippian) units, in core from 30 drill holes ranging from the Oklahoma Panhandle to the southwestern portion of the Anadarko basin. The study included inspection of ~6,500 ft of core, examination of ~100 thin sections, and a scanning-electron-microscope study of butts of the material used for thin-section preparation. The lithofacies identified are (1) fluvial-influenced coastal, which includes the deltaic facies described by Swanson (1979), (2) tidal-influenced nearshore, and (3) mixed, which shows mixed tidal and nontidal marine influence. Our interpretation is supported by the investigations of Moore (1979), Haiduk (1987), and Swanson (1979). The fluvial-influenced coastal facies is restricted to the northwestern (Panhandle) portion of the Anadarko basin.

The fluvial-influenced coastal-facies sequence consists of sandstones, siltstones, mudstones, coals, carbonaceous shales, and limestones, representing a variety of facies types, including (1) distributary-channel/overbank, (2) interdistributary bay, (3) crevasse splay, and (4) marsh-swamp facies types. These facies types include features seen in modern and Carboniferous delta-plain deposits.

The tidal-influenced nearshore-facies sequence is made up of (1) intertidal, (2) tidal-channel, (3) subtidal-bar, and (4) lagoon-facies types. The lithology and sedimentary structures typically identified in intertidal, tidal-channel, and subtidal facies types are shown in Figure 1. The core sample in Figure 2 illustrates the facies sequence representing parts of the intertidal and tidal-channel facies types. Although cores from ~30 drill holes were examined, it was only in this core that a sequence of red sandstones and siltstones alternating with gray fine-grained sediments and sandstones was observed. The occurrence of cyclic intervals of variegated sandstones and siltstones interbedded with mudstones containing mud-crack structures suggests sea-level fluctuations and subaerial exposure.

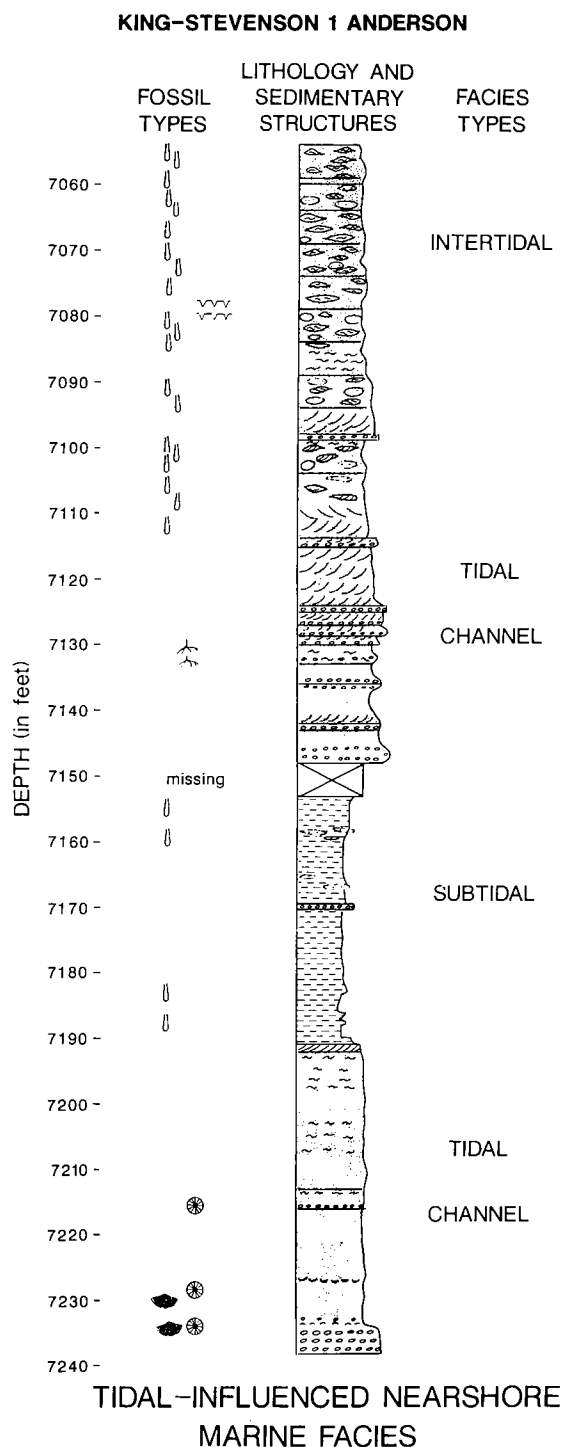
The mixed tidal-nontidal marine-facies sequence includes clastic-dominated shallow-marine facies types comprising interbedded mud-

stones, siltstones, and sandstones, as well as carbonate-dominated shallow-marine facies types consisting of interbedded limestones, sandstones, siltstones, and mudstones. The facies types are interpreted to reflect a mixed clastic-carbonate shallow-marine or open-shelf-platform environment typical of Carboniferous deposits.

Effects of diagenetic alteration are seen in all samples, which span a depth range of approximately 4,000–18,000 ft (see also Adams, 1964; Al-Shaieb and Walker, 1986; and Haiduk, 1987). Samples were studied in thin sections, and with the scanning electron microscope, to determine types and extent of diagenetic modification and the influence of diagenesis on potential reservoir properties of the sandstones. Signs of mechanical compaction, which serves to reduce porosity, are seen in all examined samples; these include deformed labile rock fragments, deformed glauconite grains, and stylolites. Chemical diagenesis is widespread—indicated by silica or carbonate cements (calcite and/or ankerite) and formation of various clay minerals, including chlorite, kaolinite, and illite. Cementation by iron-bearing carbonates (probably predominantly ankerite) has eliminated porosity in some of the sandstones, although the distribution of carbonate cements is highly variable. The most significant effect of diagenesis on reservoir properties is the generation of secondary porosity in the sandstones; most of the porosity identified in the sandstones is secondary. Some effects of chemical diagenesis are illustrated in Figure 3.

DISCUSSION

The three major lithofacies identified in this investigation are similar to those identified by Moore (1979) and Swanson (1979). The fluvial-influenced coastal and tidal-influenced nearshore lithofacies, found in and near the panhandle portion of the Anadarko basin, consist mainly of fluvial-lower-delta plain and intertidal-tidal channel-subtidal deposits. The mixed tidal-nontidal marine lithofacies, found in the deeper, southeastern, portion of the Anadarko basin, consists



primarily of clastic- and carbonate-dominated shallow-marine deposits.

It was not possible to clearly differentiate the sandstones on the basis of their petrofacies and diagenetic properties. The effects of both physical compaction and chemical diagenesis are seen throughout all the samples studied. It appears that the most widespread and probably most important effect of chemical diagenesis was the formation of secondary porosity through dissolution of glauconite grains, labile rock fragments, and to a limited degree, detrital framework grains.

Figure 1. Tidal-channel, intertidal, and subtidal facies types which occur within the tidal-influenced nearshore lithofacies, King-Stevenson 1 Anderson drill hole, sec. 26, T. 25 N., R. 20 W.



Figure 2. Core material from the King-Stevenson 1 Anderson drill hole, illustrating facies sequence and types. Depth range of core is approximately 7,080–7,114 ft.

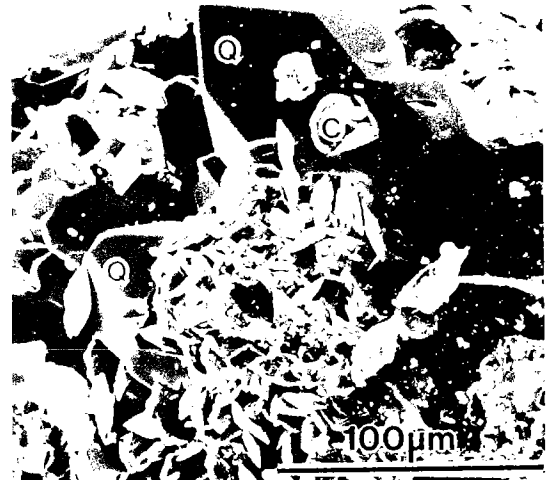


Figure 3. Scanning electron micrograph of a sandstone sample from the King-Stevenson 1 Anderson drill hole at a depth of 7,095 ft, illustrating overgrowths of authigenic quartz (Q), and an authigenic carbonate (C)—probably ankerite. This sample is not tightly cemented, but pores are typically small.

STRUCTURAL ANOMALIES IN THE DEEP ANADARKO BASIN, CADDO AND CANADIAN COUNTIES, OKLAHOMA

JOCK A. CAMPBELL

Oklahoma Geological Survey

HAROLD MCINTIRE AND RICHARD A. HAINES

Geological Data Services, Dallas

SUMMARY

Regional correlation studies by McIntire have resulted in the identification of repeated strata in several units of the Cherokee and Marmaton Groups (Desmoinesian) in four wells in the deep Anadarko basin. Vertical separations of ~30 ft to at least 120 ft occur at depths of 10,000–10,700 ft.

Interpretation of structure from chance drill-hole data is ambiguous, because the strike and dip of penetrated faults cannot be known without more detailed information. Furthermore, it is not known whether the four drill holes penetrate one, two, three, or four faults, or whether the faults have the same or different strikes. In the absence of knowledge of the number and geometry of the faults, interpretations of their origin and significance are speculative. However, it may be instructive to analyze these anomalies for their possible value to better understanding of basin structure. The present knowledge of regional structure limits the possibilities for the probable geometry of the faults.

For the purpose of this investigation it is assumed that faults strike WNW, parallel to the major structural grain of the Wichita Mountains and much of the basin (Harlton, 1972; Evans, 1987; Fig. 1). Repetition of strata indicates reverse separation in all four wells. Misinterpretation of structure due to crooked wells is unlikely, as surveys taken during the course of drilling demonstrate that the maximum deviation from vertical in any of the subject wells in the faulted interval is only 1.5°.

With the above evidence, two major possibilities as to slip of the faults exist: strike slip, or reverse dip slip, although each may also include some element of the other, resulting in oblique slip. If strike-slip is responsible for the observed structural relations, the fault or faults may dip either N or S. However, the slip would have to be left-lateral in order to move shallower structure contours into juxtaposition with deeper ones (Fig. 2). Structure contours (Fritz, 1978) indicate a dip of ~7° SW in the subject area. However, dip parallel to the strike of the faults is much less, ~3°

N. 70° W. Accordingly, a left horizontal slip of ~2,290 ft (0.43 mi) would be required to produce vertical separation of 120 ft. Left-lateral displacement is consistent with interpretation of structures to the southeast by Wickham (1978a), Harding (1974), and Harding and others (1983).

If true reverse faults are responsible for the observed structural relations, then the separation may be up on either the north or the south side of the faults. However, considering the structural style of the region, it is difficult to develop a process, or a model for the occurrence of significant up-to-the-north faults. Down-to-the-north reverse (overthrust) faulting is the major structural style of the Wichita Mountains front, and such faults are well documented in the region (Harlton, 1972; Evans, 1987); blind thrusts occur in the basin where latest Pennsylvanian and Permian strata have overlapped them (Brewer, 1982; Brewer and others, 1983). Therefore, it is concluded that separation on the faults is down to the north, and that the dip is S. Although some element of strike slip is possible, and would contribute to reverse separation in the area, the subject faults most likely are primarily overthrust, reverse-slip faults. The Mills Ranch field (Jemison, 1979; Petersen, 1983) and West Mayfield and Erick fields (Solter, 1980) are on structural highs associated with deep thrust faults. The geologic structure is similar in the Gotebo area (Takken, 1963) and in the vicinity of West Sentinel field (Gelphman, 1959). Many other fields in the basin occur on the relatively uplifted, south sides of blind faults that probably have similar overthrust geometry. Among these are the Cement area (Herrmann, 1961; Takken, 1974) and Knox area (Petersen, 1983). Wroblewski (1970) illustrated the structure of the Elk City field, which can only have been produced by a blind thrust. The Hunton structure-contour map of the Gageby Creek field (Young, 1977) also suggests overthrust structure. Low-angle thrusting may be much more common in the basin than previously believed, but there is little documentation of that in the public domain. Furthermore, the interpretation of seismic data may be too ambiguous to be cer-

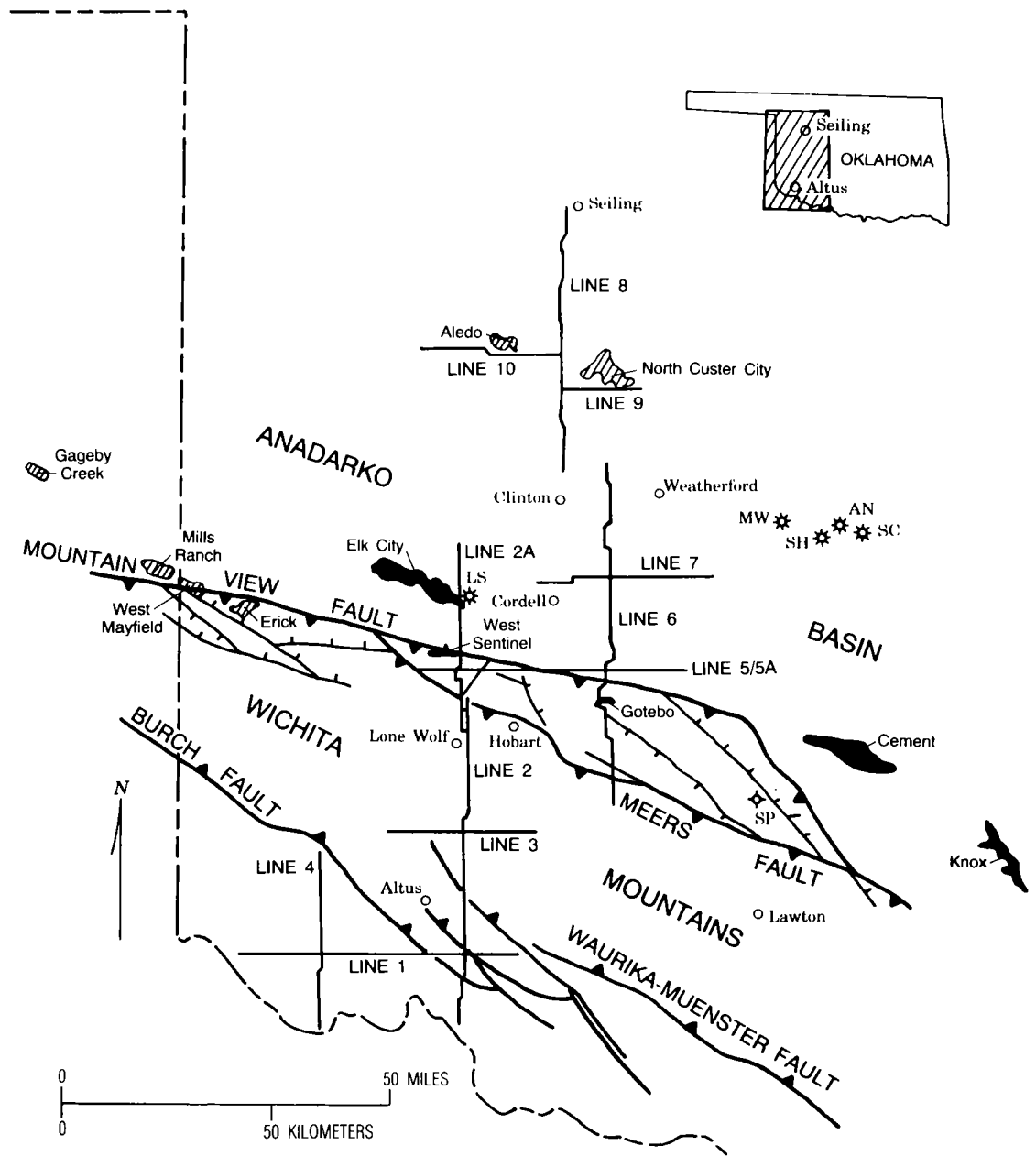


Figure 1. Map of part of the Anadarko basin in western Oklahoma. Illustrated are significant faults, wells, towns, and lines for composite COCORP seismic profile. Oil fields solid; gas fields hachured (modified after Brewer, 1982). Wells: MW, Mustang 1-7 West; SH, Slawson 3-34 Hall "B"; AN, An-Son 1 Nitzel; SC, Sun B-2 Chiles; LS, Lone Star 1 Rogers; SP, Stanolind 1 Perdasofy.

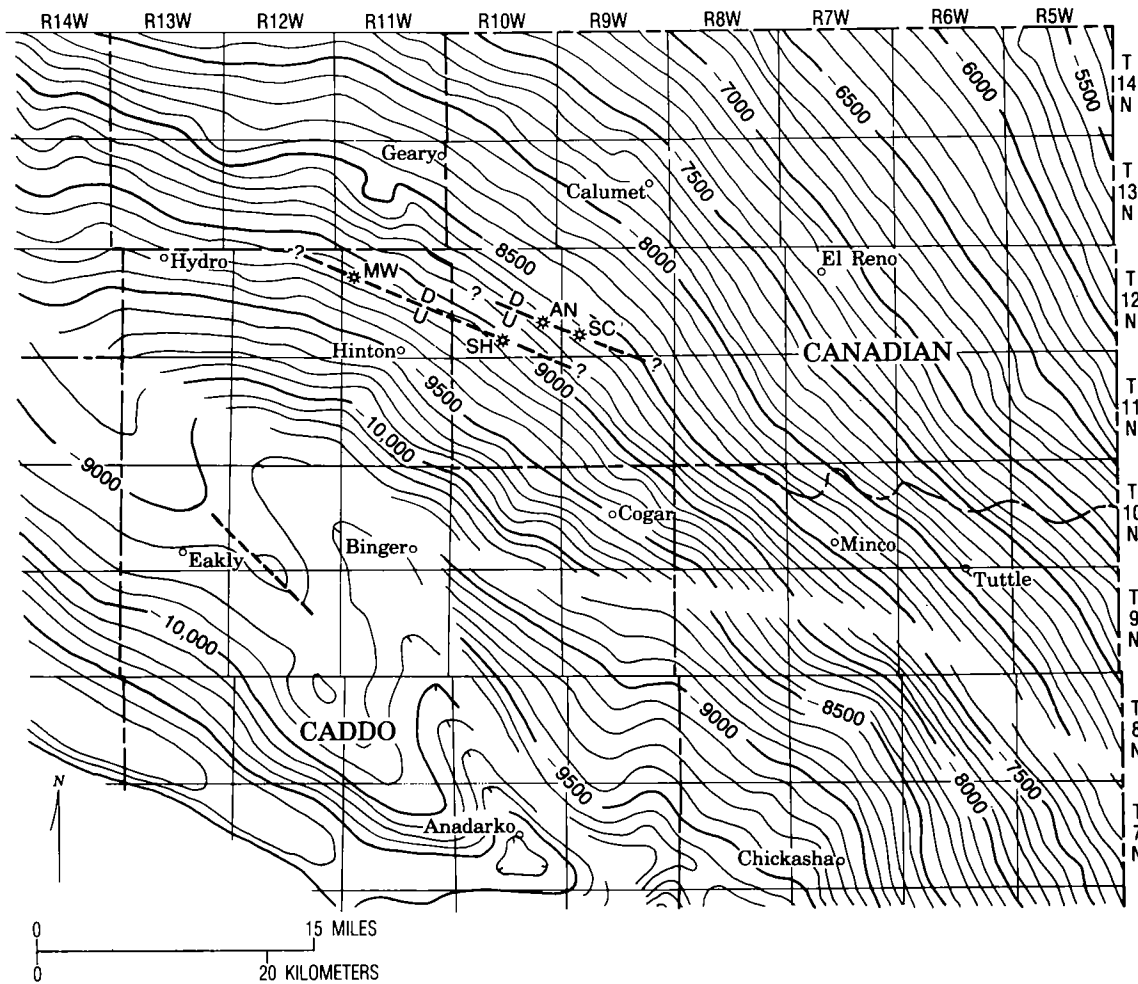


Figure 2. Structural contours on the top of the Oswego lime (Desmoinesian) in parts of Canadian, Caddo, and adjacent counties, southwestern Oklahoma. Contours are on the base of the Hoxbar Group in the southwest, and on the top of the Checkerboard Limestone in the southeast part of the area. Wells are shown as open circles. Approximate position of faults indicated by dashed lines (modified after Fritz, 1978). Explanation of wells: MW—Mustang Co., no. 1-7 West CSE $\frac{1}{4}$ sec. 7, T. 12 N., R. 11 W., Caddo Co. SH—D. C. Slawson, no. 3-34 Hall "B" CNW $\frac{1}{4}$ sec. 34, T. 12 N., R. 10 W., Canadian Co. AN—An-Son Corp. and Patrick Petroleum Co., Nitel no. 1 CNE $\frac{1}{4}$ sec. 26, T. 12 N., R. 10 W., Canadian Co. SC—Sun Oil Co., Chiles B-2 CSW $\frac{1}{4}$ sec. 29, T. 12 N., R. 9 W., Canadian Co.

tain of overthrust structure, and deep drilling has documented reverse faults in ramp zones only locally.

Four wells identified in this study exhibit repeated strata, ranging from 30 ft to at least 120 ft of repeated section (Fig. 3). Repetition of different parts of the section in the four wells suggests multiple reverse faults or fault segments. The repetition of at least 120 ft of strata in the An-Son 1 Nitel requires at least two faults. This suggests that the local structure is that of the

ramp portion of a blind, low-angle thrust, where a single fault commonly splays into several fault segments. This is interpreted to be the structure typical of the four-well area.

To the northwest of that area, and parallel to the N. 70° W. structural grain of the basin, the Aledo (Gatewood, 1980) and North Custer City (Berg, 1974) fields are both associated with down-to-the-north faults. Although the previous authors interpreted those to be normal faults, present knowledge of regional structure favors a

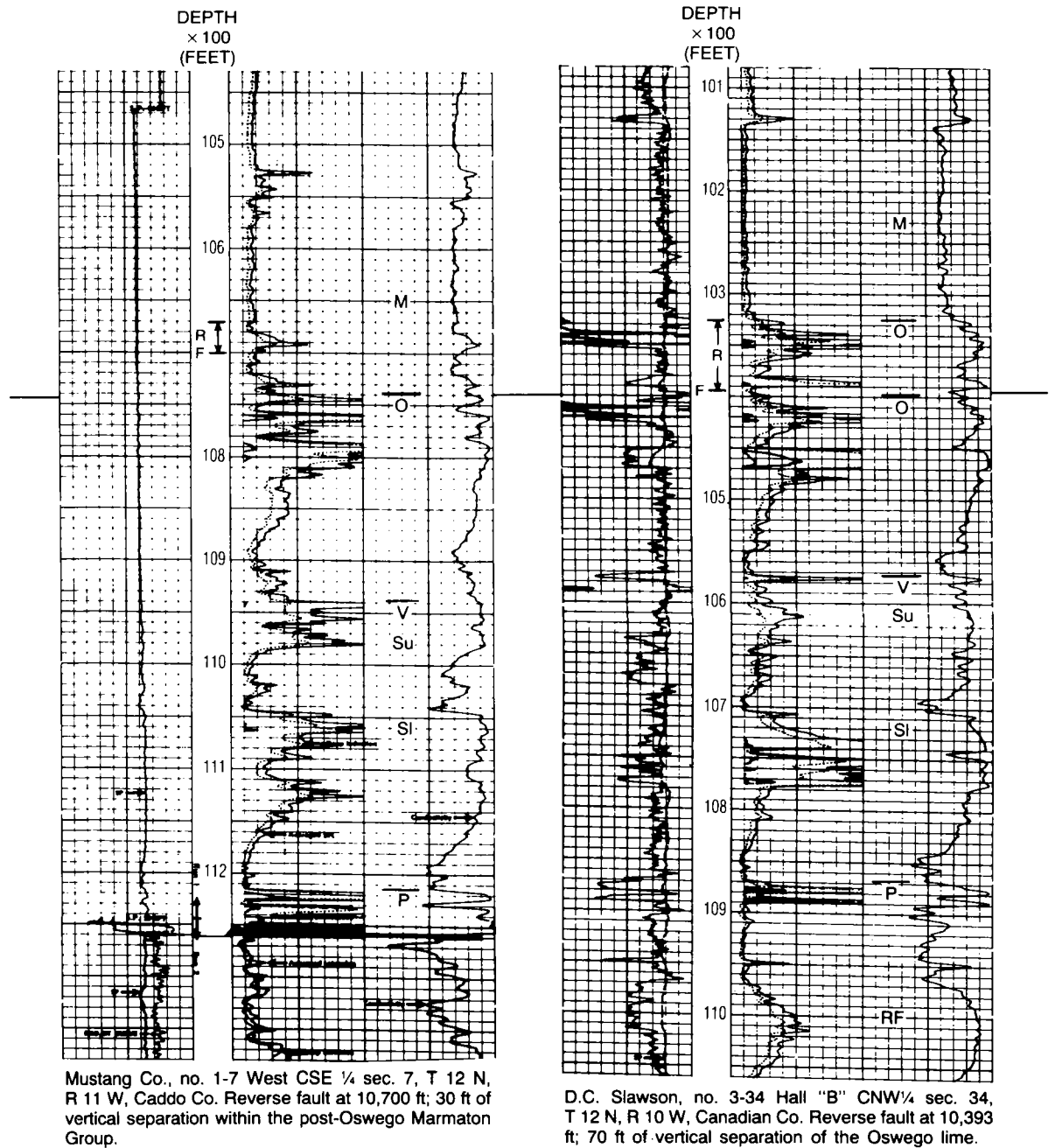
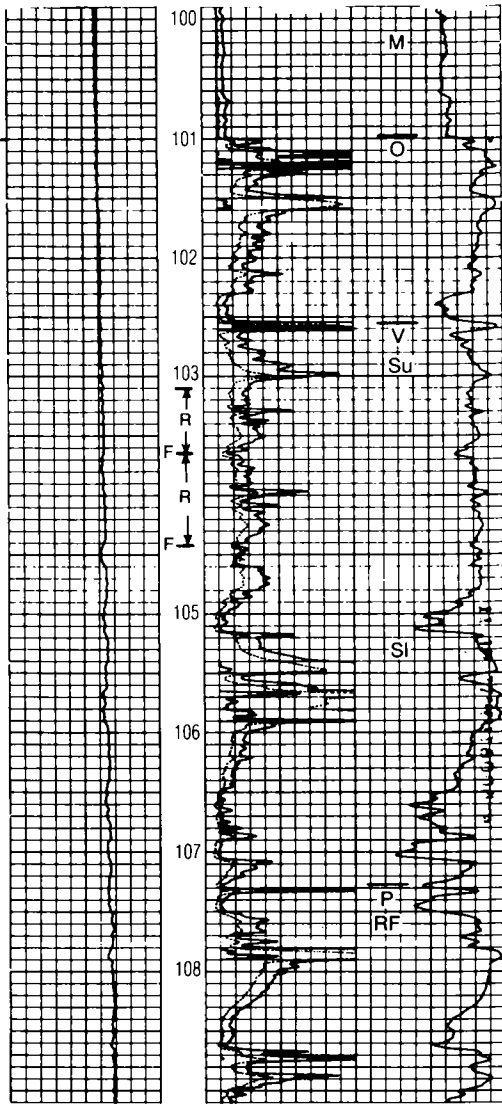


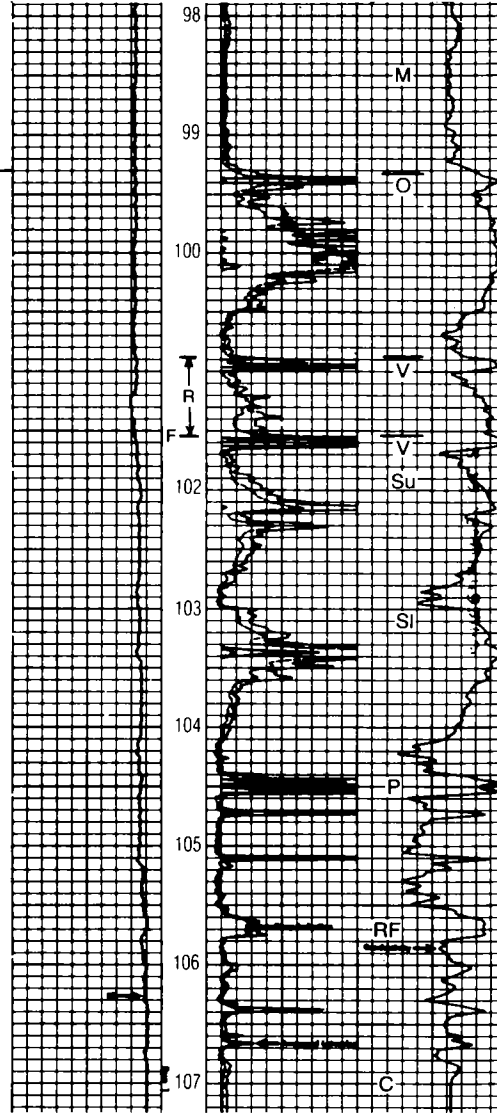
Figure 3. Wells penetrating repeated section in southwestern Canadian County and adjacent Caddo County, Oklahoma. Formations identified as follows (youngest to oldest): M—Marmaton Group (undivided). O—Oswego lime. V—Verdigris Limestone. Su—upper Skinner sand. Sl—lower Skinner sand. P—Pink lime (Tiawah Limestone). RF—Red Fork sand. C—Cherokee Group (undivided). F—position of interpreted fault. R—repeated section. Datum: Oswego lime.

DEPTH
× 100
(FEET)



An-Son Corp. and Patrick Petroleum Co., Nitzel no. 1 CNE¼ sec. 26, T 12 N, R 10 W, Canadian Co. Reverse fault at 10,363, and 10,441 ft; at least 133 ft of repetition of upper Skinner sand (sandstone thicknesses variable compared to two wells in Section 25).

DEPTH
× 100
(FEET)



Sun. Oil Co., Chiles B-2, CSW¼ sec. 29, T 12 N, R 9 W, Canadian Co. Reverse fault at 10,120 ft; 64 ft of vertical separation at the Verdigris Limestone.

Figure 3. *Continued.*

thrust-fault geometry. Sole faults may occur in more than one stratigraphic position, as interpreted farther south in the basin by Brewer (1982, fig. 28).

It is herein suggested that one or more WNW-trending blind thrust systems occur on the northern slope of the deep Anadarko basin, along a line including the Aledo and North Custer City fields, and four wells in northern Caddo and southwest-

ern Canadian Counties. The position of the suggested thrust or thrusts (Fig. 4) suggests that the Anadarko shelf may have acted as a buttress against which thrusting was directed during subsidence in Pennsylvanian time. This is the northernmost thrusting located to date in the published literature, and it may be significant in the formation of heretofore unrecognized petroleum traps.

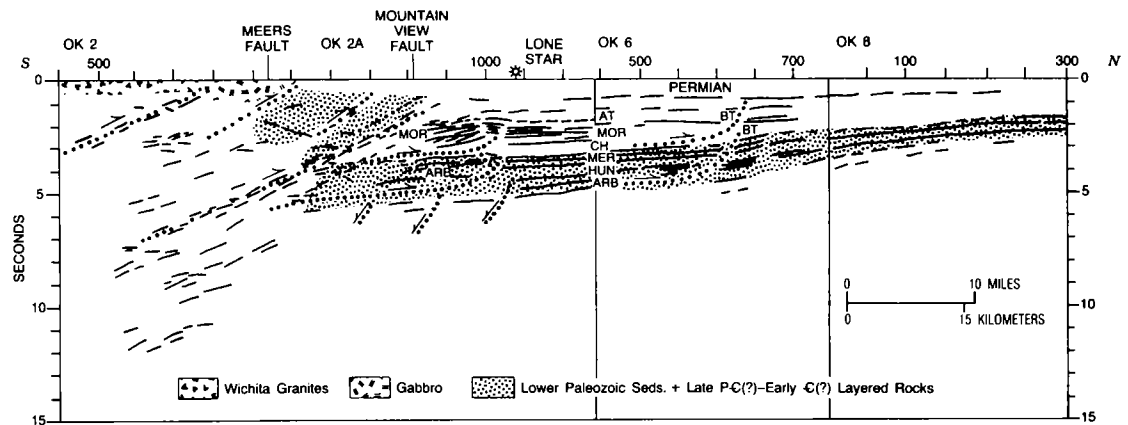


Figure 4. Interpretation of unmigrated COCORP seismic profile across the Wichita Mountains/Anadarko basin transition. Identified stratigraphic units: ARB—Arbuckle Group (Cambrian–Ordovician). HUN—Hunton Group (Silurian–Devonian). MER—Meramecian (Mississippian). CH—Chesterian (Mississippian). MOR—Morrowan (Pennsylvanian). AT—Atokan (Pennsylvanian). BT—blind thrusts interpreted in this study, projected along structural strike into line of profile (modified after Brewer, 1982).

SUBSURFACE GEOLOGY OF THE NORTHERN SHELF OF THE ANADARKO BASIN

DOROTHY J. SMITH

Oklahoma Geological Survey

A four-county study on the northern shelf of the Anadarko basin was undertaken in order to summarize the general subsurface geology of the area. The study includes Woods, Woodward, Alfalfa, and Major Counties in Oklahoma (Fig. 1). Pre-Permian sedimentary rocks in the subsurface in this area represent each geologic system from the Cambrian through the Pennsylvanian, and each system is productive of petroleum (Fig. 2). Three horizons were selected for structural mapping because they are major markers in the section and easily correlated regionally. Structure contour maps were prepared on the Viola Group (Fig. 3), on the unconformity at the base of the Pennsylvanian System, and on the top of the "big lime"—Oswego (Marmaton Group); "big lime" was chosen for the benefit of the well-site geologist because it is the top of the Marmaton carbonate sequence in the area. Although "big lime"—Oswego includes all the Marmaton carbonates, the Oswego is a more commonly used mapping horizon that is easily correlated over long distances. A gentle S-dipping homocline is apparent on all ho-

rizons. Average dip of the Oswego is 40 ft/mi, with local variations, and the Viola dips an average of 80 ft/mi, increasing slightly in Woodward and Major Counties (Fig. 3).

Structural features include a distinct closure in northwestern Woods County at the site of the Yellowstone field, where Viola, Simpson, and Arbuckle strata are the principal reservoirs (Fig. 3). The map on the basal Pennsylvanian unconformity shows an extensive low in central Woodward County, commonly referred to as the "Woodward trench." Well-developed, continuous, porous and permeable channel deposits of Morrow sands lie within this N-S feature.

In north-central Oklahoma, weathering at the top of the Mississippian, and locally within 100 ft or so of the top, has produced a zone of rubble known as "Mississippi chat." This variable zone of weathered material may be limestone, weathered chert, fractured siliceous limestone, tripolitic chert, or any combination of these lithologies. The "Mississippi chat" is Meramecian and (principally) Osagean (Mikkelsen, 1966). According to

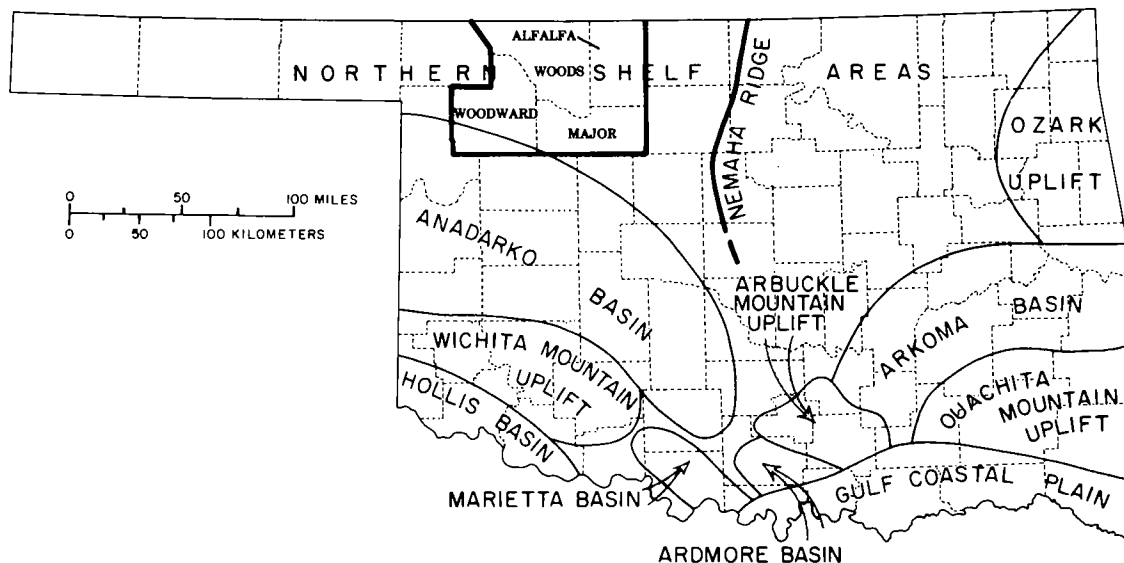


Figure 1. Map of Oklahoma showing location of the four-county study area on the northern shelf of the Anadarko basin.

SYSTEM	SERIES	GROUP or FORMATION	PRINCIPAL OIL and GAS RESERVOIR	
PENNSYLVANIAN	Virgilian	Wabunsee Group		
		Shawnee Group		
		Douglas Group	Tonkawa sand	
	Missourian	Ochelata Group	Cottage Grove sand	
		Skiatook Group	Layton sand	
	Desmoinesian	Marmaton Group	Oswego lime	
		Cherokee Group	Red Fork sand	
	Atokan	Atoka Group		
	Morrowan	Morrow Group	Morrow sands	
MISSISSIPPIAN	Chesterian	Chester Group	Chester Group	
	Meramecian	Meramec Group	Miss. ls.	Meramec lime
	Osagean	Osage Group		Osage lime
	Kinderhookian	Kinderhook shale		
DEVONIAN		Woodford Shale		
SILURIAN	Upper	Hunton Group	Hunton lime	
	Lower			
ORDOVICIAN	Upper	Sylvan Shale	Maquoketa dolomite	
		Viola Group	Viola lime	
	Middle	Simpson Group	Simpson dolomite	
		Lower		Simpson sand
CAMBRIAN	Upper	Arbuckle Group	Arbuckle lime	
		Reagan Sandstone		
PRECAMBRIAN		GRANITE		

Figure 2. Stratigraphic column of pre-Permian strata and principal reservoirs on the northern shelf of the Anadarko basin. Modified from Hills and Kottlowski (1983) and from an unpublished column by Herbert G. Davis and Robert A. Northcutt.

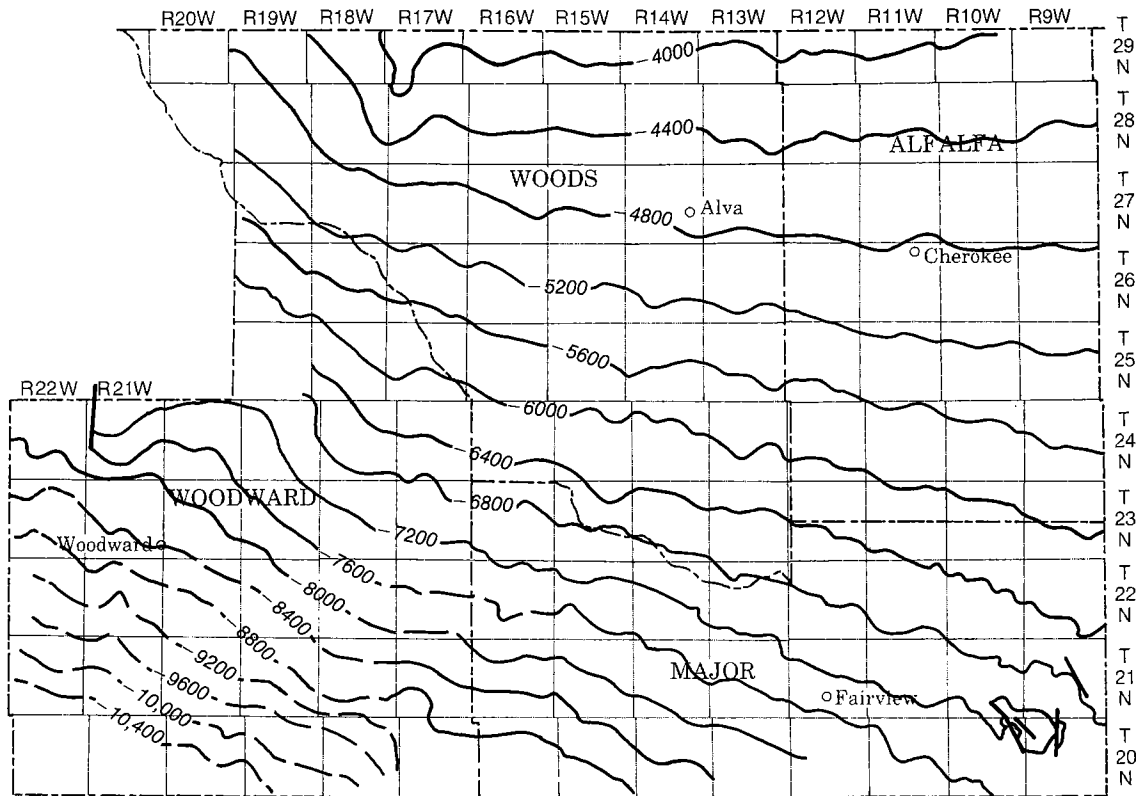


Figure 3. Structure-contour map on top of the Viola Group.

Mikkelsen (1966, p. 256) the "chat" was formed "(1) underwater during Mississippian time; (2) exposed during the hiatus between Mississippian and Pennsylvanian time; and (3) reimmersed in early Pennsylvanian time."

Petroleum production on the shelf is almost entirely from stratigraphic traps and other local variations of porosity. Offshore bars, channel sands, and sand lenses are common. Other traps are formed by dolomitization and fractures. Fractured reservoirs have been defined and are limited to those in which oil and gas would not be produced or would be seriously decreased if fractures were absent. There are two types according to this classification: those with only fracture porosity and those with a combination of fracture and intergranular porosity (Hubbert and Willis, 1955). Dolomitization forms a trapping mechanism when a porous dolomitic zone grades in all directions into impermeable strata.

Numerous parts of the stratigraphic column are productive, including the Tonkawa sand, Cottage Grove sand, Oswego (Fort Scott) lime, Cherokee sands, Morrow sands, several zones within the

Mississippian System, and the Hunton Group. Table 1 lists the major fields and their principal reservoirs.

With steadily rising oil prices from 1973 until 1981, a high level of exploration and development was reached. A slight decline began in 1982, and by 1984 development wells accounted for most of the drilling activity. Cumulative production by counties is shown in Table 2.

Several major patterns of deposition and erosion are significant. In the Pennsylvanian System, the northward thinning of the Cherokee Group due to marine onlap is apparent. The Cherokee Group includes strata from the base of the Oswego to the top of the Atoka, which in this area is the "Thirteen Finger line." Where the Atoka and Morrow Groups are missing, the Cherokee rests unconformably upon the Mississippian. The Cherokee is composed of gray shales and thin limestones and sandstones that are persistent and often are good marker beds; it was deposited by a transgressive sea onto a low, broad shelf dipping gently southward into the Anadarko basin.

The updip limit of the Morrow Group is shown

TABLE 1.—SELECTED MAJOR PETROLEUM-PRODUCING HORIZONS
IN THE FOUR-COUNTY STUDY AREA

Field Name	Field no. ^b	Discovery date	Principal producing horizons	Cumulative through 1985 ^a	
				Oil (bbls)	Gas (Mcf)
Avard NW	148	1954	Tonkawa, Red Fork, Hunton, Oswego	6,003,759	194,391,566
Cheyenne Valley	577	1958	Mississippian, Upper Red Fork	11,047,049	101,177,051
Oakdale	2000	1955	Oswego, Red Fork, Mississippian, Chester, Hunton, Simpson, Layton	9,596,420	136,582,981
Ringwood	2399	1945	Hunton, Red Fork, Oswego, Mississippian	86,347,382	550,229,464
Campbell	458	1969	Mississippian, Hunton	2,922,188	41,328,154
Cedardale NE	530	1957	Chester, Hunton, Red Fork, Oswego	2,593,934	474,773,015
Okeene NW (Blaine and Major Counties)	2021	1956	Red Fork, Chester, Mississippian, Hunton	10,930,886	331,841,224
Selling NE (Dewey, Woodward, and Major Counties)	2524	1952	Cottage Grove, Chester	6,627,301	178,258,700
Chester W	574	1959	Chester	1,179,253	204,449,093
Sharon W	2546	1965	Morrow, Cottage Grove	3,215,221	60,540,416
Waynoka NE	2940	1960	Cottage Grove, Oswego, Chester, Simpson, Tonkawa	752,121	222,825,687

^aDwights Petroleum Data Service (1985).

^bField numbers refer to those used by Burchfield (1985).

TABLE 2.—CUMULATIVE PRODUCTION THROUGH 1985
(NOT INCLUDING CONDENSATES)

County	Oil (bbls)	Gas (Mcf)
Alfalfa	118,036,325	881,966,832
Major	44,807,751	961,384,759
Woods	16,235,850	490,108,674
Woodward	14,607,665	690,813,326

Source: International Oil Scouts Association (1984-85).

in Figure 4. Updip thinning of the Morrow is due to transgressive overlap, depositional thinning of stratigraphically equivalent beds, and possibly truncation (Forgotson, 1969).

The Chester Group thins northward due to marine onlap and erosion (Fig. 5). Shales and limestones with some sandy zones are typical of the Chester on the northern shelf. The Manning zone of Chesterian age produces in the Ringwood field, where the lithology of the Manning is highly variable, ranging from sandy limestone to

a sandy dolomite, to an oolitic and oolitic to sandy limestone or dolomite, to limestone or dolomite with very little sand (Lillibridge, 1963).

Northward thinning and truncation of the Hunton (Fig. 6) is due to pre-Woodford erosion. The Henryhouse Formation and Chimneyhill Subgroup are the only Hunton units present in the study area. The irregular truncation pattern in the eastern part of the study area results from a pre-Woodford stream channel cut through the Hunton.

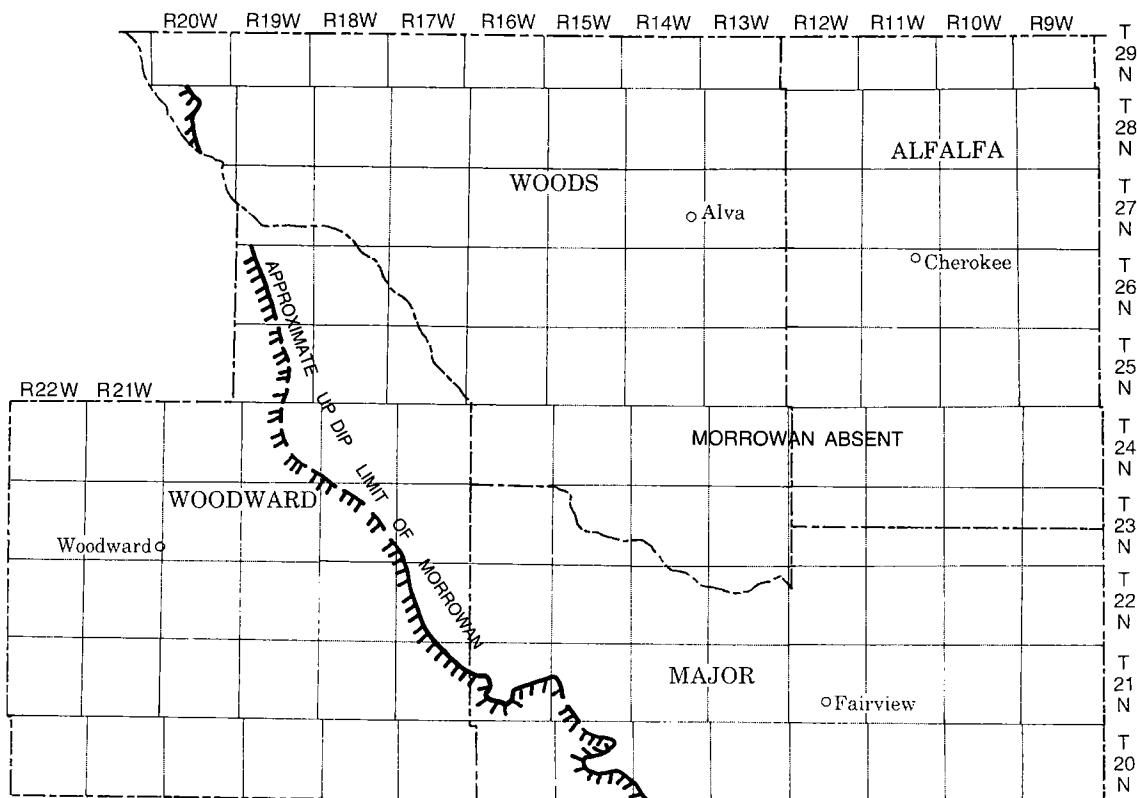


Figure 4. Map showing updip limit of Morrow Group.

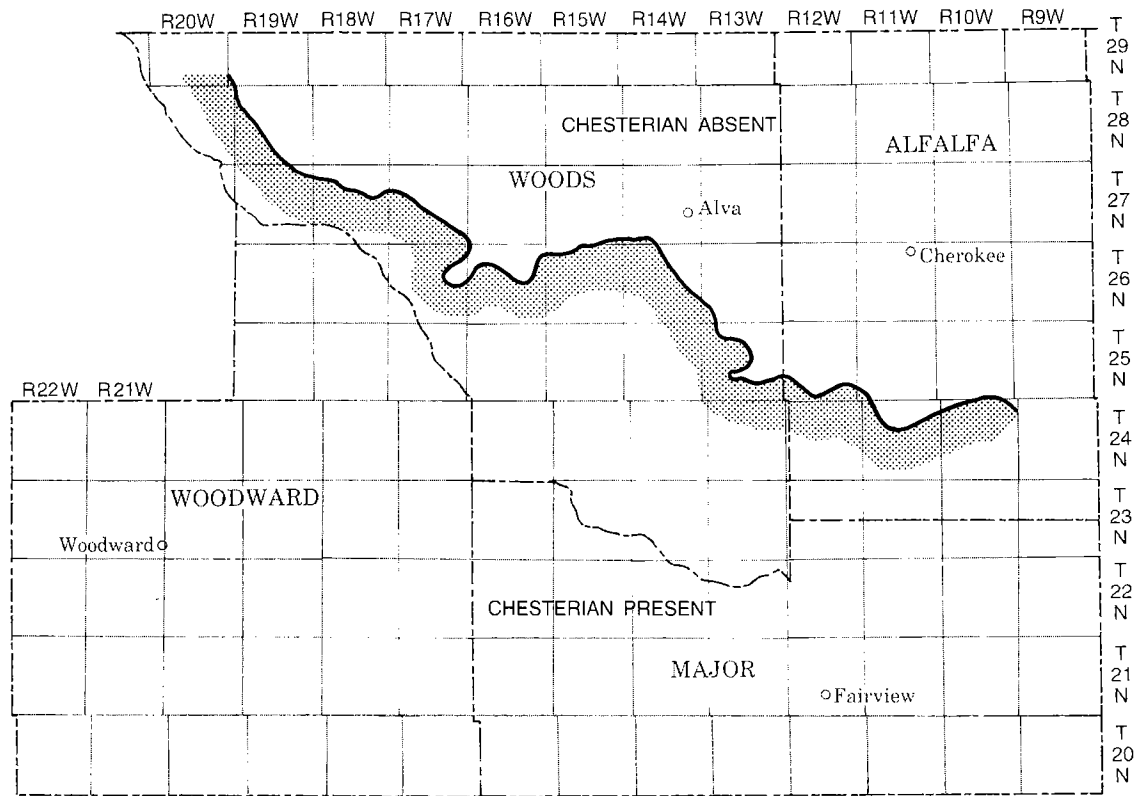


Figure 5. Map showing truncation of Chester Group.

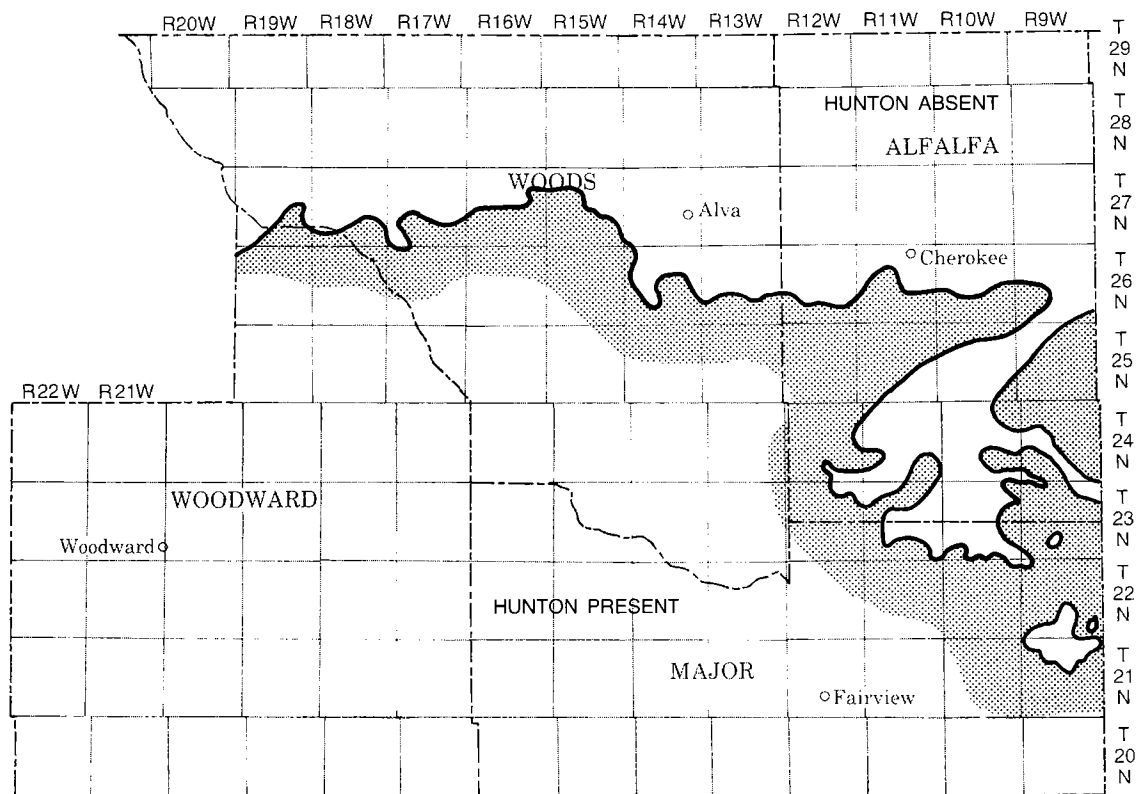


Figure 6. Map showing truncation of Hunton Group.

HABITAT OF PETROLEUM IN PERMIAN ROCKS OF THE GREATER ANADARKO BASIN

JOCK A. CAMPBELL AND CHARLES J. MANKIN

Oklahoma Geological Survey

Abstract.—Permian reservoirs offer the shallowest potential exploration play in the greater Anadarko basin. It is our contention that most of the discoveries in Permian reservoirs to date are the result of "wildcatting" and the drilling of surface structures historically, and the drilling for structural traps in pre-Permian rocks in recent decades. We believe that Permian strata deserve exploration on their own merit, based on their reservoir potential and the widespread occurrence of hydrocarbons trapped in Permian rocks.

Petroleum production is widespread from both carbonate and siliciclastic strata of Early Permian age in the Anadarko basin (Fig. 1). The world-class accumulation of the Panhandle-Guyton-Hugoton-Panoma field complex is well known to most petroleum geologists, but the regional attributes of the Permian as a focus for exploration potential have not been addressed, except in combination with the underlying Pennsylvanian strata.

Production from siliciclastic rocks of Wolfcampian age occurs in the Wichita-Amarillo Mountains area, along the Nemaha uplift, and on the central Kansas uplift. Carbonates of Wolfcampian age produce widely on the north side of the Amarillo uplift and along the Cimarron arch in the western Anadarko basin, and on the central Kansas and Nemaha uplifts.

Production from Leonardian strata is less widespread, but commonly occurs in the eastern part of the Wichita Mountains front area and, locally, in association with the Amarillo Mountains front, and locally to the north in association with the Cimarron arch (Fig. 2).

In this regional study, no attempt has been made to conduct original investigations involving correlation of stratigraphic units. However, the stratigraphic chart (Fig. 2) not only synthesizes current understanding of stratigraphic relations, but identifies the most commonly reported gas- and oil-producing reservoirs, including those in the major informally named subsurface stratigraphic units. It also attempts to place a number of informally named subsurface sandstone members, or "beds," in the Chase and Council Grove Groups accurately with respect to their original and/or most common usage. Correlation of these units has been difficult historically, because most of the petroleum discoveries were made, and the units named, prior to common use of electric logs. In addition, the sandstones are commonly channel-form bodies, and therefore are not continuous over wide areas in more than two directions. Penecontemporaneous erosion has locally removed the underlying carbonate unit, further complicating stratigraphic correlation. The lack of consistent correlation and nomenclature for these sandstone units has been a vexing problem from the outset of their recognition. Additional names have been applied to these, and probably to other sandstones in the area, but are not presented here, as they could not be placed in the section with any accuracy whatsoever.

Now that electric logs for more recent wells are generally available, a much better understanding of the continuity and correlation of these sandstone units is possible. We believe that an effort to correlate and map these units will result in prospects for shallow exploration.

A review of producing fields and reservoir rocks in the basin indicates that trap and reservoir development in Permian strata are primarily of stratigraphic and diagenetic origin in most of the Anadarko basin. However, petroleum pooled in Permian strata has been discovered primarily by virtue of the chance association of those reservoirs with anticlinal structures. We conclude that the discovered petroleum pools represent only a part of the petroleum trapped in Permian rocks in the Anadarko basin. Therefore, Permian strata offer opportunities for the development of shallow (from <1,000 to ~3,500 ft) prospects for petroleum exploration.

A complete paper has been published as a part of a symposium volume by Campbell and others (1988).

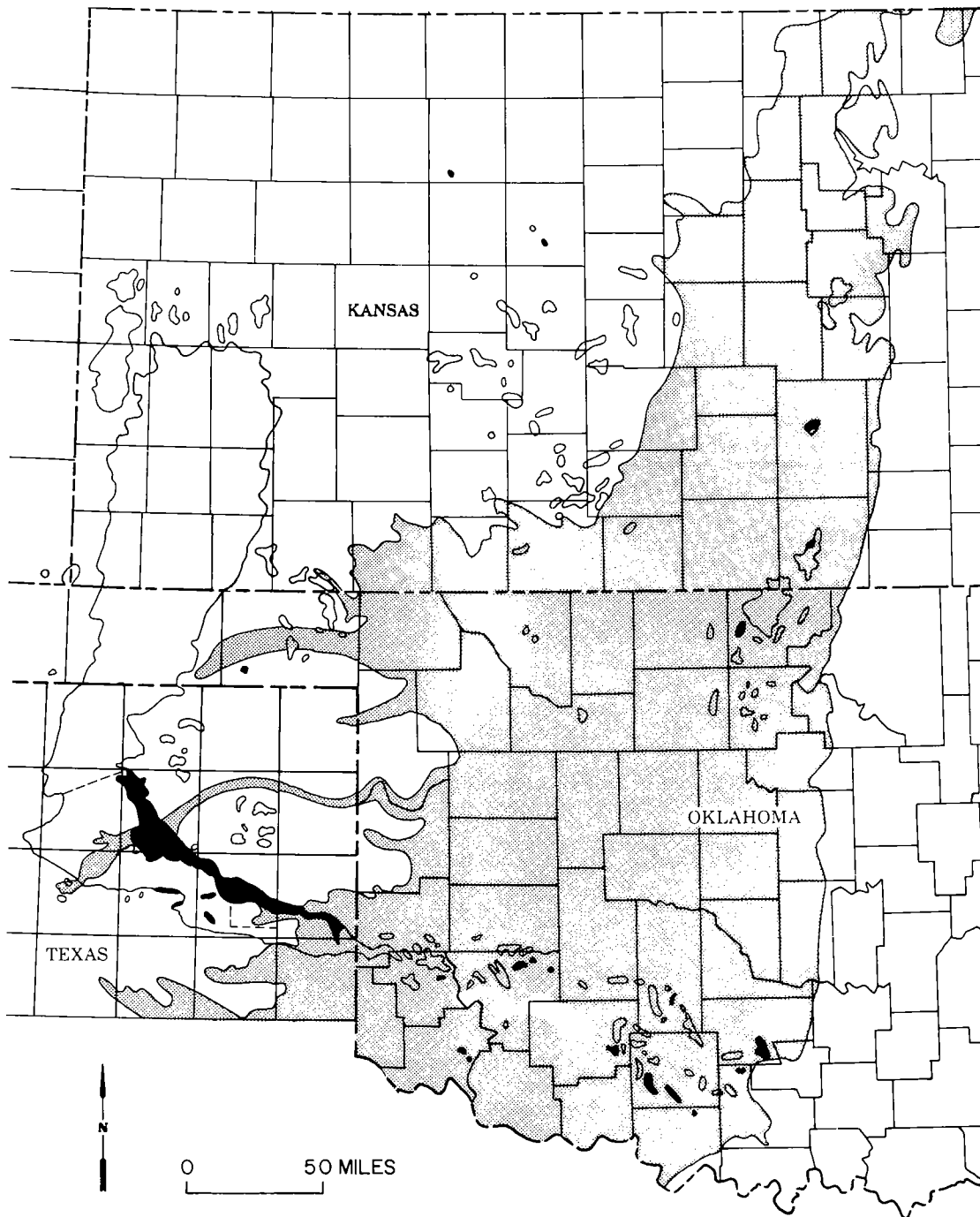


Figure 1. Petroleum production from Permian strata in the greater Anadarko basin. Oil fields, black; gas fields, outlined. Stipple pattern, area of Permian outcrop. After Pippin (1970), King and Beikman (1974), Burchfield (1985), Newell and others (1987), and unpublished sources.

THERMAL REGIME OF THE ANADARKO BASIN

JAQUIDON D. GALLARDO AND LARRY S. CARTER

Southern Methodist University

There have been various attempts at mapping the thermal structure of sedimentary basins, most often based on gradients calculated from bottom-hole temperatures (BHT). Aside from the inaccuracy of the BHT data, this approach suffers from its method of calculation. Using only one subsurface point, the BHT, to calculate the gradient gives a straight line resulting in an unrealistic representation of the true gradient. The gradient is dependent upon the lithology of the rocks, each rock type having a different thermal conductivity.

Conductivity has an inverse relationship to the gradient. Rocks with relatively higher conductivities allow heat to pass through, and therefore will have lower gradients. Rocks with relatively lower conductivities trap heat and exhibit higher gradients. As a result, the gradient of any given area is a composite of the gradients through the individual sedimentary units—and this is far from a straight line.

In this study, an attempt is being made to depict a truer picture of the temperature structure

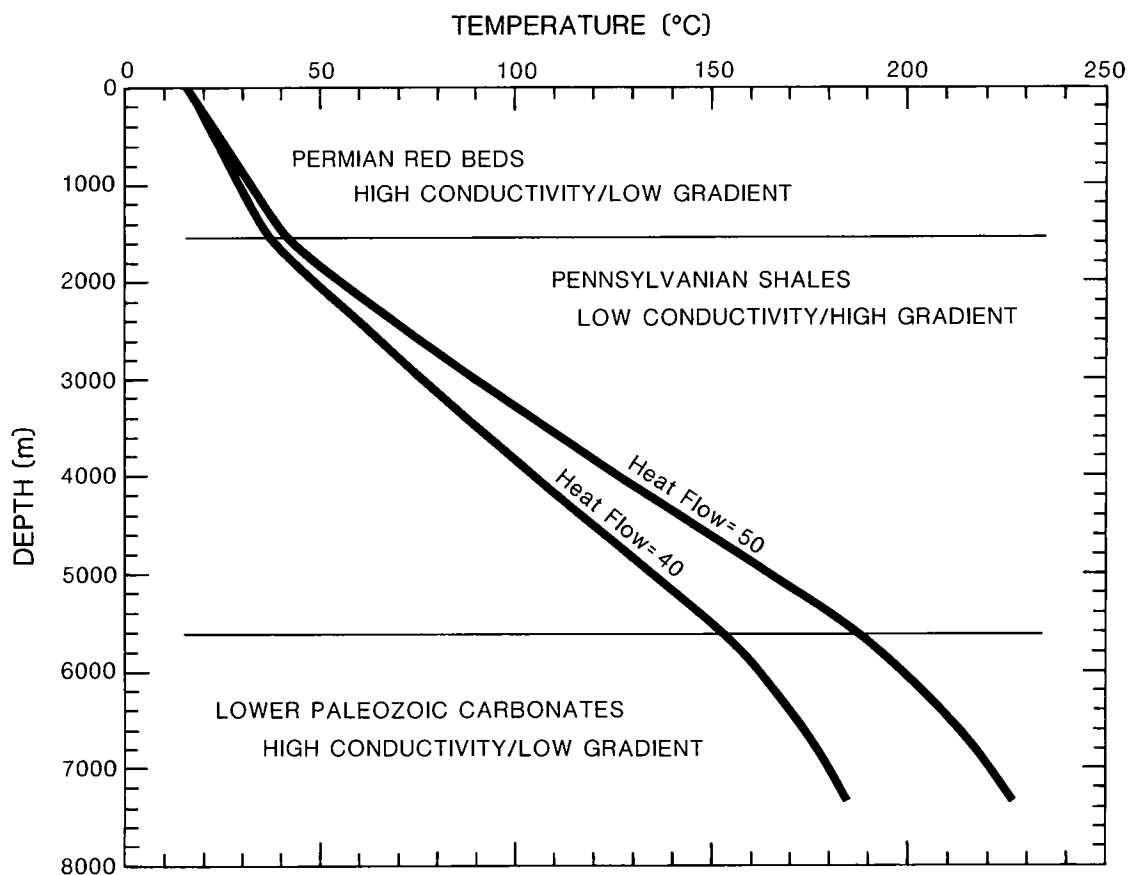


Figure 1. Relative gradients of the major sedimentary divisions of a typical Anadarko basin well, calculated at heat-flow values of 40 and 50 mW/m.

of the Anadarko basin by calculating it from the approach just described. The first step is to determine the lithologic succession in a particular well. Various types of logs (sample, mud, electric) are used to pick each lithologic unit and its thickness. Regional heat flow and thermal conductivity information are obtained by direct logging measurements. These data are then used to calculate temperature, according to the following formula:

$$T_z = T_0 + \sum_i^N Z_i(Q/K_i),$$

where T_z = temperature at depth z ,
 T_0 = surface temperature,
 Z_i = thickness of each lithologic unit,
 Q = heat flow,
 K_i = thermal conductivity of each lithologic unit.

By calculating the gradient in this manner at various points in a basin, a three-dimensional picture of the temperature structure can be built.

The Anadarko basin can be divided into three major sections based on distinctly different gradi-

ents. This is due to the relative differences in the major lithologies represented in each section. The Permian consists largely of high-conductivity red beds, the Pennsylvanian of low-conductivity shales, and the lower Paleozoic of intermediate-conductivity carbonates; this is illustrated in Figure 1. Another effect of lithology on gradient occurs in areas where "granite wash" was deposited during the Pennsylvanian. Outside the areas of "wash" deposition, the Pennsylvanian section is dominated by low-conductivity shales, and because the wash sections have a higher conductivity the gradient is lower through these sections. An expected conclusion of this study is that the geothermal gradients observed in the Anadarko basin are a normal consequence of the lithologies present, and differences across the basin can be explained by lateral differences in the stratigraphy.

The model created by this method illustrates a static, present-day representation of the temperature structure of the Anadarko basin. This can then be used as a starting point for modeling thermal conditions in the geologic past for maturation studies.

RELATIONSHIP OF CLAY-MINERAL DIAGENESIS TO TEMPERATURE, AGE, AND HYDROCARBON GENERATION—AN EXAMPLE FROM THE ANADARKO BASIN, OKLAHOMA

RICHARD M. POLLASTRO AND JAMES W. SCHMOKER
U.S. Geological Survey, Denver

Abstract.—Randomly interstratified illite/smectite (I/S) is present in Springeran and Morrowan rocks (Late Mississippian and Early Pennsylvanian) of the Anadarko basin, Oklahoma, at present-day depths <2,750 m, but disappears at depths of 2,750–3,050 m. Only ordered I/S is found in samples below 3,050 m. The work reported here relates the diagenesis of I/S to burial history and oil generation in the Anadarko basin and tests the dependence of the smectite-to-illite reaction on temperature and time.

Published temperature models of clay diagenesis suggest that, for Tertiary and Cretaceous rocks, the transition from randomly interstratified I/S to ordered I/S occurs at 100–110°C. Burial reconstructions for the Anadarko basin indicate that maximum temperatures of 100–110°C correspond to present-day burial depths between 2,700 and 3,100 m. These independently calculated depths for the 100–110°C isotherm match the depths at which randomly interstratified I/S is observed to disappear in Morrowan–Springeran rocks. Thus, random I/S disappears at the same temperature in rocks that differ in age by some 300 m.y. Although the extent of the smectite-to-illite reaction is controlled by kinetics, and effects of time are apparent in laboratory experiments and short-lived geologic systems, the results of this study suggest that time plays a secondary role in long-term diagenetic settings.

INTRODUCTION

Various techniques can be used to study the thermal history of sedimentary basins. Changes in degree of ordering and composition of clay minerals serve as geothermometers; vitrinite reflectance (R_o) is commonly used to assess the thermal maturity of kerogen; Lopatin's time-temperature index (TTI) is a mathematical measure of time-temperature exposure.

The conversion of smectite to illite is the major clay-mineral reaction in sedimentary rocks during progressive burial (Hower, 1981). This reaction—originally defined by X-ray powder diffraction (XRD) patterns interpreted according to the “mixed-layer” concept (Reynolds and Hower, 1970)—results in a progressive and irreversible decrease in the amount of expandable (smectite) layers and a corresponding increase in illite layers.

Although clay diagenesis appears to be a function of depth in well profiles, reactions are in fact controlled primarily by increasing temperature. Regional depth variations in I/S composition and ordering are thus explained, in large part, by differences in geothermal gradient and burial history.

Hoffman and Hower (1979) first proposed the use of clay minerals as geothermometers and documented the temperatures at which clay miner-

als, as well as zeolites and other minerals, are formed, transformed, or destroyed. However, they cautioned that their temperature model was based only on rocks of Tertiary and Cretaceous age, and that the appearance or disappearance of an index mineral could also be dependent on geologic time.

Although little is known of the relationship, the age of the rocks and “residence time” at a given temperature have been recognized as factors possibly influencing the smectite-to-illite reaction (Eberl and Hower, 1976; Ramseyer and Boles, 1986). Bethke and others (1988) have applied computer modeling techniques in basin analysis. Using varying burial rates, they considered time as a factor in smectite diagenesis in modeling basin histories. Weaver (1979), in a review of published data, plotted the temperature of conversion of random I/S to ordered I/S (the disappearance of the 17-Å glycol reflection) as a function of time. Weaver found good agreement between the composition and degree of ordering of I/S and temperature, and no apparent dependence on geologic age. He concluded that time had little effect on the smectite-to-illite reaction.

This study compares temperature of the smectite-to-illite reaction in rocks of Paleozoic age to those of the Cretaceous–Tertiary model. In addition, I/S diagenesis is related to burial history and stages of hydrocarbon generation in the Anadarko basin, Oklahoma.

METHODOLOGY

Morrow and Springer sands (Lower Pennsylvanian and Upper Mississippian) were chosen for this study because they contain appreciable smectite, are prolific producers of hydrocarbons in the Anadarko basin, and could be sampled in numerous cores. Clay mineralogy was determined by X-ray powder diffraction (XRD) on 80 samples of sandstone, shale, and shale partings in sandstone from core from 13 wells. The wells form a general northwest-southeast trend across the Anadarko basin of Oklahoma, and the samples span a present depth range from about 1,200–5,500 m (Fig. 1).

Samples for clay mineral analysis were prepared using the methods described by Pollastro (this volume). Composition and ordering of the I/S clay were determined on oriented, ethylene-glycol-saturated specimens of both the $<2\text{-}\mu\text{m}$ and $<0.25\text{-}\mu\text{m}$ fractions, and interpreted by the methods of Reynolds and Hower (1970) and Reynolds (1980), with the understanding that XRD patterns of illite and I/S may also be interpreted (and perhaps better explained) as physical mixtures of fundamental illite and smectite particles (Nadeau and others, 1984a,b), rather than as mixed-layer clays.

A number of models have been proposed for estimating the thermal maturity of kerogen at points in the sedimentary section where direct geochemical measurements are not available. Lopatin's (1971) time-temperature index of thermal maturity (TTI), as described and calibrated by Waples (1980), is a widely accepted mathematical index whose utility has been demonstrated in numerous case studies. Schmoker (1986) has published details of TTI calculations for the Anadarko basin of Oklahoma.

Change in degree of ordering of I/S is combined here with TTI modeling and burial history reconstructions, first to test the dependence of the smectite-to-illite reaction on temperature and time, and second to relate smectite diagenesis to burial history and stages of hydrocarbon generation.

RESULTS AND INTERPRETATIONS

The composition and ordering of I/S versus depth for sandstone and shale are plotted in Figure 2. Randomly interstratified I/S (defined by the presence of a $17\text{-}\text{\AA}$ glycol reflection on XRD profiles) is interpreted to disappear at a present-day depth range of about 2,750–3,050 m (Fig. 2). The transition from randomly interstratified I/S ($R = 0$) to short-range ordered I/S ($R = 1$), according to the model proposed by Hoffman and Hower (1979) for Cretaceous and Tertiary rocks, occurs in the temperature range 100–110°C. Average

surface erosion for the central Anadarko basin is ~ 800 m (Schmoker, 1986; this volume). The maximum burial depth of the zone where randomly interstratified I/S disappears was therefore about 3,550–3,850 m. Reconstructions of the temperature history of the Anadarko basin using the model proposed by Schmoker (1986; this volume) show that corresponding maximum temperatures of the zone where randomly interstratified I/S disappears (~ 60 m.y. ago) were approximately 102–109°C.

Randomly interstratified I/S thus disappears in Morrowan and Springeran rocks at essentially the same maximum temperature (100–110°C) as in Cretaceous and Tertiary rocks. The similarity in temperature for the onset of I/S ordering in rocks which span some 300 m.y. suggests that time plays a secondary role in the smectite-to-illite reaction in long-term diagenetic settings.

Weaver (1979) and Foster and Custard (1983) suggested that the smectite-to-illite reaction is largely controlled by temperature when heating durations exceed several million years. However, time is a significant parameter in the initial stages of the smectite-to-illite reaction over shorter time intervals, as demonstrated in laboratory experiments with heating durations of hundreds of days (e.g., Eberl and Hower, 1976; Inoue, 1983; Howard and Roy, 1985; Whitney and Northrop, 1988). Time also appears to be a factor in geothermal systems with heating durations of thousands of years (G. Thompson, University of Montana, personal communication, 1988), and where heating durations are within a specific temperature window or range of TTI values (Ramseyer and Boles, 1986).

Figure 3 relates the change in I/S ordering to stages of oil generation in the Anadarko basin. The nonparallelism between the 100–110°C temperature band and the oil-generation window reflects the different time dependence assumed for clay diagenesis and kerogen maturation. The burial histories relate clay-mineral diagenesis in two areas of the basin (A and B, Fig. 3) to geologic time, show the stages of tectonic development at which clays entered critical temperature windows, and show the length of time spent at or above critical temperatures.

The burial curve in Figure 3 for location A (Fig. 1) illustrates that Morrowan rocks in this area have never reached the temperatures required for conversion of randomly interstratified I/S to ordered I/S. XRD profiles confirm this conclusion by showing a well-developed $17\text{-}\text{\AA}$ reflection in Morrowan samples from wells near location A. Thus, although these rocks have been deeply buried and remained at temperatures slightly cooler for some 250 m.y., they have not converted all I/S to the ordered variety. In contrast, the burial curve in Figure 3 for location B (Fig. 1) indicates that Morrowan rocks in this

CROSS SECTION OF X-X'

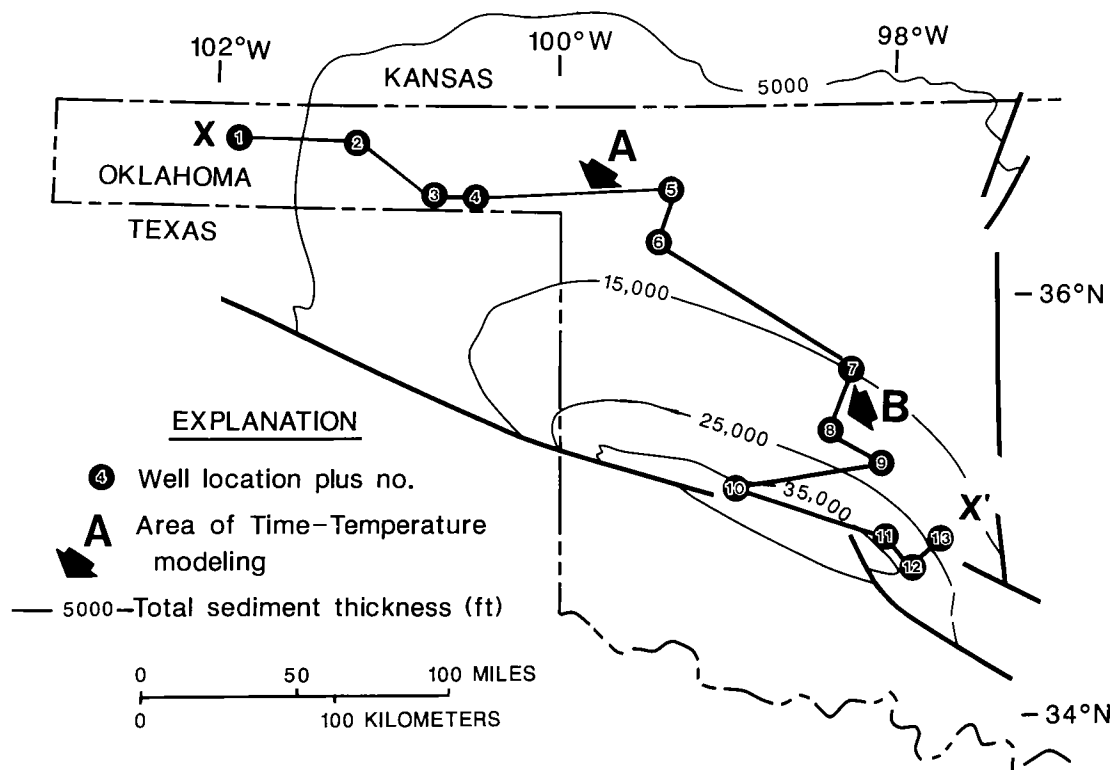
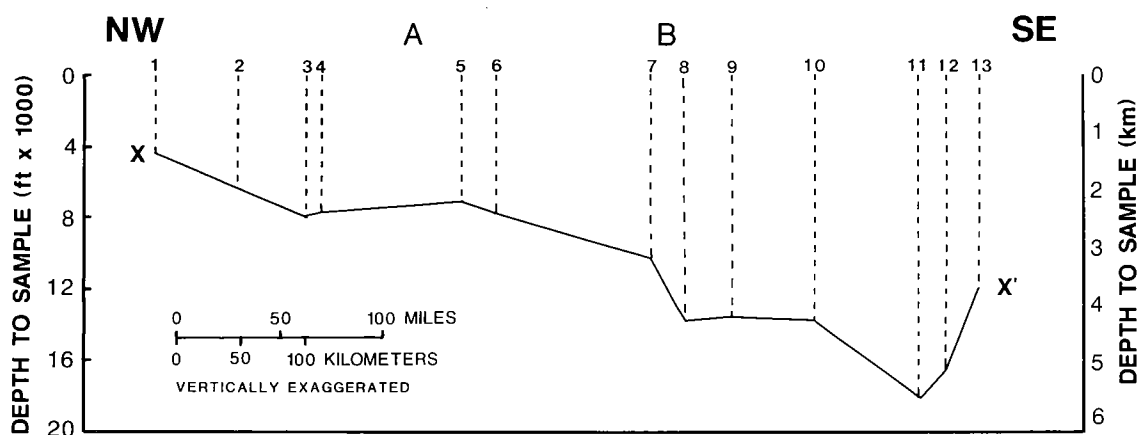


Figure 1. Sediment thickness in the Anadarko basin, cross section through sampled wells, and areas of time-temperature modeling.

area reached temperatures required for the ordering of I/S ~265 m.y. ago; these rocks have remained at burial temperatures $>110^{\circ}\text{C}$ to the present time. XRD profiles show that only ordered I/S is present in Morrowan samples from wells near location B.

At location B (Fig. 3) the conversion of randomly interstratified I/S to ordered I/S occurred just prior to the onset of oil generation (i.e., a large proportion of smectite was converted to illite). Relations like those shown in Figure 3 may prove helpful in testing effects of the smectite-to-

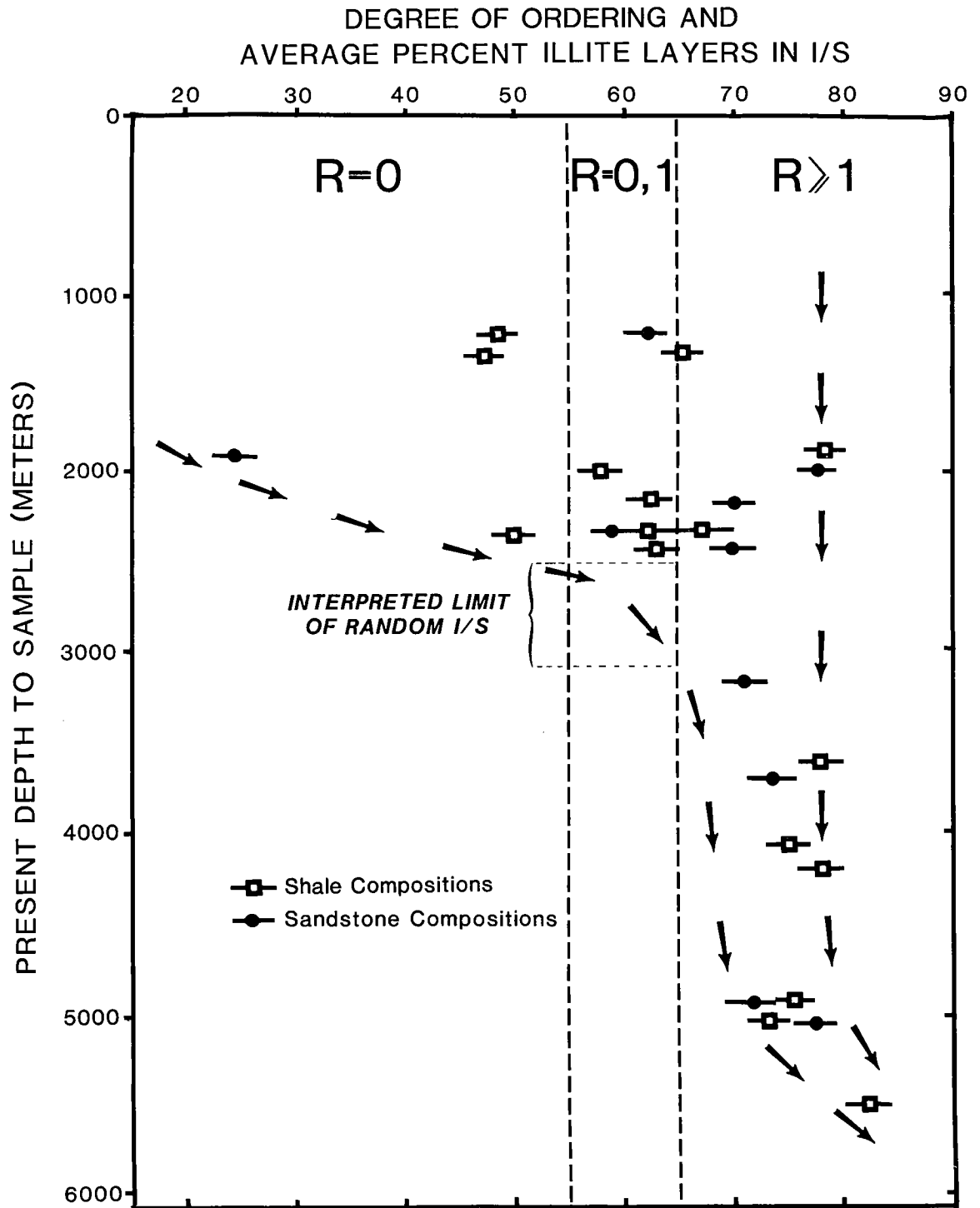


Figure 2. Composition and ordering of interstratified illite/smectite (I/S) in Springeran and Morrowan rocks versus depth. Arrows define composition "window" for I/S versus depth. Samples from cores of 13-well profile, Anadarko basin, Oklahoma (Fig. 1). $R = 0$, random I/S; $R = 0,1$, both random and ordered I/S; $R \geq 1$, only ordered I/S.

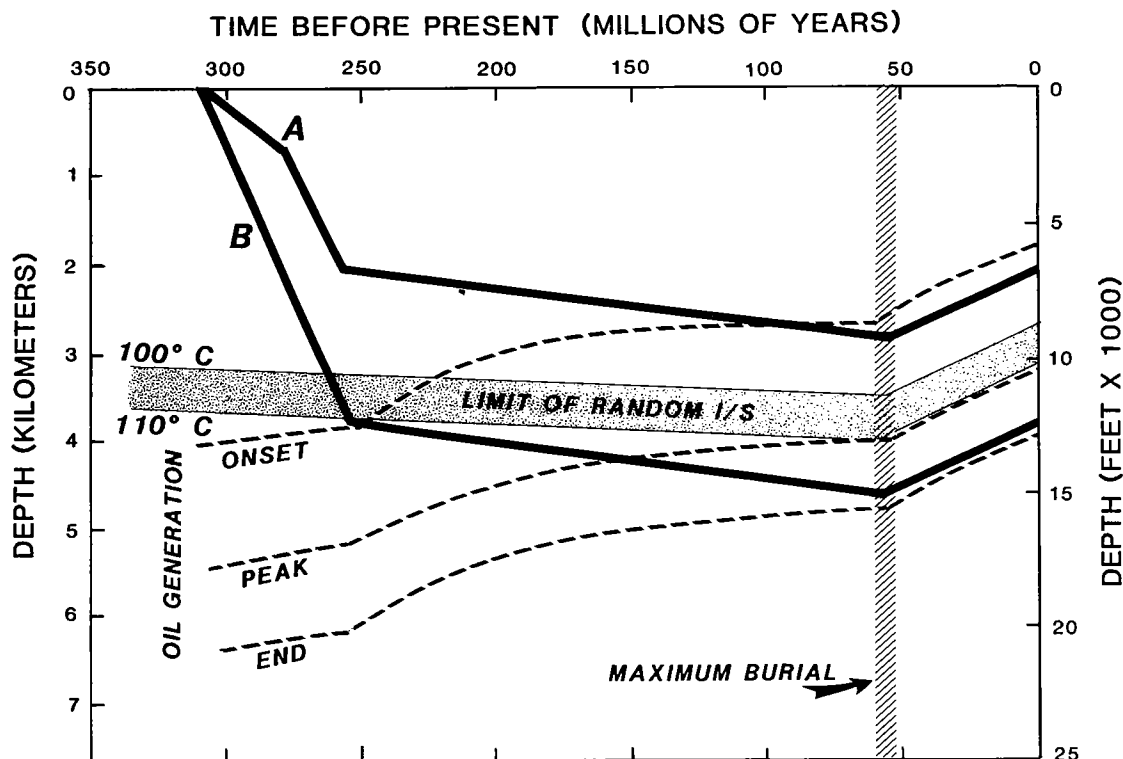


Figure 3. Lopatin, burial, and temperature reconstructions for Morrowan rocks, Anadarko basin, Oklahoma, relating ordering changes in interstratified illite/smectite (I/S) to burial history and the oil window. Solid lines are burial reconstructions for top of Morrowan near wells with (A) randomly interstratified I/S and (B) only ordered I/S (locations for A and B are shown on Figure 1). Dashed lines are time-depth reconstructions for oil generation, based on Lopatin modeling. Shaded zone shows 100–110°C temperature band and represents predicted upper limit for randomly interstratified I/S.

illite reaction upon reservoir cementation (Boles and Franks, 1979a), and the relations among smectite dehydration, geopressure, and hydrocarbon migration and emplacement (Bruce, 1984; Colton-Bradley, 1987).

SUMMARY

Randomly interstratified I/S is common in shale and sandstone of Springeran and Morrowan age in the Anadarko basin, Oklahoma, at present-day depths less than about 2,750 m. Only ordered I/S is found below 3,050 m. Thermal and burial reconstructions for the Anadarko basin indicate that randomly interstratified I/S disappeared in Springeran and Morrowan rocks at maximum temperatures between 100 and 110°C, which were reached ~60 m.y. ago. These temperatures are

nearly identical to those temperatures documented for the disappearance of randomly interstratified I/S in Cretaceous and Tertiary rocks.

In rocks of Morrowan age that have remained at temperatures slightly cooler than 100°C for 250 m.y. or more (area A, Fig. 1), all I/S has not converted to the ordered form. The results of this study suggest that time is of limited importance in the smectite-to-illite reaction in long-term burial diagenetic settings where heating durations are several millions of years.

ACKNOWLEDGMENTS

The manuscript has benefited greatly from the critical reviews of the manuscript and informal discussions by Gene Whitney and Dennis Eberl. We thank them both for their help and interest.

FORMATION RESISTIVITY AS AN INDICATOR OF THE ONSET OF OIL GENERATION IN THE WOODFORD SHALE, ANADARKO BASIN, OKLAHOMA

JAMES W. SCHMOKER AND TIMOTHY C. HESTER
U.S. Geological Survey, Denver

Abstract.—The Upper Devonian and Lower Mississippian Woodford Shale is a black, organic-rich shale that is a major hydrocarbon source rock in the Anadarko basin. With the onset of oil generation, nonconductive hydrocarbons begin to replace conductive pore water in the Woodford, and formation resistivity increases. Crossplots of formation resistivity versus either vitrinite reflectance (R_o) or Lopatin's time-temperature index of thermal maturity (TTI) define two data populations that represent immature shales and shales that have generated oil. The midpoint of the resistivity zone marking the transition between immature and mature shales is ~ 35 ohm-m. The onset of appreciable oil generation in the Woodford Shale of the study area occurs at maturity levels of R_o near 0.57% and of TTI between 33 and 48.

INTRODUCTION

The Upper Devonian and Lower Mississippian Woodford Shale is a highly radioactive dark-gray to black shale widely regarded as an important hydrocarbon source rock in the Anadarko basin (e.g., Cardott and Lambert, 1985). The Woodford contains predominantly type-II kerogen, admixed with varying amounts of terrestrial (type-III) kerogen. Organic-carbon content generally exceeds source-rock minimums and can average as high as 6% by weight on the northeast shelf (Hester and Schmoker, 1987, table 2).

The Woodford Shale is a laterally extensive formation with regional variations in physical and geochemical properties. The particular area of the Woodford represented by the data of this report is shown in Figure 1.

Formation resistivity of the Woodford Shale is shown here to increase sharply in response to the generation of oil. Crossplots of resistivity versus the thermal maturation indices of vitrinite reflectance (R_o) and Lopatin's time-temperature index (TTI) are used to determine the level of thermal maturation at the onset of appreciable oil generation.

CONCEPT

Fundamental factors affecting formation resistivity are illustrated by a rearrangement and simplification of the Archie equation:

$$R_T = R_w / (\phi^2 S_w^2), \quad (1)$$

where R_T is formation resistivity (ohm-m), R_w is pore-water resistivity (ohm-m), ϕ is fractional po-

rosity, and S_w is fractional water saturation. Although highly oversimplified for the case of shales, equation 1 serves to illustrate the fact that, all else being equal, the displacement of pore water by oil causes formation resistivity to increase.

With the onset and continuation of oil generation in organic-rich shales, nonconductive petroleum replaces conductive pore water. As this occurs and S_w decreases, resistivity increases from low levels that are associated with thermal immaturity (equation 1). Formation resistivity as measured by logs can approach hundreds of ohm-meters if sufficient oil is generated to displace most pore water and thus drive S_w to near-zero values.

The increase of source-rock resistivity associated with the onset of oil generation has been noted in the literature. Meyer and Nederlof (1984) observed that resistivity of source rocks can increase by a factor of 10 or more with attainment of thermal maturity. Smagala and others (1984) noted a relation between resistivity and vitrinite reflectance for the calcareous Upper Cretaceous Niobrara Formation of the Denver basin. Murray (1968) equated high resistivity in shales of the Upper Devonian and Lower Mississippian Bakken Formation of the Williston basin with hydrocarbon-saturated pore space. Meissner (1978) discussed the association between black-shale resistivity and oil generation, and used resistivity logs to map areas of source-rock maturity of shales of the Bakken Formation in parts of the Williston basin.

A black shale might have sufficient kerogen content to generate and perhaps to expel oil without being rich enough to effectually displace pore water and thus significantly increase resistivity.

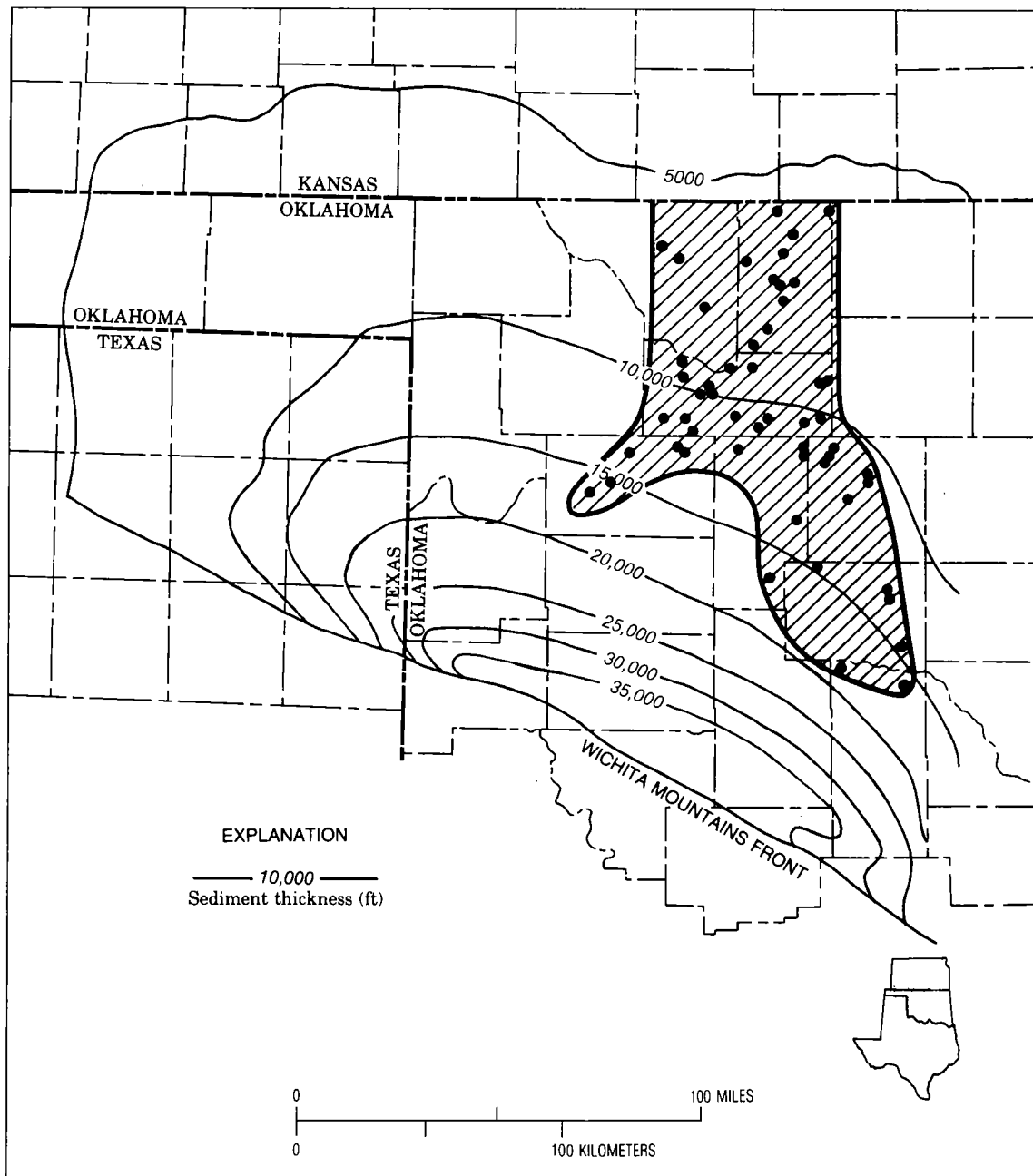


Figure 1. Index map of Anadarko basin showing area of Woodford Shale (hachured) represented by data of this report. Wells from which resistivity data were obtained are located by dots. Contours show total sediment thickness in feet.

For the concept outlined here to be applicable, a source rock must generate enough oil to disrupt the internal electrical-conduction paths formed by saline water.

The Woodford Shale is characterized by vertical resistivity variations that probably reflect nonuniform displacement of pore water by internally generated oil, as well as changes in chemical and physical properties such as organic-matter type and content, porosity and pore geometry, water salinity, and shale mineralogy. The interval or facies of the Woodford Shale with highest resistivity at each well location is assumed to be most representative of source-rock maturity and is used here for the crossplots of Figures 2 and 3.

SUPPORTING EVIDENCE FROM PYROLYSIS DATA

Volatile hydrocarbons (S_1) in source-rock samples can be measured by Rock-Eval thermal analysis. The onset of oil generation is frequently indicated by a marked increase in S_1 . Low resistivities in the Woodford Shale are associated with low values of S_1 that probably reflect thermally immature source rocks (Fig. 2). Resistivities greater than ~ 30 ohm-m are associated with elevated values of S_1 that are indicative of oil generation. The data are too sparse to define with precision the resistivity zone corresponding to the onset of oil generation, but the data support the

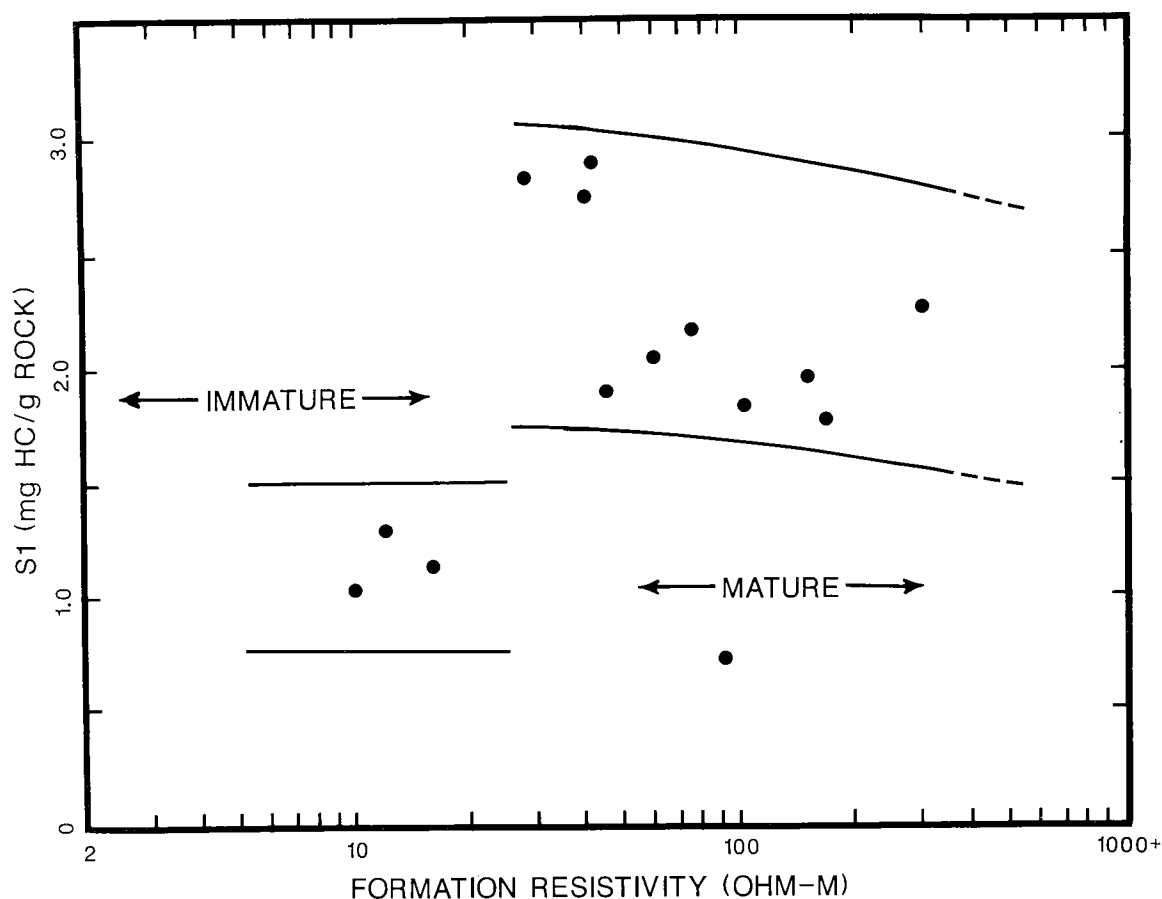


Figure 2. Volatile hydrocarbons (S_1) versus formation resistivity for the Woodford Shale of the study area (Fig. 1). Thermally mature source rocks, marked by an abrupt increase in S_1 , have high resistivities.

concept that formation resistivity is a measure of free hydrocarbons, and thus of oil generation, in the Woodford Shale.

ONSET OF OIL GENERATION

Data in plots of vitrinite-reflectance versus formation-resistivity for the Woodford Shale of the study area group into two quadrants (Fig. 3A). In accordance with the preceding discussion, points in the upper-left quadrant represent thermally immature shales, and points in the lower-right quadrant represent shales that are thermally mature and have generated oil. An analogous plot (Fig. 3B) using Lopatin's time-temperature index of thermal maturity (Waples, 1980)—a second, independent measure of the level of thermal maturation—shows a similar pattern. Again, data group into two quadrants representing immature (low-resistivity) and mature (high-resistivity) shales.

A resistivity of ~ 35 ohm-m marks the center of the zone of transition between immature and mature source rocks in Figure 3. This value is in accord with the approximate transition suggested by the pyrolysis data of Figure 2. A choice for the midpoint resistivity of the transition zone that is appreciably higher or lower than 35 ohm-m tends to blur the distinction between mature- and immature-shale quadrants by placing data points in a category that is neither mature nor immature.

The level of thermal maturity (R_o or TTI) marking the onset of appreciable oil generation in the highest-resistivity Woodford Shale intervals of the study area is defined by Figures 3A and 3B as the maturity corresponding to the transition zone between low (<35 ohm-m) and high resistivities. Oil generation sufficient to displace pore water occurs at a vitrinite-reflectance level of about 0.56–0.57% (Fig. 3A). Note that the Woodford Shale is not homogeneous, and the onset of oil generation defined by Figure 3A does not apply to all areas and facies of the formation.

Black shales such as the Woodford have varying kerogen compositions, so that precise levels of thermal maturity required for oil generation cannot be predicted *a priori*. The approach illustrated by Figure 3A offers a means to quantify the onset of oil generation in such rocks in terms of vitrinite reflectance.

Oil generation sufficient to displace pore water, measured in terms of a calculated time-tempera-

ture history of the Woodford Shale, corresponds to TTI values of about 33 to 48 (Fig. 3B). TTI values are rarely linked directly to the onset of oil generation, as in Figure 3B, but are usually calibrated to vitrinite reflectance, which in turn is correlated with stages of oil generation. However, problems may arise with such indirect calibrations of TTI. R_o may be systematically biased by laboratory practices or by geologic factors, and TTI may be systematically biased by incorrect time-temperature reconstructions. In addition, the level of thermal maturation required for oil generation is a function of kerogen composition. Crossplots of TTI versus resistivity, as illustrated by Figure 3B, provide a direct calibration between TTI and the onset of appreciable oil generation.

SUMMARY

In black shales with sufficient organic richness, such as some facies of the Woodford Shale, formation resistivity increases in response to oil generation and thus offers a means to "observe" the in situ formation of petroleum. Using resistivity data alone, the Woodford Shale can be categorized as either thermally immature or mature. As a working hypothesis, a resistivity of ~ 35 ohm-m can be taken as a general indicator of the onset of oil generation.

If measurements of vitrinite reflectance are available, R_o at the onset of significant oil generation can be determined from the R_o -resistivity crossplot, as illustrated by Figure 3A. The onset of oil generation varies with kerogen composition and thus provides insight into source-rock properties. TTI corresponding to the onset of significant oil generation can be determined from the TTI-resistivity crossplot, as illustrated by Figure 3B. Problems of indirect calibration of TTI values are circumvented, and TTI is directly linked to oil generation.

ACKNOWLEDGMENTS

B. J. Cardott of the Oklahoma Geological Survey generously made available unpublished vitrinite-reflectance data for the Woodford Shale, and T. A. Daws of the U.S. Geological Survey performed pyrolysis analyses. This work was done as part of the U.S. Geological Survey's Evolution of Sedimentary Basins Program.

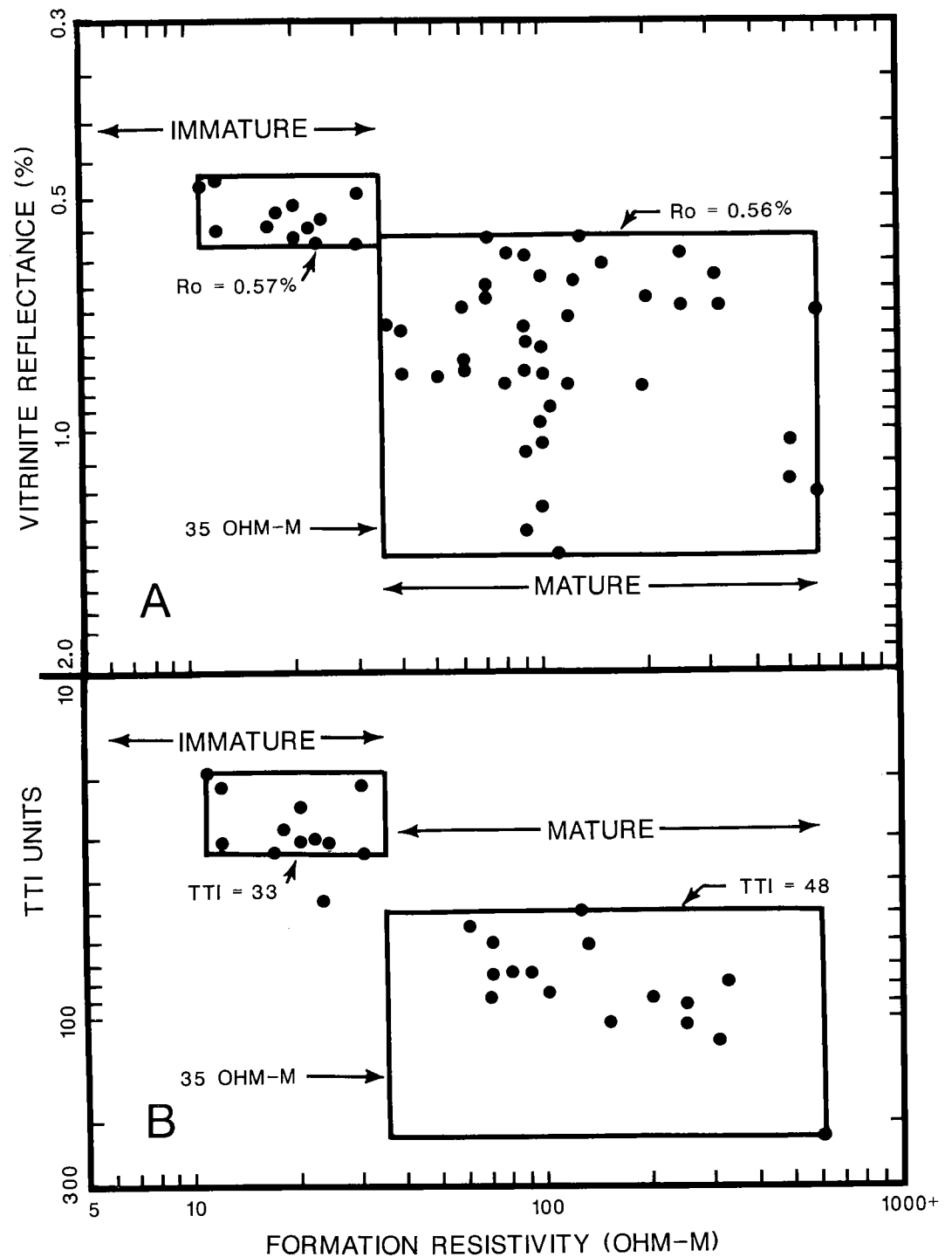


Figure 3. A—Vitrinite reflectance (Cardott and Lambert, 1985; B. J. Cardott, personal communication, 1986) versus formation resistivity for Woodford Shale at well locations shown in Figure 1. B—Lopatin's time-temperature index of thermal maturity (TTI) versus formation resistivity for Woodford Shale at well locations (Fig. 1) where vitrinite reflectance of the Woodford is $<0.7\%$. TTI calculations are after Schmoker (1986). In both panels, data form an upper-left quadrant representing thermally immature shales and a lower-right quadrant representing thermally mature shales that have generated oil.

EVIDENCE OF EARLY OIL GENERATION IN THE WOODFORD SHALE, WITCHER FIELD, CENTRAL OKLAHOMA

TERRY SMITH
University of Tulsa

Abstract.—Vitrinite-reflectance (R_o) values of Woodford Shale in the Witcher Field of central Oklahoma indicate that the local Woodford is too immature to generate petroleum. This seems to be confirmed by the lack of significant correlation between the GC/MS terpane “fingerprints” of Woodford Shale extracts and reservoirized Hunton crude oil within the field. However, extracts of Pennsylvanian Red Fork Sandstone lying directly above the Woodford contain migrated petroleum that correlates with the crude oil in the terpane fingerprints, but which is significantly less mature than the crude oil in GC/MS sterane isomer distributions and the hopane series T_s/T_m ratio. In thin section, the sandstone formation lacks indigenous organic matter; therefore, it must be assumed that the petroleum represents a mixture of mature crude oil similar to that found in the reservoirs and less-mature oil generated in and expelled from the local Woodford.

MODELING OF HYDROCARBON GENERATION AND MIGRATION FOR THE WOODFORD SHALE IN THE ANADARKO BASIN

LONGJIANG WANG

University of Tulsa

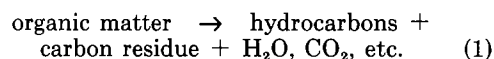
In recent years computer modeling of oil generation in a sedimentary basin has been widely used in the oil industry, and a variety of models have been proposed (e.g., Lopatin, 1971; Tissot and Espitalié, 1975; Sweeney and others, 1987). A similar feature of all these models is to simulate the oil-generation process from the beginning of oil generation. The kinetic parameters and the initial amount of organic matter are assumed to be known. Unfortunately, no models have been developed to determine directly the amount of oil generated from a source rock based on the study of the present rock. At present what we can deduce from studying a source rock is the end results of the source rock after oil generation and migration. We do not know the initial amount of organic matter in the source rock, the amount of oil that has been generated, or the amount of oil which has migrated from the source rock. However, we do know the mechanism of oil generation, and we can infer the geothermal history of the source rock. From the study of the present rock, we can determine the amount of bitumen, the generation potential of the rock, and kerogen type. The question is whether it is possible to use these results and the knowledge of the oil-generation mechanism to find out the amount of oil generated and migrated out of the source rock. The purpose of this paper is to develop a method using pyrolysis data to do this work.

A kinetic model of oil generation and migration has been developed. It incorporates a mass balance of all of the organic matter and can be used to calculate the amount of oil generated for a given source rock, the amount migrated out of the source rock, and the oil-expulsion efficiency. The model can also be used to establish the time of oil generation and migration, as well as the thermal maturity of the source rock.

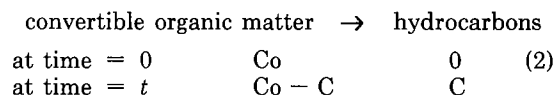
The model is based on two assumptions: (1) oil generation obeys first-order kinetic law; and (2) the total amount of oil that can be generated from a source rock is a constant. The input data required for the model are the amount of bitumens (S1), the amount of pyrolysates from kerogen (S2), the kinetic parameters for kerogen, and the geothermal history of the source rock.

Figure 1 is a schematic diagram showing the evolution of the organic matter in a source rock through its geologic history. The figure also shows

laboratory pyrolysis for the rock. The overall oil-generation process can be described by the following reaction:



Let us assume that the organic matter in a source rock can be divided into two parts. One part is called convertible organic matter. Upon heating, this part of the organic matter will transform only to hydrocarbons. If enough time and heat energy are available, it will completely convert to hydrocarbons. Another part is called nonconvertible organic matter, and it either remains unchanged (forming a carbon residue) or forms nonhydrocarbons (water, carbon dioxide, and other gases) during oil generation. Oil generation can be modeled by considering the convertible organic matter. Terms in the following equations are explained in Table 1.



If we assume that there are n reactions in the oil-generation process and each reaction has its own kinetic parameters, the following two equations can be derived:

$$\begin{aligned} \text{CG} &= \text{CK} \sum_{i=1}^n \text{Xi} [1 - \exp(-\int_0^t \text{Ai} \exp(-\text{Ei}/\text{RT}(t)) dt)] / \\ &[1 - \sum_{i=1}^n (\text{Xi} (1 - \exp(-\int_0^t \text{Ai} \exp(-\text{Ei}/\text{RT}(t)) dt))] \end{aligned} \quad (3)$$

$$C = \text{Co} \sum_{i=1}^n [\text{Xi} (1 - \exp(-\int_0^t \text{Ai} \exp(-\text{Ei}/\text{RT}(t)) dt))] \quad (4)$$

The relationships among different hydrocarbons for a source rock are given in Figure 2. Equation (3) is first used to calculate CG; then equation (4) is used to calculate the hydrocarbons generated at any time throughout the geologic evolution of a source rock.

Several useful parameters can also be defined as follows:

1. The amount of hydrocarbons migrated out of a source rock, CM:

$$\text{CM} = \text{CG} - \text{CB} + \text{Yo}$$

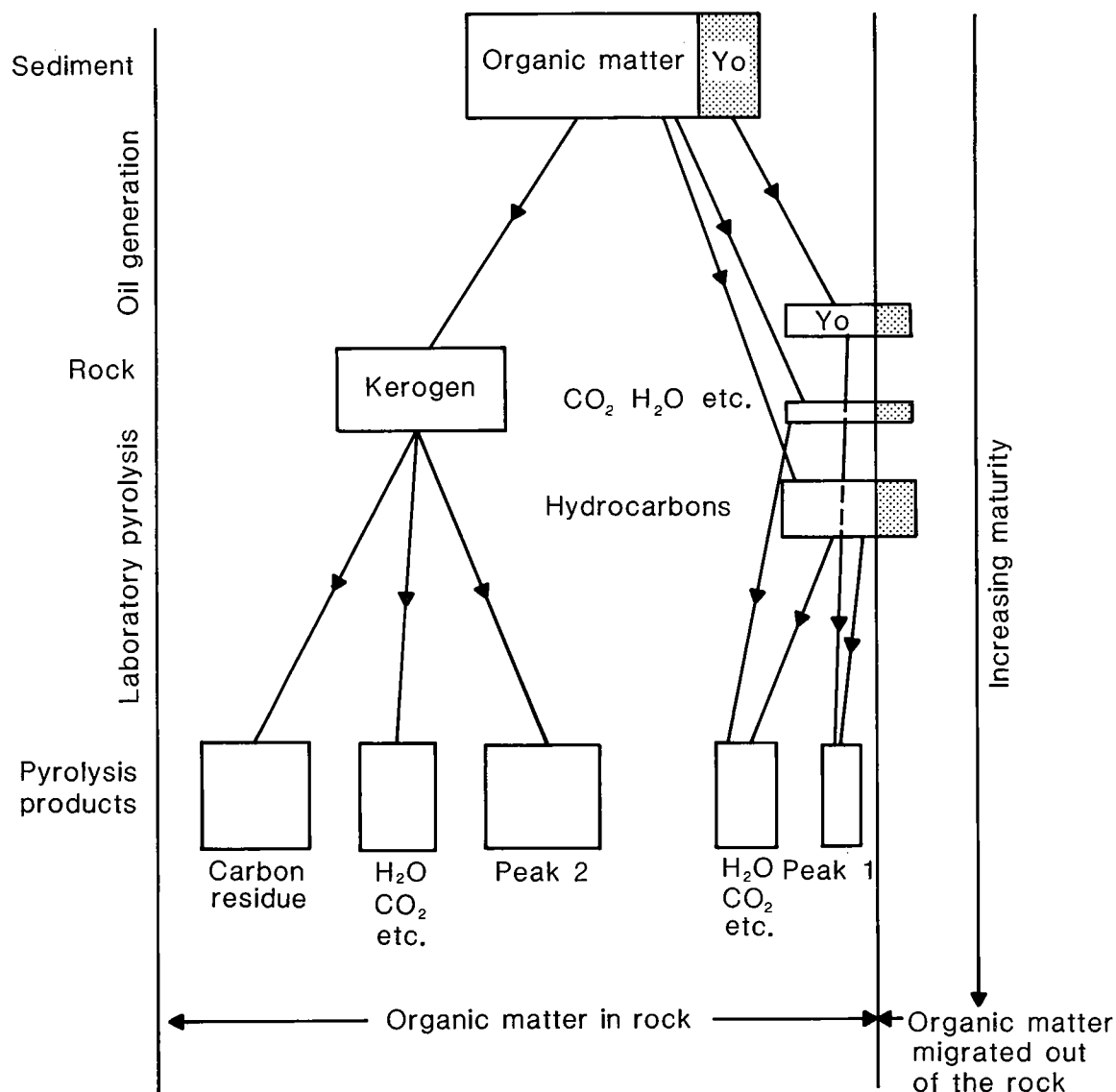


Figure 1. Schematic diagram showing the evolution of organic matter in the process of oil generation and laboratory pyrolysis. Yo = fossil hydrocarbons.

2. Expulsion efficiency, EE:

$$EE + CM/(CG + Yo) = (CG - CB + Yo)/(CG - Yo) = 1 - CB/(CG + Yo)$$

3. Conversion ratio, CR:

$$CR = CG/(CG + CK)$$

4. Total generation potential of the rock, TP:

$$TP = CG + CK + Yo$$

The input data for the model are the amount of bitumen ($S1 = CB$), the generation potential ($S2 = CK$), the geothermal history of the rock ($T(t)$), and the kinetic parameters of kerogen in the rock (E and A). If immature samples are available for the source rock, the kinetic parameters of kerogen in the rock can be determined in the laboratory (Burnham and Braun, 1985; Ungerer and others, 1986; Quigley and others, 1987).

TABLE 1. —SYMBOLS USED
IN KINETIC MODELING

S1:	Peak 1
S2:	Peak 2
Co:	Initial amount of convertible organic matter in a source rock; $Co = CG + CK$
C:	Amount of hydrocarbons generated at time t (m.y.)
X_i :	Fraction of the i th reaction at time zero
i :	The i th reaction ($i = 1, 2, \dots, n$)
n :	The number of reactions in the oil generation process
E_i :	Activation energy of the i th reaction
A_i :	Arrhenius constant of the i th reaction
$T(t)$:	Geothermal history of a source rock
t :	Any time during a source rock evolution (m.y.)
t_p :	Present time of a source rock (m.y.)
CB:	Amount of bitumen
CK:	Generation potential of a source rock
CG:	Amount of hydrocarbons already generated by a source rock
CM:	Amount of hydrocarbons migrated out of a source rock
Yo:	Amount of fossil hydrocarbons in a rock before oil generation
TP:	Total generation potential of a source rock
CR:	Conversion ratio
EE:	Expulsion efficiency
R:	Universal gas constant

If no immature samples are available, the published results for the kerogen type can be used (e.g., Tissot and Espitalié, 1975).

The model has been used to simulate oil generation and migration for two source rocks. The maturity data (CR) determined from the new model were compared with Lopatin's TTI and Tissot and Espitalié's transformation ratio. The model is now being used to simulate oil generation and migration for the Woodford Shale in the Anadarko basin.

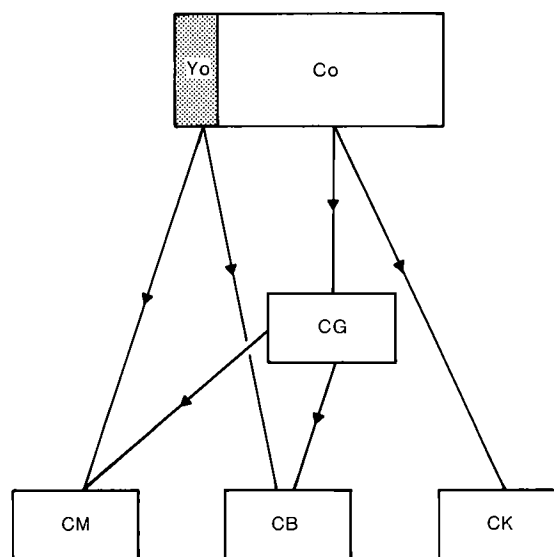


Figure 2. Block diagram showing the distribution of different hydrocarbons. See Table 1 for the meaning of symbols.

BIOMARKER CHARACTERIZATION OF WOODFORD-TYPE OIL AND CORRELATION TO SOURCE ROCK, AYLESWORTH FIELD, MARSHALL COUNTY, OKLAHOMA

JENNIFER REBER

University of Tulsa

Abstract.—In several counties in southern Oklahoma, crude oil is commercially produced out of fractures and stylolites from the Woodford Formation. Source-rock data here indicate that the Woodford, while extremely organic-rich, is too thermally immature ($R_o = 0.46$) to have expelled a significant amount of oil. Core samples analyzed in this study have an average total organic carbon of 7.7%. Elemental O/C ratios of 0.07 and H/C ratios of 1.14 indicate samples with type-II oil-prone kerogen that fall within the primary zone of oil generation on a van Krevelen diagram.

Three Woodford crudes from the Madill and Aylesworth fields and rock extracts from an immature Woodford core from the Aylesworth Field, Marshall County, Oklahoma, were geochemically analyzed for carbon isotopes, light-end distribution, and pristane/phytane. A stepwise extraction technique was developed in an attempt to sample bitumen in fractures and stylolites, as well as indigenous bitumen. A special emphasis was placed on biomarker distributions, determined by a combination of gas chromatography and mass spectrometry, in an attempt to determine if the commercially produced Woodford crude was sourced by the local immature Woodford Shale, or migrated into stylolites and fractures from a more thermally mature source. A secondary purpose of the study was to determine if biomarker distributions and ratios change with lengthy extraction time.

Based on the aforementioned geochemical parameters, maturity calculations using C_{27} trisnorhopanes (Ts/Tm), S and R isomers of C_{31} homohopane, S and R isomers of C_{28} ethyl cholesterol, $\beta\beta$ steranes/total steranes, and percent of $C_{20}/(C_{20} + C_{28})$ triaromatics, the Woodford oils and source-rock extracts analyzed in this study appear to be of the same maturity; therefore, they correlate. If the correlation is real, it is suggested that source rocks at the immature threshold of the oil-generation window may indeed be able to expel a commercial quantity of oil.

Results of biomarker analysis also show that isomer ratios and biomarker distributions do not change significantly with lengthy extraction time (>700 hr).

COLLECTED REFERENCES

- Abdullah, T. Y., 1985, Depositional facies in the Funston cycle (Lower Permian) of southwestern Kansas, in Watney, W. L.; Walton, A. N.; and Doveton, J. H. (compilers); and Adkins-Heljeson, M. D. (ed.), *Core studies in Kansas: Kansas Geological Survey Subsurface Geology Series 6*, p. 161-171.
- Adams, W. L., 1964, Diagenetic aspects of lower Morrowan, Pennsylvanian, sandstones, northwestern Oklahoma: American Association of Petroleum Geologists Bulletin, v. 48, p. 1568-1580.
- Addison, W. L., 1972, Stratigraphy and structure of Middle and Upper Ordovician rocks in the Sedgewick basin and adjacent areas, south and central Oklahoma: U.S. Geological Survey Professional Paper 702, 33 p.
- Adler, F. J., 1971, Anadarko basin and central Oklahoma area, in Cram, I. H. (ed.), *Future petroleum provinces of the United States—their geology and potential: American Association of Petroleum Geologists Memoir 15*, v. 2, p. 1061-1070.
- Adler, F. J.; and others, 1971, Future petroleum provinces of the Mid-Continent, region 7, in Cram, I. H. (ed.), *Future petroleum provinces of the United States—their geology and potential: American Association of Petroleum Geologists Memoir 15*, v. 2, p. 985-1120.
- Almon, W. R.; and Davies, D. K., 1981, Formation damage and the crystal chemistry of clays, in Longstaffe, F. J. (ed.), *Clays and the resource geologist: Mineralogical Society of Canada Short Course Handbook*, v. 7, p. 81-103.
- Al-Shaieb, Zuhair; and Walker, Patty, 1986, Evolution of secondary porosity in Pennsylvanian Morrow sandstones, Anadarko basin, Oklahoma, in Spencer, C. W.; and Mast, R. F. (eds.), *Geology of tight gas reservoirs: American Association of Petroleum Geologists Studies in Geology 24*, p. 45-67.
- Amadei, Bernard; Swolfs, H. S.; and Savage, W. Z., 1988, Gravity-induced stresses in stratified rock masses: *Rock Mechanics and Rock Engineering*, v. 21, p. 1-20.
- American Society for Testing and Materials, 1987, Annual book of ASTM standards: gaseous fuels; coal and coke: American Society for Testing and Materials, sec. 5, v. 5.05, 559 p.
- Amsden, T. W., 1949, Stratigraphy and paleontology of the Brownsport Formation (Silurian) of western Tennessee: Yale University, Peabody Museum of Natural History Bulletin 5, 138 p.
- 1955, Lithofacies map of Lower Silurian deposits in central and eastern United States and Canada: American Association of Petroleum Geologists Bulletin, v. 39, p. 60-74.
- 1960, Hunton stratigraphy, pt. 6 of Stratigraphy and paleontology of the Hunton Group in the Arbuckle Mountain region: Oklahoma Geological Survey Bulletin 84, 311 p.
- 1968, Articulate brachiopods of the St. Clair Limestone (Silurian), Arkansas, and the Clarita Formation (Silurian), Oklahoma: Paleontological Society Memoir 1 [Journal of Paleontology, v. 42, no. 3, suppl.], 117 p.
- 1969, A widespread zone of pentamerid brachiopods in subsurface Silurian strata of Oklahoma and the Texas Panhandle: Journal of Paleontology, v. 43, p. 961-975.
- 1974, Late Ordovician and Early Silurian articulate brachiopods from Oklahoma, southwestern Illinois, and eastern Missouri: Oklahoma Geological Survey Bulletin 119, 154 p.
- 1975, Hunton Group (Late Ordovician, Silurian, and Early Devonian) in the Anadarko basin of Oklahoma: Oklahoma Geological Survey Bulletin 121, 214 p.
- 1980, Hunton Group (Late Ordovician, Silurian, and Early Devonian) in the Arkoma basin of Oklahoma: Oklahoma Geological Survey Bulletin 129, 136 p.
- 1981, Biostratigraphic and paleoenvironmental relations: a Late Silurian example, in Broadhead, T. W. (ed.), *Lophophorates, notes for a short course organized by J. T. Dutro, Jr., and R. S. Boardman: University of Tennessee, Department of Geological Sciences, Studies in Geology 5*, p. 154-169.
- Amsden, T. W.; and Barrick, J. E., 1986, Late Ordovician-Early Silurian strata in the central United States and the Hirnantian Stage: Oklahoma Geological Survey Bulletin 139, 95 p.
- 1988, Late Ordovician through Early Devonian annotated correlation chart and brachiopod range charts for the southern Midcontinent region, U.S.A., with a discussion of Silurian and Devonian conodont faunas: Oklahoma Geological Survey Bulletin 143, 66 p.
- Amsden, T. W.; and Rowland, T. L., 1965, Silurian stratigraphy of northeastern Oklahoma: Oklahoma Geological Survey Bulletin 105, p. 174.
- Amsden, T. W.; Toomey, D. F.; and Barrick, J. E., 1980, Paleoenvironment of Fitzhugh Member of Clarita Formation (Silurian, Wenlockian), southern Oklahoma: Oklahoma Geological Survey Circular 83, 54 p.
- Anders, D. E.; Magoon, L. B.; and Lubeck, C., 1987, Geochemistry of surface oil shows and potential source rocks, in Bird, K. J.; and Magoon, L. B. (eds.), *Petroleum geology in the northern part of the Arctic National Wildlife Refuge, northeast Alaska: U.S. Geological Survey Bulletin 1778*, p. 181-198.
- Babaei, A., 1980, The structural geology of part of the Limestone Hills in the Wichita Mountains, Caddo and Comanche Counties, Oklahoma: Oklahoma State University unpublished M.S. thesis, 63 p.
- Bailey, N. J. L.; Krouse, H. R.; Evans, C. R.; Rogers, M. A., 1973, Alteration of crude oil by waters and bacteria—evidence from geochemical and isotope studies: American Association of Petroleum Geologists Bulletin, v. 57, p. 1276-1290.
- Bambach, R. K.; Scotese, C. R.; and Ziegler, A. M., 1980, Before Pangaea—the geographies of the Paleozoic world: American Scientist, v. 68, p. 26-38.
- Barker, C., 1979, Organic geochemistry in petroleum exploration: American Association of Petroleum Geologists Continuing Education Course Note Series 10, 160 p.
- Barnes, V. E.; Cloud, P. E., Jr.; and Warren, L. E., 1947, Devonian rocks of central Texas: Geological Society of America Bulletin, v. 48, p. 125-140.
- Barrett, C. M., 1980, A gravity and magnetic study of the Kingfisher anomaly, north-central Oklahoma:

- University of Oklahoma unpublished M.S. thesis, 45 p.
- Bartlett, W. L.; Friedman, M.; and Logan, J. M., 1981, Experimental folding and faulting of rocks under confining pressure. Part 9. Wrench faults in limestone layers: *Tectonophysics*, v. 79, p. 255-277.
- Barwise, A. J., 1986, High performance liquid chromatography analysis of free base porphyrins. I. An improved method: *Journal of Chromatography*, v. 368, p. 1-9.
- Barwise, A. J.; and Park, P. J. D., 1983, Petroporphyrin fingerprinting as a geochemical marker, in Bjorøy, M.; and others (eds.), *Advances in organic geochemistry 1981*: John Wiley, London, p. 667-674.
- Barwise, A. J.; and Whitehead, E. V., 1979, Separation and structure of petroporphyrins, in *Advances in organic geochemistry 1979*: Pergamon Press, Oxford, p. 181-191.
- Batschelet, Edward, 1965, Statistical methods for the analysis of problems in animal orientation and certain biological rhythms: *American Institute of Biological Sciences Monograph*, 57 p.
- Beauchamp, W. H., 1983, The structural geology of the southern Slick Hills, Oklahoma: Oklahoma State University unpublished M.S. thesis, 119 p.
- Beaumont, C.; Boutilier, R.; Mackenzie, A. S.; and Rullkötter, J., 1985, Isomerization and aromatization of hydrocarbons and the paleothermometry and burial history of Alberta foreland basin: *American Association of Petroleum Geologists Bulletin*, v. 69, p. 546-566.
- Becker, C. M., 1927, Geology of Caddo and Grady Counties: *Oklahoma Geological Survey Bulletin* 40-I, 18 p.
- Bell, J. S.; and Gough, D. I., 1979, Northeast-southwest compressive stress in Alberta—evidence from oil wells: *Earth and Planetary Science Letters*, v. 45, p. 475-482.
- 1982, The use of borehole breakouts in the study of crustal stress, in Zoback, M. D.; and Haimson, B. C. (eds.), *Proceedings of workshop on hydraulic fracturing stress measurements*: U.S. Geological Survey Open-File Report 82-1575, p. 539-557.
- Bennison, A. P.; and Chenoweth, P. A. [no date], Geologic highway map of northern Great Plains region: *American Association of Petroleum Geologists Map* 12, 1 sheet, scale 1:1,875,000.
- Berg, O. R., 1974, North Custer City field, in Berg, O. R.; Koinm, D. N.; and Richardson, D. E. (eds.), *Oil and gas fields of Oklahoma, reference report, supplement I*: Oklahoma City Geological Society, p. 10.
- Berg, R. R., 1962, Mountain flank thrusting in Rocky Mountain foreland, Wyoming and Colorado: *American Association of Petroleum Geologists Bulletin*, v. 46, p. 2019-2032.
- Berry, W. B. N.; and Boucot, A. J., 1970, Correlation of the North American Silurian rocks: *Geological Society of America Special Paper* 102, 289 p.
- Bertrand, R.; and Héroux, Y., 1987, Chitinozoan, graptolite, and scolecodont reflectance as an alternative to vitrinite and pyrobitumen reflectance in Ordovician and Silurian strata, Anticosti Island, Quebec, Canada: *American Association of Petroleum Geologists Bulletin*, v. 71, p. 951-957.
- Bethke, C. M., 1986, Hydrologic constraints on genesis of the upper Mississippi Valley Mineral District from Illinois basin brines: *Economic Geology*, v. 81, no. 2, p. 233-249.
- Bethke, C. M.; Harrison, W. J.; Upson, C.; and Altaner, S. P., 1988, Supercomputer analysis of sedimentary basin: *Science*, v. 239, p. 261-267.
- Blümling, Peter, 1986, In situ spannungsmessung in Tiefbohrungen mit hilfe von Bohrlochrandausbrüchen und die spannungsverteilung in der kruste mitteleuropas und Australiens: Karlsruhe University, West Germany, unpublished Ph.D. dissertation.
- Bockmeulen, H.; Barker, C.; and Dickey, P. A., 1983, Geology and geochemistry of crude oils, Bolivar Coastal fields, Venezuela: *American Association of Petroleum Geologists Bulletin*, v. 67, p. 242-270.
- Boles, J. R., 1982, Active abtization of plagioclase Gulf Coast Tertiary: *American Journal of Science*, v. 282, p. 165-180.
- Boles, J. R.; and Franks, S. G., 1979a, Clay diagenesis in Wilcox sandstones of southwest Texas: implications of smectite diagenesis on sandstone cementation: *Journal of Sedimentary Petrology*, v. 49, p. 55-70.
- 1979b, Clay diagenesis in Wilcox sandstones of southwest Texas: implications of smectite diagenesis on sandstone cementation, in Scholle, P. A.; and Schluger, P. A. (eds.), *Aspects of diagenesis: Society of Economic Paleontologists and Mineralogists Special Publication* 26, p. 185-207.
- Booth, S. L., 1981, Structural analysis of a portion of the Washita Valley fault zone, Arbuckle Mountains, Oklahoma: *Shale Shaker*, v. 31, p. 107-120.
- Borjeson, R. W.; and Lamb, T. J., 1987, Geotechnical borehole testing report Holtzclaw No. 1 well (PD-10), Palo Duro basin: Stone and Webster Engineering Corporation, 312 p.
- Bostick, N. H., 1979, Microscopic measurement of the level of catagenesis of solid organic matter in sedimentary rocks to aid exploration for petroleum and to determine former burial temperatures—a review, in Scholle, P. A.; and Schluger, P. A. (eds.), *Aspects of diagenesis: Society of Economic Paleontologist and Mineralogists Special Publication* 26, p. 17-43.
- Bostick, N. H.; and Foster, J. N., 1975, Comparison of vitrinite reflectance in coal seams and in kerogen of sandstone, shale, and limestones in the same part of a sedimentary section, in Alpern, B. (ed.), *Pétrographie de la matière organique des sédiments, relations avec la paléotempérature et le potentiel pétrolier*: Centre National de la Recherche Scientifique, Paris, p. 13-25.
- Bradfield, H. H., 1968, Stratigraphy and structure of the deeper Marietta basin of Oklahoma and Texas, in Wendell, J. S. (ed.), *Basins of the Southwest*: American Association of Petroleum Geologists, Tulsa, v. 1, p. 54-70.
- Branson, C. C., 1962, Pennsylvanian System of the Mid-Continent, in Branson, C. C. (ed.), *Pennsylvanian System in the United States—a symposium*: American Association of Petroleum Geologists, Tulsa, p. 431-460.
- Brevetti, D. A.; Greer, G. K.; and Weis, B. R., 1984, Evaluation of fractured carbonates in the Mid-Continent region: *Society of Professional Well Log Analysts, 26th Annual Logging Symposium*, Schlumberger Reprint, 19 p.
- Brewer, J. A., 1982, Study of southern Oklahoma aulacogen, using COCORP deep seismic-reflection profiles, in Gilbert, M. C.; and Donovan, R. N. (eds.), *Geology of the eastern Wichita Mountains, southwestern Oklahoma*: Oklahoma Geological Survey Guidebook 21, p. 31-39.

- Brewer, J. A.; Good, R.; Oliver, J. E.; Brown, L. D.; and Kaufman, S., 1983, COCORP profiling across the southern Oklahoma aulacogen: overthrusting of the Wichita Mountains and compression within the Anadarko basin: *Geology*, v. 11, p. 109-114.
- 1984, COCORP deep seismic reflection traverse across the southern Oklahoma aulacogen, in Borger, J. G., III (ed.), Technical proceedings of the American Association of Petroleum Geologists, Mid-Continent Section, 1981 regional meeting: Oklahoma City Geological Society, p. 191-194.
- Bridge, Josiah, 1930, *Geology of the Eminence and Cardareva Quadrangles*: Missouri Bureau of Geology and Mines, v. 24 (2nd series), p. 134-150.
- Bridges, S. D., 1985, Mapping, stratigraphy, and tectonic implications of Lower Permian strata, eastern Wichita Mountains, Oklahoma: Oklahoma State University unpublished M.S. thesis, 129 p.
- Brown, L. F., Jr., 1969, Late Pennsylvanian paralic sediments, in Brown, L. F., Jr.; and Wermund, E. G. (eds.), *A guidebook to the Late Pennsylvanian shelf sediments, north-central Texas*: Dallas Geological Society, p. 21-33.
- Brown, R. O., 1978, Application of fracture identification logs in the Cretaceous of north Louisiana and Mississippi: *Gulf Coast Association of Geological Societies Transactions*, v. 28, p. 75-91.
- Brown, W. G., 1984, Washita Valley fault system: a new look at an old fault, in Borger, J. G., III (ed.), Technical proceedings of the American Association of Petroleum Geologists, Mid-Continent Section, 1981 regional meeting: Oklahoma City Geological Society, p. 68-80.
- Bruce, C. H., 1984, Smectite dehydration—its relation to structural development and hydrocarbon accumulation in northern Gulf of Mexico basin: *American Association of Petroleum Geologists Bulletin*, v. 68, p. 673-683.
- Budnick, R. T., 1983, Recurrent motion on Precambrian-age basement faults, Palo Duro basin, Texas Panhandle [abstract]: *American Association of Petroleum Geologists Bulletin*, v. 67, p. 433.
- 1986, Left-lateral intraplate deformation along the Ancestral Rocky Mountains: implications for Late Paleozoic plate reconstructions: *Tectonophysics*, v. 132, p. 195-214.
- 1987, Late Miocene reactivation of Ancestral Rocky Mountain structures in the Texas Panhandle—a response to basin and range extension: *Geology*, v. 15, p. 163-166.
- Budnik, Roy; and Smith, Dale, 1982, Regional stratigraphic framework of the Texas Panhandle, in *Geology and geohydrology of the Palo Duro basin, Texas Panhandle—a report on the progress of nuclear waste isolation feasibility studies*: Texas Bureau of Economic Geology Circular 82-7, p. 38-86.
- Burchett, R. R.; Luza, K. V.; Van Eck, O. J.; and Wilson, F. W., 1985, Seismicity and tectonic relationships of the Nemaha uplift and Midcontinent geophysical anomaly (final project summary): Oklahoma Geological Survey Special Publication 85-2, 33 p.
- Burchfield, M. R., 1985, Map of Oklahoma oil and gas fields: Oklahoma Geological Survey GM-28, 1 sheet, scale 1:500,000.
- Burnham, A. K.; and Braun, R. L., 1985, General kinetic model of oil shale pyrolysis: *In Situ*, v. 9, p. 1-23.
- Burruss, R. C., 1981, Hydrocarbon fluid inclusions in studies of sedimentary diagenesis, in Hollister L. S.; and Crawford, M. L. (eds.), *Fluid inclusions: applications to petrology*: Mineralogical Association of Canada Short Course Notes, v. 6, p. 138-156.
- Burruss, R. C.; and Hatch, J. R., 1987, Regional variations in crude oil geochemistry, Anadarko basin, Oklahoma, Texas, and Kansas—evidence for multiple sources, mixing and migration distances [abstract]: *American Association of Petroleum Geologists Bulletin*, v. 71, p. 535.
- Burruss, R. C.; Cercone, K. R.; and Harris, P. M., 1985, Timing of hydrocarbon migration: evidence from fluid inclusions in calcite cements, tectonics, and burial history, in Harris, P. M.; and Schneidermann, N. M. (eds.), *Carbonate cements revisited: Society of Economic Paleontologists and Mineralogists Special Publication 36*, p. 277-289.
- Burst, J. F., 1969, Diagenesis of Gulf Coast clayey sediments and its possible relation to petroleum migration: *American Association of Petroleum Geologists Bulletin*, v. 53, p. 73-93.
- Burtner, R. L.; and Warner, M. A., 1986, Relationship between illite/smectite diagenesis and hydrocarbon generation in Lower Cretaceous Mowry and Skull Creek shales of the northern Rocky Mountain area: *Clays and Clay Minerals*, v. 34, p. 390-402.
- Burwood, R.; Drozd, R. J.; Halpern, H. I.; and Sedivy, R. A., 1988, Carbon isotopic variations of kerogen pyrolyzates: *Organic Geochemistry*, v. 12, p. 195-205.
- Busch, D. A., 1959, Prospecting for stratigraphic traps: *American Association of Petroleum Geologists Bulletin*, v. 43, p. 2829-2843.
- Bustin, R. M.; Cameron, A. R.; Grieve, D. A.; and Kalkreuth, W. D., 1985, *Coal petrology—its principles, methods, and applications* [2nd revised edition]: Geological Association of Canada Short Course Notes 3, 230 p.
- Campbell, J. A.; Mankin, C. J.; Schwarzkopf, A. B.; and Raymer, J. H., 1988, Habitat of petroleum in Permian rocks of the Midcontinent region, in Morgan, W. A.; and Babcock, J. A. (eds.), *Permian rocks of the Midcontinent region*: Society of Economic Paleontologists and Mineralogists Special Publication 1, p. 13-25.
- Cardott, B. J.; and Lambert, M. W., 1985, Thermal maturation by vitrinite reflectance of Woodford Shale, Anadarko basin, Oklahoma: *American Association of Petroleum Geologists Bulletin*, v. 69, p. 1982-1998.
- 1987, Thermal maturation by vitrinite reflectance of Woodford Shale, Anadarko basin, Oklahoma—reply: *American Association of Petroleum Geologists Bulletin*, v. 71, p. 898-899.
- Carlson, M. P., 1963, Lithostratigraphy and correlation of the Mississippian System in Nebraska: *Nebraska Geological Survey Bulletin* 21, 63 p.
- Carr, J. E.; and Bergman, D. L., 1976, Reconnaissance of the water resources of the Clinton Quadrangle, west-central Oklahoma: Oklahoma Geological Survey Hydrologic Atlas 5, 4 sheets, scale 1:250,000.
- Carson, B.; and Arcaro, N. P., 1983, Control of clay-mineral stratigraphy by selective transport in Late Pleistocene-Holocene sediments of northern Cascadia basin—Juan de Fuca Abyssal Plain: implications for studies of clay-mineral provenance: *Journal of Sedimentary Petrology*, v. 53, p. 395-406.
- Chenoweth, P. A., 1972, *Principal structural features of Oklahoma*: PennWell Maps, Tulsa, scale 1:500,000.
- Chicarelli, M. I.; Wolff, G. A.; and Maxwell, J. R., 1986,

- High-performance liquid chromatography analysis of free-base porphyrins. II. Structure and retention behavior: *Journal of Chromatography*, v. 368, p. 11–19.
- Christie-Blick, N.; and Biddle, K. T., 1985, Deformation and basin formation along strike-slip faults, in Biddle, K. T.; and Christie-Blick, N. (eds.), *Strike-slip deformation on basin formation and sedimentation*: Society of Economic Paleontologists and Mineralogists Special Publication 37, p. 1–34.
- Clayton, J. L.; King, J. D.; Threlkeld, C. N.; and Vuletic, A., 1987, Geochemical correlation of Paleozoic oils, northern Denver basin—implications for exploration: *American Association of Petroleum Geologists Bulletin*, v. 71, p. 103–109.
- Clement, W. A. [in press], The subsurface geology of the upper Red Fork in East Clinton and adjacent fields in Custer and Caddo Counties, Oklahoma: American Association of Petroleum Geologists.
- Cole, V. B., 1975, Subsurface Ordovician–Cambrian rocks in Kansas: Kansas Geological Survey Subsurface Geology Series 2.
- 1976, Precambrian structure of Kansas: Kansas Geological Survey Map 7, scale 1:500,000.
- Coleman, J. M., 1976, Deltas: processes of deposition and models for exploration: Continuing Education Publication Co., Inc., Champaign, 102 p.
- Collins, K., 1985, The evolution of the Meers Valley in the Wichita Mountains, Oklahoma: Oklahoma State University unpublished M.S. thesis, 128 p.
- Colton-Bradley, V. A., 1987, Role of pressure in smectite dehydration—effects on geopressure and smectite-to-illite transformation: *American Association of Petroleum Geologists Bulletin*, v. 71, p. 1414–1427.
- Comer, J. B.; and Hinch, H. H., 1987, Recognizing and quantifying expulsion of oil from the Woodford Formation and age-equivalent rocks in Oklahoma and Arkansas: *American Association of Petroleum Geologists Bulletin*, v. 71, p. 844–858.
- Condie, K. C., 1982, Plate-tectonics model for Proterozoic continental accretion in the southwestern United States: *Geology*, v. 10, p. 37–42.
- Connan, J., 1984, Biodegradation of crude oils in reservoirs, in Brooks, J.; and Welte, D. H. (eds.), *Advances in petroleum geochemistry*: Academic Press, New York, v. 1, p. 299–335.
- Cox, J. W., 1970, The high resolution dipmeter reveals dip-related borehole and formation characteristics: Society of Professional Well Log Analysts, 11th Annual Logging Symposium, p. 1–25.
- Craig, L. C.; and Varnes, K. L., 1979, History of the Mississippian System—an interpretive summary, in Craig, L. C.; Connor, C. W.; and others, *Interpretive summary and special features of the Mississippian System, pt. 2 of Paleotectonic investigations of the Mississippian System in the United States*: U.S. Geological Survey Professional Paper 1010, p. 371–406.
- Craig, L. C.; Connor, C. W.; and others, 1979, Paleotectonic investigations of the Mississippian System in the United States: U.S. Geological Survey Professional Paper 1010, parts 1–3.
- Crisp, P. T.; Ellis, J.; Hutton, A. C.; Korth, J.; Martin, F. A.; and Saxby, J. D., 1987, Australian oil shales: a compendium of geological and chemical data: Department of Geology, University of Wollongong, Australia, 109 p.
- Crone, A. J.; and Luza, K. V., 1986, Holocene deformation associated with the Meers fault, southwestern Oklahoma, in Donovan, R. N. (ed.), *The Slick Hills of southwestern Oklahoma—fragments of an aulacogen?*: Oklahoma Geological Survey Guidebook 24, p. 68–74.
- Crossey, L. J.; Hagen, E. S.; Surdan, R. C.; and Papoint, T. W., 1986, Correlation of organic parameters derived from elemental analysis and programmed pyrolysis of kerogen, in Gautier, D. L. (ed.), *Roles of organic matter in sediment diagenesis*: Society of Economic Paleontologists and Mineralogists Special Publication 38, p. 35–45.
- Crowell, J. C., 1959, Problems of fault nomenclature: *American Association of Petroleum Geologists Bulletin*, v. 43, p. 2653–2674.
- Dake, C. L., 1930, *Geology of Potosi and Edgehill Quadrangles*: Missouri Bureau of Geology and Mines, v. 23 (2nd series), p. 193–197.
- Dart, R. L., 1987, South-central United States well-bore breakout-data catalog: U.S. Geological Survey Open-File Report 87-405, 95 p.
- Dart, R. L.; and Zoback, M. L., 1987, Principal stress directions on the Atlantic continental shelf inferred from the orientations of borehole elongations: U.S. Geological Survey Open-File Report 87-283, 43 p.
- [in press], Well bore-breakout stress analysis within the Continental United States: *The Log Analyst Journal*.
- David, M.; Campiglio, C.; and Darling, R., 1974, Progresses in *R*- and *Q*-mode analysis: correspondence analysis and its application to the study of geological processes: *Canadian Journal of Earth Sciences*, v. 11, p. 131–146.
- David, M.; Dagbert, M.; and Beauchamin, Y., 1977, Statistical analysis in geology; correspondence analysis method: *Colorado School of Mines Quarterly*, v. 72, no. 1, 60 p.
- Davis, D. V., Jr., 1976, *Geology of Panoma gas area, southwestern Kansas* [abstract]: *American Association of Petroleum Geologists Bulletin*, v. 60, p. 318.
- Davis, J. C., 1973, *Statistics and data analysis in geology*: John Wiley, New York, 550 p.
- 1986, *Statistics and data analysis in geology* [2nd edition]: John Wiley, New York, 646 p.
- Davis, R. M., 1959, Patterson field, Kearny County, Kansas, in *Western Kansas, v. 2 of Kansas oil and gas fields*: Kansas Geological Society, p. 126–130.
- Decker, C. E.; and Merritt, C. A., 1931, The stratigraphy and physical characteristics of the Simpson Group: *Oklahoma Geological Survey Bulletin* 55, 112 p.
- Dembicki, H., Jr., 1984, An interlaboratory comparison of source rock data: *Geochimica et Cosmochimica Acta*, v. 48, p. 2641–2649.
- Denison, R. E., 1982, Geologic cross-section from the Arbuckle Mountains to the Muenster arch, southern Oklahoma and Texas: *Geological Society of America Map and Chart Series MC-28R*, 8 p.
- Denison, R. E.; Lidiak, E. G.; Bickford, M. E.; and Kisvarsanyi, E. B., 1984, Geology and geochronology of Precambrian rocks in the central interior region of the United States: U.S. Geological Survey Professional Paper 1241-C, 20 p.
- Dickinson, W. R.; and Suczek, C. A., 1979, Plate tectonics and sandstone compositions: *American Association of Petroleum Geologists Bulletin*, v. 63, p. 2164–2182.
- Dickson, J. A. D., 1966, Carbonate identification and genesis as revealed by staining: *Journal of Sedimentary Petrology*, v. 36, p. 491–505.

- Dietz, R. S.; and Holden, J. C., 1970, The breakup of Pangaea: *Scientific America*, v. 223, no. 4, p. 30-41.
- Dixon, G. H., 1967, Northeastern New Mexico and Texas-Oklahoma Panhandles, in McKee, E. D.; Oriel, S. S.; and others, Paleotectonic investigations of the Permian System in the United States: U.S. Geological Survey Professional Paper 515-D, p. 65-80.
- Donovan, R. N., 1982, Geology of Blue Creek Canyon, Wichita Mountains area, in Gilbert, M. C.; and Donovan, R. N. (eds.), Geology of the eastern Wichita Mountains, southwestern Oklahoma: Oklahoma Geological Survey Guidebook 21, p. 65-77.
- 1986a, Geology of the Slick Hills, in Donovan, R. N. (ed.), The Slick Hills of southwestern Oklahoma—fragments of an aulacogen?: Oklahoma Geological Survey Guidebook 24, p. 1-12.
- (ed.), 1986b, The Slick Hills of southwestern Oklahoma—fragments of an aulacogen?: Oklahoma Geological Survey Guidebook 24, 112 p.
- Donovan, R. N.; Babaei, A.; and Sanderson, D. J., 1982, Stop 10—Blue Creek Canyon, in Gilbert, M. C.; and Donovan, R. N. (eds.), Geology of the eastern Wichita Mountains, southwestern Oklahoma: Oklahoma Geological Survey Guidebook 21, p. 148-153.
- Donovan, R. N.; Gilbert, M. C.; Luza, K. V.; Marchini, David; and Sanderson, David, 1983, Possible Quaternary movement on the Meers fault, southwestern Oklahoma: Oklahoma Geology Notes, v. 43, p. 124-133.
- Donovan, R. N.; Morgan, K.; Wilhelm, S.; Marchini, W. R. D.; and Bridges, S., 1987, Lineaments in the Slick Hills, southwestern Oklahoma—an application of remote sensing technology: American Association of Petroleum Geologists, Southwest Section, Transactions, p. 74-79.
- Dow, W. G., 1977, Kerogen studies and geological interpretations: *Journal of Geochemical Exploration*, v. 7, p. 79-99.
- Dow, W. G.; and O'Connor, D. I., 1982, Kerogen maturity and type by reflected light microscopy applied to petroleum exploration, in Staplin, F. L.; and others, How to assess maturation and paleotemperatures: Society of Economic Paleontologists and Mineralogists Short Course 7, p. 133-157.
- Drever, J., 1973, The preparation of oriented clay mineral specimens for X-ray diffraction analysis by a filter membrane peel technique: *American Mineralogist*, v. 58, p. 395-406.
- Drisdale, J. K., 1982, Anadarko shows unique problems, economics: *Oil and Gas Journal*, v. 80, no. 32, p. 153-162.
- Dunham, R. J., 1955, Pennsylvanian conglomerates, structure, and orogenic history of the Lake Classen area, Arbuckle Mountains, Oklahoma: American Association of Petroleum Geologists Bulletin, v. 39, p. 1-30.
- Durand, B.; Alpern, B.; Pittion, J. L.; and Pradier, B., 1986, Reflectance of vitrinite as a control of thermal history of sediments, in Burrus, Jean (ed.), Thermal modeling in sedimentary basins: Éditions Technip, Collection Colloques et Séminaires No. 44, Paris, p. 441-474.
- Dutton, S. P., 1984, Fan-delta granite wash of the Texas Panhandle: Oklahoma City Geological Society Short Course Notes, 42 p.
- Dutton, S. P.; and Land, L. S., 1985, Meteoric burial diagenesis of Pennsylvania arkosic sandstones, southwestern Anadarko basin, Texas: American Association of Petroleum Geologists Bulletin, v. 69, p. 22-38.
- Dutton, S. P.; Goldstein, A. G.; and Ruppel, S. C., 1982, Petroleum potential of the Palo Duro basin, Texas Panhandle: Texas Bureau of Economic Geology Report of Investigations 123, 80 p.
- Dyman, T. S., 1987, Petrographic data for Atokan through Virgilian sandstones in Oklahoma: U.S. Geological Survey Open-File Report 87-137, 15 p.
- Ebanks, W. J., Jr., 1979, Correlation of Cherokee (Desmoinesian) sandstones of the Missouri-Kansas-Oklahoma Tri-State area, in Hyne, N. J. (ed.), Pennsylvanian sandstones of the Mid-Continent: Tulsa Geological Society Special Publication 1, p. 295-312.
- Eberl, D. D.; and Hower, J., 1976, Kinetics of illite formation: *Geological Society of America Bulletin*, v. 87, p. 1326-1330.
- Eberl, D. D.; Srodon, J.; Lee, M.; Nadeau, P. H.; and Northrup, H. R., 1987, Sericite from the Silverton Caldera, Colorado: correlation among structure, composition, origin, and particle thickness: *American Mineralogist*, v. 72, p. 914-934.
- Ebukanson, E. J.; and Kinghorn, R. R. F., 1985, Kerogen facies in the major Jurassic mudrock formations of southern England and the implication on the depositional environments of their precursors: *Journal of Petroleum Geology*, v. 8, p. 435-462.
- El-Etr, H. A., 1967, Technique of lineaments and linear analyses and its application on the minerogenic province of southeast Missouri: University of Missouri, Columbia, unpublished Ph.D. dissertation, 249 p.
- Ellis, W. L.; and Swolfs, H. S., 1983, Preliminary assessment of in situ geomechanical characteristics in drill hole USW G-1, Yucca Mountain, Nevada: U.S. Geological Survey Open-File Report 83-401, 18 p.
- Engel, M. H.; Imbus, S. W.; and Zumberge, J. E., 1988, Organic geochemical correlation of Oklahoma crude oils using R- and Q-mode factor analysis: *Organic Geochemistry*, v. 12, p. 157-170.
- Ervine, W. B.; and Bell, J. S., 1987, Subsurface in situ stress magnitudes from oil well drilling records, an example from the Venture area, offshore eastern Canada: *Canadian Journal of Earth Sciences*, v. 24, p. 1748-1759.
- Espitalié, J.; Laporte, J. L.; Madec, M.; Marquis, F.; Leplat, P.; Paulet, J.; and Botefu, A., 1977, Méthode rapide de caractérisation des roches mères, de leur potentiel pétrolier et de leur degré d'évolution: *Revue de l'Institut du Pétrole*, v. 32, p. 23-42.
- Evans, J. L., 1979, Major structural and stratigraphic features of the Anadarko basin, in Hyne, N. J. (ed.), Pennsylvanian sandstones of the Mid-Continent: Tulsa Geological Society Special Publication 1, p. 97-113.
- 1987, Major structural features of the Anadarko basin, in Rascoe, B., Jr.; and Hyne, N. J. (eds.), Petroleum geology of the Midcontinent: Tulsa Geological Society Special Publication 3, p. 6-9.
- Feinstein, Shimon, 1981, Subsidence and thermal history of southern Oklahoma aulacogen—implications for petroleum exploration: American Association of Petroleum Geologists Bulletin, v. 65, p. 2521-2533.
- Ferm, J. C., 1970, Allegheny deltaic deposits, in Morgan, J. P. (ed.), Deltaic sedimentation, modern and ancient: Society of Economic Paleontologist and Mineralogists Special Publication 15, p. 246-255.
- Fertl, W. H., 1984, Well logging and its applications in cased holes: *Journal of Petroleum Technology*, v. 36, p. 249-266.

- Fertl, W. H.; Chilingarian, G. V.; and Yen, T. F., 1982, Use of natural gamma ray spectral log in evaluation of clay minerals: *Energy Sources*, v. 6, p. 335-360.
- Folk, R. F., 1968, *Petrology of sedimentary rocks*: Hemphills, Austin, Texas, 170 p.
- Forgotson, J. M., Jr., 1969, Factors controlling occurrence of Morrow Sandstones and their relation to production in the Anadarko basin: *Shale Shaker Digest* 6, p. 135-149.
- Foster, W. R.; and Custard, H. C., 1983, Role of clay composition on extent of illite/smectite diagenesis [abstract]: *American Association of Petroleum Geologists Bulletin*, v. 67, p. 462.
- Frederickson, E. A.; and Redman, R. H., 1965, *Geology of Love County, pt. 1 of Geology and petroleum of Love County, Oklahoma*: Oklahoma Geological Survey Circular 63, p. 7-47.
- Freie, A. J., 1930, Sedimentation in the Anadarko basin: *Oklahoma Geological Survey Bulletin* 48, 80 p.
- Frezon, S. E.; and Dixon, G. H., 1975, Texas Panhandle and Oklahoma, in McKee, E. D.; Crosby, E. J.; and others (eds.), *Introduction and regional analyses of the Pennsylvanian System, pt. 1 of Paleotectonic investigations of the Pennsylvanian System in the United States*: U.S. Geological Survey Professional Paper 853-J, p. 177-195.
- Frezon, S. E.; and Jordon, Louise, 1979, Oklahoma, in Craig, L. C.; Connor, C. W.; and others (eds.), *Introduction and regional analysis of the Mississippian System, pt. 1 of Paleotectonic investigations of the Mississippian System in the United States*: U.S. Geological Survey Professional Paper 1010-I, p. 147-159.
- Fritz, R. D., 1978, Structural contour map of Oklahoma on the Pennsylvanian Wapanucka Limestone, Oswego limestone, base of the Hoxbar Group, and Checkerboard Limestone: Oklahoma State University unpublished M.S. thesis.
- Garner, D. L.; and Turcotte, D. L., 1984, The thermal and mechanical evolution of the Anadarko basin: *Tectonophysics*, v. 107, p. 1-24.
- Gatewood, L. E., 1970, Oklahoma City field—atomy of a giant, in Halbouty, M. T. (ed.), *Geology of giant petroleum fields*: American Association of Petroleum Geologists Memoir 14, p. 223-254.
- 1980, Map of geologic structure on top of the Arbuckle (Ellenburger) Formation, Oklahoma and Texas Panhandle: Copyright, L. E. Gatewood, Oklahoma City, scale 1:32,000.
- 1985, Arbuckle structure map: Copyright, L. E. Gatewood, Oklahoma City, scale 1:32,000.
- Gautier, D. L. (ed.), 1986, *Roles of organic matter in sediment diagenesis*: Society of Economic Paleontologists and Mineralogists Special Publication 38, 203 p.
- Gelphman, N. R., 1959, West Sentinel oil field, Washita County, Oklahoma: sedimentology of the "granite wash" and structural geology: University of Oklahoma unpublished M.S. thesis, 94 p.
- Gilbert, M. C., 1982, Geologic setting of the eastern Wichita Mountains with a brief discussion of unresolved problems, in Gilbert, M. C.; and Donovan, R. N. (eds.), *Geology of the eastern Wichita Mountains, southwestern Oklahoma*: Oklahoma Geological Survey Guidebook 21, p. 1-30.
- 1983a, The Meers fault—unusual aspects of possible tectonic consequences [abstract]: *Geological Society of America Abstracts with Programs*, v. 15, p. 1.
- 1983b, The Meers fault of southwestern Oklahoma—evidence for possible Quaternary seismicity in the Midcontinent [abstract]: *American Geophysical Union, EOS*, v. 64, no. 18, p. 313.
- 1983c, Timing and chemistry of igneous events associated with the southern Oklahoma aulacogen: *Tectonophysics*, v. 94, p. 439-455.
- (ed.), 1986, *Petrology of the Cambrian Wichita Mountains igneous suite*: Oklahoma Geological Survey Guidebook 23, 188 p.
- Gilbert, M. C.; and Donovan, R. N. (eds.), 1982, *Geology of the eastern Wichita Mountains, southwestern Oklahoma*: Oklahoma Geological Survey Guidebook 21, 160 p.
- Gish, W. G.; and Carr, R. M., 1929, Garber field, Garfield County, Oklahoma, in *Structure of typical American oil fields*: American Association of Petroleum Geologists, Tulsa, v. 1, p. 176-191.
- Glossa, J. M., 1982, Depositional environments and diagenetic history of the Nolans Limestone (Upper Wolfcampian), Rice County, Kansas: Kansas Geological Survey Open-File Report 82-23.
- Godson, R. H., 1980, Program COLOR: U.S. Geological Survey unpublished report, 13 p.
- Goodarzi, F., 1985, Reflected light microscopy of chitinozoan fragments: *Marine and Petroleum Geology*, v. 2, p. 72-78.
- Goodarzi, F.; and Norford, B. S., 1985, Graptolites as indicators of the temperature histories of rocks: *Journal of the Geological Society, London*, v. 142, pt. 6, p. 1089-1099.
- Goodwin, N. S.; Park, P. J. D.; and Rawlinson, A. P., 1983, Crude oil biodegradation under simulated and natural conditions, in Bjorøy, M.; and others (eds.), *Advances in organic geochemistry 1981*: John Wiley, London, p. 650-658.
- Gough, D. I.; and Bell, J. S., 1981, Stress orientations from oil-well fractures in Alberta and Texas: *Canadian Journal of Earth Sciences*, v. 18, p. 638-645.
- 1982, Stress orientation from borehole wall fractures with examples from Colorado, east Texas and northern Canada: *Canadian Journal of Earth Sciences*, v. 19, p. 1958-1970.
- Gould, C. N., 1924, A new classification of the Permian red beds of southwestern Oklahoma: *American Association of Petroleum Geologists Bulletin*, v. 8, 1 map, p. 322-341.
- Gustavson, T. C.; and Budnik, R. T., 1985, Structural influences on geomorphic processes and physiographic features, Texas Panhandle—technical issues in siting a nuclear-waste repository: *Geology*, v. 13, p. 173-176.
- Gustavson, T. C.; and Finley, R. J., 1985, Late Cenozoic geomorphic evolution of the Texas Panhandle and northeastern New Mexico—case studies of structural control on regional drainage development: Texas Bureau of Economic Geology Report of Investigations 148, 42 p.
- Haiduk, J. P., 1987, Facies analysis, paleoenvironmental interpretation, and diagenetic history of the Britt Sandstone (Upper Mississippian), southeastern Anadarko basin, Oklahoma [abstract]: *American Association of Petroleum Geologists Bulletin*, v. 71, p. 993.
- Haimson, B. C.; and Herrick, C. G., 1985, In situ stress evaluation from borehole breakouts, experimental studies: *Proceedings of the 26th U.S. Symposium on Rock Mechanics*, Rapid City, South Dakota, v. 2, p. 1207-1218.
- Halbouty, M. T., 1970, *Geology of giant petroleum*

- fields: introduction, in Halbouty, M. T. (ed.), *Geology of giant petroleum fields*: American Association of Petroleum Geologists Memoir 14, p. 5.
- Haley, B. R., 1976, Geological map of Arkansas: U.S. Geological Survey, scale 1:500,000.
- Ham, W. E.; and Wilson, J. L., 1967, Paleozoic epeirogeny and orogeny in the central United States: *American Journal of Science*, v. 265, p. 332-407.
- Ham, W. E.; Denison, R. E.; and Merritt, C. A., 1964, Basement rocks and structural evolution of southern Oklahoma: *Oklahoma Geological Survey Bulletin* 95, 302 p.
- Ham, W. E.; Amsden, T. W.; Denison, R. E.; Derby, J. R.; Fay, R. O.; Graffham, A. A.; Rowland, T. L.; Squires, R. L.; Stitt, J. H.; and Wiltse, E. W., 1973, Regional geology of the Arbuckle Mountains, Oklahoma: *Oklahoma Geological Survey Special Publication* 73-3, 61 p.
- Harding, T. P., 1974, Petroleum traps associated with wrench faults: *American Association of Petroleum Geologists Bulletin*, v. 58, p. 1270-1304.
- 1976, Tectonic significance and hydrocarbon consequences of sequential folding synchronous with San Andreas faulting, San Joaquin Valley, California: *American Association of Petroleum Geologists Bulletin*, v. 60, p. 356-378.
- Harding, T. P.; and Lowell, J. D., 1979, Structural styles, their plate-tectonic habitats and hydrocarbon traps in petroleum provinces: *American Association of Petroleum Geologists Bulletin*, v. 63, p. 1016-1058.
- Harding, T. P.; Gregory, R. F.; and Stephens, L. H., 1983, Convergent wrench fault and positive flower structure, Ardmore basin, Oklahoma, in Bally, A. W. (ed.), *Seismic expression of structural styles—a picture and work atlas*: *American Association of Petroleum Geologists, Studies in Geology* 15, v. 3, p. 4.2-13-4.2-17.
- Hare, B. D., 1970, Petrology of the Thurman Sandstone (Desmoinesian), Hughes and Coal Counties, Oklahoma: *The Compass of Sigma Gamma Epsilon*, v. 48, no. 1, p. 45-55.
- Harlton, B. H., 1951, Faults in the sedimentary part of Wichita Mountains of Oklahoma: *American Association of Petroleum Geologists Bulletin*, v. 35, p. 988-999.
- 1963, Frontal Wichita fault system of southwestern Oklahoma: *American Association of Petroleum Geologists Bulletin*, v. 47, p. 1552-1580.
- 1972, Faulted fold belts of southern Anadarko basin adjacent to frontal Wichitas: *American Association of Petroleum Geologists Bulletin*, v. 56, p. 1544-1551.
- Harris, S. A., 1975, Hydrocarbon accumulation in "Meramec-Osage" (Mississippian) rocks, Sooner trend, northwest-central Oklahoma: *American Association of Petroleum Geologists Bulletin*, v. 59, p. 633-664.
- Harrison, W. E.; and Burchfield, M. R., 1984, Tar-sand potential of selected areas in Carter and Murray Counties, south-central Oklahoma: U.S. Department of Energy, DE-AS20-81LC10730, 221 p.
- Harrison, W. E.; Mankin, C. J.; Weber, S. J.; and Curiale, J. A., 1981, Oil-sand and heavy-oil potential of Oklahoma, in Meyer, R. F.; and Steele, C. T. (eds.), *The future of heavy crude oils and tar sands*: McGraw-Hill, New York, p. 83-89.
- Harrison, W. E.; Luza, K. V.; Prater, M. L.; and Cheung, P. K., 1983, Geothermal resource assessment in Oklahoma: *Oklahoma Geological Survey Special Publication* 83-1, 42 p.
- Hatch, J. R.; Rice, D. D.; Burruss, R. C.; Schmoker, J. W.; and Clayton, J. L., 1986, Thermal maturity modeling and geochemical characterization of hydrocarbon source rocks, oils, and natural gases of the Anadarko basin [abstract], in Carter, J. M. H. (ed.), *USGS research on energy resources—1986, program and abstracts*: U.S. Geological Survey Circular 974, p. 21-23.
- Hatch, J. R.; Jacobson, S. R.; Witzke, B. J.; Risatti, J. B.; Anders, D. E.; Watney, W. L.; Newell, K. D.; and Vuletich, A. K., 1987, Possible late middle Ordovician organic carbon isotope excursion: evidence from Ordovician oils and hydrocarbon source rocks, Mid-Continent and east-central United States: *American Association of Petroleum Geologists Bulletin*, v. 71, p. 1342-1354.
- Havens, J. S., 1977, Reconnaissance of the water resources of the Lawton Quadrangle, southwestern Oklahoma: *Oklahoma Geological Survey Hydrologic Atlas* 6, 4 sheets, scale 1:250,000.
- Hayes, J. B., 1979, Sandstone diagenesis—the hole truth, in Scholle, P. A.; and Schluger, P. A. (eds.), *Aspects of diagenesis*: Society Economic Paleontologists and Mineralogists Special Publication 26, p. 127-139.
- Hayes, W. C., 1962, Precambrian surface showing major lineaments: *Missouri Geological Survey Map*, 1 sheet, scale 1:500,000.
- Healy, J. H.; Hickman, S. H.; Zoback, M. D.; and Ellis, W. L., 1984, Report on televiwer log and stress measurements in core hole USW-G1, Nevada Test Site, December 13-22, 1981: U.S. Geological Survey Open-File Report 84-15, 47 p.
- Heckel, P. H., 1980, Paleogeography of eustatic model for deposition of Midcontinent upper Pennsylvanian cyclothems, in Fouch, T. D.; and Magathan, E. R. (eds.), *Paleozoic paleogeography of the west-central United States*: Society of Economic Paleontologists and Mineralogists, Rocky Mountain Section, Paleogeography Symposium 1, p. 197-215.
- Hempton, M. R.; and Neher, Kurt, 1986, Experimental fracture, strain and subsidence patterns over en echelon strike-slip faults—implications for the structural evolution of pull-apart basins: *Journal of Structural Geology*, v. 8, no. 6, p. 597-605.
- Henry, G. E., 1968, Recent development in the Marietta basin, in Wendell, J. S. (ed.), *Basins of the Southwest*: American Association of Petroleum Geologists, Tulsa, v. 1, p. 71-78.
- Herrmann, L. A., 1961, Structural geology of Cement-Chickasha area, Caddo and Grady Counties, Oklahoma: *American Association of Petroleum Geologists Bulletin*, v. 45, p. 1971-1993.
- Hester, T. C.; and Schmoker, J. W., 1987, Determination of organic content from formation-density logs, Devonian-Mississippian Woodford Shale, Anadarko basin, Oklahoma: U.S. Geological Survey Open-File Report 87-20, 11 p.
- Hevia, V.; and Virgos, J. M., 1977, The rank and anisotropy of anthracites: the indicating surface of reflectivity in uniaxial and biaxial substances: *Journal of Microscopy*, v. 109, pt. 1, p. 23-28.
- Hickman, S. H.; Healy, J. H.; and Zoback, M. D., 1985, In situ stress, natural fracture distribution, and borehole elongation in the Auburn geothermal well, Auburn, New York: *Journal of Geophysical Research*, v. 90, no. B7, p. 5497-5512.
- Hill, G. W., Jr., 1984, The Anadarko basin: a model for

- regional petroleum accumulations, in Borger, J. G., III (ed.), Technical proceedings of the American Association of Petroleum Geologists, Mid-Continent Section, 1981 regional meeting: Oklahoma City Geological Society, p. 1-23.
- Hill, G. W., Jr.; and Clark, R. H., 1980, The Anadarko basin—a regional petroleum accumulation—a model for future exploration and development: *Shale Shaker*, v. 31, p. 36-49.
- Hills, J. M.; and Kottowski, F. E. (coordinators), 1983, Correlation of Stratigraphic Units in North America (COSUNA)—southwest/southwest Mid-Continent correlation chart: American Association of Petroleum Geologists, Tulsa.
- Hoffman, J., 1976, Regional metamorphism and K-Ar dating of clay minerals in Cretaceous sediments of the disturbed belt of Montana: Case Western Reserve University, Cleveland, Ohio, unpublished Ph.D. dissertation, 266 p.
- Hoffman, J.; and Hower, J., 1979, Clay mineral assemblages as low-grade metamorphic geothermometers: application to the thrust faulted disturbed belt of Montana, U.S.A., in Scholle, P. A.; and Schluger, P. A. (eds.), Aspects of diagenesis: Society of Economic Paleontologists and Mineralogists Special Publication 26, p. 55-79.
- Hoffman, P.; Dewey, J. F.; and Burke, K., 1974, Aulacogens and their genetic relation to geosynclines and a Proterozoic example from Great Slave Lake, Canada, in Dott, R. H., Jr.; and Shaver, R. H. (eds.), Modern and ancient geosynclinal sedimentation: Society of Economic Paleontologists and Mineralogists Special Publication 19, p. 38-55.
- Hollister, L. S.; Crawford, M. L.; Roedder, E.; Burruss, R. C.; Spooner, C. T. C.; and Touret, J., 1981, Practical aspects of microthermometry, in Hollister, L. S.; and Crawford, M. L. (eds.), Fluid inclusions: applications to petrology: Mineralogical Association of Canada Short Course Notes, v. 6, p. 278-304.
- Hooker, V. B.; and Johnson, C. F., 1969, Near-surface horizontal stresses, including the effects of rock anisotropy: U.S. Bureau of Mines Report of Investigations 7654.
- Houseknecht, D. W., 1988, Intergranular pressure solution in four quartzose sandstones: *Journal of Sedimentary Petrology*, v. 58, p. 228-246.
- Houseknecht, D. W.; and Hathorn, L. A., 1987, Hydrocarbons in an overmature basin: II. Is there a thermal maturity limit to methane production in Arkoma basin? [abstract]: American Association of Petroleum Geologists Bulletin, v. 71, p. 994.
- Houseknecht, D. W.; and Matthews, S. M., 1985, Thermal maturity of carboniferous strata, Ouachita Mountains: American Association of Petroleum Geologists Bulletin, v. 69, p. 335-345.
- Howard, J. J.; and Roy, D. M., 1985, Development of layer charge and kinetics of experimental smectite alteration: *Clays and Clay Minerals*, v. 33, p. 81-88.
- Hower, J., 1981, Shale diagenesis, in Longstaffe, F. J. (ed.), Clays and the resource geologist: Mineralogical Association of Canada Short Course Handbook, v. 6, p. 60-80.
- Hower, J.; Eslinger, E.; Hower, M.; and Perry, E., 1976, The mechanism of burial diagenetic reactions in argillaceous sediments. 1. Mineralogical and chemical evidence: *Geological Society of America Bulletin*, v. 87, p. 725-737.
- Hubbert, M. K.; and Willis, D. C., 1955, Fractured reservoirs in the United States: Fourth World Petroleum Congress Proceedings, sec. 1, p. 57-81.
- Huffman, G. G., 1959, Pre-Desmoinesian isopachous and paleogeologic studies in central Mid-Continent region: American Association of Petroleum Geologists Bulletin, v. 43, p. 2541-2574.
- Hunt, J. M., 1979, Petroleum geochemistry and geology: W. H. Freeman, San Francisco, 617 p.
- Hutton, A. C.; and Cook, A. C., 1980, Influence of alginite on the reflectance of vitrinite from Joadja, NSW, and some other coals and oil shales containing alginite: *Fuel*, v. 59, p. 711-714.
- Illich, H. A.; Haney, F. R.; and Mendoza, M., 1981, Geochemistry of oil from Santa Cruz basin, Bolivia: case study of migration-fractionation: American Association of Petroleum Geologists Bulletin, v. 65, p. 2388-2402.
- Imbus, S. W.; Engel, M. H.; and Zumbege, J. E., 1987, A geochemical correlation study of Oklahoma crude oils using a multivariate statistical method [abstract]: American Association of Petroleum Geologists Bulletin, v. 71, p. 570.
- Inoue, A., 1983, Potassium fixation by clay minerals during hydrothermal treatment: *Clays and Clay Minerals*, v. 31, p. 81-91.
- International Association of Geodesy, 1971, Geodetic reference system, 1967: International Association of Geodesy Special Publication 3, 116 p.
- International Oil Scouts Association, 1987, Production, pt. 2 of International oil and gas development, Yearbook (review of 1984-85), v. 55/56, 999 p.
- Jacob, H., 1985, Disperse solid bitumens as an indicator for migration and maturity in prospecting for oil and gas: *Erdöl und Kohle-Erdgas-Petrochemie*, v. 38, p. 365.
- Jacobson, Lynn, 1959, Petrology of Pennsylvanian sandstones and conglomerates of the Ardmore basin: Oklahoma Geological Survey Bulletin 79, 144 p.
- Jemison, R. M., Jr., 1979, Geology and development of Mills Ranch Complex—world's deepest field: American Association of Petroleum Geologists Bulletin, v. 63, p. 804-808.
- Jiang, Z.; Philp, R. P.; and Lewis, C. A., 1988, Identification of novel bicyclic alkanes from steroid precursors in crude oils from Kelamayi Oilfield of China: *Geochimica et Cosmochimica Acta*, v. 52, p. 491-498.
- Johnson, K. S., 1971, Introduction, guidelines, and geologic history of Oklahoma, book 1 of Guidebook for geologic field trips in Oklahoma: Oklahoma Geological Survey Educational Publication 2, 15 p.
- 1978, Stratigraphy and mineral resources of Guadalupian and Ochoan rocks in the Texas Panhandle and western Oklahoma, in Austin, G. S. (compiler), Geology and mineral deposits of Ochoan rocks in Delaware basin and adjacent areas: New Mexico Bureau of Mines and Mineral Resources Circular 159, p. 57-62.
- Johnson, K. S.; and Denison, R. E., 1973, Igneous geology of the Wichita Mountains and economic geology of Permian rocks in southwest Oklahoma: Geological Society of America Guidebook for Field Trip No. 6, 35 p.
- Johnson, K. S.; Branson, C. C.; Curtis, N. M., Jr.; Ham, W. E.; Marcher, M. V.; and Roberts, J. F., 1972, Geology and earth resources of Oklahoma—an atlas of maps and cross sections: Oklahoma Geological Survey Educational Publication 1, 8 p.
- Johnson, K. S.; Burchfield, M. R.; and Harrison, W. E.,

- 1984, Guidebook for Arbuckle Mountain field trip, southern Oklahoma: Oklahoma Geological Survey Special Publication 84-1, 21 p.
- Johnson, K. S.; Amsden, T. W.; Denison, R. E.; Dutton, S. P.; Goldstein, A. G.; Rascoe, B., Jr.; Sutherland, P. K.; and Thompson, D. M., 1988, Southern Midcontinent region, in Sloss, L. L. (ed.), *Sedimentary cover—North American craton, U.S.: The Geology of North America*, Geological Society of America, Boulder, v. D-2, p. 307–359.
- Jones, J. M.; Murchison, D. G.; and Saleh, S. A., 1972, Variation of vitrinite reflectivity in relation to lithology, in *Advances in organic geochemistry 1971*: Pergamon Press, Oxford, p. 601–612.
- Jones, P. J., 1984, Maturity parameters of Woodford Shale, Anadarko basin, Oklahoma [abstract]: American Association of Petroleum Geologists Bulletin, v. 68, p. 493–494.
- 1986, The petroleum geochemistry of the Pauls Valley area, Anadarko basin, Oklahoma: University of Oklahoma unpublished M.S. thesis, 175 p.
- Jones, P. J.; Lewis, C. A.; Philp, R. P.; Lin, L. H.; and Michael, G. E., 1987, Geochemical study of oils, source rocks, and tar sands in Pauls Valley area, Anadarko basin, Oklahoma [abstract]: American Association of Petroleum Geologists Bulletin, v. 71, p. 574.
- Jordan, Louise, 1957, Subsurface stratigraphic names of Oklahoma: Oklahoma Geological Survey Guidebook 6, 220 p.
- 1962, Geologic map and section of pre-Pennsylvanian rocks in Oklahoma, showing surface and subsurface distribution: Oklahoma Geological Survey Map GM-5, scale 1:750,000.
- 1967, Geology of Oklahoma—a summary: Oklahoma Geology Notes, v. 27, p. 215–228.
- Jordan, Louise; and Vosburg, D. L., 1963, Permian salt and associated evaporites in the Anadarko basin of the western Oklahoma-Texas Panhandle region: Oklahoma Geological Survey Bulletin 102, 76 p.
- Jorgensen, D. G.; Helgesen, J. O.; Imes, J. L. [in press], Regional aquifers in Kansas, Nebraska, and parts of Arkansas, Colorado, Missouri, New Mexico, Oklahoma, South Dakota, Texas, and Wyoming—geologic framework: U.S. Geological Survey Professional Paper 1414-B.
- Juckes, L. M.; and Pitt, G. J., 1977, The standardization of petrographic analysis of coal: *Journal of Microscopy*, v. 109, pt. 1, p. 13–21.
- Kasino, R. E.; and Davies, D. K., 1979, Environments and diagenesis, Morrow sands, Cimarron County (Oklahoma), and significance to regional exploration, production and well completion practices, in Hyne, N. J. (ed.), *Pennsylvanian sandstones of the Midcontinent*: Tulsa Geological Society Special Publication 1, p. 169–194.
- Katz, B. J.; and Liro, L. M., 1987, Thermal maturation by vitrinite reflectance of Woodford Shale, Anadarko basin, Oklahoma—discussion: American Association of Petroleum Geologists Bulletin, v. 71, p. 897.
- Katz, B. J.; Liro, L. M.; Lacey, J. E.; and White, H. W., 1982, Time and temperature formation: application of Lopatin's method to petroleum exploration—discussion: American Association of Petroleum Geologists Bulletin, v. 66, p. 1150–1151.
- Kennedy, C. L.; Miller, J. A.; Kelso, J. B.; Lago, O. K.; and Peterson, D. S., 1982, The deep Anadarko basin: Petroleum Information Corporation, Denver, 359 p.
- Khaiwka, M. H., 1968, Geometry and depositional environments of Pennsylvanian reservoir sandstones, northwestern Oklahoma: University of Oklahoma unpublished Ph.D. dissertation, 126 p. [Published in part in *Shale Shaker Digest* 7, p. 170–193.]
- 1972, Geometry and depositional environment of Morrow reservoir sandstones, northwestern Oklahoma: *Shale Shaker*, v. 22, p. 170.
- King, P. B., 1951, The tectonics of middle North America—east of the Cordilleran system: Princeton University Press, Princeton, 203 p.
- 1968, Tectonic map of North America: U.S. Geological Survey National Atlas, 1 sheet, scale 1:7,500,000.
- King, P. B.; and Beikman, H. M., 1974, Geologic map of the United States: U.S. Geological Survey, 2 sheets, scale 1:2,500,000.
- Kluth, C. F.; and Coney, P. J., 1981, Plate tectonics of the Ancestral Rocky Mountains: *Geology*, v. 9, p. 10–15.
- Knight, R. J.; and Dalrymple, R. W., 1975, Intertidal sediments from the south shore of Cobequid Bay, Bay of Fundy, Nova Scotia, Canada, in Ginsburg, R. N. (ed.), *Tidal deposits: a casebook of Recent examples and fossil counterparts*: Springer-Verlag, New York, p. 47–55.
- Krumme, G. W., 1981, Stratigraphic significance of limestones of the Marmaton Group (Pennsylvanian, Desmoinesian) in eastern Oklahoma: Oklahoma Geological Survey Bulletin 131, 67 p.
- Ku, Chao-Cheng; Sun, S.; Soffel, H.; and Scharon, L., 1967, Paleomagnetism of the basement rocks, Wichita Mountains, Oklahoma: *Journal of Geophysical Research*, v. 72, no. 2, p. 731–737.
- Kumar, N.; and Sanders, J. E., 1974, Inlet sequence: a vertical succession of sedimentary structures and textures created by the lateral migration of tidal inlets: *Sedimentology*, v. 21, p. 491–532.
- Landes, K. K., 1970, Petroleum geology of the United States: Wiley-Interscience, New York, 571 p.
- Larson, E. E.; Patterson, P. E.; Curtis, G.; Drake, R.; and Mutschler, F. E., 1985, Petrologic, paleomagnetic, and structural evidence of a Paleozoic rift system in Oklahoma, New Mexico, Colorado, and Utah: *Geological Society of America Bulletin*, v. 96, p. 1364–1372.
- Lawson, J. E., Jr.; and Luza, K. V., 1980, Oklahoma earthquakes, 1979: Oklahoma Geology Notes, v. 40, p. 95–105.
- 1981, Oklahoma earthquakes, 1980: Oklahoma Geology Notes, v. 41, p. 140–149.
- 1982, Oklahoma earthquakes, 1981: Oklahoma Geology Notes, v. 42, p. 126–137.
- 1983, Oklahoma earthquakes, 1982: Oklahoma Geology Notes, v. 43, p. 24–35.
- 1984, Oklahoma earthquakes, 1983: Oklahoma Geology Notes, v. 44, p. 32–42.
- 1985, Oklahoma earthquakes, 1984: Oklahoma Geology Notes, v. 45, p. 52–61.
- 1986, Oklahoma earthquakes, 1985: Oklahoma Geology Notes, v. 46, p. 44–52.
- 1987, Oklahoma earthquakes, 1986: Oklahoma Geology Notes, v. 47, p. 65–72.
- 1988, Oklahoma earthquakes, 1987: Oklahoma Geology Notes, v. 48, p. 54–63.
- Lawson, J. E., Jr.; DuBois, R. L.; Foster, P. H.; and Luza, K. V., 1979, Earthquake map of Oklahoma (earthquakes shown through 1978): Oklahoma Geological Survey Map GM-19, 15 p., 1 sheet, scale

- 1:750,000.
- Lee, W. T., 1918, Early Mesozoic physiography of the southern Rocky Mountains: Smithsonian Miscellaneous Collections, v. 69, 41 p.
- Lewan, M. D., 1983, Effects of thermal maturation on stable organic carbon isotopes as determined by hydrous pyrolysis of Woodford Shale: *Geochimica et Cosmochimica Acta*, v. 47, p. 1471-1479.
- Lewis, R. D., 1982, Depositional environments and paleoecology of the Oil Creek Formation (Middle Ordovician), Arbuckle Mountains and Criner Hills, Oklahoma: University of Texas, Austin, unpublished Ph.D. dissertation, 351 p.
- Lillibridge, Margaret, 1963, Ringwood District in oil and gas fields of Oklahoma: Oklahoma City Geological Society Reference Report, v. 1, p. 100-A.
- Lin, L. H., 1987, Effect of biodegradation on tar sand bitumen of south Woodford area, Carter County, Oklahoma: University of Oklahoma unpublished M.S. thesis, 91 p.
- Lindquist, S. J., 1978, How mineral content affects reservoir quality of sands: *World Oil*, April 1978, p. 99-102.
- Longman, M. W., 1976, Depositional history, paleoecology, and diagenesis of the Bromide Formation (Ordovician), Arbuckle Mountains, Oklahoma: University of Texas, Austin, unpublished Ph.D. dissertation, 327 p.
- Lopatin, N. V., 1971, Temperature and geologic time as factors in coalification [in Russian]: *Akademiya Nauk SSSR Izvestiya, Seriya Geologicheskaya* 3, Moscow, p. 95-106.
- Loucks, R. G.; Dodge, M. M.; and Galloway, W. E., 1979, Contract Report EG-77-5-05-5554: Texas Bureau of Economic Geology, Austin, 97 p.
- Luza, K. V., 1978, Regional seismic and geologic evaluations of Nemaha uplift, Oklahoma, Kansas, and Nebraska: *Oklahoma Geology Notes*, v. 38, p. 49-58.
- Luza, K. V.; Harrison, W. E.; Laguros, G. A.; Prater, M. L.; and Cheung, P. K., 1984, Geothermal resources and temperature gradients of Oklahoma: Oklahoma Geological Survey Map GM-27, scale 1:500,000.
- Luza, K. V.; Madole, R. F.; and Crone, A. J., 1987, Investigation of the Meers fault, southwestern Oklahoma: Oklahoma Geological Survey Special Publication 87-1, 75 p.
- Lyday, J. R., 1985, Atokan (Pennsylvanian) Berlin field: genesis of recycled detrital dolomite reservoir, deep Anadarko basin, Oklahoma: American Association of Petroleum Geologists Bulletin, v. 69, p. 1931-1949.
- Mackenzie, A. S., 1984, Applications of biological markers in petroleum geochemistry, in Brooks, J.; and Welte, D. H. (eds.), *Advances in petroleum geochemistry* 1983, volume 1: Academic Press, London, p. 115-214.
- MacLachlan, M. E., 1967, Oklahoma, in *Paleotectonic investigations of the Permian System in the United States*: U.S. Geological Survey Professional Paper 515-E, p. 81-92.
- Madole, R. F., 1986, The Meers fault: Quaternary stratigraphy and evidence for late Holocene movement, in Donovan, R. N. (ed.), *The Slick Hills of southwestern Oklahoma—fragments of an aulacogen?*: Oklahoma Geological Survey Guidebook 24, p. 55-67.
- 1988, Stratigraphic evidence of Holocene faulting in the Mid-Continent: the Meers fault, southwestern Oklahoma: *Geological Society of America Bulletin*, v. 100, p. 392-401.
- Mankin, C. J. (coordinator), 1983, Correlation of Stratigraphic Units in North America (COSUNA)—Texas-Oklahoma tectonic region correlation chart: American Association of Petroleum Geologists, Tulsa.
- Mapel, W. J.; Johnson, R. B.; Bachman, G. O.; and Varnes, K. L., 1979, Southern Midcontinent and southern Rocky Mountains region, in Craig, L. C.; Connor, C. W.; and others (eds.), *Introduction and regional analysis of the Mississippian System, pt. 1 of Paleotectonic investigations of the Mississippian System in the United States*: U.S. Geological Survey Professional Paper 1010-J, p. 161-187.
- Marchini, W. R. D., 1986, Transpression: an application to the Slick Hills, southwest Oklahoma: Queen's University of Belfast, Northern Ireland, unpublished Ph.D. dissertation, 286 p.
- Marriott, P. J.; Gill, J. P.; Evershed, R. P.; Hein, C. S.; and Eglinton, G., 1984, Computerized gas chromatography-mass spectrometric analysis of complex mixtures of alkyl porphyrins: *Journal of Chromatography*, v. 301, p. 107-128.
- Mason, J. W., 1968, Hugoton Panhandle field, Kansas, Oklahoma and Texas, in Beebe, B. W. (ed.), *Natural gases of North America: American Association of Petroleum Geologists Memoir* 9, v. 2, p. 1539-1547.
- Mastin, L. G., 1984, The development of borehole breakouts in sandstone: Stanford University unpublished M.S. thesis, 101 p.
- McBride, M. H.; Franks, P. C.; and Larese, R. E., 1987, Chlorite grain coats and preservation of primary porosity in deeply buried Springer Formation and lower Morrowan sandstones, southeastern Anadarko basin, Oklahoma [abstract]: *American Association of Petroleum Geologists Bulletin*, v. 71, p. 994.
- McConnell, D., 1983, The mapping and interpretation of the structure of the northern Slick Hills, southwest Oklahoma: Oklahoma State University unpublished M.S. thesis, 131 p.
- McConnell, D. A., 1987, Paleozoic structural evolution of the Wichita uplift, southwestern Oklahoma: Texas A&M University unpublished Ph.D. dissertation, 221 p.
- McConnell, D. A.; Beauchamp, W. H.; Donovan, R. N.; Marchini, W. R. D.; and Sanderson, D. J., 1986, Structural evolution of the frontal fault zone, Wichita uplift, southwestern Oklahoma [abstract]: *Geological Society of America Abstracts with Programs*, v. 18, p. 687.
- McCoss, A. M., 1986, Simple constructions for deformation in transpression/transension zones: *Journal of Structural Geology*, v. 8, p. 715-718.
- McCoss, A. M.; and Donovan, R. N., 1986, Application of a construction for determining deformation in zones of transpression to the Slick Hills in southern Oklahoma, in Donovan, R. N. (ed.), *The Slick Hills of southwestern Oklahoma—fragments of an aulacogen?*: Oklahoma Geological Survey Guidebook 24, p. 40-44.
- McDonald, D. A.; and Surdam, R. C., 1984, Clastic diagenesis: American Association Petroleum Geologists Memoir 37, 434 p.
- McGookey, D. A.; and Goldstein, A. G., 1982, Structural influence on deposition and deformation at the northwest margin of the Palo Duro basin, in *Geology and geohydrology of the Palo Duro basin, Texas Panhandle—a report on the progress of nuclear waste isolation feasibility studies*: Texas Bureau of Economic Geology Circular 82-7, p. 28-37.

- McHargue, T. R.; and Price, R. C., 1982, Dolomite from clay in argillaceous or shale-associated marine carbonates: *Journal of Sedimentary Petrology*, v. 51, p. 553-562.
- McKee, E. D.; Oriol, S. S.; Swanson, V. E.; MacLachlan, M. E.; MacLachlan, J. C.; Kitner, K. B.; Goldsmith, J. W.; Bell, R. Y.; Jameson, D. J.; and Imlay, R. W., 1956, Paleotectonic maps of the Jurassic System: U.S. Geological Survey Miscellaneous Geologic Investigations Map I-175, 6 p., 9 sheets, scale 1:500,000.
- McKee, E. D.; Oriol, S. S.; Ketner, K. B.; MacLachlan, M. E.; Goldsmith, J. W.; MacLachlan, J. C.; and Mudge, M. R., 1959, Paleotectonic map of the Triassic System: U.S. Geological Survey Miscellaneous Geologic Investigations Map I-300, 33 p., 9 sheets, scale 1:500,000.
- McKee, E. D.; Oriol, S. S.; and others, 1967a, Paleotectonic investigations of the Permian System in the United States: U.S. Geological Survey Professional Paper 515, 271 p.
- 1967b, Paleotectonic maps of the Permian System: U.S. Geological Survey Miscellaneous Geologic Investigations Map I-450, 164 p.
- McKee, E. D.; Crosby, E. J.; and others, 1975, Paleotectonic investigations of the Pennsylvanian System in the United States: U.S. Geological Survey Professional Paper 853, parts 1-3.
- McLean, T. R.; and Stearns, D. W., 1986, Stop 7—Hale Spring locality, in Gilbert, M. C. (ed.), *Petrology of the Cambrian Wichita Mountains igneous suite*: Oklahoma Geological Survey Guidebook 23, p. 172-178.
- Meissner, F. F., 1978, Petroleum geology of the Bakken Formation, Williston basin, North Dakota and Montana, in Estelle, Duane; and Miller, Roger (eds.), *The economic geology of the Williston basin*: Montana Geological Society 24th Annual Conference, Williston Basin Symposium, p. 207-227.
- Merriam, D. F., 1963, The geologic history of Kansas: *Kansas Geological Survey Bulletin* 162, 317 p.
- Merriam, D. F.; and Smith, Polly, 1961, Preliminary regional structural contour map on top of Arbuckle rocks (Cambrian-Ordovician) in Kansas: *Kansas Geological Survey Oil and Gas Investigations Map* 25.
- Meyer, B. L.; and Nederlof, M. H., 1984, Identification of source rocks on wireline logs by density/resistivity and sonic transit time/resistivity crossplots: *American Association of Petroleum Geologists Bulletin*, v. 68, p. 121-129.
- Michael, G. E., 1987, Effect of biodegradation upon porphyrin biomarkers in Upper Mississippian tar sands and related oils, southern Oklahoma: University of Oklahoma unpublished M.S. thesis, 118 p.
- Mikkelsen, D. H., 1966, The origin and age of the Mississippian "chat" in north-central Oklahoma: *Shale Shaker Digest* 5, p. 255-265.
- Miser, H. D., 1954, Geologic map of Oklahoma: Oklahoma Geological Survey and U.S. Geological Survey, 2 sheets, scale 1:500,000.
- Molnia, C. L.; Roberts, L. N. R.; and Boger, L. W., Jr., 1988, Additional geologic applications of the computerized Stratigraphic Analysis Techniques System "STRATS": U.S. Geological Survey Open-File Report 88-58, 20 p.
- Moody, J. D.; and Hill, M. J., 1956, Wrench-fault tectonics: *Geological Society of America Bulletin*, v. 67, p. 1207-1246.
- Moore, B. J., 1976, Analyses of natural gases, 1917-1974: U.S. Department of Commerce, National Technical Information Service PB-251 202, 889 p.
- Moore, G. E., 1979, Pennsylvanian paleogeography of the southern Mid-Continent, in Hyne, N. J. (ed.), *Pennsylvanian sandstones of the Mid-Continent*: Tulsa Geological Society Special Publication 1, p. 2-12.
- Morelli, C. (ed.), 1974, The international gravity standardization net, 1971: International Association of Geodesy Special Publication 4, 194 p.
- Morin, R. H.; Anderson, R. M.; and Barton, C. A. [in press] Analysis and interpretation of the borehole televiwer log—information on the state of stress and the lithostratigraphy at hole 504B: *Proceedings—Initial Reports of the Ocean Drilling Program Leg 111*.
- Morris, R. C., 1974, Sedimentary and tectonic history of the Ouachita Mountains, in Dickinson, W. R. (ed.), *Tectonics and sedimentation*: Society of Economic Paleontologists and Mineralogists Special Publication 22, p. 120-142.
- Mount, V. S.; and Suppe, J., 1987, State of stress near the San Andreas fault: implications for wrench tectonics: *Geology*, v. 15, p. 1143-1146.
- Murphy, M. E.; Narayanan, S.; Gould, G.; Lawler, S.; Noonan, J.; and Prentice, J., 1972, Organic geochemistry of some Upper Pennsylvanian and Lower Permian Kansas shales: hydrocarbons, in Kellogg, JoAnne (ed.), *Short papers on research in 1971*: *Kansas Geological Survey Bulletin* 204, pt. 1, p. 19-25.
- Murray, G. H., Jr., 1968, Quantitative fracture study—Sanish pool, McKenzie County, North Dakota: *American Association of Petroleum Geologists Bulletin*, v. 52, p. 57-65.
- Nadeau, P. H., 1985, The physical dimensions of fundamental clay particles: *Clay Minerals*, v. 20, p. 499-514.
- Nadeau, P. H.; Wilson, M. J.; McHardy, W. J.; and Tait, J. M., 1984a, Interparticle diffraction: a new concept for interstratified clays: *Clay Minerals*, v. 19, p. 757-769.
- Nadeau, P. H.; Tait, J. M.; McHardy, W. J.; and Wilson, M. J., 1984b, Interstratified XRD characteristics of physical mixtures of elementary clay particles: *Clay Minerals*, v. 19, p. 67-76.
- Nadeau, P. H.; Wilson, M. J.; McHardy, W. J.; and Tait, J. M., 1985, The conversion of smectite to illite during diagenesis: evidence from some illitic clays from bentonites and sandstones: *Mineralogical Magazine*, v. 49, p. 393-400.
- Newell, K. D.; Watney, W. L.; and Cheng, S. W. L., 1987, Stratigraphic and spatial distribution of Kansas oil and gas production: *Kansas Geological Survey Subsurface Geology Series* 9.
- Nicholson, J. H., 1960, *Geology of the Texas Panhandle*, in *Aspects of the geology of Texas: a symposium*: University of Texas Publication 6017, p. 51-64.
- Nicholson, J. H.; Kozak, F. D.; Leach, G. W.; and Bogart, L. E., 1955, Stratigraphic correlation chart of Texas Panhandle and surrounding region: *Panhandle Geological Society, Amarillo*.
- Northcutt, R. A., 1985, Oil and gas development in Oklahoma, 1891-1984: *Shale Shaker*, v. 35, p. 123-132.
- O'Donnell, M. R., 1983, Regressive shelf deposits in the Pennsylvanian Arkoma basin, Oklahoma and Kansas: *Shale Shaker*, v. 33, p. 23-37.
- Oetking, Philip; Feray, D. E.; and Renfro, H. L. B., 1967, Geologic highway map of the southern Rocky

- Mountain region, Utah, Colorado, Arizona, and New Mexico: American Association of Petroleum Geologists Map 2, 1 sheet, scale 1:1,875,000.
- Oil and Gas Journal, 1988, Production depth records in U.S.: Oil and Gas Journal, v. 86, no. 10, p. 62.
- Ottman, J. D., 1984, Evaluation of formation fluids in the "J" sandstone, Denver basin, Colorado, in Jorgensen, D. G.; and Signor, D. C. (eds.), *Geohydrology of the Dakota aquifer*: National Water Well Association, Dublin, Ohio, 247 p.
- Overshine, A. T., 1975, Tidal origin of parts of the Karheem Formation (Lower Ordovician), southeastern Alaska, in Ginsburg, R. N. (ed.), *Tidal deposits: a casebook of Recent examples and fossil counterparts*: Springer-Verlag, New York, p. 127-133.
- Palmer, S. E., 1983, Porphyrin distributions in degraded oils from Columbia [abstract]: American Chemical Society National Meeting, Division of Geochemistry, Washington D.C., Aug. 28-Sept. 2, abstr. no. 23.
- Panhandle Geological Society, 1969, Pre-Pennsylvanian geology of the western Anadarko basin: Panhandle Geological Society, Amarillo, 34 p.
- Pate, J. D., 1968, Laverne gas area, Beaver and Harper Counties, Oklahoma, in Beebe, B. W. (ed.), *Natural gases of North America*: American Association of Petroleum Geologists Memoir 9, v. 2, p. 1509-1524.
- Perry, E. A.; and Hower, J., 1970, Burial diagenesis of Gulf Coast pelitic sediments: *Clays and Clay Minerals*, v. 18, p. 165-177.
- Perry, W. J., Jr. [in press], Tectonic evolution of the Anadarko Basin region, Oklahoma, in Stoesser, Judy (ed.), *Evolution of sedimentary basin studies on the evolution of the Anadarko basin*: U.S. Geological Survey Bulletin 1866A.
- Petersen, F. A., 1983, Foreland detachment structures, in Lowell, J. D.; and Gries, R. (eds.), *Rocky Mountain foreland basins and uplifts*: Rocky Mountain Association of Geologists, Denver, p. 65-77.
- Petroleum Information Corporation, 1982, The deep Anadarko basin: A. C. Nielsen Company, Denver, 359 p.
- 1983, Oil and gas map of the United States including basins, uplifts, and basement rocks: Petroleum Information Corporation, Denver, scale 1:3,500,000.
- Petzet, G. A., 1988, Upper Red Fork trend pays off in Oklahoma: *Oil and Gas Journal*, v. 86, no. 11, p. 78-79.
- Philp, R. P.; and Lewis, C. A., 1987, Organic geochemistry of biomarkers: *Annual Review of Earth and Planetary Sciences*, v. 15, p. 363-395.
- Pierce, A. P.; Gott, G. B.; and Myton, J. W., 1964, Uranium and helium in the Panhandle gas field, Texas and adjacent areas: U.S. Geological Survey Professional Paper 454-G, 57 p.
- Pindell, J. L., 1985, Alleghanian reconstruction and subsequent evolution of the Gulf of Mexico, Bahamas, and Proto-Caribbean: *Tectonics*, v. 4, p. 1-39.
- Pippin, Lloyd, 1970, Panhandle-Hugoton field, Texas-Oklahoma-Kansas—the first fifty years, in Halbouty, M. T. (ed.), *Geology of giant petroleum fields*: American Association of Petroleum Geologists Memoir 14, p. 204-222.
- Plouff, Donald, 1977, Preliminary documentation for a FORTRAN program to compute gravity terrain corrections based on topography digitized on a geographic grid: U.S. Geological Survey Open-File Report 77-535, 45 p.
- Plumb, R. A.; and Hickman, S. H., 1985, Stress-induced borehole elongation: a comparison between the four-arm dipmeter and the borehole televiewer in the Auburn geothermal well: *Journal of Geophysical Research*, v. 90, no. B7, p. 5513-5521.
- Pollastro, R. M., 1977, A reconnaissance analysis of the clay mineralogy and major element geochemistry in the Silurian and Devonian carbonates of western New York: a vertical profile: State University of New York, Buffalo, unpublished M.S. thesis, 119 p.
- 1982, A recommended procedure for the preparation of oriented clay-mineral specimens for X-ray diffraction analysis: modifications to Drever's filter-membrane-peel technique: U.S. Geological Survey Open-File Report 82-71, 10 p.
- 1983, The formation of illite at the expense of illite/smectite: mineralogical and morphological support for a hypothesis [abstract]: Clay Minerals Society, 20th Annual Meeting Program and Abstracts, p. 82.
- 1985, Mineralogical and morphological evidence for the formation of illite at the expense of illite/smectite: *Clays and Clay Minerals*, v. 33, p. 265-274.
- [in press], Mineral composition, petrography, and diagenetic modification of lower Tertiary and Upper Cretaceous sandstones and shales, northern Green River basin, Wyoming: U.S. Geological Survey Bulletin.
- Pollastro, R. M.; and Barker, C. E., 1986, Application of clay-mineral, vitrinite reflectance, and fluid inclusion studies to the thermal and burial history of the Pindale anticline, Green River basin, Wyoming, in Gautier, D. L. (ed.), *Roles of organic matter in sediment diagenesis*: Society of Economic Paleontologists and Mineralogists Special Publication 38, p. 73-83.
- Pollastro, R. M.; and Martinez, C. J., 1985, Whole-rock, insoluble residue, and clay mineralogies of marl, chalk, and bentonite, Smoky Hill Shale Member, Niobrara Formation near Pueblo, Colorado—depositional and diagenetic implications, in Pratt, L. M.; Kauffman, E. G.; and Zelt, F. B. (eds.), *Fine-grained deposits and biofacies of the Cretaceous Western Interior Seaway: evidence of cyclic sedimentary processes*: Society of Economic Paleontologists and Mineralogists Field Trip Guidebook, p. 215-222.
- Pollastro, R. M.; and Pillmore, C. L., 1987, Mineralogy and petrology of the Cretaceous-Tertiary boundary clay bed and adjacent clay-rich rocks, Raton basin, New Mexico and Colorado: *Journal of Sedimentary Petrology*, v. 57, p. 456-466.
- Pollastro, R. M.; and Schmoker, J. W., 1988, Relationship of clay diagenesis to temperature, age, and hydrocarbon generation—an example from the Anadarko basin, Oklahoma [abstract], in Carter, L. N. H. (ed.), *U.S. geological research on energy resources 1988*: U.S. Geological Survey Circular 1025, p. 49-50.
- Pollastro, R. M.; and Scholle, P. A., 1986, Diagenetic relationships in a hydrocarbon-productive chalk: the Cretaceous Niobrara Formation, in Mumpton, F. A. (ed.), *Studies in diagenesis*: U.S. Geological Survey Bulletin 1578, p. 219-236.
- Precht, W. F.; and Pollastro, R. M., 1985, Organic and inorganic constituents of the Niobrara Formation in Weld County, Colorado, in Pratt, L. M.; Kauffman, E. G.; and Zelt, F. B. (eds.), *Fine-grained deposits and biofacies of the Cretaceous Western Interior Seaway: evidence of cyclic sedimentary processes*: Society

- of Economic Paleontologists and Mineralogists Field Trip Guidebook, p. 223-233.
- Presley, M. W., 1980, Upper Permian salt-bearing stratigraphic units, in Gustavson, T. C.; and others, Geology and geohydrology of the Palo Duro basin, Texas Panhandle—a report on the progress of nuclear waste isolation feasibility studies (1979): Texas Bureau of Economic Geology Circular 80-7, p. 12-23.
- Preston, P. A.; Harrison, W. E.; Luza, K. V.; Prater, Lynn; and Raja, Reddy, 1982, An evaluation of water resources for enhanced oil-recovery operations, Cement Field, Caddo and Grady Counties, Oklahoma: Oklahoma Geological Survey Special Publication 82-5, 64 p.
- Price, L. C., 1976, Aqueous solubility of petroleum as applied to its origin and primary migration: American Association of Petroleum Geologists Bulletin, v. 60, p. 213-244.
- Price, L. C.; and Barker, C. E., 1985, Suppression of vitrinite reflectance in amorphous rich kerogen—a major unrecognized problem: Journal of Petroleum Geology, v. 8, p. 59-84.
- Purucker, Michael, 1986, Interpretation of an aeromagnetic survey along the Wichita frontal fault zone, in Gilbert, M. C. (ed.), Petrology of the Cambrian Wichita Mountains igneous suite: Oklahoma Geological Survey Guidebook 23, p. 129-136.
- Quigley, T. M.; Mackenzie, A. S.; and Gray, J. R., 1987, Kinetic theory of petroleum generation, in Doligez, B. (ed.), Migration of hydrocarbons in sedimentary basins: Editions Technip, Paris, p. 649-666.
- Ramelli, A. R.; and Slemmons, D. B., 1986, Neotectonic activity of the Meers fault, in Donovan, R. N. (ed.), The Slick Hills of southwestern Oklahoma—fragments of an aulacogen?: Oklahoma Geological Survey Guidebook 24, p. 45-54.
- Ramelli, A. R.; Slemmons, D. B.; and Brocoum, S. J., 1987, The Meers fault; tectonic activity in southwestern Oklahoma: U.S. Nuclear Regulatory Commission, NUREG/CR-4852, 51 p.
- Ramseyer, K.; and Boles, J. R., 1986, Mixed-layer illite/smectite minerals in Tertiary sandstones and shales, San Joaquin basin, California: Clays and Clay Minerals, v. 34, p. 115-124.
- Rascoe, Bailey, Jr.; and Adler, F. J., 1983, Permo-Carboniferous hydrocarbon accumulations, Mid-Continent, U.S.A.: American Association of Petroleum Geologists Bulletin, v. 67, p. 979-1001.
- Reagor, B. G.; Stover, C. W.; and Algermissen, S. T., 1982, Seismicity map of the state of Texas: U.S. Geological Survey Miscellaneous Field Studies Map MF-1388, scale 1:1,000,000.
- Reineck, H. E.; and Singh, I. B., 1980, Depositional sedimentary environments with reference to terrigenous clastics: Springer-Verlag, New York, 549 p.
- Renfro, H. B. [no date], Geologic highway map of Texas: American Association of Petroleum Geologists Map 7, 1 sheet, scale 1:1,875,000.
- Reynolds, R. C., Jr., 1980, Interstratified clay minerals, in Brindley, G. W.; and Brown, G. (eds.), Crystal structure of clay minerals and their X-ray identification: Mineralogical Society, London, p. 247-303.
- Reynolds, R. C., Jr.; and Hower, J., 1970, The nature of interlayering in mixed-layer illite-montmorillonite: Clays and Clay Minerals, v. 18, p. 25-36.
- Rice, D. D., 1983, Relation of natural gas composition to thermal maturity and source rock type in San Juan basin, northwestern New Mexico and southwestern Colorado: American Association of Petroleum Geologists Bulletin, v. 67, p. 1199-1218.
- Rice, D. D.; Hatch, J. R.; and Krystinik, K. B., 1987, Composition, origin, and source of natural gases in the Anadarko basin, Kansas, Oklahoma, and Texas [abstract]: Geological Society of America Abstracts with Programs, v. 19, no. 7, p. 818.
- Roberts, D. G.; and Caston, V. N. D., 1975, Petroleum potential of the deep Atlantic Ocean: Proceeding of the Ninth World Petroleum Congress, v. 2, p. 281-298.
- Rogers, D. A., 1984, Analysis of pull-apart basin development produced by an echelon strike-slip faults, in Sylvester, A. G. (compiler), Wrench fault tectonics: American Association of Petroleum Geologists Reprint Series No. 28, p. 345-360.
- Ross, R. J.; and others, 1982, The Ordovician System in the United States: International Union of Geological Sciences Publication 12, Correlation Chart, 73 p.
- Rowland, T. L., 1974a, The historic 1 Baden unit and a brief look at exploration in the Anadarko basin: Oklahoma Geology Notes, v. 34, p. 3-9.
- 1974b, Lone Star 1 Rogers unit captures world depth record: Oklahoma Geology Notes, v. 34, p. 185-189.
- Rubinstein, I.; Strausz, O. P.; Spyckerelle, C.; Crawford, R. J.; and Westlake, D. W. S., 1977, The origin of the oil sand bitumens of Alberta: a chemical and a microbiological simulation study: Geochimica et Cosmochimica Acta, v. 41, p. 1341-1353.
- Saltus, R. W.; and Blakely, R. J., 1983, HYPERMAG—an interactive, 2-dimensional gravity and magnetic modeling program: U.S. Geological Survey Open-File Report 83-241, 91 p.
- Sanderson, D. J.; and Marchini, W. R. D., 1984, Transpression: Journal of Structural Geology, v. 6, p. 449-458.
- Santiago, D. J., 1979, A gravity and magnetic study of the Medford anomaly, north-central Oklahoma: University of Oklahoma unpublished M.S. thesis, 105 p.
- Saxby, J. D., 1982, A reassessment of the range of kerogen maturities in which hydrocarbons are generated: Journal of Petroleum Geology, v. 5, p. 117-127.
- Schmidt, C. J.; and Garihan, J. M., 1983, Laramide tectonic development of the Rocky Mountain foreland of southwestern Montana, in Lowell, J. D.; and Gries, R. R. (eds.), Rocky Mountain foreland basins and uplifts: Rocky Mountain Association of Geologists, Denver, p. 271-294.
- Schmoker, J. W., 1986, Oil generation in the Anadarko basin, Oklahoma and Texas: modeling using Lopatin's method: Oklahoma Geological Survey Special Publication 86-3, 40 p.
- Schoell, M., 1983, Genetic characterization of natural gases: American Association of Petroleum Geologists Bulletin, v. 67, p. 2225-2238.
- Scholle, P. A.; and Schluger, P. R. (eds.), 1979, Aspects of diagenesis: Society of Economic Paleontologists and Mineralogists Special Publication 26, 443 p.
- Schoonmaker, J.; Mackenzie, F. T.; and Speed, R. C., 1986, Tectonic implications of illite/smectite diagenesis, Barbados accretionary prism: Clays and Clay Minerals, v. 34, p. 465-472.
- Schramm, M. W., Jr., 1964, Paleogeologic and quantitative lithofacies analysis, Simpson Group, Oklahoma: American Association of Petroleum Geologists Bulletin, v. 48, p. 1164-1195.
- Schultz, L. G., 1964, Quantitative interpretation of min-

- eralogical composition from X-ray and chemical data for the Pierre Shale: U.S. Geological Survey Professional Paper 391-C, 31 p.
- 1978, Sample packer for randomly oriented powders in X-ray diffraction analysis: *Journal of Sedimentary Petrology*, v. 48, p. 627–629.
- Schultz, L. G.; Tourtelot, H. A.; Gill, J. R.; and Boerngen, J. G., 1980, Composition and properties of the Pierre Shale and equivalent rocks, Northern Great Plains Region: U.S. Geological Survey Professional Paper 1064-B, 114 p.
- Schwalb, H. R., 1982, Geologic-tectonic history of the area surrounding the northern end of the Mississippi embayment, in Proctor, P. D. (ed.), *Selected structural basins of the Midcontinent, U.S.A.*: University of Missouri—Rolla, UMR Journal, v. 3, p. 31–42.
- Scotchman, I. C., 1987, Clay diagenesis in the Kimmeridge Clay Formation, onshore UK, and its relation to organic maturation: *Mineralogical Magazine*, v. 51, p. 535–551.
- Seifert, W. K.; and Moldowan, J. M., 1978, Applications of steranes, terpanes and monoaromatics to the maturation, migration and source of crude oils: *Geochimica et Cosmochimica Acta*, v. 42, p. 77–95.
- 1979, The effect of biodegradation on steranes and terpanes in crude oils: *Geochimica et Cosmochimica Acta*, v. 43, p. 111–126.
- Seifert, W. K.; Moldowan, J. M.; and Demaison, G. J., 1984, Source correlation of biodegraded oils: *Organic Geochemistry*, v. 6, p. 633–643.
- Seni, S. J., 1980, Sand-body geometry and depositional systems, Ogallala Formation, Texas: Texas Bureau of Economic Geology Report of Investigations 105, 36 p.
- Shelby, J. M., 1980, Geologic and economic significance of the Upper Morrow chert conglomerate reservoir of the Anadarko basin: *Journal of Petroleum Technology*, v. 32, no. 3, p. 489–495.
- Sides, J. R., 1978, A study of emplacement of a shallow granite batholith—St. Francois Mountains, Missouri: University of Kansas unpublished Ph.D. dissertation, 124 p.
- Signor, D. C.; Helgesen, J. O.; Jorgensen, D. G.; and Leonard, R. L. [in preparation], Hydrology of regional aquifer systems in Cretaceous and older rocks underlying Kansas, Nebraska, and parts of Arkansas, Colorado, Missouri, New Mexico, Oklahoma, South Dakota, Texas, and Wyoming: U.S. Geological Survey Professional Paper 1414-C.
- Simon, D. E.; Kaul, F. W.; and Culbertson, J. N., 1977, Anadarko basin Morrow–Springer sandstone stimulation study: Society of Petroleum Engineers 52nd Annual Technical Conference, Preprint 6757, 11 p.
- Simpson, R. W.; Jachens, R. C.; and Blakely, R. J., 1983, AIRYROOT: a FORTRAN program for calculating the gravitational attraction of an Airy isostatic root out to 166.7 km: U.S. Geological Survey Open-File Report 83-883, 66 p.
- Sims, P. K., 1985, Precambrian basement map of northern Midcontinent, U.S.A.: U.S. Geological Survey Open-File Report 85-0604, 16 p., 1 sheet, scale 1:1,000,000.
- Smagala, T. M.; Brown, C. A.; and Nydegger, G. L., 1984, Log-derived indicator of thermal maturity, Niobrara Formation, Denver basin, Colorado, Nebraska, Wyoming, in Woodward, J.; Meissner, F. F.; and Clayton, J. L. (eds.), *Hydrocarbon source rocks of the greater Rocky Mountain region*: Rocky Mountain Association of Geologists, Denver, p. 355–363.
- Smithson, S. B.; Brewer, J. A.; Kaufman, S.; Oliver, J. E.; and Hurich, C., 1978, Nature of the Wind River thrust, Wyoming, from COCORP deep seismic reflection data and from gravity data: *Geology*, v. 6, p. 648–652.
- Society of Professional Well Log Analysts, 1984, Glossary of terms and expressions used in well logging [2nd edition]: Society of Professional Well Log Analysts, 116 p.
- Solter, D. D., Jr., 1980, West Mayfield, in Pipes, P. B., *Oil and gas fields of Oklahoma*, reference report, supplement II: Oklahoma City Geological Society, p. 17–19.
- Springer, J. E., 1987, Stress orientations from well bore breakouts in the Coalinga region: *Tectonics*, v. 6, no. 5, p. 667–676.
- Stach, E.; Mackowsky, M.-Th.; Teichmüller, M.; Teichmüller, R.; Taylor, G. H.; and Chandra, D., 1982, Stach's textbook of coal petrology [3rd revised edition]: Gebrüder Borntraeger, Berlin-Stuttgart, 535 p.
- Statler, A. T., 1965, Stratigraphy of the Simpson Group in Oklahoma: *Tulsa Geological Society Digest*, v. 33, p. 162–211.
- Steeple, D. W., 1984, Earthquakes: Kansas Geological Survey, 11 p.
- Stock, J. M.; Healy, J. H.; Hickman, S. H.; and Zoback, M. D., 1985, Hydraulic fracturing stress measurements at Yucca Mountain, Nevada, and relationship to the regional stress field: *Journal of Geophysical Research*, v. 90, no. B10, p. 8691–8706.
- Stone and Webster Engineering Corporation, 1983, Area geological characterization report for the Palo Duro and Dalhart basins, Texas: Technical Report DOE/CH/10140-1, 429 p.
- Stover, C. W.; Reager, B. G.; and Algermissen, S. T., 1981a, Seismicity map of the state of Kansas: U.S. Geological Survey Miscellaneous Field Map MF-1351, scale 1:1,000,000.
- Stover, C. W.; Reager, B. G.; Algermissen, S. T.; and Lawson, J. E., Jr., 1981b, Seismicity map of the state of Oklahoma: U.S. Geological Survey Miscellaneous Field Map MF-1352, scale 1:1,000,000.
- Sun, R. J., 1986, Regional aquifer-system analysis program of the U.S. Geological Survey—summary of projects, 1978–84: U.S. Geological Survey Circular 1002, 264 p.
- Sutherland, P. K. (ed.), 1982, Lower and Middle Pennsylvanian stratigraphy in south-central Oklahoma: Oklahoma Geological Survey Guidebook 20, 44 p.
- Swanson, D. C., 1979, Deltaic deposits in the Pennsylvanian upper Morrow Formation of the Anadarko basin, in Hyne, N. J. (ed.), *Pennsylvanian sandstones of the Mid-Continent*: Tulsa Geological Society Special Publication 1, p. 115–168.
- Sweeney, J. J.; Burnham, A. K.; and Braun, R. L., 1987, A model of hydrocarbon generation from Type I kerogen: application to Unita basin, Utah: *American Association of Petroleum Geologists Bulletin*, v. 71, p. 967–985.
- Swesnik, R. M., 1948, Geology of West Edmond oil field, Oklahoma, Logan, Canadian, and Kingfisher Counties, Oklahoma, in Howell, J. V. (ed.), *Structure of typical American oil fields*: American Association of Petroleum Geologists, Tulsa, v. 3, p. 359–398.
- Takken, Suzanne, 1963, North Gotebo area, in Cramer, R. D.; Gatlin, L.; and Wessman, H. G. (eds.), *Oil and gas fields of Oklahoma*, reference report, v. 1:

- Oklahoma City Geological Society, p. 50A-53A.
- 1968, Subsurface geology of north Gotebo area, Kiowa and Washita Counties, Oklahoma, in Beebe, B. (ed.), *Natural gases of North America: American Association of Petroleum Geologists Memoir 9*, v. 2, p. 1492-1508.
- 1974, East Cement Springer (deep) field, in Berg, O. R.; Koinm, D. N.; and Richardson, D. E. (eds.), *Oil and gas fields of Oklahoma*, reference report, supplement I: Oklahoma City Geological Society, p. 9.
- Tanner, J. H., III, 1967, Wrench fault movement along the Washita Valley fault, Arbuckle Mountain area, Oklahoma: *American Association of Petroleum Geologists Bulletin*, v. 51, p. 126-141.
- Tarafa, M. E.; Whelan, J. K.; and Farrington, J. W., 1988, Investigation on the effects of organic solvent extraction on whole-rock pyrolysis: multiple-lobed and symmetrical P₂ peaks: *Organic Geochemistry*, v. 12, p. 137-149.
- Tassone, J. A.; and Visser, G. S., 1978, Economic potential of a canyon-fan unit in the Anadarko basin [abstract]: *American Association of Petroleum Geologists Bulletin*, v. 62, p. 567.
- Teichmüller, Marlies, 1986, Organic petrology of source rocks, history and state of the art, in Leythaeuser D.; and Rullkötter, J. (eds.), *Petroleum geochemistry, pt. 1 of Advances in organic geochemistry 1985: Organic Geochemistry*, v. 10, nos. 1-3, p. 581-599.
- 1987, Organic material and very low-grade metamorphism, in Frey, M. (ed.), *Low temperature metamorphism: Chapman and Hall*, New York, p. 114-161.
- Terwilliger-Robertson, S. J., 1986, Petrology and depositional sequences of the Council Grove Group (Lower Permian), Panoma field, Grant and Haskell Counties, Kansas: *Shale Shaker*, v. 36, no. 4, p. 204-208.
- Teufel, L. W., 1985, Insights into the relationship between well bore breakouts, natural fractures, and in situ stress, in Ashworth, Eileen (ed.), *26th U.S. Symposium on Rock Mechanics, Proceedings*, v. 2, p. 1199-1206.
- Thompson, C. L.; and Dembicki, H., Jr., 1986, Optical characteristics of amorphous kerogens and the hydrocarbon-generating potential of source rocks: *International Journal of Coal Geology*, v. 6, p. 229-249.
- Tilford, N. R.; and Westen, D. P., 1984, Morphological evidence for young multiple surface ruptures along the Meers fault in southwestern Oklahoma [abstract]: *Association of Engineering Geologists Abstracts and Program*, p. 79.
- 1985, The Meers fault in southwestern Oklahoma—implications of the sense of recent movement [abstract]: *Association of Engineering Geologists Abstracts and Program*, p. 77.
- Ting, F. T. C., 1978, Petrographic techniques in coal analysis, in Karr, C., Jr. (ed.), *Analytical methods for coal and coal products: Academic Press*, New York, v. 1, p. 3-26.
- Tissot, B. P.; and Espitalié, L., 1975, L'évolution thermique de la matière organique des sédiments: applications d'une simulation mathématique: *Institut Français du Pétrole, Revue*, v. 30, p. 734-777.
- Tissot, B. P.; and Welte, D. H., 1978, *Petroleum formation and occurrence: a new approach to oil and gas exploration: Springer-Verlag*, New York, 538 p.
- 1984, *Petroleum formation and occurrence* [2nd revised edition]: *Springer-Verlag*, New York, 699 p.
- Tissot, B. P.; Durand, B.; Espitalié, J.; and Combaz, A., 1974, Influence of nature and diagenesis of organic matter in formation of petroleum: *American Association of Petroleum Geologists Bulletin*, v. 58, p. 499-506.
- Tomlinson, C. W.; and McBee, William, Jr., 1959, Pennsylvanian sediments and orogenies of Ardmore district, Oklahoma, in *Petroleum geology of southern Oklahoma: American Association of Petroleum Geologists, Tulsa*, v. 2, p. 3-52.
- Ungerer, P. J.; Espitalié, F. M.; and Durand, B., 1986, Use of kinetic models of organic matter evolution for the reconstruction of paleotemperature: application to the case of the Girinville well [France], in Burris, J. (ed.), *Thermal modeling in sedimentary basins: Editions Technip*, Paris, p. 531-546.
- U.S. Department of Energy, 1986, Seismicity, in *Environmental assessment, Deaf Smith County site, Texas: U.S. Department of Energy, Office of Civilian Radioactive Waste Management, DOE/RW-0069*, v. 1 of 3, p. 3-76-3-82.
- U.S. Geological Survey, 1975, Aeromagnetic map of the Wichita Mountains area, southwestern Oklahoma: *U.S. Geological Survey Open-File Report 75-16*, 1 oversized plate.
- Urban, J. B., 1960, *Microfossils of the Woodford Shale (Devonian) of Oklahoma: University of Oklahoma unpublished M.S. thesis*, 77 p.
- Van de Meent, D.; Brown, S. C.; Philp, R. P.; and Simoneit, B. R. T., 1980, Pyrolysis high resolution gas chromatography and pyrolysis-gas chromatography-mass spectrometry of kerogen and kerogen precursors: *Geochimica et Cosmochimica Acta*, v. 44, p. 999-1013.
- Ver Wiebe, W. A., 1930, *Ancestral Rocky Mountains: American Association of Petroleum Geologists Bulletin*, v. 14, p. 765-788.
- Viele, G. W., 1986, The subduction of Texas [abstract]: *Geological Society of America Abstracts with Programs*, v. 18, p. 779.
- Volkman, J. K.; Alexander, R.; Kagi, R. I.; Woodhouse, G. W., 1983, Demethylated hopanes in crude oils and their applications in petroleum geochemistry: *Geochimica et Cosmochimica Acta*, v. 47, p. 785-794.
- Volkman, J. K.; Alexander, R.; Kagi, R. I.; Rowland, S. J.; Sheppard, P. N., 1984, Biodegradation of aromatic hydrocarbons in crude oils from the Barrow sub-basin of western Australia, in Schenck, P. A.; De Leeuw, J. W.; and Lijmbach, G. W. M. (eds.), *Advances in organic geochemistry 1983: Pergamon Press*, Oxford, p. 619-632.
- von Almen, W. F., 1970, Palynomorphs of the Woodford Shale of south central Oklahoma with observations on their significance in zonation and paleoecology: *Michigan State University unpublished Ph.D. dissertation*, 179 p.
- von Schonfeldt, H. A.; Kehle, R. O.; and Gray, K. E., 1973, Mapping of stress field in the upper earth's crust of the U.S.; final technical report, grant 14-08-0001-1222: *U.S. Geological Survey*, Reston, Virginia, 78 p.
- Walker, J. R., 1985, Development and economic significance of Springer-Britt sandstone, Eakly field, Caddo, Custer, and Washita Counties [abstract]: *American Association of Petroleum Geologists Bulletin*, v. 69, p. 1320.
- Walters, R. F., 1958, Differential entrapment of oil and gas in Arbuckle dolomite of central Kansas: *American*

- Association of Petroleum Geologists Bulletin, v. 42, p. 2133-2173.
- Wanless, H. R.; Boroffio, J. R.; Gamble, J. C.; Horne, J. C.; Orlopp, D. R.; Rocha-Campos, A.; Souter, J. E.; Prescott, T. C.; Vail, R. S.; and Wright, C. R., 1970, Late Paleozoic deltas in the central and eastern United States, in Morgan, J. P. (ed.), *Deltaic sedimentation, modern and ancient*: Society of Economic Paleontologists and Mineralogists Special Publication 15, p. 215-245.
- Waples, D. W., 1980, Time and temperature in petroleum formation: application of Lopatin's method to petroleum exploration: American Association of Petroleum Geologists Bulletin, v. 64, p. 916-926.
- 1985, *Geochemistry in petroleum exploration*: International Human Resources Development Corporation, Boston, 232 p.
- Wardroper, A. M. K.; Hoffmann, C. F.; Maxwell, J. R.; Barwise, A. J. G.; Goodwin, N. S.; Park, P. J. D., 1984, Crude oil biodegradation under simulated and natural conditions. II. Aromatic steroid hydrocarbons: *Organic Geochemistry*, v. 6, p. 605-617.
- Warner, L. Q., 1980, Colorado lineaments, in Kent, H. C.; and Porter, K. W. (eds.), *Colorado geology: Rocky Mountain Association of Geologists, Symposium on Colorado*, p. 11-21.
- Weaver, C. E., 1979, Geothermal alteration of clay minerals and shales: Office of Nuclear Waste Isolation Technical Report 21, 176 p.
- Webb, G. W., 1976, Oklahoma City oil-second crop from pressured subunconformity source rocks: American Association of Petroleum Geologists Bulletin, v. 60, p. 115-122.
- Weber, S. J., 1987, Petrography and diagenesis of the McLish Formation, Simpson Group (Middle Ordovician), southeastern Anadarko basin, Oklahoma: Oklahoma State University unpublished M.S. thesis, 98 p.
- Webring, Michael, 1981, MINC—a gridding program based on minimum curvature: U.S. Geological Survey Open-File Report 81-1224, 43 p.
- 1985, SAKI—a FORTRAN program for generalized linear inversion of gravity and magnetic profiles: U.S. Geological Survey Open-File Report 85-122, 108 p.
- Webster, R. E., 1977, Evolution of a major petroleum province: the southern Oklahoma aulacogen: *The Compass of Sigma Gamma Epsilon*, v. 54, p. 59-71.
- 1980, Evolution of s. Oklahoma aulacogen: *Oil and Gas Journal*, v. 78, no. 7, p. 150-172.
- Weeks, J. B.; and Gutentag, E. D., 1981, Bedrock geology, altitude of base, and 1980 saturated thickness of the High Plains aquifer in parts of Colorado, Kansas, Nebraska, New Mexico, Oklahoma, South Dakota, Texas, and Wyoming: U.S. Geological Survey Hydrologic Investigations Atlas HA-648, 2 sheets, scale 1:2,500,000.
- Welte, D. H.; Kratochvil, H.; Rullkötter, J.; Ladwein, H.; and Schaefer, R. G., 1982, Organic geochemistry of crude oils from the Vienna basin and an assessment of their origin: *Chemical Geology*, v. 35, p. 33-68.
- Wenger, L. M.; and Baker, D. R., 1987, Variations in vitrinite reflectance with organic facies—examples from Pennsylvanian cyclothem of the Midcontinent, U.S.A.: *Organic Geochemistry*, v. 11, p. 411-416.
- Werner, Eberhard, 1976, Graphic display of orientation data for visual analysis, in Prodwysocki, M. H.; and Earle, J. L. (eds.), *Proceedings of the Second International Conference on Basement Tectonics*, p. 521-527.
- Whitney, G.; and Northrop, H. R., 1988, Experimental investigation of the smectite to illite reaction: dual reaction mechanisms and oxygen-isotope systematics: *American Mineralogist*, v. 73, p. 77-90.
- Wickham, J. S., 1978a, The southern Oklahoma aulacogen, in *Structural style of the Arbuckle region*: Geological Society of America, South-Central Section, Guidebook for Field Trip No. 3, p. 9-41.
- 1978b, The southern Oklahoma aulacogen, in *Structure and stratigraphy of the Ouachita Mountains and the Arkoma basin*: Oklahoma City Geological Society Guidebook, p. 1-34.
- Wickham, John; Roeder, Dietrich; and Briggs, Garrett, 1976, Plate tectonics models for the Ouachita foldbelt: *Geology*, v. 4, p. 173-176.
- Wilcox, R. E.; Harding, T. P.; and Seely, D. R., 1973, Basic wrench tectonics: American Association of Petroleum Geologists Bulletin, v. 57, p. 74-96.
- Wilhelm, S. J.; and Morgan, K. M., 1986, Utilization of Landsat thematic-mapper data for lineament analysis of the Slick Hills area, in Donovan, R. N. (ed.), *The Slick Hills of southwestern Oklahoma—fragments of an aulacogen?*: Oklahoma Geological Survey Guidebook 24, p. 35-39.
- Wilson, J. L.; and Majewske, O. P., 1960, Conjectured Middle Paleozoic history of central and west Texas, in *Aspects of the geology of Texas: a symposium*: University of Texas Publication 6017, p. 65-86.
- Wilson, L. R.; and Skvarla, J. J., 1967, Electron-microscope study of the wall structure of *Quisquilites* and *Tasmanites*: *Oklahoma Geology Notes*, v. 27, p. 54-63.
- Wilson, L. R.; and Urban, J. B., 1963, An Incertae sedis palynomorph from the Devonian of Oklahoma: *Oklahoma Geology Notes*, v. 23, p. 16-19.
- Wingenter, H. R., 1958, Greenwood gas field, Kansas, Colorado, and Oklahoma, in Beebe, B. W. (ed.), *Natural gases of North America*: American Association of Petroleum Geologists Memoir 9, v. 2, p. 1557-1566.
- Winters, J. C.; and Williams, J. A., 1969, Microbiological alteration of crude oil in the reservoir: American Chemical Society, Division of Petroleum Chemistry, Sym. Pet. Transform. Geol. Environ., New York, Sept. 7-12, Preprints 14 (4), E-22-E-31.
- World Oil, 1988, Producing depth records set in two states despite slow recovery: *World Oil*, v. 206, no. 2, p. 72.
- Wright, W. F., 1979, Petroleum geology of the Permian basin: West Texas Geological Society, Midland, 98 p.
- Wroblewski, E. F., 1970, New look at a major deep-drilling area—the Anadarko basin: *World Oil*, v. 171, no. 2, p. 292.
- Yarger, H. L., 1982, Regional interpretations of Kansas aeromagnetic data, in Steeples, D. W.; and Stearnes, S. A. (eds.), *Assessment of geothermal resources of Kansas*: Kansas Geological Survey Report to Geothermal Division of U.S. Department of Energy, 260 p.
- Young, S. D., 1977, Gageby Creek, in Taylor, I. D., *Selected gas fields of the Texas Panhandle*: Panhandle Geological Society, Amarillo, p. 19-26.
- Zeller, D. E. (ed.), 1968, The stratigraphic succession in Kansas: *Kansas Geological Survey Bulletin* 189, 81 p.
- Zemmels, I.; Tappmeyer, D. M.; and Walters, C. C., 1987, Source of shallow Simpson Group oils in Murray County, Oklahoma [abstract]: American Association of Petroleum Geologists Bulletin, v. 61, p. 1-2.

- tion of Petroleum Geologists Bulletin, v. 71, p. 245.
- Zoback, M. D.; and Zoback, M. L., 1981, State of stress and intraplate earthquakes in the United States: *Science*, v. 213, p. 96–104.
- Zoback, M. D.; Moss, Daniel; Mastin, R. L.; and Anderson, R. M., 1985, Well bore breakouts and in situ stress: *Journal of Geophysical Research*, v. 90, no. B7, p. 5523–5530.
- Zoback, M. L.; and Zoback, Mark, 1980, State of stress in the conterminous United States: *Journal of Geophysical Research*, v. 85, no. B11, p. 6113–6156.